AQUATIC INVERTEBRATE IMMUNITY AGAINST INFECTIOUS DISEASES

EDITED BY: Chaozheng Li, Kunlaya Somboonwiwat and Luciane M. Perazzolo
PUBLISHED IN: Frontiers in Immunology

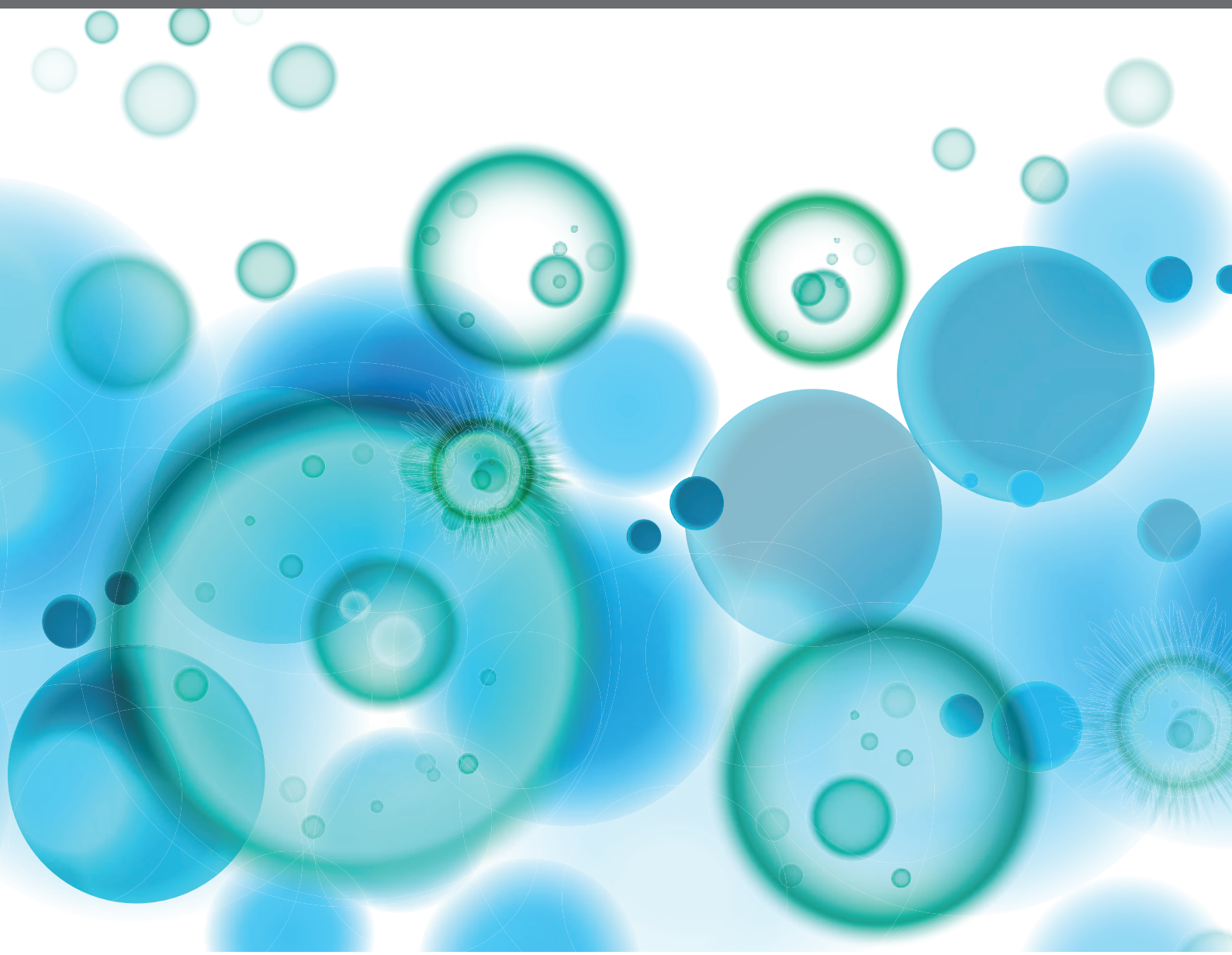

frontiers Research Topics

frontiers

ISSN 1664-8714
ISBN 978-2-88971-610-4
DOI 10.3389/978-2-88971-610-4

About Frontiers

Frontiers is more than just an open-access publisher of scholarly articles: it is a pioneering approach to the world of academia, radically improving the way scholarly research is managed. The grand vision of Frontiers is a world where all people have an equal opportunity to seek, share and generate knowledge. Frontiers provides immediate and permanent online open access to all its publications, but this alone is not enough to realize our grand goals.

Frontiers Journal Series

The Frontiers Journal Series is a multi-tier and interdisciplinary set of open-access, online journals, promising a paradigm shift from the current review, selection and dissemination processes in academic publishing. All Frontiers journals are driven by researchers for researchers; therefore, they constitute a service to the scholarly community. At the same time, the Frontiers Journal Series operates on a revolutionary invention, the tiered publishing system, initially addressing specific communities of scholars, and gradually climbing up to broader public understanding, thus serving the interests of the lay society, too.

Dedication to Quality

Each Frontiers article is a landmark of the highest quality, thanks to genuinely collaborative interactions between authors and review editors, who include some of the world's best academicians. Research must be certified by peers before entering a stream of knowledge that may eventually reach the public - and shape society; therefore, Frontiers only applies the most rigorous and unbiased reviews.
Frontiers revolutionizes research publishing by freely delivering the most outstanding research, evaluated with no bias from both the academic and social point of view. By applying the most advanced information technologies, Frontiers is catapulting scholarly publishing into a new generation.

What are Frontiers Research Topics?

Frontiers Research Topics are very popular trademarks of the Frontiers Journals Series: they are collections of at least ten articles, all centered on a particular subject. With their unique mix of varied contributions from Original Research to Review Articles, Frontiers Research Topics unify the most influential researchers, the latest key findings and historical advances in a hot research area! Find out more on how to host your own Frontiers Research Topic or contribute to one as an author by contacting the Frontiers Editorial Office: frontiersin.org/about/contact

AQUATIC INVERTEBRATE IMMUNITY AGAINST INFECTIOUS DISEASES

Topic Editors:
Chaozheng Li, Sun Yat-sen University, China
Kunlaya Somboonwiwat, Chulalongkorn University, Thailand
Luciane M. Perazzolo, Federal University of Santa Catarina, Brazil

Citation: Li, C., Somboonwiwat, K., Perazzolo, L. M., eds. (2021). Aquatic Invertebrate Immunity Against Infectious Diseases. Lausanne: Frontiers Media SA. doi: 10.3389/978-2-88971-610-4

Table of Contents

frontiers in Immunology

EDITORIAL
published: 22 September 2021
doi: 10.3389/fimmu.2021.762082

Editorial: Aquatic Invertebrate Immunity Against Infectious Diseases

Luciane Maria Perazzolo[1]*, *Chaozheng Li*[2] and *Kunlaya Somboonwiwat*[3]

[1] Laboratory of Immunology Applied to Aquaculture, Department of Cell Biology, Embryology and Genetics, Federal University of Santa Catarina, Florianópolis, Brazil, [2] Southern Marine Science and Engineering Guangdong Laboratory (Zhuhai)/ State Key Laboratory of Biocontrol, School of Marine Sciences, Sun Yat-Sen University, Guangzhou, China, [3] Center of Excellence for Molecular Biology and Genomics of Shrimp, Department of Biochemistry, Faculty of Science, Chulalongkorn University, Bangkok, Thailand

Keywords: farmed aquatic invertebrates, host-pathogen-microbiota interactions, antiviral immunity, antimicrobial defense, crustaceans, mollusks

Editorial on the Research Topic

Aquatic Invertebrate Immunity Against Infectious Diseases

OPEN ACCESS

Edited and reviewed by:
Miki Nakao,
Kyushu University, Japan

***Correspondence:**
Luciane Maria Perazzolo
l.m.perazzolo@ufsc.br

Specialty section:
This article was submitted to Comparative Immunology, a section of the journal Frontiers in Immunology

Received: *20 August 2021*
Accepted: *06 September 2021*
Published: *22 September 2021*

Citation:
Perazzolo LM, Li C and Somboonwiwat K (2021) Editorial: Aquatic Invertebrate Immunity Against Infectious Diseases. Front. Immunol. 12:762082. doi: 10.3389/fimmu.2021.762082

Aquatic invertebrates farming represents an important trade in the food supply of the global economy. Despite the expanding commercial relevance of shellfish farming, emerging diseases have caused catastrophic losses by limiting aquaculture sustainability. Crustaceans and mollusks cultures face numerous challenges, notably viral, bacterial, and fungal infections. Invertebrates lack classical adaptive immunity and only rely on innate responses to protect them from pathogens. Shrimp, oysters, scallops, mussels, crayfish, and crabs are among the most valuable farmed invertebrates. Understanding interactions between its immunity and pathogens is critical to controlling farming diseases. In light of this, nowadays, research on shellfish immunity has received remarkable efforts to unravel the molecular mechanisms that drive the immune responses against pathogens and, ultimately, to reach new non-antibody-based therapies to protect both cultivated and wild species. This Research Topic compiles 13 articles, including original studies and reviews by renowned scientists and research groups, which integrate current progress and understanding regarding antiviral and antimicrobial defenses triggered by aquatic invertebrates to control infectious diseases.

PATHOGEN RECOGNITION AND ANTIMICROBIAL DEFENSES

Like other invertebrates, shellfish possess cellular and humoral defenses to protect them against pathogens. However, defense responses must be tightly regulated to allow the destruction of pathogens without harming the host. In this Research Topic, Bouallegui reviews crayfish immunity, addressing plague disease, molecular aspects of hematopoiesis, and highlighting cell-mediated responses associated with Extracellular trap cell death (ETosis). During pathogen recognition, the host's pattern recognition receptors/proteins (PRRs/PRPs) recognize and bind to microbial/pathogen-associated molecular patterns (MAMPs/PAMPs), inducing PAMP-triggered immunity (PTI). C-type lectins are crucial PRPs for immobilizing microorganisms by agglutination; shrimp lectins are also implicated in antibacterial and antiviral defenses (1). Qiu et al. describe a novel C-type lectin widely distributed in adult mud crab tissues, *Scylla paramamosain* (*Sp*CTL6), and discuss

its immunoprotective effect against bacteria. In turn, Cao et al. report a new lectin expressed by the hepatopancreas of the red swamp crayfish (*Procambarus clarkii*) and discuss its agglutinating ability to promote bacterial clearance.

ANTIVIRAL IMMUNITY

In penaeid shrimp farming, selective breeding and biosecurity have become essential to prevent viral diseases based on the host's robust resistance to specific pathogens (2). Both disease prevention and genetic improvement have been based on theoretical support for the interaction between host immunity and virus pathogenesis (3). In this Research Topic, Zhang et al. report and discuss that glycogen synthase kinase-3β (GSK3β) from shrimp *Litopenaeus vannamei* (*Lv*GSK3β) negatively regulates the activity of NF-κB pathway; RNAi mediated knockdown of *Lv*GSK3β raise the survival of the shrimp infected by White spot syndrome virus (WSSV). In turn, Li et al. reveal that the TRAF3 ortholog from the *L. vannamei* (*Lv*TRAF3) could protect shrimp against WSSV infection by mediating antiviral defense throughout the IRF-Vago pathway, but not by the NF-κB pathway. Altogether, these findings describe shrimp immune responses against WSSV and suggest potential candidate genes for resistance-based antiviral defense. Another relevant contribution is made by Liao et al. concerning the decapod iridescent virus 1 (DIV1), an emergent virus responsible for recent economic troubles in Asian shrimp farming (4). Comparative transcriptome analysis reveals that DIV1 could hijack the triosephosphate isomerase-like genes (LvTPI) to facilitate virus replication in shrimp (Liao et al.). Consequently, LvTPI gene silencing reduces shrimp mortality by inhibiting viral replication. This study provides a theoretical basis for the epidemiological investigation of DIV1 infection and may help prevent viral diseases in shrimp farming.

CELL-MEDIATED RESPONSES

Hemocytes represent the immunocompetent cells of crustaceans and mollusks, responsible for cell-mediated responses against invading microorganisms and parasites. Regarding oyster immunity, cell-mediated responses include infiltration, phagocytosis, extracellular trap cell death, encapsulation, immune genes induction, and effectors secretion (5). In light of this, Lu et al. report and discuss the alteration in some hemato-immunological parameters in oyster *Crassostrea hongkongensis* associated with gender and subpopulation in oysters under bacterial challenge. Estrada et al. evaluated and discuss the occurrence of programmed cell death (PCD), apoptosis and pyroptosis-like, in hemocytes from *Crassostrea gigas* triggered by marine toxins produced by microalgae and bacteria.

HOST-PATHOGEN AND MICROBIOTA INTERACTIONS

Recent studies have revealed exciting aspects of the immune defense triggered by aquatic invertebrates in response to strategies used by pathogens to circumvent them. Insights into host-pathogen and microbiota interactions in fighting invaders have only recently started to emerge. In line with this notion, Petton et al. review and shed light on how the polymicrobial and multifactorial factors operate in the Pacific oyster mortality syndrome (POMS), the most prevalent disease in *C. gigas*. The authors underline the effect of environmental culture conditions and the oyster microbiota imbalance (dysbiosis) in promoting the POMS pathogenesis. Bivalves are sessile filter feeders that live closely associated with large and diverse communities of microorganisms that form their microbiota. In light of this, González et al. provide new insights into the interaction between the immune responses of scallop *Argopecten purpuratus* and its microbiota. Scallop antimicrobial peptides and proteins are implicated in maintaining microbial homeostasis and are critical molecules in orchestrating host-microbiota interactions. In turn, aspects of the infection of Chinese crab, *Eriocheir sinensis* by the pathogenic yeast are described by Jiang et al., using proteomic analysis. The disease caused by *Metschnikowia bicuspidata* seems to induce some antimicrobial mechanisms (proPO activation system, ROS, and phagocytosis), while the fungal infection suppresses hemolymph coagulation and tissue regeneration.

HOST SUSCEPTIBILITY VERSUS TOLERANCE TO MICROBIAL AND VIRAL INFECTIONS

As already mentioned, microbial and viral infections have impacted aquatic invertebrates farming, and selective breeding and biosecurity in farms have become essential to prevent diseases based on the host's robust resistance to specific pathogens (2). Surprisingly, the molecular mechanisms that drive the susceptibility and tolerance of aquatic invertebrates against pathogens remain elusive. A study conducted by Mai et al. report molecular aspects of differential gene expression in susceptible and resistant strains of shrimp to acute hepatopancreatic necrosis disease (AHPND). A set of candidate genes is proposed to be involved in bacterial pathogenesis, and these findings may aid in breeding programs to select AHPND resistant/tolerant shrimp. In turn, Escobedo-Bonilla provides a broad overview of the viral interference phenomenon in cultivated crustacean species. Exclusion of superinfection, virus-virus interaction, host cell receptor blockade, viral co-infection, and current assays to assess viral interference are widely discussed. Ultimately, a heterologous virus interference mechanism is proposed as a natural strategy to control the incidence of viral diseases in shrimp farming.

CONCLUDING REMARKS

This Research Topic brings new studies and insights into the molecular, cellular, and physiological mechanisms implicated in

antimicrobial and antiviral defenses triggered by the aquatic invertebrates. Original articles and reviews provide novel sharpness into the intricate puzzle of pathogen-host interaction, the role of microbiota in host health and homeostasis, intracellular pathways driving immune effectors/regulators, viral interference phenomena, host susceptibility and tolerance to infections, and other issues. Elucidating the multifaceted mechanisms driving the immunity of farmed aquatic invertebrates is crucial to building new non-antibody-based therapies and controlling aquaculture diseases. Hopefully, the exciting outcomes displayed here can contribute to developing tools that increase shellfish immunocompetence and ultimately promote health security in aquaculture.

AUTHOR CONTRIBUTIONS

All authors co-edited the Research Topic. LMP substantially contributed to the conception, drafting, and editing of the final version of the Editorial. CL and KS contributed by drafting part of the work and approved it for publication. All authors contributed to the article and approved the submitted version.

ACKNOWLEDGMENTS

The Editors would like to thank all Research Topic Authors and additional editors for their contributions.

REFERENCES

1. Wang XW, Vasta GR, Wang JX. The Functional Relevance of Shrimp C-Type Lectins in Host-Pathogen Interactions. *Dev Comp Immunol* (2020) 109:103708. doi: 10.1016/j.dci.2020.103708
2. Moss SM, Moss DR, Arce SM, Lightner DV, Lotz JM. The Role of Selective Breeding and Biosecurity in the Prevention of Disease in Penaeid Shrimp Aquaculture. *J Invertebr Pathol* (2012) 110:247–50. doi: 10.1016/J.JIP.2012.01.013
3. Li C, Weng S, He J. WSSV–host Interaction: Host Response and Immune Evasion. *Fish Shellfish Immunol* (2019) 84:558–71. doi: 10.1016/j.fsi.2018.10.043
4. Qiu L, Chen MM, Wan XY, Li C, Zhang QL, Wang RY, et al. Characterization of a New Member of Iridoviridae, Shrimp Hemocyte Iridescent Virus (SHIV), Found in White Leg Shrimp (*Litopenaeus Vannamei*). *Sci Rep* (2017) 7:11834. doi: 10.1038/s41598-017-10738-8
5. Bachère E, Rosa RD, Schmitt P, Poirier AC, Merou N, Charrière GM, et al. The New Insights Into the Oyster Antimicrobial Defense: Cellular, Molecular and Genetic View. *Fish Shellfish Immunol* (2015) 46:50–64. doi: 10.1016/j.fsi.2015.02.040

Conflict of Interest: The authors declare that the research was conducted in the absence of any commercial or financial relationships that could be construed as a potential conflict of interest.

Publisher's Note: All claims expressed in this article are solely those of the authors and do not necessarily represent those of their affiliated organizations, or those of the publisher, the editors and the reviewers. Any product that may be evaluated in this article, or claim that may be made by its manufacturer, is not guaranteed or endorsed by the publisher.

frontiers in Immunology

ORIGINAL RESEARCH
published: 28 August 2020
doi: 10.3389/fimmu.2020.01904

Comparative Transcriptome Analysis of *Litopenaeus vannamei* Reveals That Triosephosphate Isomerase-Like Genes Play an Important Role During Decapod Iridescent Virus 1 Infection

Xuzheng Liao[1†], Chenggui Wang[1†], Bo Wang[1], Haipeng Qin[1], Shikang Hu[1], Ping Wang[2], Chengbo Sun[1,3,4] and Shuang Zhang[1,5*]*

[1] College of Fisheries, Guangdong Ocean University, Zhanjiang, China, [2] Hainan Zhongzheng Aquatic Science and Technology Co., Ltd., Hainan, China, [3] Guangdong Provincial Laboratory of Southern Marine Science and Engineering, Zhanjiang, China, [4] Guangdong Provincial Key Laboratory of Pathogenic Biology and Epidemiology for Aquatic Economic Animals, Zhanjiang, China, [5] Aquatic Animals Precision Nutrition and High Efficiency Feed Engineering Research Center of Guangdong Province, Zhanjiang, China

Decapod iridescent virus 1 (DIV1) results in severe economic losses in shrimp aquaculture. However, little is known about the physiological effect of DIV1 infection on the host. In this study, we found that the lethal dose 50 of DIV1-infected *Litopenaeus vannamei* after 48, 72, 96, and 156 h were 4.86×10^6, 5.07×10^5, 2.13×10^5, and 2.38×10^4 copies/μg DNA, respectively. In order to investigate the mechanisms of DIV1 infection, a comparative transcriptome analysis of hemocytes from *L. vannamei*, infected or not with DIV1, was conducted. The BUSCO analysis showed that the transcriptome was with high completeness (complete single-copy BUSCOs: 57.3%, complete duplicated BUSCOs: 41.1%, fragmentation: 0.8%, missing: 0.8%). A total of 168,854 unigenes were assembled, with an average length of 601 bp. Based on homology searches, Kyoto Encyclopedia of Genes and Genomes (KEGG), gene ontology (GO), and cluster of orthologous groups of proteins (KOG) analysis, 62,270 (36.88%) unigenes were annotated. Among them, 1,112 differentially expressed genes (DEGs) were identified, of which 889 genes were up-regulated and 223 genes were down-regulated after DIV1 infection. These genes were mainly annotated to the major metabolic processes such as fructose and mannose metabolism, carbon metabolism, and inositol phosphate metabolism. Among these metabolic pathways, the triosephosphate isomerase (*TPI*) family was the most eye-catching DEG as it participates in several metabolic processes. Three types of *TPI*, *LvTPI-like*, *LvTPI-Blike*, and *LvTPI-Blike1*, were obtained for gene silencing by RNA interference. The results showed that *LvTPI-like* and *LvTPI-Blike1* silencing caused a high mortality rate among *L. vannamei.*

OPEN ACCESS

Edited by:
Luciane M. Perazzolo, Federal University of Santa Catarina, Brazil

Reviewed by:
Chris Hauton, University of Southampton, United Kingdom
Shengkang Li, Shantou University, China

***Correspondence:**
Chengbo Sun
scb248@126.com
Shuang Zhang
zshuang@gdou.edu.cn

[†]These authors have contributed equally to this work

Specialty section:
This article was submitted to Comparative Immunology, a section of the journal Frontiers in Immunology

Received: *27 April 2020*
Accepted: *15 July 2020*
Published: *28 August 2020*

Citation:
Liao X, Wang C, Wang B, Qin H, Hu S, Wang P, Sun C and Zhang S (2020) Comparative Transcriptome Analysis of Litopenaeus vannamei Reveals That Triosephosphate Isomerase-Like Genes Play an Important Role During Decapod Iridescent Virus 1 Infection. Front. Immunol. 11:1904. doi: 10.3389/fimmu.2020.01904

However, *LvTPI-like* and *LvTPI-Blike* silencing reduced DIV1 replication in DIV1-infected *L. vannamei*. All the results indicated that *TPI-like* genes play an important role during DIV1 infection, which provides valuable insight into the infection mechanism of DIV1 in shrimp and may aid in preventing viral diseases in shrimp culture.

Keywords: *Litopenaeus vannamei*, DIV1, triosephosphate isomerase, transcriptome analysis, RNA interference

INTRODUCTION

Litopenaeus vannamei is a widely cultured shrimp species all around the world, with a huge production per year (1). The development of farmed shrimp has led to high-density growth conditions, large-scale production, and unsanitary aquaculture wastewater discharge, resulting in disease overflow, ecological imbalance, and environmental deterioration. The shrimp industry is now faced with finding solutions for these serious problems (2, 3). Over the past decades, diseases caused by various bacterial, fungal, parasitic, and viral species have significantly constrained the productivity of the *L. vannamei* industry (4). For a long time, the most concerning viruses were the white spot syndrome virus (WSSV), the Taura syndrome virus (TSV), and the infectious hypodermal and hematopoietic necrosis virus (IHHNV) (5). However, in 2014, the decapod iridescent virus 1 (DIV1) caused huge losses in farmed *L. vannamei* in Zhejiang Province in China. DIV1 was isolated and identified by Qiu et al. in 2017 (6). Since then, the prevention and the control of DIV1 have attracted much attention in shrimp culture.

In 1993, Lightner and Redman first discovered the iridescent virus in shrimp in Ecuador (7). In 2004, Tang et al. found the iridescent virus in *Acetes erythraeus* grown in Madagascar and, *via* sequencing, found that it was a new type of iridescent virus (*Sergestid iridovirus*, SIV) (8). In 2016, Xu et al. detected a new iridescent virus, *Cherax quadricarinatus* iridovirus (CQIV), from *Cherax quadricarinatus* on a farm in China (9). In 2017, Qiu et al. detected shrimp hemocyte iridescent virus (SHIV) from *L. vannamei* and determined that SHIV is a member of the new genus *Xiairidovirus*, which also belongs to the Iridoviridae family. The complete genome sequence of SHIV is 165,908-bp long with 34.6% G + C content and 170 open reading frames. Qiu et al. used intermuscular injection and reverse gavage methods to infect *L. vannamei* with SHIV, resulting in a 100% cumulative mortality rate. Results from the histopathological study using transmission electron microscopy of ultrathin sections and *in situ* hybridization indicated that SHIV mainly infects the hematopoietic tissue and hemocytes in the Pacific white shrimp (6). In 2019, the Executive Committee of the International Committee on Taxonomy of Viruses (ICTV) identified two virus isolates, SHIV and CQIV, as decapod iridescent virus 1 (DIV1) (10). Crustaceans in the coastal region of China, including *L. vannamei*, *Fenneropenaeus chinensis*, *Exopalaemon carinicauda*, and *Macrobrachium rosenbergii*, can all carry DIV1 (6, 11, 12). Until now, most of the studies on DIV1 focused on the virus itself or the histopathological changes in the host. Latest studies in 2020 based on transcriptome analysis showed that the phagosome and the MAPK signaling pathway were positively modified during DIV1 infection in *C. quadricarinatus* (13), while lysosome and phagosome were induced during DIV1 infection in *Fenneropenaeus merguiensis* (14). However, little is known about the mechanism of the host response to DIV1 infection.

Shrimp rely on their innate immune system to defend against invading viruses and microbes. Shrimp cells can recognize the invading virus *via* unique host pattern recognition proteins with pathogen-associated molecular patterns, which can activate the host immune response (15). The innate immune system includes the humoral immune system and the cellular immune system. The humoral responses are mediated by macromolecules in the hemolymph. Humoral responses are mainly divided into melanin synthesis by the prophenoloxidase system, the blood clotting system, and the generation of circulating antimicrobial peptides (16). The cellular immune response involves different types of hemocytes, which clear harmful substances in the hemolymph by defensive reactions such as phagocytosis and encapsulation (17). Recent studies confirmed that hemocytes are an important source of several humoral effector molecules, which are required in killing foreign invaders in shrimp (18, 19). It is necessary to understand the immune system of shrimp in order to develop methods that can successfully control and reduce the loss of shrimp production due to infectious diseases. High-throughput RNA sequencing (RNA-Seq) is an efficient technology to analyze gene expression, discover transcripts, and select differentially expressed genes (DEGs) (20). This technology has been used to study the molecular basis of certain gene transcription processes (21). Ren et al. found several genes related to immunity through the transcriptome profiles of *M. japonicus* following infection with *V. parahemolyticus* or WSSV (22). Additional research into the function of these immune genes, such as *caspase 4*, *integrin*, *crustin*, *ubiquitin-conjugating enzyme E2*, *C-type lectin*, and α_2*-macroglobulin*, is required to understand the molecular interactions between *V. parahemolyticus* and WSSV in *M. japonicus* and to provide valuable information for preventing diseases (22). However, no information is available on the gene expression profiles of DIV1-infected *L. vannamei*.

In the present study, the lethal concentration 50 (LD_{50}) of DIV1-infected *L. vannamei* was determined, and RNA-Seq was applied to compare the transcriptome difference between the DIV1-infected and non-infected *L. vannamei.* This study aims to gain a better insight into the DIV1–shrimp interaction and may help better understand the innate immune mechanism in shrimp, which would be beneficial to disease prevention in shrimp culture.

MATERIALS AND METHODS

Shrimp Culture

The study protocol was approved by the ethics review board of the Institutional Animal Care and Use Committee in Guangdong Ocean University. *L. vannamei* (body weight 11.2 ± 2.4 g) was purchased from Hainan Zhongzheng Aquatic Science and Technology Co., Ltd., in Dongfang (Hainan, China). The shrimps were acclimatized for 1 week in 0.3-m^3 tanks with aerated and filtered seawater in East Island Marine Biological Research Base, Guangdong Ocean University in Zhanjiang, Guangdong, China. The holding seawater conditions were as follows: salinity at 28.5 ± 0.26 ‰, pH at 8.17 ± 0.01, and temperature at 29.3 ± 0.5°C. Commercial feed was used to feed the shrimp three times a day. The shrimps were then randomly sampled and tested by PCR to ensure that they were free from WSSV, IHHNV, and DIV1 using the primers shown in **Table S1**.

LD_{50} Test

DIV1 was obtained from a Peihua prawn farm in Wuchuan, Guangdong, China, and the virus was extracted from the infected tissue of *L. vannamei*, as conducted previously (23). The DIV1 inoculation was tested by PCR to ensure that it was not contaminated with the DNA of any other known crustacean virus (e.g., WSSV and IHHNV). DNA was extracted using the EasyPure Marine Animal Genomic DNA Kit (Transgen, Beijing, China). Extracted DNA was quantified using SimpliNano (GE Healthcare, US). The DNA samples of the pleopods were used to detect the viral loads by real-time PCR performed in a LightCycler (Roche) with the following program: denaturation at 95°C for 30 s, followed by 40 cycles at 95°C for 5 s and 60°C for 30 s, using the primers qRT-DIV1-F, qRT-DIV1-R, and Taqman Probe (**Table S1**) (24). Toxicity tests were performed with the same method as in the study of WSSV in shrimp (25). Six groups of healthy *L. vannamei* were intramuscularly injected at the third abdominal segment with 50 μl of DIV1 supernatants at five concentrations (2.14×10^8, 2.14×10^7, 2.14×10^6, 2.14×10^5, and 2.14×10^4 copies/μg DNA) and phosphate-buffered saline (PBS; pH 7.4) as a control. Three replicates of 30 shrimps per replicate were used in each group. The conditions of the LD_{50} test were the same as discussed in "Shrimp Culture" section. The cumulative mortality was recorded every 4 h for the LD_{50} calculation. To investigate the copies of DIV1, total DNA was extracted from hemocyte, hepatopancreas, intestine, gill, and muscle of *L. vannamei* at 6, 12, 24, 48, and 72 h after DIV1 injection on the concentration at LD_{50} 48 h from infection.

Transcriptome Sequencing and Analysis

Sample Collection

L. vannamei was intramuscularly injected with 50 μl of DIV1 supernatant based on LD_{50} 48 h after infection. *L. vannamei* injected with PBS was used as controls. At 48 h post-injection (hpi), the hemocytes from three shrimp were combined as one sample for transcriptome sequencing. The hemolymph was withdrawn into modified ACD anticoagulant solution, and the hemocytes were separated from plasma by centrifugation (3,000 × *g* for 5 min at 4°C) (26). The hemocytes of *L. vannamei* were immediately frozen in liquid nitrogen and stored at −80°C until RNA extraction. Three biological replicates were performed for the infection and the control groups, for a total of six samples. The extracted RNA was pooled for transcriptome sequencing.

RNA Extraction and Transcriptome Sequencing

Total RNA from the hemocytes of *L. vannamei* was isolated using TransZol Up Plus RNA Kit (Transgen, Beijing, China), and the RNA concentration was determined using SimpliNano (GE Healthcare, US). Fragmentation buffer was used to break the mRNA into short fragments. Using mRNA as a template, the first-strand cDNA strand was synthesized using random hexamers, followed by the addition of buffer, dNTPs, RNase H, and DNA polymerase I to synthesize the second-strand cDNA. Poly(A) was added to connect to the sequencing adaptor. Finally, the Illumina HiSeqTM platform was used to sequence the library at Guangzhou Sagene Biotech Co., Ltd. (Guangzhou, China).

De novo Assembly and Data Analysis

Raw reads were filtered to remove adaptor and low-quality sequences. After filtering, an RNA assembly of clean data from the mock and the DIV1-infected samples was performed with Trinity Assembly Software. The completeness of the assembly was assessed using BUSCO/v3.0.2 with the BUSCO arthropod dataset (27). Six functional databases were used to search for the unigenes, including NCBI protein NR (https://blast.ncbi.nlm.nih.gov/Blast.cgi), COG (https://www.ncbi.nlm.nih.gov/COG/), SWISS-PROT (https://www.expasy.org/), KEGG (https://www.genome.jp/kegg/), GO (http://geneontology.org/), and Pfam (http://asia.ensembl.org/index.html). In addition, Gene Ontology (GO) and metabolic pathway analysis were conducted using the Blast2GO program and KEGG program (https://www.genome.jp/kegg/), respectively.

Differential Expression Analysis and Functional Annotation

Log_2(FC) was used as an indicator of the genetic transcriptome differences between the DIV1-infected and the control groups. Fragments per kilobase million was used as the measurement unit to estimate the expression level of each transcript in the study. False discovery rate (FDR) was also used to correct the calculated *p*-values (28). Genes with FDR ≤ 0.05 and $|\log_2(FC)| > 1$ were considered to be DEGs. In addition, KEGG and GO were also used for DEGs pathway and GO enrichment analysis, respectively.

Validation of DEGs by qRT-PCR

To validate the transcriptome data, 2 μg of high-quality hemocyte RNA samples from the DIV1-infected group and the PBS control group was reverse-transcribed using the 5X All-in-One RT Master Mix (Applied Biological Materials, Vancouver, Canada) according to the manufacturer's protocol. The RNA concentration of the DIV1-infected group and the PBS control group was 120.48 and 156.64 μg/ml, respectively. A total of eight differentially expressed unigenes from the hemocyte transcriptome data of *L. vannamei* were selected for qPCR

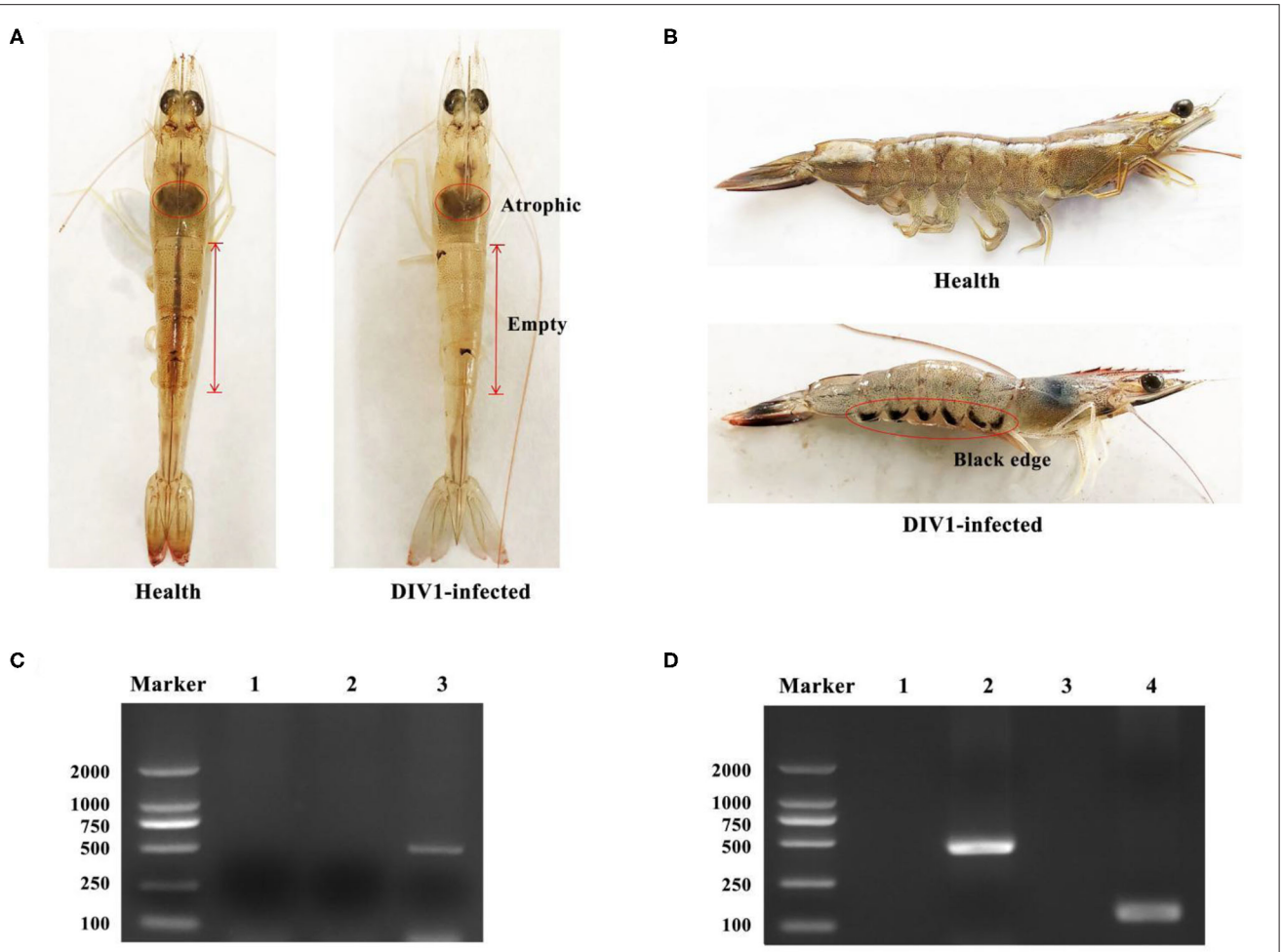

FIGURE 1 | Clinical symptoms and virus detection of *Litopenaeus vannamei*. **(A,B)** Clinical symptoms of DIV1-infected *L. vannamei*. **(C)** Virus detection of infected *L. vannamei* used for the DIV1 inoculation in LD_{50} test. Marker: DL2000 molecular mass marker; lane 1: PCR amplified products of WSSV detection; lane 2: PCR-amplified products of IHHNV detection; lane 3: PCR amplified products of DIV1detection. **(D)** DIV1 detection of *L. vannamei* in LD_{50} test using nested PCR method. Marker: DL2000 molecular mass marker; lanes 1 and 3: PCR amplified products of DIV1 detection in healthy *L. vannamei*; lanes 2 and 4: PCR-amplified products of DIV1 detection in dead *L. vannamei*.

analysis to validate the transcriptome. All DEGs were validated by qPCR using a Light Cycler® 96 system (Roche Applied Science, Switzerland) in a final reaction volume of 20 μl, which was comprised of 2 μl of 1:10 cDNA diluted with ddH_2O, 7.2 μl of ddH_2O, 10 μl of TB Green Premix Ex Taq II (Takara Biomedical Technology, Beijing, China; Code No. RR420Q), and 10 μM of specific primers. The cycling program was as follows: 1 cycle at 95°C for 30 s, followed by 40 cycles at 95°C for 15 s, 62°C for 1 min, and 65°C for 15 s. Cycling ended at 95°C, with a 4.4°C/s calefactive velocity to create the melting curve. The primers used in the qPCR analysis are listed in **Table S1**. $2^{-\Delta\Delta Ct}$ method was used to calculate gene expression (29). The amplification efficiencies (*E*) were calculated using the formula provided by Bustin et al. (30). The expression level of each gene was normalized by *EF1α* (GenBank accession no. GU136229).

Knockdown of *TPI* of *L. vannamei in vivo* Expression by Double-Stranded RNA-Mediated RNA Interference

Three types of triosephosphate isomerase (TPI)-specific primer sequences were linked to the T7 promoter by using the T7 RiboMAX™ Express Large Scale RNA Production System (Promega) to synthesize double-stranded RNAs (dsRNAs) following the method as previously described (31). The primers used for the synthesis of dsRNAs are shown in **Table S1**. The experimental group was injected with dsRNA-*LvTPI-likes* (2 μg/g), while the control groups were injected with equivalent dsRNA-EGFP. RNA interference efficiency was investigated using qPCR. The hemocyte samples were taken from nine shrimp in each challenge group at 24 and 48 hpi, and three shrimp were pooled together. Total RNA was extracted and reverse-transcribed into cDNA for qPCR. LvEF1-α was used

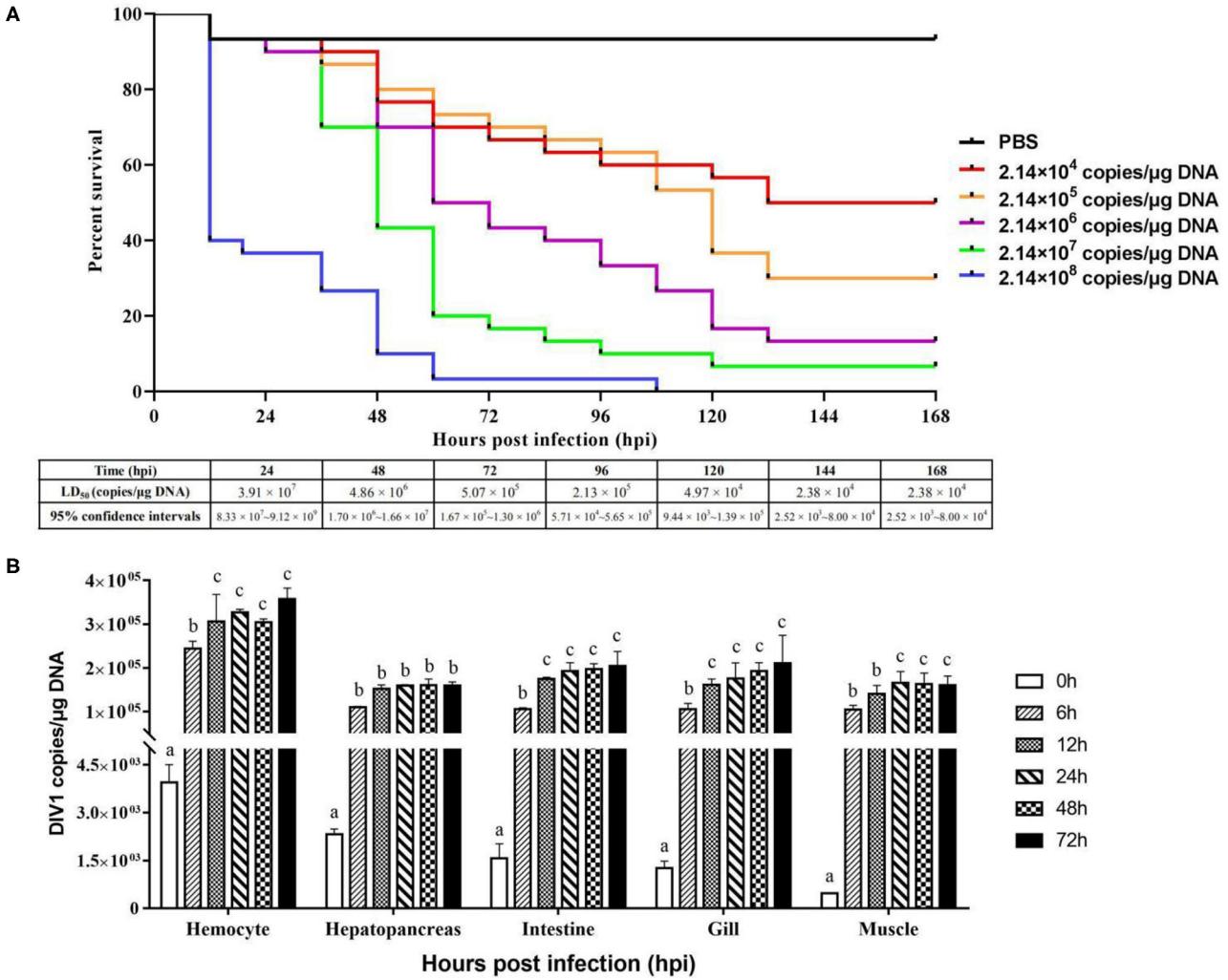

Time (hpi)	24	48	72	96	120	144	168
LD_{50} (copies/μg DNA)	3.91×10^7	4.86×10^6	5.07×10^5	2.13×10^5	4.97×10^4	2.38×10^4	2.38×10^4
95% confidence intervals	8.33×10^7–9.12×10^9	1.70×10^6–1.66×10^7	1.67×10^5–1.30×10^6	5.71×10^4–5.65×10^5	9.44×10^3–1.39×10^5	2.52×10^3–8.00×10^4	2.52×10^3–8.00×10^4

FIGURE 2 | Cumulative survival rates of *Litopenaeus vannamei* injected by DIV1 **(A)** and genome copies of DIV1 in infected *L. vannamei* **(B)**. **(A)** Six groups of healthy *L. vannamei* were intramuscularly injected at the third abdominal segment with 50 μl of DIV1 supernatants at five concentrations and phosphate-buffered saline as a control. **(B)** The DIV1 copies were investigated in the hemocyte, hepatopancreas, intestine, gill, and muscle of *L. vannamei* infected by DIV1 at the concentration of LD50 after 48 h of infection. Dissimilar letters show a significant difference ($p < 0.05$).

TABLE 1 | Summary of *de novo* assembly of *Litopenaeus vannamei* hemocyte transcriptome.

Type	Total number (*n*)	Total length (nt)	Mean length (nt)	N50 (bp)	GC (%)
Genes	168,854	101,529,805	601	807	44.5415
Transcripts	185,058	123,045,518	664	975	44.7676

as the internal control. The primer sequences are listed in **Table S1**.

Bioassay of DIV1 and PBS Challenge Tests in *TPI*-Knockdown *L. vannamei*

Healthy *L. vannamei* (7.12 ± 1.05 g, $n = 40$) received an intramuscular injection of dsRNA-*LvTPI-like*, dsRNA-*LvTPI-Blike*, dsRNA-*LvTPI-Blike1*, dsRNA-EGFP, or PBS. dsRNA was injected at a concentration of 2 μg/g shrimp. Four replicates (three replicates for mortality calculation and one for the sample collection) were analyzed for each group. After 48 h, the shrimp were injected again with 2.01×10^4 copies of DIV1 particles and mock-challenged with PBS as a control. The shrimp were cultured in tanks with air-pumped circulating seawater and were fed with artificial diet three times a day at 5% of body weight for about 7 days following the infection. The mortality of each group was counted every 4 h. At 24 and 48 h after DIV1 challenge, the hepatopancreas, intestines,

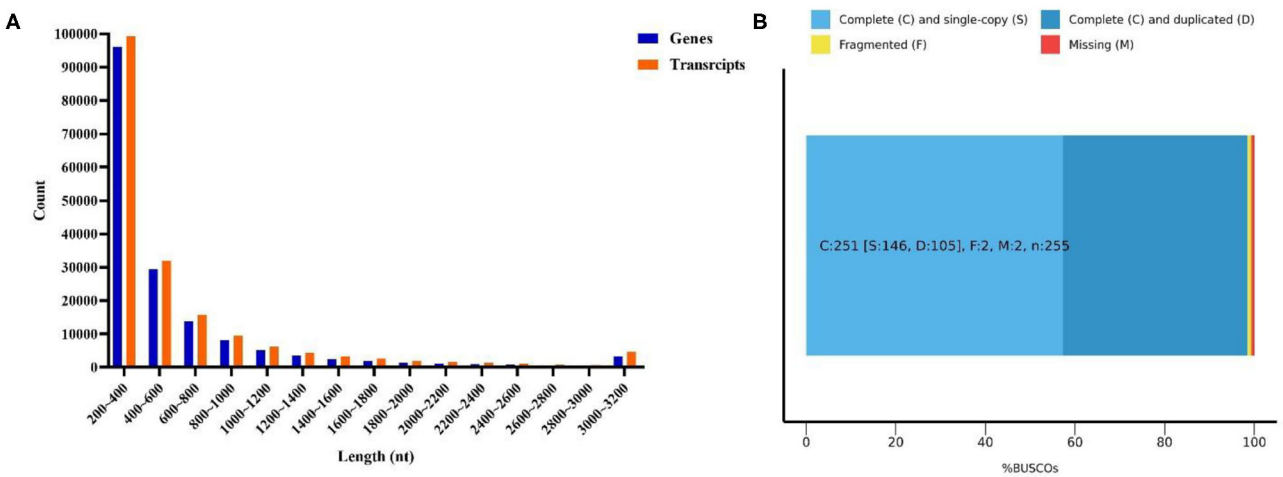

FIGURE 3 | Transcriptome sequence length distribution **(A)** and assembly quality analysis **(B)**.

TABLE 2 | Annotation of unigenes from transcriptome.

Values	Total	Nr	KEGG	SWISS-PROT	KOG	Annotated	Without annotation
Number	168,854	48,135	28,835	53,506	43,824	62,270	106,584
Percentage	100%	28.51%	17.08%	31.69%	25.95%	36.88%	63.12%

gill, muscle, and hemocyte of shrimp were collected for viral load detection.

Statistical Analysis

Data are expressed as mean ± standard deviation (SD). Statistical analyses were performed using SPSS software (version 18.0), with one-way ANOVA using Duncan's test to evaluate whether the means were significantly different ($P < 0.05$). Differences between groups were analyzed by using the Mantel–Cox (log-rank χ^2 test) method with the GraphPad Prism software.

The formula for calculating the LD_{50} of the virus is:

$$lgLD50 = \frac{1}{2}(x_i + x_{i+1})(\rho_{i+1} - \rho_i)$$

where x_i is the logarithm of the dose or concentration and ρ_i is the mortality rate.

The 95% confidence interval for $LD50 = lg^{-1}\left(lg\,Lc50 \pm 1.96 \times S_m\right)$, where S_m is the standard error (32).

RESULT

LD_{50} of DIV1 for *L. vannamei*

L. vannamei had obvious symptoms after being infected with DIV1, including empty stomach and intestine in all diseased shrimp, atrophy, and lightening of hepatopancreas, and soft shell in partially infected shrimp (**Figure 1A**). Part of the dead shrimps because of DIV1 infection showed symptoms of black edge of the abdominal shell (**Figure 1B**). As shown in **Figures 1C,D**, only DIV1 was found in the infected *L. vannamei* used for the DIV1 inoculation and the dead *L. vannamei* in the LD_{50} test. Results on the survival rate of *L. vannamei* after exposure to different DIV1 concentrations and the copies of DIV1 in the *L. vannamei* at different DIV1 injections are shown in **Figure 2**. The shrimp mortality rate increased as the DIV1 concentration increased. Probit analysis showed that the LD_{50} values for DIV1 determined are 3.91×10^7, 4.86×10^6, 5.07×10^5, 2.13×10^5, 2.38×10^4, and 2.38×10^4 copies/μg DNA for 24, 48, 72, 96, 120, 144, and 168 h after injection, respectively (**Figure 2A**). The copies of DIV1 in all the five detected tissues of infected *L. vannamei* were significantly increased at all the detected timepoints after injection (**Figure 2B**).

De novo Assembly and Annotation of Unigenes

Six cDNA libraries from *L. vannamei* were sequenced on the Illumina HiSeqTM platform. As **Table S2** shows, a total of 328,670,602 raw reads were generated, and 328,555,316 clean reads were left after removing the adapters filtering the low-quality sequences. Therefore, 163,056,696 clean reads were generated from 163,103,692 raw reads in the DIV1-infected group, and 165,498,620 clean reads were generated from 165,566,910 raw reads in the control group. The whole *de novo* assembly reads, from six libraries, yielded a total length of 101,529,805 bp, with 168,854 unigenes and an N50 length of 807 bp. The clean read data were deposited to the NCBI Sequence Read Archive (SRA, http://www.ncbi.nlm.nih.gov/Traces/sra) with the accession number SRP252506. A detailed summary of

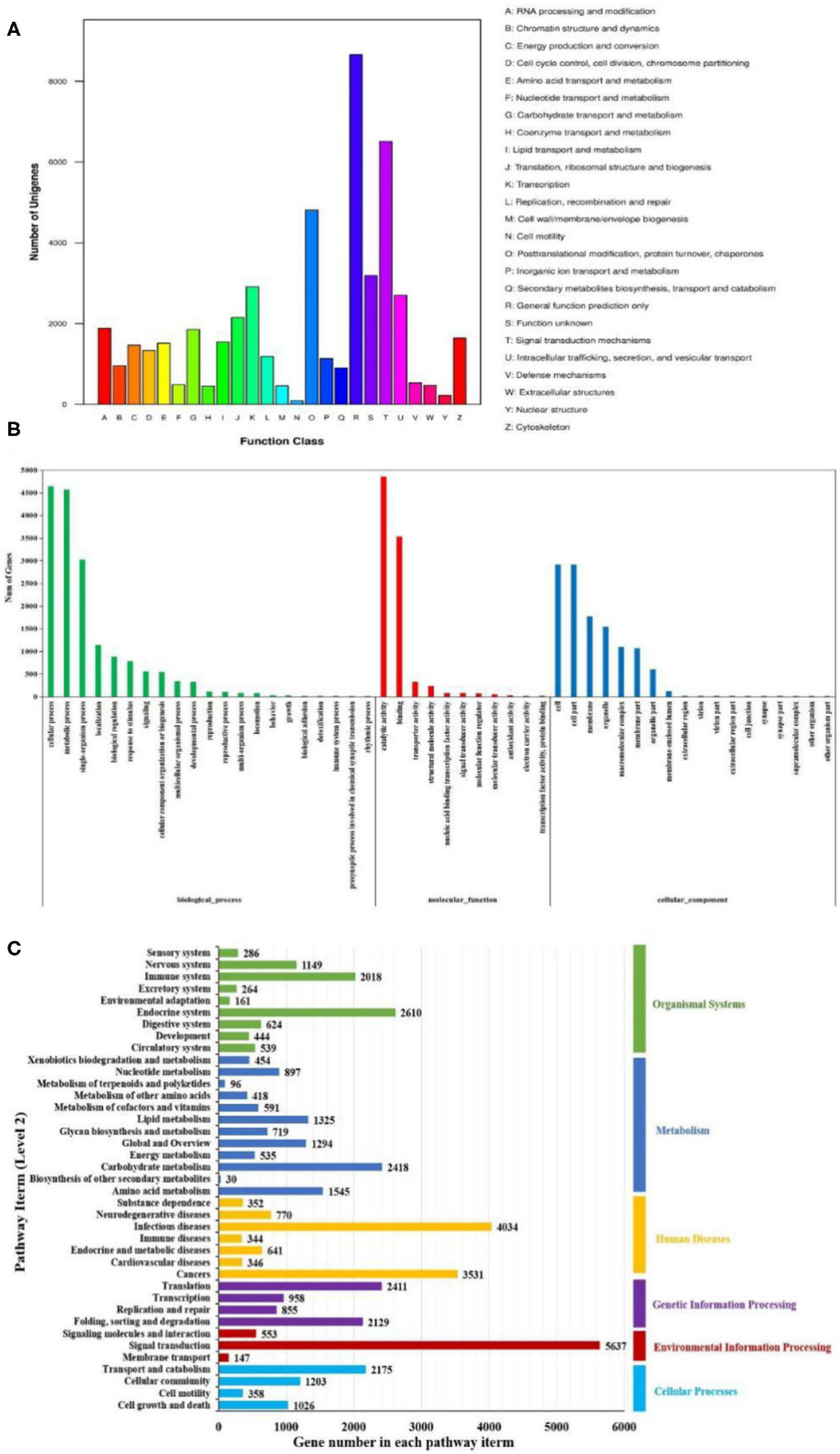

FIGURE 4 | Functional enrichment of unigenes from *Litopenaeus vannamei*. **(A)** KOG classification of unigenes. Each bar represents the number of unigenes classified into each of the 26 KOG functional categories. **(B)** Gene Ontology (GO) classification of unigenes. Three major GO categories were enriched: biological process, cellular component, and molecular function. **(C)** Kyoto Encyclopedia of Genes and Genomes (KEGG) classification of unigenes. The unigenes were assigned to six special KEGG pathways, including organismal systems, metabolism, human diseases, genetic information processing, environmental information processing, and cellular processes.

the sequencing and the assembly results is shown in **Table 1**. The sequence length (nt) ranges from 200 to ≥3,000 nt, with the distribution shown in **Figure 3A**. The most abundant unigenes were clustered in a group with 200–400 nt in length. Based on BUSCO, we compared the transcriptome with 1,066 conserved arthropod genes. A total of 98.4% of the transcriptome (251 genes) were encoded as complete proteins. Among these genes, 57.3% (146 genes) were complete and single-copy BUSCOs, 41.1% (105 genes) were complete and duplicated BUSCOs, 0.8% (two genes) were fragmented BUSCOs, and 0.8% (two genes) were missing BUSCOs (**Figure 3B**).

Functional Annotation and Classification of Unigenes

All unigenes were annotated using BLASTx with the NCBI nonredundant (Nr), KEGG, SWISS-PROT, and KOG protein database. Annotation information was retrieved from proteins with the highest sequence similarity. In this study, 62,270 (36.88%) unigenes were annotated. Among them, a total of 48,135, 28,835, 53,506, and 43,824 unigenes were annotated in the Nr, KEGG, SWISS-PROT, and KOG database, respectively (**Table 2**). The Blast hits a total of 940 species, the top five of which were *Branchiostoma belcheri* (5,329, 11.07%), *Hyalella azteca* (4,687, 9.74%), *Saccoglossus kowalevskii* (2,350, 4.88%), *Lingula anatine* (1,954, 4.06%), and *Limulus polyphemus* (1,266, 2.62%).

The KOG analysis showed that 49,048 unigenes were classified into 25 functional categories (**Figure 4A**). The largest three groups were "general function prediction only" (8,658, 17.65%), "signal transduction mechanisms" (6,511, 13.27%), and "posttranslational modification, protein turnover, chaperones" (4,809, 9.81%). The smallest cluster was "cell motility," which only contained 91 unigenes. By GO analysis, 17,321, 8,281, and 12,146 unigenes were classified into biological process, molecular function, and cellular component by Blast2GO suite, respectively (**Figure 4B**). Within the biological process category, "cellular process" (4,644 unigenes) and "metabolic process" (4,566 unigenes) were the dominant groups. Within the cellular component category, "cell" (2,909 unigenes) and "cell part" (2,909 unigenes) were the most abundant groups. Within the molecular function category, "catalytic activity" (4,859 unigenes) and "binding" (3,534 unigenes) were the dominant groups. Using KEGG, a total of 15,902 unigenes were mapped to six specific pathways, including cellular processes, environmental information processing, genetic information processing, metabolism, human diseases, and organism system (**Figure 4C**). These annotated unigenes were further divided into 39 level 2 subcategory pathways. The largest subcategory group, signal transduction, had 5,637 annotated genes, followed by infection diseases (4,034), cancers (3,531), the endocrine system (2,610), carbohydrate metabolism (2,418), and translation (2,412). Apart from these, 302 level 3 KEGG subcategories were annotated and are listed in **Table S3**.

Classification and Analysis of DEGs

To analyze and characterize the DEGs in *L. vannamei* following DIV1 infection, a cutoff false discovery rate (FDR) was set at <0.05 and a $|\log_2 \text{ratio}| \geq 1$ was employed as threshold. Based on this, 1,112 genes were observed to be dysregulated in DIV1-infected group compared to the control, including 889 up-regulated genes and 223 down-regulated genes. These DEGs were visualized by volcano plot in **Figure 5**.

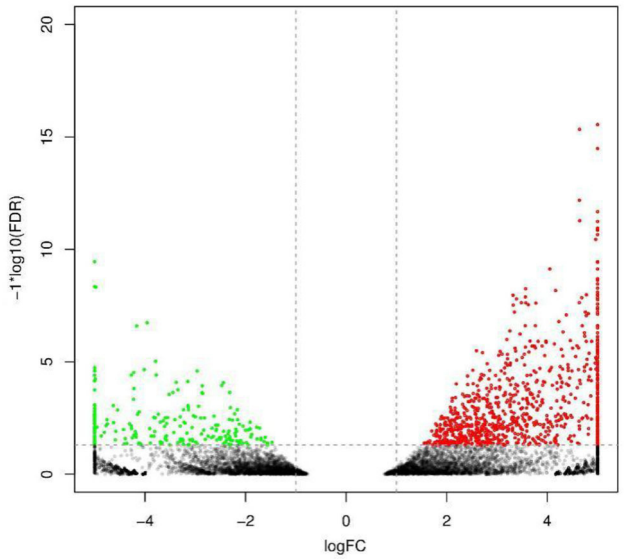

FIGURE 5 | Volcano diagram of differentially expressed genes (DEGs) in *Litopenaeus vannamei* with and without DIV1 infection. The x-axis indicates the fold change, and the y-axis indicates the statistical significance of the differences. Red dots represent the significantly up-regulated DEGs, while green dots represent the significantly down-regulated DEGs (FDR < 0.05 and |log2 ratio| ≥ 1). The gray dots represent the DEGs which are not significantly different.

The DEGs were further annotated with GO and KEGG databases. In the GO enrichment analysis, the 197 up-regulated and the 41 down-regulated genes expressed in the DIV1-infected group were enriched in several categories: biological process (106 up-regulated and 23 down-regulated), molecular function (38 up-regulated and 11 down-regulated), and cellular component (53 up-regulated and seven down-regulated) (**Figure 6**). For the KEGG pathway enrichment analysis, 121 DEGs were annotated into 108 pathways. Among them, metabolism was a crucial pathway. The category that contained the higher number of DEGs was "protein processing in endoplasmic reticulum." The top 20 KEGG enrichment pathways influenced by DIV1 infection are shown in **Figure 7**. KEGG analysis showed that 28 DEGs were presented in seven immune system pathways, including NOD-like receptor signaling pathway (four), MAPK signaling pathway (seven), Wnt signaling pathway (two), Toll-like receptor signaling pathway (two), phagosome (seven), RIG-I-like receptor signaling pathway (two), and p53 signaling pathway (four) (**Table 3**). In these pathways, *TPI* genes received particular attention for their participation in several distinct pathways, such as fructose and mannose metabolism, glycolysis/gluconeogenesis, biosynthesis of amino acids, inositol phosphate metabolism, and carbon metabolism (**Table 4**).

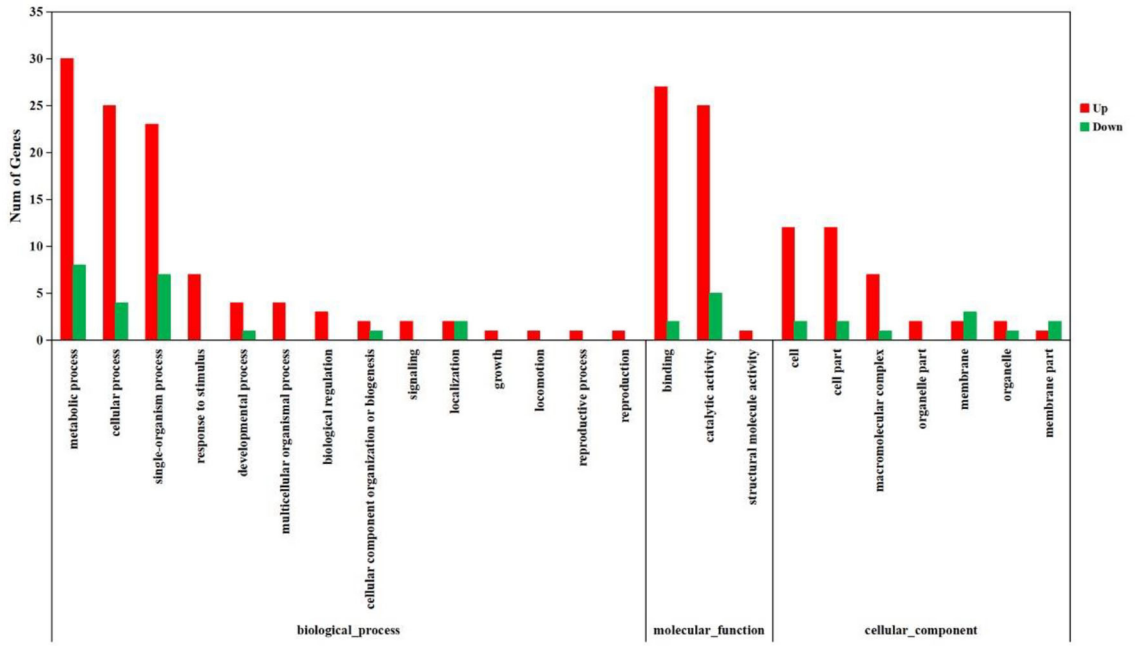

FIGURE 6 | Analysis of GO term functional enrichment of differentially expressed genes between DIV1-infected and control groups. The x-axis indicates the Gene Ontology processes, and the y-axis indicates the number of unigenes in a process.

Validation of RNA-Seq Results by qRT-PCR

To further evaluate our DEG library, eight unigenes were randomly selected, including four up-regulated and four down-regulated DEGs for qPCR analysis. The amplification efficiency (*E*) of all unigenes and EF1α ranged from 95.2 to 98.2% (**Table S1**). As shown in **Figure 8**, the qPCR results showed significant, identical expression tendencies as the high-throughput sequencing data. However, some quantitative differences in the expression level were seen for Unigene064464, Unigene072846, Unigene027278, and Unigene040974. The qPCR analysis results, therefore, confirmed the expressions of DEGs which were detected in the high-throughput sequencing analysis.

Functional Analysis of *LvTPI* in *L. vannamei* During DIV1 Infection

Silencing of *LvTPI-likes* Led to *L. vannamei* Death

According to the transcriptome information in this study and the genome information from NCBI, three full-length TPI types were obtained and named as *LvTPI-like* (accession no. MT123334), *LvTPI-Blike* (accession no. MT107901), and *LvTPI-Blike1* (accession no. MN996302). The silencing efficiency was checked using qPCR. At 24 and 48 h post-dsRNA injection, the mRNA level of *LvTPI-likes* was remarkably downregulated in dsRNA-*LvTPI-likes*-treated shrimp ($p < 0.05$), whereas there was no suppressive effect on *LvTPI-likes* in the dsRNA-EGFP-treated group (**Figure 9A**). The *L. vannamei* started to die after dsRNA-*LvTPI-like* and dsRNA-*LvTPI-Blike1* injection, with a cumulative mortality of 50 and 82.5% at 48 hpi, respectively. The final mortality rates at 144 hpi were 72.5 and 92.5% for the dsRNA-*LvTPI-like* and the dsRNA-*LvTPI-Blike1* groups, respectively. However, there was no effect on the survival rate of *L. vannamei* by dsRNA-*LvTPI-Blike* injection (**Figure 9B**).

LvTPI-like and *LvTPI-Blike* Suppression Did Not Affect the Survival Rates of *L. vannamei* but Reduced DIV1 Replication

Due to the mass death of *L. vannamei* when *LvTPI-Blike1* was silenced, the function of *LvTPI-like* and *LvTPI-Blike* in DIV1-infected *L. vannamei* was investigated. The shrimp were challenged with DIV1 at 48 h post-dsRNA injection in the following experiments. As shown in **Figure 9C**, the cumulative survival rate in the dsRNA-*LvTPI-Blike* group was lower than those in the dsRNA-EGFP group. However, there was no significant difference between the cumulative survival rate of the dsRNA-*LvTPI-like* and dsRNA-*LvTPI-Blike* groups compared with the dsRNA-EGFP group during DIV1 infection. The final survival rates were 30.0, 11.1, and 28.95% for dsRNA-*LvTPI-like*, dsRNA-*LvTPI-Blike*, and dsRNA-EGFP groups, respectively. However, both dsRNA-*LvTPI-like* and dsRNA-*LvTPI-Blike* suppression reduced DIV1 replication. The virus copies in five tissues—hemocyte, hepatopancreas, intestine, gill, and muscle—were measured in shrimp at 24 and 48 h post-DIV1 infection in each double-stranded RNA silencing group. As shown in **Figure 10**, the DIV1 copy numbers for both the dsRNA-*LvTPI-like* and the dsRNA-*LvTPI-Blike* groups were not significantly different from that for the dsRNA-EGFP group at 24 hpi. At 48 hpi, the viral loads in the hemocyte,

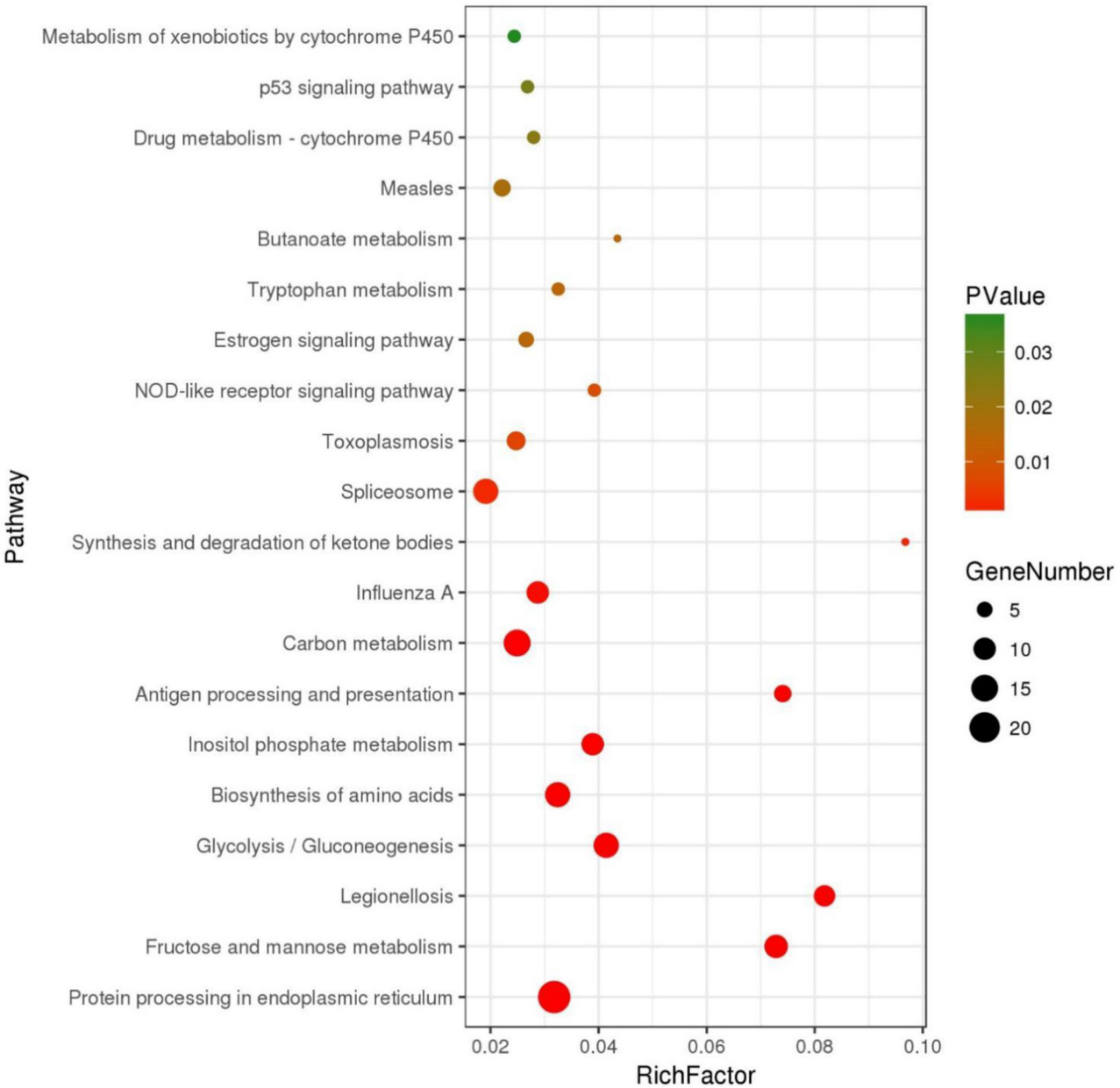

FIGURE 7 | Top 20 of pathway enrichment. The x-axis indicates the ratio of the number of genes in the pathway of the DEGs and all genes. The y-axis indicates the pathway.

hepatopancreas, intestine, gill, and muscle of the ds*LvTPI-Blike* + DIV1 group was 3.10×10^2, 1.75×10^3, 1.34×10^3, 2.64×10^3, and 6.95×10^2 copies/μg DNA, respectively. The viral loads in all the detected tissues of the ds*LvTPI-Blike* + DIV1 group were significantly lower than those of the dsRNA-EGFP + DIV1 control group ($p < 0.05$). In the ds*LvTPI-like* + DIV1 group, the number of copies of DIV1 at 48 hpi decreased in the hemocyte and muscle but increased in the hepatopancreas, intestine, and gill, with a significantly different level only in the hepatopancreas.

DISCUSSION

DIV1 is a new disease prevalent in shrimp cultures in China. DIV1 mainly affects the hematopoietic tissue and the hemocytes of shrimp (6). The emergence of DIV1 poses a new biological risk to the shrimp farming industry (33). However, there are no reports on the harmful effects of DIV1 on *L. vannamei* until now. In this study, the toxicity of DIV1 for *L. vannamei* was measured at different time points, and a comparative transcriptome analysis of *L. vannamei* challenged by DIV1 was conducted. The results

TABLE 3 | Differentially expressed genes associated with immune responses during DIV1 infection.

Category or gene ID	Gene description	Species	FC[a]
NOD-like receptor signaling pathway			
Unigene024064_All	Endoplasmin	*Bemisia tabaci*	2.64
Unigene056132_All	Caspase-2	*Cerapachys biroi*	1.96
Unigene067577_All	NACHT, LRR, and PYD domain-containing protein 3-like	*Branchiostoma belcheri*	4.64
Unigene072846_All	Protein NLRC5-like	*Acropora digitifera*	3.60
MAPK signaling pathway			
Unigene011119_All	Cytosolic heat shock protein 70, partial	*Mytilus galloprovincialis*	6.08
Unigene039540_All	Heat shock protein 70 kDa, partial	*Bythograea thermydron*	2.83
Unigene045522_All	Heat shock cognate protein 70, partial	*Latrodectus hesperus*	3.50
Unigene055746_All	70-kDa heat shock protein C, partial	*Euphausia superba*	3.72
Unigene055749_All	High-molecular-weight heat shock protein	*Acanthamoeba castellanii str. Neff*	2.52
Unigene055750_All	Heat shock cognate protein 70	*Haliotis diversicolor*	2.53
Unigene123680_All	NPKL2	*Oryza sativa Japonica Group*	3.83
Wnt signaling pathway			
Unigene031735_All	Calcyclin-binding protein-like	*Parasteatoda tepidariorum*	5.67
Unigene031736_All	SGS domain-containing protein	*Toxoplasma gondii*	7.07
Toll-like receptor signaling pathway			
Unigene056132_All	Caspase-2	*Cerapachys biroi*	1.96
Unigene137202_All	Interleukin-1 receptor-associated kinase 4-like	*Parasteatoda tepidariorum*	3.59
Phagosome			
Unigene001107_All	Calnexin-like protein	*Littorina littorea*	2.32
Unigene025407_All	Calreticulin	*Dictyostelium lacteum*	1.98
Unigene047081_All	C-type lectin	*Litopenaeus vannamei*	6.68
Unigene061835_All	Thrombospondin II	*Penaeus monodon*	7.68
Unigene068957_All	Cathepsin L	*Penaeus monodon*	2.93
Unigene117499_All	Ervatamin-B	*Oryza sativa japonica* group	−4.25
Unigene155244_All	Cathepsin L-like cysteine proteinase	*Longidorus elongatus*	−3.34
RIG-I-like receptor signaling pathway			
Unigene041866_All	ATP-dependent RNA helicase DDX3X-like protein	*Rhinopithecus roxellana Saccoglossus kowalevskii*	5.54
Unigene056132_All	Caspase-2	*Cerapachys biroi*	1.96
p53 signaling pathway			
Unigene018326_All	Cytochrome c-like isoform X1	*Galendromus occidentalis*	3.26
Unigene027278_All	Ribonucleoside-diphosphate reductase subunit M2 B-like	*Limulus polyphemus*	−4.54
Unigene056132_All	Caspase-2	*Cerapachys biroi*	1.96
Unigene064926_All	Cytochrome c	*Litopenaeus vannamei*	2.73

[a] *Fold changes (log_2 ratio) in expression.*

showed that several metabolisms and immune function signaling pathways participated in the *L. vannamei* response to DIV1. In addition, *TPI* genes play an outstanding role.

As an important parameter of virulence, LD_{50} was often used to evaluate the effect of virus on shrimp. In crustaceans, the LD_{50} of several disease-causing viruses including WSSV, IHHNV, and TSV have been reported (34–36); however, the LD_{50} of DIV1 in shrimp has not been found. To our knowledge, this is the first report on the virulence of DIVI in crustaceans. The detection of DIV1 replication in LD_{50} test showed that the copies of DIV1 in the hemocyte, hepatopancreas, intestine, gill, and muscle of infected *L. vannamei* were significantly increased at all the detected timepoints after injection. A consistent conclusion was confirmed by Qiu et al. A histological analysis of ultrathin sections imaged under transmission electron microscopy revealed that enveloped icosahedral virus-like particles were present in hemocytes localized to the hemal sinus, hepatopancreas, and muscle of *L. vannamei* infected by DIV1 (6). It can be inferred that the mortality of *L. vannamei* was the result of virus replication.

Transcriptome sequencing, a powerful tool in biological research, has been used to analyze the immune response to many shrimp pathogens (37). Xue et al. compared the transcriptome profiles in hemocytes of uninfected and WSSV-infected *L. vannamei* and found 1,179 immune-related unigenes (38). Zeng et al. performed transcriptome sequencing in the hepatopancreas of *L. vannamei* infected with TSV and found 1,311 differential genes, including a large number of immune-related genes (39).

TABLE 4 | Triosephosphate isomerase genes and the pathways and the genes related to them in differentially expressed genes.

Category or gene ID	Gene description	Species	FC[a]
Fructose and mannose metabolism			
Unigene015918	CLUMA_CG013551, isoform A	*Clunio marinus*	2.79
Unigene068542	Triosephosphate isomerase	*Penaeus monodon*	4.31
Unigene068543	Triosephosphate isomerase	*Palaemon carinicauda*	4.83
Unigene046663	Fructose-bisphosphate aldolase	*Dictyostelium lacteum*	−5.41
Unigene051281	Triosephosphate isomerase	*Penaeus monodon*	5.22
Unigene064463	Triosephosphate isomerase	*Litopenaeus vannamei*	5.17
Unigene064464	Triosephosphate isomerase	*Penaeus monodon*	5.25
Unigene064465	Triosephosphate isomerase	*Penaeus monodon*	5.21
Unigene068538	Triosephosphate isomerase	*Penaeus monodon*	3.90
Unigene068539	Triosephosphate isomerase	*Penaeus monodon*	4.42
Unigene068541	Triosephosphate isomerase	*Penaeus monodon*	4.29
Glycolysis/gluconeogenesis			
Unigene038694	Multiple inositol polyphosphate phosphatase	*Daphnia magna*	−2.59
Unigene046663	Fructose-bisphosphate aldolase	*Dictyostelium lacteum*	−5.41
Unigene051281	Triosephosphate isomerase	*Penaeus monodon*	5.22
Unigene062010	Phosphoenolpyruvate carboxykinase	*Litopenaeus vannamei*	3.92
Unigene064463	Triosephosphate isomerase	*Litopenaeus vannamei*	5.17
Unigene064464	Triosephosphate isomerase	*Penaeus monodon*	5.25
Unigene064465	Triosephosphate isomerase	*Penaeus monodon*	5.21
Unigene068538	Triosephosphate isomerase	*Penaeus monodon*	3.90
Unigene068539	Triosephosphate isomerase	*Penaeus monodon*	4.42
Unigene068541	Triosephosphate isomerase	*Penaeus monodon*	4.29
Unigene068542	Triosephosphate isomerase	*Penaeus monodon*	4.31
Unigene068543	Triosephosphate isomerase	*Palaemon carinicauda*	4.83
Unigene074167	Acetyl-coenzyme A synthetase 2-like, mitochondrial	*Crassostrea gigas*	1.79
Biosynthesis of amino acids			
Unigene018569	Kynurenine aminotransferase 4	*Dictyostelium discoideum AX4*	2.95
Unigene046663	Fructose-bisphosphate aldolase	*Dictyostelium lacteum*	−5.41
Unigene051281	Triosephosphate isomerase	*Penaeus monodon*	5.22
Unigene059719	S-adenosylmethionine synthetase	*Polysphondylium pallidum PN500*	2.09
Unigene064463	Triosephosphate isomerase	*Litopenaeus vannamei*	5.17
Unigene064464	Triosephosphate isomerase	*Penaeus monodon*	5.25
Unigene064465	Triosephosphate isomerase	*Penaeus monodon*	5.21
Unigene068538	Triosephosphate isomerase	*Penaeus monodon*	3.90
Unigene068539	Triosephosphate isomerase	*Penaeus monodon*	4.42
Unigene068541	Triosephosphate isomerase	*Penaeus monodon*	4.29
Unigene068542	Triosephosphate isomerase	*Penaeus monodon*	4.31
Unigene068543	Triosephosphate isomerase	*Palaemon carinicauda*	4.83
Unigene083661	Phosphoserine aminotransferase, chloroplastic	*Sphaeroforma arctica JP610*	2.81
Inositol phosphate metabolism			
Unigene038694	Multiple inositol polyphosphate phosphatase	*Daphnia magna*	−2.59
Unigene051281	Triosephosphate isomerase	*triosephosphate isomerase*	5.22
Unigene064463	Triosephosphate isomerase	*Litopenaeus vannamei*	5.17
Unigene064464	Triosephosphate isomerase	*Penaeus monodon*	5.25
Unigene064465	Triosephosphate isomerase	*Penaeus monodon*	5.21
Unigene068538	Triosephosphate isomerase	*Penaeus monodon*	3.90
Unigene068539	Triosephosphate isomerase	*Penaeus monodon*	4.42
Unigene068541	Triosephosphate isomerase	*Penaeus monodon*	4.29
Unigene068542	Triosephosphate isomerase	*Penaeus monodon*	4.31
Unigene068543	Triosephosphate isomerase	*Palaemon carinicauda*	4.83

(Continued)

TABLE 4 | Continued

Category or gene ID	Gene description	Species	FC[a]
Carbon metabolism			
Unigene018569	Aspartate aminotransferase	*Dictyostelium discoideum AX4*	2.95
Unigene046663	Fructose-bisphosphate aldolase	*Dictyostelium lacteum*	−5.41
Unigene051281	Triosephosphate isomerase	*Penaeus monodon*	5.22
Unigene061564	Putative uncharacterized protein DDB_G0277255	*Hyalella azteca*	2.35
Unigene064463	Triosephosphate isomerase	*Litopenaeus vannamei*	5.17
Unigene064464	Triosephosphate isomerase	*Penaeus monodon*	5.25
Unigene064465	Triosephosphate isomerase	*Penaeus monodon*	5.21
Unigene068538	Triosephosphate isomerase	*Penaeus monodon*	3.90
Unigene068539	Triosephosphate isomerase	*Penaeus monodon*	4.42
Unigene068541	Triosephosphate isomerase	*Penaeus monodon*	4.29
Unigene068542	Triosephosphate isomerase	*Penaeus monodon*	4.31
Unigene068543	Triosephosphate isomerase	*Palaemon carinicauda*	4.83
Unigene074167	Acetyl-coenzyme A synthetase 2-like, mitochondrial	*Crassostrea gigas*	1.79
Unigene083661	Phosphoserine aminotransferase, chloroplastic	*Sphaeroforma arctica JP610*	2.81
Unigene150662	Malate dehydrogenase	*malate dehydrogenase*	3.23

[a]*Fold changes (log_2 ratio) in expression.*

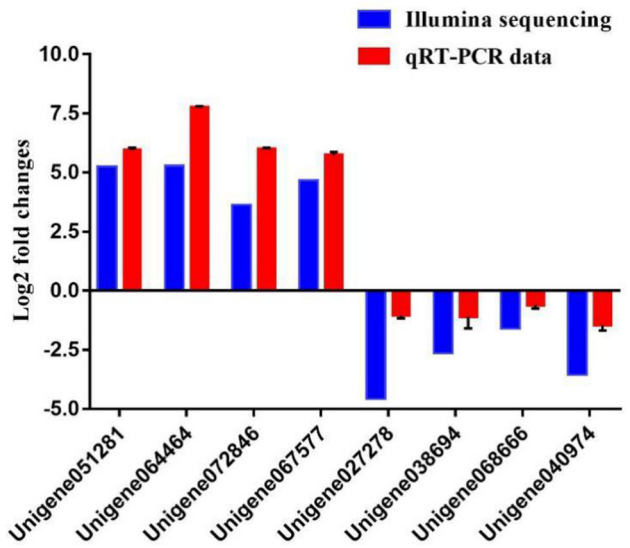

FIGURE 8 | Comparison of the expression profiles of six selected genes as determined by Illumina sequencing and qRT-PCR.

Hui et al. used transcriptome analysis to reveal a large number of immune-related genes in the intestine of *M. rosenbergii* infected with WSSV (40). By using transcriptome sequencing, Cao et al. also obtained an abundant number of immune-related genes, such as toll-like receptors, C-type lectins, and scavenger receptors, during WSSV infection of *M. rosenbergii* (41). In the present study, transcriptome analysis was conducted to identify genes and pathways in *L. vannamei* which may play a role during the infection of DIV1. Similarly, a large number of immune-related genes were found, participating in several immune-related pathways, including NOD-like receptor, MAPK, Wnt, Toll-like receptor, phagosome, RIG-I-like receptor, and p53 signaling pathways. The results indicated that immune response was necessary when the shrimps suffered the attacks of the virus. It is noteworthy that KEGG analysis showed that several metabolism-related pathways such as fructose and mannose metabolism, glycolysis/gluconeogenesis, biosynthesis of amino acids, inositol phosphate metabolism, and carbon metabolism are members of the top 20 KEGG enrichment pathways influenced by DIV1 infection. A previous study showed that the replication and the packaging of DIV1 not only requires nucleic acids and proteins but also phospholipids to form the inner limiting envelope (6). Thinking of the increased copies of DIV1 in the infected *L. vannamei*, it can be seen that infection with DIV1 results in a metabolic disorder of *L. vannamei*, which supported the general model of viral pathogenesis causing a systemic disruption to metabolic pathways as the host physiology is taken over to support viral replication (42). Consistent results have been reports in other two crustacean species, *C. quadricarinatus* and *F. merguiensis*. Yang et al. found that DIV1 infection induced changes in carbohydrate metabolism, lipid metabolism, and amino acid metabolism in *C. quadricarinatus* (13). Our previous study in *F. merguiensis* found that DIV1 affected not only some immune-related pathways but also some metabolic pathways such as amino sugar and nucleotide sugar metabolism, glycolysis/gluconeogenesis, and inositol phosphate metabolism (14). However, the key factors that play important roles during DIV1 infection in these species are still unclear.

Another notable result in our transcriptome analysis was that lots of DEGs annotated as TPI participated in several members of the top 20 KEGG enrichment pathways. *TPI* was known as an important factor which plays a role in both glycolysis and phospholipid biosynthesis in all organisms (43). *TPI* is an enzyme in the glycolytic pathway, which catalyzes the reversible

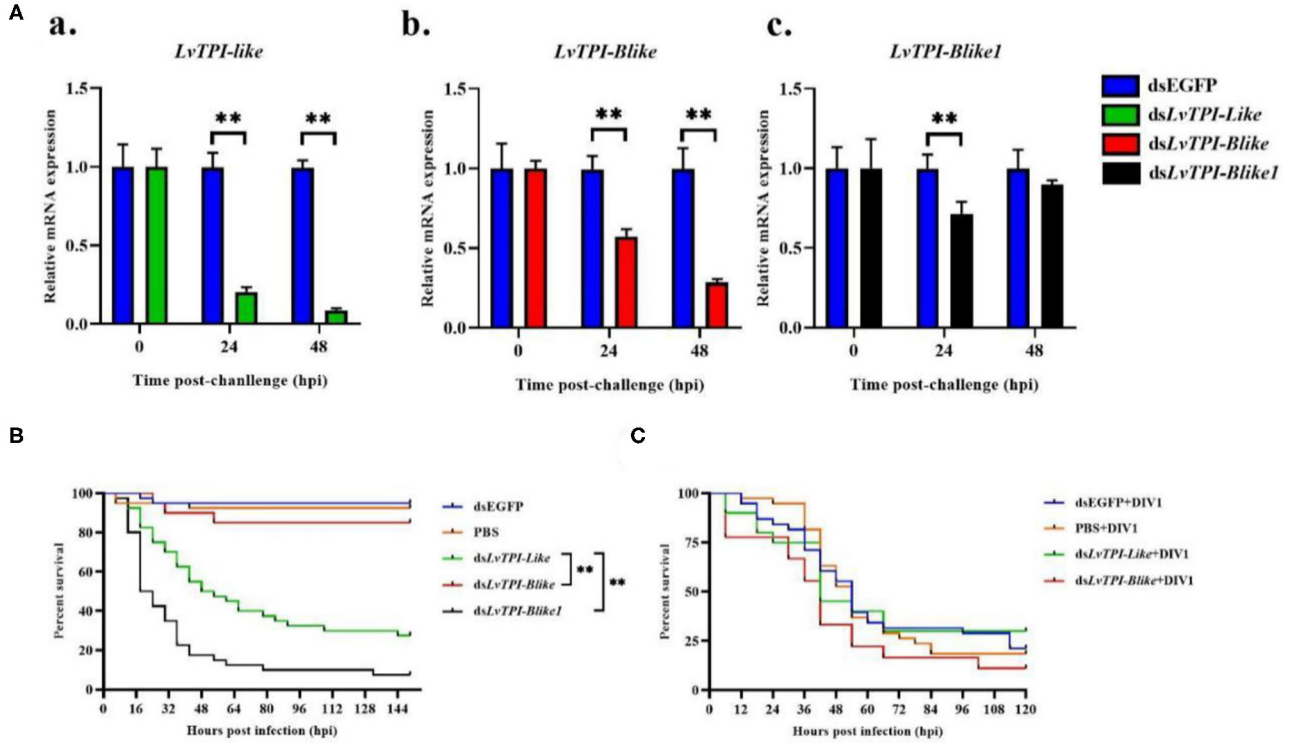

FIGURE 9 | Function of *LvTPI-likes* during DIV1 infection. **(A)** qPCR analysis of the silencing efficiencies of *LvTPI-likes*. (a) *LvTPI-like*, (b) *LvTPI-Blike*, and (c) *LvTPI-Blike1*. EF1α was used as the internal control. **(B)** Cumulative survival rates of *Litopenaeus vannamei* injected by *LvTPI-likes* dsRNA. **(C)** Cumulative survival rates of *LvTPI-likes*-RNAi *L. vannamei* during DIV1 infection. Error bars represent ± SD of three replicates. Data were analyzed with the GraphPad Prism software using the log-rank (Mantel–Cox) method. All data are given in terms of means ± standard error (SE). Asterisks indicate significant differences. $^{*}P < 0.05$ and $^{**}P < 0.01$ ($n = 3$).

interconversion of dihydroxyacetone phosphate (DHAP) and the triose phosphate glyceraldehyde 3-phosphate (GAP) (44–47). *TPI* is vital to an organism's response to external factors (48). Besides that, *TPI* could be used to develop vaccines against parasitic diseases in mammals (49, 50). In shrimp, the only study in *Exopalaemon carinicauda* showed that TPI facilitated the replication of WSSV (51). In this study, three types of TPI genes (namely, *LvTPI-like*, *LvTPI-Blike*, and *LvTPI-Blike1*) were obtained in *L. vannamei*, and their functions during DIV1 infection were identified using RNAi. To our surprise, the results showed that the silence of *LvTPI-like* or *LvTPI-Blike1* significantly reduced the survival rate of *L. vannamei*. This result can be attributed to the important role of TPI in both glycolysis and phospholipid biosynthesis, and the silence of *LvTPI-like* or *LvTPI-Blike1* caused the metabolic disorders, affecting the normal life activities of *L. vannamei* (43). It is notable that *LvTPI-Blike1* expression at 48 h post-dsRNA injection was not significantly lower than the control. That may be because the *L. vannamei*, in which *LvTPI-Blike1* was knocked down, died before the detection time point. On these bases, only the survival rates of *LvTPI-like* and *LvTPI-Blike* knock-down *L. vannamei* after DIV1 infection were investigated. It was shown that the silence of *LvTPI-like* and *LvTPI-Blike* did not lead to a significant difference in shrimp survival, but the DIV1 copies were significantly reduced in all the detected tissues of *LvTPI-Blike* knock-down *L. vannamei* and the hemocytes and the muscle of *LvTPI-like* knock-down *L. vannamei* at 48 hpi. Similar results have been reported in the function analysis of immune genes in *L. vannamei*. Shi et al. showed that the cumulative mortality of *L. vannamei* after WSSV infection had no significant difference between laccase knockdown and the control groups, but the WSSV copies were significantly reduced in laccase knock-down *L. vannamei* (52). Similarly, the knockdown *LvTube*, *LvPelle*, and *LvTAB2* did not affect the mortality of *L. vannamei* caused by WSSV infection, but could slow down the replication of WSSV in the infected *L. vannamei* (53, 54). All these findings were in accordance with the viewpoint that host physiology could be taken over by the virus to support their replication, and the physiological disorder of the host is not conducive to the replication of the virus. In this study, the reduced DIV1 copies may probably be due to the physiological disorder caused by *LvTPI-like* or *LvTPI-Blike* silence. Considering the important role of TPI in metabolism, it can be speculated that a viral-induced Warburg effect could also be induced in DIV1-infected *L. vannamei*, which is similar to the effect of WSSV infection in shrimp (42). In *E. carinicauda* infected with WSSV, glycolysis was affected and TPI was up-regulated, which produced more GAP which became DHAP, which is necessary for the synthesis

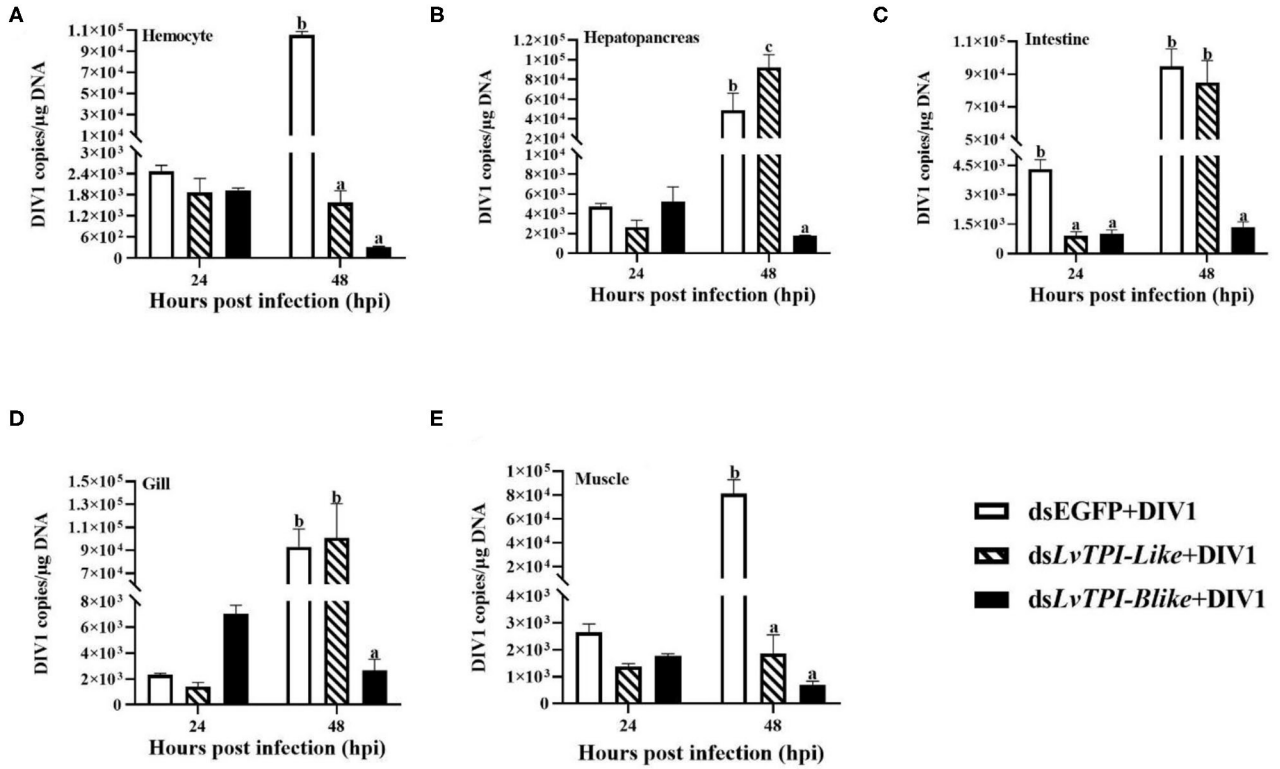

FIGURE 10 | Detection of DIV1 copy numbers in hemocyte **(A)**, hepatopancreas **(B)**, intestine **(C)**, gill **(D)**, and muscle **(E)** of *Litopenaeus vannamei* following treatment with ds*LvTPI-like* and *dsLvTPI-Blike*. Data are shown as mean ± SD of three animals. Dissimilar letters show a significant difference ($p < 0.05$).

of phospholipids. The production of phospholipids then affected WSSV replication (51). However, the mechanism of TPI shrimp during DIV1 infection could not be clarified in this study. Further studies are needed. In addition, what could not be ignored was that the DIV1 copies were not significantly different in the hepatopancreas, intestines, and gill of *LvTPI-like* knock-down *L. vannamei* when compared with the control. It may be related to the functional specificity of the gene in different tissues. In any case, there is no doubt about the fact that TPI-like genes play an important role during DIV1 infection in *L. vannamei*.

In conclusion, we determined the LD_{50} values of DIV1-infected *L. vannamei* and found that *TPI-like* genes played an important role during DIV1 infection in *L. vannamei*. The results were helpful to better understand the immune response mechanism of disease resistance in shrimp, which could provide a theoretical basis for the prevention and the control of the viral disease in shrimp culture and be of great significance for promoting the health and the sustainable development of the shrimp industry.

DATA AVAILABILITY STATEMENT

The datasets presented in this study can be found in online repositories. The names of the repository/repositories and accession number(s) can be found in the article/**Supplementary Material**.

AUTHOR CONTRIBUTIONS

XL, CS, and SZ conceived and designed the experiments. XL, CW, BW, HQ, SH, and PW collected the samples and performed the experiments. XL and SZ analyzed the data as well as wrote the paper. All authors contributed to the article and approved the submitted version.

FUNDING

This work was supported by the National Key R&D Program of China (grant no. 2019YFD0900200), the National Natural Science Foundation of China (grant no. 31702377), the Project of 2019 Annual Guangdong Provincial Special Financial Fund (grant no. 2319412525), the Fangchenggang Science and Technology Plan Project (grant no. AD19008017), and the Guangdong Provincial Special Fund for Modern Agriculture Industry Technology Innovation Teams (grant no. 2019KJ149).

ACKNOWLEDGMENTS

We would like to acknowledge NATIVE English Editing (www.nativeee.com) for its linguistic assistance during the preparation of this manuscript.

SUPPLEMENTARY MATERIAL

The Supplementary Material for this article can be found online at: https://www.frontiersin.org/articles/10.3389/fimmu.2020.01904/full#supplementary-material

REFERENCES

1. Hernandez-Palomares MLE, Godoy-Lugo JA, Gomez-Jimenez S, Gamez-Alejo LA, Ortiz RM, Munoz-Valle JF, et al. Regulation of lactate dehydrogenase in response to WSSV infection in the shrimp *Litopenaeus vannamei*. *Fish Shellfish Immunol.* (2018) 74:401–9. doi: 10.1016/j.fsi.2018.01.011
2. Miandare HK, Yarahmadi P, Abbasian M. Immune related transcriptional responses and performance of *Litopenaeus vannamei* post-larvae fed on dietary probiotic PrimaLac®. *Fish Shellfish Immunol.* (2016) 55:671–8. doi: 10.1016/j.fsi.2016.06.053
3. Smith VJ, Brown JH, Hauton C. Immunostimulation in crustaceans: does it really protect against infection? *Fish Shellfish Immunol.* (2003) 15:71–90. doi: 10.1016/S1050-4648(02)00140-7
4. Wang L, Chen H, Xu J, Xu Q, Wang M, Zhao D, et al. Crustacean hyperglycemic hormones directly modulate the immune response of hemocytes in shrimp *Litopenaeus vannamei*. *Fish Shellfish Immunol.* (2017) 62:164–74. doi: 10.1016/j.fsi.2017.01.007
5. Thitamadee S, Prachumwat A, Srisala J, Jaroenlak P, Salachan PV, Sritunyalucksana K, et al. Review of current disease threats for cultivated penaeid shrimp in Asia. *Aquaculture.* (2016) 452:69–87. doi: 10.1016/j.aquaculture.2015.10.028
6. Qiu L, Chen MM, Wan XY, Li C, Zhang QL, Wang RY, et al. Characterization of a new member of Iridoviridae, Shrimp hemocyte iridescent virus (SHIV), found in white leg shrimp (*Litopenaeus vannamei*). *Scientific Reports.* (2017) 7:11834. doi: 10.1038/s41598-017-10738-8
7. Lightner DV, Redman RM. A putative iridovirus from the penaeid shrimp protrachypene precipua burkenroad (Crustacea: Decapoda). *J Invert Pathol.* (1993) 62:107–9. doi: 10.1006/jipa.1993.1084
8. Tang KF, Redman RM, Pantoja CR, Groumellec ML, Duraisamy P, Lightner DV. Identification of an iridovirus in *Acetes erythraeus* (Sergestidae) and the development of *in situ* hybridization and PCR method for its detection. *J Invertebr Pathol.* (2007) 96:255–60. doi: 10.1016/j.jip.2007.05.006
9. Xu LM, Wang TT, Li F, Yang F. Isolation and preliminary characterization of a new 472 pathogenic iridovirus from redclaw crayfish Cherax quadricarinatus. *Dis Aquat Organ.* (2016) 120:17–26. doi: 10.3354/dao03007
10. Qiu L, Chen X, Zhao RH, Li C, Gao W, Zhang QL, et al. Description of a natural infection with decapod iridescent virus 1 in farmed giant freshwater prawn, *Macrobrachium rosenbergii*. *Viruses.* (2019) 11:354. doi: 10.3390/v11040354
11. Chen X, Qiu L, Wang H, Zou P, Dong X, Li F, et al. Susceptibility of *Exopalaemon carinicauda* to the infection with shrimp hemocyte iridescent virus (SHIV 20141215), a strain of decapod iridescent virus 1 (DIV1). *Viruses.* (2019) 11:387. doi: 10.3390/v11040387
12. Miao HZ, Tong SL, Xu B, Jiang M, Liu XY. Viral and Pathological observation in cultured lymphoid tissues of shrimp Penaeus chinensis. *J Fish China.* (1999) 2:169–73.
13. Yang HZ, Wei XX, Wang R, Zeng L, Yang YH, Huang GH, et al. Transcriptomics of Cherax quadricarinatus hepatopancreas during infection with Decapod iridescent virus 1 (DIV1). *Fish Shellfish Immunol.* (2020) 98:832–42. doi: 10.1016/j.fsi.2019.11.041
14. Liao XZ, Wang CG, Wang B, Qin HP, Hu SK, Zhao JC, et al. Research into the hemocyte immune response of *Fenneropenaeus merguiensis* under decapod iridescent virus 1 (DIV1) challenge using transcriptome analysis. *Fish Shellfish Immunol.* (2020) 104:8–17. doi: 10.1016/j.fsi.2020.05.053
15. Christophides GK, Vlachou D, Kafatos FC. Comparative and functional genomics of the innate immune system in the malaria vector *Anopheles gambiae*. *Immunol Rev.* (2004) 198:127–48. doi: 10.1111/j.0105-2896.2004.0127.x
16. Tassanakajon A, Rimphanichyakit V, Visetnan S, Amparyup P, Tang S. Shrimp humoral responses against pathogens: antimicrobial peptides and melanization. *Dev Comp Immunol.* (2017) 80:81–93. doi: 10.1016/j.dci.2017.05.009
17. Jiravanichpaisal P, Lee BL, Soderhall K. Cell-mediated immunity in arthropods: hematopoiesis, coagulation, melanization and opsonization. *Immunobiology.* (2006) 211:213–36. doi: 10.1016/j.imbio.2005.10.015
18. Koiwai K, Kondo H, Hirono I. The immune functions of sessile hemocytes in three organs of kuruma shrimp *Marsupenaeus japonicus* differ from those of circulating hemocytes. *Fish Shellfish Immunol.* (2018) 78:109–13. doi: 10.1016/j.fsi.2018.04.036
19. Koiwai K, Alenton RR, Shiomi R, Nozaki R, Kondo H, Hirono I. Two hemocyte sub-populations of kuruma shrimp *Marsupenaeus japonicus*. *Mol Immunol.* (2017) 85:1–8. doi: 10.1016/j.molimm.2017.01.024
20. Mutz KO, Heilkenbrinker A, Lonne M, Walter JG, Stahl F. Transcriptome analysis using next-generation sequencing. *Curr Opin Biotechnol.* (2013) 24:22–30. doi: 10.1016/j.copbio.2012.09.004
21. Chen YH, Yuan FH, Bi HT, Zhang ZZ, Yue HT, Yuan K, et al. Transcriptome analysis of the unfolded protein response in hemocytes of *Litopenaeus vannamei*. *Fish Shellfish Immunol.* (2016) 54:153–63. doi: 10.1016/j.fsi.2015.10.027
22. Ren X, Liu P, Li J. Comparative transcriptomic analysis of Marsupenaeus japonicus hepatopancreas in response to *Vibrio parahaemolyticus* and white spot syndrome virus. *Fish Shellfish Immunol.* (2019) 87:755–64. doi: 10.1016/j.fsi.2019.02.030
23. Ye T, Tang W, Zhang X. Involvement of Rab6 in the regulation of phagocytosis against virus infection in invertebrates. *J Proteome Res.* (2012) 11:4834–46. doi: 10.1021/pr300274k
24. Sun YM, Li FH, Xiang JH. Analysis on the dynamic changes of the amount of WSSV in Chinese shrimp *Fenneropenaeus chinensis* during infection. *Aquaculture.* (2013) 376:124–32. doi: 10.1016/j.aquaculture.2012.11.014
25. Durand SV, Lightner DV. Quantitative real time PCR for the measurement of white spot syndrome virus in shrimp. *J Fish Dis.* (2002) 25:381–9. doi: 10.1046/j.1365-2761.2002.00367.x
26. Vargas-Albores F, Yepiz-Plascencia G, Jimenez-Vega F, Avila-Villa A. Structural and functional differences of *Litopenaeus vannamei* crustins. *Comp Biochem Physiol B Biochem Mol Biol.* (2004) 138:415–22. doi: 10.1016/j.cbpc.2004.05.007
27. Simão FA, Waterhouse RM, Ioannidis P, Kriventseva EV, Zdobnov EM. BUSCO: assessing genome assembly and annotation completeness with single-copy orthologs. *Bioinformatics.* (2015) 31:3210–12. doi: 10.1093/bioinformatics/btv351
28. Reiner A, Yekutieli D, Benjamini Y. Identifying differentially expressed genes using false discovery rate controlling procedures. *Bioinformatics.* (2003) 19:368–75. doi: 10.1093/bioinformatics/btf877
29. Livak KJ, Schmittgen TD. Analysis of relative gene expression data using real-time quantitative PCR and the $2^{-\Delta\Delta CT}$ Method. *Methods.* (2001) 25:402–8. doi: 10.1006/meth.2001.1262
30. Bustin SA, Benes V, Garson JA, Hellemans J, Huggett J, Kubista M, et al. The MIQE guidelines: minimum information for publication of quantitative real-time PCR experiments. *Clin Chem.* (2009) 55:611–22 doi: 10.1373/clinchem.2008.112797
31. Vatanavicharn T, Prapavorarat A, Jaree P, Somboonwiwat K, Tassanakajon A. PmVRP15, a novel viral responsive protein from the black tiger shrimp, Penaeus monodon, promoted white spot syndrome virus replication. *PLoS ONE.* (2014) 9:e91930. doi: 10.1371/journal.pone.0091930
32. Finney DJ. *Probit Analysis*. Cambridge: Cambridge University Press. (1971).
33. Qiu L, Chen MM, Wan XY, Zhang QL, Li C, Dong X, et al. Detection and quantification of shrimp hemocyte iridescent virus by

TaqMan probe based real-time PCR. *J Invertebr Pathol.* (2018) 154:95–101. doi: 10.1016/j.jip.2018.04.005
34. Yin R, Guo YY, Wei ZL, Shi DJ, He PM, Jia R. Pathogenicity of white-spot syndrome virus in *Macrobrachium nipponensis.* via different infection routes. *Chin J Biotechnol.* (2017) 33:946–56. doi: 10.13345/j.cjb.170005
35. Kathy FJ, Bonnie TP, Jun W, Rita MR, Hsiu-Hui, S, Lightner DV. Geographic variations among infectious hypodermal and hematopoietic necrosis virus (IHHNV) isolates and characteristics of their infection. *Dis Aquatic Organ.* (2003) 53:91–9. doi: 10.3354/dao053091
36. Laxminath T, Eleanor FS, Allan ES, Craig LB. Effects of endosulfan exposure and taura syndrome virus infection on the survival and molting of the marine penaeid shrimp, *Litopenaeus vannamei*. *Chemosphere.* (2012) 86:912–8. doi: 10.1016/j.chemosphere.2011.10.057
37. Qin Z, Babu VS, Wan Q, Zhou M, Liang R, Muhammad A, et al. Transcriptome analysis of Pacific white shrimp (*Litopenaeus vannamei*) challenged by *Vibrio parahaemolyticus* reveals unique immune-related genes. *Fish Shellfish Immunol.* (2018) 77:164–74. doi: 10.1016/j.fsi.2018.03.030
38. Xue S, Liu Y, Zhang Y, Sun Y, Geng X, Sun J. Sequencing and *de novo* analysis of the hemocytes transcriptome in *Litopenaeus vannamei* response to white spot syndrome virus infection. *PLoS ONE.* (2013) 8:e76718. doi: 10.1371/journal.pone.0076718
39. Zeng D, Chen X, Xie D, Zhao Y, Yang C, Li Y, et al. Transcriptome analysis of Pacific white shrimp (*Litopenaeus vannamei*) hepatopancreas in response to Taura syndrome Virus (TSV) experimental infection. *PLoS ONE.* (2013) 8:e57515. doi: 10.1371/journal.pone.0057515
40. Hui K, Ren Q, Cao J. Insights into the intestine immune of Marsupenaeus japonicus under the white spot syndrome virus challenge using RNA sequencing. *Vet Immunol Immunopathol.* (2019) 208:25–33. doi: 10.1016/j.vetimm.2018.12.001
41. Cao J, Wu L, Jin M, Li T, Hui K, Ren Q. Transcriptome profiling of the *Macrobrachium rosenbergii* lymphoid organ under the white spot syndrome virus challenge. *Fish Shellfish Immunol.* (2017) 67:27–39. doi: 10.1016/j.fsi.2017.05.059
42. Su MA, Huang YT, Chen IT, Lee DY, Hsieh YC, Li CY, et al. An invertebrate warburg effect: a shrimp virus achieves successful replication by altering the host metabolome via the PI3K-Akt-mTOR Pathway. *PLOS Pathog.* (2014) 10:e1004196. doi: 10.1371/journal.ppat.1004196
43. Knowles JR. To Build an Enzyme. *Philos Trans.* (1991) 332:115–21. doi: 10.1098/rstb.1991.0039
44. Merkle S, Pretsch W. Characterization of triosephosphate isomerase mutants with reduced enzyme activity in Mus musculus. *Genetics.* (1989) 123:837–44.
45. Roland BP, Stuchul KA, Larsen SB, Amrich CG, Vandemark AP, Celotto AM, et al. Evidence of a triosephosphate isomerase non-catalytic function crucial to behavior and longevity. *J Cell Sci.* (2013) 126(Pt 14):3151–8. doi: 10.1242/jcs.124586
46. Yang Y, Chen ZW, Hurlburt BK, Li GL, Zhang YX, Fei DX, et al. Identification of triosephosphate isomerase as a novel allergen in *Octopus fangsiao*. *Mol Immunol.* (2017) 85:35–46. doi: 10.1016/j.molimm.2017.02.004
47. Yang Y, Zhang YX, Liu M, Maleki SJ, Zhang ML, Liu QM, et al. Triosephosphate isomerase and filamin C share common epitopes as novel allergens of *Procambarus clarkii*. *J Agricult Food Chem.* (2017) 65:950–63. doi: 10.1021/acs.jafc.6b04587
48. Anuar TS, Azreen SN, Salleh FM, Moktar N. Molecular epidemiology of giardiasis among Orang Asli in Malaysia: application of the triosephosphate isomerase gene. *Bmc Infect Dis.* (2014) 14:78. doi: 10.1186/1471-2334-14-78
49. Dai Y, Wang X, Zhao S, Tang J, Zhang L, Dai J, et al. Construction and evaluation of replication-defective recombinant optimized triosephosphate isomerase adenoviral vaccination in *Schistosoma japonicum* challenged mice. *Vaccine.* (2014) 32:771–8. doi: 10.1016/j.vaccine.2013.12.059
50. Kumar K, Bhargava P, Roy U. Cloning, overexpression and characterization of *Leishmania donovani* triosephosphate isomerase. *Exp Parasitol.* (2012) 130:430–6. doi: 10.1016/j.exppara.2012.01.016
51. Liu F, Li S, Liu G, Li F. Triosephosphate isomerase (TPI) facilitates the replication of WSSV in *Exopalaemon carinicauda*. *Dev Comp Immunol.* (2017) 71:28–36. doi: 10.1016/j.dci.2017.01.018
52. Shi LL, Chan SM, Li CZ, Zhang S. Identification and characterization of a laccase from *Litopenaeus vannamei* involved in anti-bacterial host defense. *Fish Shellfish Immunol.* (2017) 66:1–10. doi: 10.1016/j.fsi.2017.04.026
53. Li CZ, Chen YX, Weng SP, Li SD, Zuo HL, Yu XQ et al. Presence of Tube isoforms in *Litopenaeus vannamei* suggests various regulatory patterns of signal transduction in invertebrate NF-κB pathway. *Dev Comp Immunol.* (2014) 42:174–85. doi: 10.1016/j.dci.2013.08.012
54. Wang S, Li HY, Qian Z, Song X, Zhang ZJ, Zuo HL et al. Identification and functional characterization of the TAB2 gene from *Litopenaeus vannamei*. *Fish Shellfish Immunol.* (2015) 46:206–16. doi: 10.1016/j.fsi.2015.06.024

Conflict of Interest: PW was employed by Hainan Zhongzheng Aquatic Science and Technology Co., Ltd.

The remaining authors declare that the research was conducted in the absence of any commercial or financial relationships that could be construed as a potential conflict of interest.

frontiers in Immunology

ORIGINAL RESEARCH
published: 11 September 2020
doi: 10.3389/fimmu.2020.02110

TNF-Receptor-Associated Factor 3 in *Litopenaeus vannamei* Restricts White Spot Syndrome Virus Infection Through the IRF-Vago Antiviral Pathway

Haoyang Li[1], Qihui Fu[1], Sheng Wang[1], Rongjian Chen[2], Xiewu Jiang[2], Peng Zhu[3], Jianguo He[1] and Chaozheng Li[1]**

[1] Southern Marine Science and Engineering Guangdong Laboratory (Zhuhai)/State Key Laboratory of Biocontrol, School of Marine Sciences, Sun Yat-sen University, Guangzhou, China, [2] Guangdong Hisenor Group Co., Ltd., Guangzhou, China, [3] Guangxi Key Laboratory of Beibu Gulf Marine Biodiversity Conservation, Beibu Gluf University, Qinzhou, China

OPEN ACCESS

Edited by:
Chu-Fang Lo,
National Cheng Kung University, Taiwan

Reviewed by:
Anchalee Tassanakajon,
Chulalongkorn University, Thailand
Hidehiro Kondo,
Tokyo University of Marine Science and Technology, Japan
Ikuo Hirono,
Tokyo University of Marine Science and Technology, Japan

***Correspondence:**
Jianguo He
lsshjg@mail.sysu.edu.cn
Chaozheng Li
lichzh5@mail.sysu.edu.cn

Specialty section:
This article was submitted to Comparative Immunology, a section of the journal Frontiers in Immunology

Received: 05 May 2020
Accepted: 04 August 2020
Published: 11 September 2020

Citation:
Li H, Fu Q, Wang S, Chen R, Jiang X, Zhu P, He J and Li C (2020) TNF-Receptor-Associated Factor 3 in Litopenaeus vannamei Restricts White Spot Syndrome Virus Infection Through the IRF-Vago Antiviral Pathway. Front. Immunol. 11:2110. doi: 10.3389/fimmu.2020.02110

Tumor necrosis factor receptor (TNFR)-associated factors (TRAFs) are vital signaling adaptor proteins for the innate immune response and are involved in many important pathways, such as the NF-κB- and interferon regulatory factor (IRF)-activated signaling pathways. In this study, the TRAF3 ortholog from the shrimp *Litopenaeus vannamei* (LvTRAF3) was cloned and characterized. LvTRAF3 has a transcript of 3,865 bp, with an open reading frame (ORF) of 1,002 bp and encodes a polypeptide of 333 amino acids, including a conserved TRAF-C domain. The expression of LvTRAF3 in the intestine and hemocyte was up-regulated in response to poly (I:C) challenge and white spot syndrome virus (WSSV) infection. RNAi knockdown of LvTRAF3 *in vivo* significantly increased WSSV gene transcription, viral loads, and mortality in WSSV-infected shrimp. Next, we found that LvTRAF3 was not able to induce the activation of the NF-κB pathway, which was crucial for synthesis of antimicrobial peptides (AMPs), which mediate antiviral immunity. Specifically, in dual-luciferase reporter assays, LvTRAF3 could not activate several types of promoters with NF-κB binding sites, including those from WSSV genes (*wsv069*, *wsv056*, and *wsv403*), *Drosophila* AMPs or shrimp AMPs. Accordingly, the mRNA levels of shrimp AMPs did not significantly change when TRAF3 was knocked down during WSSV infection. Instead, we found that LvTRAF3 signaled through the IRF-Vago antiviral cascade. LvTRAF3 functioned upstream of LvIRF to regulate the expression of *LvVago4* and *LvVago5* during WSSV infection *in vivo*. Taken together, these data provide experimental evidence of the participation of LvTRAF3 in the host defense to WSSV through the activation of the IRF-Vago pathway but not the NF-κB pathway.

Keywords: *Litopenaeus vannamei*, TRAF3, NF-κB, IRF, WSSV

INTRODUCTION

Tumor necrosis factor receptor (TNFR)-associated factors (TRAFs) are intracellular signal transducers for a number of members of the immune receptor superfamily, which converge on inducing the production of proinflammatory factors, interferons (IFNs) and/or antimicrobial peptides (AMPs) (1). A total of six TRAF families, TRAF1–6, have been identified in mammals, most of which are implicated with several innate immune responses (1). Upon pathogenic infection, a TRAF6 forms a signal transduction complex with myeloid differentiation factor 88 (MyD88), IL-1 receptor-associated kinase-4 (IRAK4) and IRAK1 to activate the downstream NF-κB pathway and trigger the expression of immune-related effectors (2–4). Conversely, TRAF3 plays a negative regulatory role in the MyD88-dependent Toll like receptor (TLR) pathway through inhibiting the formation of the complexes for IRAK1, IRAK4, and TRAF6 (5). In addition to the NF-κB pathway, TRAF family members are involved in signaling regulation in the interferon regulatory factor (IRF)-IFN pathway. In mammals, TRAF2, TRAF3, and TRAF6 can bind with TRIF, the adaptor protein of the TLR3/4 pathway, to regulate the activation of IRF3 and finally promote the expression of type I IFNs (5, 6). In the RIG-I-like receptor (RLR) pathway, the activated mitochondrial antiviral-signaling protein (MAVS) can recruit TRAF2, TRAF3, TRAF5, and/or TRAF6, then these TRAFs are ubiquitinated, followed by the recruitment of the TANK/IKKε/TBK1 complex, and finally IRF3 is recruited and phosphorylated (7). In addition, TRAF3 is involved in the STING-mediated activation of IRF3 (8). In general, most TRAF family members participate in the regulation of the NF-κB and IRF-mediated innate immune pathways.

In *Drosophila melanogaster*, three TRAFs, named dTRAF4 (also called dTRAF1), dTRAF6 (also called dTRAF2) and dTRAF3, have been identified. dTRAF4 is homologous to mammalian TRAF4, and has a conserved TRAF-C domain and seven zinc fingers (9). dTRAF4 was found to regulate JNK pathway activation and participate in *Drosophila* embryo development and differentiation (10). dTRAF6 is homologous to mammalian TRAF6 and has similar functions in inducing the activation of the NF-κB pathway (9). Interestingly, dTRAF3 is likely to have derived from a common precursor to the mammalian TRAF1, 2, 3, and 5 genes (9). A recent study showed that viral infection can enhance lipolysis through the TRAF3-AMPK/WTS-Atg1 pathway to increase intestinal resistance (11). In all, the regulatory relationship between invertebrate TRAFs and classical innate immune signaling pathways remains unclear.

The shrimp species *Litopenaeus vannamei* has become one of the most important cultured species in the world. With high-density tolerance and a rapid growth rate, *L. vannamei* production accounts for 75% of the world's shrimp production each year (12). Recently, several kinds of shrimp diseases have threatened shrimp aquaculture, especially the white spot syndrome (WSS) caused by white spot syndrome virus (WSSV) (13). Within 3–10 days of infection, the mortality rate of WSSV-infected shrimp can reach up to 100%, which has led to serious economic losses in shrimp cultures (14). In addition, to prevent and control the diseases of cultured shrimp, the selection and breeding of shrimp with strong disease resistance have become an important measure for fundamentally improving the disease resistance of shrimp. Both shrimp disease prevention and genetic improvement are based on theoretical support from the study of immune genes. In shrimp, the IRF-Vago and NF-κB pathways have been demonstrated to be crucial for antiviral immunity (12), but the mechanism underlying their signal transduction in WSSV infection is still poorly understood.

In this study, we cloned a new TRAF3 ortholog from *L. vannamei* and explored its function during WSSV infection. We found that LvTRAF3 could signal through the IRF-Vago pathway, but not the NF-κB pathway, to confer protective immunity for shrimp from viral infection. These results provide some insights into the antiviral function of invertebrate TRAF3 members.

MATERIALS AND METHODS

Cloning of Full Length of LvTRAF3 cDNA

An expressed sequence tag (EST) encoding a putative TRAF3 protein was retrieved from *L. vannamei* transcriptome data to obtain the 3′- and 5′-ends of LvTRAF3 using gene specific primers via the rapid amplification of cDNA ends (RACE) method as previously described (**Table 1**) (15). The cDNA template for RACE-PCR was prepared with the SMARTer PCR cDNA Synthesis Kit (Clontech, Japan). The first-round PCR amplifications were conducted on 10-fold dilutions of SMARTer RACE cDNA with either Universal Primer A Mix (UPM)/LvTRAF3-5RACE1 (for 5′-RACE) or UPM/LvTRAF3-3RACE1 (for 3′-RACE), respectively. The products from the first-round PCR were diluted 50-fold as templates for a second round of PCR. Primers of Nested Universal Primer A (NUP) and LvTRAF3-5RACE2 or 3RACE2 were used for a second round of 5′- and 3′-RACE PCR, respectively. The final products were cloned into the pMD-20T Cloning Vector (TaKaRa, Japan) and 12 positive clones were selected and sequenced.

Sequence and Phylogenetic Analysis of LvTRAF3

Protein domains for LvTRAF3 were predicted using the SMART program[1] (16). Protein sequences of TRAFs from other species were found using the National Center for Biotechnology Information (NCBI[2]) database. Sequences of LvTRAF3 and TRAF3 homologs from other species were aligned using Clustal X v 2.0 (17) and visualized using GeneDoc software[3] (18). Phylogenetic trees were constructed via MEGA 5.0 with the neighbor joining (NJ) method (19).

Plasmid Construction

A GFP coding sequence was synthesized and cloned into pAc5.1/V5-His A (Invitrogen) using *Bst*BI/*Pme*I sites to replace the V5-His tag, generating pAc5.1A-GFP for GFP-tagged protein

[1]http://smart.embl-heidelberg.de/

[2]http://www.ncbi.nlm.nih.gov/

[3]http://www.nrbsc.org/gfx/genedoc/

TABLE 1 | Summary of primers in this study.

RACE	
LvTRAF3-5RACE1	CTGGGCAATGGCTAGGAGATCCGGT
LvTRAF3-5RACE2	ACTCAATCTCCTCGTTGCCCTGCTG
LvTRAF3-3RACE1	GTTGTCACACTAACTTTGTCTTTTG
LvTRAF3-3RACE2	TTCATAGGGTGCAATACCTTGGCTT
Protein expression	
LvTRAF3-F	GGGGTACCATGGAGCGAGCGGTGCTGTTGTGTG
LvTRAF3-R	TTGGGCCCTTAGTAGTAGGTGAAGACCCTCCAGCCG
LvDorsal-F	AGGGGTACCATGTTTGTTGCCCAGCGTACTTCC
LvDorsal-R	AACGGGCCCTCACATATCAGAAAATATCCAAAAC
LvRelish-F	AGGGGTACCATGGTGAGAGGTGACAGAGGTGG
LvRelish-R	AACGGGCCCTCACGCCTGGTCCAGTACAGCTACA CATTCC
DmDorsal-F	CGGGGTACCATGTTTCCGAACCAGAACAATGGAGCCG
DmDorsal-R	TGCTCTAGATTACGTGGATATGGACAGGTTCGATATCT
DmRelish-F	CCGGAATTCATGAACATGAATCAGTACTACGACC
DmRelish-R	TGCTCTAGATTATCAAGTTGGGTTAACCAGTAGGG
qRT-PCR	
LvTRAF3-F	CTCCTAGCCATTGCCCAGAG
LvTRAF3-R	GGTCCACCACCTGTTTCTGC
LvEF-1α-F	TATGCTCCTTTTGGACGTTTTGC
LvEF-1α-R	CCTTTTCTGCGGCCTTGGTAG
VP28-F	AACACCTCCTCCTTCACCC
VP28-R	GGTCTCAGTGCCAGAGTAGGT
wsv056-F	TCTGGCAAGGAGATTATGGAGAACCG
wsv056-R	TTTCTTCGTATTTTCTTCATTGTTGGAGGG
wsv069-F	ACAACAACAGACCCTACCCGCCCCA
wsv069-R	GTTGCTGATAAACTCTTGAAGGAAT
wsv249-F	CCCGGACGGAGACGTGATAA
wsv249-R	ATGATGATGGGCCTTTCTTCTCT
wsv403-F	GGGTGGTTGCTTCAACTCCGT
wsv403-R	TCGGTATAGGTTTGGTGTACGTCTCA
LvLYZ1-F	TACGCGACCGATTACTGGCTAC
LvLYZ1-R	AGTCTTTGCTGCGACCACATTC
LvALF1-F	TTACTTCAATGGCAGGATGTGG
LvALF1-R	GTCCTCCGTGATGAGATTACTCTG
LvCTL3-F	ATGTTCTTCGTGCTCCTGCTGT
LvCTL3-R	GCAGTGGTCGTAAATGTTGTG
LvCTL4-F	GCTTTTACTTCCATCAAGACCAG
LvCTL4-R	TGTTAGGATGTACTCATAAAATTCCCT
LvVago4-F	ACGACGAGTTCACGAATTGGATC
LvVago4-R	ACGGCATCTTACCTCAAGAGTC
LvVago5-F	CTCCATAGCCAGGCACGAAAG
LvVago5-R	GTCAGCACAAGCAGCATCACA
Absolute qPCR	
WSSV32678-F	TGTTTTCTGTATGTAATGCGTGTAGGT
WSSV32753-R	CCCACTCCATGGCCTTCA
TaqMan probe-WSSV32706	CAAGTACCCAGGCCCAGTGTCATACGTT
dsRNA templates amplification	
LvTRAF3-F	CTCAGGACCCAAGACAAGC
LvTRAF3-R	GTCAGCCCGACGTGAATAT
LvTRAF3-T7-F	GGATCCTAATACGACTCACTATAGGCTCAGGAC CCAAGACAAGC
LvTRAF3-T7-R	GGATCCTAATACGACTCACTATAGGGTCAGC CCGACGTGAATAT

(Continued)

TABLE 2 | Continued

GFP-F	CGACGTAAACGGCCACAAGTT
GFP-R	ATGGGGGTGTTCTGCTGGTAG
GFP-T7-F	GGATCCTAATACGACTCACTATAGGCGACGTAAA CGGCCACAAGTT
GFP-T7-R	GGATCCTAATACGACTCACTATAGGATGGGGGTG TTCTGCTGGTAG
LvIRF-F	ATGCCGCCATCTTTCACCAATG
LvIRF-R	CTACGGCAACGTCCTCTCGCCGGCA
LvIRF-T7-F	GGATCCTAATACGACTCACTATAGGATGCCGCCAT CTTTCACCAATG
LvIRF-T7-R	GGATCCTAATACGACTCACTATAGGCTACGGCAACGTC CTCTCGCCGGCA

expression (15). The open reading frame (ORF) without a stop codon of *LvTRAF3* was then cloned into pAc5.1A-GFP. The ORFs without stop codons of *LvTRAF3*, *LvDorsal* (Accession No. ROT84343.1), *LvRelish* (Accession No. ABR14713.1), *DmDorsal* (Accession No. NP_724052.1), and *DmRelish* (Accession No. NP_477094.1) were cloned into the *Kpn*I/*Apa*I sites of pAc5.1A vector for the expression of V5-tagged proteins, respectively. The 5′ flanking regulatory regions of *Lysozyme 1* (*LYZ1*) (Accession No. ABD65298), *anti-lipopolysaccharide (LPS) factor 1* (*ALF1*) (Accession No. AHG99284.1), *C-type lectin 3* (*CTL3*) (Accession No. AGV68681.1), and *C-type lectin 4* (*CTL4*) (Accession No. AKA64754.1) were cloned into the pGL3-Basic vector (Promega). Primer sequences are listed in **Table 1** and **Supplementary Table S1**.

Confocal Laser Scanning Microscopy

Drosophila S2 cells were seeded onto glass slides in 12-well plates. After being cultured 24 h, S2 cells were then transfected with pAc5.1A-LvTRAF3-GFP or pAc5.1A-GFP (as a control) using the FuGENE HD Transfection Reagent (Promega). After 36 h, cells were fixed with 4% paraformaldehyde. Hochest 33258 (Beyotime, China) was used to stain cells for 5 min, and then the cells were washed three times with PBS, and finally, visualized with confocal laser scanning microscopy (Leica TCS-SP5, Germany).

The hemocytes from double stranded RNAs (dsRNA)-injected shrimp at 48 hpi were centrifuged at 3000 *g* for 10 min at 4°C. The cells were washed twice with PBS and spread onto cover slips in a 24-well plate (Corning, Untied States). After 30 min, remove PBS and fixed cells in 4% paraformaldehyde diluted in PBS at 25°C for 15 min. The cells were then permeabilized with methanol at −20°C for 10 min. After washing slides for three times, the hemocytes were blocked with 3% bovine serum albumin (BSA) (diluted in PBS) for 1 h at 25°C and then incubated with a mixture of primary antibodies (1:100, diluted in blocking reagent) overnight (about 8 h) at 4°C. The primary antibodies used in immunofluorescence (IF) were rabbit anti-LvIRF antibody (20) and mouse anti-β-actin antibody (Sigma-Aldrich, United States). The slides were washed with PBS six times and then incubated with 1:1000 diluted anti-rabbit IgG (H + L), F (ab′)2 fragment Alexa Fluor 488 Conjugate (CST, United States), and anti-mouse IgG(H + L), F (ab′)2 Fragment Alexa Fluor 594 Conjugate (CST, United States) for 1 h at 25°C. The cell nuclei were stained with

Hoechst 33258 Solution (Beyotime, China) for 10 min. Finally, the slides were observed with a confocal microscope (Leica, Germany) after washing six times with PBS.

SDS-PAGE and Western Blotting

Hemocytes of dsRNA-injected shrimps were sampled with each sample collected and pooled from five shrimps. The nuclear and cytoplasmic fractions of hemocytes were extracted according to the protocol of NE-PER Nuclear and Cytoplasmic Extraction Reagents (Thermo Fisher Scientific, United States). Samples were boiled for 5 min, separated on SDS-PAGE gels followed by transfer to polyvinylidene difluoride (PVDF) membranes. After blocking in 5% BSA in TBS with 0.1% Tween-20 (TBS-T) for 1 h, membranes were incubated with anti-LvIRF, anti-HSP90 (Abcam, United States) and anti-Histone H3 (CST, United States) for 15 h at 4°C. After washing in TBS-T, membranes were incubated for 1 h at 25°C with horseradish peroxidase (HRP)-labeled Goat secondary antibody to Goat anti-Rabbit IgG (H + L)-HRP or Goat anti-Mouse IgG (H + L)-HRP. Both primary and secondary antibodies were incubated in TBS-T with 0.5% BSA. Membranes were developed with the enhanced chemiluminescent (ECL) blotting substrate (Thermo Fisher Scientific) and chemiluminescence was detected using the 5200 Chemiluminescence Imaging System (Tanon, China).

qRT-PCR Analysis of LvTRAF3 Expression

Healthy shrimp were provided by a shrimp farm (Guangdong Hisenor Group) in Maoming, Guangdong province, China. Tissues from the gills, hepatopancreases, hemocytes, and intestines were sampled and pooled from 15 shrimp for assaying tissue expression distribution. For immune stimulation assays, the treated groups were injected with 5 μg of poly (I:C) or WSSV (1×10^6 particles, newly extracted) in 50 μl PBS at the second abdominal segment of each shrimp, and the control group was injected with a PBS solution. The hemocytes and intestines of challenged shrimp were sampled at 0, 4, 8, 12, 24, 36, 48, and 72 h post-injection (hpi), and each sample was collected and pooled from 15 shrimp. Total RNA and qRT-PCR were performed as described previously (21). Expression levels of *LvTRAF3* were calculated using the Livak ($2^{-\Delta\Delta CT}$) method after normalization to *L. vannamei EF-1a* (Accession No. GU136229). Primer sequences are listed in **Table 1**. Each experiment was repeated at least three times.

Knockdown of LvTRAF3 Expression by dsRNA-Mediated RNAi

Double stranded RNAs specifically targeting the LvTRAF3 gene, as well as GFP, as a control, were synthesized by *in vitro* transcription as previously described with the gene-specific primers listed in **Table 1** (22). The lengths of LvTRAF3 and GFP dsRNA were 422 and 504 bp, respectively. The experimental group was injected with LvTRAF3 dsRNA (2 μg/g shrimp), while the control groups were injected with GFP dsRNA (2 μg/g shrimp) and PBS, respectively. The RNA interference efficiency was measured by qRT-PCR. Briefly, total RNA was extracted from hemocytes sampled from the experimental and control groups (nine shrimp from each group) at 48 h post injection and subsequently reverse transcribed into cDNA as a template for qRT-PCR. *L. vannamei EF-1a* was used as an internal control. Primer sequences are listed in **Table 1**. Each experiment was performed at least three times.

WSSV Challenge Experiments in LvTRAF3-Knockdown Shrimp

To explore whether LvTRAF3 plays a role in defense against WSSV, healthy shrimp (5 ± 0.5 g) were divided into two groups. The control group received GFP dsRNA injection and the RNAi group received LvTRAF3 dsRNA. Forty-eight hours later, shrimp were injected again with 1×10^5 copies of WSSV particles or 50 μl PBS. Shrimp were kept in culture flasks for about 7 days following infection. The survival number was recorded every 4 h. Differences in the mortality levels between treatments were tested for statistical significance using a Kaplan–Meier plot (log-rank χ^2 test) in GraphPad Prism software.

A parallel experiment was also performed to monitor WSSV replication in LvTRAF3-knockdown shrimp. Briefly, eight samples of hemocytes or gills (each sample pooled from one shrimp) were collected from each group at 48 h post infection for RNA and DNA extraction. Hemocyte RNA was extracted for detecting RNAi efficiency (*LvTRAF3*), and for measuring the expression changes of both viral and host genes, including WSSV genes (*wsv056*, *wsv069*, *wsv249*, *wsv403,* and *VP28*), shrimp NF-κB-mediated genes (*LvALF1*, *LvLYZ1*, *LvCTL3,* and *LvCTL4*) and shrimp IRF-mediated genes (*LvVago4* and *LvVago5).* Gill DNA was also extracted with the TIANGEN Marine Animals DNA Kit (TIANGEN, China) according to the user's introduction. The viral loads were measured by absolute quantitative PCR with primers WSSV32678-F/WSSV32753-R and a TaqMan fluorogenic probe (**Table 1**). The WSSV genome copy numbers in 0.1 μg of shrimp gill DNA were then calculated. Primer sequences are listed in **Table 1**. Each experiment was performed at least three times.

Dual-Luciferase Reporter Assays

In this study, *Drosophila* S2 cells were used for dual-luciferase reporter assays. Before plasmid transfection, S2 cells were seeded into 96-well plate (TPP, Switzerland), and LvTRAF3 plasmids were transfected the next day using the FuGENE Transfection Reagent (Promega) according to the manufacturer's recommendations. For dual-luciferase reporter assays, S2 cells in each well of a 96-well plate were transfected with 0.1 μg of reporter gene plasmids (pGL3-*DmMtk*, pGL3-*DmDef*, pGL3-*DmCecA*, pGL3-*DmDipt*, pGL3-*DmAttA*, pGL3-*DmDrs*, pGL3-*LvALF1*, pGL3-*LvLYZ1*, pGL3-*LvCTL3,* or pGL3-*LvCTL4*), 0.01 μg of pRL-TK renilla luciferase plasmid (as an internal control), and 0.1 μg of expression plasmids (pAc5.1A-LvTRAF3) or the empty pAc5.1/V5-His A plasmid (as control). At 48 h post transfection, the activities of the firefly and renilla luciferases were measured according to manufacturer's instructions. Each experiment was conducted at least three times.

WSSV Challenge Experiments in Double LvTRAF3/LvIRF-Knockdown Shrimp

In shrimp, the IRF-Vago cascade is crucial for defense against WSSV infection (20). We try to figure out whether LvTRAF3 regulates the expression of LvVago4/5 through LvIRF during WSSV infection, thus a double gene (LvTRAF3/LvIRF) knockdown was performed. Forty-eight hours after dsRNAs injection, shrimp were injected again with 1×10^5 copies of WSSV particles. Shrimp were then kept in culture flasks for about 7 days following infection. The cumulative mortality was recorded every 4 h. Differences in the mortality levels between treatments were tested for statistical significance using a Kaplan–Meier plot (log-rank χ^2 test) in GraphPad Prism software.

A parallel experiment was also performed to monitor the RNA interference of dsRNA, viral envelope protein *VP28* transcription and WSSV replication. After 48 h after WSSV infection, the hemocytes and gills were collected for RNA extraction and DNA extraction (9 shrimp for RNA extraction and 12 shrimp for DNA extraction from each group). The RNAi efficiency (*LvTRAF3*) and WSSV genes (*wsv056*, *wsv069*, *wsv249*, *wsv403,* and *VP28*) transcription was measured by qRT-PCR, and WSSV replication detection was performed by absolute quantitative PCR. Primer sequences are listed in **Table 1**. Each experiment was conducted at least three times.

RESULTS

Sequence Analysis of LvTRAF3

The transcript of *LvTRAF3* was found to be 3,865 bp long, consisting of a 368 bp 5′-untranslated region (UTR), a 2,495 bp 3′-UTR including a poly (A) tail, and a 1,002 bp ORF encoding a polypeptide of 333 amino acids with a calculated molecular weight of 38.6 kDa (Accession No. MN037815). The predicted domain analysis of LvTRAF3 indicated that there was a TRAF-C domain (MATH domain) located at 197–330 amino acids (**Figure 1A**).

Multiple sequence analysis showed that the TRAF-C domain of *L. vannamei* TRAF3 was similar to that of *Homo sapiens* TRAF3 (32% identity), *H. sapiens* TRAF5 (29% identity), *H. sapiens* TRAF1 (32% identity), *H. sapiens* TRAF2 (32% identity), *H. sapiens* TRAF4 (25% identity), *D. melanogaster* TRAF4 (28% identity), *L. vannamei* TRAF6 (23% identity), *H. sapiens* TRAF6 (23% identity), *D. melanogaster* TRAF6 (23% identity), and *D. melanogaster* TRAF3 (24% identity) (**Figure 1B**). In general, the TRAF-C domain of LvTRAF3 showed conservation to those of *Drosophila* and human TRAFs, suggesting that LvTRAF3 was a TRAF family member.

According to the NJ phylogenetic tree, the TRAFs from various species could be divided into nine groups, namely vertebrate TRAF4, invertebrate TRAF4, vertebrate TRAF1, vertebrate TRAF2, vertebrate TRAF5, vertebrate TRAF3, invertebrate TRAF6, vertebrate TRAF6, and invertebrate TRAF3. *L. vannamei* TRAF3 (LvTRAF3) was clustered with TRAF3 homologs from invertebrates, including *D. melanogaster*, *Anopheles gambiae*, *Culex quinquefasciatus*, and *Aedes aegypti*, further suggesting that LvTRAF3 was a TRAF3 family member (**Figure 2**).

Expression of *LvTRAF3* in Healthy and Immune-Challenged Shrimp

Tissue distribution analysis showed that *LvTRAF3* was expressed highly in the intestine and hemocyte, with ∼22-fold and ∼43-fold levels over that in the gill (set to 1.0), respectively (**Figure 3A**).

The shrimp hemocytes are leukocyte-like blood cells with phagocytic functions, while the intestine is the crucial organ involved in immune defense against bacterial infection (23). In the hemocyte of WSSV-infected shrimp, the expression of *LvTRAF3* was dramatically up-regulated at 4 h with a 3.99-fold increase, and then stayed at a high level (8.99-fold) at 48 h. Infected with WSSV, *LvTRAF3* expression in the intestine was induced to a peak (2.55-fold) at 4 h, remained at a high level during 24–48 h with 3. 55-, 3. 77-, and 2.95-fold increases at 24, 36, and 48 h, respectively (**Figure 3B**). Then we explored the effect of poly (I:C), a viral nucleic acid mimic, on *LvTRAF3* expression. The expression of *LvTRAF3* in hemocyte was gradually up-regulated from 4 to 72 h, with a 13.29-fold peak at 24 h. In intestine, the injection of poly (I:C) induced *LvTRAF3* transcription from 4 to 12 h, with 3. 11-, 2. 62-, and 2.43-fold increases at 4, 8, and 12 h, respectively, and then reached a peak at 72 h with a 4.33-fold increase. The control group injected with PBS did not show obvious changes in *LvTRAF3* expression (**Figure 3C**).

Subcellular Localization of LvTRAF3

Subcellular localization plays an important role in the study of protein function. Vector pAc5.1A-LvTRAF3-GFP was constructed by inserting the full-length coding sequences of *LvTRAF3* into the pAc5.1A-GFP vector. To investigate the subcellular distribution of LvTRAF3, pAc5.1A-LvTRAF3-GFP plasmids were transfected into *Drosophila* S2 cells, and the GFP-fusion proteins were visualized using confocal laser scanning microscopy. **Figure 4** shows that LvTRAF3 aggregated in the cytoplasm and nucleus, while GFP was distributed uniformly.

Critical Role of LvTRAF3 in Defense Against WSSV

To determine the function of LvTRAF3 faced with WSSV, we suppressed LvTRAF3 expression *in vivo* via the RNAi strategy. Several studies have reported that nucleic acid mimics, especially dsRNA, can strongly induce non-specific antiviral immune responses in insects, shrimp, and oyster (24). GFP was the specific gene from jellyfish, and did not exist in shrimp. To eliminate the sequence-non-specific effect of dsRNA, we selected dsRNA-GFP as the treatment for control groups, which could keep the sequence-non-specific effect without targeting any genes in shrimp. Forty-eight hours after dsRNA injection, shrimp were injected with WSSV or PBS, and their survival numbers were counted every 4 h. The silencing efficiency of *LvTRAF3* was checked by qRT-PCR at 48 h post WSSV infection. The injection of dsRNA-LvTRAF3 resulted in a significant

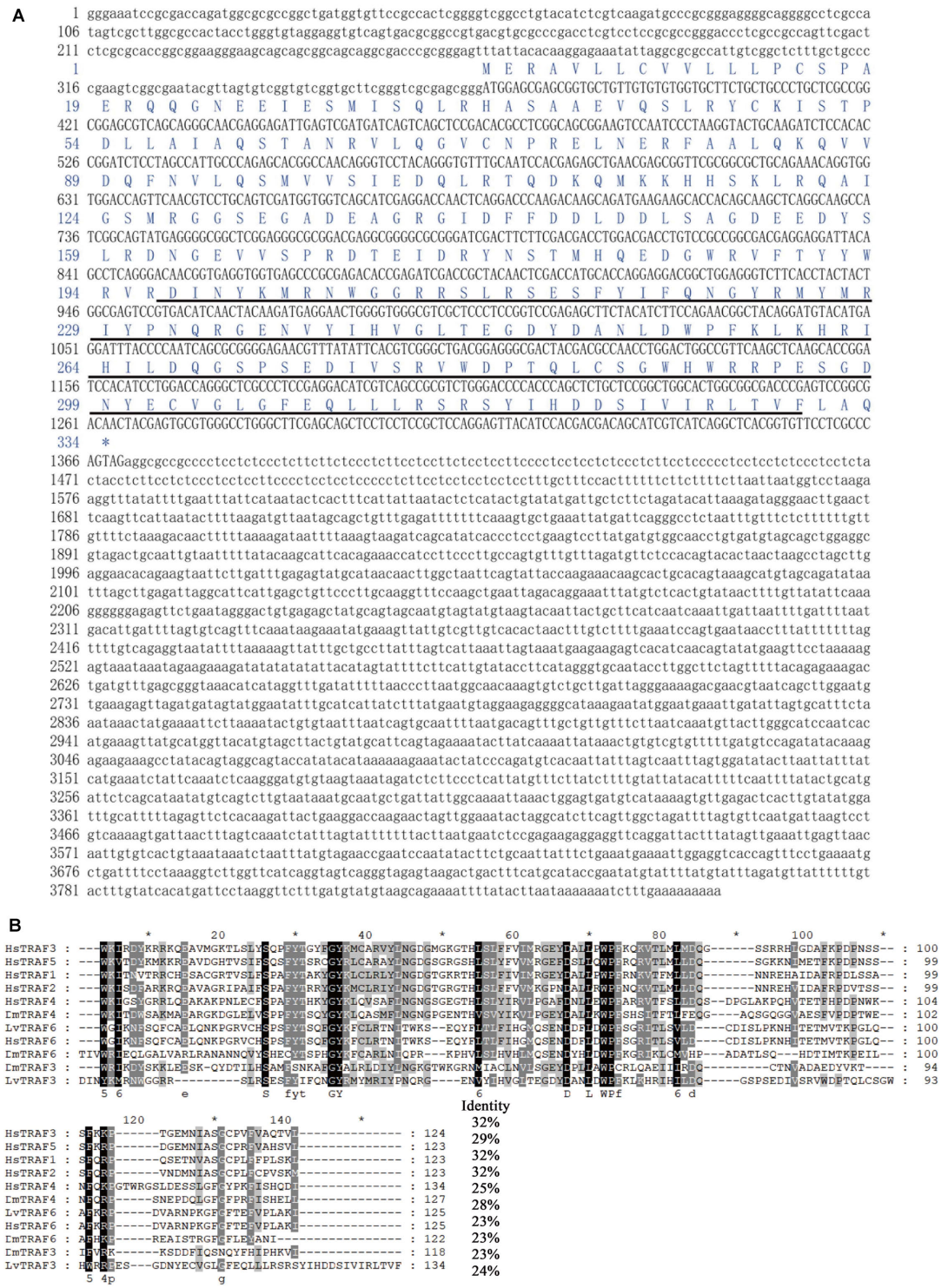

FIGURE 1 | Full-length cDNA and amino acid sequence of LvTRAF3, and multiple sequence alignment with TRAFs. **(A)** The ORF of the nucleotide sequence is shown in upper-case letters, while the 5′ and 3′-UTR sequences are shown in lowercase. Amino acid sequence is represented with one-letter codes above the nucleotide sequence. The TRAF-C domain in the C-terminal is underlined. **(B)** Identical amino acid residues are shaded in black and similar residues are in gray. Amino acid identities of the LvTRAF3 with other TRAFs are shown on the right. Proteins analyzed are listed below: LvTRAF3, *L. vannamei* TRAF3 (Accession No. MN037815); LvTRAF6, *L. vannamei* TRAF6 (113823573); HsTRAF1, *Homo sapiens* TRAF1 (NP_005649.1); HsTRAF2, *H. sapiens* TRAF2 (ADQ89802.1); HsTRAF3, *H. sapiens* TRAF3 (NP_003291.2); HsTRAF4, *H. sapiens* TRAF4 (NP_004286.2); HsTRAF5, *H. sapiens* TRAF5 (CAG38794.1); HsTRAF6, *H. sapiens* TRAF6 (NP_004611.1); DmTRAF4, *D. melanogaster* TRAF4 (NP_477416.1); DmTRAF6, *D. melanogaster* TRAF6 (AAD47895.1); DmTRAF3, *D. melanogaster* TRAF3 (NP_727976.1).

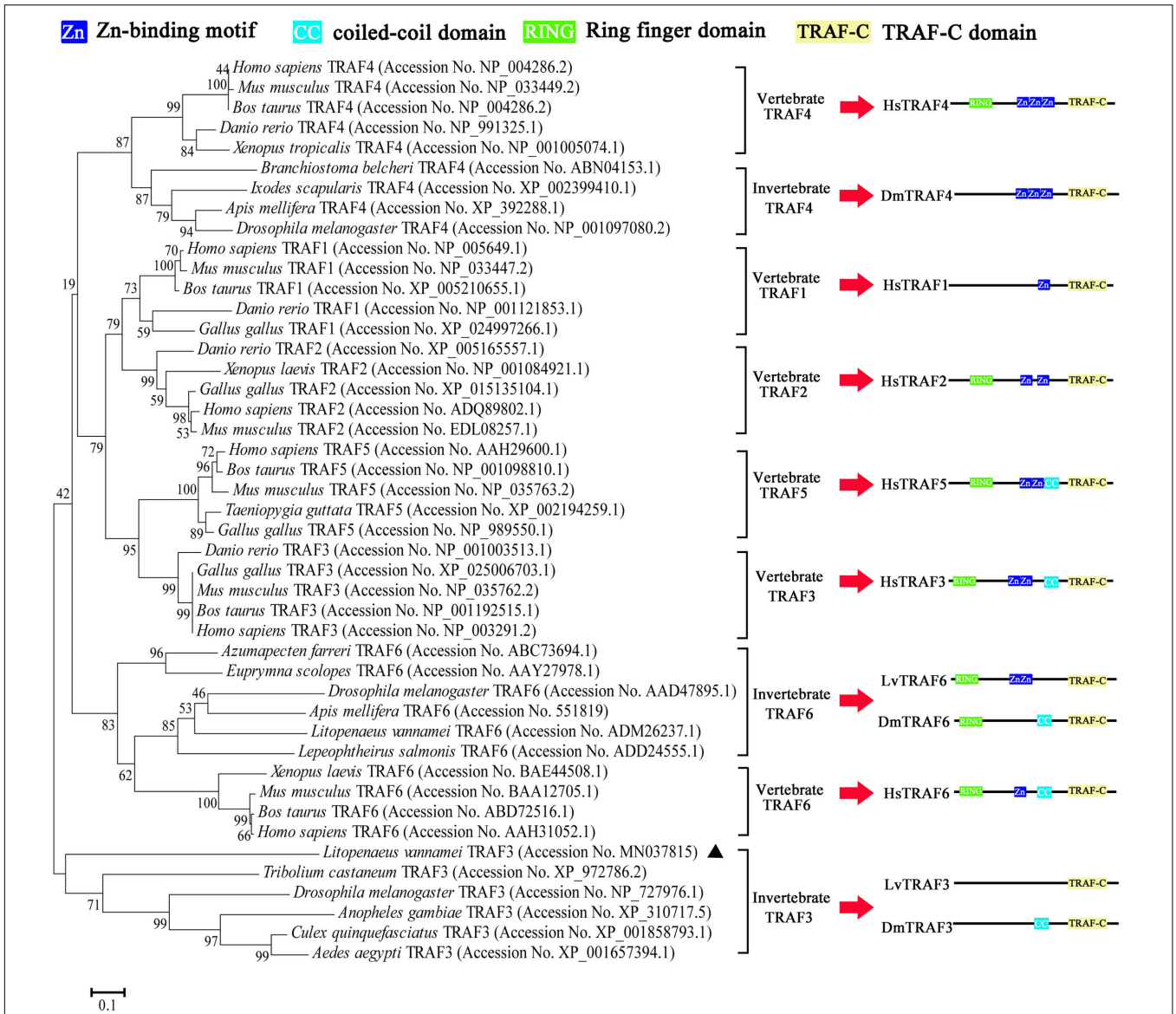

FIGURE 2 | Phylogenetic tree of TRAFs using full-length amino acid sequences from various species. GenBank accession numbers are shown after scientific names of their species. The right side shows the structure of TRAFs belonging to human, *Drosophila*, and shrimp.

decrease in the *LvTRAF3* transcription levels, which was down-regulated to 0.18-fold of the GFP dsRNA injection groups (control) (**Figure 5A**).

The expression of WSSV immediate early (IE) genes somewhat reflects viral pathogenesis (25). We chose several viral genes to investigate their expression in LvTRAF3-knockdown shrimp. We found that the expression of *wsv056*, *wsv069*, *wsv249*, and *wsv403* in the LvTRAF3-knockdown group was 7. 16-, 10. 26-, 10. 10-, and 11.35-fold higher than that in the dsRNA-GFP group, respectively (**Figure 5B**). These results showed that LvTRAF3 was involved in the antiviral defense against WSSV. We also found that the expression of *VP28*, a WSSV structural protein, was 10.23-fold higher in LvTRAF3-knockdown shrimp (**Figure 5B**). Consistent with the upregulated expression of WSSV genes, higher viral loads were observed at corresponding time points after WSSV infection. As shown in **Figure 5C**, the viral loads of the dsRNA-LvTRAF3 group were significantly higher than those of the control group, with a 10-fold increase being apparent. In addition, at 12 h post WSSV infection, shrimp from two groups (dsRNA-GFP and dsRNA-LvTRAF3) started to die. However, the survival rate of the dsRNA-LvTRAF3 group reached 0 post WSSV infection (108 h) faster compared with the control group (144 h). Meanwhile the survival rate of shrimp in the LvTRAF3-knockdown group was significantly lower than that in the GFP-knockdown group (χ^2: 12.25, $p = 0.0066 < 0.01$) (**Figure 5D**). All of the results above indicated that LvTRAF3 played a crucial role in the innate immune defense against WSSV infection.

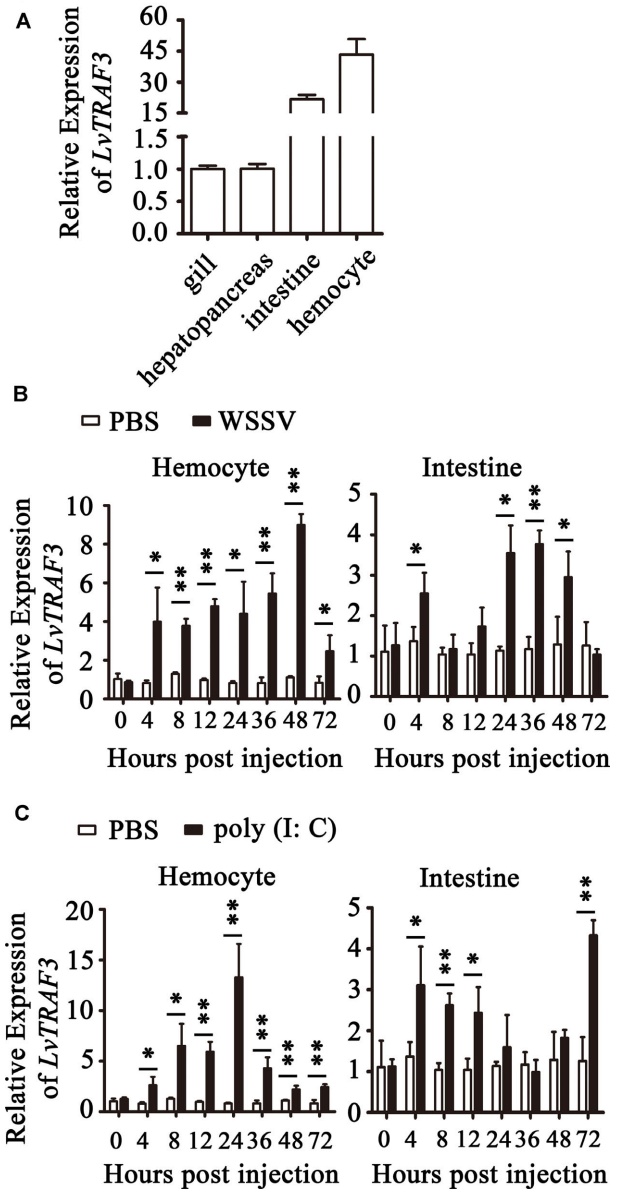

FIGURE 3 | Expression of *LvTRAF3* in healthy and immune challenged shrimp. Expression of *LvTRAF3* was normalized to that of *EF-1α* using the Livak ($2^{-\Delta\Delta CT}$) method and the data is provided as the mean ± SD from triplicate assays. **(A)** Tissue distribution of LvTRAF3 in healthy *L. vannamei*. Expression level in the gill was used as control and set to 1.0. **(B)** Expression profiles of *LvTRAF3* after WSSV infection in hemocytes and the intestine. The expression level at each time point was normalized to PBS-injected group. (*$p < 0.05$, **$p < 0.01$). **(C)** Expression profiles of *LvTRAF3* after poly (I:C) stimulation in hemocyte and intestine. The expression level at each time point was normalized to the PBS-injected group. (*$p < 0.05$, **$p < 0.01$).

LvTRAF3 Not Involved in NF-κB Mediated Immune Response

It has been reported that shrimp NF-κB can induce the expression of some WSSV IE genes that contain NF-κB binding sites in their promoters, such as *wsv069* (25). In addition to *wsv069*, NF-κB binding sites were also found in the promoters of *wsv056* and *wsv403* (**Figure 6A**). Dual luciferase reporter assays in *Drosophila* S2 cells showed that both shrimp NF-κBs (LvDorsal and LvRelish) were able to upregulate the promoter activities of *wsv056*, *wsv069,* and *wsv403* significantly, whereas ectopic expression of LvTRAF3 had no effect on the promotor activities of *wsv056*, *wsv069,* or *wsv403* (**Figure 6B**).

In *Drosophila*, AMP expression is mainly regulated by NF-κB (DmDorsal, DmRelish). In details, DmRelish regulates the expression of *DmDpt* (*Diptericin*), *DmAttA* (*Attacin A*), and *DmCecA* (*Cecropin A*), while DmDorsal regulates the expression of *DmDrs* (*Drosomycin*) (26). Both DmRelish and DmDorsal can regulate the expression of both *DmMtk* (*Metchnikowin*) and *DmDef* (*Defensin*) (26). Dual luciferase reporter experiments showed that both DmDorsal and DmRelish upregulated the promoter activities of *DmMtk*, *DmDef*, *DmCecA*, *DmDipt*, *DmAttA,* and *DmDrs*, whereas over-expression of LvTRAF3 had no effect on the promoter activities of these NF-κB-mediated AMPs (**Figure 6C**). Likewise, *L. vannamei* NF-κB was shown to induce a lot of immune effectors, such as LvALF1 (anti-LPS-factor 1), LvCTL3 (C-type lectin 3), LvCTL4 (C-type lectin 4), and LvLYZ1 (lysozyme 1) (27–29). As shown in **Figure 6D**, we found that LvRelish and LvDorsal, but not LvTRAF3, could upregulate the promoter activities of *LvALF1*, *LvLYZ1*, *LvCTL3,* and *LvCTL4*. These results suggested that LvTRAF3 was not able to induce NF-κB driven *Drosophila* and shrimp AMPs *in vitro*.

To further explore whether LvTRAF3 exerted a regulatory effect on NF-κB pathway targeted genes *in vivo*, we determined the expression levels of these AMPs in LvTRAF3-silenced shrimp during WSSV infection. At 48 h post WSSV infection, dsRNA-LvTRAF3 resulted in a significant decrease of LvTRAF3 transcription levels [0.18-fold of the GFP dsRNA injection group (control)]. Yet, the mRNA levels of shrimp AMPs did not change significantly due to the knockdown of TRAF3 (**Figure 6E**). Together, our results revealed that LvTRAF3 could not participate in regulation of the NF-κB pathway *in vitro* or *in vivo*.

Participation of LvTRAF3 in IRF-Vago Mediated Antiviral Responses

In mammals, several TRAF family members can modulate IRF activity to trigger an IFN-mediated immune response (7). Interestingly, it has been reported that shrimp possess an IFN system-like antiviral pathway, as evidenced by the fact that shrimp LvIRF is able to induce the activation of LvVago4/5, invertebrate IFN-like molecules, to defend against viral infection (20). In this study, we were curious about the relationship between LvTRAF3 and the LvIRF-LvVago4/5 pathway. We firstly investigated the effect of TRAF3 on IRF nuclear translocation by immunofluorescence staining in shrimp hemocytes. The results showed that dsRNA-LvTRAF3 injection inhibited LvIRF translocated from the cytoplasm to the nucleus, while the control treatment of dsRNA-GFP did not (**Figures 7A,B**). To confirm the above results, we probed LvIRF translocation from the cytoplasm to the nucleus upon

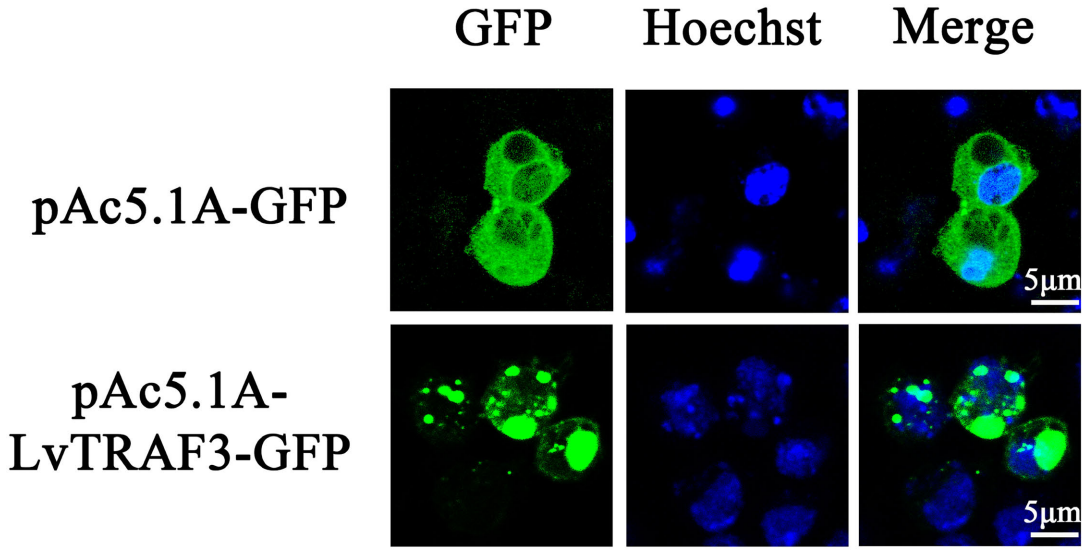

FIGURE 4 | Subcellular localization of LvTRAF3 in *Drosophila* S2 cells. *Drosophila* S2 cells were transfected with plasmids pAc5.1A-LvTRAF3-GFP and pAc5.1A-GFP. At 36 h post-transfection, cells were observed using a Leica laser scanning confocal microscope.

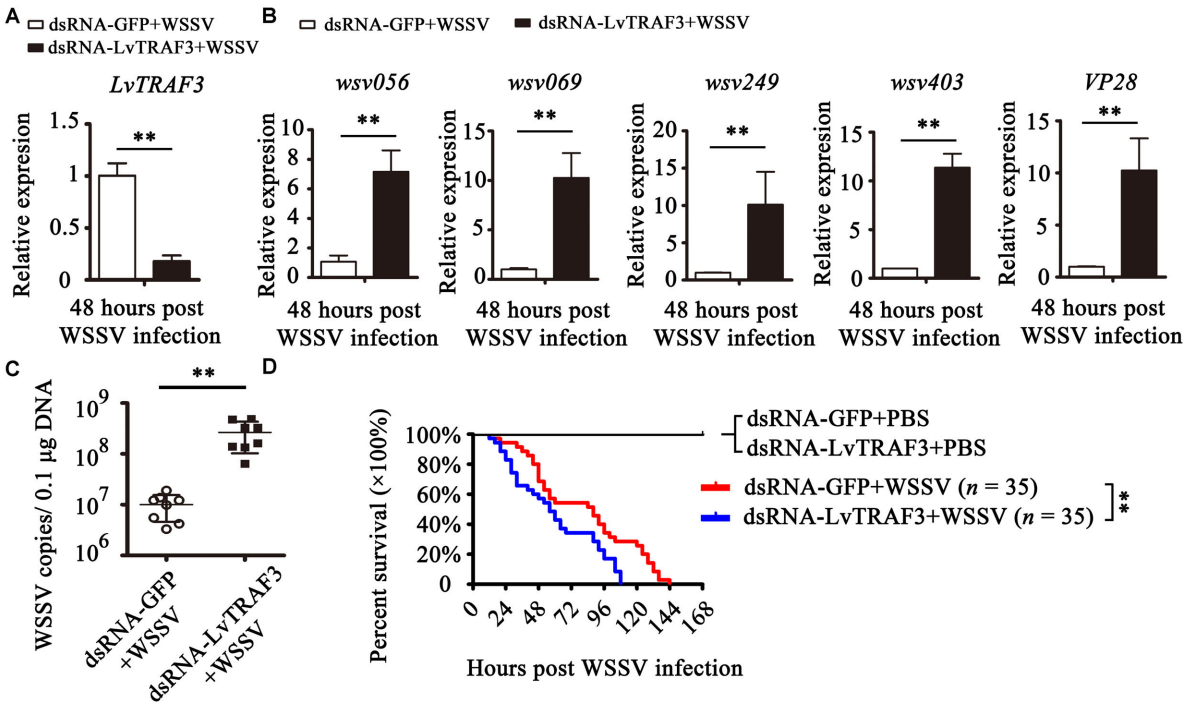

FIGURE 5 | Functional analysis of LvTRAF3 in WSSV infection by RNAi. **(A)** The silencing efficiency of LvTRAF3 was confirmed by qRT-PCR normalized to *EF-1a*. **(B)** Expression levels of *wsv056*, *wsv069*, *wsv249*, *wsv403,* and *VP28* in dsRNA-GFP treated or dsRNA-LvTRAF3 treated shrimp 48 h post WSSV infection. **(C)** Copy number of WSSV in dsRNA-LvTRAF3 or dsRNA-GFP treated shrimp at 48 h post WSSV infection. The data is provided as the mean ± SD from triplicate assays and analyzed statistically by Student's *t*-test ($p < 0.01$). **(D)** Survival of WSSV challenged LvTRAF3-silenced shrimp and GFP dsRNA treated shrimp. The data is provided as the mean ± SD of triplicate assays and analyzed statistically by Student's *t*-test (**$p < 0.01$) **(A–C)**. Experiments were performed three times with similar results and analyzed statistically by Kaplan–Meier plot (log-rank χ^2 test) (**$p < 0.01$) **(D)**.

LvTRAF3-knockdown by using an LvIRF specific antibody. In good agreement with the results of immunofluorescence staining, we were able to detect less nuclear import of IRF in shrimp hemocytes during LvTRAF3-knockdown (**Figure 7C**). Our data suggested that LvTRAF3 was a key factor for mediating downstream LvIRF activation.

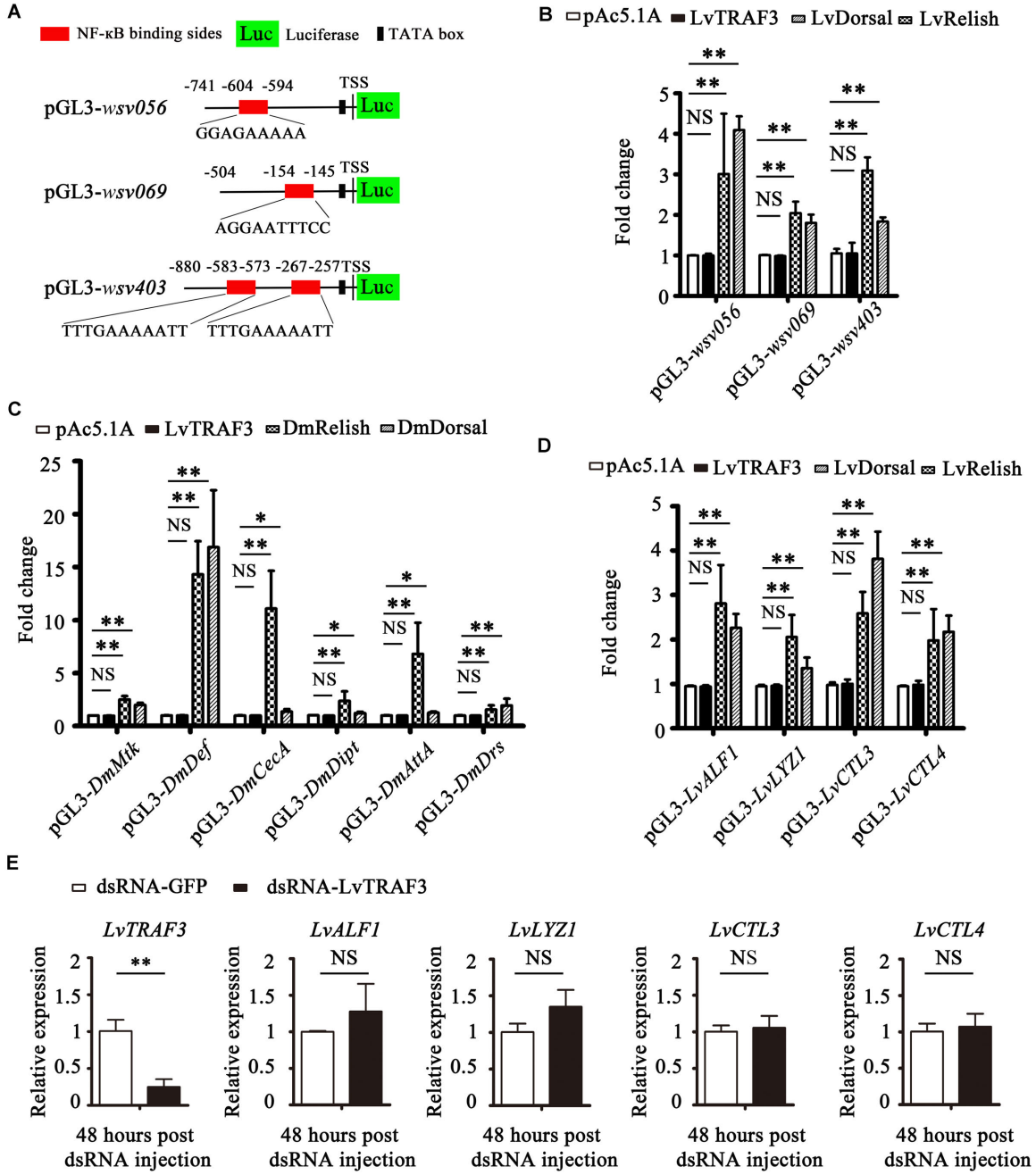

FIGURE 6 | LvTRAF3 fails to regulate the expression of NF-κB pathway driven genes *in vitro* and *in vivo*. **(A)** Schematic diagram of the *wsv056*, *wsv069,* and *wsv403* promotors regions in luciferase reporter gene constructs. **(B)** Relative luciferase activities of the WSSV genes *wsv056*, *wsv069,* and *wsv403* in S2 cells. **(C)** Relative luciferase activities of *Drosophila* AMPs in S2 cells. **(D)** Relative luciferase activities of shrimp AMPs in S2 cells. **(E)** The expression of *LvTRAF3* and the shrimp immune effectors *LvALF1*, *LvLYZ1*, *LvCTL3,* and *LvCTL4* in dsRNA-LvTRAF3 or dsRNA-GFP treated shrimp at 48 h post WSSV infection. All of the data are plotted as the mean ± SD from triplicate assays and analyzed statistically by Student's *t*-test (*$p < 0.05$, **$p < 0.01$, NS, non significant) **(A–E)**.

Then, we explored the potential function of LvTRAF3 involved in IRF-Vago pathway. As shown in **Figure 8A**, during WSSV infection, the suppression of LvTRAF3 by RNAi led to down-regulated expression of *LvVago4* (0.17-fold) and *LvVago5* (0.23-fold), which suggested that LvTRAF3 might be involved in the regulation of *LvVago4/5*. Next, we performed a double knockdown experiment to investigate whether LvTRAF3 regulated the expression of LvVago4/5 through upstream LvIRF. First, we observed that LvTRAF3- or LvIRF-knockdown reduced the expression of *LvVago4* and *LvVago5* during WSSV infection. qPCR assays then demonstrated that the reduction of *LvVago4* and *LvVago5* in dsRNA-LvIRF-injected shrimps became more

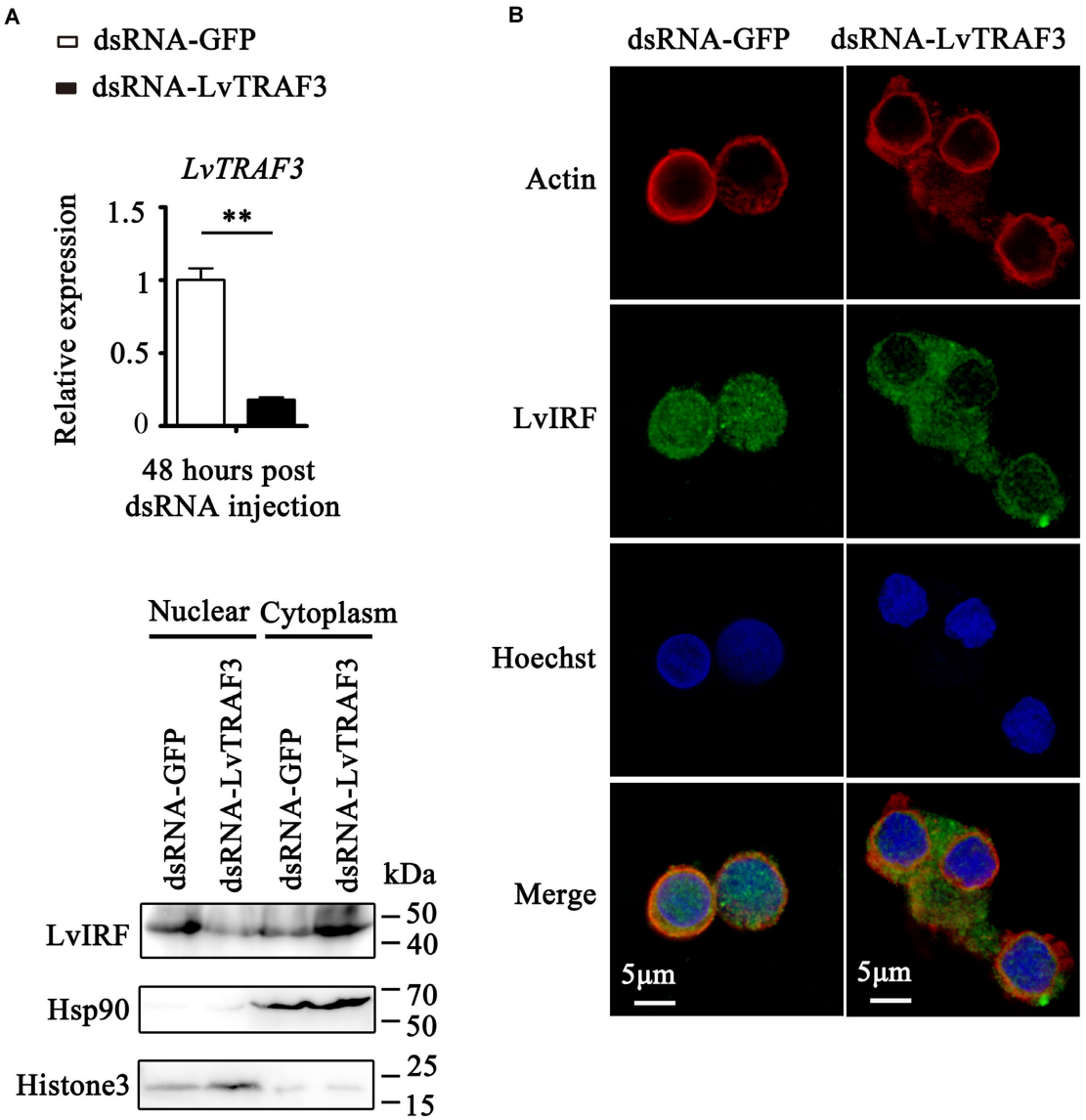

FIGURE 7 | LvTRAF3 could activate LvIRF nuclear translocation. **(A)** Knockdown efficiencies of LvTRAF3 were checked by qRT-PCR (**$p < 0.01$). **(B)** LvIRF nuclear translocation was inhibited in LvTRAF3 silenced hemocytes. The hemocytes were collected at 48 h post dsRNA injection, and then subjected to immunofluorescence staining. β-actin was used here in order to define the shape and cytoplasmic region of cells. **(C)** The subcellular distribution of LvIRF in LvTRAF3 silenced hemocytes was detected at 48 h post dsRNA injection by western blotting. The GFP dsRNA treated hemocytes was used as a control.

obvious when LvTRAF3 was silenced (**Figure 8B**). Accordingly, dsRNA-LvTRAF3 or dsRNA-LvIRF injection led to upregulate the expressional levels of *wsv056*, *wsv069*, *wsv249*, *wsv403,* and *VP28*, while the double gene knockdown caused a more increased in the expression of those genes (**Figure 8C**). In agreement with this finding, enhancement of viral replication and pathogenicity by LvTRAF3 suppression was observed in LvIRF-silenced shrimp (**Figures 8D,E**). In detail, knockdown of LvTRAF3 caused a lower cumulative mortality in LvIRF-silenced shrimp (χ^2: 12.42, $p = 0.0145 < 0.05$), suggesting that LvTRAF3 might defend against WSSV infection via LvIRF (**Figure 8E**). Taken together, these results suggested that LvTRAF3 could trigger an antiviral response via the LvIRF-LvVago4/5 pathway during WSSV infection.

DISCUSSION

Tumor necrosis factor receptor-associated factor family proteins play important roles in the innate immune response to viral invasion (30). In this study, we identified a TRAF3 homolog from *L. vannamei* (LvTRAF3) for the first time, explored its antiviral function and the relationship involving related immune pathways in shrimp.

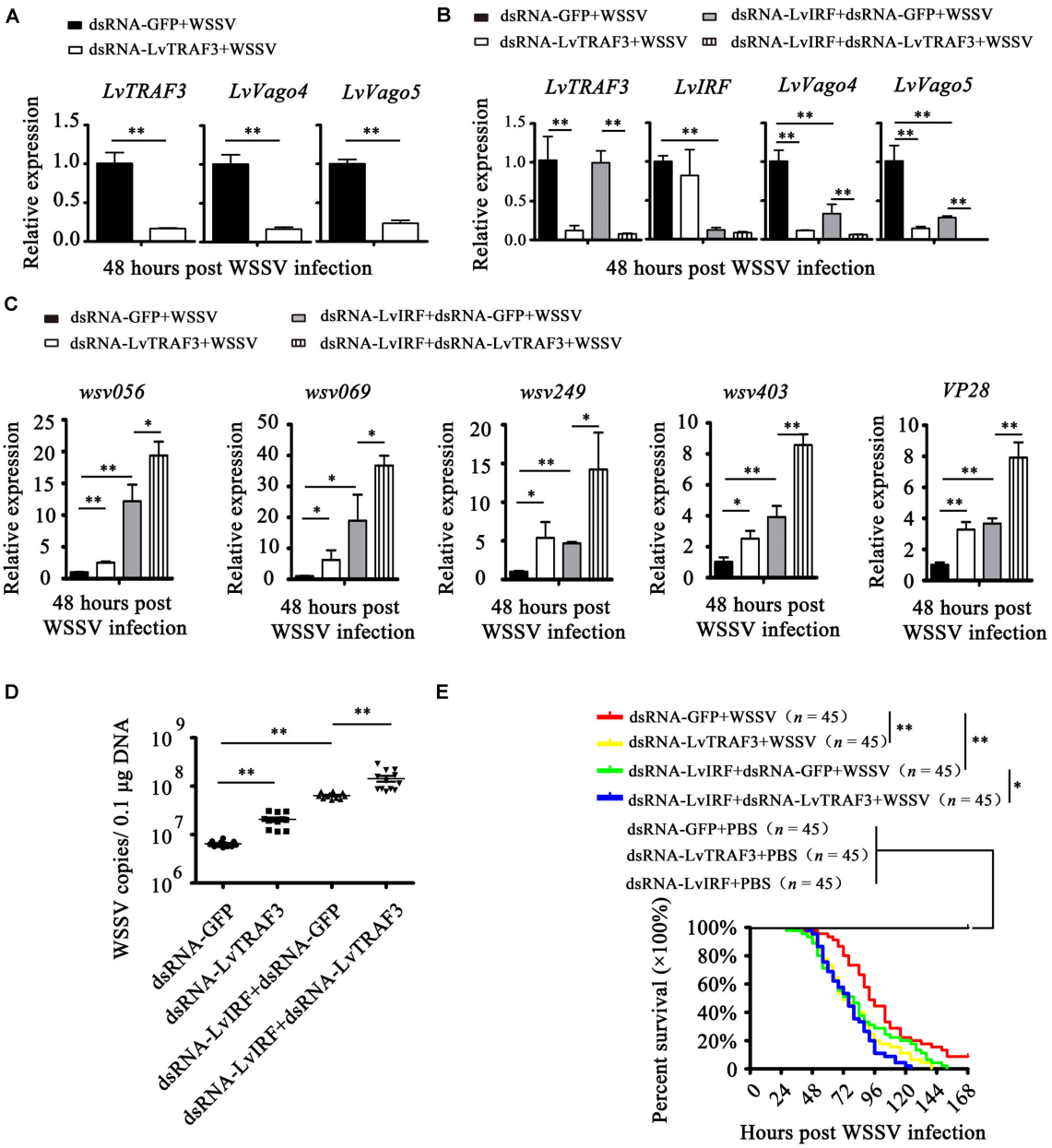

FIGURE 8 | LvTRAF3 functions upstream of the LvIRF-LvVago4/5 antiviral pathway. **(A)** The expression of *LvTRAF3* and the antiviral genes *LvVago4* and *LvVago5* in dsRNA-LvTRAF3 or dsRNA-GFP treated shrimp at 48 h post WSSV infection. **(B)** The expression of *LvTRAF3* and antiviral genes *LvIRF*, *LvVago4,* and *LvVago5* in dsRNA-LvTRAF3 or dsRNA-GFP treated shrimp with or without dsRNA-LvIRF injection at 48 h post WSSV infection. **(C)** WSSV genes *wsv056*, *wsv069*, *wsv249*, *wsv403,* and *VP28* transcription in dsRNA-LvTRAF3 or dsRNA-GFP treated shrimp with or without dsRNA-LvIRF injection 48 h post WSSV infection. **(D)** WSSV copy number in dsRNA-LvTRAF3 or dsRNA-GFP treated shrimp with or without dsRNA-LvIRF injection 48 h post WSSV infection. The experiments were repeated three times with similar results. One dot represents 1 shrimp and the horizontal line represents the median of the results. The results were analyzed statistically by Student's *t*-test (**$p < 0.01$). **(E)** Survival of WSSV challenged dsRNA-LvTRAF3 or dsRNA-GFP treated shrimp with or without dsRNA-LvIRF injection. Experiments were performed three times with similar results and analyzed statistically by Kaplan–Meier plot (log-rank χ^2 test) (**$p < 0.01$, *$p < 0.05$). All of the data are plotted as the mean ± SD from triplicate assays and analyzed statistically by Student's *t*-test (*$p < 0.05$, **$p < 0.01$) **(A–C)**.

In mammals, TRAFs 1 through 6 share a conserved TRAF-C terminus, which is required for the hetero- and homo-oligomerization of TRAF proteins, and recruitment to TRAF binding motifs in the cytoplasmic domains of cell surface receptors, as well as certain cytoplasmic and nuclear proteins (1). LvTRAF3 also has a TRAF-C domain at its C terminus. A sequence alignment revealed that the TRAF-C domain of LvTRAF3 was homologous to those from other species. Phylogenetic tree analysis showed that LvTRAF3 was closer to invertebrate TRAFs across evolution, suggesting that LvTRAF3

belonged to the TRAF family. Compared with mammalian TRAF2–6 and *Drosophila* TRAF6, LvTRAF3 lacks RING and zinc-finger domains, which are vital for triggering downstream kinase activity in some signaling pathways, such as the NF-κB pathway (9). Additionally, LvTRAF3 lacks coiled-coil domains, which are conserved between dTRAF3 and mammalian TRAF3 (31). The deficiency of some classical domains makes LvTRAF3 structurally different from other members, which may lead to the diversity of LvTRAF3 functions.

Studying subcellular localization can help us better understand the function of a protein. TRAF family proteins exist in the cytoplasm, which corresponds to their roles as adaptor proteins in the cytoplasm. Human TRAF4 is special in the TRAF family because it contains nuclear localization signals (NLS) and is distributed in both cytoplasm and nucleus (31). Of note, human TRAF6 lacks a NLS, and under genotoxic stress, translocation of TRAF6 from the cytosol to the nucleus facilitates the ubiquitination of p53, thus reducing apoptosis and tumorigenesis (32). Interestingly, LvTRAF3 was found to be mainly distributed in the cytoplasm with some in the nucleus, although there was no obvious NLS in the structure of this protein. We speculated that LvTRAF3 may be able to interact with some proteins that can enter the nucleus and translocated with them into the nucleus together. To our knowledge, this is the first report of the nuclear localization of an invertebrate TRAF3, and this interesting phenomenon is worthy of further exploration.

Tumor necrosis factor receptor-associated factors function as the adaptor proteins in multiple signaling pathways, and they are involved in a diversity of biological processes. It has been reported that TRAF family members from different species play crucial immunoregulatory roles in innate immune response. Faced with poly (I:C) stimuli and Sendai virus infection, *Anas platyrhynchos* TRAF6 (ApTRAF6) mediates NF-κB activation and interferon-β expression (33). In invertebrates, *Crassostrea gigas* TRAF2 (CgTRAF2) can be induced by *Vibrio alginolyticus* or Ostreid herpesvirus 1 (OsHV-1) (34), while *L. vannamei* TRAF6 (LvTRAF6) induces several kinds of AMPs during *Vibrio parahaemolyticus* or WSSV (35). In this study, we found that the expression of LvTRAF3 in the hemocyte and intestine were induced by the treatments of WSSV and poly (I:C), the conservative pathogen-associated molecular pattern (PAMP) mimics of RNA virus, which indicated that LvTRAF3 could be involved in the innate immune response for both DNA virus and RNA virus infection. Furthermore, by RNAi, LvTRAF3 was found to be crucial for shrimp to oppose WSSV infection.

Emerging studies have shown that TRAFs can signal through various pathways to stimulate the production of related effectors for defense against pathogenic invasion. For example, *Epinephelus punctatus* TRAF6 (EpTRAF6) was thought to activate an immune response via NF-κB activation, and *Danio rerio* TRAF6 (DrTRAF6) plays a protective role against pathogen invasion by inducing AMPs (36, 37). At present, the NF-κB and IRF-mediated pathways are the two well-identified ones for shrimp in response to microbial infection (12). In *L. vannamei*, NF-κB contains LvDorsal and LvRelish, which can regulate the expression of several kinds of AMPs, such as ALFs, PENs, CTLs, and LYZs, to resist diverse microbes, including WSSV (13). However, the shrimp IRF-mediated pathway, namely, the IRF-Vago-JAK/STAT axis, has been found to function similar to the invertebrate IFN system, and played vital roles in the defense against viral (WSSV) infection (20). How, unfortunately, the invertebrate TRAFs, including LvTRAF3, mediated signaling pathways are largely unknown. In our study, we found that knockdown of LvTRAF3 had no effect on the expression of NF-κB-mediated AMPs, which indicated that LvTRAF3 was not able to signal through the NF-κB pathway. This result was consistent with LvTRAF3 protein structure, which lacks a conserved RING domain or a Zinc finger domain. In previous reports, the RING domain and Zinc finger domain were found to be required for the activation of the NF-κB pathway (9). Instead, we discovered that LvTRAF3 could activate LvIRF translocation, and trigger the shrimp IRF-Vago pathway in response to WSSV infection. Interestingly, in insects, the recognition of viral dsRNA by *Drosophila* Dicer2 can induce Vago activation, and *Culex* TRAF-Rel2 signaling pathway is involved in the activation of Vago (38). Nevertheless, the definite molecular mechanism by which LvTRAF3 modulated shrimp IRF-Vago pathways remains unknown and requires for further investigation.

Collectively, we identified the TRAF3 homolog from *L. vannamei* and explored its function during WSSV infection. Our results demonstrated that LvTRAF3 responded to WSSV infection and altered resistance to viral infection. In addition, we found that LvTRAF3 defended against WSSV infection via mediating the activation of the IRF-Vago pathway but not the NF-κ B pathway.

DATA AVAILABILITY STATEMENT

The datasets presented in this study can be found in online repositories. The names of the repository/repositories and accession number(s) can be found in the article/**Supplementary Material**.

AUTHOR CONTRIBUTIONS

CL conceived and designed the experiments. HL, QF, SW, RC, XJ, and PZ performed the experiments and analyzed the data. HL wrote the draft manuscript. JH, HL, and CL acquired the funding. CL was responsible for forming the hypothesis, project development, data coordination, and writing, finalizing, and submitting the manuscript. All authors discussed the results and approved the final version.

FUNDING

This research was supported by Key-Area Research and Development Program of Guangdong Province (2018B020204001); National Key Research and Development

Program of China (2018YFD0900600 and 2018YFD0900500), National Natural Science Foundation of China (31802326 and 31930113); Guangdong Natural Science Funds for Distinguished Young Scholars (2016A030306041), and Tip-top Scientific and Technical Innovative Youth Talents of Guangdong Special Support Program (2016TQ03N504). The funders had no role in study design, data collection and analysis, decision to publish, or preparation of the manuscript.

SUPPLEMENTARY MATERIAL

The Supplementary Material for this article can be found online at: https://www.frontiersin.org/articles/10.3389/fimmu.2020.02110/full#supplementary-material

TABLE S1 | 5′ flanking regions of reporter gene plasmids, including WSSV genes, *D. melanogaster* and *L. vannamei* antimicrobial peptides.

REFERENCES

1. Dhillon B, Aleithan F, Abdul-Sater Z, Abdul-Sater AA. The evolving role of TRAFs in mediating inflammatory responses. *Front Immunol.* (2019) 10:104. doi: 10.3389/fimmu.2019.00104
2. Suzuki N, Saito T. IRAK-4–a shared NF-κB activator in innate and acquired immunity. *Trends Immunol.* (2006) 27:566–72. doi: 10.1016/j.it.2006.10.003
3. Gottipati S, Rao NL, Fung-Leung W-P. IRAK1: a critical signaling mediator of innate immunity. *Cell Signal.* (2008) 20:269–76. doi: 10.1016/j.cellsig.2007.08.009
4. Muroi M, Tanamoto KI. TRAF6 distinctively mediates MyD88−and IRAK−1−induced activation of NF-κB. *J Leuk Biol.* (2008) 83:702–7. doi: 10.1189/jlb.0907629
5. Häcker H, Tseng P-H, Karin M. Expanding TRAF function: TRAF3 as a tri-faced immune regulator. *Nat Rev Immunol.* (2011) 11:457–68. doi: 10.1038/nri2998
6. Sasai M, Tatematsu M, Oshiumi H, Funami K, Matsumoto M, Hatakeyama S, et al. Direct binding of TRAF2 and TRAF6 to TICAM-1/TRIF adaptor participates in activation of the Toll-like receptor 3/4 pathway. *Mol Immunol.* (2010) 47:1283–91. doi: 10.1016/j.molimm.2009.12.002
7. Liu S, Chen J, Cai X, Wu J, Chen X, Wu Y-T, et al. MAVS recruits multiple ubiquitin E3 ligases to activate antiviral signaling cascades. *Elife.* (2013) 2:e00785. doi: 10.7554/eLife.00785
8. Chen X, Yang X, Zheng Y, Yang Y, Xing Y, Chen Z. SARS coronavirus papain-like protease inhibits the type I interferon signaling pathway through interaction with the STING-TRAF3-TBK1 complex. *Protein Cell.* (2014) 5:369–81. doi: 10.1007/s13238-014-0026-3
9. Grech A, Quinn R, Srinivasan D, Badoux X, Brink R. Complete structural characterisation of the mammalian and Drosophila TRAF genes: implications for TRAF evolution and the role of RING finger splice variants. *Mol Immunol.* (2000) 37:721–34. doi: 10.1016/S0161-5890(00)00098-5
10. Preiss A, Johannes B, Nagel AC, Maier D, Wajant H. Dynamic expression of *Drosophila* TRAF1 during embryogenesis and larval development. *Mechan Dev.* (2001) 100:109–13. doi: 10.1016/S0925-4773(00)00506-2
11. Lee K-A, Cho K-C, Kim B, Jang I-H, Nam K, Kwon YE, et al. Inflammation-modulated metabolic reprogramming is required for DUOX-dependent gut immunity in *Drosophila*. *Cell Host Microbe.* (2018) 23:338–52. doi: 10.1016/j.chom.2018.01.011
12. Li C, Weng S, He J. WSSV–host interaction: host response and immune evasion. *Fish Shellfish Immunol.* (2019) 84:558–71. doi: 10.1016/j.fsi.2018.10.043
13. Li C, Wang S, He J. The two NF-κB pathways regulating bacterial and WSSV infection of shrimp. *Front Immunol.* (2019) 10:1785. doi: 10.3389/fimmu.2019.01785
14. Leu JH, Yang F, Zhang X, Xu X, Kou GH, Lo CF. Whispovirus, lesser known large dsDNA viruses. *Curr Topics Microbiol Immunol.* (2009) 328:197–227. doi: 10.1007/978-3-540-68618-7_6
15. Li C, Chen Y, Weng S, Li S, Zuo H, Yu X, et al. Presence of Tube isoforms in *Litopenaeus vannamei* suggests various regulatory patterns of signal transduction in invertebrate NF-κB pathway. *Dev Comparat Immunol.* (2014) 42:174–85. doi: 10.1016/j.dci.2013.08.012
16. Letunic I, Doerks T, Bork P. SMART: recent updates, new developments and status in 2015. *Nucleic Acids Res.* (2014) 43:D257–60. doi: 10.1093/nar/gku949
17. Larkin MA, Blackshields G, Brown NP, Chenna R, McGettigan PA, McWilliam H, et al. Clustal X version 2.0. *Bioinformatics.* (2007) 23:2947–8. doi: 10.1093/bioinformatics/btm404
18. Nicholas KB. *Genedoc: A Tool for Editing and Annoting Multiple Sequence Alignments*. (1997). Available online at: http://wwwpscedu/biomed/genedoc (accessed April 9, 2019).
19. Tamura K, Peterson D, Peterson N, Stecher G, Nei M, Kumar S. MEGA5: molecular evolutionary genetics analysis using maximum likelihood, evolutionary distance, and maximum parsimony methods. *Mol Biol Evol.* (2011) 28:2731–9. doi: 10.1093/molbev/msr121
20. Li C, Li H, Chen Y, Chen Y, Wang S, Weng SP, et al. Activation of Vago by interferon regulatory factor (IRF) suggests an interferon system-like antiviral mechanism in shrimp. *Sci Rep.* (2015) 5:15078. doi: 10.1038/srep15078
21. Li C, Weng S, Chen Y, Yu X, Lü L, Zhang H, et al. Analysis of *Litopenaeus vannamei* transcriptome using the next-generation DNA sequencing technique. *PLoS One.* (2012) 7:e47442. doi: 10.1371/journal.pone.0047442
22. Li H, Wang S, Chen Y, Lu K, Yin B, Li S, et al. Identification of two p53 isoforms from *Litopenaeus vannamei* and their interaction with NF-κB to induce distinct immune response. *Scientific reports* (2017) 7:45821. doi: 10.1038/srep45821
23. Tassanakajon A, Piti A, Kunlaya S, Premruethai S. Cationic antimicrobial peptides in penaeid shrimp. *Mar Biotechnol.* (2010) 13:639–57. doi: 10.1007/s10126-011-9381-8
24. Wang PH, Weng SP, He JG. Nucleic acid-induced antiviral immunity in invertebrates: an evolutionary perspective. *Dev Comparat Immunol.* (2015) 48:291–6. doi: 10.1016/j.dci.2014.03.013
25. Huang X-D, Zhao L, Zhang H-Q, Xu X-P, Jia X-T, Chen Y-H, et al. Shrimp NF-κB binds to the immediate-early gene ie1 promoter of white spot syndrome virus and upregulates its activity. *Virology.* (2010) 406:176–80. doi: 10.1016/j.virol.2010.06.046
26. Tanji T, Ip YT. Regulators of the toll and imd pathways in the *Drosophila* innate immune response. *Trends Immunol.* (2005) 26:193–8. doi: 10.1016/j.it.2005.02.006
27. Li H, Yin B, Wang S, Fu Q, Xiao B, Lu K, et al. RNAi screening identifies a new Toll from shrimp *Litopenaeus vannamei* that restricts WSSV infection through activating Dorsal to induce antimicrobial peptides. *PLoS Pathogens.* (2018) 14:e1007109. doi: 10.1371/journal.ppat.1007109
28. Li H, Chen Y, Li M, Wang S, Zuo H, Xu X, et al. lectin (LvCTL4) from *Litopenaeus vannamei* is a downstream molecule of the NF-κB signaling pathway and participates in antibacterial immune response. *Fish Shellfish Immunol.* (2015) 43:257–63. doi: 10.1016/j.fsi.2014.12.024
29. Li M, Li C, Ma C, Li H, Zuo H, Weng S, et al. Identification of a C-type lectin with antiviral and antibacterial activity from pacific white shrimp Litopenaeus vannamei. *Dev Comparat Immunol.* (2014) 46:231–40. doi: 10.1016/j.dci.2014.04.014
30. Xie P. TRAF molecules in cell signaling and in human diseases. *J Mol Signal.* (2013) 8:1–31. doi: 10.1186/1750-2187-8-7
31. Wajant H, Scheurich P. *Analogies Between Drosophila and Mammalian TRAF Pathways, Invertebrate Cytokines and the Phylogeny of Immunity*. Berlin: Springer (2003). p. 47–72. doi: 10.1007/978-3-642-18670-7_3
32. Zhang X, Li C-F, Zhang L, Wu C-Y, Han L, Jin G, et al. TRAF6 restricts p53 mitochondrial translocation, apoptosis, and tumor suppression. *Mol Cell.* (2016) 64:803–14. doi: 10.1016/j.molcel.2016.10.002
33. Zhai Y, Luo F, Chen Y, Zhou S, Li Z, Liu M, et al. Molecular characterization and functional analysis of duck TRAF6. *Dev Comparat Immunol.* (2015) 49:1–6. doi: 10.1016/j.dci.2014.11.006

34. Baoyu H, Linlin Z, Yishuai D, Li XT, Guofan Z. Molecular characterization and functional analysis of tumor necrosis factor receptor-associated factor 2 in the Pacific oyster. *Fish Shellfish Immunol.* (2016) 48:12–9. doi: 10.1016/j.fsi.2015.11.027
35. Wang PH, Wan Z-H, Fau DH, Gu X-X, Gu ZH, Fau D, et al. Litopenaeus vannamei tumor necrosis factor receptor-associated factor 6 (TRAF6) responds to Vibrio alginolyticus and white spot syndrome virus (WSSV) infection and activates antimicrobial peptide genes. *Dev Comparat Immunol.* (2011) 35:105–14. doi: 10.1016/j.dci.2010.08.013
36. Li Y-W, Li X, Xiao X-X, Zhao F, Luo X-C, Dan X-M, et al. Molecular characterization and functional analysis of TRAF6 in orange-spotted grouper (Epinephelus coioides). *Dev Comparat Immunol.* (2014) 44:217–25. doi: 10.1016/j.dci.2013.12.011
37. Stockhammer OW, Rauwerda H, Wittink FR, Breit TM, Meijer AH, Spaink HP. Transcriptome analysis of Traf6 function in the innate immune response of zebrafish embryos. *Mol Immunol.* (2010) 48:179–90. doi: 10.1016/j.molimm.2010.08.011
38. Paradkar PN, Duchemin J-B, Voysey R, Walker PJ. Dicer-2-dependent activation of Culex Vago occurs via the TRAF-Rel2 signaling pathway. *PLoS Neglect Trop Dis.* (2014) 8:e2823. doi: 10.1371/journal.pntd.0002823

Conflict of Interest: RC and XJ where employed by Guangdong Hisenor Group Co., Ltd.

The remaining authors declare that the research was conducted in the absence of any commercial or financial relationships that could be construed as a potential conflict of interest.

frontiers in Immunology

ORIGINAL RESEARCH
published: 12 November 2020
doi: 10.3389/fimmu.2020.599625

Host Defense Effectors Expressed by Hemocytes Shape the Bacterial Microbiota From the Scallop Hemolymph

*Roxana González[1,2], Ana Teresa Gonçalves[3], Rodrigo Rojas[4], Katherina Brokordt[5], Rafael Diego Rosa[6] and Paulina Schmitt[2]**

[1] Doctorado en Acuicultura. Programa Cooperativo Universidad de Chile, Universidad Católica del Norte, Pontificia Universidad Católica de Valparaíso, Valparaiso, Chile, [2] Laboratorio de Genética e Inmunología Molecular, Facultad de Ciencias, Instituto de Biología, Pontificia Universidad Católica de Valparaíso, Valparaíso, Chile, [3] GreenCoLab, Centro de Ciências do Mar, Universidade do Algarve, Faro, Portugal, [4] Laboratorio de Patobiología Acuática, Departamento de Acuicultura, Universidad Católica del Norte, Coquimbo, Chile, [5] Laboratorio de Fisiología Marina (FIGEMA), Departamento de Acuicultura, Facultad de Ciencias del Mar, Universidad Católica del Norte, Antofagasta, Chile, [6] Laboratory of Immunology Applied to Aquaculture, Department of Cell Biology, Embryology and Genetics, Federal University of Santa Catarina, Florianópolis, Brazil

OPEN ACCESS

Edited by:
Kunlaya Somboonwiwat, Chulalongkorn University, Thailand

Reviewed by:
Yong-hua Hu, Chinese Academy of Tropical Agricultural Sciences, China
Jing Xing, Ocean University of China, China
Timothy James Green, Vancouver Island University, Canada

***Correspondence:**
Paulina Schmitt
paulina.schmitt@pucv.cl

Specialty section:
This article was submitted to Comparative Immunology, a section of the journal Frontiers in Immunology

Received: *27 August 2020*
Accepted: *19 October 2020*
Published: *12 November 2020*

Citation:
González R, Gonçalves AT, Rojas R, Brokordt K, Rosa RD and Schmitt P (2020) Host Defense Effectors Expressed by Hemocytes Shape the Bacterial Microbiota From the Scallop Hemolymph. Front. Immunol. 11:599625. doi: 10.3389/fimmu.2020.599625

The interaction between host immune response and the associated microbiota has recently become a fundamental aspect of vertebrate and invertebrate animal health. This interaction allows the specific association of microbial communities, which participate in a variety of processes in the host including protection against pathogens. Marine aquatic invertebrates such as scallops are also colonized by diverse microbial communities. Scallops remain healthy most of the time, and in general, only a few species are fatally affected on adult stage by viral and bacterial pathogens. Still, high mortalities at larval stages are widely reported and they are associated with pathogenic *Vibrio*. Thus, to give new insights into the interaction between scallop immune response and its associated microbiota, we assessed the involvement of two host antimicrobial effectors in shaping the abundances of bacterial communities present in the scallop *Argopecten purpuratus* hemolymph. To do this, we first characterized the microbiota composition in the hemolymph from non-stimulated scallops, finding both common and distinct bacterial communities dominated by the Proteobacteria, Spirochaetes and Bacteroidetes phyla. Next, we identified dynamic shifts of certain bacterial communities in the scallop hemolymph along immune response progression, where host antimicrobial effectors were expressed at basal level and early induced after a bacterial challenge. Finally, the transcript silencing of the antimicrobial peptide big defensin *ApBD1* and the bactericidal/permeability-increasing protein *ApLBP/BPI1* by RNA interference led to an imbalance of target bacterial groups from scallop hemolymph. Specifically, a significant increase in the class Gammaproteobacteria and the proliferation of *Vibrio* spp. was observed in scallops silenced for each antimicrobial. Overall, our results strongly suggest that scallop antimicrobial peptides and proteins are implicated in the maintenance of microbial homeostasis and are key molecules in orchestrating host-microbiota

interactions. This new evidence depicts the delicate balance that exists between the immune response of *A. purpuratus* and the hemolymph microbiota.

Keywords: host-microbiota interactions, invertebrate immunity, mollusk, *Vibrio*, host defense effectors, big defensin, bactericidal/permeability-increasing protein

INTRODUCTION

Scallops are a cosmopolitan family of bivalve mollusks. In recent years, interest in scallop immunity has increased due to its economic importance for aquaculture, and because the group occupies a key position within the phylogeny and evolution of the animal kingdom (1). Bivalves have a semi-open circulatory system where the hemolymph, the analogue of vertebrate blood, and the organs are constantly exposed to high and diverse bacterial loads (~10^6 cfu/ml) (2). Still, scallops remain healthy most of the time, and in general, only a few species are fatally affected on adult stage by viral and bacterial pathogens (3–5).

Like the rest of invertebrates, scallops possess only innate immune mechanisms of defense, where cellular and humoral components act in a coordinated and synergistic manner (6). Hemocytes, the immunocompetent cells, circulate within hemolymph and infiltrate tissues, constantly producing a great diversity of antimicrobial effectors (7). When scallops are exposed to microorganisms, many of these effectors are released by the hemocytes to the hemolymph or into infiltrated tissues, where they classically inactivate or destroy foreign invaders (8, 9). Antimicrobial peptides from the big defensin family such as *ApBD1* (10–12), hydrolytic enzymes (13, 14), lipopolysaccharide binding/bactericidal permeability increasing proteins (LBP/BPIs) (15), and an antimicrobial peptide derived from histone (HDAP) (16) have been described to be expressed by scallop hemocytes. Furthermore, the recent genome sequencing and *de novo* assemblies of transcriptomes from several scallop species suggests the existence of many other gene candidates for antimicrobial effectors (17–20).

In recent years, the interaction between the immune response and the microbiota has become a fundamental aspect of animal health (21, 22). This interaction allows the conformation of the microbial communities, which participate in a variety of processes in the host species, such as stimulating the immune system (23, 24), nutrition (25), protection against pathogens (26–28), among others. In higher vertebrates as well as in model and non-model invertebrates, a delicate balance exists between the basal expression of immune effectors and the microbial host associations (22, 29, 30). If this balance is disrupted, pathogenic microorganisms can proliferate causing damage and host mortality (22, 31). In the oyster *Crassostrea gigas*, microbiota destabilization caused by viral infection and subsequently host immunosuppression ended in bacteremia and host death (32). In addition, differential basal expression of immune genes has been related with oyster resistance to this polymicrobial disease (33). Recently, changes in the structure and diversity of bacterial microbiota associated with scallops has been identified during the immune response of *Argopecten purpuratus* in field (34). Overall, these results suggest that functional interaction between host immune effectors and associated microbiota could also exist in pectinids.

To give new insights into the scallop-microbiota interactions, we assessed the involvement of two host antimicrobial effectors, *ApBD1* and *ApLBP/BPI1* in shaping the hemolymph scallop microbiota. We first characterized the structure and relative abundances of bacterial communities present in hemolymph from non-stimulated scallops. Then, we identified significant shifts and restorations of specific bacterial groups along immune response progression. In here, antimicrobial effectors were expressed at basal levels and early induced after bacterial challenges. Finally, we investigated the effect of silencing the antimicrobials *ApBD1* and *ApLBP/BPI1* expressions in the bacterial abundances from non-stimulated scallops. Results obtained here suggest that antimicrobial peptides and proteins effectors are implicated in the maintenance of microbial homeostasis and are key molecules in orchestrating host-microbiota interactions in scallops.

MATERIAL AND METHODS

Scallop Maintenance, Experimental Challenges, and Sample Collection

US National Research Council guidelines for the care and use of laboratory animals were strictly followed during this research (35). Adult *Argopecten purpuratus* (n = 123; 60 mm length) were obtained from the aquaculture concession of the Universidad Católica del Norte (UCN) located at Tongoy Bay, Coquimbo, Chile. Scallops were transferred to the Central Laboratory of Marine Cultures on the premises of UCN, acclimatized and kept in 200-L tanks for two weeks prior to each experiment. Animals were constantly maintained with aeration and replacement of filtered water at 16°C. Animals were fed daily with a mixture of microalgae (50% *Isochrysis galbana* and 50% *Nannochloris* spp.; 6x10^6 cells/ml/day). *Vibrio splendidus* bacterial strain VPAP18 was used in challenge experiments (36). The bacteria were cultivated in Trypticase Soy Broth (Difco) supplemented with 2% NaCl at 18°C for 24 h. Subsequently, the bacterial suspension was inactivated for 2 h at 90°C and centrifuged at 12,000 × g for 10 min. The obtained pellet was washed twice with 0.22 μm microfiltered sterile seawater, and bacterial solution concentration was adjusted to 1 ×10^8 cfu/ml. *V. splendidus* VPAP18 was heat inactivated and washed to eliminate microbe-microbe interaction between *V. splendidus* VPAP18 and scallop microbiota.

Two independent scallop immune challenges were performed, both including the following experimental conditions: (i) *Vibrio*-injected scallops (5×10^6 cells in 50 μl), (ii) seawater-injected (SW) scallops (50 μl) and (iii) non-stimulated scallops. Samples were

obtained after 12, 24, 48, 72 and 168 h. For the RNAi experiment [RNAi, ribonucleic acid (RNA) interference], experimental conditions considered scallops injected with 20 µg in 100 µl of: (i) *Ap*BD1-dsRNA (dsRNA, double-stranded ribonucleic acid), (ii) *Ap*LBP/BPI1-dsRNA and (iii) GFP-dsRNA (green fluorescent protein). Samples were obtained after 48 h. Scallop sample size for each experiment is shown in **Figure S1**. All animals were injected with sterile syringes (25G × ⅝) into the adductor muscle. To obtain hemocytes, 2 ml of hemolymph per individual were extracted and centrifuged at 800 × g for 10 min at 4°C to separate cells from plasma. Then, cells were lysed in Trizol® reagent (ThermoFisher) at 4°C and stored at -80°C until total RNA purification. To obtain hemolymph bacteria, 2 ml of hemolymph were deep-frozen in liquid nitrogen and stored at -80°C for subsequent extraction of genomic DNA (gDNA).

RNA Extraction and Gene Expression Analysis by RT-qPCR

Total hemocyte RNA was extracted using Trizol® reagent (ThermoFisher) according to manufacturer's instructions. Genomic DNA was removed with DNase I (Ambion). The integrity of RNA was verified on agarose gels, and purity and concentration were determined on an Epoch™ microplate spectrophotometer (BioTek). The cDNA was synthesized by reverse transcription from 1 µg of total RNA, using the RevertAid First Strand cDNA Synthesis Kit (ThermoFisher), according to manufacturer's instructions. RT-qPCR (quantitative polymerase chain reaction prior to reverse transcription) assays were performed in triplicate on a Stratagene Mx3005p Real Time PCR System thermocycler (Agilent Technologies), using the specific gene primers (**Table S1**). Amplification was performed in a final reaction volume of 20 µl composed of: 10 µl of Takyon ™ Rox SYBR® MasterMix dTTP Blue (Eurogentec), 0.6 µl of each primer (10 mmol L^{-1}) and 2 µl of cDNA (1:5). The amplification program consisted of an initial denaturation at 3 min at 95°C, followed by 40 cycles of 15 s at 95°C and 30 s at 60°C. Through serial dilutions of cDNA, the efficiencies of RT-qPCR were verified in the range between 95%–110% ($E = 10^{(-1/slope)}$). The relative expression of the immune response genes was calculated by the Pfaffl method (37). Differences in gene expression with the control groups (SW) were verified with two-way ANOVA test and Tukey´s posterior test ($P < 0.05$).

Genomic DNA Extraction and Deep Amplicon Sequencing of the 16S rDNA Gene

Genomic DNA (gDNA) present in *A. purpuratus* hemolymph was extracted with the Wizard Genomic DNA purification kit (Promega) according to manufacturer's instructions. The integrity, concentration and purity of the gDNA was verified by 1% agarose gel, Qubit 3.0 (Life Technologies) and Epoch™ microplate spectrophotometer (BioTek), respectively. The 16S rDNA gene of bacterial communities was amplified and sequenced, targeting the variable regions V3-V4 (341F: 5'-CCTACGGGNGGCWGCAG-3'; 805R: 5'-159 GACTACHVGGGTATCTAATCC-3') and using ~12.5 ng of gDNA from 5 biological replicates from each experimental condition: *Vibrio*-injected and SW-injected scallops at 48 h and 168 h, and non-stimulated scallops at 0 h. Paired-end multiplex sequencing (2×300 bp read length) was performed from individual samples by Macrogen Inc. on a MiSeq system (Illumina®) using the MiSeq Reagent Kit v3 according to manufacturer's instruction. Raw sequence data are available in the SRA database BioProject PRJNA639911.

16S rDNA Deep Amplicon Sequencing Analysis

Raw reads were processed using QIIME2 version 2019.1 (http://qiime2.org) and developed based on standards described by (38, 39) for microbiota community evaluation. Demultiplexed paired-end reads were imported as artifacts and denoised using DADA2 (40). In this step of the analysis, quality control as well as phiX reads (commonly present in marker gene Illumina sequence data) and chimera sequence filtering were applied to ensure the retainment of only high-quality reads. Amplicon sequence variants (ASVs), a higher resolution analog to operative taxonomic units (OTUs) (41), were obtained and further processed for taxonomic assignment and diversity analysis. Taxonomy was assigned based on the Green Genes database (gg-13_8 99%) (42, 43). Features assigned to the class Chloroplast (Phylum Cyanobacteria) and Family Mitochondria (Phylum Proteobacteria) were filtered out due to their contaminant character. Samples were rarefied to the maximum depth of the sample with less sequencing depth, and rarefaction curves were plotted. Alpha diversity was evaluated using the Shannon and Simpson Diversity Index, the richness index was evaluated by Chao1 y Faith PD (Faith's Phylogenetic Diversity) and beta diversity was evaluated by assessing weighted and unweighted UniFrac distances (44, 45). Differences in alpha diversity between groups were analyzed using the Kruskal-Wallis (pairwise) test in QIIME2. A principal coordinate analysis was performed to visualize phylogenetic beta diversity and differences between experimental groups based on the distances were assessed by PERMANOVA considering 999 permutations in QIIME2. Significant differences between relative abundances among groups were evaluated using two-way ANOVA and Tukey-Kramer tests on STAMP (Statistical Analysis of Metagenomic Profiles) (46), significant differences were only considered when $P \leq 0.05$ and a q-value < 0.3. Bacterial groups showing abundances greater than 1% were considered for analysis.

Absolute Quantification of 16S rDNA by qPCR and Determination of Relative Abundances of Bacterial Groups

The 16S rDNA gene of four bacterial strains belonging to the Gammaproteobacteria, Epsilonproteobacteria, Betaproteobacteria, and Firmicutes taxa (**Table S2**), plus the 16S rDNA gene from *Vibrio splendidus* VPAP18 were amplified by PCR using the 16S rDNA universal primers 16SEUBAC (**Table S1**). The 16S rDNA fragments were cloned into the pCR2.1 vector included in the TOPO TA kit following manufacturer's instructions. Specific cloning of each 16S rDNA bacterial strain was verified by plasmid sequencing. Then, seven-serial dilutions of each plasmid, ranging from 10^{10} to 10^{3} plasmid copies/µl were prepared to construct standard curves and to obtain absolute quantifications of the 16S rDNA gene copy number of each bacterial group by qPCR. Plasmid copies were calculated by the following formula: Number of copies/µl = 6.022×10^{23} (molecules/mole) × DNA concentrations (g/µl)/Number of bases pairs × 660

Da, were 6.022×10^{23} (molecules/mole) is Avogadro´s number and 660 Da is the average weight for a single base pair.

Specific primers for the 16S rDNA of each bacterial group were previously designed and validated (**Table S1**). qPCR assays were performed in triplicate on a Stratagene Mx3005p Real Time PCR System thermocycler (Agilent Technologies), using a final reaction volume of 20 µl composed of: 10 µl of Takyon ™ Rox SYBR® MasterMix dTTP Blue (Eurogentec), 0.6 µl of each primer (10mmol * L-1) and 2 µl of plasmid DNA. The amplification program consisted of an initial denaturation at 10 min at 95°C, followed by 40 cycles of 30 s at 95°C and 1 min at 60°C and dissociation curve detection. Standard curves were obtained by plotting the threshold cycle (C_q) on the Y-axis and the natural log of concentration (copies/µl) on the X-axis. We considered the following criteria: PCR efficiency (95-110%) and correlation coefficient R^2 (0.99), which validates the linear relation between the threshold cycle and the natural log of concentration (copies/µl). Next, 50 ng of gDNA from scallop hemolymph was analyzed by qPCR using the same settings. The copy numbers of 16S rDNA gene of each bacterial group in the sample were obtained by relating the C_q value to the respective standard curve. Eubacteria universal primers were used to obtain the total copies of bacterial 16S rDNA in each sample and it was considered as the 100% to calculate the relative abundance of each bacterial group. Differences in the relative abundance of the bacterial groups between treatments were verified with ANOVA two-way and the Sidak´s posterior test (P <0.05).

dsRNA Synthesis for RNA Interference Assay of Antimicrobial Effectors

Sequence specific primers were designed to amplify fragments of *ApBD1* (401 bp) and *ApLBP/BPI1* (543 bp) from hemocyte cDNA as template and to add the T7 promoter sequence TAATACGACTCACTATAGGG by PCR (**Table S1**). A plasmid containing the sequence for the green fluorescent protein (GFP) gene (GenBank no. HM640279) which is not present in *A. purpuratus* was amplified with specific primers and included as a dsRNA control of specific gene silencing. The PCR products were verified on agarose gel and then purified using E.Z.N.A.® Gel Extraction Kit (Omega Biotek). PCR products were confirmed by sequencing. T7 RiboMAX® Express RNAi System was used to synthesize the dsRNA in accordance with manufacturer's instructions. The quantity and quality of the RNAi were determined using a Qubit 3.0 (Life Technologies) and agarose gel electrophoresis, respectively.

Determination of Cultivable *Vibrio* spp. in Scallop Hemolymph After Gene Silencing of Antimicrobial Effectors

Thiosulfate-citrate-bile salts-sucrose (TCBS) selective agar plates for *Vibrio* spp. (Difco) were prepared in sterile sea water (50%): distilled water 1: 1 following the manufacturer's instructions. Aliquots of 0.1 ml and their dilutions from scallop hemolymph from the RNA interference experiment were plated separately in the selective agar plates and incubated at 25°C. Three independent aliquots from each scallop hemolymph were plated (5 scallops per experimental condition). After 24 h of plate incubation, visible colonies were counted. Then, average colony forming units (c.f.u.) number with the corresponding standard deviation were calculated for each sample. Differences in the c.f.u. number of *Vibrio* spp. between treatments were verified with Welch's t-test (P <0.05).

RESULTS

Characterization of Common and Variable Bacterial Communities Present in Scallop Hemolymph

The gDNA extracted from bacteria present in the hemolymph of i) heat-inactivated *Vibrio*-injected scallops, ii) SW-injected scallops, and iii) non-stimulated control scallops was analyzed by 16S rDNA deep amplicon sequencing. As a result, a total of 2,546 million bases were sequenced complying 4,229,314 joined sequences, with an average length of 300 bp, and 92.7% presented a quality score above Q20 whereas 84.6% were above Q30. After filtering, denoising and chimera removal, 3,159,967 high quality reads were obtained, ranging per individual between 108,842 and 150,048 reads, representing all the phylotypes present in the *A. purpuratus* hemolymph bacterial microbiota (**Table S3**). After filtering the rare OTUs, 478 taxonomic groups were identified in the *A. purpuratus* hemolymph. Analysis of rarefaction curves indicated that the sequencing depth was sufficient to identify all unique OTUs among all experimental groups (**Figure S2**).

We first focused on the analysis of bacterial groups present in non-stimulated scallops to determine how variable was the scallop microbiota between control individuals. Common bacterial groups among five non-stimulated scallops were determined by Venn diagrams (**Figure 1**). From the 37 phyla identified, 35% (13 phyla) were common to the 5 individuals (**Figure 1A**). Within these 13 phyla, a 54% were predominant groups, displaying relative abundances around or higher than 1% of the total (**Figure 1B**). Those phyla were identified as Proteobacteria (71.04%), Spirochaetes (12.58%), Bacteroidetes (9.86%), Gracilibacteria (1.95%), and Firmicutes (0.92). Venn diagram analysis indicated that the number of phyla shared among the five individuals was higher than the specific phyla number found for each individual. Accordingly, two scallops lacked specific phyla, two scallops presented two specific phyla and one scallop (namely N3) displayed six particular phyla (**Figure 1A**).

From the 90 bacterial classes identified, 23% (21 classes) corresponded to common groups among all scallops (**Figure 1C**). Within these classes, 43% were predominant, displaying relative abundances higher than 1% of the total, such as: Gammaproteobacteria (18.16%), Brachyspirae (10.32%), Alphaproteobacteria (6.54%), Deltaproteobacteria (6.52%), Flavoproteobacteria (6.36%), Epsilonproteobacteria (4.28%), and Betaproteobacteria (1.16%) (**Figure 1D**). Venn diagram analysis also indicated that the number of classes shared among the five individuals was higher than the specific classes found for each individual. Therefore, four scallops presented between one to four distinct classes, and N3 scallop displayed a higher number of 16 particular classes (**Figure 1C**).

At the genus level, from the 329 bacterial genera identified in from the 5 non-stimulated scallops, 7.5% (25 genera) corresponded to

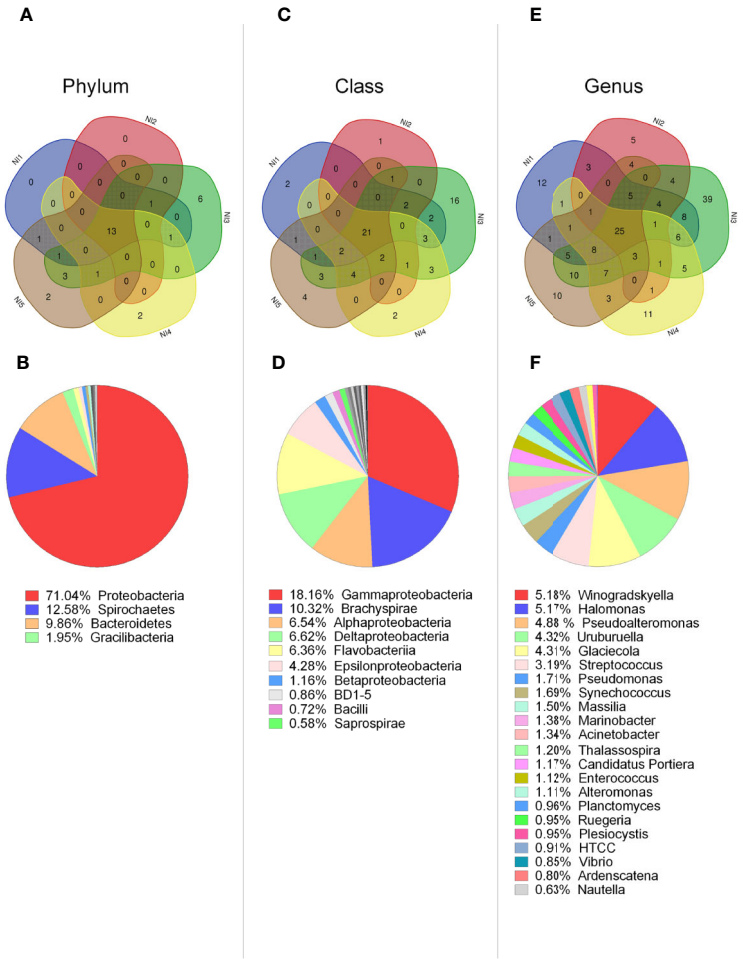

FIGURE 1 | Characterization of bacterial communities present in hemolymph from single scallops determined by 16S rDNA deep amplicon sequencing. Upper panel: Venn diagrams indicate the number of common and distinct bacterial groups at phylum **(A)**, class **(C)**, and genus **(E)** levels between five non-stimulated individuals. Lower panel: Relative abundances of common bacterial groups at phylum **(B)**, class **(D)**, and genus **(F)** levels. Bacterial groups with relative abundances higher or closer to 1% are shown for each taxonomic level.

common groups (**Figure 1E**). From these common genera, 88% had relative abundances higher than 1%. The most relative abundant were *Winogradskyella* (5.18%), *Halomonas* (5.17%), *Pseudoalteromonas* (4.87%), *Uruburuella* (4.32%), *Glaciecola* (4.31%), *Streptococcus* (3.19%), and *Pseudomonas* (1.71%) (**Figure 1F**). Venn diagram analysis indicated again that four scallops presented more common than particular genera, presenting between five to twelve specific genera. At this level, N3 scallop differed from the others in terms of variable groups, displaying 39 particular genera (**Figure 1E**). Overall, results suggested that control scallops share more common taxa compared to specific taxa, except for one individual that harbored an elevated number of particular groups (**Figures 1A, C, E**). In agreement, N3 individual displayed higher species richness compared to other control scallops, determined by Chao1 and Faith PD indices (**Figures S3C and D**). Similarly, the Unweighted UniFrac distance analysis confirmed that the bacterial communities from N3 individual differed from the rest of the non-stimulated scallops (**Figure S4A**).

Shifts and Restoration of Specific Bacterial Group Abundances Are Detected in Hemolymph Along Scallop Immune Response Progression

A previous study identified bacterial shifts in structure and composition from whole scallop microbiota at 48 h after immune challenge (34). To determine whether imbalances in bacterial communities are sustained or restored over time after the immune response, we analyzed the bacterial composition present in the scallop hemolymph at 48 h and 168 h after challenge them. Then, the bacterial relative abundances at class and genus taxonomic levels obtained by deep amplicon sequencing analysis were compared between *Vibrio*- and SW-injected scallops (**Figure 2**). We found that the most noticeable changes on bacterial abundances between experimental conditions were observed at 48 h post challenge, at both class (**Figure 2A**) and genus (**Figure 2B**) levels. As expected, the relative abundance of Gammaproteobacteria was significantly higher in *Vibrio*-injected scallops (46%) compared to seawater scallops

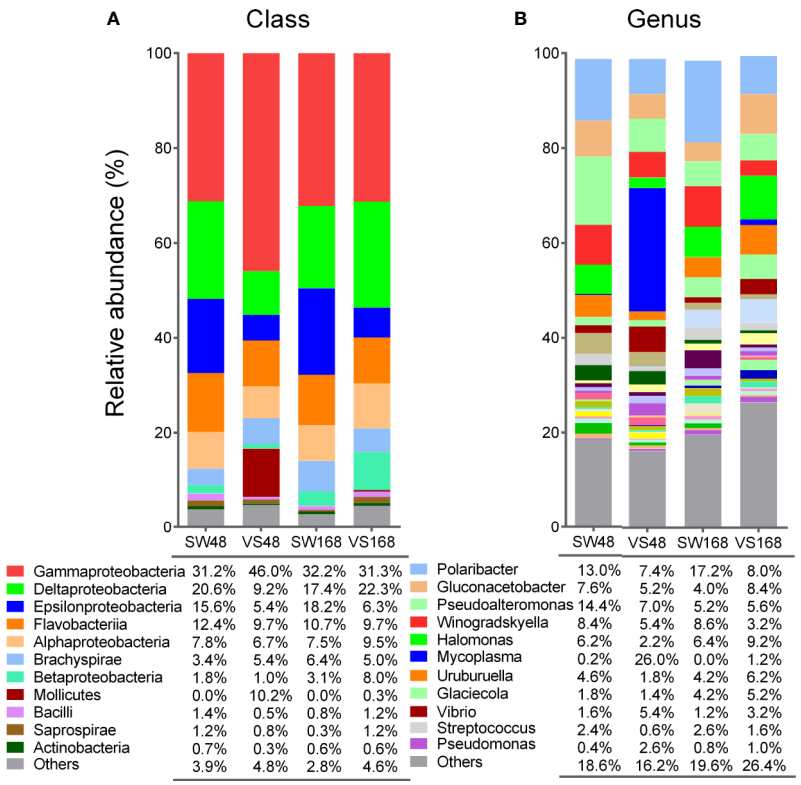

FIGURE 2 | Relative abundances of bacterial groups present in scallop hemolymph after immune stimulation determined by 16S rDNA deep amplicon sequencing. Stack bar graphs indicate the average relative abundance of major bacterial groups found in *Vibrio*-injected scallops (VS) and seawater-injected scallops (SW) after 48 h and 168 h, at class **(A)** and genus **(B)** taxonomic levels. Bacterial groups with relative abundances higher or closer to 1% are shown for each taxonomic level.

(31.2%) ($P<0.05$). Concomitantly, the classes Delta- and Epsilonproteobacteria displayed a lower abundance in *Vibrio*-injected (9.2% and 5.4%, respectively) when compared to SW-injected scallops (20.6% and 15.6%, respectively) ($P<0.05$). The class Mollicutes, which were found at 0.023% in SW-injected scallops, displayed an 10.2% of relative abundance in *Vibrio*-injected scallops at 48 h after immune challenge. At 168 h after immune challenge, relative abundances of Gamma-, Delta-, and Epsilonproteobacteria in *Vibrio*-injected scallops were statistically comparable to those from SW-injected scallops, suggesting a restoration of those communities after that time (**Figure 2A**). Betaproteobacteria showed no significant variation at 48 h among injected groups, though a slightly increase of this class was observed in the *Vibrio*-injected group (8%) compared to the SW-injected group (3.1%) at 168 h.

When we compared the relative abundances of bacteria at genera level, we found that *Mycoplasma* (from Mollicutes class) displayed the principal shift, although slightly non-significant ($P = 0.065$). Specifically, *Mycoplasma* increased from 0.2% in SW-injected scallops up to 26% in *Vibrio*-injected scallops at 48 h. As expected, *Vibrio* displayed significant increase in its relative abundance *in Vibrio*-injected scallops (5.4%) when compared to SW-injected scallops at 48 h (1.6%) ($P<0.05$). Remarkably, *Vibrio* genus abundance was only a fraction (11%) of total increase of Gammaproteobacteria abundance in *Vibrio*-injected scallops, revealing that the higher abundance found in this group was not only due to the immunostimulation approach. Other bacterial genera displayed shifts on their relative abundances among groups at 48 h, but still non-significant. For instance, *Streptococcus* and *Halomonas* were found in lower abundance in *Vibrio*-injected scallops (0.6% and 2.2%, respectively) when compared to SW-injected scallops at 48 h (2.4% and 6.2%, respectively). *Pseudomonas* displayed the opposite pattern at the same time point, showing a relative abundance of 2.6% in *Vibrio*-injected and 0.4% SW-injected scallops (**Figure 2B**). After 168 h of challenge, bacterial abundances at the genus level in *Vibrio*-injected scallops were also statistically similar to those from SW-injected scallops, although a higher variability in bacterial abundances were observed at this taxonomic level (**Figure 2B**). For instance, *Mycoplasma* relative abundance decreased in *Vibrio*-injected scallops after 168 h (1.2%) when compared to 48 h (26%) but it was still higher when compared to the SW-injected group which did not show any presence of this genera. Analogous variation in their relative abundances were found for *Streptococcus, Halomonas, Pseudomonas*, and *Vibrio* genera at 168 h (**Figure 2B**). Overall, our data revealed the existence of dynamic shifts of bacterial communities in the scallop hemolymph along immune response progression. Certain bacterial group shift abundances were sustained over time, while a greater proportion of bacterial groups were restored after 168 h.

Alpha diversity was evaluated using the Simpson and Shannon Diversity indices, while the species richness was evaluated by Chao1 y Faith PD indices (**Figure S3**). The Simpson index determined that *Vibrio*-injected scallops at 48 h presented more diverse bacterial communities than the other experimental conditions, specifically compared to non-stimulated scallops and SW-injected scallops at 168 h ($P<0.05$) (**Figure S3**). Shannon index presented a similar trend than the Simpson index but differences were non-significant. Similarly, the Chao1 and Faith PD richness indices suggested that *Vibrio*-injected scallops at 48 h and 168 h, respectively, tended to display a higher species richness compared to other injected scallops, although the differences were non-significant ($P>0.05$) (**Figure S3**). PCoA based on weighted (quantitative) and unweighted (qualitative) UniFrac distances suggested not distinct microbiota community among experimental conditions (**Figure S4**), with the exception of the weighted UniFrac distance between bacterial communities from SW-injected scallops at 168 h (SW168) and *Vibrio*-injected scallops at the same time (VS168) that was significant (PERMANOVA pseudo-F=2.43, P=0.023). The variance explained in the PCoA using the unweighted UniFrac was 19.08% (PC1 10.94% and PC2 8.14%) (**Figure S4A**) and the explained variance obtained using the weighted UniFrac was 54.19% (PC1 37.29% and PC2 16.91%) (**Figure S4B**).

Significant Changes in the Bacterial Abundances From Hemolymph Occurred After the Activation of Scallop Immune Response

We next investigated the expression of antimicrobial effectors that could be involved in host-microbiota interaction during scallop immune response. For that, we focused on the transcription patterns of four antimicrobial effectors expressed by hemocytes from the same analyzed scallops. The relative expression of the antimicrobial peptide big defensin *ApBD1*, the antimicrobial proteins *ApLBP/BPI1* and *ApLBP/BPI2*, and the hydrolytic enzyme lysozyme *ApGlys* were assessed in all experimental conditions at 12, 24, 48, 72, and 168 h by RT-qPCR (**Figure 3**). Results showed that all antimicrobials were first overexpressed in *Vibrio*-injected scallops within the first 24 h compared to the sea water-injected control group. Thus, *ApLBP/BPI1* was overexpressed 15- and 5.7- folds at 15 and 24 h, respectively whereas *ApLBP/BPI2* was slightly overexpressed 2.3- fold at 15 h. *ApBD1* was overexpressed 9.1- and 6.3- folds s at 24 and 72 h, respectively. The *ApGlys* gene was overexpressed 17- fold at 24 h (**Figure 3**). No significant overexpression was detected for the four immune genes after 72 h post injection. Also, all genes were expressed at basal level by hemocytes of non-stimulated scallops

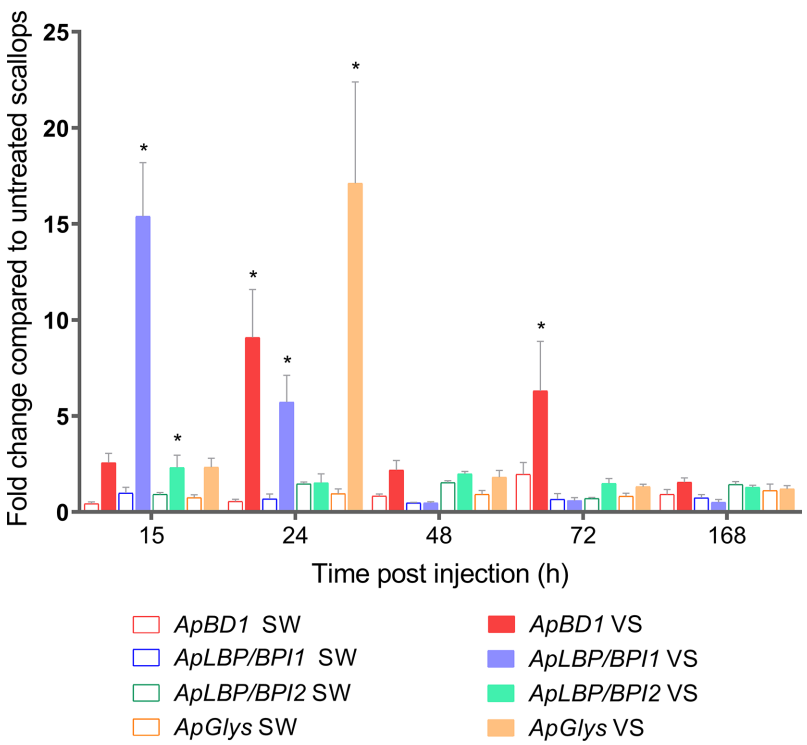

FIGURE 3 | Transcript expression of *ApBD1, ApLBP/BPI1, ApLBP/BPI2*, and *ApGlys* in scallop hemocytes during immune response. Bar graphs indicate the relative expression of antimicrobial effectors genes in *Vibrio*-injected scallops (VS) and seawater-injected scallops (SW) after 12, 24, 48, 72, and 168 h. SW-injected scallops were considered as injury control condition. Relative expression was calculated using non-stimulated scallops as control group, where gene expression values were considered 1. Graphed data are represented as the mean ± ES (n = 7). Asterisks indicate significant differences compared to SW-injected scallops (*$P < 0.05$).

(**Figure S5**). Overall, the significant changes observed in the scallop bacterial communities occurred after the activation of the immune response and the expression of antimicrobial effectors.

Significant Shifts of Target Bacterial Groups Are Early Detected During Scallop Immune Response

In an attempt to assess the changes of target bacterial groups in scallop hemolymph during the expression of immune effectors, we determined their relative abundances by qPCR and absolute quantification of 16S rDNA. To do this, a second immune challenge was performed and the significant overexpression of antimicrobial effectors in scallop hemocytes was confirmed at 24 h post challenge (**Figure S6**). Then, we examined the relative abundances of Gamma-, Epsilon-, and Betaproteobacteria, Firmicutes, as well as the specific quantification of *Vibrio* spp. from scallop hemolymph at 24 and 48 h after challenge (**Figure 4**). Results showed that significant shifts in bacterial relative abundances could be detected in scallop hemolymph as early as 24 h after challenge (**Figure 4A**). Furthermore, the relative abundances of Gamma-, Epsilon- and Betaproteobacteria, and Firmicutes were similar in *Vibrio*-injected scallops compared to SW-injected scallops at both 24 h and 48 h (**Figures 4A, B**). We observed a significant increase in the Gammaproteobacteria ($P<0.001$) and a significant decrease in undetermined bacterial groups (others) ($P<0.05$) in *Vibrio*-injected scallops at both time points. Still, Gammaproteobacteria exhibited a higher relative abundance at 48 h (65.8%) compared to 24 h (59%) after *Vibrio* injection. Betaproteobacteria and Firmicutes relative abundances did not vary between groups or time points. Epsilonproteobacteria abundance decreased in *Vibrio*-injected scallops at 24 h and 48 h, still those changes were non-significant ($P>0.05$). When comparing data obtained by absolute quantification of 16S rDNA and the deep amplicon sequencing from samples at 48 h, results showed a consistent shift trend for Epsilon-, Beta-, and Gammaproteobacteria but not for Firmicutes.

We further determined the number of total copies of specific bacterial 16S rDNA gene of the genus *Vibrio* to explain the contribution of the *Vibrio* injection to the Gammaproteobacteria abundance observed in scallop hemolymph (**Figures 4C, D**). As determined by the deep amplicon sequencing analysis, the increase *Vibrio* spp. was only a fraction of total Gammaproteobacteria relative abundance. Indeed, in terms of relative abundance, *Vibrio* spp. correspond to the 50% and 16% of total Gammaproteobacteria at 24 and 48 h respectively. Thus, other bacteria belonging to the Gammaproteobacteria class increased their abundances in *Vibrio*-injected scallops.

Gene Silencing of ApBD1 and ApLBP/BPI1 by RNAi in Non-Stimulated Scallops Leads to an Imbalance of Bacterial Groups From the Hemolymph Which Is Associated With *Vibrio* spp. Proliferation

Since we detected significant shifts of bacterial groups in scallop hemolymph together with the overexpression of antimicrobial effectors, we focused on the role of *ApBD1* and *ApLBP/BPI1* in

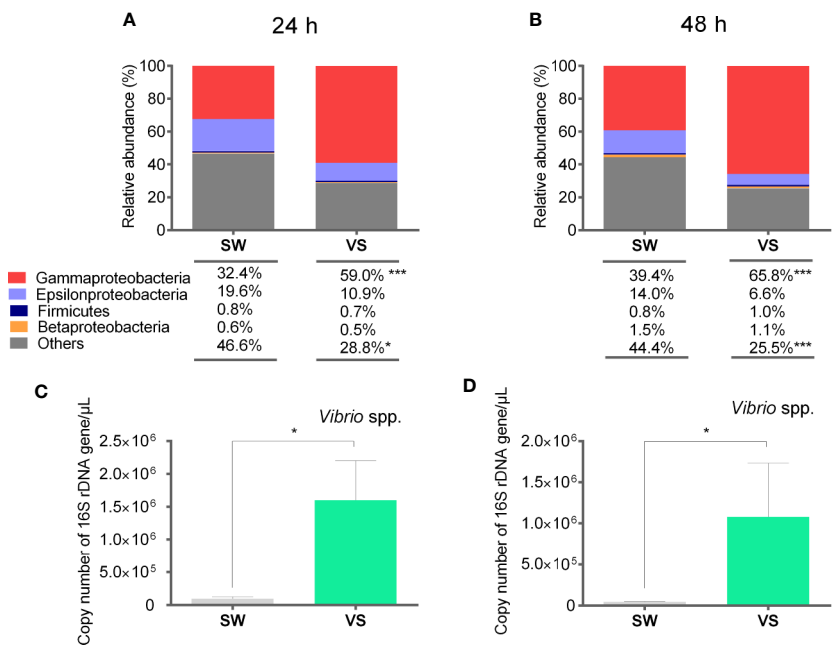

FIGURE 4 | Relative abundances of target bacterial groups present in scallop hemolymph after immune stimulation determined by qPCR and absolute quantification. Stack bar graphs indicate the average relative abundance of target bacterial groups in Vibrio-injected scallops (VS) and seawater-injected scallops (SW) at 24 h **(A)** and 48 h **(B)** after challenge. Number of total copies of specific bacterial 16S rDNA gene for *Vibrio* spp. at 24 h **(C)** and 48 h **(D)** after challenge are represented as the mean ± SE, and asterisks indicate significant differences compared to SW-injected scallops (***$P < 0.005$; *$P < 0.05$).

shaping the scallop microbiota. Thus, we performed a RNA interference silencing approach by injecting sequence-specific dsRNA in non-immune stimulated scallops. Subsequently, we quantified the 16S rDNA of target bacterial groups present in scallop hemolymph by qPCR (**Figure 5**). Results showed that transcript expressions of *ApBD1* and *ApLBP/BPI1* in hemocytes from scallops injected with *Ap*BD1-dsRNA and *Ap*LBP/BPI1-dsRNA were significant suppressed by ~94% and ~45%, respectively, compared to scallops injected with GFP-dsRNA as control after 48 h (**Figure 5A**). In addition, the expressions of *ApBD1* and *ApLBP/BPI1* in scallops injected with GFP-dsRNA were consistent with the basal expression levels observed in hemocytes from non-stimulated scallops (**Figure S6**). Then, we assessed the relative abundances of Gamma-, Epsilon-, and Betaproteobacteria, and Firmicutes from every experimental group. Particularly, Gammaproteobacteria significantly increased when the expression of antimicrobial effectors was suppressed compared to the control group (**Figure 5B**). We observed the highest relative abundance of Gammaproteobacteria in *Ap*LBP/BPI1-dsRNA injected scallops (81.8%) followed by *Ap*BD1-dsRNA (69.3%) and GFP-dsRNA (35.9%) injected scallops. Concomitantly, the increase in Gammaproteobacteria was associated with a significant decrease in undetermined bacterial groups (named as others). Specifically, *Ap*LBP/BPI1-dsRNA injected scallops displayed the lowest abundance of undetermined groups (9.3%) followed by *Ap*BD1-dsRNA (18.4%) and GFP-dsRNA (35.9%) injected scallops. Epsilonproteobacteria also displayed a significant decrease in *Ap*LBP/BPI1-dsRNA injected (5.7%) compared to control scallops (28.7%). Firmicutes and Betaproteobacteria did not show any significant shift in their relative abundances among experimental conditions. Moreover, relative abundances of bacterial groups from scallops injected with GFP-dsRNA were non-significantly different from SW-injected scallops.

In parallel, we detected a significant increase of the number of total copies of specific bacterial 16S rDNA gene from the genus *Vibrio* in scallops silenced for *ApBD1* or *ApLBP/BPI1* (**Figure 5C**). In terms of the relative abundance, *Vibrio* spp. corresponded to 29% and 22% of total bacteria in *Ap*LBP/BPI1- and *Ap*BD1-dsRNA injected scallops, respectively, while *Vibrio* spp. only represented 2% of total bacteria in GFP-dsRNA injected scallops. Finally, to confirm that the increase in *Vibrio* was due to cultivable *Vibrio* spp., hemolymph from all dsRNA-injected scallops were plated onto TCBS selective media. Results showed a significant increased number of *Vibrio* spp. c.f.u. in *Ap*LBP/BPI1- and *Ap*BD1-dsRNA injected scallops compared to the GFP-control group ($P<0.05$) (**Figure 5D**).

DISCUSSION

Results obtained in the present study shows that relative abundances of different bacterial groups found in the scallop hemolymph could rapidly change during the immune response.

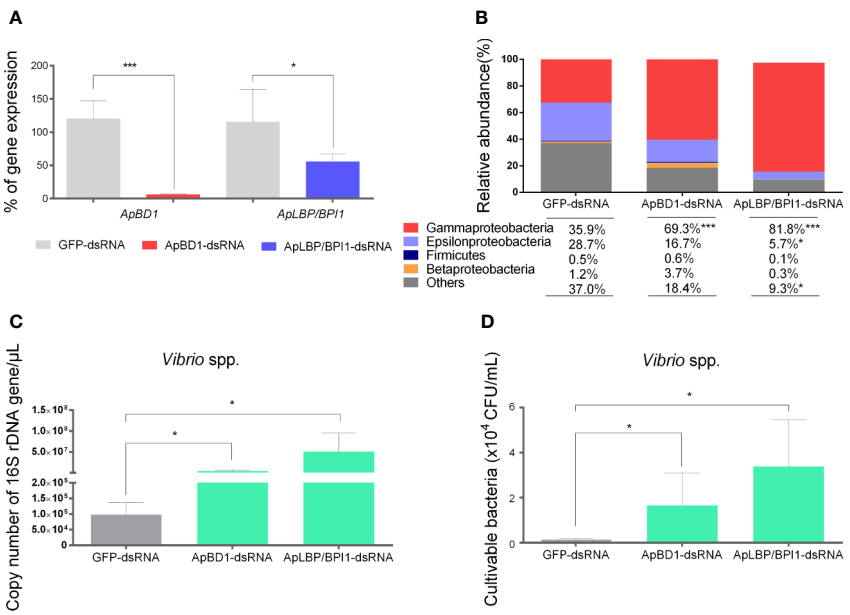

FIGURE 5 | Effect of the silencing of *ApBD1* and *ApLBP/BPI1* expression in scallop by RNAi on the relative abundances of target bacterial groups. **(A)** Transcript expression of *ApBD1* and *ApLBP/BPI1* in scallop hemocytes injected with *Ap*BD1-dsRNA (red bar) and *Ap*LBP/BPI1dsRNA (blue bar) compared to GFP-dsRNA (gray bar), considered as control of specific gene silencing. Values are represented as the mean ± SE, considering the gene expression in GFP-dsRNA-injected animals as 100%. **(B)** Relative abundances of target bacterial groups present in the hemolymph of dsRNA injected scallops determined by qPCR and absolute quantification. **(C)** Number of total copies of specific bacterial 16S rDNA gene for *Vibrio* spp. present in dsRNA injected scallops. Values are represented as the mean ± SE and asterisks indicate significant differences compared with GFP-dsRNA-injected scallops (*$P < 0.05$, ***$P < 0.005$). **(D)** cultivable *Vibrio* spp. present in hemolymph from dsRNA injected scallops. Values are represented as the mean number of colony forming units/ml of hemolymph ± SE.

We also establish that the abundances of major shifted bacterial groups were restored within a period of 7 days after immune challenge in a controlled environment. Importantly, the silencing of expression of the two antimicrobial effectors in non-immune stimulated scallops demonstrate that shifts of some major bacterial groups' abundances are related to the expression of antimicrobial effectors. Indeed, silenced scallops for both, *ApBD1* and *ApLBP/BPI1* antimicrobials exhibited proliferation of *Vibrio* spp. in their hemolymph. Overall, these results depict the delicate balance that exists between the immune response of *A. purpuratus* and hemolymph microbiota, indicating that host antimicrobial peptides and proteins could modulate the abundances of certain groups of bacteria such as *Vibrio*.

The analysis of hemolymph bacterial composition from non-stimulated scallops at the individual level reveal that scallops display a variable bacterial community, with both common and distinct bacterial groups among individuals. Considering the common phyla, scallop hemolymph is dominated by Proteobacteria, Spirochaetes, Bacteroidetes, Firmicutes and Gracilibacteria. Some of these phyla have been described also as predominant bacterial groups in other marine invertebrates. For example, Proteobacteria and/or Bacteroidetes are dominant phyla in the hemolymph of the mussel *Mytilus coruscus* (47), the oyster *Crassostrea gigas* (48), certain crustaceans (49), and in gonads from the scallop *Pecten maximus* (50). Yet, high variability in bacterial community composition and the lack of a common bacterial core between all scallop individuals is more evident at the class and genera level. Considering that scallops were acclimatized for two weeks in controlled conditions prior experiments, the variability on bacterial communities found between individuals is unlikely associated to the marine environment, as proposed in a previous study which characterized the microbiota from scallops sampled from the field (34). One single individual displays a microbiota composition quite different from the observed for the other individuals, which suggests the existence of higher microbiota variability in non-stimulated scallops. In oysters, the stability of the hemolymph microbiota and the assembly of the microbial community has been related to the host genotype (51), suggesting that the hemolymph microbiome is not a simple reflection of bivalve filtering lifestyle (48). Consequently, both extrinsic (environmental) and intrinsic (host) factors are at play in shaping and mediating the bacterial communities of aquatic organisms (52). As well, bacterial community variability has been related to different levels of basal expression of certain antimicrobial effectors among individuals (29), so each animal would represent bacterial niches with unique characteristics (30, 53). Indeed, consistent differences have been reported between host microbiota and environmental bacterial communities in a large number of marine invertebrates. These evidences suggest the existence of mechanisms for selection, adaptation, and regulation between hosts and associated microorganisms (30, 54–57).

The composition of the hemolymph microbiota significantly changed at 48 h post immune challenge, a result previously observed from whole scallops directly sampled from the field (34). The evidence that scallop microbiota shifts during the immune response at both, controlled conditions and natural environment, suggests a strong host genetic effect in this process, as previously demonstrated in *Hydra* (56). In the present study, we found that (i) significant shifts in bacterial groups can be detected as early as 24 h after immune challenge and (ii) shifted abundances of most bacterial groups are reestablished within 7 days post immunostimulation. These results give new insights into the kinetics of the scallop microbiota modulation, showing that abundances of some bacterial populations can be rapidly shifted and restored in the scallop after the immune response. In the oyster *C. gigas*, recent studies have shown that hemolymph microbiota dynamics are subject to internal microbiome forces and host-related factors, such as genetics, that contribute to long-term stability (48, 58). Indeed, no significant bacterial shifts were detected in scallop hemolymph at phylum level, and the significant changes observed at class level during immunostimulation were reestablished within 7 days, supporting the idea of stability in the dynamics of the marine bivalve hemolymph microbiome (48, 58).

The significant increase in the Gammaproteobacteria class, in which *Vibrio* only corresponds to a minor fraction of total Gammaproteobacteria abundance, together with the significant decrease of Epsilonproteobacteria and Deltaproteobacteria, is considered as a clear sign of microbiota destabilization in immunostimulated scallops. Studies from other marine bivalves have proposed that processes such as infections, temperature stress, contaminants, among others, can trigger the destabilization of the microbiota, "opening the door" to opportunistic pathogens (32, 48, 59–61). In the present work, we specifically induce the immune activation with a heat-killed *Vibrio* to exclude the pathogen-microbe interaction that could occur during a real pathogenic infection. The selection of the four antimicrobial effectors to confirm scallop immune activation was based on their involvement in the immune response and on their antibacterial properties described in this and others bivalves species (12, 15, 62–64). Thus, bacterial shifts observed were possibly shaped in part by the host response and consequently, the silencing of antimicrobial effectors expressed by the host was a functional approach to validate this premise.

*Ap*BD1 and *Ap*LBP/BPI1 effectors were previously characterized as *A. purpuratus* antimicrobial effector genes (12, 15). Both genes exhibited high levels of expression during bacterial challenge and were expressed at basal level by hemocytes and other tissues. Furthermore, *Ap*BD1 was recently shown to entrap *Staphylococcus aureus* in peptide aggregates similar to those reported to the oyster Big defensin *Cg*-BigDef1 (63). Although *Ap*LBP/BPI1 has not been functional characterized yet, its oyster homologue *Cg*BPI display strong antibacterial activity by membrane permeabilization of gram-negative bacteria (62). The transcript silencing of these genes in non-stimulated scallops indicate that both antimicrobials are involved in the regulation of *A. purpuratus* bacterial microbiota. Interestingly, consistent changes in Gamma- and Epsilonproteobacteria abundances were detected when these effectors were overexpressed or silenced. This result suggests that changes in bacterial groups abundances might be occurring at lower taxonomic levels within those bacterial classes.

Certainly, considering the antibacterial activities reported for these effectors, *Ap*BD1 and *Ap*LBP/BPI1 could specifically regulate certain target bacterial groups, controlling their abundance in the hemolymph. Also, antimicrobials could be acting indirectly through the modulation of certain bacterial groups that interact with the bacterial groups targeted in this study, for instance by antagonistic interactions (65). In parallel, diverse cellular reactions and humoral effectors are produced during the scallop immune response. Thus, additional immune processes might be associated with bacterial shifts regulation, such as expression of further antimicrobial effectors, immunomodulators, and cellular responses (22, 30, 34, 55).

Overall, our results bring out the importance of the scallop humoral immune response not only in defense against external pathogens, but also in regulating the proliferation and maintaining specific levels of certain bacterial groups. In other invertebrate species such as *Marsupenaeus japonicus* or *Drosophila melanogaster*, silencing or knockdown of antimicrobial peptides can cause host death, due to an exacerbated proliferation of bacteria in hemolymph or tissues (22, 29). Antimicrobial peptides expressed in *Hydra* select specific bacterial colonization, changing the structure of the bacterial community when their expression is altered (66). In this study, we depicted the kinetics of microbiota modification during the scallop immune response. We also defined the functional interaction between the expression of two antimicrobial effectors and the hemolymph microbiota of *A. purpuratus*. Future research on the beneficial or detrimental effect of bacterial composition shifts in the immune capacity of scallops will allow us to contribute with the design of management aquaculture strategies. Also, which antimicrobial peptides and proteins specifically shaped target bacterial groups from scallop microbiota will be a pertinent information to implement future genetic breading programs in *A. purpuratus*.

DATA AVAILABILITY STATEMENT

The datasets presented in this study can be found in online repositories. The names of the repository/repositories and accession number(s) can be found below: https://www.ncbi.nlm.nih.gov/genbank/, PRJNA639911.

AUTHOR CONTRIBUTIONS

RG, RDR, KB, and PS contributed to the conception and design of the study. RG, AG, and RR contributed to the acquisition of data. RG and AG created the databases and performed the statistical analysis. RG and PS worked on analysis, interpretation of data, and wrote the first draft of the manuscript. All authors contributed to the article and approved the submitted version.

FUNDING

This study was supported by the following research funding programs: FONDECYT No 11150009 to PS. RG. was supported by the PhD student fellowship CONICYT-PFCHA/DOCTORADO NACIONAL/2016 – 21160980. RDR was supported by the Brazilian funding agency CNPq (Grant Numbers 406530/2016-5 and 307032/2018-3).

ACKNOWLEDGMENTS

We thank German Lira for all his support with scallop maintenance and procurement. We gratefully acknowledge Katherine Muñoz, Ana Mercado, Katherine Jeno, Elisa Torres and Esteban Revilla for their helpful technical assistance.

SUPPLEMENTARY MATERIAL

The Supplementary Material for this article can be found online at: https://www.frontiersin.org/articles/10.3389/fimmu.2020.599625/full#supplementary-material

REFERENCES

1. Wang S, Zhang J, Jiao W, Li J, Xun X, Sun Y, et al. Scallop genome provides insights into evolution of bilaterian karyotype and development. *Nat Ecol Evol* (2017) 1(5):120. doi: 10.1038/s41559-017-0120
2. Gram L, Melchiorsen J, Bruhn JB. Antibacterial activity of marine culturable bacteria collected from a global sampling of ocean surface waters and surface swabs of marine organisms. *Mar Biotechnol (NY)* (2010) 12(4):439–51. doi: 10.1007/s10126-009-9233-y
3. Inglis SD, Kristmundsson A, Freeman MA, Levesque M, Stokesbury K. Gray meat in the Atlantic sea scallop, *Placopecten magellanicus*, and the identification of a known pathogenic scallop apicomplexan. *J Invertebr Pathol* (2016) 141:66–75. doi: 10.1016/j.jip.2016.10.008
4. Xing J, Lin T, Zhan W. Variations of enzyme activities in the haemocytes of scallop *Chlamys farreri* after infection with the acute virus necrobiotic virus (AVNV). *Fish Shellfish Immunol* (2008) 25(6):847–52. doi: 10.1016/j.fsi.2008.09.008
5. Liu R, Qiu L, Yu Z, Zi J, Yue F, Wang L, et al. Identification and characterisation of pathogenic *Vibrio splendidus* from Yesso scallop (*Patinopecten yessoensis*) cultured in a low temperature environment. *J Invertebr Pathol* (2013) 114(2):144–50. doi: 10.1016/j.jip.2013.07.005
6. González R, Muñoz K, Brokordt K, Schmitt P. Scallop Immunology. In: *Reference Module in Life Sciences*. Massachusetts: Elsevier (2019). doi: 10.1016/B978-0-12-809633-8.20896-0
7. Escoubas J-M, Gourbal B, Duval D, Green TJ, Charrière GM, Destoumieux-Garzón D, et al. Immunity in Molluscs. In: MJH Ratcliffe, editor. *Encyclopedia of Immunobiology*. Oxford: Academic Press (2016). doi: 10.1016/B978-0-12-374279-7.12004-1
8. Gerdol M, De Moro G, Manfrin C, Venier P, Pallavicini A. Big defensins and mytimacins, new AMP families of the Mediterranean mussel *Mytilus galloprovincialis*. *Dev Comp Immunol* (2012) 36(2):390–9. doi: 10.1016/j.dci.2011.08.003
9. Allam B, Espinosa EP. Bivalve immunity and response to infections: Are we looking at the right place? *Fish Shellfish Immunol* (2016) 53:4–12. doi: 10.1016/j.fsi.2016.03.037

10. Yang J, Luo J, Zheng H, Lu Y, Zhang H. Cloning of a big defensin gene and its response to *Vibrio parahaemolyticus* challenge in the noble scallop *Chlamys nobilis* (Bivalve: Pectinidae). *Fish Shellfish Immunol* (2016) 56:445–449. doi: 10.1016/j.fsi.2016.07.030
11. Zhao J, Song L, Li C, Ni D, Wu L, Zhu L, et al. Molecular cloning, expression of a big defensin gene from bay scallop *Argopecten irradians* and the antimicrobial activity of its recombinant protein. *Mol Immunol* (2007) 44 (4):360–8. doi: 10.1016/j.molimm.2006.02.025
12. Gonzalez R, Brokordt K, Carcamo CB, Coba de la Pena T, Oyanedel D, Mercado L, et al. Molecular characterization and protein localization of the antimicrobial peptide big defensin from the scallop *Argopecten purpuratus* after *Vibrio splendidus* challenge. *Fish Shellfish Immunol* (2017) 68:173–9. doi: 10.1016/j.fsi.2017.07.010
13. Zhao J, Song L, Li C, Zou H, Ni D, Wang W, et al. Molecular cloning of an invertebrate goose-type lysozyme gene from *Chlamys farreri*, and lytic activity of the recombinant protein. *Mol Immunol* (2007) 44(6):1198–208. doi: 10.1016/j.molimm.2006.06.008
14. He C, Yu H, Liu W, Su H, Shan Z, Bao X, et al. A goose-type lysozyme gene in Japanese scallop (*Mizuhopecten yessoensis*): cDNA cloning, mRNA expression and prom oter sequence analysis. *Comp Biochem Physiol B Biochem Mol Biol* (2012) 162(1-3):34–43. doi: 10.1016/j.cbpb.2012.02.002
15. González R, Brokordt K, Rojas R, Schmitt P. Molecular characterization and expression patterns of two LPS binding /bactericidal permeability-increasing proteins (LBP/BPIs) from the scallop *Argopecten purpuratus*. *Fish Shellfish Immunol* (2020) 97:12–7. doi: 10.1016/j.fsi.2019.12.032
16. Li C, Song L, Zhao J, Zhu L, Zou H, Zhang H, et al. Preliminary study on a potential antibacterial peptide derived from histone H2A in hemocytes of scallop *Chlamys farreri*. *Fish Shellfish Immunol* (2007) 22(6):663–72. doi: 10.1016/j.fsi.2006.08.013
17. Jiang W, Lin F, Fang J, Gao Y, Du M, Fang J, et al. Transcriptome analysis of the Yesso scallop, *Patinopecten yessoensis* gills in response to water temperature fluctuations. *Fish Shellfish Immunol* (2018) 80:133–40. doi: 10.1016/j.fsi.2018.05.038
18. Pauletto M, Milan M, Moreira R, Novoa B, Figueras A, Babbucci M, et al. Deep transcriptome sequencing of *Pecten maximus* hemocytes: a genomic resource for bivalve immunology. *Fish Shellfish Immunol* (2014) 37(1):154–65. doi: 10.1016/j.fsi.2014.01.017
19. Ventoso P, Pazos AJ, Pérez-Parallé ML, Blanco J, Triviño JC, Sánchez JL. RNA-Seq Transcriptome Profiling of the Queen Scallop (*Aequipecten opercularis*) Digestive Gland after Exposure to Domoic Acid-Producing Pseudo-nitzschia. *Toxins* (2019) 11(2):97. doi: 10.3390/toxins11020097
20. Flores-Herrera P, Farlora R, Gonzalez R, Brokordt K, Schmitt P. De novo assembly, characterization of tissue-specific transcriptomes and identification of immune related genes from the scallop *Argopecten purpuratus*. *Fish Shellfish Immunol* (2019) 89:505–15. doi: 10.1016/j.fsi.2019.03.069
21. Hooper LV, Littman DR, Macpherson AJ. Interactions between the microbiota and the immune system. *Science* (2012) 336(6086):1268–73. doi: 10.1126/science.1223490
22. Ryu JH, Kim SH, Lee HY, Bai JY, Nam YD, Bae JW, et al. Innate immune homeostasis by the homeobox gene caudal and commensal-gut mutualism in Drosophila. *Science* (2008) 319(5864):777–82. doi: 10.1126/science.1149357
23. Zhao Q, Elson CO. Adaptive immune education by gut microbiota antigens. *Immunology* (2018) 154(1):28–37. doi: 10.1111/imm.12896
24. Abt MC, Osborne LC, Monticelli LA, Doering TA, Alenghat T, Sonnenberg GF, et al. Commensal bacteria calibrate the activation threshold of innate antiviral immunity. *Immunity* (2012) 37(1):158–70. doi: 10.1016/j.immuni.2012.04.011
25. Valdes AM, Walter J, Segal E, Spector TD. Role of the gut microbiota in nutrition and health. *BMJ* (2018) 361:k2179. doi: 10.1136/bmj.k2179
26. Salzman NH. Paneth cell defensins and the regulation of the microbiome: detente at mucosal surfaces. *Gut Microbes* (2010) 1(6):401–6. doi: 10.4161/gmic.1.6.14076
27. Sassone-Corsi M, Raffatellu M. No vacancy: how beneficial microbes cooperate with immunity to provide colonization resistance to pathogens. *J Immunol* (2015) 194(9):4081–7. doi: 10.4049/jimmunol.1403169
28. You JS, Yong JH, Kim GH, Moon S, Nam KT, Ryu JH, et al. Commensal-derived metabolites govern *Vibrio cholerae* pathogenesis in host intestine. *Microbiome* (2019) 7(1):132. doi: 10.1186/s40168-019-0746-y
29. Wang XW, Xu JD, Zhao XF, Vasta GR, Wang JX. A shrimp C-type lectin inhibits proliferation of the hemolymph microbiota by maintaining the expression of antimicrobial peptides. *J Biol Chem* (2014) 289(17):11779–90. doi: 10.1074/jbc.M114.552307
30. Franzenburg S, Walter J, Künzel S, Wang J, Baines JF, Bosch TC, et al. Distinct antimicrobial peptide expression determines host species-specific bacterial associations. *Proc Natl Acad Sci U S A* (2013) 110(39):E3730–8. doi: 10.1073/pnas.1304960110
31. Wang GL, Xia XL, Li XL, Dong SJ, Li JL. Molecular characterization and expression patterns of the big defensin gene in freshwater mussel (*Hyriopsis cumingii*). *Genet Mol Res* (2014) 13(1):704–15. doi: 10.4238/2014.January.29.1
32. Clerissi C, de Lorgeril J, Petton B, Lucasson A, Escoubas JM, Gueguen Y, et al. Microbiota Composition and Evenness Predict Survival Rate of Oysters Confronted to Pacific Oyster Mortality Syndrome. *Front Microbiol* (2020) 11:311. doi: 10.3389/fmicb.2020.00311
33. de Lorgeril J, Lucasson A, Petton B, Toulza E, Montagnani C, Clerissi C, et al. Immune-suppression by OsHV-1 viral infection causes fatal bacteraemia in Pacific oysters. *Nat Commun* (2018) 9(1):4215. doi: 10.1038/s41467-018-06659-3
34. Muñoz K, Flores-Herrera P, Gonçalves AT, Rojas C, Yáñez C, Mercado L, et al. The immune response of the scallop *Argopecten purpuratus* is associated with changes in the host microbiota structure and diversity. *Fish Shellfish Immunol* (2019) 91:241–50. doi: 10.1016/j.fsi.2019.05.028
35. L. Committee on Acute Exposure Guideline, T. Committee on, T. Board on Environmental Studies and, S. Division on Earth and Life and and C. National Research. *Acute Exposure Guideline Levels for Selected Airborne Chemicals: Volume 16*. Washington (DC: National Academies Press (US) Copyright 2014 by the National Academy of Sciences (2014). All rights reserved. doi: 10.17226/18707
36. Rojas R, Miranda CD, Opazo R, Romero J. Characterization and pathogenicity of *Vibrio splendidus* strains associated with massive mortalities of commercial hatchery-reared larvae of scallop *Argopecten purpuratus* (Lamarck, 1819). *J Invertebr Pathol* (2015) 124:61–9. doi: 10.1016/j.jip.2014.10.009
37. Pfaffl MW. A new mathematical model for relative quantification in real-time RT-PCR. *Nucleic Acids Res* (2001) 29(9):e45–5. doi: 10.1093/nar/29.9.e45
38. Caporaso JG, Kuczynski J, Stombaugh J, Bittinger K, Bushman FD, Costello EK, et al. QIIME allows analysis of high-throughput community sequencing data. *Nat Methods* (2010) 7(5):335–6. doi: 10.1038/nmeth.f.303
39. Bolyen E, Rideout JR, Dillon MR, Bokulich NA, Abnet CC, Al-Ghalith GA, et al. Reproducible, interactive, scalable and extensible microbiome data science using QIIME 2. *Nat Biotechnol* (2019) 37(8):852–7. doi: 10.1038/s41587-019-0209-9
40. Callahan BJ, McMurdie PJ, Rosen MJ, Han AW, Johnson AJA, Holmes SP. DADA2: High-resolution sample inference from Illumina amplicon data. *Nat Methods* (2016) 13(7):581–3. doi: 10.1038/nmeth.3869
41. Callahan BJ, McMurdie PJ, Holmes SP. Exact sequence variants should replace operational taxonomic units in marker-gene data analysis. *Isme J* (2017) 11(12):2639–43. doi: 10.1038/ismej.2017.119
42. McDonald D, Price MN, Goodrich J, Nawrocki EP, DeSantis TZ, Probst A, et al. An improved Greengenes taxonomy with explicit ranks for ecological and evolutionary analyses of bacteria and archaea. *Isme J* (2012) 6(3):610–8. doi: 10.1038/ismej.2011.139
43. Edgar RC. Updating the 97% identity threshold for 16S ribosomal RNA OTUs. *Bioinformatics* (2018) 34(14):2371–5. doi: 10.1093/bioinformatics/bty113
44. Lozupone C, Knight R. UniFrac: a new phylogenetic method for comparing microbial communities. *Appl Environ Microbiol* (2005) 71(12):8228–35. doi: 10.1128/AEM.71.12.8228-8235.2005
45. Lozupone CA, Hamady M, Kelley ST, Knigh R. Quantitative and qualitative beta diversity measures lead to different insights into factors that structure microbial communities. *Appl Environ Microbiol* (2007) 73(5):1576–85. doi: 10.1128/aem.01996-06
46. Parks DH, Tyson GW, Hugenholtz P, Beiko RG. STAMP: statistical analysis of taxonomic and functional profiles. *Bioinformatics* (2014) 30(21):3123–4. doi: 10.1093/bioinformatics/btu494
47. Li YF, Chen YW, Xu JK, Ding WY, Shao AQ, Zhu YT, et al. Temperature elevation and *Vibrio cyclitrophicus* infection reduce the diversity of

haemolymph microbiome of the mussel *Mytilus coruscus*. *Sci Rep* (2019) 9 (1):16391. doi: 10.1038/s41598-019-52752-y
48. Lokmer A, Mathias Wegner K. Hemolymph microbiome of Pacific oysters in response to temperature, temperature stress and infection. *Isme J* (2015) 9 (3):670–82. doi: 10.1038/ismej.2014.160
49. Ooi MC, Goulden EF, Smith GG, Bridle AR. Haemolymph microbiome of the cultured spiny lobster *Panulirus ornatus* at different temperatures. *Sci Rep* (2019) 9(1):1677. doi: 10.1038/s41598-019-39149-7
50. Lasa A, Mira A, Camelo-Castillo A, Belda-Ferre P, Romalde JL. Characterization of the microbiota associated to *Pecten maximus* gonads using 454-pyrosequencing. *Int Microbiol* (2016) 19(2):93–9. doi: 10.2436/20.1501.01.267
51. Wegner KM, Volkenborn N, Peter H, Eiler A. Disturbance induced decoupling between host genetics and composition of the associated microbiome. *BMC Microbiol* (2013) 13:252. doi: 10.1186/1471-2180-13-252
52. Melissa LP, Ward JE. Microbial Ecology of the Bivalvia, with an Emphasis on the Family Ostreidae. *J Shellfish Res* (2018) 37(4):793–806. doi: 10.2983/035.037.0410
53. Wang XW, Wang JX. Crustacean hemolymph microbiota: Endemic, tightly controlled, and utilization expectable. *Mol Immunol* (2015) 68(2 Pt B):404–11. doi: 10.1016/j.molimm.2015.06.018
54. Augustin R, Schröder K, Murillo Rincón AP, Fraune S, Anton-Erxleben F, Herbst E-M, et al. A secreted antibacterial neuropeptide shapes the microbiome of Hydra. *Nat Commun* (2017) 8(1):698. doi: 10.1038/s41467-017-00625-1
55. Bevins CL, Salzman NH. The potter's wheel: the host's role in sculpting its microbiota. *Cell Mol Life Sci* (2011) 68(22):3675–85. doi: 10.1007/s00018-011-0830-3
56. Fraune S, Bosch TCG. Long-term maintenance of species-specific bacterial microbiota in the basal metazoan Hydra. *Proc Natl Acad Sci U S A* (2007) 104 (32):13146–51. doi: 10.1073/pnas.0703375104
57. Cullen TW, Schofield WB, Barry NA, Putnam EE, Rundell EA, Trent MS, et al. Gut microbiota. Antimicrobial peptide resistance mediates resilience of prominent gut commensals during inflammation. *Science* (2015) 347 (6218):170–5. doi: 10.1126/science.1260580
58. Lokmer A, Goedknegt MA, Thieltges DW, Fiorentino D, Kuenzel S, Baines JF, et al. Spatial and Temporal Dynamics of Pacific Oyster Hemolymph Microbiota across Multiple Scales. *Front Microbiol* (2016) 7:1367. doi: 10.3389/fmicb.2016.01367
59. Egan S, Gardiner M. Microbial Dysbiosis: Rethinking Disease in Marine Ecosystems. *Front Microbiol* (2016) 7:991. doi: 10.3389/fmicb.2016.00991
60. Bachere E, Rosa RD, Schmitt P, Poirier AC, Merou N, Charriere GM, et al. The new insights into the oyster antimicrobial defense: Cellular, molecular and genetic view. *Fish Shellfish Immunol* (2015) 46(1):50–64. doi: 10.1016/j.fsi.2015.02.040
61. Destoumieux-Garzón D, Canesi L, Oyanedel D, Travers M-A, Charrière GM, Pruzzo C, et al. Vibrio–bivalve interactions in health and disease. *Environ Microbiol* (2020) 4323–41. doi: 10.1111/1462-2920.15055
62. Gonzalez M, Gueguen Y, Destoumieux-Garzon D, Romestand B, Fievet J, Pugniere M, et al. Evidence of a bactericidal permeability increasing protein in an invertebrate, the *Crassostrea gigas* Cg-BPI. *Proc Natl Acad Sci U S A* (2007) 104(45):17759–64. doi: 10.1073/pnas.0702281104
63. Stambuk F, Ojeda C, Schmitt P. Big Defensin BD1 from the scallop *Argopecten purpuratus* is an antimicrobial peptide which entraps bacteria through nanonets formation. *bioRxiv* (2020). doi: 10.1101/2020.02.25.965327
64. Zhao J, Song L, Li C, Zou H, Ni D, Wang W, et al. Molecular cloning of an invertebrate goose-type lysozyme gene from *Chlamys farreri*, and lytic activity of the recombinant protein. *Mol Immunol* (2007) 44(6):1198–208. doi: 10.1016/j.molimm.2006.06.008
65. García-Bayona L, Comstock LE. Bacterial antagonism in host-associated microbial communities. *Science* (2018) 361(6408):eaat2456. doi: 10.1126/science.aat2456
66. Fraune S, Augustin R, Anton-Erxleben F, Wittlieb J, Gelhaus C, Klimovich VB, et al. In an early branching metazoan, bacterial colonization of the embryo is controlled by maternal antimicrobial peptides. *Proc Natl Acad Sci U S A* (2010) 107(42):18067–72. doi: 10.1073/pnas.1008573107

Conflict of Interest: The authors declare that the research was conducted in the absence of any commercial or financial relationships that could be construed as a potential conflict of interest.

frontiers in Immunology

ORIGINAL RESEARCH
published: 26 November 2020
doi: 10.3389/fimmu.2020.607543

GSK3β Plays a Negative Role During White Spot Syndrome Virus (WSSV) Infection by Regulating NF-κB Activity in Shrimp *Litopenaeus vannamei*

Shuang Zhang[1,2,3], *Lulu Zhu*[1], *Cuihong Hou*[1], *Hang Yuan*[1], *Sheng Yang*[1], *Mustafa Abdo Saif Dehwah*[4] *and Lili Shi*[1,5*]

[1] College of Fisheries, Guangdong Ocean University, Zhanjiang, China, [2] Key Laboratory of Aquatic, Livestock and Poultry Feed Science and Technology in South China, Ministry of Agriculture, Zhanjiang, China, [3] Aquatic Animals Precision Nutrition and High Efficiency Feed Engineering Research Center of Guangdong Province, Zhanjiang, China, [4] Department of Medical Laboratories, Faculty of Medical and Health Science, Taiz University/AL-Turba Branch, Taiz, Yemen, [5] Guangdong Provincial Key Laboratory of Marine Resources and Coastal Engineering, Guangzhou, China

OPEN ACCESS

Edited by:
Chaozheng Li,
Sun Yat-sen University, China

Reviewed by:
Hongliang Zuo,
Sun Yat-sen University, China
Muting Yan,
South China Agricultural University, China

***Correspondence:**
Lili Shi
shill@gdou.edu.cn

Specialty section:
This article was submitted to Comparative Immunology, a section of the journal Frontiers in Immunology

Received: *17 September 2020*
Accepted: *30 October 2020*
Published: *26 November 2020*

Citation:
Zhang S, Zhu L, Hou C, Yuan H, Yang S, Dehwah MAS and Shi L (2020) GSK3β Plays a Negative Role During White Spot Syndrome Virus (WSSV) Infection by Regulating NF-κB Activity in Shrimp Litopenaeus vannamei. Front. Immunol. 11:607543. doi: 10.3389/fimmu.2020.607543

Glycogen synthase kinase-3 (GSK3), a cytoplasmic serine/threonine-protein kinase involved in a large number of key cellular processes, is a little-known signaling molecule in virus study. In this study, a GSK3 protein which was highly similar to GSK3β homologs from other species in *Litopenaeus vannamei* (designated as LvGSK3β) was obtained. LvGSK3β was expressed constitutively in the healthy *L. vannamei*, at the highest level in the intestine and the lowest level in the eyestalk. White spot syndrome virus (WSSV) reduced LvGSK3β expression was in immune tissues including the hemocyte, intestine, gill and hepatopancreas. The inhibition of LvGSK3β resulted in significantly higher survival rates of *L. vannamei* during WSSV infection than the control group, and significantly lower WSSV viral loads in LvGSK3β-inhibited *L. vannamei* were observed. Knockdown of LvGSK3β by RNAi resulted in increases in the expression of LvDorsal and several NF-κB driven antimicrobial peptide (AMP) genes (including ALF, PEN and crustin), but a decrease in LvCactus expression. Accordingly, overexpression of LvGSK3β could reduce the promoter activity of LvDorsal and several AMPs, while the promoter activity of LvCactus was increased. Electrophoretic mobility shift assays (EMSA) showed that LvDorsal could bind to the promoter of LvGSK3β. The interaction between LvGSK3β and LvDorsal or LvCactus was confirmed using co-immunoprecipitation (Co-IP) assays. In addition, the expression of LvGSK3β was dramatically reduced by knockdown of LvDorsal. In summary, the results presented in this study indicated that LvGSK3β had a negative effect on *L. vannamei* by mediating a feedback regulation of the NF-κB pathway when it is infected by WSSV.

Keywords: glycogen synthase kinase 3β, nuclear factor κB, negative regulation, white spot syndrome virus, *Litopenaeus vannamei*

INTRODUCTION

Shrimp is one of the main internationally traded aquatic products, which has important economic value. As an important aquaculture shrimp species, the produce of *Litopenaeus vannamei* accounts for nearly two-thirds of the total output of shrimp worldwild (1). In recent years, emerging diseases caused by various pathogens have been the main menace for sustainable development of the shrimp industry worldwide. Among these pathogens, white spot syndrome virus (WSSV) has always been a viral agent of greatest concern, although other viruses such as Taura syndrome virus (TSV), infectious hypodermal and hematopoietic necrosis virus (IHHNV) and decapod iridescent virus 1 (DIV1) were reported to cause losses in farmed shrimp (2–5). As an invertebrate, the innate immunity is the first defense line against viral infections in shrimp (6). Although a considerable number of scientific studies have focused on this for several years, knowledge of the host-virus interaction is quite insufficient. Thus, it is in urgent need to investigate the mechanisms of immune defence for disease controling in shrimp culture.

Glycogen synthase kinase 3 (GSK3), a multifunctional serine/threonine-protein kinase, initially identified as a key regulator of glycogen metabolism and insulin signaling, has been verified as being involved in various physiological and pathological processes, such as protein synthesis, signal transduction, cell proliferation and differentiation, immune response, inflammation and tumorigenesis, and so on (7, 8). GSK3 is highly conserved in species from the amoeba, *Dictyostelium discoideum*, to humans. In vertebrates, there are two isoforms of GSK3 (GSK3α and GSK3β) known, which share a highly conserved catalytic domain but differ at both termini (9). GSK3α and GSK3β perform different functions in many biological processes. GSK3α is mainly involved in glycogen metabolism, while GSK3β functions as a convergence point for multiple signaling pathways, including nuclear factor κB (NF-κB), Wnt/β-catenin, phosphatidylinositide 3-kinase/protein kinase B (PI3K/Akt), Hedgehog and STAT signaling pathways (10–12). Recent studies have unearthed GSK3β's role in viral infections through its alteration of viral entry, replication and egress. GSK3β is known as an AKT substrate which plays a crucial role in influenza viral entry (13, 14). GSK3β silence could decrease the hepatitis C virus (HCV) replication and the production of infectious particle while GSK3β overexpression enhanced HCV replication (15). Studies *in vitro* displayed that specific inhibitors (small molecules) of GSK3β significantly decreased Tat-dependent replication of human immunodeficiency virus 1 (HIV1) (16). In addition, GSK3β inhibitors could effectively prevent the assembly and release of HCV because of the key role in HCV virion assembly and release GSK3β played, through inhibiting apolipoprotein synthesis (17). But overall, studying on the function of GSK3β and its related signaling pathways in the research field of virology is still in its initial stage, especially in invertebrates.

GSK3β has been demonstrated to play a role in the interaction between host and virus in shrimp, but studies on its specific regulation mechanism during the anti-viral immune reaction in shrimp is required, as GSK3β is a cross point in several signal pathways (18). An important pro-inflammatory pathway promoted by GSK3β is the activation of NF-κB (19). GSK3β plays a vital role in gene transcription by the way of regulating the promoter-specific recruitment of NF-κB (20). Through restraining the transcriptional activation of NF-κB, GSK3β inhibitors could lessen the inflammatory cytokine production of the TLR pathway (21). Consistently, activation of the PI3K/Akt/GSK3β signaling pathway reduced the NF-κB nuclear translocation and the pathway acts as the influencing factor in inflammatory protection (22). NF-κB plays an essential role in the antiviral immunity and is an obstacle to the survival of virus (23). The Toll and immune deficiency (IMD) pathways are Two NF-κB related signaling pathways which are considered as the main regulatory factors of the anti-viral immune response in shrimp (24). Building on the current research, the mechanism behind GSK3β mediation of NF-κB during WSSV infection in *L. vannamei* was studied in this paper. The results showed that *L. vannamei* GSK3β (LvGSK3β) has a negative effect for the shrimp during WSSV infection by regulating NF-κB activity, which is beneficial for the study on the host-virus interactional mechanisms and may offer potential strategies for disease prevention in shrimp industry.

MATERIALS AND METHODS

Shrimp and WSSV

L. vannamei (approximately 4–6 g each) were purchased from a local shrimp farm in Zhanjiang City, Guangdong Province, China. As our previous study (25) described, *L. vannamei* were cultured in a recirculating water tank system for over 7 days before the experiments with water salinity and temperature maintained at 27‰ salinity at 25–27 °C. The shrimp were fed with a commercial shrimp pellet diet (Haid Group, Guangzhou, China) twice daily. At the beginning of all experimental treatments, shrimp (5% of the total) were analyzed and ensured to be free of WSSV via PCR method performed according to published standard operating procedures. The WSSV (Chinese strain, AF332093) was extracted from WSSV-infected shrimp muscle tissue and stored at −80 °C. Before injection, the muscle tissue was homogenised and prepared as a WSSV inoculum with approximately 1×10^5 copies/μl, as previously described (26).

Cloning the cDNA and Genome of LvGSK3β

Total RNA and the genomic DNA were extracted from the shrimp tissues using the RNeasy Mini kit (Qiagen, Hilden, Germany) and TIANGEN Marine Animals DNA Kit (TIANGEN, Guangzhou, China), respectively. First-strand cDNA synthesis was performed using a cDNA Synthesis Kit (Takara, Dalian, China) following the manufacturer's instructions. The partial cDNA sequence of LvGSK3β was obtained from transcriptomic sequencing of *L. vannamei* (27) and its full-length cDNA sequence was cloned by a rapid amplification of cDNA ends (RACE) PCR using the SMARTer™ RACE cDNA Amplification kit (Clontech, Japan),

following the user manual and the specific primers used are listed in **Table 1**. The genomic DNA sequences of LvGSK3β were obtained via PCR, according to a previously published method (28) and were based on the genome sequences of *Penaeus vannamei* breed Kehai No.1 (GenBank No. NW_020869560). The PCR products were cloned into the pMD-20 vector (Takara, Japan) and sequenced. The gene sequences obtained in this study have been deposited in the NCBI GenBank (http://www.ncbi.nlm.nih.gov/genbank/).

TABLE 1 | PCR primers used in this study.

Primers	Primer sequences (5'-3')
cDNA cloning	
LvGSK3β-5RACE1	TTTGCTGTGATGCCTTGCTACT
LvGSK3β-5RACE2	GCAGCACCCTCAGAAGAGTCAA
LvGSK3β-3RACE1	TATAAACCTGGTGTCACGACTG
LvGSK3β-3RACE2	GACTACCCAACAATCGGGAGTT
Genomic DNA cloning	
GLvGSK3β-1F	AGTCTTGAGCCAGGTCTGTCGT
GLvGSK3β-1R	ATTTGTTCTCTTTACCCATACACTCA
GLvGSK3β-2F	TCTCATACATCGTCCTCGGTCTT
GLvGSK3β-2R	TGTGTGGTGGACTCGGCTG
GLvGSK3β-3F	AAGATTACCACAGTTATTGCCACC
GLvGSK3β-3R	CCTTTCGTTGTCACATCTTCATC
GLvGSK3β-4F	TAAAGTAGCAAGGCATCACAGCA
GLvGSK3β-4R	AATAGCGGGAGCAGATGTACG
GLvGSK3β-5F	GTTGTTCCGAAGCCTTGCCT
GLvGSK3β-5R	GCAGGCACAGTCTTGTCAGC
GLvGSK3β-6F	TCTTTCAGTGCTGCCCTTGT
GLvGSK3β-6R	CCCTCAGAAGAGTCAACGGC
Genome walking	
AP1	GTAATACGACTCACTATAGGGC
AP2	ACTATAGGGCACGCGTGGT
LvGSK3β-GWR1	CAGCCTTTCCGAGATGCG
LvGSK3β-GWR2	GTCGCTGCGGAGTCAAAGAA
qPCR	
qLvEF1α-F	GAAGTAGCCGCCCTGGTTG
qLvEF1α-R	CGGTTAGCCTTGGGGTTGAG
qLvGSK3β-F	GGTGGGAGTGGGGAGGGT
qLvGSK3β-R	TCCTTCCAGCCTCATTGTTGTG
qLvDorsal-F	AGATGGAATGATAGAATGGGAAGC
qLvDorsal-R	GTACACCTTTATGGGGTTCTCTATCTC
qLvCactus-F	GGAGGCGTGCCAGTGACTATG
qLvCactus-R	GAAGTAACGATCTGCATTGAAGGG
qLvALF1-F	GGATGTGGTGTCCTGGATGG
qLvALF1-R	GCGTCGTCCTCCGTGATG
qLvALF2-F	GCGAACAAACTCACTGGACTG
qLvALF2-R	ACATGCGACCCTGGAATACAG
qLvALF3-F	GACCTGTCCAACCCTGAGC
qLvALF3-R	TCGCCTCCTCCTCCGTTATC
qLvPEN2-F	TTCTCAGATGTCCGCATTTGC
qLvPEN2-R	ACGTTGTCAAGCCAGGTTTCC
qLvPEN3-F	TACAACGGTTGCCCTGTCTCA
qLvPEN3-R	ACCGGAATATCCCTTTCCCAC
qLvPEN4-F	GGTGCGATGTATGCTACGGAA
qLvPEN4-R	CATCGTCTTCTCCATCAGCCA
qLvCru1-F	GTAGGTGTTGGTGGTGGTTTC
qLvCru1-R	CTCGCAGCAGTAGGCTTGAC
qLvCru2-F	GGTACGTCTGCTGCAAGCC
qLvCru2-R	CTGAGAACCTGCCACGATGG
qLvCru3-F	TCCACAATGGTCAGCGTCAAG
qLvCru3-R	CTGTCCGACAAGCAGTTCCTC
WSSV32678-F	TGTTTTCTGTATGTAATGCGTGTAGGT
WSSV32753-R	CCCACTCCATGGCCTTCA
TaqMan probe-WSSV32706	CAAGTACCCAGGCCCAGTGTCATACGTT
dsRNA synthesis	
dsLvGSK3β-T7F[a]	TAATACGACTCACTATAGGAGGTGCTTCAGGACAAACGC
dsLvGSK3β-T7R[a]	TAATACGACTCACTATAGGTAGCGGGAGCAGATGTACGATA
dsLvGSK3β-F	AGGTGCTTCAGGACAAACGC
dsLvGSK3β-R	TAGCGGGAGCAGATGTACGATA
dsLvDorsal-T7F[a]	TAATACGACTCACTATAGGGTAGGATACAAAGGACCTGCTG
dsLvDorsal-T7R[a]	TAATACGACTCACTATAGGTGGAAATCACCGAAGGCT
dsLvDorsal-F	GTAGGATACAAAGGACCTGCTG
dsLvDorsal-R	TGGAAATCACCGAAGGCT
dsGFP-T7F[a]	TAATACGACTCACTATAGGATGGTGAGCA AGGGCGAGGAG
dsGFP-T7R[a]	TAATACGACTCACTATAGGTTACTTGTACA GCTCGTCCATGCC
dsGFP-F	ATGGTGAGCAAGGGCGAGGAG
dsGFP-R	TTACTTGTACAGCTCGTCCATGCC
EMSA probes	
Bio-probe1	CCTTTCCAATGAAACAGAAAAACCTCGCGCACAGACGA
Unbio-probe1	CCTTTCCAATGAAAGCGCACAGACGACTCCCGAC
Bio-probe2	TAGCGATGAATGGGGTGTGTTTCACTGTGAGAATCTT
Unbio-probe2	TAGCGATGAATGGTGTGAGAATCTTGATTTTGGATGCT
Protein expression	
pAcLvGSK3β-F[b]	CCG**CTCGAG**ATGAGTGGACGACCCAGGACT
pAcLvGSK3β-R[b]	CGG**GGGCCC**ATTATCATTTACAGCAGCAGCT
pAcLvDorsal-F[b]	GGGGTACC**ATCAAA**ATGTTTGTTGCCCAGCGTACTTC
pAcLvDorsal-R[b]	TT**GGGCCC**ATATCAGAAAATATCCAAAACTTACCC
pAcLvCactus-F[b]	GGGGTACC**ATCAAA**ATGTGGCACATTGGCAGTGCCCA
pAcLvCactus-R[b]	TT**GGGCCC**GAAGTAACGATCTGCATTGAAGG

[a]*T7 RNA polymerase promoter sequence are underlined.*
[b]*Nucleotides in bold represent the restriction sites introduced for cloning.*

Genomic Walking

The 5' flanking regulatory regions of LvGSK3β were cloned by genome walking PCR amplification via the GenomeWalker Universal Kit (Clontech, Dalian, China), according to the methods of a previous paper (29). Two pairs of primers, AP1/LvGSK3β-R1 and AP2/LvGSK3β-R2, were used to perform the primary and nested genome walking PCR amplification. The PCR products were cloned into the pMD-20T vector (Takara, Dalian, China) and sequenced. Primers are listed in **Table 1**.

Bioinformatics Analyses

The protein domain topologies and the genome sequences were analysed using the SMART program (http://smart.embl-heidelberg.de/) and Splign program (https://www.ncbi.nlm.nih.gov/sutils/splign/splign.cgi). Protein sequences of GSK3β homologues from other species were selected from the NCBI databases. Multiple sequence alignments were performed using the ClustalX 2.0 program (http://www.ebi.ac.uk/tools/clustalw2) and visualized using GeneDoc. The similarities among the GSK3β proteins were calculated in GeneDoc. The neighbor-joining phylogenetic trees were constructed based on the amino acid sequences using MEGA 5.0 (http://www.megasoft-ware.net/download_form), applying the Poisson distribution substitution

and bootstrapping procedure with a minimum of 1,000 bootstraps. The LvGSK3β promoter sequence was analyzed using Consite (http://consite.genereg.net/).

Tissue Distribution, Immune Challenge, and Gene Expression Analyses

Eleven tissues, including the hemocytes, hepatopancreas, gill, heart, stomach, pyloric caecum, nerve, epithelium, eyestalk, intestine and muscle, were obtained from 10 healthy *L. vannamei* for RNA extraction. For the challenge experiments, 60 healthy *L. vannamei* divided into two groups (n = 30) were intramuscularly injected with WSSV (10^6 copies/g) in the third abdominal segment. *L. vannamei* injected with PBS were used as controls. At 0, 4, 8, 12, 24, 48, and 72 h post-injection (hpi), three animals from each group were randomly sampled for hemocyte, hepatopancreas, gill and intestine collection. Total RNA extraction, reverse transcription and real-time PCR (qPCR) analysis were performed as detailed in previous research (30). The qPCR was performed in a Roche Light Cycler480 thermal cycler (Roche Applied Science, Germany). Elongation factor 1α (EF1α, GenBank accession No. GU136229) was used as the internal control. The expression level of LvGSK3β was calculated using the Livak($2^{-\Delta\Delta Ct}$) method after normalization to LvEF1α. All samples were tested in triplicate. Primer sequences are listed in **Table 1**.

RNA Interference

As described in our previous studies (31, 32), the double-stranded RNAs (dsRNAs) specific to LvGSK3β, LvDorsal and GFP (as control) were synthesized using an *in vitro* transcription method, by using the T7 RiboMAX™ Express RNAi System (Promega, USA), and the quality and amount of dsRNA were checked after annealing via gel electrophoresis. For the RNA interference efficiency determination, healthy *L. vannamei* were injected with 50 μl PBS containing 5 μg LvGSK3β, LvDorsal or GFP dsRNA. At 24 and 48 hpi, the hemocytes from each group were sampled for qPCR to detect the RNAi efficiency, the effects of LvGSK3β on the expression of LvDorsal, LvCactus and nine antimicrobial peptides (AMP) genes and the effects of LvDorsal on the expression of LvGSK3β in *L. vannamei*. Primer sequences are listed in **Table 1**.

WSSV Challenge Experiments in LvGSK3β-Inhibited *L. vannamei*

LvGSK3β was inhibited both on the enzyme activity and mRNA expression levels by injecting with the specific inhibitor and dsRNA. Specific inhibitor of LvGSK3β, named TWS-119 (Selleck Chemicals, USA) was used with the dose refer to the Inhibitory concentration 50 (IC50) (33). At 4, 8 and 12 hpi, the hemocytes from each group were sampled for the detection of inhibition efficiency of LvGSK3β activities, using the GSK3β Kinase Activity Quantitative Detection Kit (Genmed, China). The expression of LvGSK3β was inhibited by RNAi as described above in Section *RNA Interference*. For the mortality test, *L. vannamei* were injected with 50 μl PBS containing or not containing 10^6 WSSV after 8 h of TWS-119 injection or 48 h of dsRNA injection. Cumulative mortality was recorded every 4 h and the differences between groups were analysed using the Mantel–Cox (log-rank χ^2 test) method with the software GraphPad Prism. To investigate the genome copies of WSSV, total DNA was extracted from muscle at 48, 72 and 96 hpi and absolute real-time PCR was performed using primers WSSV32678-F/WSSV32753-R and a Taq Man fluorogenic probe, as in a previous study (34).

Dual-Luciferase Reporter Assays

The gene-specific primers were designed to amplify the ORF of LvGSK3β without introducing a stop codon. The amplified product was cloned into a pAc5.1/V5-His A vector (Invitrogen) to allow subsequent expression of V5-tagged LvGSK3β proteins. All of the vectors with reporter genes used in this paper, including Dorsal, Cactus and AMPs in shrimp or *Drosophila*, were obtained from our previous studies (30, 35). Since no permanent shrimp cell line was available, *Drosophila* Schneider 2 (S2) cells were cultured for promoter activity analysis at 28 °C in Schneider's Insect Medium (Sigma, USA) containing 10% fetal bovine serum (Gibco, USA) for the *in vitro* experiments. After 24 h of culturing in a 96-well plate, the S2 cells of each well were transfected with 0.05 μg of firefly luciferase reporter-gene plasmids, 0.01 μg of pRL-TK renilla luciferase plasmid (Promega, as an internal control) and 0.05 μg of (otherwise indicated) either pAc-LvGSK3β-V5 plasmids or pAc5.1-Basic plasmids (control). Each experiment was repeated in 6 wells. 48 hours post-transfection, the activity of the luciferases was detected in order to calculate the relative ratios of firefly and renilla luciferase activity using the Dual-Glo® Luciferase Assay System kit (Promega, USA), according to the manufacturer's instructions.

Electrophoretic Mobility Shift Assay

An electrophoretic mobility shift assay (EMSA) was performed using a Light Shift Chemiluminescent EMSA kit (Thermo Fisher Scientific, Waltham, MA, USA) according to a previously published method (36). Briefly, the biotin-labeled or unbiotin-labeled probes were designed using the Dorsal binding motif sequence. The mutant probe was designed by deleting the Dorsal-binding motif sequence. All of the probes were synthesized by Life Technologies (Shanghai, China) and the sequences are listed in **Table 1**. RHD domain of Dorsal (Dorsal-RHD) was cloned into the modified pGEX-4T plasmid to get rDorsal-RHD-GST. GST tag of rDorsal-RHD-GST was then removed using rPorcine Enterokinase from Glutathione Resin Kit. The purification productions of rDorsal-RHD-GST and rDorsal-RHD were analyzed using SDS-PAGE and stained with Coomassie blue. Purified rDorsal-RHD protein (10 μg) was incubated with 20 fmol of the probes for the binding reactions. The reactions were separated on a 5% native PAGE gel, transferred to positively charged nylon membranes (Roche, Germany) and cross-linked by UV light. Then, the biotin-labeled DNA on the membrane was detected by chemiluminescence and developed on X-ray film, followed by enhanced chemiluminescence (ECL) visualisation (Tanon, Shanghai, China).

Co-Immunoprecipitation Assays

Co-immunoprecipitation (Co-IP) assays were performed as described in the previous study (36). To investigate the interaction of LvGSK3β with LvDorsal or LvCactus, pAc-LvGSK3β-GFP or pAc5.1-GFP (control) were co-transfected with individual plasmids along with pAc-LvDorsal-HA or pAc-LvCactus-HA into the S2 cells. Forty eight hours post transfection, cells were harvested and washed with ice-cold PBS three times, and then lysed in IP Lysis Buffer with a protease inhibitor cocktail (Sigma, USA). Both Co-IP and reciprocal Co-IP experiments were carried out using anti-HA affinity gel (Sigma, USA) and samples were subjected to SDS-PAGE assay. The precipitated protein was examined using western-blots, with rabbit anti-GFP antibody as the primary antibody, and alkaline phosphatase-conjugated goat anti-rabbit as the secondary antibody (Sigma, USA). A standardized aliquot (5%) of each total input cell lysates was also examined as control.

Statistical Analyses

The relative gene expression data were statistically analysed and all data were presented as mean ± SD. Student's t-tests were used to make comparisons among groups. For the mortality analysis, the data were statistically analysed using GraphPad Prism (Graphpad, San Diego, CA, USA) to obtain Kaplan–Meier plots (log-rank χ^2 test).

RESULTS

Bioinformatics Analyses of LvGSK3β

As shown in **Figure 1A**, the transcript of LvGSK3β was 2,382 bp in length, with a 286 bp 5'-untranslated region (UTR), an 863 bp 3'-UTR containing a poly (A) tail and a 1233 bp open reading frame (ORF) encoded a protein of 410 amino acids at the calculated molecular weight of 46,098.78 Da and an estimated pI of 8.70 (GenBank No. KU641425). Additionally, a protein kinase ATP-binding region signature (between amino acids 61 and 85), a serine/threonine protein kinases active site signature (between amino acids 176 and 188) and two candidate regulatory residues at positions 9 (serine) and 216 (tyrosine) were identified. The genomic sequence of LvGSK3β (GenBank No. MT891030) was also obtained, showing that the LvGSK3β gene consists of eight exons and seven introns (**Figure 1B**). Analysis of the genome sequences showed that all of the exon-intron boundaries in LvMyD88 conform to the consensus GT/AG rule for splicing (37). SMART analysis revealed that the LvGSK3β protein contained one protein kinase domain named STKc_GSK3 between residues 54 and 338 (**Figure 1C**).

Multiple sequence alignment indicated that LvGSK3β shares a high similarity of more than 80% with GSK3β proteins from invertebrates to vertebrates, with the lowest homology (80%) to GSK3β from *Aplysia californica* and the highest homology (100%) to GSK3β from *Penaeus monodon* (**Figure 2A**), which is also a shrimp species. The neighbour-joining (NJ) phylogenetic tree showed that GSK3α and GSK3β were closely related to their own homologues from other species. All of the GSK3β proteins used in this study were separated into five clades including the crustacea, insecta, arachnids, molluscs and vertebrates groups (**Figure 2B**). GSK3β from *L. vannamei*, *P. monodon*, *Daphnia pulex* and *Eriocheir sinensis* were clustered together in the crustacea group. *L. vannamei* GSK3β and *P. monodon* GSK3β showed the closest evolutionary relationship. As shown in **Figure 3A**, the promoter region of LvGSK3β (1,169 bp in length) contained two potential Dorsal binding sites (−700 to −711 bp and −962 to −973 bp) (**Figure 3B**).

Expression Profiles of LvGSK3β in Healthy and WSSV Challenged *L. vannamei*

LvGSK3β was detected in all of the examined tissues (**Figure 4**). The relative expression levels of LvGSK3β in the other tissues were normalised to that in eyestalk, which was the lowest and set as the baseline (1.0). LvGSK3β was expressed highest in the intestine, in which the expression level of LvGSK3β was 14.07-fold over the baseline. As shown in **Figure 4**, LvGSK3β expression in the gill, muscle, nerve, heart, hepatopancreas and hemocyte were all nearly 5.00-fold over the baseline and not significantly different from each other.

Using the four important immune tissues, including hemocytes, hepatopancreas, intestine and gill, LvGSK3β expression after WSSV challenge was investigated using qPCR (**Figure 5**). The expression of LvGSK3β was reduced to different degrees by WSSV challenge in the haemocytes, intestine and gill but not in the hepatopancreas. In the hepatopancreas there was no significant difference in LvGSK3β expression between the infection group and the control group at all of the sampled timepoints (**Figure 5B**). In the hemocyte, LvGSK3β expression was significantly down-regulated starting at 4 hpi, reaching a low-point at 12 hpi at 25.21% of the control. At 72 hpi, LvGSK3β expression recovered to a level not perceptibly different from the control (**Figure 5A**). In the intestine, the expression of LvGSK3β in the infection group was notably lower than the control group at 4, 8 and 72 hpi, with the lowest level at 8 hpi at 21.00% of the control (**Figure 5C**). When compared with the control group, LvGSK3β expression in the gill of the infection group was significantly decreased at 12, 24 and 48 hpi by 72.02%, 54.78% and 65.16%, respectively (**Figure 5D**).

Function of LvGSK3β in WSSV Infection

Refer to IC50 of TWS-119 in animals (33), a dose of 5 μg/g TWS-119 per shrimp was chosen for the LvGSK3β-inhibition test. As **Figure 6A** shows, the enzyme activity of LvGSK3β was significantly reduced at 4, 8 and 12 hpi, with the lowest level at 8 hpi, which was the timepoint chosen for the following WSSV challenge experiment. In the TWS-119 + WSSV group, the survival rates of *L. vannamei* were notably higher than that of the PBS + WSSV group starting at 56 hpi (**Figure 6B**). At 124 hpi, the survival rate of *L. vannamei* in the TWS-119 + WSSV group was 43.60% but the *L. vannamei* in the PBS+WSSV group had all died. The final survival rate of *L. vannamei* at 144 hpi was 10.30% for the TWS-119 + WSSV group. Consistently, the WSSV genome copies in the muscle of the TWS-119 injected *L. vannamei* at 48, 72 and 96 hpi were significantly less than those in the PBS injected *L. vannamei* (**Figure 6C**).

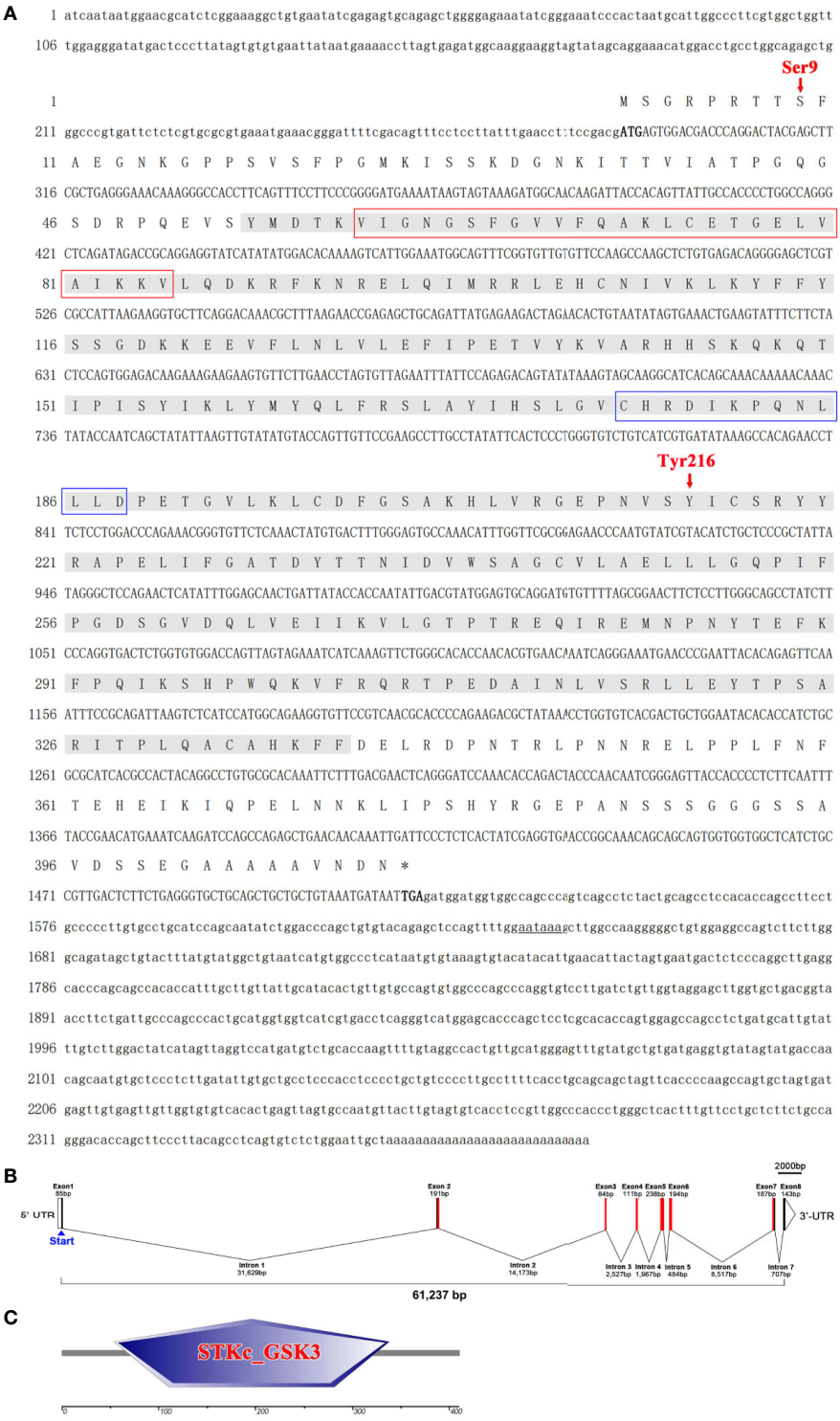

FIGURE 1 | The sequence analysis of LvGSKβ. **(A)** The full-length cDNA sequence and deduced amino acid sequences of LvGSKβ. The ORF of the nucleotide sequence was shown in upper-case letters, while the 5' and 3'-UTR sequences were shown in lowercase. The nucleotide (lower row) and deduced amino acid (upper row) sequences are shown and numbered on the left. The translation initiation codon (ATG) and stop codon (TAA) are in bold. The STKc_GSK3 domain is shaded and protein kinase ATP-binding region, serine/threonine protein kinases active site and two candidate regulatory residues (Ser9 and Tyr216) are marked out. The poly A signal (aataaa) are underlined. **(B)** Gene structure of LvGSKβ. Boxes in represent exons, and lines in represent introns. The numbers indicate the length (bp) of the exons and introns. **(C)** Structural features of LvGSKβ. Conserved domains of LvGSKβ are predicted by SMART program.

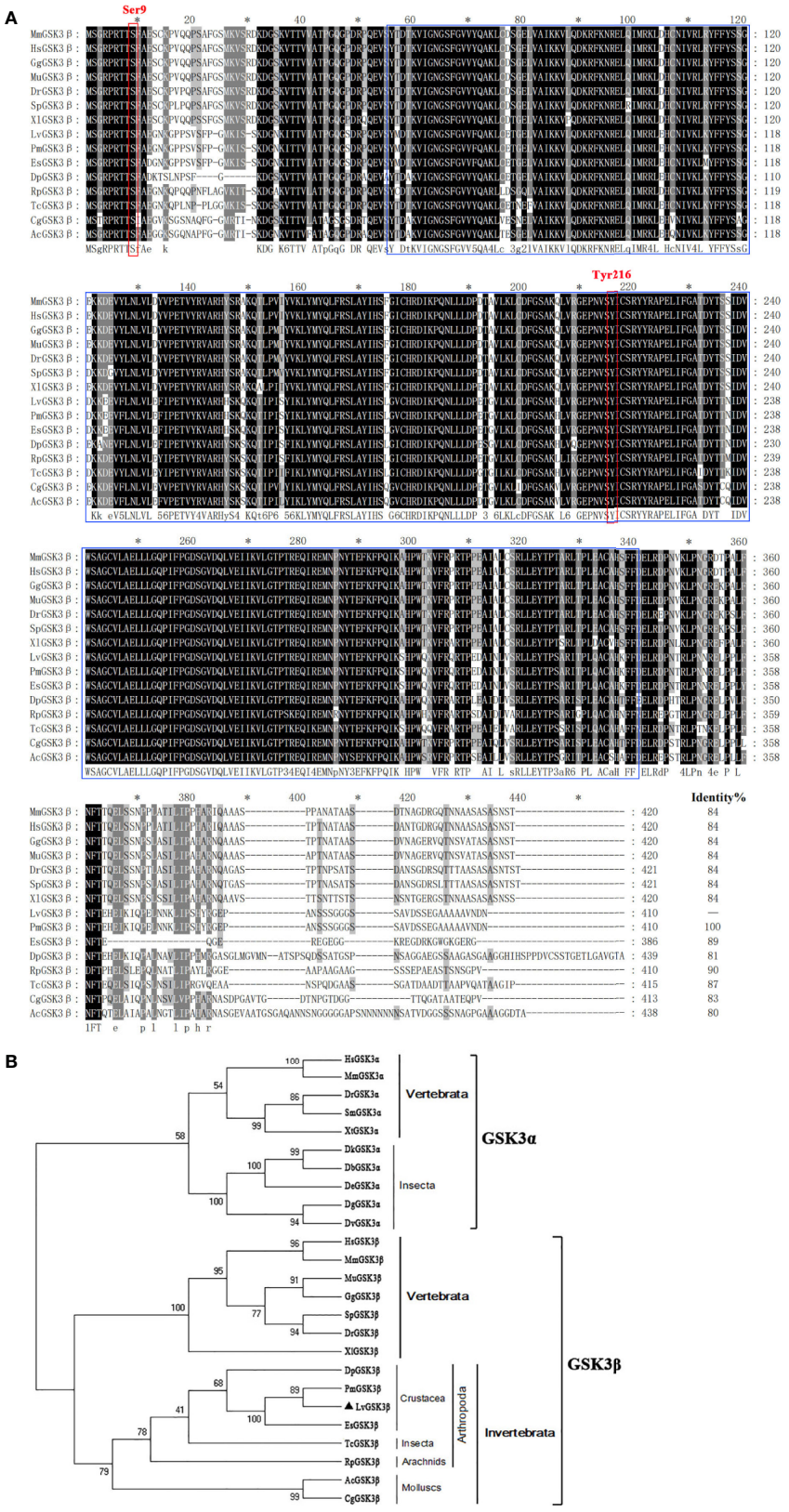

FIGURE 2 | Continued

FIGURE 2 | Multiple sequence alignment and phylogenetic tree analysis of GSK3β from *L. vannamei* and other species. **(A)** Multiple sequence alignment of GSK3β proteins. The amino acid sequences of GSK3β from typical organisms were aligned using the ClustalX 2.0 program. The black shade represent 100% identity, dark gray represented 80% identity, light gray represented 60% identity. The region of STKc_GSK3 domain was boxed in blue and two candidate regulatory residues Ser9 and Tyr216 were boxed in red. **(B)** Neighborjoining phylogenetic tree analysis. A rooted tree was constructed via the neighbor-joining method and was bootstrapped 1000 times using MEGA 5.0 software (http://www.megasoftware.net/index.html). LvGSK3β is denoted by ▲. The genes used are listed as follows, GSK3α isoform: HsGSK3α, *Homo sapiens* GSK3α (Accession No. NP_001139628); MmGSK3α, *Mus musculus* GSK3α (Accession No. AAD39258); DrGSK3α, *Danio rerio* GSK3α (Accession No. NP_571465); DrGSK3α, *Scophthalmus maximus* (Accession No. AWP21281); DrGSK3α, *Xenopus tropicalis* (Accession No. XP_002936450); DbGSK3α, *Drosophila bipectinata* (Accession No. XP_017108632); DeGSK3α, *Drosophila elegans* (Accession No. XP_017115500); DtGSK3α, *Drosophila takahashii* (Accession No. 017013230); DvGSK3α, *Drosophila virilis* (Accession No. XP_002051677); DgGSK3α, *Drosophila grimshawi* (Accession No. XP_001988855); GSK3β isoform: LvGSK3β, *L. vannamei* GSK3β (Accession No. KU641425); HsGSK3β, *Homo sapiens* GSK3β (Accession No. AAH00251); MmGSK3β, *Mus musculus* GSK3β (Accession No. AAD39258); MuGSK3β, *Melopsittacus undulatus* GSK3β (Accession No. XP_005143085); GgGSK3β, *Gallus gallus* GSK3β (Accession No. XP_004938236); SpGSK3β, *Schizothorax prenanti* GSK3β (Accession No. AKA09693); DrGSK3β, *Danio rerio* GSK3β (Accession No. NP_571456); XlGSK3β, *Xenopus laevis* GSK3β (Accession No. AAA84444); DpGSK3β, *Daphnia pulex* GSK3β (Accession No. EFX72595); PmGSK3β, *Penaeus monodon* GSK3β (Accession No. QIK00339); EsGSK3β, *Eriocheir sinensis* GSK3β (Accession No. ANZ22981); TcGSK3β, *Tribolium castaneum* GSK3β (Accession No. XP_008192199); RpGSK3β, *Rhipicephalus pulchellus* GSK3β (Accession No. JAA60305); AcGSK3β, *Aplysia californica* GSK3β (Accession No. XP_005107895); CgGSK3β, *Crassostrea gigas* GSK3β (Accession No. EKC35379).

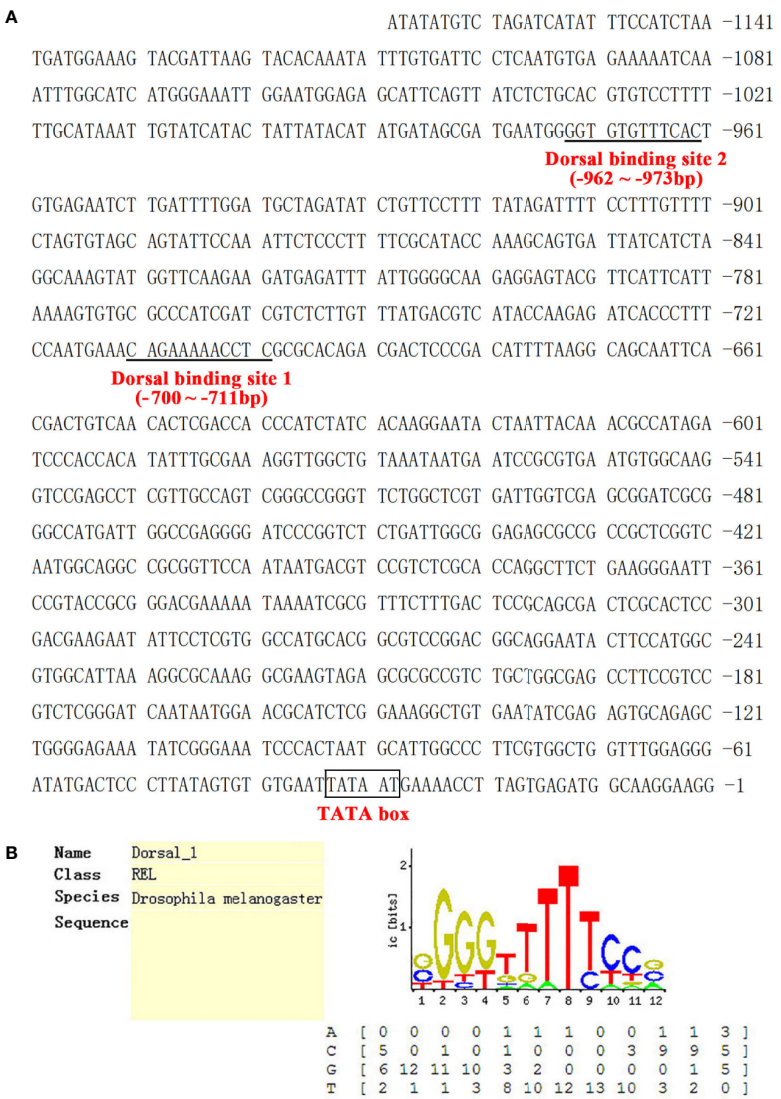

FIGURE 3 | The sequence analysis of the LvGSK3β promoter. **(A)** The promoter sequence of LvGSK3β. The predicted TATA-box was boxed and the putative Dorsal binding sites were underlined. **(B)** Prediction of the Dorsal binding sites sequence in LvGSK3β promoter using Consite software.

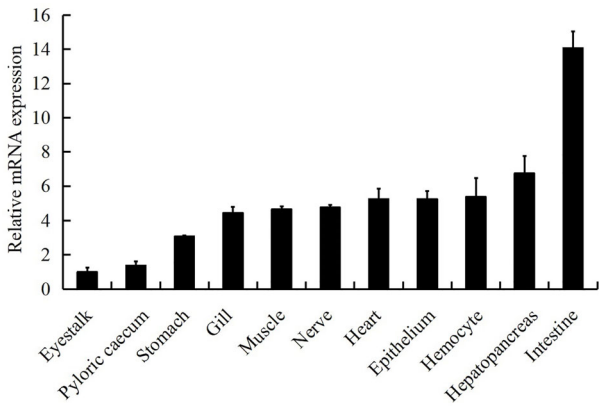

FIGURE 4 | Tissue distribution of LvGSK3β expression in healthy *L. vannamei*. Ten animals were used for tissue sampling. The expression of LvGSK3β in eyestalk was set as 1.0. LvEF1α was used as the internal control to normalize the cDNA template used for qPCR analysis. The results were based on three independent experiments and expressed as mean values ± SD.

RNAi was also performed to investigate the role of LvGSK3β during WSSV infection. qPCR was used to check the silencing efficiency of LvGSK3β. As shown in **Figure 6D**, at 48 h after injection of LvGSK3β dsRNA, the expression levels of LvGSK3β at 24 and 48 hpi were significantly down-regulated to ~0.43-fold and ~0.21-fold of the GFP dsRNA injection group, respectively. Similarly as for the results when LvGSK3β were inhibited by TWS-119, the survival rates of *L. vannamei* in the LvGSK3β dsRNA + WSSV group were also significantly higher than that of the GFP dsRNA + WSSV group, and the final survival rate of *L. vannamei* at 144 hpi was 53.85 and 14.29% for the TWS-119 + WSSV group and GFP dsRNA + WSSV group, respectively (**Figure 6E**). Furthermore, the viral loads of the LvGSK3β dsRNA + WSSV group were significantly lower than those of the GFP dsRNA + WSSV control group, with a ~15.52-fold, ~40.78-fold and~7.06-fold decrease at 48, 72 and 96 h, respectively (**Figure 6F**).

Influence of LvGSK3β on Expression of NF-κB Related Genes in *L. vannamei*

NF-κB has important roles in the regulation of AMP genes in shrimp (2). Considering the fact that the promoter of LvGSK3β contained two potential Dorsal binding sites, the expression of NF-κB related genes (Dorsal, Cactus and AMP genes) in LvGSK3β dsRNA injected shrimp were investigated to primarily explore the underlying mechanism of LvGSK3β during WSSV infection. When compared with the control GFP dsRNA, the LvGSK3β dsRNA significantly increased LvDorsal

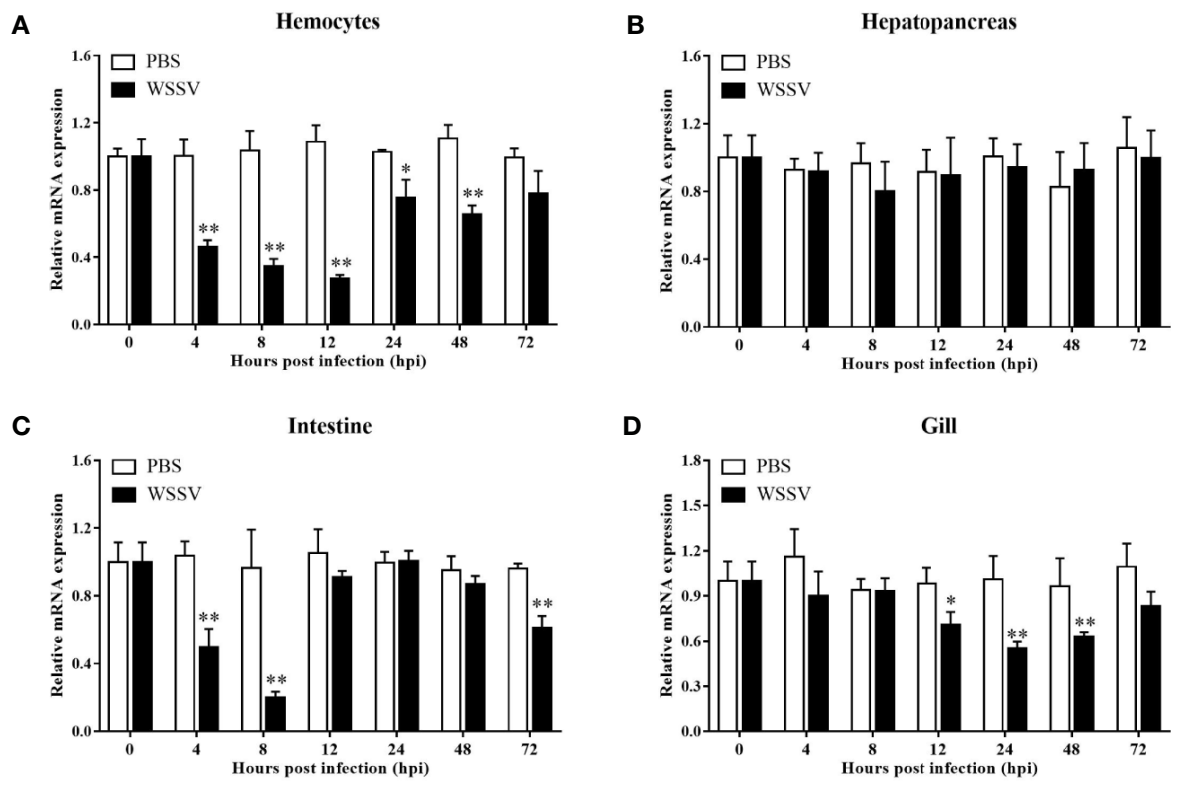

FIGURE 5 | Expression profiles of LvGSK3β in haemocytes **(A)**, hepatopancreas **(B)**, gill **(C)** and intestine **(D)** from WSSV or PBS challenged *L. vannamei*. qPCR was performed in triplicate for each sample. Expression values were normalized to those of LvEF1α using the Livak ($2^{-\Delta\Delta Ct}$) method and the data were provided as the means ± SD of triplicate assays. The statistical significance was calculated using Student's t-test (*$p < 0.05$, **$p < 0.01$).

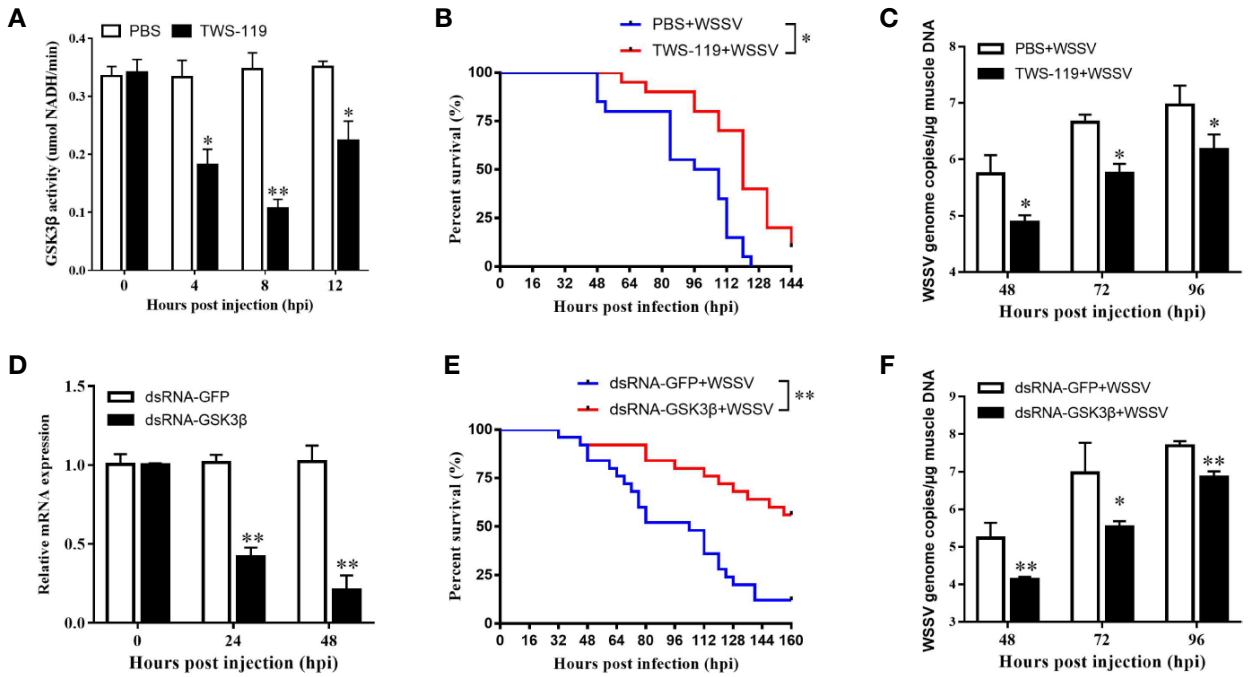

FIGURE 6 | Functional analysis of LvGSK3β in WSSV infection. The inhibiting efficiencies of LvGSK3β by TWS-119 **(A)** or dsRNA-LvGSK3β **(C)** injection. The detection of LvGSK3β activities and expression was performed in triplicate for each sample. Expression values were normalized to those of LvEF1α using the Livak ($2^{-\Delta\Delta Ct}$) method and the data were provided as the means ± SD of triplicate assays. Cumulative mortalities of TWS-119 **(B)** and dsRNA-LvGSK3β **(D)** treated *L. vannamei* during WSSV infection. The experiments were performed two times with identical results. Differences in cumulative mortality levels between treatments were analyzed by using the log-rank χ^2 test (*p <0.05, **p <0.01). WSSV genome copies in muscle tissue of TWS-119 **(C)** and dsRNA-LvGSK3β **(E)** treated *L. vannamei* post WSSV infection. Absolute real-time PCR was performed using primers WSSV32678-F/WSSV32753-R and a Taq Man fluorogenic probe. Each bar represented the mean ± SD of three samples. Statistically significant differences were represented with asterisks (**p < 0.01 and * p < 0.05).

expression but decreased LvCactus expression in the haemocyte of *L. vannamei*. Consistent with this, the expression of several AMP genes, including three antilipopolysaccharide factors (LvALF1, LvALF2, LvALF3), two penaeidins (LvPEN3, LvPEN4) and one crustin (LvCRU1) were significantly up-regulated at 48 h after injection with LvGSK3β dsRNA (**Figure 7A**).

Influence of LvDorsal on Expression of LvGSK3β in *L. vannamei*

The expression of LvGSK3β in LvDorsal dsRNA injected shrimp was also investigated. When LvDorsal was knocked down by dsRNA injection, the expression of LvGSK3β in the hemocyte of *L. vannamei* was significantly higher than the control GFP dsRNA injected group (**Figure 7B**).

Regulatory Effects of LvGSK3β on the Promoter Activities of NF-κB Related Genes

Previous results *in vivo* showed that LvGSK3β could regulate the expression of NF-κB related genes, so the effects of LvGSK3β on the promoter activities of NF-κB related genes were further explored *in vitro* using dual-luciferase reporter assays. As shown in **Figure 8**, overexpression of LvGSK3β dramatically down-regulated the promoter activities of LvDorsal (56.61%) and the AMP genes including the *L. vannamei* AMPs LvALF2 (65.80%), LvPEN2 (28.29%), LvPEN3 (41.18%), LvCru1 (65.96%), LvCru2 (59.04%) and LvCru3 (64.23%), the *Penaeus monodon* AMP PmPEN536 (66.05%), and the *Drosophila* AMPs, DmCecA (44.37%), DmDpt (49.16%), DmDrs (65.76%) and DmDef (21.23%). However, the promoter activity of LvCactus was significantly induced by ~1.88 fold.

Interaction Between LvDorsal and the LvGSK3β Promoter

To further investigate the interaction between LvDorsal and the LvGSK3β promoter, EMSA was performed using the purified 6His-tagged RHD domain of Dorsal protein (rDorsal-RHD) expressed in *E. coli* cells. As shown in **Figure 9**, rLvDorsal-RHD, but not the control rTrx, effectively retarded the mobility of the bio-labeled probes 1 and 2. The DNA/protein complex was markedly reduced by the competitive unlabeled probe 1 at the level of 10×, 50× and 100×. Contrarily, the DNA/protein complex was only faintly reduced by the competitive 10× and 50× unlabeled probe 2 but markedly reduced by the competitive 100× unlabeled probe 2. These results indicate the specificity of the interaction between rLvDorsal-RHD and the two probes.

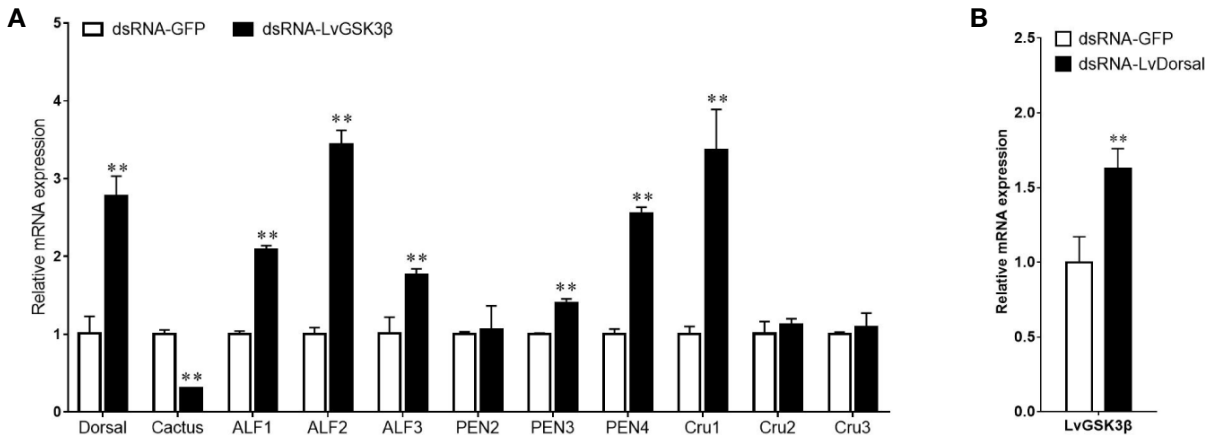

FIGURE 7 | Influence of LvGSK3β on expression of NF-κB related genes **(A)** and LvDorsal on expression of LvGSK3β **(B)** in *L. vannamei* The mRNA levels of NF-κB related genes and LvGSK3β in *L. vannamei* at 48 h post dsRNA injection were detected using qPCR with LvEF1α gene as internal control. For each gene, the value in the dsRNA-GFP injected sample was set as the baseline (1.0) for comparison (**$p < 0.01$).

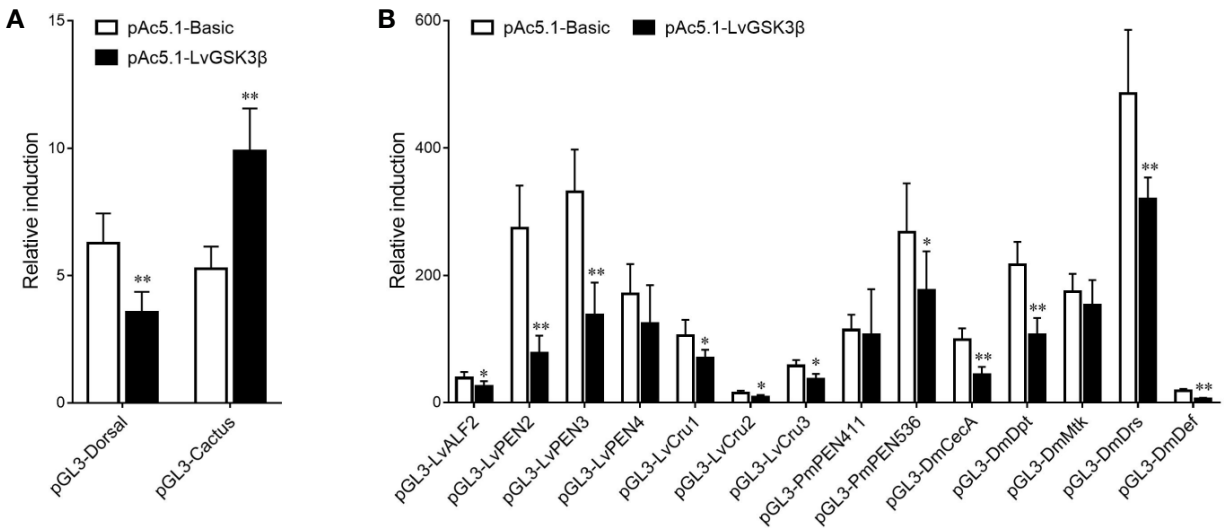

FIGURE 8 | Effects of LvGSK3β on the promoter activities of NF-κB related genes in *L. vannamei.* **(A)** LvDorsal and LvCactus promoters; **(B)** AMPs promoters. *Drosophila* S2 cells were transfected with the protein expression vectors (LvGSK3β and the pAc5.1 empty vector as a control), the reporter gene plasmid, and the pRL-TK Renilla luciferase plasmid (as an internal control). After 48 h, the cells were harvested for measurement of luciferase activity using the dualluciferase reporter assay system (Promega). The bars indicated the mean ± SD of the luciferase activity (n = 6). The statistical significance was calculated using Student's t-test (*$p < 0.05$, **$p < 0.01$).

Interaction of LvGSK3β With LvDorsal and LvCactus

To explore whether the interaction of LvGSK3β with LvDorsal or LvCactus occurs in *L. vannamei*, Co-IP analyses were carried out by using the S2 cell line. GFP-tagged LvGSK3β or GFP (as a control) were co-expressed with HA-tagged LvDorsal or HA-tagged LvCactus, respectively. The results showed that both LvDorsal-HA and LvCactus-HA co-precipitated with GFP-tagged LvGSK3β but not the control GFP (**Figures 10A, B**), indicating an interaction of LvGSK3β with LvDorsal and LvCactus.

DISCUSSION

Previous studies on GSK3, concentrating on vertebrates, have shown that it is a multifunctional enzyme involved in glycogen metabolism, insulin signaling, inflammatory response and innate

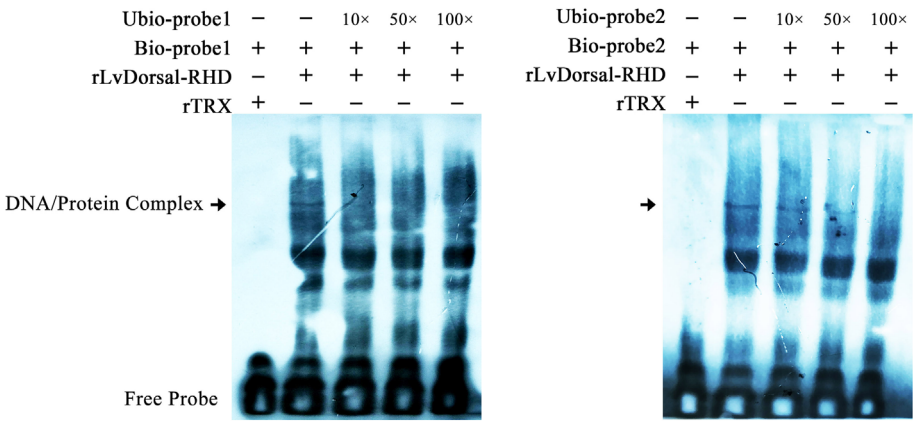

FIGURE 9 | Dorsal interacted with the predicted binding motifs of LvGSK3β promoter *in vitro*. An EMSA was performed using biotin-labeled (Bio-) or unlabeled (Unbio-) probes containing or not containing the Dorsal binding motifs of LvGSK3β. Biotin-labeled or mutated biotin-labeled dsDNA probes were incubated with 10 μg of purified rLvDorsal-RHD protein. Unlabeled probe was added to compete with binding, and an rTrx protein was used as a control. Probe1 and probe 2 referred to the Dorsal binding motif 1 and 2, respectively. All experiments were performed three times with similar results.

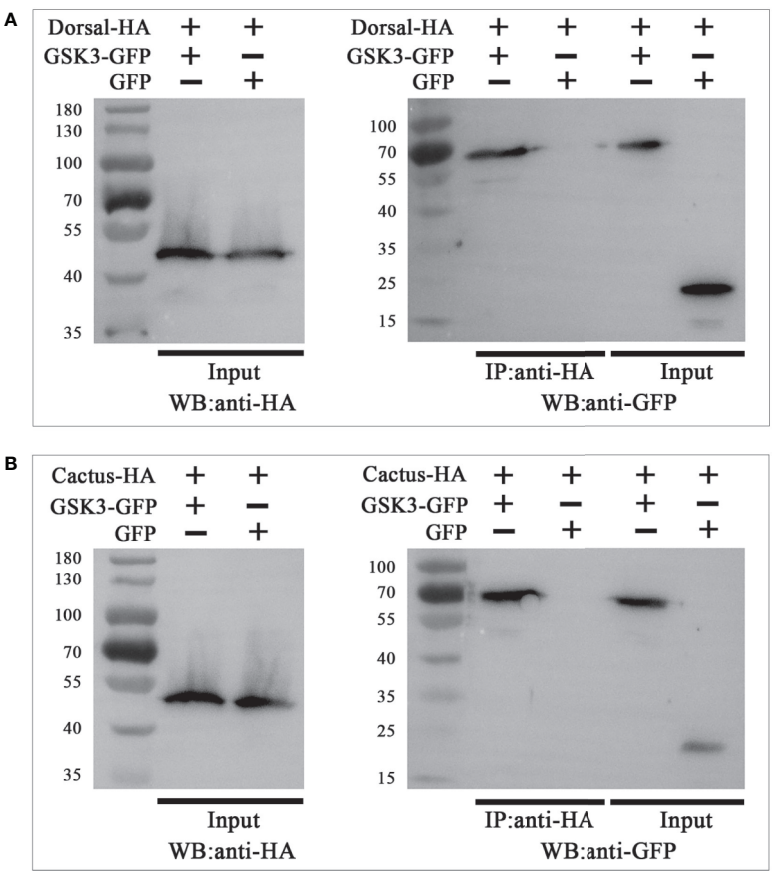

FIGURE 10 | LvGSK3β interacted with LvDorsal **(A)** and LvCactus **(B)**. Co-immunoprecipitation (Co-IP) assays showed that the GFP-tagged LvGSK3β but not the control GFP protein can be co-precipitated by HA-tagged LvDorsal or LvCactus. Input: western-blotting analysis of the input cell lysates (5%) before immunoprecipitation.

immunity (38). However, the function of GSK3 in invertebrates has rarely been reported. In the present study, a GSK3β homolog was cloned from *L. vannamei* (LvGSK3β) and was found to be strongly downregulated *in vivo* after WSSV infection, while the inhibition of LvGSK3β significantly increased the survival rate of *L. vannamei* in response to WSSV infection. The effects of inhibition and overexpression of LvGSK3β on NF-κB related genes were the opposite. In addition, interaction between LvDorsal and the LvGSK3β promoter, and the interaction of LvGSK3β with LvDorsal/LvCactus were revealed. All of the results indicated that LvGSK3β has a negative effect on the shrimp by negatively regulating NF-κB activity in *L. vannamei* when it is infected by WSSV.

In vertebrates, GSK3 comprises two homologues, GSK3α and GSK3β, encoded by two similar genes, which share similar Serine/Threonine kinase domains but differ substantially in their termini (39). Unique to the GSK3α is an N-terminal domain consisting of 63 residues that is glycine-rich. Resembling the previously identified GSK3β, *L. vannamei* GSK3β has Ser9 and Tyr216 phosphorylation sites, a STKc_GSK3 domain but no glycine-rich extension at the N-terminus, and the NJ phylogenetic tree showed that LvGSK3β belonged to the cluster of GSK3β homologues from other species, which suggested that LvGSK3β was a member of the β isoform of the GSK3 family in *L. vannamei*. Based on the information on NCBI, most of the GSK3 genes identified were GSK3β in invertebrates including *P. monodon*, *D. pulex* and *E. sinensis*, and GSK3α was only reported in *Drosophila* species. In fact, only GSK3β could be found in *L. vannamei* through scanning the transcriptome and genomic data published on NCBI. The reason why GSK3β but not GSK3α is common in invertebrates has not yet been revealed.

In *E. sinensis*, GSK3β regulated hemocyte phagocytosis in the immune response (40). A previous study reported that LvGSK3β played an important role in shrimp immunomodulation, and shrimp might promote the apoptosis to restrain WSSV infection by inhibition of LvGSK3β (18). Similarly, it was also found that LvGSK3β expression decreased with WSSV challenge, and LvGSK3β inhibition by injection with a specific inhibitor or RNAi reduced the WSSV loads in *L. vannamei* in this study. More intuitively, our study showed that the survival rates of LvGSK3β inhibited *L. vannamei* after the WSSV challenge was greater. All of the results further verified the close relationship between LvGSK3β and WSSV infection, implying the positive function of LvGSK3β on WSSV replication. To our knowledge, this study was a rare report about the role GSK3β plays during viral infection in invertebrates. Comparatively speaking, many more studies about the effect of GSK3β on viral replication have been performed on vertebrates. In humans, there was a significant drop in GSK3β expression in response to Japanese encephalitis virus (JEV) infection (41), and the replication of HCV (15), HIV-1 (16), varicella zoster virus (VZV) (42) and severe acute respiratory syndrome coronavirus (SARS-CoV) (43) was decreased by silencing GSK3β. In addition, GSK3β functioned in inhibiting porcine epidemic diarrhoea virus (PEDV) replication *in vitro* (44). Thus, it can be seen that the effect of GSK3β on viral replication is consistent in vertebrates and invertebrates, indicating the functional conservatism of GSK3β in different animal species.

As an intersection of multiple cell signaling pathways such as Wnt/β-catenin, NF-κB and PI3K/AKT, the function of GSK3β in proliferation, differentiation, apoptosis, and immune responses could not be ignored (10–12). This raises difficulties for clarifying the role of GSK3β and the associated regulatory mechanisms regarding virology. Nevertheless, great progress has been made in humans. For example, the downregulation of GSK3β resulted in a long viral persistence of JEV by enhancing the stability of cyclin D1 (39). For the herpes simplex virus type 1 (HSV-1) -induced Kaposi's sarcoma-associated herpesvirus (KSHV) reactivation, the activation of the MAPK and the PTEN/PI3K/AKT/GSK3β pathways was required (45). VZV benefited its own survival and replication through activating AKT signaling that induces the phosphorylation of GSK3β, which in turn blocks Bad's pro-apoptotic pathway (40). In addition, the decrease of GSK3β expression can also inhibit replication of the influenza virus by positively regulating the virus-induced host cell apoptosis (46). Similar results were presented in the functional study of GSK3β in shrimp. LvGSK3β play an important role in WSSV clearance by mediating apoptosis (18). Consistently, this study found that the expression of LvGSK3β was inhibited in *L. vannamei* upon WSSV challenge and the mortality rates of LvGSK3β-inhibited *L. vannamei* in response to WSSV infection were significantly reduced when compares with the control group. Besides, LvGSK3β expression has a great impact on the expression and transcriptional regulation of LvDorsal, LvCactus and AMP genes, and LvGSK3β interacted with LvDorsal and LvCactus. Furthermore, knockdown of LvDorsal significantly reduced the expression of LvGSK3β. All these results implied that LvGSK3β plays a role during virus infection by regulating NF-κB activity in *L. vannamei* and there was a feedback regulatory loop existed. Briefly speaking, the silence of LvGSK3β by dsRNA resulted in upregulation of LvDorsal and downregulation of LvCactus. The downregulation of LvCactus could indirectly increase the expression of LvDorsal, followed by the increased expression of AMP genes which acted as important effectors of host defense against WSSV (24). At the same time, the increase of LvDorsal brought about the downregulation of LvGSK3β could enhance the effect. When suffer WSSV infection, the inhibition of LvGSK3β expression was also strengthened. All the series of reactions led to the final result was that the survival rates of LvGSK3β-inhibited *L. vannamei* significantly increased when suffer WSSV infection. To our knowledge, although the role of the GSK3β or NF-κB related signaling pathways in viral infection and the control of NF-κB signaling activity by GSKβ has been confirmed separately (18–23, 37), no previous studies have explored the functional mechanisms of GSKβ in viral infection from the perspective of the regulation of NF-κB; therefore, this study is the first such report.

In conclusion, this study revealed that LvGSK3β has a negative effect on *L. vannamei* by negatively regulating NF-κB activity when it is infected by WSSV. The results detail the immune mechanisms and provide a theoretical basis for enhancing the immunity and improving the disease resistance

of shrimp, which lays the foundation for the establishment of effective prevention and control of WSS.

DATA AVAILABILITY STATEMENT

The raw data supporting the conclusions of this article will be made available by the authors, without undue reservation.

AUTHOR CONTRIBUTIONS

The experiments were conceived and designed by SZ and LS. SZ, L-LZ, CH, HY, and SY collected samples and performed the experiments. MD, SZ, and LS analyzed the data and completed the writing of the paper. All authors contributed to the article and approved the submitted version.

FUNDING

This work was supported by the National Key R&D Program of China (Grant No. 2019YFD0900200), National Natural Science Foundation of China (Grant Nos. 31702377 and 32072988), General Program of Natural Science Foundation of Guangdong Province, China (Grant Nos. 2018A030313963 and 2020A1515010319) and Research Fund Program of Guangdong Provincial Key Laboratory of Marine Resources and Coastal Engineering.

ACKNOWLEDGMENTS

We would like to acknowledge NATIVE English Editing (www.nativeee.com) for its linguistic assistance during the preparation of this manuscript.

REFERENCES

1. Alday-Sanz V, Brock J, Flegel TW, Mcintosh R, Bondad-Reantaso M, Salazar M, et al. Facts, truths and myths about spf shrimp in aquaculture. *Rev Aquaculture* (2018) 1:1–9. doi: 10.1111/raq.12305
2. Li CZ, Weng SP, He JG. WSSV-host interaction: Host response and immune evasion. *Fish Shellfish Immunol* (2019) 84:558–71. doi: 10.1016/j.fsi.2018.10.043
3. Thitamadee S, Prachumwat A, Srisala J, Jaroenlak P, Salachan PV, Sritunyalucksana K, et al. Review of current disease threats for cultivated penaeid shrimp in Asia. *Aquaculture* (2016) 452:69–87. doi: 10.1016/j.aquaculture.2015.10.028
4. Qiu L, Chen MM, Wan XY, Li C, Zhang QL, Wang RY, et al. Characterization of a new member of Iridoviridae, Shrimp hemocyte iridescent virus (SHIV), found in white leg shrimp (*Litopenaeus vannamei*). *Sci Rep* (2017) 7(1):11834. doi: 10.1038/s41598-017-10738-8
5. Liao XZ, Wang CG, Wang B, Qin HP, Hu SK, Zhao JC, et al. Research into the hemocyte immune response of *Fenneropenaeus merguiensis* under decapod iridescent virus 1 (DIV1) challenge using transcriptome analysis. *Fish Shellfish Immunol* (2020) 104:8–17. doi: 10.1016/j.fsi.2020.05.053
6. Flegel TW, Sritunyalucksana K. Shrimp molecular responses to viral pathogens. *Marine Biotechnol (NewYork NY)* (2011) 13(4):587–607. doi: 10.1007/s10126-010-9287-x
7. Larner J, Villar-Palasi C, Goldberg ND, Bishop JS, Huijing F, Wenger JI, et al. Hormonal and non-hormonal control of glycogen synthesis-control of transferase phosphatase and transferase I kinase. *Adv Enzyme Regul* (1968) 6:409–23. doi: 10.1016/0065-2571(68)90025-3
8. Patel P, Woodgett JR. Glycogen Synthase Kinase 3: A Kinase for All Pathways? *Curr Topics Dev Biol* (2017) 123:277–302. doi: 10.1016/bs.ctdb.2016.11.011
9. Woodgett JR. Molecular cloning and expression of glycogen synthase kinase-3/factor A. *EMBO J* (1990) 9(8):2431–8. doi: 10.1002/j.1460-2075.1990.tb07419.x
10. Lin J, Song T, Li C, Mao W. GSK-3β in DNA repair, apoptosis, and resistance of chemotherapy, radiotherapy of cancer. *Biochim Biophys Acta (BBA) - Mol Cell Res* (2020) 1867(5):118659. doi: 10.1016/j.bbamcr.2020.118659
11. Zhang S, Chen C, Ying J, Wei C, Qi F. Alda-1, an Aldehyde Dehydrogenase 2 Agonist, Improves Cutaneous Wound Healing by Activating Epidermal Keratinocytes *via* Akt/GSK-3β/β-Catenin Pathway. *Aesthetic Plast Surg* (2020) 44(3):993–1005. doi: 10.1007/s00266-020-01614-4
12. Terzioglu-Usak S, Nalli A, Elibol B, Ozek E, Hatiboglu MA. Anvirzel™ regulates cell death through inhibiting GSK-3 activity in human U87 glioma cells. *Neurol Res* (2020) 42(1):68–75. doi: 10.1080/01616412.2019.1709744
13. Müller KH, Kakkola L, Nagaraj AS, Cheltsov AV, Anastasina M, Kainov DE. Emerging cellular targets for influenza antiviral agents. *Trends Pharmacol ences* (2012) 33(2):89–99. doi: 10.1016/j.tips.2011.10.004
14. Hirata N, Suizu F, Matsuda-Lennikov M, Edamura T, Bala J, Noguchi M. Inhibition of Akt kinase activity suppresses entry and replication of influenza virus. *Biochem Biophys Res Commun* (2014) 450(1):891–8. doi: 10.1016/j.bbrc.2014.06.077
15. Saleh M, Rüschenbaum S, Welsch C, Zeuzem S, Moradpour D, Gouttenoire J, et al. Glycogen Synthase Kinase 3β Enhances Hepatitis C Virus Replication by Supporting miR-122. *Front Microbiol* (2018) 9:2949. doi: 10.3389/fmicb.2018.02949
16. Guendel I, Iordanskiy S, Van DR, Kylene KH, Mohammed S, Ravi D, et al. Novel neuroprotective GSK-3β inhibitor restricts Tat-mediated HIV-1 replication. *J Virol* (2014) 88(2):1189–208. doi: 10.1128/JVI.01940-13
17. Sarhan MA, Abdel-Hakeem MS, Mason AL, Tyrrell DL, Houghton M. Glycogen synthase kinase 3β inhibitors prevent hepatitis C virus release/assembly through perturbation of lipid metabolism. *Sentific Rep* (2017) 7(1):2495. doi: 10.1038/s41598-017-02648-6
18. Ruan LW, Liu HC, Shi H. Characterization and function of GSK3β from *Litopenaeus vannamei* in WSSV infection. *Fish Shellfish Immunol* (2018) 82:220–8. doi: 10.1016/j.fsi.2018.08.032
19. Cortés-Vieyra R, Bravo-Patiño A, Valdez-Alarcón JJ, Juárez MC, Finlay BB, Baizabal-Aguirre VM. Role of glycogen synthase kinase-3 beta in the inflammatory response caused by bacterial pathogens. *J Inflammation (London England)* (2012) 9(1):23. doi: 10.1186/1476-9255-9-23
20. Steinbrecher KA, Wilson W, Cogswell PC, Baldwin AS. Glycogen synthase kinase 3beta functions to specify gene-specific, NF-kappaB-dependent transcription. *Mol Cell Biol* (2005) 25(19):8444–55. doi: 10.1128/MCB.25.19.8444-8455.2005
21. Martin M, Rehani K, Jope RS, Michalek SM. Toll-like receptor-mediated cytokine production is differentially regulated by glycogen synthase kinase 3. *Nat Immunol* (2005) 6(8):777–84. doi: 10.1038/ni1221
22. Choi JY, Park HJ, Lee YJ, Byun J, Youn YS, Choi JH, et al. Upregulation of Mer receptor tyrosine kinase signaling attenuated lipopolysaccharide-induced lung inflammation. *J Pharmacol Exp Ther* (2013) 344(2):447–58. doi: 10.1124/jpet.112.199778
23. Deng LY, Zeng QR, Wang MS, Cheng AC, Jia RY, Chen S, et al. Suppression of NF-κB Activity: A Viral Immune Evasion Mechanism. *Viruses* (2018) 10(8):409. doi: 10.3390/v10080409
24. Li CZ, Wang S, He JG. The Two NF-κB Pathways Regulating Bacterial and WSSV Infection of Shrimp. *Front Immunol* (2019) 10:1785. doi: 10.3389/fimmu.2019.01785
25. Panichareon B, Khawsak P, Deesukon W, Sukhumsirichart W. Multiplex real-time PCR and high-resolution melting analysis for detection of white spot syndrome virus, yellow-head virus, and Penaeus monodon densovirus in penaeid shrimp. *J Virol Methods* (2011) 178(1-2):16–21. doi: 10.1016/j.jviromet.2011.07.010
26. Zhang S, Li CZ, Yang QH, Dong XH, Chi SY, Liu HY, et al. Molecular cloning, characterization and expression analysis of Wnt4, Wnt5, Wnt6, Wnt7, Wnt10 and Wnt16 from *Litopenaeus vannamei*. *Fish Shellfish Immunol* (2016) 54:445–55. doi: 10.1016/j.fsi.2016.04.028
27. Liao XZ, Wang CG, Wang B, Qin HP, Hu SK, Wang P, et al. Comparative Transcriptome Analysis of *Litopenaeus vannamei* Reveals That Triosephosphate Isomerase-Like Genes Play an Important Role During Decapod Iridescent Virus 1 Infection. *Front Immunol* (2020) 11:1–17. doi: 10.3389/fimmu.2020.01904

28. Zuo HL, Gao JF, Yuan J, Deng HW, Yang LW, Weng SP, et al. Fatty acid synthase plays a positive role in shrimp immune responses against *Vibrio parahaemolyticus* infection. *Fish Shellfish Immunol* (2017) 60:282–8. doi: 10.1016/j.fsi.2016.11.054
29. Zhang S, Li CZ, Yan H, Qiu W, Chen YG, Wang PH, et al. Identification and function of myeloid differentiation factor 88 (MyD88) in *Litopenaeus vannamei*. *PloS One* (2012) 7:e47038. doi: 10.1371/journal.pone.0047038
30. Zhang S, Shi LL, Lǚ K, Li HY, Wang SP, He JG, et al. Cloning, identification and functional analysis of a β-catenin homologue from Pacific white shrimp, *Litopenaeus vannamei*. *Fish Shellfish Immunol* (2016) 54:411–8. doi: 10.1016/j.fsi.2016.03.162
31. Shi LL, Chan SM, Li CZ, Zhang S. Identification and characterization of a laccase from *Litopenaeus vannamei* involved in anti-bacterial host defense. *Fish Shellfish Immunol* (2017) 66:1–10. doi: 10.1016/j.fsi.2017.04.026
32. Li HY, Wang S, Qian Z, Wu ZZ, Lǚ K, Weng SP, et al. MKK6 from pacific white shrimp *Litopenaeus vannamei* is responsive to bacterial and WSSV infection. *Mol Immunol* (2016) 70:72–83. doi: 10.1016/j.molimm.2015.12.011
33. Gattinoni L, Zhong XS, Palmer DC, Ji Y, Hinrichs CS, Yu Z, et al. Wnt signaling arrests effector T cell differentiation and generates CD8+ memory stem cells. *Nat Med* (2009) 15:808–13. doi: 10.1038/nm.1982
34. Li CZ, Chen YH, Weng S, Li SD, Zuo HL, Yu XQ, et al. Presence of Tube isoforms in *Litopenaeus vannamei* suggests various regulatory patterns of signal transduction in invertebrate NF-κB pathway. *Dev Comp Immunol* (2014) 42:174–85. doi: 10.1016/j.dci.2013.08.012
35. Qiu W, He JH, Zuo HL, Niu SW, Xu XP. Identification, characterization, and function analysis of the NF-κB repressing factor (NKRF) gene from *Litopenaeus vannamei*. *Dev Comp Immunol* (2017) 76:83–92. doi: 10.1016/j.dci.2017.05.020
36. Li CZ, Li HY, Chen YX, Chen YG, Wang S, Weng SP, et al. Activation of Vago by interferon regulatory factor (IRF) suggests an interferon system-like antiviral mechanism in shrimp. *Sci Rep* (2015) 5:15078. doi: 10.1038/srep15078
37. Sharp PA, Burge CB. Classification of introns: U2-type or U12-type. *Cell* (1997) 91(7):875–9. doi: 10.1016/s0092-8674(00)80479-1
38. Alfhili MA, Alsughayyir J, McCubrey JA, Akula SM. GSK-3-associated signaling is crucial to virus infection of cells. *Biochim Biophys Acta (BBA) - Mol Cell Res* (2020) 1867:118767. doi: 10.1016/j.bbamcr.2020.118767
39. Chen X, Wang RZ, Liu X, Wu YM, Zhou T, Yang YJ, et al. A Chemical-Genetic Approach Reveals the Distinct Roles of GSK3α and GSK3β in Regulating Embryonic Stem Cell Fate. *Dev Cell* (2017) 43(5):563–76.e4. doi: 10.1016/j.devcel.2017.11.007
40. Li XW, Jia ZH, Wang WL, Wang LL, Liu ZQ, Yang B, et al. Glycogen synthase kinase-3 (GSK3) regulates TNF production and haemocyte phagocytosis in the immune response of Chinese mitten crab *Eriocheir sinensis*. *Dev Comp Immunol* (2017) 73:144–55. doi: 10.1016/j.dci.2017.03.022
41. Kim JY, Park SY, Lyoo HR, Koo ES, Kim MS, Jeong YS. Extended stability of cyclin D1 contributes to limited cell cycle arrest at G1-phase in BHK-21 cells with Japanese encephalitis virus persistent infection. *J Microbiol* (2015) 53:77–83. doi: 10.1007/s12275-015-4661-z
42. Rahaus M, Desloges N, Wolff MH. Varicella-zoster virus requires a functional PI3K/Akt/GSK-3α/β signaling cascade for efficient replication. *Cell Signal* (2007) 19(2):312–20. doi: 10.1016/j.cellsig.2006.07.003
43. Wu CH, Yeh SH, Tsay YG, Shieh YH, Kao CL, Chen YS, et al. Glycogen synthase kinase-3 regulates the phosphorylation of severe acute respiratory syndrome coronavirus nucleocapsid protein and viral replication. *J Biol Chem* (2009) 284(8):5229–39. doi: 10.1074/jbc.M805747200
44. Ning K, Wu Y, Meng Q, Wang Z, Zuo Y, Xi P, et al. Suppression of Virulent Porcine Epidemic Diarrhea Virus Proliferation by the PI3K/Akt/GSK-3α/β Pathway. *PloS One* (2016) 11:e0161508. doi: 10.1371/journal.pone.0161508
45. Qin D, Feng N, Fan W, Ma X, Yan Q, Lv Z, et al. Activation of PI3K/AKT and ERK MAPK signal pathways is required for the induction of lytic cycle replication of Kaposi's Sarcoma-associated herpesvirus by herpes simplex virus type 1. *BMC Microbiol* (2011) 11:240. doi: 10.1186/1471-2180-11-240
46. Dai X. The Impact of GSK-3β on the Replication of Influenza Virus in A549 Cells. *Open J Natural ence* (2016) 04:371–7. doi: 10.12677/OJNS.2016.44045

Conflict of Interest: The authors declare that the research was conducted in the absence of any commercial or financial relationships that could be construed as a potential conflict of interest.

frontiers in Immunology

REVIEW
published: 18 February 2021
doi: 10.3389/fimmu.2021.630343

The Pacific Oyster Mortality Syndrome, a Polymicrobial and Multifactorial Disease: State of Knowledge and Future Directions

*Bruno Petton[1], Delphine Destoumieux-Garzón[2], Fabrice Pernet[1], Eve Toulza[2], Julien de Lorgeril[2], Lionel Degremont[3] and Guillaume Mitta[2]**

[1] Ifremer, LEMAR UMR 6539, UBO/CNRS/IRD/Ifremer, Argenton-en-Landunvez, France, [2] IHPE, Université de Montpellier, CNRS, Ifremer, Université de Perpignan Via Domitia, Montpellier, France, [3] Ifremer, SG2M, LPGMM, La Tremblade, France

OPEN ACCESS

Edited by:
Chaozheng Li,
Sun Yat-Sen University, China

Reviewed by:
Timothy James Green,
Vancouver Island University, Canada
Kunlaya Somboonwiwat,
Chulalongkorn University, Thailand

***Correspondence:**
Guillaume Mitta
mitta@univ-perp.fr

Specialty section:
This article was submitted to Comparative Immunology, a section of the journal Frontiers in Immunology

Received: *17 November 2020*
Accepted: *06 January 2021*
Published: *18 February 2021*

Citation:
Petton B, Destoumieux-Garzón D, Pernet F, Toulza E, de Lorgeril J, Degremont L and Mitta G (2021) The Pacific Oyster Mortality Syndrome, a Polymicrobial and Multifactorial Disease: State of Knowledge and Future Directions. Front. Immunol. 12:630343. doi: 10.3389/fimmu.2021.630343

The Pacific oyster (*Crassostreae gigas*) has been introduced from Asia to numerous countries around the world during the 20th century. *C. gigas* is the main oyster species farmed worldwide and represents more than 98% of oyster production. The severity of disease outbreaks that affect *C. gigas*, which primarily impact juvenile oysters, has increased dramatically since 2008. The most prevalent disease, Pacific oyster mortality syndrome (POMS), has become panzootic and represents a threat to the oyster industry. Recently, major steps towards understanding POMS have been achieved through integrative molecular approaches. These studies demonstrated that infection by Ostreid herpesvirus type 1 µVar (OsHV-1 µvar) is the first critical step in the infectious process and leads to an immunocompromised state by altering hemocyte physiology. This is followed by dysbiosis of the microbiota, which leads to a secondary colonization by opportunistic bacterial pathogens, which in turn results in oyster death. Host and environmental factors (*e.g.* oyster genetics and age, temperature, food availability, and microbiota) have been shown to influence POMS permissiveness. However, we still do not understand the mechanisms by which these different factors control disease expression. The present review discusses current knowledge of this polymicrobial and multifactorial disease process and explores the research avenues that must be investigated to fully elucidate the complexity of POMS. These discoveries will help in decision-making and will facilitate the development of tools and applied innovations for the sustainable and integrated management of oyster aquaculture.

Keywords: Pacific oyster mortality syndrome, polymicrobial disease, multifactorial disease, *Crassostrea gigas*, OsHV-1, opportunistic bacterial pathogens

INTRODUCTION

Aquaculture is one of the fastest-growing food industries, representing more than 50% of worldwide seafood production (1). Mollusk aquaculture, in which oysters are the most important taxonomic group (by volume), has become one of the largest animal food-producing industries.

The Pacific oyster *Crassostrea gigas* was introduced from Asia to numerous countries throughout the world (*e.g.* Canada, the USA, Brazil, Australia, New Zealand, Chile, Mexico, Argentina, South Africa, Namibia, and numerous European countries including France) during the 20th century (2). Worldwide production of *C. gigas* is estimated at 4.7 million tons per year (3). China is, by far, the leading producer, followed by South Korea, Japan, and France.

For decades, *C. gigas* has suffered from mortality due to disease (4), but the severity of these outbreaks has increased dramatically since 2008. These outbreaks affect the juvenile stages of the oyster, killing more than 35% of the cultivated and natural oysters in France every year (5, 6). The corresponding syndrome, referred to as Pacific oyster mortality syndrome (POMS) (7), has become panzootic; it is observed in all the coastal regions of Franc, and in numerous other countries worldwide (8). The ecological and economic consequences of POMS can be dramatic (9), and POMS represents a threat to the worldwide oyster industry.

POMS is a disease with complex etiology. Research efforts have revealed a series of factors that contribute to the disease, including interactions between infectious agents and seawater temperature, oyster genetics, food availability, and oyster growth (9–17).

In this review, we present the research performed in the past decade that has contributed to a better understanding of POMS. These studies have deciphered the polymicrobial nature of the disease. Although this is a first and important step, POMS remains an incompletely understood multifactorial disease that is controlled by a series of host and environmental factors. It is crucial that POMS be fully deciphered by the determination of which factors control disease expression, how these factors control disease expression, the weight of these different factors, and their putative synergistic and antagonistic effects. Only once this work is complete will we completely understand POMS and be able to propose solutions to ensure the durability of the oyster industry.

POMS IS A POLYMICROBIAL DISEASE

Dramatic increases in oyster mortality (observed since 2008) have been found to coincide with the recurrent detection of *Ostreid herpesvirus* (OsHV-1) variants in moribund oysters in France (17–19) and worldwide (9, 20–23). Because of this, research efforts have historically focused on the viral etiology of POMS and a series of diagnostic assays such as PCR, real-time PCR, and *in situ* hybridization have been developed to detect OsHV-1 (18, 19, 24–26). Nevertheless, the involvement of other etiological agents was suspected (15). In particular, bacterial strains of the genus *Vibrio* had been shown to be associated with POMS (27, 28). However, the role of these different putative pathogens has been tested in isolation, using experimental systems (bacterial or viral filtrate injections) that did not reproduce the natural route of infection. Consequently, the complex POMS infectious process remained misunderstood.

Several breakthroughs have advanced our understanding of the complexity of POMS. The development of an ecologically realistic model of infection was the first major progress (16, 29). Briefly, this method of infection uses pathogen-free oysters that are reared in bio-secured conditions from birth to 3 months of age. Some of these pathogen-free oysters are then naturally infected in the field to become "donors," while the remaining oysters are maintained in bio-secured conditions as "recipients." Recipients are subsequently exposed to donor oysters through cohabitation. This method retains the complexity of the infectious environment (OsHV-1 and populations of virulent bacteria) and mimics the natural route of infection (16, 29). This method also allows simultaneous triggering of disease in all recipients and parallels the dynamics of the disease through time on oysters that are phased according to the infectious process in which they are engaged. A second important breakthrough was the use of oyster biparental families selected for higher disease resistance (10). By reducing genetic diversity, which is particularly high in oysters, the disease dynamics can be monitored in oysters that have contrasting phenotypes (susceptible or resistant) during pathogen challenge. A final breakthrough was the use of integrative molecular approaches that allowed the observation of the dynamics of the host response and the microbiota, including putative pathogens, in the same experimental framework.

One recent study that combined an ecologically realistic model of infection, the use of susceptible and resistant oyster families, and integrative molecular approaches (dual RNAseq, 16S rDNA metabarcoding, and histology) deciphered the mechanism of POMS (30). This study demonstrated that POMS is a polymicrobial disease (**Figure 1**). Early gill damages, infection of hemocytes by OsHV-1, and bacterial colonization both inside and outside the gill tissues were evidenced in susceptible oysters only (30). This study revealed that infection by OsHV-1 is the first critical step in POMS and leads to an immunocompromised state by infecting and altering hemocyte physiology (30). This immunosuppression subsequently evolves towards bacteremia, which involves a series of opportunistic bacteria (30). This bacteremia leads to oyster death. Indeed, POMS requires both OsHV-1 and opportunistic bacteria: preventing either viral replication or bacterial proliferation with poly-IC injection or antibiotics, respectively, blocks the infectious process and prevents mortality (30).

Primary Viral Infection

Infection by OsHV-1 µVar is the first event in the infectious process of POMS, and intense viral replication is a prerequisite for the development of the disease. The inability of susceptible oysters to control viral replication during POMS is associated

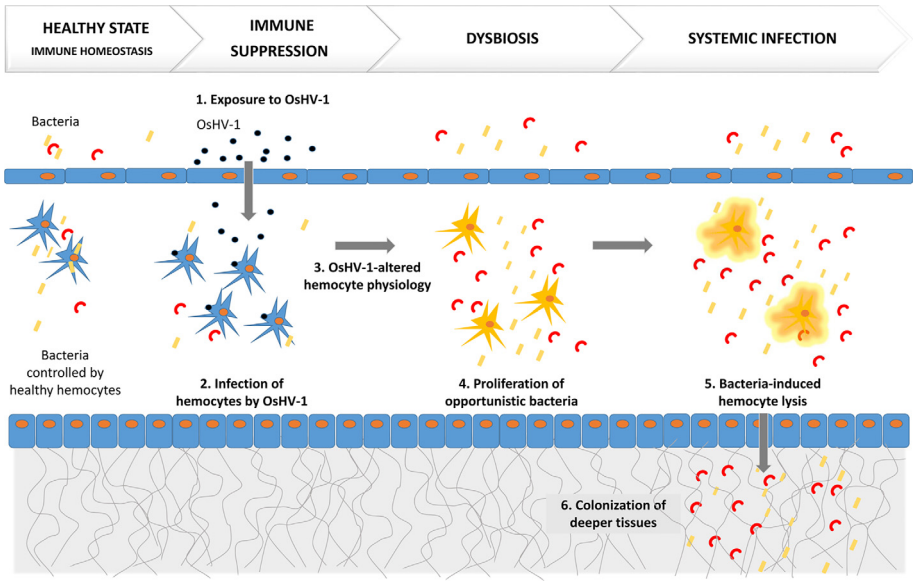

FIGURE 1 | POMS is a polymicrobial disease induced by a primary infection by OsHV-1, which alters hemocyte physiology. This is followed by secondary bacteremia that leads to oyster death.

with a strong, but late, antiviral response (30). Concomitant with the intense replication of the virus, oysters intensively express several genes that encode endogenous Inhibitors of Apoptosis (IAPs) (30). Although the pathway by which OsHV-1 could control endogenous IAP expression is unknown, such a mechanism has been described in a human Gammaherpesvirus, Epstein–Barr virus, which is able to increase the expression of IAP-2 to inhibit apoptosis (31). Remarkably, intense OsHV-1 replication is also associated with high expression of exogenous IAPs of viral origin (30). Such viral proteins, which are of the BIR family, are known to have anti-apoptotic activities that favor viral replication (32). These results suggest that both endogenous and exogenous anti-apoptotic processes, which are strongly activated in susceptible oysters, play a key role in the success of OsHV-1 infection (30).

Oyster immune cells, called hemocytes, are targeted by OsHV-1 (30, 33). Infection of hemocytes by OsHV-1 impacts hemocyte physiology and impairs the expression of antimicrobial peptides (30), either directly (through transcriptional regulation) or indirectly (through the induction of cell death or lysis processes) (33).

Since the description of the first OsHV-1 µVar genotype in 2010 (17), increasing NGS sequencing data have revealed the diversity of OsHV-1 µVar genotypes (17, 22, 23, 34, 35). This observation, similar to observations made in a number of RNA and DNA viruses (36–39), raises the question of what impact this genetic diversity has on the fitness of the virus and the consequences of the disease. Many viruses produce diverse genetically linked variants that can be defined as viral populations. These populations are maintained by mutation-selection equilibrium (40, 41), and have the potential to generate beneficial interactions and cooperation which increase viral fitness and adaptability to the host (42–45).

A recent study investigated these possibilities in OsHV-1 (46). Different biparental families of oysters were confronted with two different infectious environments. Because susceptibility to POMS can differ not only between families within the same environment, but also within the same family between the two environments, viral diversity was analyzed between families and environments (46). This analysis revealed distinct viral populations in the two infectious environments (46). Moreover, the different oyster families were infected by distinct viral populations within the same infectious environment (46). These results suggest that there are co-evolutionary processes at play between OsHV-1 µVar, and that oyster populations have selected for a diversity of viral populations that could, in turn, facilitate viral adaptation to various environments and various host genotypes.

Secondary Bacterial Infection

Until recently, the bacterial component of POMS has mainly been studied using culture-based approaches. These approaches revealed a clear association between some *Vibrio* species and POMS, which has led to extensive characterization of the roles and contributions of *Vibrio* bacteria to oyster mortality.

Using pathogen-free oyster spats and field-based approaches, Le Roux and collaborators characterized the population structure of *Vibrio* species found in naturally infected oysters during POMS episodes on the French Atlantic coast. Members of the *Splendidus* clade (*e.g. V. tasmaniensis, V. splendidus, V. cyclitrophicus, V. harveyi, V. aestuarianus*, and *V. crassostreae*) have been systematically isolated from diseased juvenile oysters,

as have (to a lesser extent) *V. harveyi* and *V. aestuarianus*, which fall outside the clade (17, 27, 47). Bruto et al. demonstrated that the *Vibrio* population structure is seasonal and varies in oysters affected by POMS (27). Notably, *Vibrio* of the *Splendidus* clade are present in healthy oysters when no mortalities occur (27), but they only express low to moderate pathogenic potential in these circumstances (48). *V. crassostreae* is predominant during mortalities and is almost exclusively associated with oyster tissues (27). *V. crassostreae* has been shown to replace the resident *Vibrio* community during a POMS episode (49).

Some factors that contribute to *Vibrio* virulence in oysters have been discovered in species that exhibit pathogenic potential in experimental infections (*e.g.* bacteria injected in the adductor muscle). These factors have mostly been described in *V. crassostreae* and *V. tasmaniensis* [a facultative intracellular pathogen of oyster hemocytes (50)] isolated from the Atlantic during POMS episodes (27, 28, 49–52). Bruto et al. (28) found that the r5.7 gene is required for virulence and is ancestral in the Splendidus clade. The R5.7 protein itself is not cytotoxic (28); however, to mediate cytotoxicity, R5.7-expressing *V. crassostreae* requires physical contact with hemocytes (51). Interestingly, upon the loss of the ancestral r5.7 gene, *V. tasmaniensis* has acquired a type 6 secretion system (T6SS) on chromosome 1. This T6SS intracellularly delivers cytotoxic effectors to oyster hemocytes (51). These findings show that *Vibrio* cytotoxicity is a key determinant of oyster colonization that allows *Vibrio* to escape from potent cellular defenses and cause systemic infection (51). Furthermore, these findings show that distinct molecular determinants can confer similar dampening of host immune defenses in *Vibrio* species associated with POMS.

To date, *Vibrio* is the only bacterial group that has been studied in detail as an etiological agent of POMS, in part because *Vibrio* species are readily cultured and amenable to functional studies. Other bacterial groups (*e.g. Arcobacter* and *Shewanella*) have been associated with oyster mortality (30, 53, 54). However, their particular contributions to, and potential cooperation with other bacterial communities that participate in, fatal dysbiosis remain unknown, largely due to technical limitations.

Recently, we studied the structure of bacterial communities (as determined by 16S metabarcoding) and the functions expressed by different bacterial genera (as determined by metatranscriptomics) in different oyster biparental families submitted to different infectious environment (55). Five bacterial genera (*Arcobacter, Marinobacterium, Marinomonas, Vibrio*, and *Pseudoalteromonas)* that colonize oysters during POMS were remarkably consistent between families and environments. These genera are referred to as the POMS pathobiota.

The core functions identified by metatranscriptomics in POMS pathobiota reveal the importance of general metabolism and adaptation to stress (imposed by host defenses) in the success of colonization (55). Beyond general metabolism, detoxifying enzymes (such as alkylhydroxyperoxydases) involved in the resistance to or tolerance of host immune defenses are expressed by all successful colonizers. Most of the successful genera also express enzymes required for tolerance/resistance to oxidative stress. Reactive Oxygen Species (ROS) and Reactive Nitrogen Species (RNS) are major players at the oyster-microbiota interface (56). Thus, it is not surprising that successful colonizers express ROS/RNS detoxifying enzymes during oyster colonization.

A number of genus-specific functions that likely confer cross-benefits at the community level are also expressed during pathogenesis (55). These include genes related to metal homeostasis (siderophore production), iron uptake, and virulence (*e.g.* T6SS), all of which contribute to suppression of oyster cellular defenses (51, 57). The expression of these genes is likely beneficial to the entire bacterial community. From a metabolic point of view, cross-benefits are best exemplified by sulfur metabolism, a pathway which is non-redundantly encoded by five different genera. This suggests that sulfur cycling is a core property of the colonizing microbiota as a whole, rather than of a single genus. Such metabolic interdependence between, and cooperation of, microbial communities is likely a key determinant of the structure of the POMS pathobiota, and may dictate its conservation across distinct environments and oyster genetic backgrounds.

Many questions remain to be studied, including how *Vibrio* and/or other bacterial genera collaborate with OsHV-1 to kill oysters. It is known that the molecular manipulation of hemocyte molecular responses by OsHV-1 (i.e. the inhibition of antimicrobial peptide expression) is a key determinant of bacterial colonization, without which *Vibrio* species fail to efficiently colonize oysters and express their pathogenic potential (30). It is also known that the dampening of oyster cellular defenses by *Vibrio* (through active hemocyte lysis), or possibly by other pathogenic bacteria, is key in the development of systemic infection (51). Because hemocytes are composed of diverse populations of cells that play different roles in infection control, better identification of the cell populations targeted by each POMS-associated pathogen is required to understand the polymicrobial nature of POMS at the cellular and molecular scales.

POMS IS A MULTIFACTORIAL DISEASE

The risk of POMS outbreaks has been linked to subtle interactions between not only host and pathogens, but also environmental factors. Thus, POMS is a not only a polymicrobial disease, but also a multifactorial disease. In this review, we focus on the five main environmental and host factors associated with disease expression: i) temperature, ii) oyster genetics, iii) oyster age, iv) oyster energetic status, and v) microbiota.

Temperature

Temperature increases linked to climate warming are a major driver of disease outbreaks (58). In different invertebrate–pathogen interactions, temperature has been found to affect the outcome of the interaction by influencing host and/or pathogen physiology (59–63). A permissive temperature range for POMS has been clearly identified, specifically, 16°C to 24°C (5, 6, 64).

The same trend was observed in mesocosm experiments in which recipient oysters were confronted to disease donors at different temperature [**Figure 2A**, (16)].

Although higher temperatures decrease oyster susceptibility to POMS, viral infectivity is quite similar to infectivity at permissive temperatures (66). This reinforces the hypothesis that other factors (*e.g.* bacterial virulence or oyster physiology) could be influenced by high temperatures and thereby affect POMS permissiveness. Although the effect of high temperatures on bacterial virulence remains to be investigated, a recent work demonstrated that oyster immunity is modulated, and apoptotic processes induced, by high temperatures, which could explain the observed decrease of permissiveness (11).

With respect to lower temperatures, diseased oysters exposed to low temperature (13°C) over the course of 40 days exhibited no mortality, were negative for OsHV-1, and did not transmit the disease to healthy oysters (16). The mechanisms by which low temperatures affect POMS permissiveness remain to be investigated.

Oysters Genetics

Some oysters, particularly those able to limit infection by OsHV-1, are resistant to POMS. Such resistant oysters were first described in field challenges (67), and subsequently in laboratory challenges, as exhibiting a 3 log of decrease in viral DNA copies (30, 68, 69). Genetic studies of oyster resistance have revealed a significant additive genetic component of survival during OsHV-1 infection (10, 70–72). Over the past decade, many oyster genomic tools [including a reference genome (73) and SNP arrays (74)] have been developed to expand the study of the genetic underpinnings of *C. gigas* resistance to OsHV-1 infection.

The results of genome-wide association studies in juvenile oysters experimentally challenged with OsHV-1 and genotyped using a high-density linkage map constructed for the Pacific oyster (75) suggest that OsHV-1 resistance is polygenic in nature. These studies also highlighted that region of linkage group 6 contains a significant QTL which affects host resistance (75). Several SNPs, associated with survival and/or viral load, were located in several genes that encode RAN Binding Protein 9, a Coronin and Myo10 (an actin motor protein). However, the specific roles of these genes in the resistance process remain to be elucidated.

A recent transcriptomic study on several oyster biparental families that exhibited different susceptibilities to POMS revealed that the early induction of genes involved in antiviral defense is a hallmark of resistant oyster families (30). However, the specific genetic components responsible for this early induction remain unidentified. To identify putative transcriptomic determinants associated with POMS resistance, basal transcriptomes (no disease challenge) of three resistant oyster families were compared to the basal transcriptomes of three susceptible families (76). POMS resistant oysters showed constitutive differences in the expression of genes involved in stress responses, protein modification, maintenance of DNA integrity and DNA repair, and immune and antiviral pathways. Similarities and differences between molecular pathways were observed among the resistant families. For example, several genes related to the TLR-NF-κB, JAK-STAT, and STING-RLR pathways were identified (76). Among them, only one transcript was overrepresented in the three resistant families (76). This transcript corresponded to an endosomal Toll-like Receptor that displays similarities to TLR 13, which can act as a sensor of viral and bacterial RNA in the TLR-NF-κB signaling

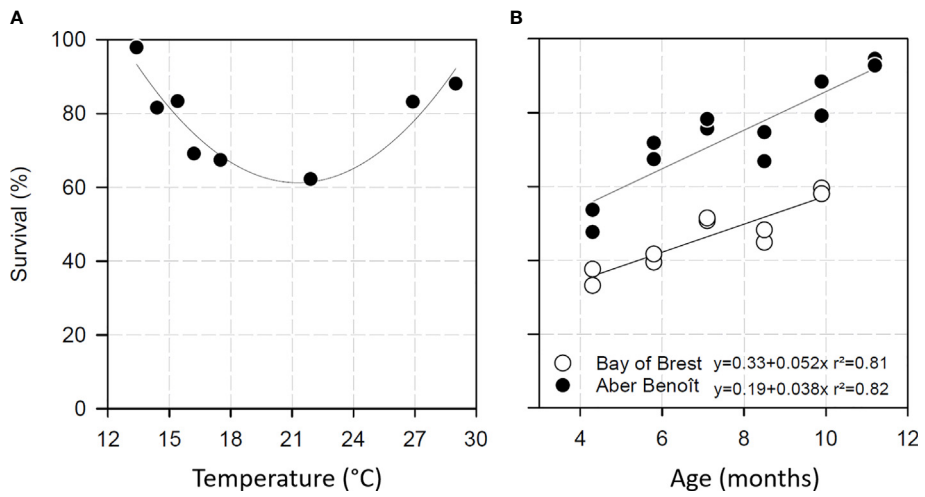

FIGURE 2 | Survival of Pacific oysters exposed to POMS according to temperature **(A)** and age **(B)**. **(A)** *C. gigas* survival after exposition to POMS in mesocosm. Oyster mortalities after 16 days of exposition were maximal at temperatures ranging from 16.2 and 21.9°C. Lower and upper temperatures diminished POMS permissiveness. Data were extracted from (17). **(B)** Survival of Pacific oysters exposed to POMS according to their age in two Atlantic coast locations (Aber Benoît and Bay of Brest). The data are modified from (65).

pathway (77, 78). This gene is particularly interesting because its function could explain how these resistant oyster families detect viral infection early, which allows them to mount a more rapid and efficient antiviral response (30). Given this putative antiviral role, TLR 13 represents a good candidate for future study.

Overall, the results of these studies suggest that the POMS resistance process is polygenic and varies somewhat with oyster genotype.

Oyster Age

A series of studies have reported that POMS-induced mortality rates are lower in adult oysters than in spat and juvenile oysters (13, 20, 79). The experimental design of these studies, however, did not allow researchers to disentangle the effect of selection on resistance and age. In fact, the adult oysters analyzed in these studies had survived one or more POMS events, and thus might have been selected for resistance to POMS over time.

To further investigate the effect of oyster age on mortality, healthy oysters at different developmental stages (juveniles and adults) were exposed to the Marennes-Oléron Bay (France) infectious environment (80). In this study, oyster age was found to be inversely correlated with mortality. This result was confirmed both in the same infectious environment (10) and in another infectious environment (Brest Bay, France) (65). In the Brest Bay study, healthy oysters of different ages were simultaneously confronted with the same infectious environment. Most oysters appear to become resistant to POMS with age (**Figure 2B**), and resistance appears to be acquired after 24 months (10, 65). It is expected that the maturation of the immune system underlies the acquisition of resistance; however, the underlying molecular mechanisms remain to be investigated.

Food Availability, Growth, and Energy Reserves

Food availability is known to influence disease risk and outcome in two ways. First, food availability improves the physiological condition of the host and lowers their susceptibility to infectious disease, which reflects a tradeoff between immunity and other functions [*e.g.* (81, 82)]. Second, food scarcity limits the resources available to the pathogen, because it slows the growth and metabolism of the host, which the pathogen depends on in order to proliferate (83–87). Therefore, food availability can have both positive and negative effects on the severity of infectious diseases.

Previous studies have demonstrated that fed oysters are at a higher risk of death than starved oysters (88, 89). Paradoxically, the energy reserves of oysters, which reflect food availability, are associated with increased resistance or tolerance to OsHV-1 (13, 64, 90). In light of these results, Pernet et al. (14) investigated how food availability, growth rate, and energy reserves drive the outcome of POMS. Briefly, the authors selected fast- and slow-growing oysters and exposed these oysters to high and low food rations. The oysters were evaluated for energy reserves, challenged with POMS, and monitored for survival. The study found that although higher food levels and oyster growth are associated with an increased mortality risk, higher energy reserves are associated with decreased mortality risk (14). Thus, food availability both enables mortality by increasing oyster growth and limits mortality by increasing energy reserves (**Figure 3**). This study clarifies the impact of food resources on disease susceptibility and suggests how host physiological condition could mitigate epidemics (14).

The specific mechanisms by which food availability, growth rate, and energy reserves modulate oyster susceptibility to infection remain to be elucidated. We hypothesize that the positive association between food level and mortality risk reflects increased host growth and metabolic rate, which in turn amplifies pathogen replication. Like other viruses, OsHV-1 uses host cellular machinery to replicate (91, 92), thus stimulation of host cellular growth could amplify viral gene expression and replication. However, there is currently no evidence that demonstrates increased viral replication in response to increased food availability and host growth rate. Furthermore, we cannot exclude the possibility that food availability, growth rate, and energy reserves act on susceptibility to secondary bacterial infection. Finally, the lower mortality risk observed at low food levels may also reflect induced autophagy, an evolutionarily conserved cell recycling process that is activated in response to stress (including starvation) (93). Autophagy also controls microbial infections, both through direct destruction of the pathogen, and indirectly as a key mediating factor in host innate and adaptive immunity (93). The autophagy pathway is functional in oysters and could explain why starvation reduces mortality during OsHV-1 infection (89). Further investigations are needed to assess

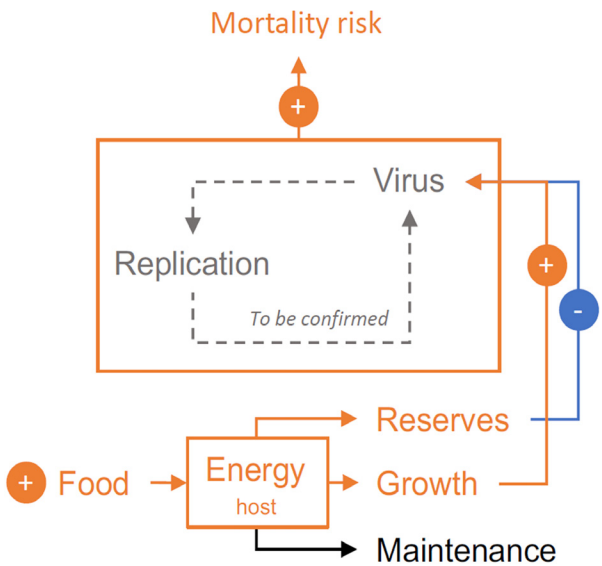

FIGURE 3 | Food availability both enables mortality by increasing oyster growth (and possibly viral replication), and limits mortality by increasing oyster energy. The net effect of increased food availability is an increased risk of mortality in oysters exposed to POMS. Orange, blue and, black lines indicate positive, negative, and neutral feedback, respectively. Gray dashed line indicates hypothetical mechanism.

whether and how food levels, growth, and energy reserves control viral proliferation, bacteremia, and/or autophagy.

Microbiota

Several independent studies used 16S metabarcoding to investigate uncultivable bacterial microbiota. These studies identified shifts in the composition of the microbiota community (dysbiosis) associated with POMS. In a large-scale analysis of the microbiota of diseased oysters from three different sites in Europe, Lasa and colleagues identified dysbiosis in OsHV-1 positive oysters. This dysbiosis was characterized by the emergence of a pathobiota composed of opportunistic pathogens (including *Vibrio* and *Arcobacter* species) (54). In the most integrative study of POMS to date, ecologically realistic infection demonstrated that bacterial dysbiosis is subsequent to viral infection, that viral infection leads to antibacterial defense impairment, and that this impairment allows opportunistic pathogens to colonize oysters (30).

In addition, oyster genotype-specific microbial associations have been identified between genetically differentiated oyster beds especially for the rare phylotype assembling (94). This association disappeared under environmental stress. Constitutive differences in microbiota have also been identified in 35 healthy oyster breeds displaying different levels of resistance to POMS (95). Operational Taxonomic Units (OTUs) of the *Photobacterium, Vibrio, Aliivibrio, Streptococcus*, and *Roseovarius* genera were significantly associated with the most susceptible oyster families, as was a higher background load of rare *Vibrio* OTUs in the healthy state. This suggests that these susceptible families exhibit a decreased immune response to these pathogens (95).

In another study, the Mycoplasmataceae, Rhodospirillaceae, and Vibrionaceae bacterial families, as well as the *Photobacterium* genus, were associated with susceptible oyster families (96). The proportion of specific taxa, including Cyanobacteriaceae, Colwelliaceae, and Rhodobacteraceae, was significantly higher in resistant oyster families that survived POMS after transplant into the field during an infectious period. Resistant oysters also displayed a higher evenness of the bacterial colonizers, suggesting that a decrease in microbial diversity may be associated with a loss of microbiota function, which could allow colonization by opportunistic pathogens (96).

This research raises questions about the role of microbiota composition and stability in oyster health and susceptibility to POMS. Whether differences in bacterial community composition and dynamics are responsible for different disease resistance levels, or are only related to the host-genotype specificity of the microbiota, remains to be elucidated. Future studies are needed to identify the relative contributions of the oyster microbiota to disease outcome, including studies of direct interactions with pathobiota and possible immune stimulation of the host.

CONCLUSIONS AND PERSPECTIVES

Determination of the mechanism of POMS pathogenesis and identification of host, pathogen, and environmental factors that influence POMS are important achievements. However, these are only initial steps in the development of new approaches to counter POMS and its devastating effects on the oyster industry.

The research discussed above, along with future studies, will help identify the main factors involved in permissiveness to POMS. It will also be necessary to evaluate the relative weights of, and interactions between, these factors during pathogenesis. This can be achieved through the study of different markers (including oyster genes, viral and bacterial load and genes, *etc.*) identified in real farming conditions with oysters of different ages and genetic backgrounds in different environmental conditions and under different physiological conditions. Such studies are necessary for the implementation of predictive models of the epidemiological risk of POMS.

Theoretical approaches to the study of bivalve infections are still in their infancy (97). Moreover, only a few epidemiological models have been developed for multiple infections, and these models usually oversimplify within-host dynamics (98). Consequently, an additional research objective could be the development of models that synthetically represent POMS under the influence of relevant host, pathogen, and environmental factors. Importantly, these models will help quantify the relative benefits and risks of changes in oyster farming practices (e.g. provision of food resources, age of the oysters at the time of transfer from the bio-secured hatcheries to the natural farming environment).

To conclude, we cannot exclude that other factors could influence the disease. As an example, we can mention field studies indicating that POMS could be influenced by the presence of particles (*e.g.* plankton) carrying OsHV-1 (90, 99–101). Future studies will focus on these factors and their weight in POMS expression, and they can be included in the proposed modeling approaches to get a comprehensive view of POMS and predict as faithfully as possible the epidemiological risk.

AUTHOR CONTRIBUTIONS

DD-G, BP, and FP contributed equally to the content of the review and figures. JD, ET, and LD contributed to the content of the review. GM supervised, edited, and added references in the review. All authors contributed to the article and approved the submitted version.

FUNDING

The present study was supported by the ANR projects DECIPHER (ANR-14-CE19-0023) and DECICOMP (ANR-19-CE20-0004), and by Ifremer, CNRS, Université de Montpellier, and Université de Perpignan *via* Domitia. This study is set within the framework of the "Laboratoires d'Excellence (LABEX)" TULIP (ANR-10-LABX-41) and CEMEB (ANR-10-LABX-04-01).

REFERENCES

1. FAO. (2015). https://ourworldindata.org/grapher/capture-fisheries-vs-aquaculture-farmed-fish-production.
2. Ruesink JL, Lenihan HS, Trimble AC, Heiman KW, Micheli F, Byers JE, et al. Introduction of Non-Native Oysters: Ecosystem Effects and Restoration Implications. *Annu Rev Ecology Evol System* (2005) 36 (1):643–89. doi: 10.1146/annurev.ecolsys.36.102003.152638
3. FAO. *Fishery and aquaculture statistics*. Rome: FAO yearbook (2014).
4. Samain J-F, Mc Combie H. Summer mortality of Pacific oyster Crassostrea gigas. *MOREST Project* (2008).
5. ECOSCOPA. (2020). https://wwz.ifremer.fr/observatoire_conchylicole/.
6. Fleury E, Barbier P, Petton B, Normand J, Thomas Y, Pouvreau S, et al. Latitudinal drivers of oyster mortality: deciphering host, pathogen and environmental risk factors. *Sci Rep* (2020) 10(1):7264. doi: 10.1038/s41598-020-64086-1
7. Paul-Pont I, Dhand NK, Whittington RJ. Influence of husbandry practices on OsHV-1 associated mortality of Pacific oysters Crassostrea gigas. *Aquaculture* (2013) 412:202–14. doi: 10.1016/j.aquaculture.2013.07.038
8. Barbosa Solomieu V, Renault T, Travers MA. Mass mortality in bivalves and the intricate case of the Pacific oyster, Crassostrea gigas. *J Invertebr Pathol* (2015) 131:2–10. doi: 10.1016/j.jip.2015.07.011
9. EFSA PoAHW. Oyster mortality. *EFSA J* (2015) 13(6):4122–n/a. doi: 10.2903/j.efsa.2015.4122
10. Azéma P, Lamy JB, Boudry P, Renault T, Travers MA, Dégremont L. Genetic parameters of resistance to Vibrio aestuarianus, and OsHV-1 infections in the Pacific oyster, Crassostrea gigas, at three different life stages. *Genet Selection Evol* (2017) 49:1–16. doi: 10.1186/s12711-017-0297-2
11. Delisle L, Pauletto M, Vidal-Dupiol J, Petton B, Bargelloni L, Montagnani C, et al. High temperature induces transcriptomic changes in Crassostrea gigas that hinders progress of Ostreid herpesvirus (OsHV-1) and promotes survival. *J Exp Biol* (2020) 223(20):1–11. doi: 10.1242/jeb.226233
12. Le Roux F, Wegner KM, Polz MF. Oysters and Vibrios as a Model for Disease Dynamics in Wild Animals. *Trends Microbiol* (2016) 24(7):568–80. doi: 10.1016/j.tim.2016.03.006
13. Pernet F, Barret J, Le Gall P, Corporeau C, Dégremont L, Lagarde F, et al. Mass mortalities of Pacific oysters Crassostrea gigas reflect infectious diseases and vary with farming practices in the Mediterranean Thau lagoon, France. *Aquaculture Environ Interact* (2012) 2(3):215–37. doi: 10.3354/aei00041
14. Pernet F, Tamayo D, Fuhrmann M, Petton B. Deciphering the effect of food availability, growth and host condition on disease susceptibility in a marine invertebrate. *J Exp Biol* (2019) 222(Pt 17):1–6. doi: 10.1242/jeb.210534
15. Petton B, Bruto M, James A, Labreuche Y, Alunno-Bruscia M, Le Roux F. Crassostrea gigas mortality in France: the usual suspect, a herpes virus, may not be the killer in this polymicrobial opportunistic disease. *Front Microbiol* (2015) 6:686. doi: 10.3389/fmicb.2015.00686
16. Petton B, Pernet F, Robert R, Boudry P. Temperature influence on pathogen transmission and subsequent mortalities in juvenile Pacific oysters Crassostrea gigas. *Aquaculture Environ Interact* (2013) 3(3):257–73. doi: 10.3354/aei00070
17. Segarra A, Pepin JF, Arzul I, Morga B, Faury N, Renault T. Detection and description of a particular Ostreid herpesvirus 1 genotype associated with massive mortality outbreaks of Pacific oysters, Crassostrea gigas, in France in 2008. *Virus Res* (2010) 153(1):92–9. doi: 10.1016/j.virusres.2010.07.011
18. Martenot C, Oden E, Travaille E, Malas JP, Houssin M. Detection of different variants of Ostreid Herpesvirus 1 in the Pacific oyster, Crassostrea gigas between 2008 and 2010. *Virus Res* (2011) 160(1-2):25–31. doi: 10.1016/j.virusres.2011.04.012
19. Renault T, Moreau P, Faury N, Pepin JF, Segarra A, Webb S. Analysis of clinical ostreid herpesvirus 1 (Malacoherpesviridae) specimens by sequencing amplified fragments from three virus genome areas. *J Virol* (2012) 86(10):5942–7. doi: 10.1128/JVI.06534-11
20. Peeler EJ, Reese RA, Cheslett DL, Geoghegan F, Power A, Thrush MA. Investigation of mortality in Pacific oysters associated with Ostreid herpesvirus-1 muVar in the Republic of Ireland in 2009. *Prev Vet Med* (2012) 105(1-2):136–43. doi: 10.1016/j.prevetmed.2012.02.001
21. Lynch SA, Carlsson J, Reilly AO, Cotter E, Culloty SC. A previously undescribed ostreid herpes virus 1 (OsHV-1) genotype detected in the pacific oyster, Crassostrea gigas, in Ireland. *Parasitology* (2012) 139 (12):1526–32. doi: 10.1017/S0031182012000881
22. Abbadi M, Zamperin G, Gastaldelli M, Pascoli F, Rosani U, Milani A, et al. Identification of a newly described OsHV-1 microvar from the North Adriatic Sea (Italy). *J Gen Virol* (2018) 99(5):693–703. doi: 10.1099/jgv.0.001042
23. Burioli EAV, Prearo M, Houssin M. Complete genome sequence of Ostreid herpesvirus type 1 microVar isolated during mortality events in the Pacific oyster Crassostrea gigas in France and Ireland. *Virology* (2017) 509:239–51. doi: 10.1016/j.virol.2017.06.027
24. Corbeil S, Faury N, Segarra A, Renault T. Development of an in situ hybridization assay for the detection of ostreid herpesvirus type 1 mRNAs in the Pacific oyster, Crassostrea gigas. *J Virol Methods* (2015) 211:43–50. doi: 10.1016/j.jviromet.2014.10.007
25. Pepin JF, Riou A, Renault T. Rapid and sensitive detection of ostreid herpesvirus 1 in oyster samples by real-time PCR. *J Virol Methods* (2008) 149(2):269–76. doi: 10.1016/j.jviromet.2008.01.022
26. Renault T, Tchaleu G, Faury N, Moreau P, Segarra A, Barbosa-Solomieu V, et al. Genotyping of a microsatellite locus to differentiate clinical Ostreid herpesvirus 1 specimens. *Vet Res* (2015) 45:3. doi: 10.1186/1297-9716-45-3
27. Bruto M, James A, Petton B, Labreuche Y, Chenivesse S, Alunno-Bruscia M, et al. Vibrio crassostreae, a benign oyster colonizer turned into a pathogen after plasmid acquisition. *ISME J* (2017) 11(4):1043–52. doi: 10.1038/ismej.2016.162
28. Bruto M, Labreuche Y, James A, Piel D, Chenivesse S, Petton B, et al. Ancestral gene acquisition as the key to virulence potential in environmental Vibrio populations. *ISME J* (2018) 12(12):2954–66. doi: 10.1038/s41396-018-0245-3
29. Petton B, de Lorgeril J, Mitta G, Daigle G, Pernet F, Alunno-Bruscia M. Fine-scale temporal dynamics of herpes virus and vibrios in seawater during a polymicrobial infection in the Pacific oyster Crassostrea gigas. *Dis Aquat Organ* (2019) 135(2):97–106. doi: 10.3354/dao03384
30. de Lorgeril J, Lucasson A, Petton B, Toulza E, Montagnani C, Clerissi C, et al. Immune-suppression by OsHV-1 viral infection causes fatal bacteraemia in Pacific oysters. *Nat Commun* (2018) 9(1):4215. doi: 10.1038/s41467-018-06659-3
31. Xiong A, Clarke-Katzenberg RH, Valenzuela G, Izumi KM, Millan MT. Epstein-Barr virus latent membrane protein 1 activates nuclear factor-kappa B in human endothelial cells and inhibits apoptosis. *Transplantation* (2004) 78(1):41–9. doi: 10.1097/01.tp.0000129805.02631.ef
32. Miller LK. An exegesis of IAPs: salvation and surprises from BIR motifs. *Trends Cell Biol* (1999) 9(8):323–8. doi: 10.1016/s0962-8924(99)01609-8
33. Martenot C, Gervais O, Chollet B, Houssin M, Renault T. Haemocytes collected from experimentally infected Pacific oysters, Crassostrea gigas: Detection of ostreid herpesvirus 1 DNA, RNA, and proteins in relation with inhibition of apoptosis. *PLoS One* (2017) 12(5):e0177448. doi: 10.1371/journal.pone.0177448
34. Bai CM, Morga B, Rosani U, Shi J, Li C, Xin LS, et al. and high-throughput sequencing of Ostreid herpesvirus 1 indicate high genetic diversity and complex evolution process. *Virology* (2019) 526:81–90. doi: 10.1016/j.virol.2018.09.026
35. Burioli EAV, Varello K, Lavazza A, Bozzetta E, Prearo M, Houssin M. A novel divergent group of Ostreid herpesvirus 1 muVar variants associated with a mortality event in Pacific oyster spat in Normandy (France) in 2016. *J Fish Dis* (2018) 41(11):1759–69. doi: 10.1111/jfd.12883
36. Drake JW, Holland JJ. Mutation rates among RNA viruses. *Proc Natl Acad Sci USA* (1999) 96(24):13910–3. doi: 10.1073/pnas.96.24.13910
37. Parvez MK, Parveen S. Evolution and Emergence of Pathogenic Viruses: Past, Present, and Future. *Intervirology* (2017) 60(1-2):1–7. doi: 10.1159/000478729
38. Renner DW, Szpara ML. Impacts of Genome-Wide Analyses on Our Understanding of Human Herpesvirus Diversity and Evolution. *J Virol* (2018) 92(1):1–13. doi: 10.1128/JVI.00908-17
39. Renzette N, Pokalyuk C, Gibson L, Bhattacharjee B, Schleiss MR, Hamprecht K, et al. Limits and patterns of cytomegalovirus genomic diversity in humans. *Proc Natl Acad Sci USA* (2015) 112(30):E4120–8. doi: 10.1073/pnas.1501880112

40. Perales C, Moreno E, Domingo E. Clonality and intracellular polyploidy in virus evolution and pathogenesis. *Proc Natl Acad Sci USA* (2015) 112 (29):8887–92. doi: 10.1073/pnas.1501715112
41. Poirier EZ, Vignuzzi M. Virus population dynamics during infection. *Curr Opin Virol* (2017) 23:82–7. doi: 10.1016/j.coviro.2017.03.013
42. Brooke CB. Population Diversity and Collective Interactions during Influenza Virus Infection. *J Virol* (2017) 91(22):e01164-17. doi: 10.1128/JVI.01164-17
43. Mao ZQ, He R, Sun M, Qi Y, Huang YJ, Ruan Q. The relationship between polymorphisms of HCMV UL144 ORF and clinical manifestations in 73 strains with congenital and/or perinatal HCMV infection. *Arch Virol* (2007) 152(1):115–24. doi: 10.1007/s00705-006-0826-8
44. Pfeiffer JK, Kirkegaard K. Increased fidelity reduces poliovirus fitness and virulence under selective pressure in mice. *PLoS Pathog* (2005) 1(2):e11. doi: 10.1371/journal.ppat.0010011
45. Xiao Y, Rouzine IM, Bianco S, Acevedo A, Goldstein EF, Farkov M, et al. RNA Recombination Enhances Adaptability and Is Required for Virus Spread and Virulence. *Cell Host Microbe* (2016) 19(4):493–503. doi: 10.1016/j.chom.2016.03.009
46. Delmotte J, Chaparro C, Galinier R, de Lorgeril J, Petton B, Stenger PL, et al. Contribution of Viral Genomic Diversity to Oyster Susceptibility in the Pacific Oyster Mortality Syndrome. *Front Microbiol* (2020) 11:1579. doi: 10.3389/fmicb.2020.01579
47. Saulnier D, De Decker S, Haffner P, Cobret L, Robert M. Garcia C. A large-scale epidemiological study to identify bacteria pathogenic to Pacific oyster Crassostrea gigas and correlation between virulence and metalloprotease-like activity. *Microb Ecol* (2010) 59(4):787–98. doi: 10.1007/s00248-009-9620-y
48. Oyanedel D, Labreuche Y, Bruto M, Amraoui H, Robino E, Haffner P, et al. Vibrio splendidus O-antigen structure: a trade-off between virulence to oysters and resistance to grazers. *Environ Microbiol* (2020) 22(10):4264–78. doi: 10.1111/1462-2920.14996
49. Lemire A, Goudenege D, Versigny T, Petton B, Calteau A, Labreuche Y, et al. Populations, not clones, are the unit of vibrio pathogenesis in naturally infected oysters. *ISME J* (2015) 9(7):1523–31. doi: 10.1038/ismej.2014.233
50. Duperthuy M, Schmitt P, Garzon E, Caro A, Rosa RD, Le Roux F, et al. Use of OmpU porins for attachment and invasion of Crassostrea gigas immune cells by the oyster pathogen Vibrio splendidus. *Proc Natl Acad Sci U S A* (2011) 108(7):2993–8. doi: 10.1073/pnas.1015326108
51. Rubio T, Oyanedel D, Labreuche Y, Toulza E, Luo X, Bruto M, et al. Species-specific mechanisms of cytotoxicity toward immune cells determine the successful outcome of Vibrio infections. *Proc Natl Acad Sci U S A* (2019) 116 (28):14238–47. doi: 10.1073/pnas.1905747116
52. Vanhove AS, Rubio TP, Nguyen AN, Lemire A, Roche D, Nicod J, et al. Copper homeostasis at the host vibrio interface: lessons from intracellular vibrio transcriptomics. *Environ Microbiol* (2016) 18(3):875–88. doi: 10.1111/1462-2920.13083
53. Go J, Deutscher AT, Spiers ZB, Dahle K, Kirkland PD, Jenkins C. Mass mortalities of unknown aetiology in Pacific oysters Crassostrea gigas in Port Stephens, New South Wales, Australia. *Dis Aquat Organ* (2017) 125(3):227–42. doi: 10.3354/dao03146
54. Lasa A, di Cesare A, Tassistro G, Borello A, Gualdi S, Furones D, et al. Dynamics of the Pacific oyster pathobiota during mortality episodes in Europe assessed by 16S rRNA gene profiling and a new target enrichment next-generation sequencing strategy. *Environ Microbiol* (2019) 21(12):4548–62. doi: 10.1111/1462-2920.14750
55. Lucasson A, Luo X, Mortaza S, de lorgeril J, toulza E, Petton B, et al. A core of functionally complementary bacteria colonizes oysters in Pacific Oyster Mortality Syndrome. *bioRxiv* (2020). doi: 10.1101/2020.11.16.384644
56. Destoumieux-Garzon D, Canesi L, Oyanedel D, Travers MA, Charriere GM, Pruzzo C, et al. Vibrio-bivalve interactions in health and disease. *Environ Microbiol* (2020). doi: 10.1111/1462-2920.15055
57. Piel D, Bruto M, James A, Labreuche Y, Lambert C, Janicot A, et al. Selection of Vibrio crassostreae relies on a plasmid expressing a type 6 secretion system cytotoxic for host immune cells. *Environ Microbiol* (2020) 22 (10):4198–211. doi: 10.1111/1462-2920.14776
58. Harvell CD, Mitchell CE, Ward JR, Altizer S, Dobson AP, Ostfeld RS, et al. Climate warming and disease risks for terrestrial and marine biota. *Science* (2002) 296(5576):2158–62. doi: 10.1126/science.1063699
59. Ben-Haim Y, Zicherman-Keren M, Rosenberg E. Temperature-regulated bleaching and lysis of the coral Pocillopora damicornis by the novel pathogen Vibrio coralliilyticus. *Appl Environ Microbiol* (2003) 69(7):4236–42. doi: 10.1128/AEM.69.7.4236-4242.2003
60. Ittiprasert W, Knight M. Reversing the resistance phenotype of the Biomphalaria glabrata snail host Schistosoma mansoni infection by temperature modulation. *PLoS Pathog* (2012) 8(4):e1002677. doi: 10.1371/journal.ppat.1002677
61. Kimes NE, Grim CJ, Johnson WR, Hasan NA, Tall BD, Kothary MH, et al. Temperature regulation of virulence factors in the pathogen Vibrio coralliilyticus. *ISME J* (2012) 6(4):835–46. doi: 10.1038/ismej.2011.154
62. Vidal-Dupiol J, Dheilly NM, Rondon R, Grunau C, Cosseau C, Smith KM, et al. Thermal stress triggers broad Pocillopora damicornis transcriptomic remodeling, while Vibrio coralliilyticus infection induces a more targeted immuno-suppression response. *PLoS One* (2014) 9(9):e107672. doi: 10.1371/journal.pone.0107672
63. Vidal-Dupiol J, Ladriere O, Destoumieux-Garzon D, Sautiere PE, Meistertzheim AL, Tambutte E, et al. Innate immune responses of a scleractinian coral to vibriosis. *J Biol Chem* (2011) 286(25):22688–98. doi: 10.1074/jbc.M110.216358
64. Pernet F, Lagarde F, Jeannee N, Daigle G, Barret J, Le Gall P, et al. Spatial and temporal dynamics of mass mortalities in oysters is influenced by energetic reserves and food quality. *PLoS One* (2014) 9(2):e88469. doi: 10.1371/journal.pone.0088469
65. Petton B, Boudry P, Alunno-Bruscia M, Pernet F. Factors influencing disease-induced mortality of Pacific oysters Crassostrea gigas. *Aquaculture Environ Interact* (2015) 6(3):205–22. doi: 10.3354/aei00125
66. Delisle L, Petton B, Burguin JF, Morga B, Corporeau C, Pernet F. Temperature modulate disease susceptibility of the Pacific oyster Crassostrea gigas and virulence of the Ostreid herpesvirus type 1. *Fish Shellfish Immunol* (2018) 80:71–9. doi: 10.1016/j.fsi.2018.05.056
67. Dégremont L. Evidence of herpesvirus (OsHV-1) resistance in juvenile Crassostrea gigas selected for high resistance to the summer mortality phenomenon. *Aquaculture* (2011) 317(1-4):94–8. doi: 10.1016/j.aquaculture.2011.04.029
68. Segarra A, Mauduit F, Faury N, Trancart S, Degremont L, Tourbiez D, et al. Dual transcriptomics of virus-host interactions: comparing two Pacific oyster families presenting contrasted susceptibility to ostreid herpesvirus 1. *BMC Genomics* (2014) 15(580):1–13. doi: 10.1186/1471-2164-15-580
69. Divilov K, Schoolfield B, Morga B, Dégremont L, Burge CA, Mancilla Cortez D, et al. First evaluation of resistance to both a California OsHV-1 variant and a French OsHV-1 microvariant in Pacific oysters. *BMC Genet* (2019) 20(1):96. doi: 10.1186/s12863-019-0791-3
70. Camara MD, Yen S, Kaspar HF, Kesarcodi-Watson A, King N, Jeffs AG, et al. Assessment of heat shock and laboratory virus challenges to selectively breed for ostreid herpesvirus 1 (OsHV-1) resistance in the Pacific oyster, Crassostrea gigas. *Aquaculture* (2017) 469:50–8. doi: 10.1016/j.aquaculture.2016.11.031
71. Dégremont L, Nourry M, Maurouard E. Mass selection for survival and resistance to OsHV-1 infection in Crassostrea gigas spat in field conditions: response to selection after four generations. *Aquaculture* (2015) 446:111–21. doi: 10.1016/j.aquaculture.2015.04.029
72. Divilov K, Schoolfield B, Morga B, Degremont L, Burge CA, Mancilla Cortez D, et al. First evaluation of resistance to both a California OsHV-1 variant and a French OsHV-1 microvariant in Pacific oysters. *BMC Genet* (2019) 20 (1):96. doi: 10.1186/s12863-019-0791-3
73. Zhang G, Fang X, Guo X, Li L, Luo R, Xu F, et al. The oyster genome reveals stress adaptation and complexity of shell formation. *Nature* (2012) 490 (7418):49–54. doi: 10.1038/nature11413
74. Gutierrez AP, Turner F, Gharbi K, Talbot R, Lowe NR, Penaloza C, et al. Development of a Medium Density Combined-Species SNP Array for Pacific and European Oysters (Crassostrea gigas and Ostrea edulis). *G3 (Bethesda)* (2017) 7(7):2209–18. doi: 10.1534/g3.117.041780
75. Gutierrez AP, Bean TP, Hooper C, Stenton CA, Sanders MB, Paley RK, et al. A Genome-Wide Association Study for Host Resistance to Ostreid Herpesvirus in Pacific Oysters (Crassostrea gigas). *G3 (Bethesda)* (2018) 8 (4):1273–80. doi: 10.1534/g3.118.200113

76. de Lorgeril J, Petton B, Lucasson A, Perez V, Stenger PL, Degremont L, et al. Differential basal expression of immune genes confers Crassostrea gigas resistance to Pacific oyster mortality syndrome. *BMC Genomics* (2020) 21 (1):63. doi: 10.1186/s12864-020-6471-x
77. Oldenburg M, Kruger A, Ferstl R, Kaufmann A, Nees G, Sigmund A, et al. TLR13 recognizes bacterial 23S rRNA devoid of erythromycin resistance-forming modification. *Science* (2012) 337(6098):1111–5. doi: 10.1126/science.1220363
78. Shi Z, Cai Z, Sanchez A, Zhang T, Wen S, Wang J, et al. A novel Toll-like receptor that recognizes vesicular stomatitis virus. *J Biol Chem* (2011) 286 (6):4517–24. doi: 10.1074/jbc.M110.159590
79. Oden E, Martenot C, Berthaux M, Travaillé E, Malas JP, Houssin M. Quantification of ostreid herpesvirus 1 (OsHV-1) in Crassostrea gigas by real-time PCR: Determination of a viral load threshold to prevent summer mortalities. *Aquaculture* (2011) 317(1-4):27–31. doi: 10.1016/j.aquaculture.2011.04.001
80. Dégremont L. Size and genotype affect resistance to mortality caused by OsHV-1 in Crassostrea gigas. *Aquaculture* (2013) 416-417:129–34. doi: 10.1016/j.aquaculture.2013.09.011
81. Lochmiller RL, Deerenberg C. Trade-offs in evolutionary immunology: just what is the cost of immunity? *Oikos* (2000) 88(1):87–98. doi: 10.1034/j.1600-0706.2000.880110.x
82. Sheldon BC, Verhulst S. Ecological immunology: costly parasite defences and trade-offs in evolutionary ecology. *Trends Ecol Evol* (1996) 11(8):317–21. doi: 10.1016/0169-5347(96)10039-2
83. Smith VH, Jones TP, Smith MS. Host nutrition and infectious disease: an ecological view. *Front Ecol Environ* (2005) 3(5):268–74. doi: 10.1890/1540-9295(2005)003[0268:HNAIDA]2.0.CO;2
84. Civitello DJ, Fatima H, Johnson LR, Nisbet RM, Rohr JR. Bioenergetic theory predicts infection dynamics of human schistosomes in intermediate host snails across ecological gradients. *Ecol Lett* (2018) 21(5):692–701. doi: 10.1111/ele.12937
85. Hall SR, Simonis JL, Nisbet RM, Tessier AJ, Cáceres CE. Resource Ecology of Virulence in a Planktonic Host-Parasite System: An Explanation Using Dynamic Energy Budgets. *Am Nat* (2009) 174(2):149–62. doi: 10.1086/600086
86. Ayres JS, Schneider DS. The role of anorexia in resistance and tolerance to infections in Drosophila. *PLoS Biol* (2009) 7(7):e1000150. doi: 10.1371/journal.pbio.1000150
87. Murray MJ, Murray AB. Anorexia of infection as a mechanism of host defense. *Am J Clin Nutr* (1979) 32(3):593–6. doi: 10.1093/ajcn/32.3.593
88. Evans O, Hick P, Dhand N, Whittington RJ. Transmission of Ostreid herpesvirus-1 in Crassostrea gigas by cohabitation: effects of food and number of infected donor oysters. *Aquaculture Env Interact* (2015) 7 (3):281–95. doi: 10.3354/aei00160
89. Moreau P, Moreau K, Segarra A, Tourbiez D, Travers MA, Rubinsztein DC, et al. Autophagy plays an important role in protecting Pacific oysters from OsHV-1 and Vibrio aestuarianus infections. *Autophagy* (2015) 11(3):516–26. doi: 10.1080/15548627.2015.1017188
90. Pernet F, Fuhrmann M, Petton B, Mazurie J, Bouget JF, Fleury E, et al. Determination of risk factors for herpesvirus outbreak in oysters using a broad-scale spatial epidemiology framework. *Sci Rep* (2018) 8(1):10869. doi: 10.1038/s41598-018-29238-4
91. Jouaux A, Lafont M, Blin J-L, Houssin M, Mathieu M, Lelong C. Physiological change under OsHV-1 contamination in Pacific oyster *Crassostrea gigas* through massive mortality events on fields. *BMC Genomics* (2013) 14(590):1–14. doi: 10.1186/1471-2164-14-590
92. Segarra A, Mauduit F, Faury N, Trancart S, Dégremont L, Tourbiez D, et al. Dual transcriptomics of virus-host interactions: Comparing two Pacific oyster families presenting contrasted susceptibility to ostreid herpesvirus 1. *BMC Genomics* (2014) 15(1):1–13. doi: 10.1186/1471-2164-15-580
93. Desai M, Fang R, Sun J. The role of autophagy in microbial infection and immunity. *ImmunoTargets Ther* (2015) 4:13–26. doi: 10.2147/ITT.S76720
94. Wegner KM, Volkenborn N, Peter H, Eiler A. Disturbance induced decoupling between host genetics and composition of the associated microbiome. *BMC Microbiol* (2013) 13:252. doi: 10.1186/1471-2180-13-252
95. King WL, Siboni N, Williams NLR, Kahlke T, Nguyen KV, Jenkins C, et al. Variability in the Composition of Pacific Oyster Microbiomes Across Oyster Families Exhibiting Different Levels of Susceptibility to OsHV-1 muvar Disease. *Front Microbiol* (2019) 10:473. doi: 10.3389/fmicb.2019.00473
96. Clerissi C, de Lorgeril J, Petton B, Lucasson A, Escoubas JM, Gueguen Y, et al. Microbiota Composition and Evenness Predict Survival Rate of Oysters Confronted to Pacific Oyster Mortality Syndrome. *Front Microbiol* (2020) 11:311. doi: 10.3389/fmicb.2020.00311
97. Pernet F, Lupo C, Bacher C, Whittington RJ. Infectious diseases in oyster aquaculture require a new integrated approach. *Philos Trans R Soc Lond B Biol Sci* (2016) 371(1689):1–9. doi: 10.1098/rstb.2015.0213
98. Sofonea MT, Alizon S, Michalakis Y. Exposing the diversity of multiple infection patterns. *J Theor Biol* (2017) 419:278–89. doi: 10.1016/j.jtbi.2017.02.011
99. Garcia C, Thebault A, Degremont L, Arzul I, Miossec L, Robert M, et al. Ostreid herpesvirus 1 detection and relationship with Crassostrea gigas spat mortality in France between 1998 and 2006. *Vet Res* (2011) 42:73. doi: 10.1186/1297-9716-42-73
100. Paul-Pont I, Dhand NK, Whittington RJ. Spatial distribution of mortality in Pacific oysters Crassostrea gigas: reflection on mechanisms of OsHV-1 transmission. *Dis Aquat Organ* (2013) 105(2):127–38. doi: 10.3354/dao02615
101. Whittington RJ, Liu O, Hick PM, Dhand N, Rubio A. Long-term temporal and spatial patterns of Ostreid herpesvirus 1 (OsHV-1) infection and mortality in sentinel Pacific oyster spat (Crassostrea gigas) inform farm management. *Aquaculture* (2019) 513:1–15. doi: 10.1016/j.aquaculture.2019.734395

Conflict of Interest: The authors declare that the research was conducted in the absence of any commercial or financial relationships that could be construed as a potential conflict of interest.

frontiers in Immunology

ORIGINAL RESEARCH
published: 31 March 2021
doi: 10.3389/fimmu.2021.659469

Gender Differences in Hemocyte Immune Parameters of Hong Kong Oyster *Crassostrea hongkongensis* During Immune Stress

Jie Lu[1]*, *Yanyan Shi*[2], *Tuo Yao*[1], *Changming Bai*[3], *Jingzhe Jiang*[4] and *Lingtong Ye*[4]*

[1] Key Laboratory of South China Sea Fishery Resources Exploitation and Utilization, Ministry of Agriculture and Rural Affairs, South China Sea Fisheries Research Institute, Chinese Academy of Fishery Sciences, Guangzhou, China, [2] Department of Chemical and Biochemical Engineering, College of Chemistry and Chemical Engineering, Xiamen University, Xiamen, China, [3] Key Laboratory of Maricultural Organism Disease Control, Ministry of Agriculture and Rural Affairs, Qingdao Key Laboratory of Mariculture Epidemiology and Biosecurity, Yellow Sea Fisheries Research Institute, Chinese Academy of Fishery Sciences, Qingdao, China, [4] Key Laboratory of Aquatic Product Processing, Ministry of Agriculture and Rural Affairs, South China Sea Fisheries Research Institute, Chinese Academy of Fishery Sciences, Guangzhou, China

OPEN ACCESS

Edited by:
Chaozheng Li,
Sun Yat-Sen University, China

Reviewed by:
Zhaoqun Liu,
Dalian Ocean University, China
Alex Cordoba-Aguilar,
Universidad Nacional Autónoma de México, Mexico

***Correspondence:**
Jie Lu
lujie@scsfri.ac.cn
Lingtong Ye
lingtong2753@126.com

Specialty section:
This article was submitted to Comparative Immunology, a section of the journal Frontiers in Immunology

Received: *27 January 2021*
Accepted: *15 March 2021*
Published: *31 March 2021*

Citation:
Lu J, Shi Y, Yao T, Bai C, Jiang J and Ye L (2021) Gender Differences in Hemocyte Immune Parameters of Hong Kong Oyster Crassostrea hongkongensis During Immune Stress. Front. Immunol. 12:659469. doi: 10.3389/fimmu.2021.659469

Gender differences in individual immune responses to external stimuli have been elucidated in many invertebrates. However, it is unclear if gender differences do exist in the Hong Kong oyster *Crassostrea hongkongensis*, one of the most valuable marine species cultivated along the coast of South China. To clarify this, we stimulated post-spawning adult *C. hongkongensis* with *Vibrio harveyi* and lipopolysaccharide (LPS). Gender-based differences in some essential functional parameters of hemocytes were studied *via* flow cytometry. Obvious gender-, subpopulation-, and immune-specific alterations were found in the hemocyte immune parameters of *C. hongkongensis*. Three hemocyte subpopulations were identified: granulocytes, semi-granulocytes, and agranulocytes. Granulocytes, the chief phagocytes and major producers of esterase, reactive oxygen species, and nitric oxide, were the main immunocompetent hemocytes. Immune parameter alterations were notable in the accumulation of granulocyte esterase activities, lysosomal masses, nitric oxide levels, and granulocyte numbers in male oysters. These results suggest that post-spawning-phase male oysters possess a more powerful immune response than females. Gender and subpopulation differences in bivalve immune parameters should be considered in the future analysis of immune parameters when studying the impact of pathogenic or environmental factors.

Keywords: gender-based difference, cellular immunity, hemocyte subpopulations, *Crassostrea hongkongensis*, immune stimulation

INTRODUCTION

Gender-specific differences in hemocyte immuno-competence have been reported in several aquatic invertebrates (1, 2). For example, in the sea urchin *Paracentrotus lividus*, females possess more immunocytes, consisting of phagocytes, uncolored spherulocytes, and the coelomocyte lysate, than males (3). Studies on the immune system of the clam (*Ruditapes philippinarum*) showed that, during

the pre-spawning period, females have more active hemocytes than males (4). A higher phagocytic index was observed in female triploids compared with male Pacific oysters (*Crassostrea gigas*) (5). In contrast, males of the sea cucumber *Apostichopus japonicus* have a stronger antioxidant ability and more effective complement system than females after spawning (6). These studies suggest that gender-based differences in immune function and disease susceptibility are a common feature of aquatic invertebrates.

Many studies of bivalves have reported the impacts of external factors, such as pathogenic bacteria (7), salinity (8), temperature (9), and pollutants (10, 11), on hemocyte immune parameters. However, few reported investigations have examined gender-related differences in immune parameters in response to environmental factors. The phagocytic activity of female blue mussels, *Mytilus edulis*, showed a higher sensitivity to mercury than that of the males (12). Female *C. corteziensis* oysters were found to be more susceptible than males to thermic, mechanical, and mechanical-thermic stress conditions (13). Apoptosis, mortality, and oxidative stress in male New Zealand Greenshell™ mussels (*Perna canaliculus*) were observed to increase after exposure to *Vibrio* sp. DO1 (1). These studies have provided evidence of gender-based differences in some immune parameters of hemocytes toward external factors. However, bivalve hemocytes are composed of multiple functional heterogeneous cell types, and the various cell types have different functions (14). Therefore, gender-related differences in the immune parameters of hemocyte subpopulations should be investigated.

The hemocytes of bivalves can typically be separated into several subpopulations based on their morphological and cytochemical features, such as cell size, granularity, and nucleus-cytoplasm (N:C) ratio (14). Many studies have led to the characterization of the hemocyte subpopulations of different bivalves, such as green-lipped mussel (*Perna canaliculus*) (15), horse mussel (*Modiolus kurilensis*) (16), and pearl oyster (*Pteria hirundo*) (17). For example, circulating hemocytes of eastern oysters (*C. virginica*) were classified as agranulocytes, intermediate hemocytes, granulocytes, and small granulocytes (18). *C. gigas* hemocytes were grouped into three morphologically different subpopulations that included agranulocytes, semi-granulocytes, and granulocytes (19). Although different hemocyte populations have been reported for many bivalves, classifying the hemocyte morphologies in individual species is necessary, as not all bivalves have the same types and proportions of hemocytes (20, 21). Additionally, differences in hemocyte subpopulations may be important causative factors in the above-mentioned gender-based differences in the immune parameters of hemocytes. However, few reports are available on gender-related differences in the immune responses of subpopulations after immune stimulation.

In the present study, we aimed to investigate gender-specific differences in the immunological responses of different oyster hemocyte subpopulations following exposure to lipopolysaccharide (LPS) and *Vibrio harveyi*. The hemocyte subpopulations in the Hong Kong oyster *C. hongkongensis* were separated by flow cytometry based on their morphological features. Molecular probes were then used to characterize the cells' corresponding immune functions.

MATERIALS AND METHODS

Oyster and Hemocyte Collection

Healthy post-spawning adults of *C. hongkongensis* (shell height 11.23 ± 0.06 cm) were collected in July 2020 from a commercial farm in Taishan, Jiangmen, Guangdong Province, China. The oysters were maintained in aerated sand-filtered seawater at a salinity of 20 ± 1 psu and temperature of 23-25°C, and fed twice daily with *Isochrysis galbana* and *Chaetoceros muelleri* for 7 days.

Vibrio harveyi was cultured in 2216 broth at 28°C for 14 h and harvested by centrifugation (5000 × *g*, 10 min). After washing twice with aseptic seawater, *V. harveyi* was resuspended in aseptic seawater at a final concentration of approximately 1×10^7 CFU/mL. LPS (from *Escherichia coli* O111: B4, Sigma) was dissolved in aseptic seawater to a concentration of 0.5 mg/mL. We randomly divided 180 oysters into three groups, and each received injections of 100 μL LPS solution (LPS group), *V. harveyi* suspension (*V. harveyi* group), or aseptic seawater (control group) into the adductor muscle. Each group contained three replicates, with 20 oysters per replicate.

The hemolymph was sampled from the posterior adductor muscle of *C. hongkongensis* at 24 h post-injection using a 5-mL syringe fitted with a 22-G needle and mixed immediately with an equal volume of modified Alsever's solution (glucose 20.8 g/L, sodium chloride 13.5 g/L, sodium citrate 8.0 g/L, EDTA-Na_2 4.28 g/L, 600 mOsm/kg, 0.22 μm filtered), then centrifuged at 4°C, 500 × *g* for 10 min. The hemocytes pellets were resuspended to 1.5-2 × 10^6 cells/mL in modified L15 medium (Leibovitz's L15 medium with 4.42 g/L NaCl, 3.9 g/L $MgCl_2$, 1 g/L $MgSO_4$, 0.6 g/L $CaCl_2$, 0.54 g/L KCl, streptomycin 100 mg/mL, penicillin 100 IU/mL, 600 mOsm/kg, 0.22 μm filtered) for later analysis. To reduce individual variation, the hemocytes from three individuals per group were pooled into one sample, and at least five male and five female replicates were used in the following assays. Oyster sex was judged by visually inspecting the males and females releasing gametes. The hemocyte concentration in the hemolymph was evaluated using manual counting methods with a Neubauer chamber.

Subpopulations Analysis of Hemocytes

The histological characterization of hemocytes was performed under light microscopy following Wright-Giemsa staining (22). Stained slides were observed using a light microscope (Leica DM2000, Leica, Heerbrugg, Switzerland), and hemocyte subpopulations were characterized according to their morphological features.

Flow cytometric analyses of the hemocytes subpopulations were conducted with a FACS Arial II flow cytometer (Becton, Dickinson and Company). Briefly, 200 μL of hemocyte suspension was stained with SYBR-Green I (10× final concentration, Invitrogen, Life Technologies) in the dark for 1 h at 25°C. The fluorescence emissions were measured in the FL1 channel (530 nm). Hemocyte subtypes were distinguished using the SYBR Green positive cell density-plot according to their morphological parameters, side scatter (SSC) for internal granularity, and forward scatter (FSC) for relative size.

Measurement of Immune Parameters by Flow Cytometry

The hemocyte parameters were analyzed using FACS Arial II flow cytometry. A total of 10,000 events were acquired for each sample. The data were displayed as cell cryptograms indicating the relative size, internal granularity, and fluorescence channels corresponding to the fluorescent markers used. The fluorescence frequency distribution histogram of each hemocyte subpopulation was then obtained. The fluorescence recorded depended on the monitored immunological parameters: hemocyte late apoptosis or necrosis was measured in the propidium iodide (PI) channel (610/20 nm), and the others were evaluated in the FITC channel (530/30 nm). The data were analyzed using FlowJo v10.3 software (FlowJo LLC, Ashland, OR). All analyses were completed within 2 hours.

Apoptosis and necrosis in hemocytes were tested with a commercial detection kit using Annexin V-FITC and PI according to the optimized manufacturer's instructions (Beyotime Biotechnology, China). Briefly, 100·μL of hemocyte suspension (0.5-1 × 10^6 cells/mL in annexin V-FITC binding buffer adjusted with NaCl to be isotonic to the oysters' environments) was incubated with 5·μL Annexin V and 10·μL PI solutions. After a 15 min incubation at 25°C in the dark, the cell solutions were diluted 1:4 with binding buffer. Early apoptosis-associated fluorescence (FITC) and late apoptosis or necrosis-associated fluorescence (PI) were measured by flow cytometry. The bivariate analysis allowed the discrimination of viable (FITC−/PI−), early apoptotic (FITC+), and late apoptotic or necrotic hemocytes (FITC+/PI+).

The phagocytic activity was measured using 1-μm diameter yellow-green fluorescent polystyrene beads (Fluoresbrite, PolyScience 17154). The hemocytes were incubated in M-L15 in the dark for 1 h at 25°C at a 1:100 hemocyte-bead ratio before flow cytometry analysis. The phagocytic activity of each hemocyte subpopulation was expressed as the percentage that engulfed at least three fluorescent beads.

The mitochondrial mass, lysosomal mass, non-specific esterase activity, reactive oxygen species (ROS) level, nitric oxide (NO) level, and intracellular calcium concentration were measured using commercialized probes and chemical compounds (Beyotime Biotechnology, China) by following the manufacturer's instructions. Briefly, 200 μL of hemocyte suspension was mixed with the corresponding probes, then incubated at 25°C in the dark before processing with flow cytometry. The final concentration and incubation time of the probes are listed in **Table 1**. The parameters in each hemocyte subpopulation were expressed as the mean fluorescence intensity (MFI) in arbitrary units (A.U.).

TABLE 1 | Final concentration and incubation time of probes used in this study.

Immune parameters	Fluorescent probe	Final concentration	Incubation time
Mitochondrial mass	Mito-Tracker Green	100 nmol/L	15 min
Lysosomal mass	Lyso-Tracker Green DND-26	75 nmol/L	45 min
Non-specific esterase activity	Fluorescein diacetate	5 μmol/L	30 min
ROS	DCFH-DA	10 mmol/L	20 min
NO	DAF-FM DA	5 mmol/L	20 min
Calcium concentration	Flou-4 AM	2 mmol/L	20 min

Statistical Analysis

The data were first tested for normality using the Shapiro-Wilk's test and for homogeneity of variance using Levene's test. Percentage data were arcsine-transformed, and other data were log10 transformed. Principal component analysis (PCA) was used to characterize the relationships among the immune function variables. Two-way MANOVA was used to test for the gender, immune stimulation, and interaction effects on all measured parameters, and Pillai's trace was used to assess significance. Two-way ANOVA was then used to test for gender, immune stimulation, and interaction effects on each measured parameter. We used Tukey's multiple comparisons test for *post hoc* analysis to compare individual means. Spearman's correlation analysis was used to assess the relationship among the immunological parameters with the corrplot (23) and corrr (24) packages in R. Data are presented as the mean ± standard deviation (SD), and $p < 0.05$ was used to determine significance.

RESULTS

Microscopic and Flow Cytometric Characteristics of the Hemocytes

The cytological observations outlined in **Figure 1A** show that three subtypes of hemocytes, agranulocytes (A), semi-granulocytes (SG), and granulocytes (G), were identified in the Hong Kong oyster *C. hongkongensis* based on size and internal complexity on Wright-Giemsa staining. The cells were further classified using the cell density plot, which represents the relative cell size (FSC-H) and internal complexity (SSC-H) from the flow cytometry analysis (**Figure 1B**). Specifically, G, the largest cell subpopulation, was characterized by cytoplasm with many large granules and a relatively small N:C ratio; whereas A represented the smallest and the least complex cells with no granules in the cytoplasm and the largest N:C ratio. SG were identified as median types between agranulocytes and granulocytes. No significant differences were detected between males and females with regards to the size and complexity of the hemocytes.

Functional Characterization of Hemocytes Subpopulations

Multivariate Data Analyses of All Hemocyte Subpopulations

We observed strong immune stimulation, gender, and interaction effects on all measured parameters (MANOVA, Pillai's trace = 4.582, $F_{22,32} = 1.518$, $p < 0.001$; Pillai's trace = 0.730, $F_{11,15} = 3.692$, $p = 0.01$; and Pillai's trace = 1.628, $F_{22,32} = 1.980$, $p < 0.001$, respectively). Additionally, PCA was performed on the immunological parameters to identify intrinsic immunological trends and the differential immunological parameters responsible for stimulation. PCA showed that

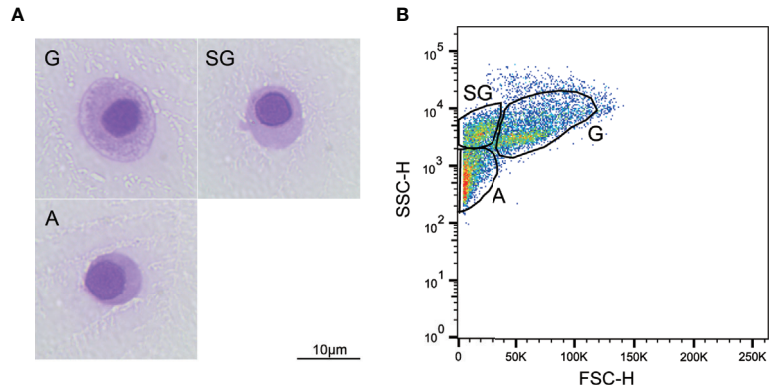

FIGURE 1 | Morphological characterization of *C. hongkongensis* hemocytes. **(A)** Light micrographs of different hemocyte subpopulations after Wright-Giemsa staining. **(B)** Flow cytometric dot plot of size (FSC) against internal complexity (SSC) of hemocyte subpopulations of a representative sample. G, granulocytes; SG, semi-granulocytes; A, agranulocytes.

56.9% of the total variance was explained by two principal components (**Figure 2**). PC1 represented 36.8% of the total variance, indicating a significant separation between males and females. The characteristics of the hemocyte functions associated with males were higher NO levels, lysosome mass, and esterase activities and late apoptotic or necrotic ratios coupled with lower early apoptotic ratios. Moreover, there was a clear separation between the four stimulation groups on PCA.

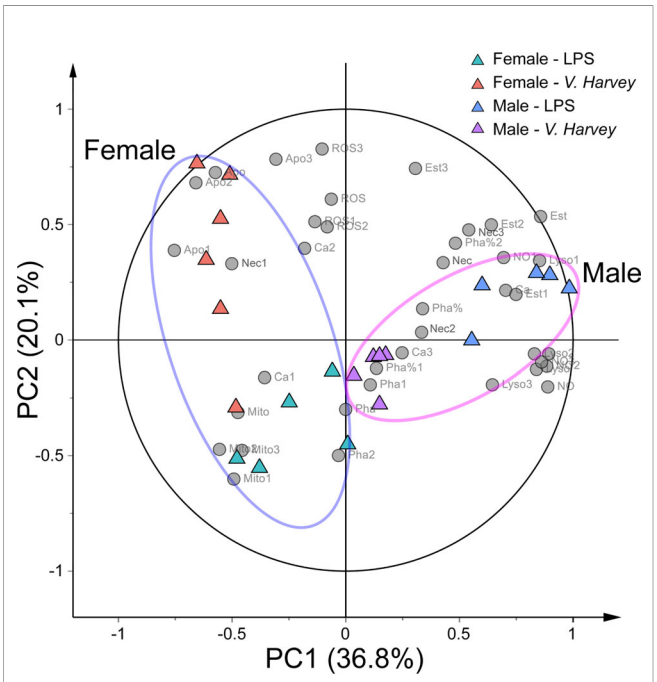

FIGURE 2 | PCA biplot showing the relationships among all immunological parameters and four exposure groups (LPS-infected males, LPS-infected females, *V. harveyi*-infected males, and V. harveyi-infected females) for all hemocyte subpopulations. 1, granulocytes; 2, semi-granulocytes; 3, agranulocytes. Mito, mitochondrial mass; NO, nitric oxideNO level; Ca, calcium content, Pha, phagocytic ratio; Est, esterase activity; ROS, ROS level; Lyso, lysosome mass; Apo, early apoptotic ratio; Nec, late apoptotic or necrotic ratio.

Composition Changes in Hemocytes After Stimulations

The hemocyte concentration in *C. hongkongensis* under the control conditions was $1.12 \pm 1.1 \times 10^6$ cells/mL. The total hemocyte count (THC) did not vary statistically between the genders under each fixed condition but was reduced by two immune stimulations. Additionally, the sizes of three hemocyte subpopulations were significantly affected by gender, immune stimulation, and their interactions, at most time points in the experiment (**Table S1**). In male oysters, granulocyte and agranulocyte numbers significantly increased and decreased, respectively, after the two immune stimulation types (**Figure 3**); however, in females, the number of semi-granulocytes significantly increased, whereas granulocytes and agranulocytes decreased, after the two immune stimulations (**Figure 3**).

Annexin V-FITC/PI Assay

Figure 4A shows representative Annexin V-FITC vs PI scatter diagrams for the different hemocyte subpopulations, with quadrant gates showing four populations. Most granulocytes were viable and non-apoptotic. Data from the four populations were further plotted in **Figures 4B, C**, which showed that both apoptotic and necrotic ratios were significantly higher in semi-granulocytes and agranulocytes than in granulocytes.

The early apoptotic ratios of total hemocytes, semi-granulocytes, and agranulocytes were significantly affected by immune stimulation, gender, and their interactions, at most time points (**Table S1**). Immune stimulation had no effect on the early apoptotic ratios of hemocyte subpopulations in male oysters but affected female oysters. Challenging the oysters with *V. harveyi* significantly increased the early apoptotic ratios of the semi-granulocytes and agranulocytes. Both LPS and *V. harveyi* stimulations significantly increased the late apoptotic or necrotic ratios of all hemocytes.

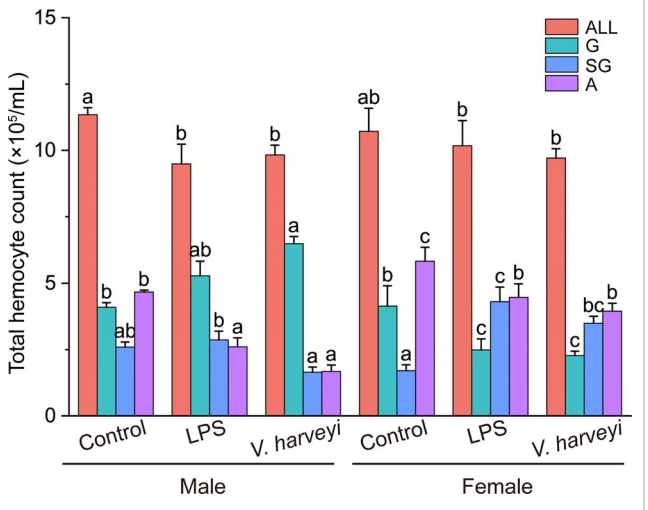

FIGURE 3 | Number of all hemocyte (ALL), granulocytes (G), semi-granulocytes (SG), and agranulocytes (A) of female and male oysters after LPS, *V. harveyi*, or control stimulation. The means denoted by different letters at each fixed hemocyte subpopulation are significantly different among different treatments ($p < 0.05$).

Phagocytic Activities of Hemocyte Subpopulations

Flow cytometry and fluorescent microspheres were used to detect the phagocytic activities of the different subpopulations. Both granulocytes and semi-granulocytes showed phagocytic capacities, whereas agranulocytes did not (**Figure 5A**). The percentage phagocytosis of granulocytes was significantly higher ($p < 0.001$) than that of semi-granulocytes (**Figure 5B**). The phagocytic ratios of total hemocytes and granulocytes were significantly affected by interactions between immune stimulation and gender during the experiment (**Table S1**), and the phagocytic indexes of granulocytes showed a significant increase after LPS stimulation (**Figure 5B**).

Six Immunological Parameters of Hemocyte Subpopulations

ROS and NO levels, lysosome and mitochondrial masses, calcium concentrations, and non-specific esterase activity were evaluated using the flow cytometer. The relative mean fluorescence intensities of the granulocytes for the six immunological parameters were significantly higher compared with the corresponding semi-granulocyte and agranulocyte readings under all situations (**Figure 6**).

After immune stimulation with LPS or *V. harveyi*, lysosomal masses in all hemocyte subpopulations were significantly altered

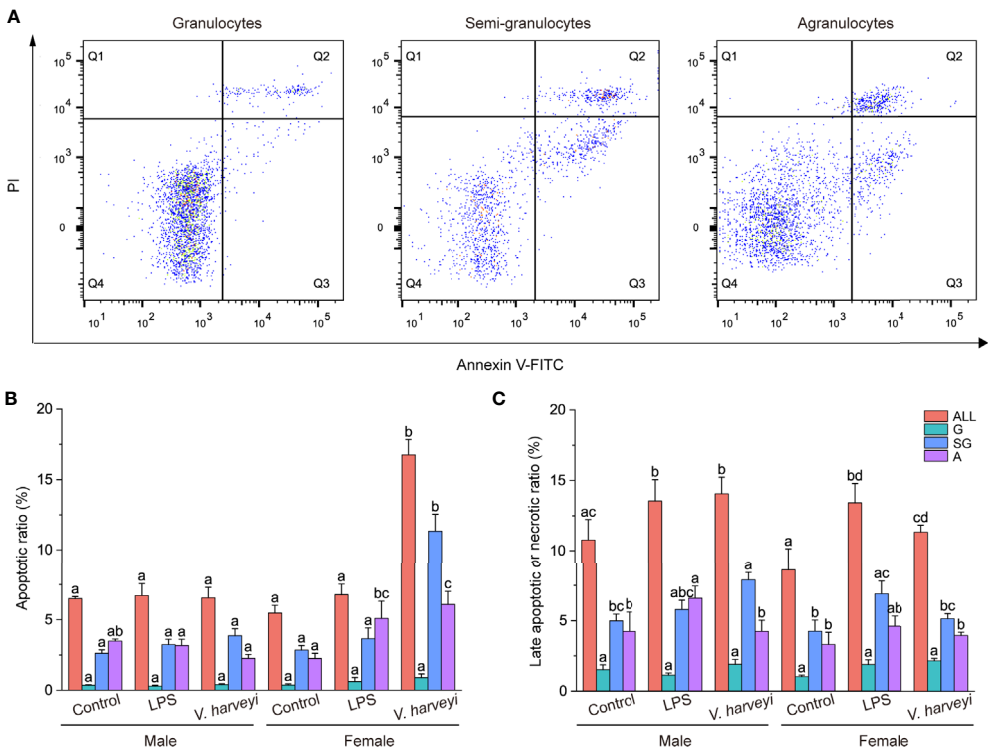

FIGURE 4 | Results of the annexin V-FITC and propidium iodide (PI) assay. **(A)** Representative scatter diagrams of three hemocyte subpopulations from *C. hongkongensis*. **(B)** Early apoptotic hemocyte ratios of different hemocyte subpopulations. **(C)** Late apoptotic or necrotic hemocyte ratios of different hemocyte subpopulations. The means denoted by different letters for each fixed hemocyte subpopulation are significantly different among different treatments ($p < 0.05$). G, granulocytes; SG, semi-granulocytes; A, agranulocytes.

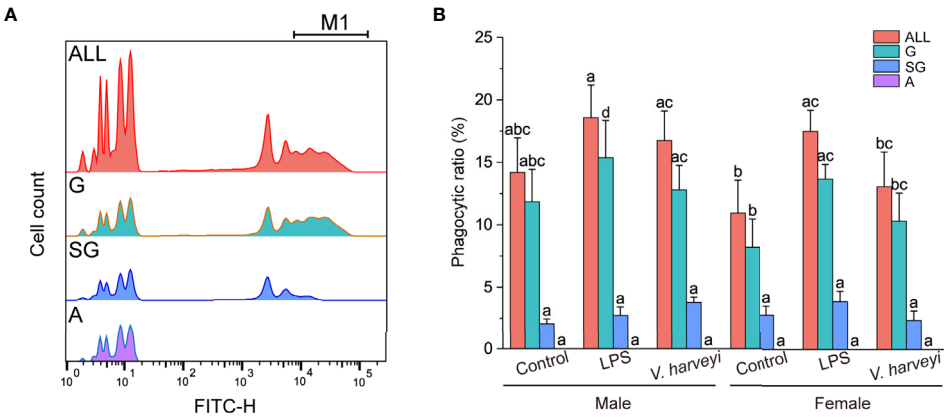

FIGURE 5 | Phagocytic capability of each hemocyte subpopulation. **(A)** Histogram of fluorescence representing phagocytic activity recorded in different hemocyte subpopulations: M1, hemocytes that engulfed three or more fluorospheres. **(B)** Phagocytic ratios of different subpopulations after stimulation. The means denoted by different letters for each fixed hemocyte subpopulation are significantly different among the different stimulation types ($p < 0.05$). G, granulocytes; SG, semi-granulocytes; A, agranulocytes.

by interactions between immune stimulation and gender (**Table S1**). Granulocytes and semi-granulocytes from male oysters exhibited significantly higher lysosomal masses after LPS stimulation (**Figure 6A**).

Mitochondrial masses of total hemocytes, granulocytes, and semi-granulocytes were significantly affected by immune stimulation, gender, and their interactions, at most time points (**Table S1**). The granulocytes of male and female oysters showed significantly lower mitochondrial masses under the two stimulation conditions (**Figure 6B**).

The esterase activity of each hemocyte subpopulation was significantly affected by interactions between immune stimulation and gender (**Table S1**). Esterase activity values in all the hemocytes of female oysters were significantly lower than those of males (**Figure 6C**). Furthermore, both LPS and *V. harveryi* challenge significantly increased the esterase activities of granulocytes from male oysters, whereas those from females exhibited no change.

Granulocyte ROS production levels were significantly affected by immune stimulation and gender (**Table S1**). As shown in **Figure 6D**, immune stimulation did not affect the intracellular ROS concentration of any hemocyte subpopulation in male oysters; whereas LPS and infection by *V. harveryi* significantly increased the ROS concentration of granulocytes in female oysters.

Immune stimulation and the interactions between immune stimulation and gender significantly affected the intracellular calcium levels of granulocytes (**Table 1**). As shown in **Figure 6E**, all hemocyte subpopulation of female oysters showed no significant response in calcium levels to immune stimulations. However, the intracellular calcium levels in male oyster granulocytes were upregulated after LPS stimulation and downregulated after *V. harveryi* challenge.

NO production levels were significantly affected by interactions between immune stimulation and gender (**Table S1**). After immune stimulation, NO production levels of total hemocytes, granulocytes, and semi-granulocytes significantly increased in both male and female oysters. However, the rate of increase in females was lower than that in males.

Correlation Analysis for Immune Parameters

A correlation heatmap and network diagram were applied to represent the Spearman's correlation coefficients among the immunological parameters of granulocytes, including lysosome and mitochondrial masses; NO, ROS and calcium levels; and phagocytic, early apoptotic, and late apoptotic or necrotic ratios of the total hemocytes. The significant correlations suggest that the parameters were in equilibrium with each other or the concentrations of correlated parameters were simultaneously controlled by the different forms of immune stimulation. As shown in **Figure 7A**, granulocyte NO levels were positively correlated with phagocytic ratio, esterase activities, and lysosome mass, and negatively associated with mitochondrial mass. Esterase activities showed a positive correlation with lysosome mass, late apoptotic or necrotic ratio, and phagocytic ratio. Moreover, in the Spearman's analysis, NO levels were adjacent to the phagocytic ratios, and esterase activities were close to lysosome masses (**Figure 7B**), indicating biological relationships between them.

DISCUSSION

The Hong Kong oyster *C. hongkongensis* is one of the most commercially farmed oysters in China. However, the frequent occurrence of infectious diseases in *C. hongkongensis*, especially after spawning, is a major problem in the oyster aquaculture industry. To prevent mortality and subsequent management in

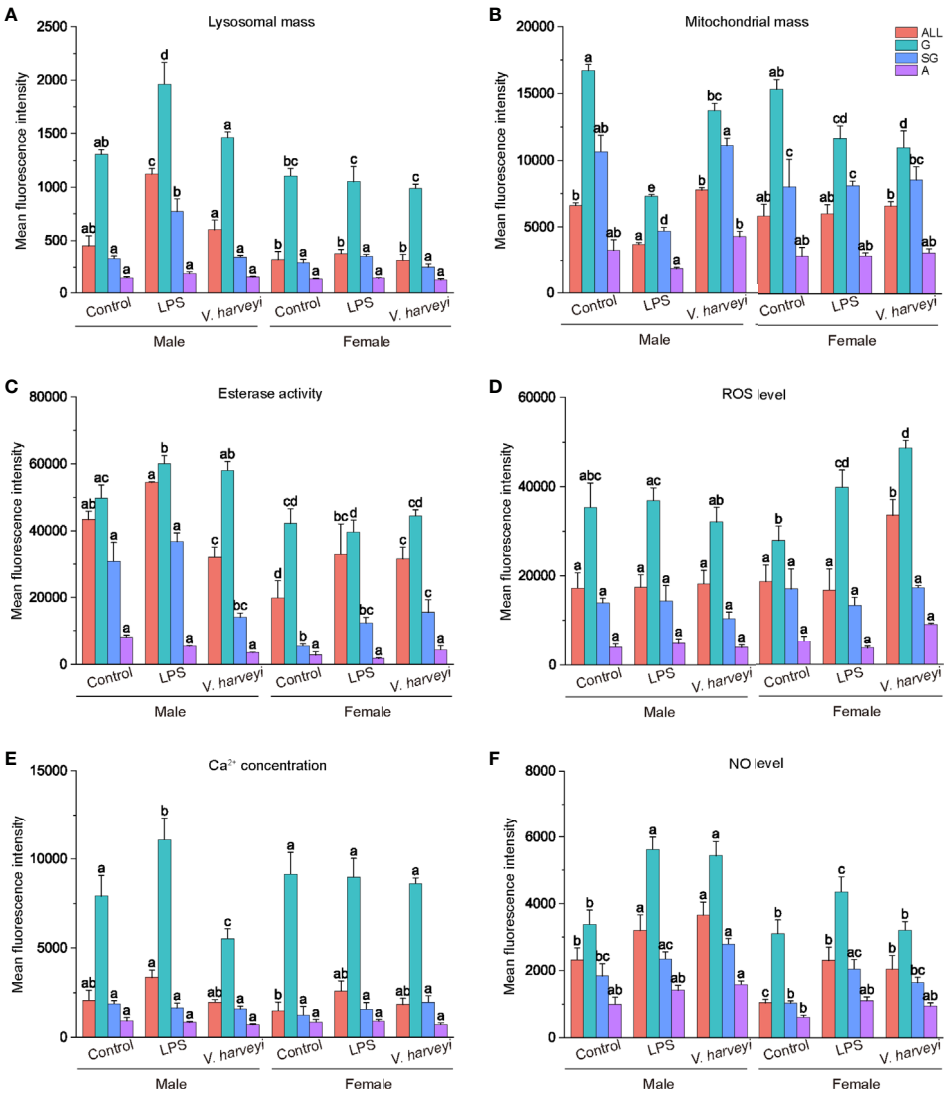

FIGURE 6 | Immunological characteristics of all hemocyte subpopulations after stimulation. **(A)** lysosomal mass, **(B)** mitochondrial mass, **(C)** esterase activity, **(D)** ROS level, **(E)** intracellular calcium concentration, **(F)** NO level. The means denoted by different letters for each fixed hemocyte subpopulation are significantly different among the different stimulations ($p < 0.05$). G, granulocytes; SG, semi-granulocytes; A, agranulocytes.

Hong Kong oyster farms, an understanding of the oyster immune system is crucial (25). Genetic studies have shown that mollusk hemocytes are essential immune cells with many functions, including phagocytosis, hemolymph clotting, encapsulation, and the production of antimicrobial compounds (22). Hemocytes in mollusks comprise morphologically and functionally diverse subpopulations characterized by different physical properties such as cell size, granularity, and nucleus-cytoplasm ratio (14). In the present study, we used Wright-Giemsa staining and flow cytometry to characterize the hemocyte subpopulations from the Hong Kong oyster *C. hongkongensis*, and agranulocytes, semi-granulocytes, and granulocytes were easily distinguished and separated. Three hemocyte subpopulations have also been identified in other oyster species: the Pacific oyster *C. gigas* (19), the Suminoe oyster *C. ariakensis* (26), and the European flat oyster *Ostrea edulis* (27). Li et al. (25) reported that the circulating hemocytes of *C. hongkongensis* could be separated into hyalinocytes and granulocytes. It is noteworthy that the osmolality of the anticoagulant used in that study was approximately 1000 mOsm/kg, which is much higher than the normal osmotic pressure in Hong Kong oysters (< 650 mOsm/kg). The high osmotic pressure may have caused cell morphology changes, and thus the hyalinocytes were suspected to be composed of semi-granulocytes and agranulocytes. Cell sorting combined with the transcriptome analysis of *C. hongkongensis* hemocytes also indicated that the semi-granulocytes and agranulocytes were two different populations (Lu et al., unpublished).

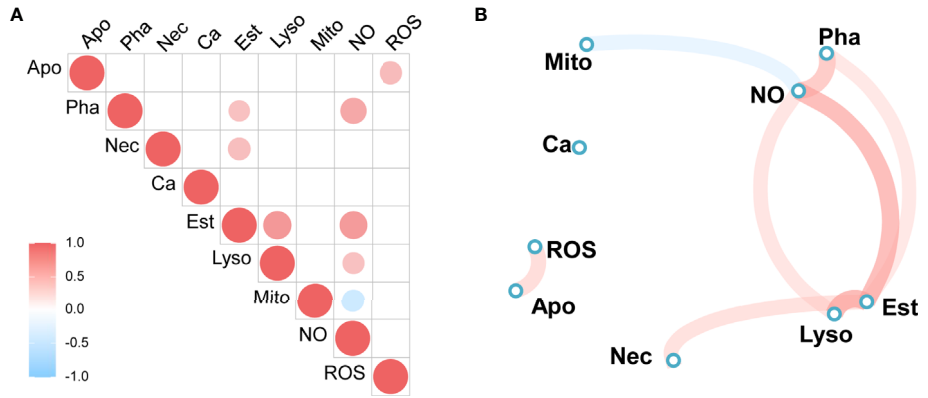

FIGURE 7 | Spearman's correlation analysis of immune parameters. **(A)** Heatmap of correlation coefficients, **(B)** Correlation network diagram. Red to sky-blue represents positive to negative correlations. Mito, mitochondrial mass; NO, NO level; Ca, calcium content, Pha, phagocytic ratio; Est, esterase activity; ROS, ROS level; Lyso, lysosome mass; Apo, early apoptotic ratio; Nec, late apoptotic or necrotic ratio.

In the present study, we discovered that lysosome and mitochondrial masses, NO and ROS levels, and phagocytic and non-specific esterase activities were mainly concentrated in granulocytes under all conditions. Granulocytes were reported to be the main immunocompetent hemocytes in *C. gigas* (19), *Pila globose*, and *Lamellidens marginalis* (28); therefore, we speculated that granulocytes are also the principal immune hemocytes in *C. hongkongensis*. Many studies have indicated that the immunological parameters of mollusk hemocytes show some variations in response to different immune stimulations (2, 4). However, only a few studies have highlighted the influence of gender on immune functions in marine mollusks; therefore, we used multivariate statistical methods to evaluate the effects of immune stimulation and gender on immunological parameters. Both the MANOVA and PCA results showed that both immune stimulation and gender affected the hemocyte immune parameters in *C. hongkongensis*, and an interaction effect was also evident. However, almost no differences in the hemocyte immune parameters of male and female oysters under normal conditions were found. To our knowledge, this is the first report describing gender-related differences in the immunological parameters of the Hong Kong oyster *C. hongkongensis* after immune stimulation.

THC is an essential immunological parameter for predicting the health of mollusks because hemocytes migrate from the circulatory system to tissues to help resist invading pathogens. This study showed that the hemolymph of *C. hongkongensis* had a hemocyte concentration of $1.12 \pm 1.1 \times 10^6$ cells/mL, which was lower than the concentration measured by Li et al. (25) ($2.52 \pm 1.1 \times 10^6$ cells/mL). Previous studies have shown that hemocyte concentrations can be affected by endogenous (e.g., age, size, gender, and reproductive period) and exogenous (e.g., temperature, salinity, pH, and pollutants) factors (29, 30). It is likely the differences in the total number of hemocytes seen in the present study and that by Li et al. (25) were due to size, reproductive period, or sampling season. In agreement with previous studies (31, 32), two immune stimulation types led to a decrease in the THC, but no significant difference in the THC was found between genders. Similarly, Cheng et al. (33) also reported no significant difference in the THC between genders of *Macrobrachium rosenbergii*, and Duchemin et al. (5) observed that THC did not differ with gender in triploid or diploid *C. gigas*. Reportedly, the percentages of the different cell subpopulations in the hemolymph can vary according to environmental and pathogenic stimulation (2, 34). We found no significant differences in the numbers of hemocyte subpopulations between male and female oysters under normal conditions in this study. However, two immune stimulations induced increases in the agranulocyte populations of male oysters and decreases in those of females. Conversely, a higher proportion of active granulocytes was observed in female *Ruditapes philippinarum* clams (4). This difference may be attributed to the different reproductive states of the animals, as Matozzo and Marin (4) sampled clams during the pre-spawning phase, whereas the population in the present study was collected after spawning. Because granulocytes were the main immunocompetent hemocytes, the increased proportion of granulocytes in males shows that the males had more active hemocytes than the females under immune-activated situations. These findings demonstrate that immune stimulation induced the gender-specific stress responses in hemocyte subpopulations.

Annexin-V assays, which are reliably used to detect apoptotic and necrotic cells in mammals, were used to quantify the innate defense mechanism of *C. hongkongensis* by adjusting the reagent osmolalities to 600 mOsm/kg. This work demonstrated the high percentages of late apoptotic or necrotic cells in total hemocytes from male and female oysters after immune stimulation. A significant inverse correlation ($r = -0.85$, $p < 0.05$) was observed between the number of total hemocytes and the percentage of late apoptotic or necrotic cells. Similar to previous findings (31), the phenomenon revealed that the disappearance of the hemocytes correlated with cell necrosis and apoptosis. Moreover, as previously observed in *C. gigas* (5), no gender difference in late apoptosis and necrosis of hemocytes

was observed in *C. hongkongensis*. Apoptosis, an orchestrated physiological process of cellular self-destruction, is essential for the correct functioning of the molluscan immune system (35). We observed lower early apoptosis rates for all granulocytes and higher apoptosis rates for semi-granulocytes in female oysters compared with males after stimulation by *V. harveyi* infection, suggesting that the semi-granulocytes in females were more susceptible to *V. harveyi* infection. The release of ROS by hemocytes is a key internal defense mechanism by which pathogens are destroyed before their phagocytosis (36). Higher ROS production was detected in female than male granulocytes, especially after LPS or *V. harveryi* stimulation. Gender-dependent differences were also reported in the abundance of ROS in the hemocytes of *Saccostrea glomerata* and *Pinctada fucata* (2). As shown in **Figure 7**, ROS was positively correlated with early apoptosis. Excess cellular levels of ROS have been shown to induce apoptosis (37). The higher levels of ROS, combined with the higher early apoptosis rate, show that *V. harveryi* challenge induced the apoptosis of female hemocytes *via* ROS generation. These findings indicate that male and female oysters use different intracellular oxidative metabolic strategies to resist LPS or *V. harveyi* infection.

Phagocytosis is an essential and effective defense mechanism against foreign pathogens. A decrease in the male and female oyster phagocytic index was witnessed in the present study, from strong phagocytosis in granulocytes, weak phagocytosis in semigranulocytes, to no phagocytosis in agranulocytes. Similar results have been reported for *C. gigas* (19). The phagocytic ratio of the total granulocytes was significantly upregulated after LPS challenge, but no significant difference was detected after *V. harveyi* challenge. Jiang et al. (38) reported that LPS, but not peptidylglycan, significantly increased phagocytic activities in *C. gigas*. These results indicated that different stimulants induced phagocytic activities *via* different strategies. Furthermore, statistical analysis revealed that male oysters had slightly (although not significantly) more phagocytic ratios than females under all corresponding conditions. Female and male diploid *C. gigas* also showed no statistically significant differences in their phagocytic index (5). NO has many biological functions related to defense and immune responses in marine invertebrates (28). In the present study, both LPS and *V. harveryi* stimulation induced a noticeable gender-specific increase in NO levels. Thus, in hemocytes, NO appears to play a pivotal role in the killing of intracellular pathogens. NO was also shown to be involved in defense mechanisms in the mollusk *Mytilus edulis* (39), and it appeared to be a cellular signal involved in the response to environmental stress in *C. virginica* (40). The NO produced by the immune cells of Wistar rats had a role in intracellular killing and phagocytic activity (41). Coincidentally, correlation analysis showed that granulocyte NO levels significantly correlated with the phagocytic ratios (**Figure 7**). Therefore, we concluded that the hemocytes of *C. hongkongensis* generate NO as a cytokine to regulate the phagocytic activities protecting the hosts from LPS or *V. harveyi* infection. Additionally, the significantly higher NO levels and the non-significant higher phagocytic ratio of males oysters after immune stimulation also indicate that males are more immunocompetent than females. Mitochondria, responsible for the energy production processes necessary for cell metabolism, vary in their number, activity, and localization in animal cells in relation to energetic needs (42). A decrease in mitochondrial function is often accompanied by an increase in proton leak, inhibition of vital mitochondrial enzymes, and elevated production of nitric oxide and reactive oxygen species (43). Notably, the mitochondrial mass showed a negative correlation with the level of nitric oxide (**Figure 7**); therefore, the lower mitochondrial mass observed in both male and female oysters after immune stimulation might be due to a higher concentration of NO. However, this needs further research.

Lysosomes, which are important bacteriolytic cellular organelles, are employed as an index to evaluate the health status and vitality of the defense system in bivalves (29) and are generally affected by environmental stress (30). Lysosomal masses of *C. gigas* granulocytes were significantly increased after stimulation with *V. splendidus* (19). Similar results were found for the male *C. hongkongensis* in this study following LPS stimulation, indicating gender-specific lysosomal responses by granulocytes to LPS stimulation. The gender-dependent differences in lysosomal masses were also reported for *Ruditapes philippinarum* (4) and *Panorpa vulgaris* (44); however, it was the hemocytes of the females of these two species that showed higher lysosomal masses. Intracellular calcium not only participates in various biological activities, such as metabolism regulation and biomineralization, but also acts as a ubiquitous second messenger to regulate intracellular or intercellular signal transduction (45, 46). The stress of organelles, including the endoplasmic reticulum, mitochondria, and lysosomes, might lead to the release of calcium into the cytoplasm (47). The concentrations of intracellular calcium in male granulocytes increased after LPS treatment, suggesting that intracellular calcium served as an essential mediator in the immune response, and much more calcium was required to maintain the lysosome mass. This speculation is supported by the higher lysosome mass in male granulocytes under LPS challenge. Increased intracellular calcium levels and lysosome masses were also observed in P1 hemocytes of *Eriocheir sinensis* (14). The hydrolase enzyme non-specific esterase plays a pivotal role in intracellular degradation and the stress response in the hemocytes of mussels (30, 48). In the present study, we observed gender differences in the esterase activities of male and female oysters, with lower levels in female oysters compared with males under all conditions. Higher hydrolytic enzyme activity has also been observed in male *R. philippinarum* compared with females. In *C. virginica*, non-specific esterase was detected and inferred to be associated with lysosome-like bodies (49); interestingly, there were significant positive correlations between the esterase activity and lysosomal mass. The esterase activity in *C. hongkongensis* granulocytes was adjacent to lysosomal mass in the Spearman's correlation analysis. Hence, the gender-specific activity of esterase could be considered a consequence of gender-specific differences in lysosomal mass. The higher esterase activities and lysosomal masses in males compared with females further suggest that gender-specific immune responses were induced in *C. hongkongensis* hemocytes.

Generally, adult females mount stronger innate and adaptive immune responses than males (50). Many theories, such as the immunocompetence handicap hypothesis (ICHH) (51), Bateman's principle (52), evolutionary-ecology approach (53), and the sicker sex principle (54), attempt to explain why gender differences exist. However, in this study, the upregulation of granulocyte esterase activities, lysosomal masses, nitric oxide levels, and granulocyte numbers was observed in male *C. hongkongensis*. These findings indicate that males have a more powerful cellular immune response level than females after spawning. Because Hong Kong Oysters reproduce using external fertilization, we speculate that females may invest more reproductive resources and have a weaker immune system after spawning. This speculation can be proved by the high mortality of post-spawning-phase female Hong Kong oysters. In the sea cucumber *A. japonicus*, the stronger antioxidant ability is also observed in males than that in females after spawning (6). In the current study, we have analyzed the differences in immunity to infections between male and female oysters based on hemocyte immune parameters, but humoral immunity systems such as the phenoloxidase system (55) also play an important role in molluscan immunity, which is worthy of further study.

CONCLUSION

In this study, gender-related differences in immune responses to LPS and *V. harveyi* were reported for the first time in the Hong Kong oyster *C. hongkongensis* during the post-spawning phase. To accurately assess the immune parameters in hemocytes, three types of hemocyte were identified: granulocytes, semi-granulocytes, and agranulocytes. Because granulocytes were identified as the primary phagocytes, with a dense mass of mitochondria and lysosomes and prominent esterase, superoxide anion, and nitric oxide activities, we concluded that granulocytes are the main immunocompetent hemocytes in *C. hongkongensis*. Our multivariate statistical results showed that gender, immune stimulation, and their interaction, affected the immune-related parameters of hemocyte subpopulations. Significantly lower THC values were recorded in both male and female oysters, but significantly higher percentages of granulocytes were found in the hemolymph of males after immune stimulation compared with that of females. Esterase activities and lysosomal masses were positively correlated, and they significantly increased in male hemocytes after immune challenge. NO levels were also upregulated in males and were positively associated with non-significantly higher phagocytic ratios in males post-immune infection. These results suggest that, during the post-spawning stage, male oysters have more effective defense responses against immune infection than females. Therefore, gender and subpopulation differences should be included in the future analysis of bivalve immune parameters when studying the impact of pathogens, environmental variables, or multiple variables.

DATA AVAILABILITY STATEMENT

The original contributions presented in the study are included in the article/**Supplementary Material**. Further inquiries can be directed to the corresponding authors.

ETHICS STATEMENT

The animal study was reviewed and approved by The Animal Care and Ethics Committee of South China Sea Fisheries Research Institute, Chinese Academy of Fishery Sciences.

AUTHOR CONTRIBUTIONS

JL: funding acquisition, methodology, validation, data curation, writing—original draft, writing—review & editing. YS: methodology, writing—review and editing. TY: Writing—review and editing. CB: Writing—review and editing. JJ: writing—review and editing. LY: funding acquisition, writing—review and editing. All authors contributed to the article and approved the submitted version.

FUNDING

This work was financially supported by National Key R&D Program of China (2019YFD0900105), Central Public-interest Scientific Institution Basal Research Fund, South China Sea Fisheries Research Institute, CAFS (2017YB22), the earmarked fund for Modern Agro-industry Technology Research System (CARS-49), the Central Public-interest Scientific Institution Basal Research Fund, CAFS (2020TD42, 2021SD05), National Key R&D Program of China (2019YFD0900105), the Science and Technology Planning Project of Guangzhou (202002030488), the Shellfish and Large Algae Industry Innovation Team Project of Guangdong Province (2021KJ146), the Professorial and Doctoral Scientific Research Foundation of Huizhou University (2020JB0650), and Provincial Rural Revitalization Strategy Special Funds (Fishery Industry Development).

ACKNOWLEDGMENTS

We thank Suzanne Leech, Ph.D., from Edanz Group (https://en-author-services.edanz.com/ac) and Jiangyong Wang, Prof., from Huizhou University for editing a draft of this manuscript.

SUPPLEMENTARY MATERIAL

The Supplementary Material for this article can be found online at: https://www.frontiersin.org/articles/10.3389/fimmu.2021.659469/full#supplementary-material

REFERENCES

1. Nguyen TV, Alfaro AC, Merien F, Young T, Grandiosa R. Metabolic and immunological responses of male and female new Zealand Greenshell mussels (*Perna canaliculus*) infected with *Vibrio* sp. *J Invertebr Pathol* (2018) 157:80–9. doi: 10.1016/j.jip.2018.08.008
2. Dang C, Tan T, Moffit D, Debouttéville JD, Barnes AC. Gender differences in hemocyte immune parameters of bivalves: the Sydney rock oyster *Saccostrea glomerata* and the pearl oyster *Pinctada fucata*. *Fish Shellfish Immunol* (2012) 33:138–42. doi: 10.1016/j.fsi.2012.04.007
3. Arizza V, Vazzana M, Schillaci D, Russo D, Giaramita FT, Parrinello N. Gender differences in the immune system activities of sea urchin *Paracentrotus lividus*. *Comp Biochem Physiol A: Mol Integr Physiol* (2013) 164:447–55. doi: 10.1016/j.cbpa.2012.11.021
4. Matozzo V, Marin MG. First evidence of gender-related differences in immune parameters of the clam *Ruditapes philippinarum* (Mollusca, Bivalvia). *Mar Biol* (2010) 157:1181–9. doi: 10.1007/s00227-010-1398-4
5. Duchemin MB, Fournier M, Auffret M. Seasonal variations of immune parameters in diploid and triploid Pacific oysters, *Crassostrea gigas* (Thunberg). *Aquaculture* (2007) 264:73–81. doi: 10.1016/j.aquaculture.2006.12.030
6. Jiang J, Zhao Z, Pan Y, Dong Y, Gao S, Li S, et al. Gender specific differences of immune competence in the sea cucumber *Apostichopus japonicus* before and after spawning. *Fish Shellfish Immunol* (2019) 90:73–9. doi: 10.1016/j.fsi.2019.04.051
7. Ciacci C, Manti A, Canonico B, Campana R, Camisassi G, Baffone W, et al. Responses of *Mytilus galloprovincialis* hemocytes to environmental strains of *Vibrio parahaemolyticus*, *Vibrio alginolyticus*, *Vibrio vulnificus*. *Fish Shellfish Immunol* (2017) 65:80–7. doi: 10.1016/j.fsi.2017.04.002
8. Gajbhiye DS, Khandeparker L. Immune response of the short neck clam *Paphia malabarica* to salinity stress using flow cytometry. *Mar Environ Res* (2017) 129:14–23. doi: 10.1016/j.marenvres.2017.04.009
9. Gagnaire B, Frouin H, Moreau K, Thomas-Guyon H, Renault T. Effects of temperature and salinity on haemocyte activities of the Pacific oyster, *Crassostrea gigas* (Thunberg). *Fish Shellfish Immunol* (2006) 20:536–47. doi: 10.1016/j.fsi.2005.07.003
10. Hong HK, Donaghy L, Kang CK, Kang HS, Lee HJ, Park HS, et al. Substantial changes in hemocyte parameters of Manila clam *Ruditapes philippinarum* two years after the Hebei Spirit oil spill off the west coast of Korea. *Mar Pollut Bull* (2016) 108:171–9. doi: 10.1016/j.marpolbul.2016.04.033
11. Sendra M, Volland M, Balbi T, Fabbri R, Yeste MP, Gatica JM, et al. Cytotoxicity of CeO2 nanoparticles using in vitro assay with *Mytilus galloprovincialis* hemocytes: Relevance of zeta potential, shape and biocorona formation. *Aquat Toxicol* (2018) 200:13–20. doi: 10.1016/j.aquatox.2018.04.011
12. Brousseau-Fournier C, Alix G, Beaudry A, Gauthier-Clerc S, Duchemin M, Fortier M, et al. Role of confounding factors in assessing immune competence of bivalves (*Mya arenaria*, *Mytilus edulis*) exposed to pollutants. *J Xenobiotics* (2013) 3:3–5. doi: 10.4081/xeno.2013.s1.e2
13. Hurtado-Oliva M.á., Gómez-Hernández SJ, Gutiérrez-Rivera JN, Estrada N, Piña-Valdez P, Nieves-Soto M, et al. Gender differences and short-term exposure to mechanical, thermic, and mechanical—thermic stress conditions on hemocyte functional characteristics and *Hsp*70 gene expression in oyster *Crassostrea corteziensis* (Hertlein, 1951). *J Shellfish Res* (2015) 34:849–59. doi: 10.2983/035.034.0314
14. Jia Z, Wang L, Jiang S, Sun M, Wang M, Yi Q, et al. Functional characterization of hemocytes from Chinese mitten crab *Eriocheir sinensis* by flow cytometry. *Fish Shellfish Immunol* (2017) 69:15–25. doi: 10.1016/j.fsi.2017.08.001
15. Rolton A, Ragg NLC. Green-lipped mussel (*Perna canaliculus*) hemocytes: A flow cytometric study of sampling effects, sub-populations and immune-related functions. *Fish Shellfish Immunol* (2020) 103:181–9. doi: 10.1016/j.fsi.2020.05.019
16. Kumeiko VV, Sokolnikova YN, Grinchenko AV, Mokrina MS, Kniazkina MI. Immune state correlates with histopathological level and reveals molluscan health in populations of *Modiolus kurilensis* by integral health index (IHI). *J Invertebr Pathol* (2018) 154:42–57. doi: 10.1016/j.jip.2018.03.014
17. Vieira GC, Da Silva PM, Barracco MA, Hering AF, Albuquerque MCP, Coelho JDR, et al. Morphological and functional characterization of the hemocytes from the pearl oyster *Pteria hirundo* and their immune responses against *Vibrio infections*. *Fish Shellfish Immunol* (2017) 70:750–8. doi: 10.1016/j.fsi.2017.09.040
18. Lau YT, Sussman L, Pales Espinosa E, Katalay S, Allam B. Characterization of hemocytes from different body fluids of the eastern oyster *Crassostrea virginica*. *Fish Shellfish Immunol* (2017) 71:372–9. doi: 10.1016/j.fsi.2017.10.025
19. Wang W, Li M, Wang L, Chen H, Liu Z, Jia Z, et al. The granulocytes are the main immunocompetent hemocytes in *Crassostrea gigas*. Dev. *Comp Immunol* (2017) 67:221–8. doi: 10.1016/j.dci.2016.09.017
20. Preziosi BM, Bowden TJ. Morphological characterization via light and electron microscopy of Atlantic jackknife clam (*Ensis directus*) hemocytes. *Micron* (2016) 84:96–106. doi: 10.1016/j.micron.2016.03.003
21. Mao F, Wong NK, Lin Y, Zhang X, Liu K, Huang M, et al. Transcriptomic evidence reveals the molecular basis for functional differentiation of hemocytes in a marine invertebrate, *Crassostrea gigas*. *Front Immunol* (2020) 11:911. doi: 10.3389/fimmu.2020.00911
22. Jiang S, Jia Z, Xin L, Sun Y, Zhang R, Wang W, et al. The cytochemical and ultrastructural characteristics of phagocytes in the Pacific oyster *Crassostrea gigas*. *Fish Shellfish Immunol* (2016) 55:490–8. doi: 10.1016/j.fsi.2016.06.024
23. Wei T, Simko V. *R package "corrplot": Visualization of a Correlation Matrix (Version 0.84)*. (2017). Available at: https://github.com/taiyun/corrplot.
24. Kuhn M, Jackson S, Cimentada J. *corrr: Correlations in R. R package version 0.4.3*. (2020). Available at: https://CRAN.R-project.org/package=corrr.
25. Li J, Zhang Y, Mao F, Lin Y, Xiao S, Xiang Z, et al. The first morphologic and functional characterization of hemocytes in Hong Kong oyster, *Crassostrea hongkongensis*. *Fish Shellfish Immunol* (2018) 81:423–9. doi: 10.1016/j.fsi.2018.05.062
26. Donaghy L, Kim BK, Hong HK, Park HS, Choi KS. Flow cytometry studies on the populations and immune parameters of the hemocytes of the Suminoe oyster, *Crassostrea ariakensis*. *Fish Shellfish Immunol* (2009) 27:296–301. doi: 10.1016/j.fsi.2009.05.010
27. Renault T, Xue QG, Chilmonczyk S. Flow cytometric analysis of European flat oyster, *Ostrea edulis*, haemocytes using a monoclonal antibody specific for granulocytes. *Fish Shellfish Immunol* (2001) 11:269–74. doi: 10.1006/fsim.2000.0312
28. Ray M, Bhunia NS, Bhunia AS, Ray S. A comparative analyses of morphological variations, phagocytosis and generation of cytotoxic agents in flow cytometrically isolated hemocytes of Indian molluscs. *Fish Shellfish Immunol* (2013) 34:244–53. doi: 10.1016/j.fsi.2012.11.006
29. Wu F, Lu W, Shang Y, Kong H, Li L, Sui Y, et al. Combined effects of seawater acidification and high temperature on hemocyte parameters in the thick shell mussel *Mytilus coruscus*. *Fish Shellfish Immunol* (2016) 56:554–62. doi: 10.1016/j.fsi.2016.08.012
30. Huang X, Jiang X, Sun M, Dupont S, Huang W, Hu M, et al. Effects of copper on hemocyte parameters in the estuarine oyster *Crassostrea rivularis* under low pH conditions. *Aquat Toxicol* (2018) 203:61–8. doi: 10.1016/j.aquatox.2018.08.003
31. Xu HS, Lyu SJ, Xu JH, Lu BJ, Zhao J, Li S, et al. Effect of lipopolysaccharide on the hemocyte apoptosis of *Eriocheir sinensis*. *J Zhejiang Univ Sci B* (2015) 16:971–9. doi: 10.1631/jzus.B1500098
32. Lv S, Xu J, Zhao J, Yin N, Lu B, Li S, et al. Classification and phagocytosis of circulating haemocytes in Chinese mitten crab (*Eriocheir sinensis*) and the effect of extrinsic stimulation on circulating haemocytes in vivo. *Fish Shellfish Immunol* (2014) 39:415–22. doi: 10.1016/j.fsi.2014.05.036
33. Cheng W, Chen JC. Effects of intrinsic and extrinsic factors on the haemocyte profile of the prawn, *Macrobrachium rosenbergii*. *Fish Shellfish Immunol* (2001) 11:53–63. doi: 10.1006/fsim.2000.0293
34. Evariste L, Auffret M, Audonnet S, Geffard A, David E, Brousseau P, et al. Functional features of hemocyte subpopulations of the invasive mollusk species *Dreissena polymorpha*. *Fish Shellfish Immunol* (2016) 56:144–54. doi: 10.1016/j.fsi.2016.06.054
35. Sokolova IM. Apoptosis in molluscan immune defense. *ISJ-Invert Surviv J* (2009) 6:49–58. doi: 10.3109/08830180903208303
36. Wu F, Cui S, Sun M, Xie Z, Huang W, Huang X, et al. Combined effects of ZnO NPs and seawater acidification on the haemocyte parameters of thick shell mussel *Mytilus coruscus*. Sci. *Total Environ* (2018) 624:820–30. doi: 10.1016/j.scitotenv.2017.12.168

37. Simon HU, Haj-Yehia A, Levi-Schaffer F. Role of reactive oxygen species (ROS) in apoptosis induction. *Apoptosis* (2000) 5:415–8. doi: 10.1023/a:1009616228304
38. Jiang S, Jia Z, Zhang T, Wang L, Qiu L, Sun J, et al. Functional characterisation of phagocytes in the Pacific oyster *Crassostrea gigas*. *PeerJ* (2016) 4:e2590. doi: 10.7717/peerj.2590
39. Gourdon I, Guerin MC, Torreilles J, Roch P. Nitric oxide generation by hemocytes of the mussel *Mytilus galloprovincialis*. *Nitric Oxide* (2001) 5:1–6. doi: 10.1006/niox.2000.0327
40. Ivanina AV, Eilers S, Kurochkin IO, Chung JS, Techa S, Piontkivska H, et al. Effects of cadmium exposure and intermittent anoxia on nitric oxide metabolism in eastern oysters, *Crassostrea virginica*. *J Exp Biol* (2010) 213:433–44. doi: 10.1242/jeb.038059
41. Tumer C, Bilgin HM, Obay BD, Diken H, Atmaca M, Kelle M. Effect of nitric oxide on phagocytic activity of lipopolysaccharide-induced macrophages: possible role of exogenous L-arginine. *Cell Biol Int* (2007) 31:565–9. doi: 10.1016/j.cellbi.2006.11.029
42. Agnello M, Morici G, Rinaldi AM. A method for measuring mitochondrial mass and activity. *Cytotechnology* (2008) 56:145–9. doi: 10.1007/s10616-008-9143-2
43. Doherty E, Perl A. Measurement of Mitochondrial Mass by Flow Cytometry during Oxidative Stress. *React Oxyg Species (Apex)* (2017) 4:275–83. doi: 10.20455/ros.2017.839
44. Kurtz J, Wiesner A, Gotz P, Sauer KP. Gender differences and individual variation in the immune system of the scorpionfly *Panorpa vulgaris* (Insecta: Mecoptera). *Dev Comp Immunol* (2000) 24:1–12. doi: 10.1016/s0145-305x(99)00057-9
45. Zheng J, Zeng X, Wang S. Calcium ion as cellular messenger. *Sci China Life Sci* (2015) 58:1–5. doi: 10.1007/s11427-014-4795-y
46. Wang X, Wang M, Wang W, Liu Z, Xu J, Jia Z, et al. Transcriptional changes of Pacific oyster *Crassostrea gigas* reveal essential role of calcium signal pathway in response to CO2-driven acidification. *Sci Total Environ* (2020) 741:140177. doi: 10.1016/j.scitotenv.2020.140177
47. Xian JA, Wang AL, Ye CX, Chen XD, Wang WN. Phagocytic activity, respiratory burst, cytoplasmic free-Ca^{2+} concentration and apoptotic cell ratio of haemocytes from the black tiger shrimp, *Penaeus monodon* under acute copper stress. *Comp Biochem Physiol C Toxicol Pharmacol* (2010) 152:182–8. doi: 10.1016/j.cbpc.2010.04.003
48. Mottin E, Caplat C, Mahaut ML, Costil K, Barillier D, Lebel JM, et al. Effect of in vitro exposure to zinc on immunological parameters of haemocytes from the marine gastropod *Haliotis tuberculata*. *Fish Shellfish Immunol* (2010) 29:846–53. doi: 10.1016/j.fsi.2010.07.022
49. Feng SY, Feng JS, Burke CN, Khairallah LH. Light and electron microscopy of the leucocytes of *Crassostrea virginica* (Mollusca: Pelecypoda). *Z Zellforsch Mikrosk Anat* (1971) 120:222–45. doi: 10.1007/BF00335537
50. Klein SL, Flanagan KL. Sex differences in immune responses. *Nat Rev Immunol* (2016) 16:626–38. doi: 10.1038/nri.2016.90
51. Folstad I, Karter AJ. Parasites, bright males, and the immunocompetence handicap. *Am Nat* (1992) 139:603–22. doi: 10.1086/285346
52. Rolff J. Bateman's principle and immunity. *Proc Biol Sci* (2002) 269:867–72. doi: 10.1098/rspb.2002.1959
53. Schmid-Hempel P. Variation in immune defence as a question of evolutionary ecology. *Proc Biol Sci* (2003) 270:357–66. doi: 10.1098/rspb.2002.2265
54. Córdoba-Aguilar A, Munguía-Steyer R. The sicker sex: understanding male biases in parasitic infection, resource allocation and fitness. *PloS One* (2013) 8:e76246. doi: 10.1371/journal.pone.0076246
55. González-Santoyo I, Córdoba-Aguilar A. Phenoloxidase: a key component of the insect immune system. *Entomol Exp Appl* (2012) 142:1–16. doi: 10.1111/j.1570-7458.2011.01187.x

Conflict of Interest: The authors declare that the research was conducted in the absence of any commercial or financial relationships that could be construed as a potential conflict of interest.

frontiers in Immunology

ORIGINAL RESEARCH
published: 01 April 2021
doi: 10.3389/fimmu.2021.659723

Proteomic Analysis of the Hemolymph After *Metschnikowia bicuspidata* Infection in the Chinese Mitten Crab *Eriocheir sinensis*

Hongbo Jiang[†], *Jie Bao*[†], *Yuenan Xing*, *Chengcheng Feng*, *Xiaodong Li* and *Qijun Chen*[*]

Key Laboratory of Livestock Infectious Diseases in Northeast China, Ministry of Education, Key Laboratory of Zoonosis, Shenyang Agricultural University, Shenyang, China

The "milky disease" of the Chinese mitten crab, *Eriocheir sinensis*, is a highly lethal fungal disease caused by *Metschnikowia bicuspidata* infection. To elucidate the immune responses of the hemolymph of *E. sinensis* to *M. bicuspidata* infection, a comparative analysis of the hemolymph of *E. sinensis* infected with *M. bicuspidata* and that treated with phosphate buffered saline was performed using label-free quantitative proteomics. A total of 429 proteins were identified. Using a 1.5-fold change in expression as a physiologically significant benchmark, 62 differentially expressed proteins were identified, of which 38 were significantly upregulated and 24 were significantly downregulated. The upregulated proteins mainly included cytoskeleton-related proteins (myosin regulatory light chain 2, myosin light chain alkali, tubulin α-2 chain, and tubulin β-1 chain), serine protease and serine protease inhibitor (clip domain-containing serine protease, leukocyte elastase inhibitor, serine protein inhibitor 42Dd), catalase, transferrin, and heat shock protein 70. Upregulation of these proteins indicated that phenoloxidase system, phagocytosis and the ROS systems were induced by *M. bicuspidata*. The downregulated proteins were mainly organ and tissue regeneration proteins (PDGF/VEGF-related factor protein, integrin-linked protein kinase homing pat-4 gene) and hemagglutination-associated proteins (hemolymph clottable protein, hemocyte protein-glutamine gamma-glutamyltransferase). Downregulation of these proteins indicated that *M. bicuspidata* inhibited hemocyte regeneration and hemolymph agglutination. Fifteen differentially expressed proteins related to immunity were verified using a parallel reaction monitoring method. The expression trend of these proteins was similar to that of the proteome. To the best of our knowledge, this is the first report on the proteome of *E. sinensis* in response to *M. bicuspidata* infection. These results not only provide new and important information on the immune response of crustaceans to yeast infection but also provide a basis for further understanding the molecular mechanism of complex host pathogen interactions between crustaceans and fungi.

Keywords: ***Metschnikowia bicuspidata***, ***Eriocheir sinensis***, **milky disease, proteome, immune response**

OPEN ACCESS

Edited by:
Chaozheng Li,
Sun Yat-Sen University, China

Reviewed by:
Qingguo Meng,
Nanjing Normal University, China
Yongxu Cheng,
Shanghai Ocean University, China

***Correspondence:**
Qijun Chen
qijunchen759@syau.edu.cn

[†]*These authors have contributed equally to this work*

Specialty section:
This article was submitted to Comparative Immunology, a section of the journal Frontiers in Immunology

Received: *28 January 2021*
Accepted: *16 March 2021*
Published: *01 April 2021*

Citation:
Jiang H, Bao J, Xing Y, Feng C, Li X and Chen Q (2021) Proteomic Analysis of the Hemolymph After Metschnikowia bicuspidata Infection in the Chinese Mitten Crab Eriocheir sinensis. Front. Immunol. 12:659723. doi: 10.3389/fimmu.2021.659723

INTRODUCTION

The Chinese mitten crab, *Eriocheir sinensis*, is a high-value economic aquatic product that is widely distributed in China's lakes and reservoirs. Fishery statistics from 2019 showed that the breeding output of *E. sinensis* reached 778,682 tons in China (1) and *E. sinensis* aquaculture has become an important pillar industry. With the rapid development of intensive culture of *E. sinensis*, various viral and bacterial diseases are causing serious damage to the aquaculture industry, leading to significant economic losses. At present, the reported diseases include *E. sinensis* tremor disease caused by *Spiroplasma eriocheiris* infection (2), vibrio disease caused by *Vibrio parahaemolyticus* and *V. anguillarum* (3, 4), hepatopancreatic necrosis disease caused by microsporidia (5), and parasitic diseases caused by ciliates (6). In 2018, some diseased *E. sinensis* with a milky-like liquid accumulated *in vivo* were found in Panjin city in the Liaoning province, and this condition was referred to as "milky disease." After infection, the activity of infected crabs was weakened, their pereiopods easily fell off, and the crabs died. The infection rate was greater than 20% (7). The pathogen was identified as *Metschnikowia bicuspidata*. The incidence of infection has now increased and the pathogen has spread to many cities and provinces in China. *M. bicuspidata* can infect not only invertebrates such as Artemia, Daphnia, *Portunus trituberculatus*, and *Macrobrachium rosenbergii*, but also fish (8–11). Similar to *P. trituberculatus* and *M. rosenbergii*, infected *E. sinensis* also showed milky symptoms. To the best of our knowledge, there are no effective prevention and control measures for "milky disease", although some progress has been made in *in vitro* experiments (12, 13).

It is well known that vertebrates have both innate and acquired immune systems; however, crustaceans only rely on innate immune systems to defend against foreign pathogens. As an important part of crustacean immunity, hemolymph plays a critical role in the process of crustacean resistance to foreign pathogens through phagocytosis, covering, and wound repair functions (14). Therefore, using hemolymph as the research object can better clarify the immune mechanism. In immunological research, transcriptomics and proteomics have been widely used to study the interaction between crustaceans and pathogens (15–17). Proteomics was able to identify the proteins and pathways involved in immune responses more accurately than transcriptomics, by analyzing the changes in host protein expression before and after pathogen invasion. In crustaceans, numerous immune-related proteins and pathways involved in pathogen infection were identified by describing their proteomic characteristics (18, 19). For example, the interaction between red claw crayfish and white spot syndrome virus (WSSV) *in vitro* was studied using proteomics (20). Twenty differential proteins in hemolymph that were involved in the immune responses of *E. sinensis* to *S. eriocheiris* infection were obtained using proteomics techniques (21). Sun et al. (22) used proteomics techniques to study the immune response of mud crabs to WSSV or *V. alginolyticus* infection. Therefore, proteomics is an excellent method for studying the immune response of crustaceans to yeast fungal infection.

The purpose of this study was to identify changes in protein expression in the hemolymph and elucidate the immune response of *E. sinensis* at the translational level after being challenged with *M. bicuspidata*. These results will not only provide new and important information on the immune response of crustaceans to yeast infection but will also provide a basis for further understanding the molecular mechanism of complex host pathogen interactions between crustaceans and fungi.

MATERIALS AND METHODS

Pathogen Challenge

Eriocheir sinensis (20 ± 3 g, 1: 1 female: male ratio) were purchased from a market in Panjin city, China, transported back to Shenyang Agricultural University, and temporarily cultured in 300 L tanks. Healthy *E. sinensis* [verified by *M. bicuspidata* negative results using PCR D1/D2 domain of the 26S rDNA sequence analyses (7)] were cultured for 7 d prior to the experimental tests. The control group (n = 30) was injected with 100 μL of phosphate-buffered saline (pH 7.4), and the experimental group (n = 30) was injected with 100 μL of *M. bicuspidata* (10^7 cells/mL). At 48 h post-infection, 15 individuals from each group were randomly selected, and the hemolymph was extracted from the last pereiopod with a 1 mL syringe and mixed with an equal volume of sterile anticoagulant citrate glucose solution B (21). Three biological replicates with five organisms mixed per replicate were performed in the two groups, amounting to six samples. The samples were frozen in liquid nitrogen and refrigerated at −80°C for further proteomic studies.

Protein Extraction

After sample refrigeration, 1% protease inhibitor was added to each group. The samples were then centrifuged at 4°C and 12000 × *g* for 10 min to remove cell debris. The supernatant was extracted and its protein concentration was determined using a BCA kit (Nanjing Jiancheng Bioengineering Institute, Nanjing, China), following the manufacturer's instructions.

Trypsin Digestion

Fifty micrograms of extracted proteins were enzymolyzed and the volume was adjusted to 200 μL with lysis buffer (8 M urea, 1% Triton 100, 10 mM dithiothreitol, and 1% protease inhibitor cocktail). An equal volume of precooled acetone was added. After vortex mixing, four times the volume of precooled acetone was added and precipitated at −20°C for 2 h. The supernatant was discarded after centrifugation at 4500 × *g* for 5 min. The precipitate was washed twice with precooled acetone and air-dried. After adding 200 mM tetraethylammonium bromide, the precipitate was dispersed using ultrasound. Next, 1:50 (trypsin: protein, M/M) trypsin was added for overnight enzymolysis. Subsequently, dithiothreitol was added (5 mM final concentration), and the sample was reduced for 30 min at 56°C. The final concentration of iodoacetamide was 11 mM, and this was incubated in the dark at 20°C for 15 min.

Analysis *via* Liquid Chromatography-Mass Spectrometry (LC-MS)/MS

The peptides were dissolved in mobile phase A and separated using an EASY-nLC 1000 ultra-performance liquid chromatography system (Thermo Fisher Scientific, Waltham, MA, USA). Both mobile phase A and B were aqueous solutions containing 0.1% formic acid and 2% acetonitrile, and 0.1% formic acid and 90% acetonitrile, respectively. The flow rate of the liquid was 450.00 nL/min, gradient settings were 0–90 min, 6–24% B; 90–114 min, 24–35% B; 114–117 min, 35–80% B; 117–120 min, 80% B. After ionization (nanoelectrospray ionization source, electrospray voltage: 2.1 kV), the peptide was analyzed using Q Exactive™ Plus (Thermo Fisher Scientific) mass spectrometry, and the parent ion and its secondary fragments were detected and analyzed using high-resolution Orbitrap. The scanning ranges and resolutions were respectively 350–1800 m/z and 70000.00 for the primary MS, and 100 m/z and 17500.00 for the secondary MS. A data-dependent scanning program was used during the data acquisition mode. The automatic gain control was set to 5E4, the signal threshold was set to 4E4 ions/s, and the maximum injection time was set to 50 ms.

Database Search

The secondary MS data were retrieved using Maxquant 1.5.2.8. Retrieval parameter settings were as follows: the database was *E. sinensis* (6843 sequences); to eliminate the influence of contaminated proteins in the identification results, a common contaminated library was added to the database. The cleavage enzyme was set as Trypsin/P; the number of missing sites was set as two. The minimum length of the peptide was set as seven amino acid residues; the maximum modification number of the peptide was set as 5. The mass error tolerance of primary parent ion was 10.0 ppm and 5 ppm for the first and main searches, respectively. The mass error tolerance of the secondary fragment ion was 0.02 Da. Carbamidomethyl on Cys was specified as fixed and acetylation modifications, and oxidation on Met and deamidation on Asn and Gln were specified as variable modifications. The quantitative method was set to label-free quantification, and the false positive rate of protein identification and peptide spectrum match identification was set to 1%.

Protein Annotation and Function Enrichment

Gene Ontology (GO) Analysis

First, the system converted the protein ID to a UniProt ID, then used the UniProt ID to match a GO ID, and extracted the corresponding information from the UniProt-GOA database based on the GO ID. If there was no protein information in the UniProt GOA database, interproscan (http://www.ebi.ac.uk/interpro/), an algorithm software based on protein sequence, was used to predict the GO function of the protein. The proteins were then classified according to cell composition, molecular function, or physiological process.

GO and Pathway Enrichment Analyses

Fisher's exact test was used to test differentially expressed proteins in the background of identified proteins. A p-value of less than 0.05 for the GO and pathway enrichment tests was considered significant. Finally, these channels were classified according to the KEGG channel level classification method.

Clustering Analysis Based on Functional Protein

First, we collected information on the functional classification and corresponding p-values of the protein groups, and then we screened out the functional classifications with significant enrichment (p-value < 0.05) in at least one protein group. The filtered p-value data matrix was first transformed by the logarithm of –log10, and then the transformed data matrix was classified using Z transformation. Finally, the hierarchical clustering (Euclidean distance, average connection clustering) method was used for unilateral clustering analysis of the data set obtained by Z-transform. The clustering relationship was visualized using the Heatmap 2 function in the R language package "gplots."

Targeted Protein Quantification *Via* Parallel Reaction Monitoring (PRM)

Fifteen differentially expressed proteins were randomly selected from different proteins for PRM verification. The peptide was derived from the remaining peptide of the proteome. The mobile phase composition, electrospray voltage, Orbitrap resolution, and mass spectrometry were consistent with the previously described methods The differences were as follows: the liquid gradient settings were 0–40 min, 6–25% B; 40–52 min, 25–35% B; 52–56 min, 35–80% B; 56–60 min, 80% B, with the flow rate maintained at 500 nL/min. Automatic gain control was set at 3E6 for full MS and 1E5 for MS/MS. The maximum injection time was set to 50 ms for full MS and 160 ms for MS/MS. For the target peptides, relative quantitative analysis was repeated three times after normalizing the quantitative information. Peptide parameters were as follows: protease was set to trypsin [KR/P] and the maximum number of missed cut sites and peptide length was set to 0 and 7–25 amino acid residues, respectively. Cysteine alkylation was set as fixed modification.

RESULTS

Proteomics Overview

In this study, 230,809 secondary spectrums were received by mass spectrometry. After searching the protein database, the number of available secondary mass spectra was 15,982 and the utilization rate was 6.9%. A total of 2892 peptides were identified *via* spectroscopic analysis, of which 2858 were found to be specific. A total of 429 proteins were identified (**Table S1**), of which 304 were quantifiable. Among the identified proteins, 62 were identified as DEPs, which used thresholds of a 1.5-fold (p < 0.05) increase or a 0.67-fold decrease (**Table S2**); of these, 38 were significantly upregulated and 24 were significantly downregulated after *M. bicuspidata* challenge (**Figure 1**). Principal component analysis results are shown in **Figure 2**. The immune-related proteins in these DEPs were shown in **Table 1**.

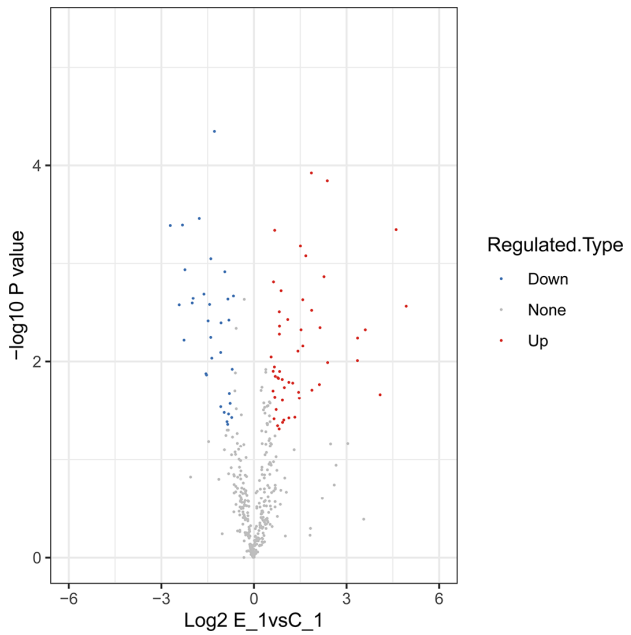

FIGURE 1 | Volcano plots of differentially-expressed proteins.

GO and KEGG Analysis of DEPs

The GO classification analysis of the DEPs showed that biological processes were mainly concentrated in cellular processes, biological regulation, the developmental process, the multicellular organismal process, response to stimulus, and the metabolic process. Cellular components were mainly concentrated in cells, organelles, extracellular regions, protein-containing complexes, and membranes; molecular functions were mainly enriched in binding, catalytic activity, molecular function regulation, and structural molecule activity (**Figure 3**).

Pathway analysis of the DEPs was conducted using GO and KEGG analyses. The results of biological processes pathway by GO analysis showed that the significant enrichment pathways included the integrin-mediated signaling pathway, regulation of toll signaling pathway, negative regulation of hydrolase activity, response to fungus, cell surface receptor signaling pathway, epithelial tube morphogenesis, and morphogenesis of an epithelium (**Figure 4A**). The results of the KEGG pathway analysis showed that the significant enrichment pathways for the upregulated proteins included those for longevity regulating pathway, gap junction, alcoholism, pathogenic *Escherichia coli* infection, phagosome, and apoptosis (**Figure 4B**). There was no significant enrichment pathway for the downregulated proteins.

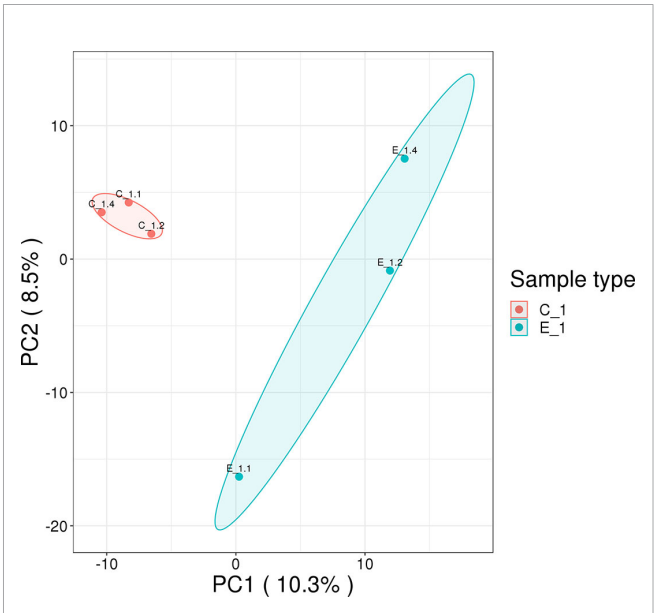

FIGURE 2 | Principal component analysis of proteomics data. The distance of each sample point represents the degree of similarity between samples. The closer the sample points, the higher the similarity between samples.

Validation of Proteome Data for Selected Proteins *via* PRM

In this research, we used the PRM method to verify the different expression proteins obtained from the proteome. Fifteen immune-related proteins from the DEPs were randomly selected for PRM analysis. Although the values of PRM and proteome were slightly different, the overall trend was highly consistent (**Table 2**), which showed that the results of our proteome study are reliable.

DISCUSSION

With analytical technology development, proteomic research has gradually become an innovative field in the search for functional proteins. In this field, the differentially expressed proteins identified between the control and experimental groups can be easily explained to a high reasonable extent (23, 24). In some cases, such research can help us understand the response of cells to various external factors.

To the best of our knowledge, this is the first study on the proteomic characteristics of the hemolymph of *E. sinensis* in response to *M. bicuspidata*, using proteomic methods. Our results showed that the proteins and biological processes in the hemolymph changed significantly when *E. sinensis* was infected with *M. bicuspidata*. A total of 304 proteins were quantifiable, of which 62 were differentially expressed. We validated 15 differentially expressed proteins using MS-based precise quantitative PRM analysis. Similar to western blotting, PRM is a useful methodology for proteomics validation (25, 26). In the absence of specific antibodies, the detection time can be greatly shortened, and high accuracy can be maintained (27). In this study, the trend of the PRM was consistent with that of proteomics. Therefore, the results of mass spectrometry experiments are technically credible.

Based on the obtained proteins, the differentially expressed proteins may directly or indirectly participate in the immune response of *E. sinensis*. The KEGG enrichment results showed that cytoskeletal proteins, proteins with gap junctions, pathogenic *E. coli* infection, and the phagosome pathway in the hemolymph

TABLE 1 | Differentially expressed immune-related proteins.

Accession no.	Protein name	Fold change	*P*-value	Regulation Type
TRINITY_DN10_c0_g3_m.452	Cystatin-A	1.8689	0.041024621	Up
TRINITY_DN1001_c0_g1_m.15	Gelsolin, cytoplasmic	2.0479	0.002688917	Up
TRINITY_DN1355_c0_g1_m.1522	Purine nucleoside phosphorylase	1.9057	0.001507337	Up
TRINITY_DN1382_c1_g3_m.1620	Myosin regulatory light chain 2	2.6698	0.036741424	Up
TRINITY_DN1537_c1_g1_m.2248	Low-density lipoprotein receptor	3.2765	0.005054685	Up
TRINITY_DN182_c0_g1_m.3315	Myosin light chain alkali	2.1011	0.008237636	Up
TRINITY_DN187_c0_g1_m.3442	Tubulin alpha-2 chain	2.1529	0.000265648	Up
TRINITY_DN215_c0_g1_m.4297	Tubulin beta-1 chain	1.5009	0.045635628	Up
TRINITY_DN21871_c0_g1_m.4382	Heat shock cognate 70 kDa protein	1.7352	0.011368734	Up
TRINITY_DN2200_c0_g1_m.4428	L-ascorbate oxidase	5.7885	0.007828275	Up
TRINITY_DN2465_c1_g1_m.5252	Prosaposin	1.5803	0.018755506	Up
TRINITY_DN2539_c0_g1_m.5462	Transferrin	3.0141	0.016913764	Up
TRINITY_DN2787_c0_g1_m.6005	C-type lectin lectoxin-Enh6	1.9349	0.029630599	Up
TRINITY_DN284_c3_g3_m.6143	Serine protease inhibitor 42Dd	4.1181	0.049267135	Up
TRINITY_DN3715_c0_g1_m.7754	Arginine kinase	2.1531	0.009807981	Up
TRINITY_DN3897_c0_g1_m.7995	Tubulin alpha-1	1.6799	0.000044299	Up
TRINITY_DN418_c1_g1_m.8384	CLIP domain-containing serine protease 2	2.4207	0.011347414	Up
TRINITY_DN600_c0_g1_m.10539	protein spätzle 5-like isoform X2	3.3422	0.009098329	Up
TRINITY_DN799_c0_g1_m.12110	Leukocyte elastase inhibitor	4.9718	0.006077766	Up
TRINITY_DN8507_c0_g2_m.12453	Tubulin alpha-2/alpha-4 chain	1.7535	0.045897205	Up
TRINITY_DN925_c0_g2_m.12943	Catalase	2.4116	0.01111043	Up
TRINITY_DN941_c0_g1_m.13028	Hemolymph clottable protein	0.2775	0.003626456	Down
TRINITY_DN10547_c0_g1_m.243	Anti-lipopolysaccharide factor	0.5259	0.012217912	Down
TRINITY_DN106_c1_g2_m.316	Annexin A11	0.517	0.005016753	Down
TRINITY_DN13_c0_g1_m.1679	Alpha-N-acetylgalactosamine-specific lectin	0.3086	0.012753786	Down
TRINITY_DN16_c0_g2_m.2902	PDGF/VEGF-related factor	0.392	0.00340923	Down
TRINITY_DN1708_c2_g1_m.2937	Putative uncharacterized oxidoreductase C513.07	0.6154	0.00158104	Down
TRINITY_DN195_c4_g3_m.3711	Integrin-linked protein kinase homolog pat-4	0.6222	0.003803178	Down
TRINITY_DN559_c0_g3_m.9998	Hemocyte protein-glutamine gamma-glutamyltransferase	0.6299	0.029494743	Down

were influenced remarkably by *M. bicuspidata* infection. Cytoskeletal proteins, including myosin regulatory light chain (MRLC), myosin light chain (MLC), and tubulin α and β chains, were found to be significantly upregulated after *M. bicuspidata* infection. It is well known that cytoskeletal proteins are essential for phagocytosis, which is an important innate immune response of crustaceans (28, 29). The basic structure of myosin in vertebrate and invertebrate muscles is identical. A complete conventional myosin molecule is a hexamer composed of two myosin heavy chains, two MLC, and two MRLC. Myosin is a vital component of muscle cells and plays a crucial role in muscle movement, material transport, cytoplasmic flow, energy supply, and signal transduction (30). Han et al. (31) found that the expression of MLC gene significantly increased in WSSV-resistant *Marsupenaeus japonicus*. RNAi experiments showed that the phagocytic rate and phagocytic index significantly decreased after silencing of the MLC gene. Similarly, MRLC phosphorylation increases after YHV infection in *Penaeus monodon*, and inhibition of phosphorylation leads to increased YHV replication (32). These results suggest that MLC and MRLC might play an important role in crustacean defense against pathogen infection by regulating hemocyte phagocytic activity. In this study, MRLC and MLC protein expression levels significantly decreased in the hemolymph after stimulation with *M. bicuspidata*. Tubulin is a type of globulin, which is a heterodimer formed by the polymerization of α- and β-tubulin molecules. Each of these dimers is combined with two nucleotide molecules, one of which binds tightly, whereas the other binds loosely, and both can be exchanged rapidly. Tubulin is one of the main components of the cytoskeleton and plays an indispensable role in many processes, including structural support, intracellular transport, and DNA separation (33). In this study, tubulin α and β protein levels were significantly higher in the infection group than in the control group. Li et al. (34) found that after WSSV infection, tubulin α-1 and β-1 chains were significantly upregulated. Meng et al. (21) also found that tubulin α gene expression in *E. sinensis* was significantly increased after *S. eriocheiris* infection. In this study, myosin and tubulin cytoskeleton proteins were significantly upregulated, which was hypothesized to promote cell adhesion and regulate hemolymph phagocytosis during *M. bicuspidata* infection.

GO analysis showed that many immune pathways were enriched in biological processes, such as regulation of the toll signaling pathway, cell surface receptor signaling pathway, response to fungus, negative regulation of hydrolase activity, and integrin-mediated signaling pathway. Many serine protease and serine protease inhibitors (serpins) are involved in these immune pathways, including clip domain-containing serine protease (CSP), leukocyte elastase inhibitor (Serpin B1) and Serpin 42Dd. CSP plays an important role in activating phenoloxidase (PO) system and induces melanization of immune response in crustaceans (35, 36). In addition to activating PO, CSP can also cleave the precursor of spätzle to activate the spätzle, which is required for Toll signaling pathway and antimicrobial peptides synthesis (37, 38). In this study, CSP and spätzle 5-like protein were significantly increased, which indicated that *E. sinensis* could activate PO system and improve antimicrobial peptides synthesis in resistance of *M. bicuspidata* infection. Serpins have been found in all higher eukaryotes, bacteria,

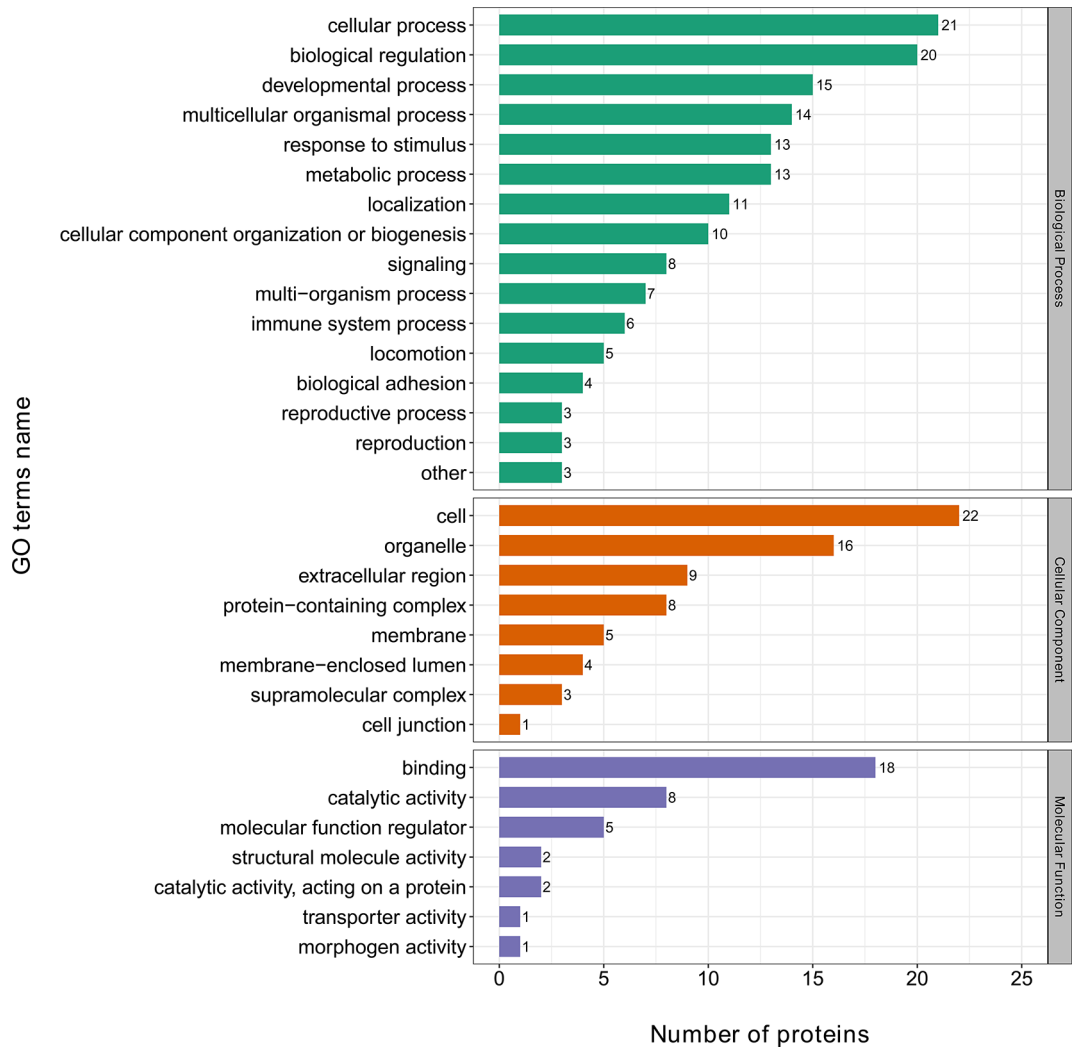

FIGURE 3 | Gene ontology (GO) analysis of differentially expressed proteins.

and viruses, and they play an important role in the immune response by regulating the protein hydrolysis cascade (39, 40). Serpin B1 is an intracellular protein that acts primarily to protect the cell from proteases released into the cytoplasm during stress (41). Serpin 42Dd isoforms may be essential for immune defense by inhibiting a large spectrum of pathogenic proteolytic enzymes (42). In this study, the expression levels of Serpin B1 and Serpin 42Dd were 5.0 and 4.1 times higher than those in the control group, respectively, indicating that Serpin B1 and Serpin 42Dd play an essential role in the immune defense against *M. bicuspidata* in *E. sinensis*, possibly by inhibiting the protease produced by *M. bicuspidata* and/or protecting cells from excess protease effects.

Among the 38 upregulated proteins, the expression levels of many immune genes (transferrin, heat shock cognate 70 kDa protein, and catalase) were significantly increased. Transferrin exists widely in most organisms, from invertebrates to vertebrates. It is a type of glycoprotein with a molecular weight of 70–80 kDa. It plays an important role in maintaining iron homeostasis and is an essential growth and non-specific immune factor (43). Toe et al. found that transferrin plays a vital role in the innate immunity of crustaceans by stimulating *M. rosenbergii* with *Aeromonas hydrophila* (44). Xu et al. used protein technology to screen the immune proteins of *E. sinensis* hemocytes stimulated by *S. eriocheiris* (45). The results showed that the expression level of transferrin was significantly increased after *S. eriocheiris* stimulation. In this study, the expression of transferrin protein in *E. sinensis* infected with *M. bicuspidata* was 3.0 times higher than that in the control group, indicating that it also plays an important role in the innate immunity of *E. sinensis* against infection by *M. bicuspidata*.

Catalase (CAT) is an important part of the body's antioxidant defense system. After superoxide dismutase converts oxygen free radicals into H_2O_2, CAT further reduces them into water and oxygen molecules, which can protect cells from hydrogen peroxide poisoning and protect the stability of the internal environment of the body (46). Therefore, changes in CAT gene expression and activity can reflect the metabolism of free radicals

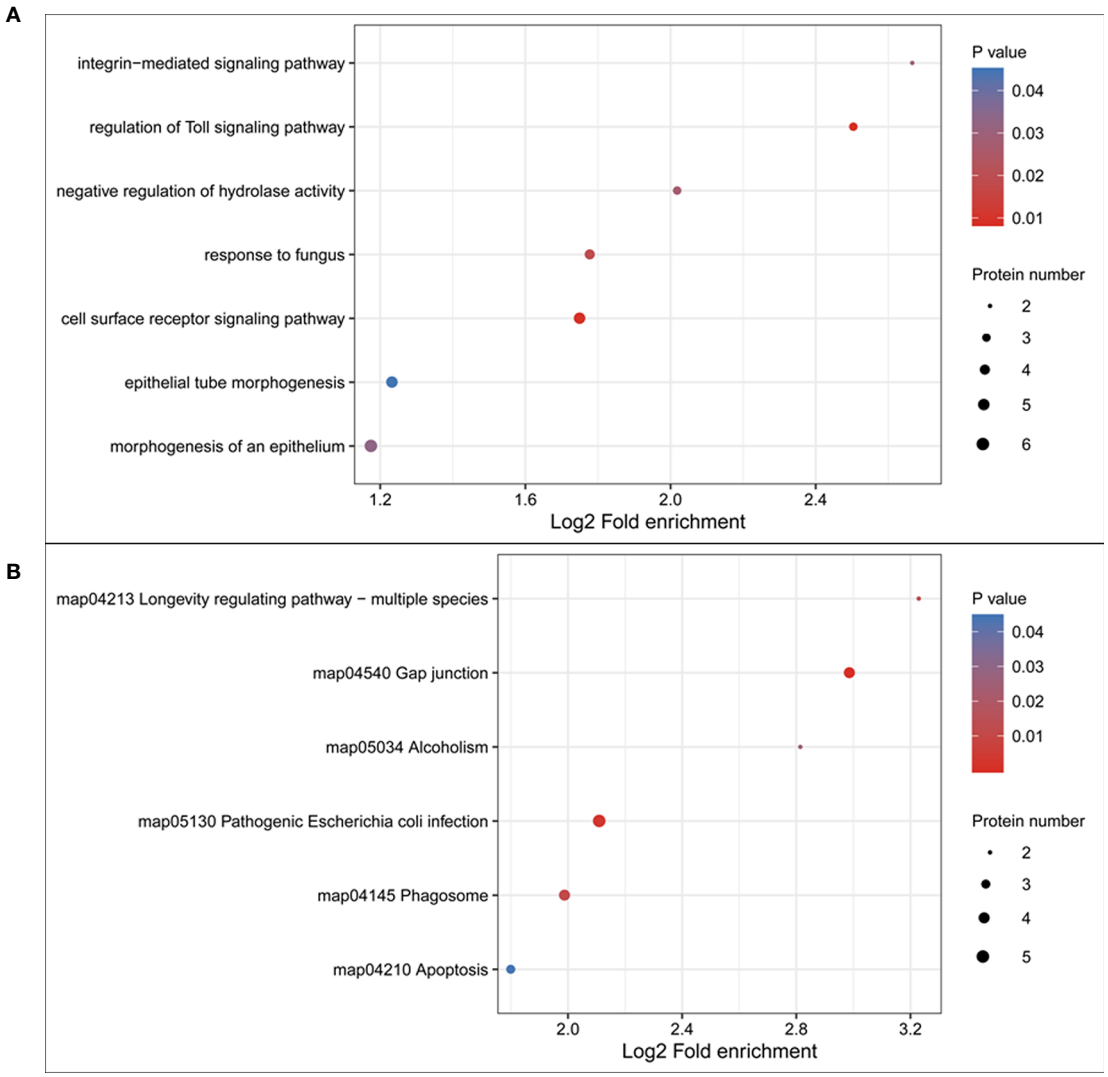

FIGURE 4 | Gene ontology (GO) and KEGG pathway enrichment of the differentially expressed proteins. **(A)** GO pathway enrichment of differentially expressed proteins; **(B)** KEGG pathway enrichment of upregulated proteins.

in the body and thereby indicate the health status of organisms. It is also an important index of antioxidant defense ability (47). After infection by *M. bicuspidata*, the CAT gene expression level in the hemolymph tissue of *E. sinensis* increased to 2.4 times higher than that of the control group. The results showed that *M. bicuspidata* infection causes phagocytosis and consumes excessive reactive oxygen species in the body to maintain the stability of the intracellular environment and then cause respiratory burst. The high amount of hydrogen peroxide protein is mainly used to scavenge oxygen free radicals to avoid body damage.

Previous studies have shown that environmental stress (such as heat stress, heavy metals, and ammonia nitrogen) can promote the synthesis of the heat shock protein HSP70 (48, 49). HSP70 can effectively reduce damage to the body caused by stress by preventing protein folding and degrading denatured protein. Recent studies have shown that HSP70 also plays a key role in immune regulation, including as a stimulator and target to stimulate innate and adaptive immunity (50, 51). Among crustaceans, HSP70 levels significantly increased in *Litopenaeus vannamei* that had been exposed to hypodermic and thermopoietic necrosis virus, WSSV, and pathogen infection, indicating that it plays an important role in the innate immunity of shrimp (52). In this experiment, the expression of HSP70 protein in the *E. sinensis* infected by *M. bicuspidata* was twice as high as that in the control group, indicating that HSP70 is also involved in the innate immune response to yeast infection.

There was no significant KEGG pathway for the 24 significantly decreased proteins. In the GO enrichment analysis, these downregulated proteins were mainly

TABLE 2 | Relative expression levels of selected proteins measured *via* parallel reaction monitoring (PRM).

Accession no.	Protein Name	Folder change of PRM	*P*-value	Folder change of proteome
TRINITY_DN21871_c0_g1_m.4382	Heat shock cognate 70 kDa protein	1.40	0.0165	1.74
TRINITY_DN2787_c0_g1_m.6005	C-type lectin lectoxin-Enh6	1.84	0.00414	1.93
TRINITY_DN1001_c0_g1_m.15	Gelsolin	1.87	0.000640	2.05
TRINITY_DN106_c1_g2_m.316	Annexin A11	0.30	0.00116	0.52
TRINITY_DN1537_c1_g1_m.2248	Low-density lipoprotein receptor	2.79	0.00429	3.28
TRINITY_DN1708_c2_g1_m.2937	Putative uncharacterized oxidoreductase	0.51	0.00217	0.62
TRINITY_DN215_c0_g1_m.4297	Tubulin beta-1 chain	1.37	0.0188	1.50
TRINITY_DN2200_c0_g1_m.4428	L-ascorbate oxidase	5.99	0.000318	5.79
TRINITY_DN2539_c0_g1_m.5462	Transferrin	2.27	0.0219	3.01
TRINITY_DN559_c0_g3_m.9998	Hemocyte protein-glutamine gamma-glutamyltransferase	0.58	0.0110	0.63
TRINITY_DN600_c0_g1_m.10539	Protein spaetzle 5-like isoform X2	2.71	0.00957	3.34
TRINITY_DN925_c0_g2_m.12943	Catalase	2.15	0.0357	2.41
TRINITY_DN10547_c0_g1_m.243	Anti-lipopolysaccharide factor	0.42	0.00140	0.53
TRINITY_DN418_c1_g1_m.8384	CLIP domain-containing serine protease 2	1.75	0.0407	2.42
TRINITY_DN941_c0_g1_m.13028	Hemolymph clottable protein	0.25	0.00205	0.28

concentrated in the biological processes related to organ genesis and formation, such as PDGF/VEGF-related factor protein and the integrin-linked protein kinase homolog pat-4 gene. The results showed that host cell regeneration was affected after yeast infection (53, 54). The typical feature of "milky disease" is that the hemolymph does not solidify and presents as a milky liquid. Crustaceans have an open circulatory system; they must heal wounds through effective coagulation reactions to prevent loss of hemolymph and capture pathogenic microorganisms to prevent them from spreading into the hemolymph. The coagulation reaction is initiated by the release of Ca^{2+}-dependent transglutaminase by hemocytes, which causes clotting protein polymerization in the hemolymph to form a stable clot (55, 56). Our research found that after 48 h of *M. bicuspidata* infection, the content of coagulation protein in the infected group decreased significantly, which was 0.28 times that of the control group, and the transglutaminase also decreased significantly. This showed that *M. bicuspidata* could reduce the coagulation reaction of the host, which is helpful for the proliferation of yeast.

CONCLUSIONS

This study investigated the protein expression changes in *E. sinensis* infected with *M. bicuspidata* using proteomics technology. The results showed that many immune-related proteins in *E. sinensis* were significantly upregulated after infection with *M. bicuspidata*, such as cytoskeleton-related proteins, serine protease and serine protease inhibitor proteins. The upregulation of these proteins indicated that the phenoloxidase system, phagocytosis and the ROS systems were induced by *M. bicuspidata*. In addition, proteins related to organ and tissue regeneration and coagulation reaction proteins were significantly downregulated by *M. bicuspidata* infection, which inhibited hemocyte regeneration and hemolymph agglutination. This finding provides an insight into the immune defense mechanism of crustacean hemolymph against pathogenic yeast.

DATA AVAILABILITY STATEMENT

The raw data supporting the conclusions of this article will be made available by the authors, without undue reservation.

ETHICS STATEMENT

The animal study was reviewed and approved by the Animal Experiments Ethics Committee of Shenyang Agricultural University.

AUTHOR CONTRIBUTIONS

HJ, JB, and QC were involved in designing of the research and wrote the manuscript. HJ, JB, YX, CF, and XL performed the majority of the experiment, data processing, analysis, and interpretation. All authors contributed to the article and approved the submitted version.

FUNDING

This work was supported by Modern Agro-industry Technology Research System (CARS-48); Liaoning province Department of Education fund item (LSNQN202002); Liaoning Science and Technology Mission Project (2020JH5/10400147; 2020JH5/10400115); and Liaoning Province Key R&D Planning Guidance Plan Project (2019JH8/10200018).

SUPPLEMENTARY MATERIAL

The Supplementary Material for this article can be found online at: https://www.frontiersin.org/articles/10.3389/fimmu.2021.659723/full#supplementary-material

REFERENCES

1. Zhang X, Cui L, Li S, Liu X, Han X, Jiang K, et al. *China Fishery Statistical Yearbook, 2020*. Beijing: China Agriculture Press (2020). p. 24.
2. Wang W, Wen B, Gasparich GE, Zhu N, Rong L, Chen J, et al. A spiroplasma associated with tremor disease in the Chinese mitten crab (*Eriocheir sinensis*). *Microbiology* (2004) 150:3035–40. doi: 10.1099/mic.0.26664-0
3. Yano Y, Kaneniwa M, Satomi M, Oikawa H, Chen SS. Occurrence and density of *vibrio parahaemolyticus* in live edible crustaceans from markets in China. *J Food Prot* (2006) 69(11):2742–6. doi: 10.4315/0362-028x-69.11.2742
4. Yang QZ, Yang ZJ, Zhang Y, Li XL, Zhang W. Molecular characteristic and expression analysis of collagenolytic serine protease from the Chinese mitten crab *Eriocheir sinensis* with defense response to *Vibrio anguillarum* challenge. *Genet Mol Res* (2014) 13(2):3885–94. doi: 10.4238/2014.April.29.1
5. Ding Z, Meng Q, Liu H, Yuan S, Zhang F, Sun M, et al. First case of hepatopancreatic necrosis disease in pond-reared Chinese mitten crab, *Eriocheir sinensis*, associated with microsporidian. *J Fish Dis* (2016) 39 (9):1043–51. doi: 10.1111/jfd.12437
6. Wu H, Feng M. Mass mortality of larval *Eriocheir sinensis* (Decapoda: Grapsidae) population bred under facility conditions: possible role of Zoothamnium sp. (*Peritrichida: Vorticellidae*) Epiphyte. *J Invertebr Pathol* (2004) 86(1-2):59–60. doi: 10.1016/j.jip.2004.03.010
7. Bao J, Jiang H, Shen H, Xing Y, Feng C, Li X, et al. First description of milky disease in the Chinese mitten crab *Eriocheir sinensis* caused by the yeast *Metschnikowia bicuspidata*. *Aquaculture* (2021) 532:735984. doi: 10.1016/j.aquaculture.2020.735984
8. Codreanu R, Codreanu-Balcescu D. On two *Metschnikowia* yeast species producing hemocoelic infections in *Daphnia magna* and *Artemia salina* (Crustacea, Phyllopoda) from Romania. *J Invertebr Pathol* (1981) 37(1):22–7. doi: 10.1016/0022-2011(81)90049-5
9. Wang X, Chi Z, Yue L, Li J, Li M, Wu L. A marine killer yeast against the pathogenic yeast strain in crab (*Portunus trituberculatus*) and an optimization of the toxin production. *Microbiol Res* (2007) 162(1):77–85. doi: 10.1016/j.micres.2006.09.002
10. Chen SC, Chen YC, Kwang J, Manopo I, Wang PC, Chaung HC, et al. *Metschnikowia bicuspidata* dominates in Taiwanese cold-weather yeast infections of *Macrobrachium rosenbergii*. *Dis Aquat Organ* (2007) 75 (3):191–9. doi: 10.3354/dao075191
11. Moore MM, Strom MS. Infection and mortality by the yeast *Metschnikowia bicuspidata* var. *bicuspidata* in chinook salmon fed live adult brine shrimp (*Artemia franciscana*). *Aquaculture* (2003) 220:43–57. doi: 10.1016/S0044-8486(02)00271-5
12. Zhang HQ, Chi Z, Liu GL, Zhang M, Hu Z, Chi ZM. *Metschnikowia bicuspidate* associated with a milky disease in *Eriocheir sinensis* and its effective treatment by *Massoia lactone*. *Microbiol Res* (2021) 242:126641. doi: 10.1016/j.micres.2020.126641
13. Wang X, Chi Z, Yue L, Li J. Purification and characterization of killer toxin from a marine yeast *Pichia anomala* YF07b against the pathogenic yeast in crab. *Curr Microbiol* (2007) 55(5):396–401. doi: 10.1007/s00284-007-9010-y
14. Huang Y, Ren Q. Research progress in innate immunity of freshwater crustaceans. *Dev Comp Immunol* (2020) 104:103569. doi: 10.1016/j.dci.2019.103569
15. Zheng Z, Wang F, Aweya JJ, Li R, Yao D, Zhong M, et al. Comparative transcriptomic analysis of shrimp hemocytes in response to acute hepatopancreas necrosis disease (AHPND) causing *Vibrio parahemolyticus* infection. *Fish Shellfish Immunol* (2018) 74:10–8. doi: 10.1016/j.fsi.2017.12.032
16. Li M, Wang J, Huang Q, Li C. Proteomic analysis highlights the immune responses of the hepatopancreas against Hematodinium infection in *Portunus trituberculatus*. *J Proteomics* (2019) 197:92–105. doi: 10.1016/j.jprot.2018.11.012
17. Tao M, Zhou H, Luo K, Lu J, Zhang Y, Wang F. Quantitative serum proteomics analyses reveal shrimp responses against WSSV infection. *Dev Comp Immunol* (2019) 93:89–92. doi: 10.1016/j.dci.2019.01.003
18. Chaikeeratisak V, Somboonwiwat K, Wang HC, Lo CF, Tassanakajon A. Proteomic analysis of differentially expressed proteins in the lymphoid organ of *Vibrio harveyi*-infected *Penaeus monodon*. *Mol Biol Rep* (2012) 39(5):6367–77. doi: 10.1007/s11033-012-1458-6
19. Hernández-Pérez A, Zamora-Briseño JA, Ruiz-May E, Pereira-Santana A, Elizalde-Contreras JM, Pozos-González S, et al. Proteomic profiling of the white shrimp *Litopenaeus vannamei* (Boone, 1931) hemocytes infected with white spot syndrome virus reveals the induction of allergy-related proteins. *Dev Comp Immunol* (2019) 91:37–49. doi: 10.1016/j.dci.2018.10.002
20. Jeswin J, Xie XL, Ji QL, Wang KJ, Liu HP. Proteomic analysis by iTRAQ in red claw crayfish, *Cherax quadricarinatus*, hematopoietic tissue cells post white spot syndrome virus infection. *Fish Shellfish Immunol* (2016) 50:288–96. doi: 10.1016/j.fsi.2016.01.035
21. Meng Q, Hou L, Zhao Y, Huang X, Huang Y, Xia S, et al. iTRAQ-based proteomic study of the effects of *Spiroplasma eriocheiris* on Chinese mitten crab *Eriocheir sinensis* hemocytes. *Fish Shellfish Immunol* (2014) 40(1):182–9. doi: 10.1016/j.fsi.2014.06.029
22. Sun B, Wang Z, Wang Z, Ma X, Zhu F. A Proteomic Study of Hemocyte Proteins from Mud Crab (*Scylla paramamosain*) Infected with White Spot Syndrome Virus or *Vibrio alginolyticus*. *Front Immunol* (2017) 8:468. doi: 10.3389/fimmu.2017.00468
23. Zhang B, Mao JL, Yao H, Aubourg SP. Label-free based proteomics analysis of protein changes in frozen whiteleg shrimp (*Litopenaeus vannamei*) pre-soaked with sodium trimetaphosphate. *Food Res Int* (2020) 137:109455. doi: 10.1016/j.foodres.2020.109455
24. Guo H, Chen T, Liang Z, Fan L, Shen Y, Zhou D. iTRAQ and PRM-based comparative proteomic profiling in gills of white shrimp *Litopenaeus vannamei* under copper stress. *Chemosphere* (2021) 263:128270. doi: 10.1016/j.chemosphere.2020.128270
25. Du W, Xiong CW, Ding J, Nybom H, Ruan CJ, Guo H. Tandem mass tag based quantitative proteomics of developing sea buckthorn berries reveals candidate proteins related to lipid metabolism. *J Proteome Res* (2019) 18 (5):1958–69. doi: 10.1021/acs.jproteome.8b00764
26. Wu X, Yan J, Wu Y, Zhang H, Mo S, Xu X, et al. Proteomic analysis by iTRAQ-PRM provides integrated insight into mechanisms of resistance in pepper to *Bemisia tabaci* (Gennadius). *BMC Plant Biol* (2019) 19(1):270. doi: 10.1186/s12870-019-1849-0
27. Peterson AC, Russell JD, Bailey DJ, Westphall MS, Coon JJ. Parallel reaction monitoring for high resolution and high mass accuracy quantitative, targeted proteomics. *Mol Cell Proteomics* (2012) 11(11):1475–88. doi: 10.1074/mcp.O112.020131
28. Li F, Xiang J. Recent advances in researches on the innate immunity of shrimp in China. *Dev Comp Immunol* (2013) 39(1-2):11–26. doi: 10.1016/j.dci.2012.03.016
29. Liu S, Zheng SC, Li YL, Li J, Liu HP. Hemocyte-mediated phagocytosis in crustaceans. *Front Immunol* (2020) 11:268. doi: 10.3389/fimmu.2020.00268
30. Sitbon YH, Yadav S, Kazmierczak K, Szczesna-Cordary D. Insights into myosin regulatory and essential light chains: a focus on their roles in cardiac and skeletal muscle function, development and disease. *J Muscle Res Cell Motil* (2020) 41(4):313–27. doi: 10.1007/s10974-019-09517-x
31. Han F, Wang Z, Wang X. Characterization of myosin light chain in shrimp hemocytic phagocytosis. *Fish Shellfish Immunol* (2010) 29(5):875–83. doi: 10.1016/j.fsi.2010.07.030
32. Taengchaiyaphum S, Havanapan PO, Roytrakul S, Lo CF, Sritunyalucksana K, Krittanai C. Phosphorylation is required for myosin regulatory light chain (PmMRLC) to control yellow head virus infection in shrimp hemocytes. *Fish Shellfish Immunol* (2013) 34(5):1042–9. doi: 10.1016/j.fsi.2012.12.022
33. Pellegrini F, Budman DR. Review: tubulin function, action of antitubulin drugs, and new drug development. *Cancer Invest* (2005) 23(3):264–73. doi: 10.1081/cnv-200055970
34. Li W, Tang X, Xing J, Sheng X, Zhan W. Proteomic analysis of differentially expressed proteins in *Fenneropenaeus chinensis* hemocytes upon white spot syndrome virus infection. *PloS One* (2014) 9(2):e89962. doi: 10.1371/journal.pone.0089962
35. Liu H, Liu Y, Song C, Ning J, Cui Z. Functional characterization of two clip-domain serine proteases in the swimming crab *Portunus trituberculatus*. *Fish Shellfish Immunol* (2019) 89:98–107. doi: 10.1016/j.fsi.2018.12.047
36. Jia Z, Wang M, Zhang H, Wang X, Lv Z, Wang L, et al. Identification of a clip domain serine proteinase involved in immune defense in Chinese mitten crab *Eriocheir sinensis*. *Fish Shellfish Immunol* (2018) 74:332–40. doi: 10.1016/j.fsi.2017.12.056

37. Jang IH, Nam HJ, Lee WJ. CLIP-domain serine proteases in *Drosophila* innate immunity. *BMB Rep* (2008) 41(2):102–7. doi: 10.5483/bmbrep.2008.41.2.102
38. Li C, Wang S, He J. The Two NF-κB Pathways Regulating Bacterial and WSSV Infection of Shrimp. *Front Immunol* (2019) 10:1785. doi: 10.3389/fimmu.2019.01785
39. He Y, Wang Y, Zhao P, Rayaprolu S, Wang X, Cao X, et al. Serpin-9 and -13 regulate hemolymph proteases during immune responses of *Manduca sexta*. *Insect Biochem Mol Biol* (2017) 90:71–81. doi: 10.1016/j.ibmb.2017.09.015
40. Wang D, Gou M, Hou J, Pang Y, Li Q. The role of serpin protein on the natural immune defense against pathogen infection in *Lampetra japonica*. *Fish Shellfish Immunol* (2019) 92:196–208. doi: 10.1016/j.fsi.2019.05.062
41. Torriglia A, Martin E, Jaadane I. The hidden side of SERPINB1/Leukocyte Elastase Inhibitor. *Semin Cell Dev Biol* (2017) 62:178–86. doi: 10.1016/j.semcdb.2016.07.010
42. Ellisdon AM, Zhang Q, Henstridge MA, Johnson TK, Warr CG, Law RH, et al. High resolution structure of cleaved Serpin 42 Da from *Drosophila melanogaster*. *BMC Struct Biol* (2014) 14:14. doi: 10.1186/1472-6807-14-14
43. Kamińska-Gibas T, Szczygieł J, Jurecka P, Irnazarow I. The many faces of transferrin: Does genotype modulate immune response? *Fish Shellfish Immunol* (2020) 102:511–18. doi: 10.1016/j.fsi.2020.05.001
44. Toe A, Areechon N, Srisapoome P. Molecular characterization and immunological response analysis of a novel transferrin-like, pacifastin heavy chain protein in giant freshwater prawn, *Macrobrachium rosenbergii* (De Man, 1879). *Fish Shellfish Immunol* (2012) 33(4):801–12. doi: 10.1016/j.fsi.2012.07.007
45. Xu X, Liu Y, Tang M, Yan Y, Gu W, Wang W, et al. The function of *Eriocheir sinensis* transferrin and iron in *Spiroplasma eriocheiris* infection. *Fish Shellfish Immunol* (2018) 79:79–85. doi: 10.1016/j.fsi.2018.05.019
46. Wang WN, Li BS, Liu JJ, Shi L, Alam MJ, Su SJ, et al. The respiratory burst activity and expression of catalase in white shrimp, *Litopenaeus vannamei*, during long-term exposure to pH stress. *Ecotoxicology* (2012) 21(6):1609–16. doi: 10.1007/s10646-012-0937-9
47. Yang HT, Yang MC, Sun JJ, Guo F, Lan JF, Wang XW, et al. Catalase eliminates reactive oxygen species and influences the intestinal microbiota of shrimp. *Fish Shellfish Immunol* (2015) 47(1):63–73. doi: 10.1016/j.fsi.2015.08.021
48. Luan W, Li F, Zhang J, Wen R, Li Y, Xiang J. Identification of a novel inducible cytosolic Hsp70 gene in Chinese shrimp *Fenneropenaeus chinensis* and comparison of its expression with the cognate Hsc70 under different stresses. *Cell Stress Chaperones* (2010) 15(1):83–93. doi: 10.1007/s12192-009-0124-y
49. Sung YY, Rahman NA, Shazili NAM, Chen S, Lv A, Sun J, et al. Non-lethal heat shock induces hsp70 synthesis and promotes tolerance against heat, ammonia and metals in post-larvae of the white leg shrimp *Penaeus vannamei* (boone, 1931). *Aquaculture* (2018) 483:21–6. doi: 10.1016/j.aquaculture.2017.09.034
50. Zhou J, Wang WN, He WY, Zheng Y, Wang L, Xin Y, et al. Expression of HSP60 and HSP70 in white shrimp, *Litopenaeus vannamei* in response to bacterial challenge. *J Invertebr Pathol* (2010) 103(3):170–8. doi: 10.1016/j.jip.2009.12.006
51. Valentim-Neto PA, Moser JR, Fraga AP, Marques MR. Hsp70 expression in shrimp *Litopenaeus vannamei* in response to IHHNV and WSSV infection. *Virusdisease* (2014) 25(4):437–40. doi: 10.1007/s13337-014-0236-6
52. Yang Y, Ye H, Huang H, Li S, Liu X, Zeng X, et al. Expression of Hsp70 in the mud crab, *Scylla paramamosain* in response to bacterial, osmotic, and thermal stress. *Cell Stress Chaperones* (2013) 18(4):475–82. doi: 10.1007/s12192-013-0402-6
53. Dai J, Rabie AB. VEGF: an essential mediator of both angiogenesis and endochondral ossification. *J Dent Res* (2007) 86(10):937–50. doi: 10.1177/154405910708601006
54. Grashoff C, Aszódi A, Sakai T, Hunziker EB, Fässler R. Integrin-linked kinase regulates chondrocyte shape and proliferation. *EMBO Rep* (2003) 4(4):432–8. doi: 10.1038/sj.embor.embor801
55. Maningas MB, Kondo H, Hirono I, Saito-Taki T, Aoki T. Essential function of transglutaminase and clotting protein in shrimp immunity. *Mol Immunol* (2008) 45(5):1269–75. doi: 10.1016/j.molimm.2007.09.016
56. Maningas MB, Kondo H, Hirono I. Molecular mechanisms of the shrimp clotting system. *Fish Shellfish Immunol* (2013) 34(4):968–72. doi: 10.1016/j.fsi.2012.09.018

Conflict of Interest: The authors declare that the research was conducted in the absence of any commercial or financial relationships that could be construed as a potential conflict of interest.

frontiers in Immunology

ORIGINAL RESEARCH
published: 01 April 2021
doi: 10.3389/fimmu.2021.634497

In vitro Evaluation of Programmed Cell Death in the Immune System of Pacific Oyster *Crassostrea gigas* by the Effect of Marine Toxins

Norma Estrada[1], Erick J. Núñez-Vázquez[2], Alejandra Palacios[3], Felipe Ascencio[3], Laura Guzmán-Villanueva[1] and Rubén G. Contreras[4]*

[1] Programa Cátedras CONACyT (Consejo Nacional de Ciencia y Tecnología), Centro de Investigaciones Biológicas del Noroeste, S.C. (CIBNOR), La Paz, Mexico, [2] Laboratorio de Toxinas Marinas y Aminoácidos, Centro de Investigaciones Biológicas del Noroeste, S.C. (CIBNOR), La Paz, Mexico, [3] Laboratorio de Patogénesis Microbiana, Centro de Investigaciones Biológicas del Noroeste, S.C. (CIBNOR), La Paz, Mexico, [4] Departamento de Fisiología, Biofísica y Neurociencias, Centro de Investigación y de Estudios Avanzados del IPN (CINVESTAV), Mexico City, Mexico

OPEN ACCESS

Edited by:
Kunlaya Somboonwiwat, Chulalongkorn University, Thailand

Reviewed by:
Annalisa Pinsino, National Research Council (CNR), Italy
Linlin Zhang, Institute of Oceanology (CAS), China

****Correspondence:***
Norma Estrada
nestrada@cibnor.mx

Specialty section:
This article was submitted to Comparative Immunology, a section of the journal Frontiers in Immunology

Received: *27 November 2020*
Accepted: *24 February 2021*
Published: *01 April 2021*

Citation:
Estrada N, Núñez-Vázquez EJ, Palacios A, Ascencio F, Guzmán-Villanueva L and Contreras RG (2021) In vitro Evaluation of Programmed Cell Death in the Immune System of Pacific Oyster Crassostrea gigas by the Effect of Marine Toxins. Front. Immunol. 12:634497. doi: 10.3389/fimmu.2021.634497

Programmed cell death (PCD) is an essential process for the immune system's development and homeostasis, enabling the remotion of infected or unnecessary cells. There are several PCD's types, depending on the molecular mechanisms, such as non-inflammatory or pro-inflammatory. Hemocytes are the main component of cellular immunity in bivalve mollusks. Numerous infectious microorganisms produce toxins that impair hemocytes functions, but there is little knowledge on the role of PCD in these cells. This study aims to evaluate *in vitro* whether marine toxins induce a particular type of PCD in hemocytes of the bivalve mollusk *Crassostrea gigas* during 4 h at 25°C. Hemocytes were incubated with two types of marine toxins: non-proteinaceous toxins from microalgae (saxitoxin, STX; gonyautoxins 2 and 3, GTX2/3; okadaic acid/dynophysistoxin-1, OA/DTX-1; brevetoxins 2 and 3, PbTx-2,-3; brevetoxin 2, PbTx-2), and proteinaceous extracts from bacteria (*Vibrio parahaemolyticus*, Vp; *V. campbellii*, Vc). Also, we used the apoptosis inducers, staurosporine (STP), and camptothecin (CPT). STP, CPT, STX, and GTX 2/3, provoked high hemocyte mortality characterized by apoptosis hallmarks such as phosphatidylserine translocation into the outer leaflet of the cell membrane, exacerbated chromatin condensation, DNA oligonucleosomal fragments, and variation in gene expression levels of apoptotic caspases 2, 3, 7, and 8. The mixture of PbTx-2,-3 also showed many apoptosis features; however, they did not show apoptotic DNA oligonucleosomal fragments. Likewise, PbTx-2, OA/DTX-1, and proteinaceous extracts from bacteria Vp, and Vc, induced a minor degree of cell death with high gene expression of the pro-inflammatory initiator caspase-1, which could indicate a process of pyroptosis-like PCD. Hemocytes could carry out both PCD types simultaneously. Therefore, marine toxins trigger PCD's signaling pathways in *C. gigas* hemocytes, depending on the toxin's nature, which appears to be highly conserved both structurally and functionally.

Keywords: programmed cell death, marine toxins, apoptosis, pyroptosis-like, bivalve mollusk, *Crassostrea gigas*

INTRODUCTION

Pacific oyster *Crassostrea gigas* (Thunberg, 1793) (Bivalvia, Mollusk) shows the highest aquaculture production in the world and is one of the best-studied bivalve mollusks (1, 2). These benthic invertebrates filter high volumes of water through their gills and accumulate pathogenic microbes and environmental toxins that continuously challenge their normal functions (3–5). To cope with this challenge, these animals have developed effective systems to detect and discriminate beneficial microorganisms from potentially harmful and pathogenic ones and are capable of keeping infections under control (6–8). Bivalve's innate immunity consists of humoral components of hemolymph (agglutinins, lysosomal enzymes, opsonizing molecules, and antimicrobial peptides) and the cellular defense that the hemocytes perform (9). Hemocytes represent the first line of internal defense against parasites, pathogens, and non-self-materials in bivalve mollusks and play a significant role in the immune system homeostasis and disease prevention. They are capable of phagocytosis, encapsulation, and enzymatic digestion (9–14), and participate in other processes, such as wound and shell repair, nutrient digestion, transport, and excretion (10, 15). Injury, toxic substances, or invasion by pathogenic microorganisms activates internal hemolymph factors such as hormones, cytokines, and other humoral factors that regulate hemocyte's function and migration to promote localized responses (14, 16, 17).

Hemocyte death is a naturally occurring phenomenon in bivalve mollusks due to internal and external stimuli, as in other multicellular organisms. There are two types of cell death: 1) programmed/regulated cell death (PCD), most commonly known as apoptosis, but including also autophagy, necroptosis, pyroptosis, and 2) necrosis, a kind of accidental cell death due to non-physiological states such as infection or injury (18, 19). PCD is a natural part of the animal cell cycle and an essential factor in animal disease progression. In a healthy animal, PCD occurs when a cell is damaged, infected, senescent, or otherwise of little use to the animal and plays crucial roles in immune system homeostasis and function, defense against parasite and pathogens, and self/non-self recognition (20–24). Hemocytes' enhanced PCD could conceivably create immunosuppression that in turn would reduce disease's resistance, increase opportunistic infections, and decline mollusk's population (25–31).

PCD involves activating a family of cysteine proteases called caspases (32, 33), that can be pro-apoptotic or pro-inflammatory. The pro-apoptotic subfamily includes the initiator caspases -2, -8, -9, and -10 that respond to the apoptotic signals and cleave and activate the effector caspases -3, -6, and -7, which in turn cleave target proteins to orchestrate apoptotic cell death (21, 28, 31, 32, 34). Apoptotic cell death is an immunologically silent death that does not induce inflammation but allows the orderly degradation and recycling of cellular components. The pro-inflammatory caspases -1, -4, -5, and -11 play a significant role in innate immune responses by inducing pyroptosis, an inflammatory cell death that clear infections by removing pathogen replication niches and releasing pro-inflammatory cytokines and danger signals (21, 34–38). Caspases induce profound changes in cells, including the hallmarks of apoptosis: phosphatidylserine (PS) translocation from the cytosolic to the exoplasmic leaflet of the plasma membrane, cell shrinkage and blebbing, chromatin condensation, and DNA nuclear fragmentation (39–41). Pyroptosis also exhibits PS translocation, resulting from plasma membrane rupture, nuclear condensation, and DNA cleavage, but nuclear integrity is maintained (42–45). **Table 1** summarizes the features of apoptosis and pyroptosis.

A wide variety of pathogenic microorganisms like viruses, bacteria, protozoan, and microalgae, cause mollusk hemocyte cell death, either as a consequence of infecting host cells or producing toxic products. The study of these effects has raised interest to solve the economic, ecologic, and health challenges of mollusk's aquaculture (5, 25, 30, 46–62). The objective of this study was to demonstrate whether marine toxins induce PCD in hemocytes. We exposed *C. gigas* hemocytes *in vitro* to non-proteinaceous microalgae marine toxins saxitoxin (STX), gonyautoxins 2 and 3 (GTX2/3), brevetoxins 2 and 3 (PbTx-2,-3), brevetoxin 2 (PbTx-2), okadaic acid/dynophysistoxin 1 (OA/DTX-1), as well as proteinaceous toxins from the bacteria *Vibrio parahaemolyticus* (Vp) and *V. campbellii* (Vc). Little is known, about how PCD processes regulates bivalve's immune defenses, and if the pathogens or xenobiotics induce hemocyte's PCD to unbalance cellular homeostasis toward higher mortality.

MATERIALS AND METHODS

Source of Oysters

Crassostrea gigas (Thunberg, 1793) oysters (11 ± 1.2 cm) cultivated in suspended cages at Rancho Bueno, Mexico (24°32 N, 111°42 W), were collected and transported to CIBNOR. The specimens were placed in 40 L plastic tanks containing filtered (1 μm) seawater (35 psu) pumped directly from the sea. The water was maintained with constant aeration through air stones. The water was replaced every 2 days. During acclimation (10 days), oysters were fed a mixture of microalgae (*Chaetoceros calcitrans*, *C. muelleri*, and *Isochrysis galbana*; 1:1:1) obtained at CIBNOR. *C. calcitrans* (CHCAL-7) and *C. muelleri* (CHM-8) were cultured in 20-L plastic bags in F/2 growth medium at 22°C under constant illumination at a salinity of 32 PSU. *I. galbana* (ISG-1) was grown in MA-F/2 medium at the same temperature, salinity, and volume under continuous illumination, and were harvested in the stationary growth phase.

Toxins and Apoptosis Inducers

Obtention, Extraction, and Quantification of Marine Toxins

Non-proteinaceous Toxins

Paralyzing Shellfish Toxins. Saxitoxin (STX) FDA Reference Standard Saxitoxin was obtained from the US National Institute of Standards and Technology (NIST, RM 8642). The saxitoxin dihydrochloride concentration is nominally 100 μg mL^{-1} in a solution of 80% acidified water (pH 3.5) and 20% ethanol (volume fractions) and provided by Marine Toxins and Amino acids Laboratory from CIBNOR. Gonyautoxins

TABLE 1 | Generalized features of apoptosis and pyroptosis.

	Features	Apoptosis	Pyroptosis
Outcome	Evolutionary conserved	Yes	Yes
	Programmed	Yes	Yes
	Regulated process	Yes	Yes
	Inflammatory	No	Yes
	Signaling pathway	Specific	Specific
	Activated by	Intrinsic or extrinsic	PAMPs and DAMPs
Intermediate signaling	Mitochondrial disfunction	Yes	Yes
	Cytochrome-c release	Yes	No
	Caspase-1	No	Yes
	Caspase-2	Yes	No
	Caspase-3	Yes	Yes*
	Caspase-7	Yes	No
	Caspase-8	Yes	Yes*
Phenotype	Membrane intact	Yes	No
	Pore formation	No	Yes
	Membrane blebbing	Yes	No
	Cell lysis	No	Yes
	Cell swelling	No	Yes
	PS exposure	Yes	Yes
	Chromatin condensation	Yes	Yes
	DNA fragmentation	Yes	Yes
	DNA laddering	Yes	No

**Variable according to cell type.*

epimers 2 and 3 (GTX 2/3) were obtained according to Estrada et al. (58) from cultured dinoflagellate *G. catenatum* (Strain GCQM-2) (https://www.cibnor.gob.mx/investigacion/colecciones-biologicas/codimar). Identity and quantification of STX and GTX 2/3 were subjected to HPLC analysis, using the post-column oxidative fluorescence method (63, 64), and the biological activity was performed by mouse bioassay (MBA) according to AOAC (65) standards.

Diarrheic Shellfish Toxins. A mixture of okadaic acid (OA) and dinophysistoxin 1 (DTX-1) were obtained from cultured of the dinoflagellate *Prorocentrum lima* (Strain PRL1) isolated from the Gulf of California (66), and provided by Marine Toxins and Amino acids Laboratory from CIBNOR. The cells were cultured in f/2+Se medium (67, 68) with filtered (0.45 μm) seawater and grown in monoalgal cultures in 500 mL Erlenmeyer flasks for 12-h light:12-h dark photocycle at 25°C under 70 W fluorescent lamps and anaerobic conditions. The concentration of OA/DTX-1 in the extract semi-purified (69) was calculated as log Mouse Unit (MU) = 2.6 log (1 + t−1); MU = 4 μg of OA (70). The DST content (OA + DTX-1) was determined by LC–MS/MS method (71).

Neurotoxic Shellfish Toxins. The brevetoxin 2 (PbTx-2) extract and the mixture of brevetoxin 2 and 3 (PbTx-2,−3) were obtained by cultivation of the dinoflagellate *Karenia brevis* (Strain Kb-3) originally isolated from the Gulf of Mexico and donated to CIBNOR by Dr. Tracy Villareal from the University of Austin, Texas, USA. The cells were cultured in GSe medium (72) with filtered (0.45 μm) seawater and grown in monoalgal cultures in 2.8 L Fernbach flasks for 12-h light:12-h dark photocycle, at 25°C under 70 W fluorescent lamps and anaerobic conditions. Extraction and semi-purification of PbTx2 and PbTx-2,-3 were performed and provided by Marine Toxins and Amino acids Laboratory from CIBNOR (73). PbTxs were identified and measured by LC-MS/MS (pers. comm. Dr. Andrew Turner, CEFAS, United Kingdom), and MBA measured biological activity according to the American Public Health Association (74).

We made aliquots for these non-proteinaceous marine toxins, and the solvents were removed by evaporation to dryness *in vacuo* and stored at −80°C. Before experiments toxins were suspended in 1% dimethyl-sulfoxide (DMSO), diluted in 0.22 μm sterile saline solution (Cs PiSA NaCl 0.9%, pH 7.2), prepared immediately before use for the desired working concentration.

Proteinaceous Toxins

Crude Extracts of Bacteria Vibrio parahaemolyticus and V. campbellii. V. parahaemolyticus (Strain VpM) and *V. campbellii* (VcA1) were isolated from white-leg shrimp (*Litopenaeus vannamei*) and Pacific oyster (*C. gigas*), respectively, with signs of illness and growth in Luria-Bertani agar (LB), and then transferred to Miller's LB Broth (37°C). Ten liters of each strain (1×10^9 cell mL^{-1}) was centrifuged at 600× g, 10 min at 4°C, and freeze. To confirm the strains' identity, we extracted DNA by the organic extraction method (75), and DNA was resuspended by the addition of TE Buffer 10 mM pH 8.0. DNA purity and concentration were estimated using the Nanodrop 1000 spectrophotometer (Thermo Fisher Scientific). DNA integrity was visualized in 1.5% agarose gel electrophoresis, under UVP Biodoc-It 2 imaging system (Analytik Jena), stained with the fluorescent dye GelRed® Nucleic Acid Gel Stain (Biotium 41003). Endpoint PCR was performed to identify the bacterial species and identify some virulence factors in the strains. The primers used are shown in **Supplementary Table 1**. PCR reactions were performed with GoTaq® Flexi DNA Polymerase (Promega M829) according to the manufacturer's instructions. The PCR products were electrophoresed and sequenced by Genewiz (South Plainfield, NJ, USA). The sequences were analyzed by Blast-NCBI (https://blast.ncbi.nlm.nih.gov/Blast.cgi). **Supplementary Table 2** shows the genes identified in bacterial strains. To obtain the protein crude extract, centrifuged bacteria were re-suspended in filtered (0.2 μm) sterile saline solution (CS PiSA NaCl 0.9%, pH 7.2), with 1X protease inhibitor (Sigma P1860), and 0.5% Triton X-100. Cells were homogenized with glass beads (300 μm) in a vortex, and the extract was centrifuged at 1,200× g, 15 min, 4°C. Protein was determined by BCA Protein Assay Kit (bicinchoninic acid, 23227, Thermo Fisher Scientific) according to the manufacturer's instructions with bovine albumin as a standard.

Commercial Apoptosis Inducers

Camptothecin (CPT, C-9911, Sigma–Aldrich, St. Louis, MO) was dissolved in DMSO and made into a stock 1 mM solution. Staurosporine (STP, 81590, Cayman Chemical, Ann Harbor, MI) was dissolved in DMSO and made into a 1 mM stock solution.

Hemolymph Extraction

Oyster shells were surface-cleaned with 70% ethanol, and hemolymph (4–5 pools of 10–30 animals) extracted from the adductor muscle using a 26-gauge hypodermic needle making a small hole in the valves of the animals close to the muscle, and immediately put on ice. No oyster was subjected to more than one sampling. Immediately after hemolymph collection, the total number of hemocytes was determined using TC20™ Automated Cell Counter (BioRad). The mean cell concentration for the hemocyte oyster population was $1.9 \pm 0.5 \times 10^6$ cell mL^{-1}. When necessary, hemocytes' concentration in the solution was adjusted by adding centrifuged hemolymph (600× g, 10 min, 4°C) without hemocytes.

Biological Activity of Toxins and Commercial Apoptosis Inducers

To assess toxins and commercial apoptosis inducer's biological activity, we carried out a hemocyte viability test with resazurin sodium salt (C-62758-13-8, Sigma-Aldrich). Each hemocyte pooled subgroup was subdivided into three aliquots (each 100 µL at densities of 1×10^6 cell mL^{-1}) for each treatment. Aliquots were placed in a 96-well sterile microplate and allowed to attach and spread for 1 h at 25°C. Samples were exposed to three different concentrations of STP, CPT, toxins, negative control (hemocytes exposed to sterile saline Cs PiSA NaCl 0.9%, pH 7.2), or positive control (hemocytes exposed to 10 mM HCl pH 2). Not more than 10 µL of toxins or apoptosis inducer's working concentration were added for every 100 mL of hemolymph to obtain the final concentrations studied. Control tests with DMSO were assayed and showed no effect on cell viability (data not shown). Hemocytes were incubated in the dark for 4 h at 25°C, in a humid chamber in triplicate. Preview studies have shown that incubation for 4–6 h is enough to induce apoptosis in bivalve hemocytes exposed to marine toxins such as PST and DST (56, 58). Following the incubation time, cell viability was measured with the resazurin reduction cell viability assay (76). From this experiment, final concentrations close to 50% mortality were chosen for the rest of the tests (**Table 2**).

Neutral Comet Assay

Neutral comet assay detects the breakage of double-stranded DNA (58, 77). Aliquots of 150 µL of hemolymph, with a cellular concentration of 1.5×10^6 cells mL^{-1}, were placed in Eppendorf tubes. The cells were exposed to toxins or apoptosis inducers, according to **Table 2**. Hemocytes were incubated for 4·h at 25°C, in a dark, humid chamber in triplicate. Hemocytes were harvested using 0.25% trypsin in filtered (0.2 µm) sterile seawater (pH 7, 33 PSU) and washed and resuspended in the same sterile volume seawater. The suspension was added to 0.75% low-temperature melting agarose at a ratio of 1:10 (v/v) and spread on glass slides that were pre-coated with 0.7% regular agarose and then air-dried. Slides with double-layered agarose were submerged in pre-cooled lysis solution (154 mM NaC1, 10 mM Tris, 10 mM EDTA, and 0.5% SLS at pH 10) at 4°C for 30 min, washed briefly to remove detergent and salt, and electrophoresed at ∼7 V cm^{-1} for 3 min in TBE solution (40 mM Tris-boric acid, 2 mM EDTA at pH 8.3) and then stained for 10 min with propidium iodide (PI; 10 µg mL^{-1}). DNA damage was quantified by measuring displacement between the nucleus's genetic material (comet head) and the resulting tail, according to Estrada et al. (58); the comet tail's intensity, relative to the head, reflects the number of DNA breaks.

Annexin V Assay

To identify PS exposure on the outer leaflet of the plasma membrane, we used the Annexin V–FITC apoptosis kit (BioVision, K101). Each of the pooled subgroups was subdivided into three aliquots (aliquots of 200 µL at densities of 1×10^6 cell mL^{-1}) for each treatment, put directly on a coverslip and allowed to attach and spread for 1 h at room temperature. The cells were exposed to toxins or apoptosis inducers, according to **Table 2**. Hemocytes were incubated for 4 h at 25°C, in a dark, humid chamber in triplicate. Following exposure to toxins or apoptosis inducers, hemocytes were washed with filtered (0.2 µm) sterile seawater (pH 7, 33 PSU). The hemocytes were processed with Annexin-V according to the manufacturer's instructions. Following incubation, the coverslip was inverted on a glass slide and observed under a phase-contrast microscope (Nikon Eclipse Ni-U) coupled with fluorescence for characterization using a dual filter set for FITC and rhodamine. At least 100 cells were counted in each sample. Categories were assigned based on the total number of hemocytes counted. Viable cells are stained for annexin V (FITC green) but not for propidium iodide (PI, red). Cells in early PCD are stained by FITC-annexin V but not by PI. Late PCD or already dead cells are stained both by FITC-annexin V and PI, or only by PI, respectively.

Chromatin Condensation

We used adherent cells stained with 4′,6-Diamidino-2-Phenylindole (DAPI, ThermoFisher D1306) to evaluate chromatin's condensation. Hemocytes (200 µL at densities of 1×10^6 cell mL^{-1}) were allowed to attach and spread onto a glass coverslip for one h at room temperature. Then they were exposed to toxins or apoptosis inducers for 4 h at 25°C, washed with filtered (0.2 µm) sterile seawater (pH 7, 33 PSU), and fixed with methanol. Fixed hemocytes were immersed in PBS buffer (137 mM NaCl, 2 mM KCl, 10 mM Na_2HPO_4, 1.8 mM KH_2PO_4, pH 7.2) for 5 min and then treated with a DAPI solution in PBS (1:1,500) for 5 min. Hemocytes were washed with PBS, and the coverslip was inverted and mounted on a glass slide and observed under a fluorescence microscope (365 nm) (Nikon Eclipse Ni-U). The percentage of nuclei with chromatin condensation was estimated by examining 200 cells per sample. Cells with intact DNA show weak fluorescence signals; in contrast, cells with condensed chromatin exhibit stronger fluorescence when observed under a fluorescence microscope. Also, condensed chromatin could be kept in the periphery of the nuclei or small fragments dispersed.

TABLE 2 | Final concentration of apoptosis inducers or marine toxins used for the experiments.

Apoptosis inducers or marine toxins	Concentration
STP	1.5 μg mL^{-1}
CPT	1.2 μg mL^{-1}
STX	5 μg STX *eq* mL^{-1}
GTX 2/3	1.25 μg STX *eq* mL^{-1}
OA/DTX-1	3 μg AO *eq* mL^{-1}
PbTx2	5 μg PbTx *eq* mL^{-1}
PbTx-2,3	4 μg PbTx *eq* mL^{-1}
Vp	6.25 μg protein mL^{-1}
Vc	5 μg protein mL^{-1}

CPT, Camptothecin; STP, Staurosporine; STX, Saxitoxin; GTX, Gonyautoxin; OA, Okadaic acid; DTX, Dynophysistoxin; PbTx, Brevetoxin; Vp, Vibrio parahaemolyticus extract; Vc, V. campbellii extract.

DNA Fragmentation Assay

Aliquots of 2 mL of hemolymph, with a cellular concentration of 2×10^6 cells mL^{-1}, were placed in Eppendorf tubes in triplicate. The cells were exposed to toxins or apoptosis inducers, according to **Table 2**. Each hemocyte triplicate was pooled to extract DNA with the Apoptotic DNA-Ladder Kit (Merck 11835246001), according to the manufacturer's instructions. DNA was visualized in 2% agarose gel electrophoresis, under UVP Biodoc-It 2 imaging system (Analytik Jena), stained with the fluorescent dye GelRed® Nucleic Acid Gel Stain (Biotium 41003).

Gene Expression Analysis by Quantitative Real-Time PCR

RNA Extraction and cDNA Synthesis

To perform RT-qPCR analysis, after hemolymph extraction, 2 mL of hemolymph with a cellular concentration of 1.5×10^6 cells mL^{-1} were placed in Eppendorf tubes and exposed to the desired final concentration of toxins or apoptosis inducers according to **Table 2**. Hemocytes were incubated for 4 h at 25°C, in a humidity chamber in triplicate. Following incubation hemocytes were centrifuged 600× g, 15 min, 4°C, and washed in filtered (0.2 μm) sterile seawater (pH 7, 33 PSU). The hemocyte pellet obtained was stored to −80°C for further analyses. For total RNA extraction pooled hemolymph samples were lysed in 1 mL of FastRNA® Pro Green Kit solution (MP Biomedicals) and processed according to the manufacturer's instructions. The extracted RNA concentration was measured by spectrophotometer (Nanodrop 1000® Thermo Scientific) at 260 nm. The purity of RNA was determined as the 260/280 nm ratio with acceptable values > 1.8. RNA concentration was estimated using the Nanodrop 1000 spectrophotometer (Thermo Fisher Scientific). A total of 1 μg total RNA was treated with 1 U DNase I (SIGMA AMPD1) for 2 h at 37°C and then heat-inactivated at 65°C for 10 min before reverse transcription to eliminate genomic DNA contamination. The integrity of total RNA was analyzed by 1% agarose gel electrophoresis under UVP Biodoc-It 2 imaging system (Analytik Jena), stained with the fluorescent dye GelRed® Nucleic Acid Gel Stain (Biotium 41003). A sample of 2.5 μg RNA was used to synthesize cDNA from each pooled sample using an oligo dT and Superscript III first-strand synthesis system for RT-PCR kit (Invitrogen, USA 11904018), according to the manufacturer's instructions. The resulting cDNA was stored at −80°C until use. cDNA synthesis was confirmed by endpoint PCR amplification of the beta actin gene (Forward 5′-CCACACCCGTAAGGGAAAG-3′; Reverse 5′-GGTTACCACCACCATGAGG-3′) with GoTaq® Flexi DNA Polymerase (Promega M829), and PCR products were electrophoresed in 1% agarose gel with GelRed® Nucleic Acid Gel Stain (Biotium 41003).

Quantitative Real-Time PCR

cDNAs were used for qPCR analysis to determine the relative expression of mRNA coding five caspases (caspase 1, 2, 3, 7, and 8) and two endogenous controls (RPL7 and RPL36). Primers were obtained from preview reports (**Supplementary Table 1**), and the primers were ordered from T4 Oligo (Irapuato, Gto, Mexico). Primers efficiency was tested using the standard curve method. For this purpose, a serial dilution (1:5, 1:10, 1:20, 1:40, 1:80) was made from a single cDNA sample consisting of a pool of all cDNAs different treatments (0.5 μg μL^{-1}). Only primers that showed efficiencies between 1.8 and 2.2 were used. The qPCR analysis was performed in tube strips in triplicate using the Rotor-Gene Q (Quiagen TM) with a total reaction volume of 10 μL. Each reaction had 5 μL of 2X SsoFast™EvaGreen®Supermix (Bio-Rad, Hercules, CA, 1725201), 0.3 mM of each primer, and 1 μL of each diluted cDNA (100 ng μL^{-1}). Amplification conditions were enzyme activation at 95°C for 1 min, followed by 40 cycles of denaturation 10 s at 95°C and annealing/extension 30 s at 59°C. The qPCR product's specificity was analyzed by a dissociation curve performed after amplification (65–95°C continuous-time), observing a single peak at the expected Tm. Relative quantification of the expression of the analyzed genes was calculated using REST 2009 (Relative Expression Software Tool) software v2.0.13 with RG mode (http://www.qiagen.com/rest), using the pair-wise fixed randomization test (78). Normalization using the housekeeping genes RPL7 and RPL36 were used to identify the expression levels of the caspase's genes. Using the take-off values obtained from Rotor-Gene Q, the program performed 3,000 iterations to determine whether there are significant differences between samples and controls while considering issues of reaction efficiency and reference gene normalization. This program's expression values are a ratio such that values above 1 denote an upregulation of gene expression in the treated group while values <1 indicate a downregulation ($^*P < 0.05$; $^{**}P < 0.01$). Expression variation for each gene is visualized in a whisker-box plot.

Statistical

For all experiments, means and SD were calculated, and results are expressed as the means ± SD of three independent experiments, except for RT-qPCR analysis as mentioned above. Comparisons between control and treatments were assessed with Student's t distribution or Wilcoxon test, according to results obtained with Shapiro-Wilk (distributions normality) and Fisher (homoscedasticity) tests. Statistical significance was set at $P <$

0.05. All analyses were performed using the SPSS for Windows statistical package (version 16.0).

RESULTS

Cytotoxicity of Hemocytes

To investigate if marine toxins cause hemocyte toxicity, we measured cell viability after 4 h of exposure to proteinaceous and non-proteinaceous toxins and apoptosis inducers (**Figure 1**). Control cells in sterile saline NaCl, 0.9% (Neg) showed negligible cell viability changes, while hemocytes treated with 10 mM HCl pH 2 (Pos) showed the expected cell death of 97%. Staurosporine (STP), camptothecin (CPT), saxitoxin (STX), gonyautoxin epimers 2 and 3 (GTX2/3), and the mixture of brevetoxins 2 and 3 (PbTx-2,-3) provoked a dose-dependent effect, with hemocyte mortality above 50% for the highest concentrations. The mixture of okadaic acid and dinophysistoxin 1 (AO/DTX-1) was not toxic at the concentration range tested, and brevetoxin 2 (PbTx-2) exerted minor toxicity only at 5 $\mu g\ mL^{-1}$. Crude extracts of *Vibrio parahaemolyticus* (Vp) and *V. campbellii* (Vc) increased cell death only at a marginal level of 5–10%, at 6.25 and 5 $\mu g\ mL^{-1}$, respectively. These results demonstrate that marine toxins induce hemocytes' cell death.

Phosphatidylserine Translocation

We used Annexin V to identify PS's translocation from the cytoplasmic to the exoplasmic leaflet of the hemocyte plasma membrane, through the binding of fluorescent annexin V at 4 h post challenged. **Figure 2A** showed hemocytes observed by fluorescence microscopy to detect viable or no measurable PCD cells (green and red staining negative, **v**), PCD cells (green, anexin V-bound, **a**), and cells in end stage of PCD and dead (red, propidium iodide stained cells, and green anexin V-bound cells, **d**). We measured the percentage of hemocytes at each of these different stages, after 4 h of incubation in media with marine toxins. We choose the lowest concentration of marine toxins that provoked 50% of hemocyte death, or the concentration that caused the highest response, to perform this experiment (**Table 2**). We observed 2% of PCD (red column) in sterile saline solution NaCl 0.9% (**Figure 2B**, SS). Incubation with CPT, STP, STX, and epimers GTX 2/3, increased PCD by ∼15–30% (**Figure 2B**), demonstrating that these toxins induce PCD.

Breakage of Double-Stranded DNA and Chromatin Condensation

A late stage of PCD pathway is the breakage of double-stranded DNA. To confirm that marine toxins induce PCD and analyze bivalves' and vertebrates' PCD pathway similitudes, we measure marine toxins' effect in double-stranded DNA breakage. Hemocytes were incubated with toxins as described above and analyzed by neutral single-cell gel electrophoresis (comet) assay. Broken DNA migrates electrophoretically faster than complete DNA material, a phenomenon that results in the formation of a "tail" susceptible to stain a measure in fluorescence images. More DNA breakage produces longer tails susceptible to categorize in the classes shown in **Figure 3A**. The statistical analysis shown in **Figure 3B** indicates that hemocytes incubated with CTP, STP, STX, GTX 2/3, and PbTx-2,-3 developed higher DNA breakage than the observed in control hemocytes exposed to sterile saline solution NaCl 0.9% ($P < 0.05$). Besides DNA breakage, PCD cells develop nuclear hyperchromasia and chromatin condensation, observable by fluorescence. We stained hemocytes incubated in the absence or presence of marine toxins with DAPI, as indicated before and measured the number of hyperchromatic and peripheral chromatin condensation nuclei following the characteristics illustrated in **Figure 4A**. The quantitative analysis presented in **Figure 4B** proves that CTP, STP, STX, and GTX 2/3, induced hyperchromasia and chromatin condensation in hemocytes ($P < 0.05$). Analyses of DNA breakage, nuclear hyperchromasia, and chromatin condensation confirm that CTP, STP, STX, and GTX 2/3 induce PCD and that bivalve mollusk and vertebrates' PCD signaling pathways are fundamentally similar. We also tested the nuclear DNA fragmentation, and **Figure 5** shows DNA laddering visualized in a 2% agarose gel. We used as a positive control (C+), DNA from U937 apoptotic cells provided by the kit. A clear DNA-ladder pattern is visible when hemocytes are treated with CPT, STP, STX, and epimers GTX 2/3. None oligonucleosomal fragments were observed in the rest of the samples.

Caspase Gene Expression

Once confirmed that some marine toxins induce PCD, we investigated what kind of PCD these substances trigger. Based on what is known in vertebrates, we hypothesized that marine toxins induce either apoptosis, a process characterized by the activation of caspases−2,−3,−7, or−8, or pyroptosis-like, identified by the increment in the expression of the proinflamatory caspase-1. We measured the amount of mRNA of these caspases by RT-qPCR, in the absence or presence of marine toxins and vertebrates' apoptosis inducers, as described before (**Figure 6** and **Table 3**). Caspase-1 mRNA underwent the most drastic downregulation in hemocytes treated with STX, GTX2/3, and PbTx-2, and a significant upregulation in the cells treated with CPT, AO/DTX1, PbTx-2,−3, Vc, and Vp. Caspase-2 mRNA decreased in hemocytes exposed to STP, GTX2/3, PbTx-2, PbTx-2,-3, while caspase-3 mRNA increased under GTX2/3 treatment and decreased with PbTx-2 incubation. Caspase-7 mRNA increased in hemocytes exposed to AO/DTX-1 and, finally, caspase-8 mRNA decreased in hemocytes incubated with CPT, and STX, and increased in hemocytes exposed to Vc crude extract. **Table 3** is a matrix that summarizes the graphical data of RT-qPCR, representing the value of significance (*P*) for each sample with a colorimetric scale (green, up-regulated; red down-regulated; yellow, no-differences).

DISCUSSION

The PCD concept applies broadly to several intracellular pathways involved in cell's self-destruction (21). PCD exhibit unique morphological characteristics and energy-dependent biochemical mechanisms, and occurs when a cell is damaged, infected, senescent, or otherwise of little use to the animal (20–24). PCD participates in the immune system (79–81), and marine toxins modulated mollusk's immune response (9, 25, 28, 29,

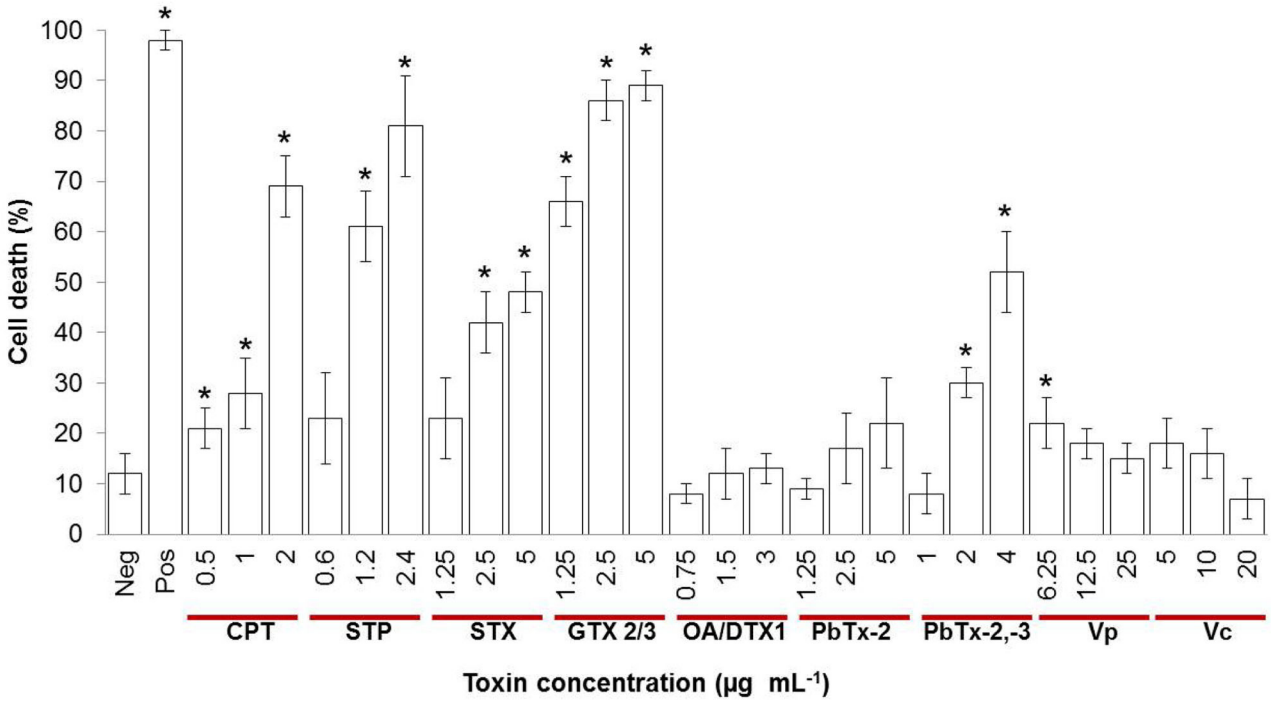

FIGURE 1 | Percentage of cell death evaluated through the resazurin assay in hemocytes treated with different concentrations of inducers of apoptosis or marine toxins during 4 h at 25°C. Hemolymph from 10 to 30 oysters was pooled to have a total of 1.5×10^6 cells mL^{-1}. Bars represent mean ± standard deviation of two independent experiments. *$P < 0.05$. Neg, negative control; Pos, positive control; CPT, camptothecin; STP, staurosporine; STX, saxitoxin; GTX, gonyautoxin; OA, okadaic acid; DTX, dynophysistoxin; PbTx, brevetoxin; Vp, *Vibrio parahaemolyticus* extract; Vc, *V. campbellii* extract.

31, 46–52, 55, 56, 58–62, 82–87). Hemocytes are the first line of defense in bivalve mollusks immune system, and here we evaluated how marine toxins modulate PCD in hemocytes from *C. gigas*. The fact that control hemocytes exhibit high PCD level indicates that this process is vital for molluscan immunity (25, 26, 88–90). Here we show that marine toxins increase hemocyte's cell mortality with PCD phenotype.

We first analyzed the cell death characteristics induced by CPT and STP, two *bona fide* PCD inducers. CPT is a potent inhibitor of topoisomerase I extracted from the Chinese tree *Camptotheca acuminata* (91). STP is a non-selective protein kinase inhibitor obtained from the bacteria *Streptomyces staurospores* (92). Both substances induce apoptosis *in vitro* in various cell types and therefore they are standard positive controls in bioassays (92–96). Both substances caused high mortality in *C. gigas* hemocytes and helped to describe how death is carried out in bivalve hemocytes, as previously shown for *Nodipecten subnodosus* (58). Like STP and CPT, hemocyte death was evident with paralyzing toxins (STX and epimers GTX2/3), and to a lesser extent, with the mixture of brevetoxins (PbTx-2,-3). The inducers and these marine toxins, showed a marked translocation of PS to the extracellular leaflet and breakage of double-stranded DNA. Early PS exposure is closely associated with plasma membrane rupture during PCD for attracting engulfing cells (43, 45, 97–99). We observed many cells expressing annexin V and PI labels and considered them to be in late PCD or result from secondary necrosis, but we thought them for the analysis only as dead cells, and it was not the study's object of this work. Recent studies showed that mammalian cell lines undergoing programmed necrosis (necroptosis), as well as necrotic cells in the nematode *Caenorhabditis elegans*, translocates PS to their outer surfaces before cell lysis to recruit phagocytes (100, 101). Chromatin condensation and DNA fragmentation are important criteria to identify PCD in terminal stages. We observed both characteristics consistently in hemocytes treated with STP, CPT, STX, and epimers GTX2/3, which induced a clear death ladder pattern. During apoptosis and pyroptosis, cells undergo chromatin condensation and DNA fragmentation, but only in apoptosis the nucleus breaks into multiple chromatin bodies, in a process called nucleosomal fragmentation, while remains intact in pyroptosis (39–44). In previous work we observed that paralyzing toxins, epimers GTX2/3, provokes nucleosomal fragmentation and apoptosis in *N. subnodosus* (58).

Caspases are a family of cysteine proteases, which play an essential role in apoptosis and inflammation, distinguishing between many cell death possibilities. Caspases involved in apoptosis are human caspase -2, -3, -6, -7, -8, -9, and -10; those participating primarily in pyroptosis are human caspase -1, -4, -5, -13, and -14, as well as murine caspase -11 and -12 (21, 28, 32, 102). *C. gigas* expresses executer caspases -1, -3, and -7 and initiator caspases -2 and -8 (30, 37, 55, 103, 104). Given that mRNA increase generally indicates the synthesis of a particular

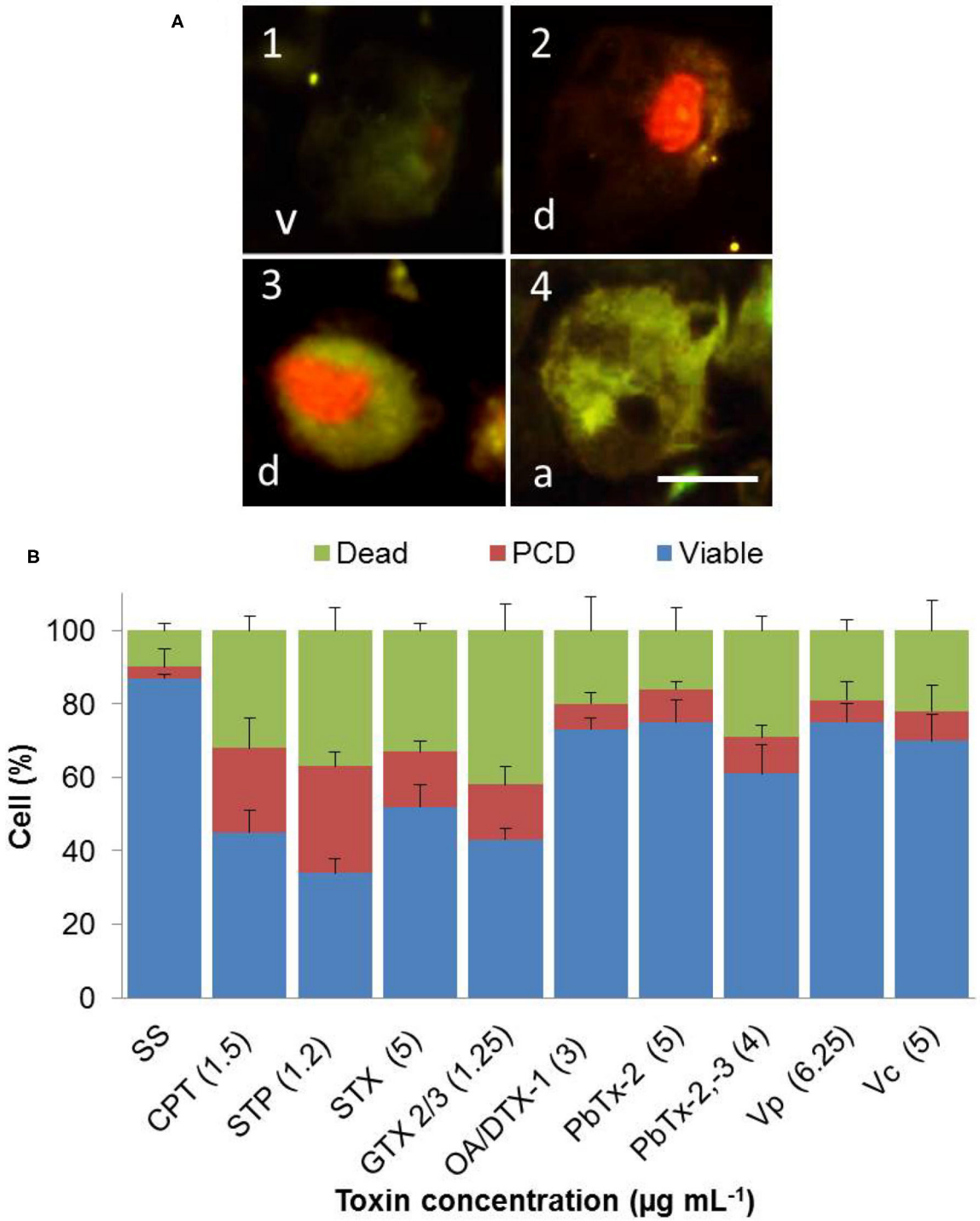

FIGURE 2 | *In vitro* phosphatidylserine translocation to the extracellular leaflet in hemocytes exposed to apoptosis inducers or marine toxins during 4 h at 25°C. (A1) Hemocytes observed by fluorescence, to detect viable or no measurable programmed cell death (PCD, green and red staining negative), (A4) PCD cells (green, annexin V-bound), and (A2 and A3) cells in end stage of PCD and dead (red, propidium iodide stained cells, and green annexin V-bound cells). **(B)** The graph shows percentages of different stages of cells of **(A)**. Results are expressed as the mean ± standard deviation. A, annexin V positive; d, dead; v, viable. Scale bar = 5 µm. SS, saline solution; CPT, camptothecin; STP, staurosporine; STX, saxitoxin; GTX, gonyautoxin; OA, okadaic acid; DTX, dynophysistoxin; PbTx, brevetoxin; Vp, *Vibrio parahaemolyticus* extract; Vc, *V. campbellii* extract.

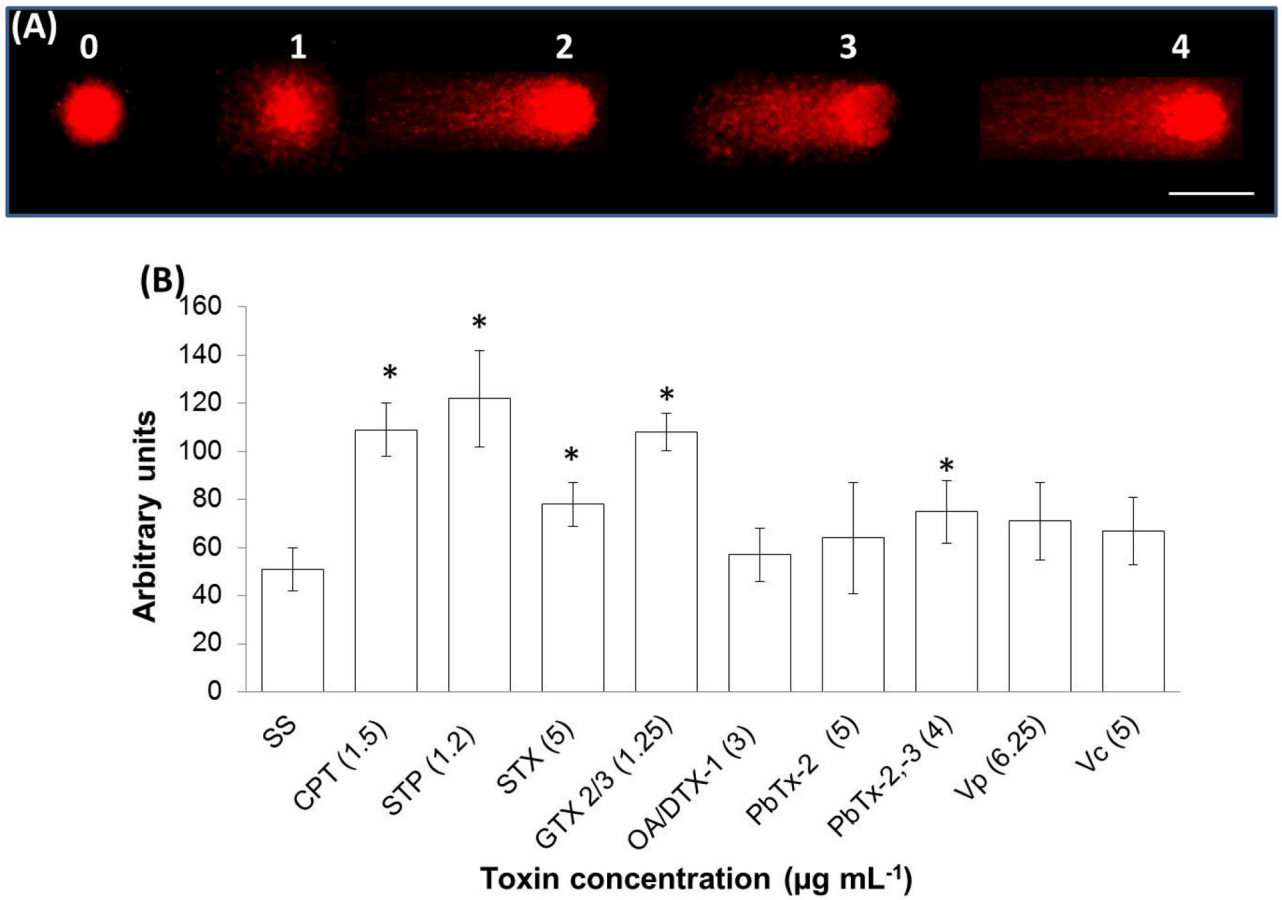

FIGURE 3 | *In vitro* DNA double-strand breakage in hemocytes exposed to apoptosis inducers or marine toxins for 4 h at 25°C. **(A)** Image of hemocyte nuclei with different DNA damage grades, assessed by neutral comet assay, stained red with propidium iodide. DNA damage categories: undamaged, low damaged, medium damage, high damage, and complete damage, using a scale of 0–4, respectively. Scale bar = 5 µm. **(B)** Frequency distribution of DNA damage in hemocytes. Data were obtained from 400 scored nuclei. Results are expressed as the mean ± standard deviation. *$P < 0.05$. SS, saline solution; CPT, camptothecin; STP, staurosporine; STX, saxitoxin; GTX, gonyautoxin; OA, okadaic acid; DTX, dynophysistoxin; PbTx, brevetoxin; Vp, *Vibrio parahaemolyticus* extract; Vc, *V. campbellii* extract.

gene product (105), we resorted to use mRNA quantitation to measure caspase expression. CPT induced upregulation of the pro-inflammatory caspase-1 and down regulation of caspase 8. Caspase-1 is a cysteine protease that cleaves and activates the pro-forms of host inflammatory cytokines, IL-1β, and IL-18 (106). On vertebrates, caspase-1 acts in pyroptosis, a pathway of host cell death stimulated by a range of microbial infections and non-infectious stimuli, associated with plasma membrane rupture and release of pro-inflammatory intracellular content (35, 38, 107, 108). Therefore, we show here that CPT could induces pyroptosis-like in *C. gigas* hemocytes, in addition to cause apoptosis. Caspase-1 mediated pyroptosis has been observed in other invertebrates such as sea cucumbers (109) and crustaceans (110). *C. gigas* hemocytes express cytoplasmic and nuclear caspase-1, capable to induce cell death (37, 111). In oysters, caspase-1 is a homolog of executioner caspase-3/7, which can activate itself, bind to other caspases and lipopolysaccharides (111). On the other hand, STP induces caspase-2 down-regulation in hemocytes of *C. gigas*. Caspase-2 keeps a high similarity among animal species (37, 51) and the pathogen-associated molecular patterns (PAMPs) provoke its downregulation in *Mytilus edulis* mussel (51). Nevertheless, STP provoked apoptosis in bivalve hemocytes of *N. subnodosus* dependent of caspases (58), which indicates that the type of PCD that STP induces depends on the species studied. The low level of variation of caspases mRNA induced by CPT and STP seems to be sufficient to induce PCD in *C. gigas*, either by apoptosis or pyroptosis-like, given that both substances induced clear morphological alterations such as the breakage of double-stranded DNA, induction of the characteristic DNA ladder pattern, and the translocation of PS to the extracellular leaflet of the plasma membrane.

Paralyzing shellfish toxins (PST) are tricyclic tetrahydropurine derivatives with potent hydrophilic neurotoxic activity. In vertebrates, PSTs inhibit the voltage gated-sodium channel with high affinity and, thus blocking action potentials in excitable

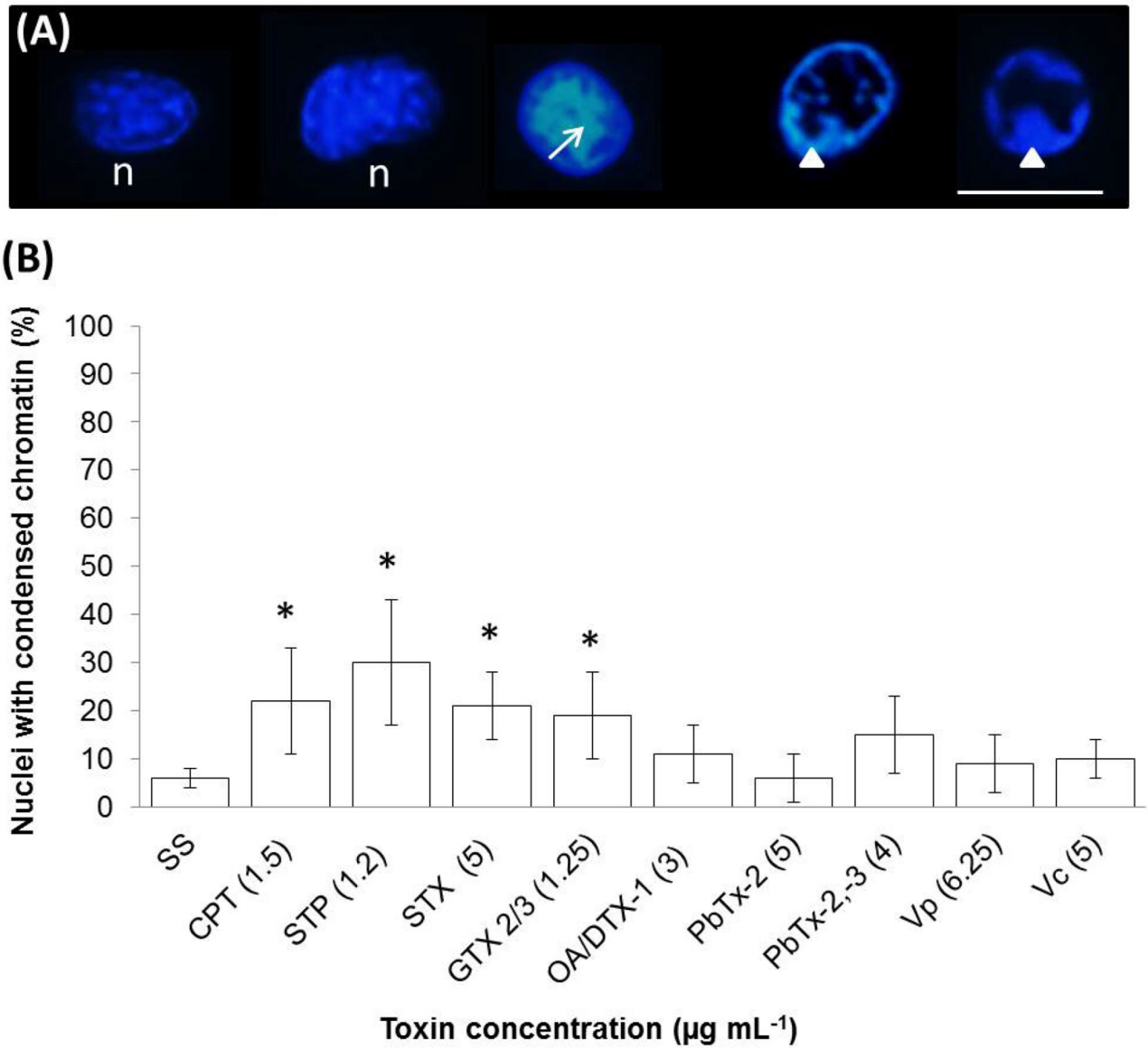

FIGURE 4 | *In vitro* chromatin condensation in nuclei of hemocytes exposed to apoptosis inducers or marine toxins for 4 h at 25°C. **(A)** DAPI staining (blue) of representative nuclei: observe the normal nuclei (n), hyperchromasia (arrow) characteristic of condensed chromatin, and nuclei with condensation of chromatin in the periphery (arrow head). **(B)** Percentages of the nuclei with condensed chromatin. In each sample, at least 100 nuclei were counted. Scale bar = 5 µm. Results are expressed as the mean ± standard deviation. *$P < 0.05$. SS, saline solution; CPT, camptothecin; STP, staurosporine; STX, saxitoxin; GTX, gonyautoxin; OA, okadaic acid; DTX, dynophysistoxin; PbTx, brevetoxin; Vp, *Vibrio parahaemolyticus* extract; Vc, *V. campbellii* extract.

membranes of neurons and muscles (112). PSTs are present in some genera of dinoflagellates such as *Alexandrium* sp., *Pyrodinium bahamense*, *Gymnodinium catenatum*, *Centrodinium punctatum* and cyanobacteria (113–116). There are more than 57 analogs of these toxins that differ in their toxicity (117), and has been stated that PSTs provoke apoptosis *in vivo* e *in vitro* in bivalve mollusks (55, 58, 87). In *C. gigas* hemocytes the epimers GTX2/3 increased expression of executioner caspase-3 and with STX a down-regulated caspase-8 was observed. Caspase-3 and caspase-8 have been previously identified in *Crassostrea* sp. (30, 37, 100, 118). These results could indicate that hemocytes are in a late stage of apoptosis, consistent with the observed oligonucleosomal fragmentation. These results further corroborate that marine toxin induce PCD by apoptosis in hemocytes of *C. gigas*. When STX is injected in the mussel *M. chilensis*, hemocytes involve numerous pattern recognition receptors (PRRs) that, subsequently, trigger a cellular response apoptotic or autophagic death (87). When epimers GTX2/3 are exposed with the hemocytes of the pectinid *N. subnodosus*, the induction of apoptosis is linked directly to caspases (58).

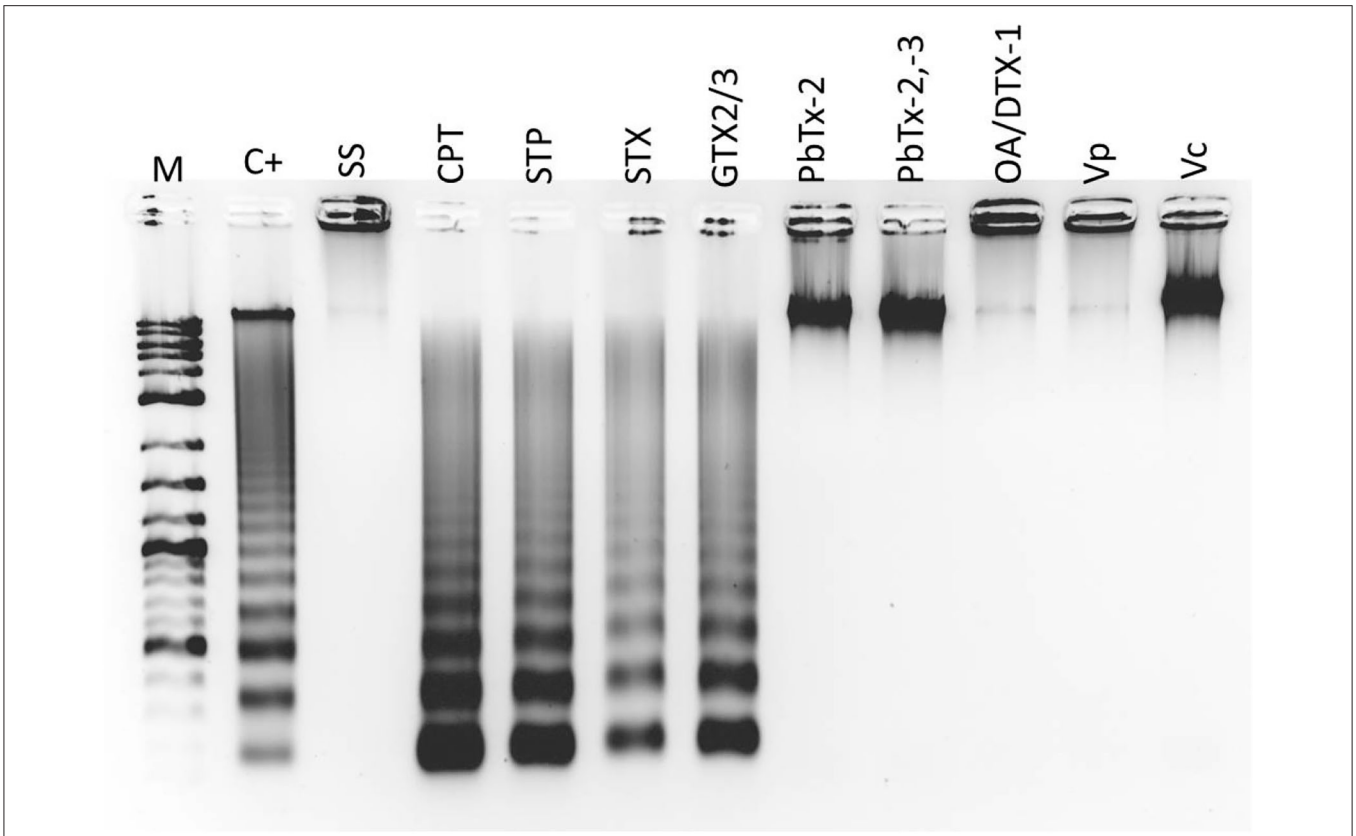

FIGURE 5 | *In vitro* DNA ladder in nuclei of hemocytes exposed to apoptosis inducers or marine toxins for 4 h at 25°C. Electrophoresis was performed on 2% agarose gel. M, kb marker; C+, Positive control (DNA from apoptotic U937 cells); SS, Saline solution; CPT, camptothecin; STP, staurosporine; STX, saxitoxin; GTX, gonyautoxin; OA, okadaic acid; DTX, dynophysistoxin; PbTx, brevetoxin; Vp, *Vibrio parahaemolyticus* extract; Vc, *V. campbellii* extract.

When *C. gigas* fed with the PST producer *A. catenella* there was a significant increase of the number of hemocytes in apoptosis after 29 h of exposure, with overexpression of two caspase executor genes (caspase-3 and caspase-7) (55). STX and GTX 2/3 also showed the down-regulation of caspase-1 in *C. gigas*, which indicates that PST inhibits pyroptosis-like processes, similar to what happens with other pathogens, conferring some ability to persist and cause disease in the host (35). On the other hand, this inhibition of caspase-1 could permit hemocytes perform apoptosis in an orderly manner, thus avoiding the inflammatory damage.

Brevetoxins (PbTxs) represent a group of polyether compounds that bind to and stimulate sodium flux through voltage-gated sodium channels in nerve and muscle, leading to uncontrolled sodium influx into the cell (119). PbTxs are produced by the marine dinoflagellate *Karenia brevis* (119, 120). The mixture of PbTx-2,-3 triggered DNA alterations, PS translocation, and mortality in *C. gigas* hemocytes. PS translocation and chromosomal DNA cleavage are observed in apoptosis and pyroptosis (35, 42–45). After hemocyte exposure to a mixture of these toxins, we did not observe the DNA ladder characteristic of apoptosis, and together with the up-regulation of caspase-1 and the absence of nuclear disintegration, suggest a PCD by a pyroptosis-like mechanism. In human lymphocytes exposed to PbTx-2,-3, results indicate a high mortality rate and extensive genotoxic damage with both toxins (121). On the contrary, when we exposed hemocytes of *C. gigas* to PbTx-2, caspase-1, initiator caspase-2, and effector caspase-3 expression decreased, and cell death was low, in agreement with the experiments carried out by Mello et al. (52), where at 4 h, high viability was observed with the same toxin in *C. gigas*. They concluded that this viability correlated with the activation of detoxification and stress genes CYP356A1, FABP and Hsp70, but not with immune or to antioxidant ones BPI, IL-17, EcSOD, Prx6, GPx, and SOD.

Diarrheic shellfish toxins (DST) are heat-stable polyether and lipophilic compounds isolated from various species of dinoflagellates, mainly of the genus *Dynophysis* and *Prorocentrum* (114). Among these toxins, okadaic acid (OA) and its derivatives named dinophysistoxins (DTX1-10) are the best known. These compounds inhibit protein phosphatase-1 and -2A *in vitro*, provoking inflammation of the intestinal tract and diarrhea in humans (122, 123). They are also tumor promoters in animal test systems (124, 125). OA and its analogs DTXs did not seem to cause the same harmful effects in bivalve hemocytes as in other studied vertebrate cell lines, where OA induced

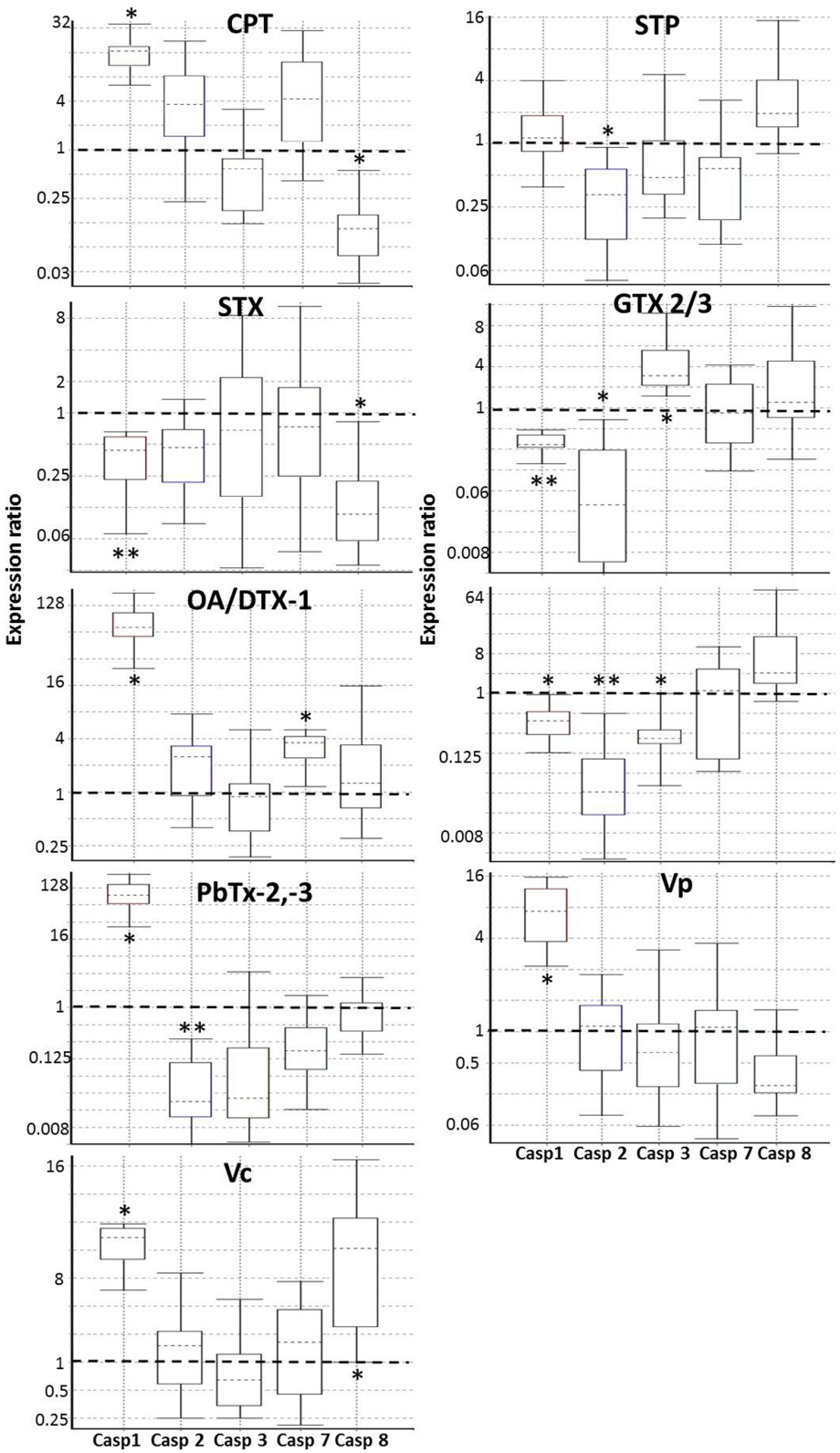

FIGURE 6 | Real-time PCR (qRT-PCR) of caspases (Casp) in hemocytes exposed to in hemocytes exposed to apoptosis inducers or marine toxins for 4 h at 25°C. Whisker-box plots of the relative expressions calculated by the REST 2009 Software of the caspase-1, caspase-2, caspase-3, caspase-7, and caspase-8 genes.

(Continued)

FIGURE 6 | Boxes represent the interquartile range, or the middle 50% of observations. The dotted line inside the box represents the median gene expression. Whiskers represent the minimum and maximum observations. The proportions over 1 indicate genes that increase expression, while proportions <1 indicate genes decrease in expression. *$P < 0.05$; **$P < 0.01$. Casp, Caspase; CPT, Camptothecin; STP, Staurosporine; STX, Saxitoxin; GTX, Gonyautoxin; OA, Okadaic acid; DTX, Dynophysistoxin; PbTx, Brevetoxin; Vp, *Vibrio parahaemolyticus* extract; Vc, *V. campbellii* extract.

TABLE 3 | *P*-value of relative expression of caspase transcripts in hemocytes of *Crassostrea gigas* exposed to apoptosis inducers or marine toxins.

Toxin	caspase-1	caspase-2	caspase-3	caspase-7	caspase-8
CPT	0.025	0.051	0.968	0.083	0.030
STP	0.326	0.013	0.142	0.146	0.223
STX	0.001	0.055	0.396	0.586	0.015
GTX2/3	0.000	0.033	0.047	0.534	0.158
OA/DTX-1	0.028	0.074	0.486	0.014	0.093
PbTx2	0.026	0.000	0.030	0.437	0.200
PbTx2/3	0.019	0.000	0.088	0.308	0.574
Vp	0.020	0.968	0.390	0.800	0.105
Vc	0.021	0.173	0.459	0.273	0.014

CPT, Camptothecin; STP, Staurosporine; STX, Saxitoxin; GTX, Gonyautoxin; OA, Okadaic acid; DTX, Dynophysistoxin; PbTx, Brevetoxin; Vp, Vibrio parahaemolyticus extract; Vc, V. campbellii extract. Red = down regulated; Green = up-regulated; Yellow = No differences comparing with control.

cytotoxicity and apoptosis (126–136). Our analyses with the mixture of OA and DTX-1, showed no evident cytotoxic effects *in vitro* in hemocytes of *C. gigas*. It has been demonstrated in *C. gigas* that ingestion of the strain of *P. lima* cells that produces OA and DTX1, provokes a clear mRNA modulation expression of the genes involved in cell cycle regulation and immune system (137). Several authors have pointed out that the low percentage of dead hemocytes in bivalve mollusks and apoptotic processes, seem to indicate *in vivo* and *in vitro*, that these organisms have protective mechanisms and resistance against harmful effects of OA and/or DTX-1, that involves OA's storage into the lysosomal system (50, 56, 60, 138). Despite low hemocyte death in our work, there was a significant increase in caspase-1 and caspase-7 when hemocytes were exposed to OA/DTX1. Caspase-1 can process proteolytically the apoptotic effector caspase-7, and both can activate simultaneously (36, 139). There are vertebrate cell types that express caspase-1 but do not undergo PCD (140). It has been described that the low level of cell death when exposed to OA indicates protective mechanisms by the presence of caspase inhibitors, which can inhibit PCD pathways (141).

Bacteria of the genus *Vibrio* sp. produce many pathogenic factors, including enterotoxins, hemolysins, and cytotoxins. *V. campbellii* and *V. parahaemolyticus* are extensively studied species because they are the causative agent of the often lethal effects in aquaculture organisms, such as fish, bivalves, and crustacean (142–145). In this study, hemocytes were exposed to the crude protein extract of *V. parahaemolyticus*, and *V. campbellii*, two bacteria that had shown high virulence against shrimp postlarvae, and were isolated from shrimp and oyster, respectively (146). The crude extracts of these bacteria showed hemolytic activity in human erythrocytes (147). Still, we did not find a cytotoxic effect at 4 h post challenged. We previously identified genes related to some protein toxins as part of this virulence, and their genomes showed many pathogenic factors such as hemolysin, enterotoxins, cytotoxins, proteases, siderophores, adhesive factors, and hemagglutinin (148). Some studies with mollusks have demonstrated the role of caspase-8 in anti-bacterial response (51, 118, 149–151), and it has been proved in *Haliotis discus discus* and *C. hongkongensis* that caspase-8 mRNA expression in hemocytes was significantly up-regulated by exposure to *Vibrio* species (118, 150). Similar results we obtained with proteinaceous extract from *V. campbellii* in *C. gigas* hemocytes. Caspase-8 was cloned and characterized in *C. hongkongensis* and *C. gigas* and showed that it is ubiquitously expressed in oysters, suggesting a role in apoptosis (100, 118). Likewise, *Vibrio* extracts showed the over-expression of caspase-1 in hemocytes from *C. gigas*. It has been recognized that moderate activity levels of caspase-1 stimulate cell host's survival responses, modulate intracellular growth of bacteria, and promote inflammatory cytokines production. When caspase-1 passes a threshold level, the cell undergoes PCD by pyroptosis, characterized by plasma-membrane pore formation, which leads to cell lysis and release of pro-inflammatory intracellular contents (35, 42, 152, 153). Pore-forming toxins are the most common *Vibrio* cytotoxic proteins, are required for virulence, and have been implicated in pyroptosis cell death (154, 155). Also, several studies have identified novel roles for caspase-8 in modulating IL-1β, inflammation, and caspase-1 processing, in response on the stimulus or stimuli that initiate the signaling cascade (156–163). In *C. gigas* a pyroptosis-like PCD could be playing a role in bacteria clearance, by removing intracellular replication niches and enhancing the host's immune responses. Also it has been documented that caspase-1 activation fails to trigger pyroptosis in many vertebrate cell lines in response to bacterial pore-forming toxins, which in turn promote cell survival upon toxin challenge possibly by facilitating membrane repair (164), a similar scenario could be relevant for infectious with *Vibrio* extracts in *C. gigas* hemocytes. It is controversial whether pyroptosis, which can also be triggered by non-bacterial pathological stimuli, truly represents a cell modality in bivalve hemocytes or whether it constitutes a special case of apoptosis or necrosis, but the activation of caspase-1 in cells could has unquestionable pathophysiological implications.

Finally, we do not rule out the importance of different cell death types that could be causing misbalance of hemocytes, such as necrosis, necroptosis, autophagy, pyroptosis, pironecrosis, etc. The marine non-proteinaceous STX, GTX2/3, and PbTx-2,-3 trigger signaling pathways that promote apoptotic cell death, as the apoptotic inducers CPT and STP, but PbTx-2,-3 did not show oligonucleosomal fragmentation. Vp and Vc extracts, OA/DTX-1, and PbTx-2 increased pro-inflammatory caspase-1 indicative of signaling pathways leading to PCD by a pyroptosis-like process; still, protective mechanisms could influence in

the low cell death observed. The results presented illustrate the complexity of the hemocyte response to marine toxins. Nevertheless, they are consistent with the role of PCD to preserve a healthy and balanced immunity, keeping hemocytes at normal levels for the systematic and regulated dismantling elimination of damaged cells in *C. gigas*.

DATA AVAILABILITY STATEMENT

The datasets generated for this study are available on request to the corresponding author.

AUTHOR CONTRIBUTIONS

NE, EN-V, AP, FA, and RC contributed to the conception and design of the study. NE, EN-V, AP, and LG-V developed the experiments and performed statistical analysis. NE, EN-V, AP, LG-V, and RC analyzed the data as well as wrote the paper. All authors contributed to revising the manuscript, reading, and approving the final version.

FUNDING

Financial support was provided by Consejo Nacional de Ciencia y Tecnología of Mexico (CONACyT, Ciencia Básica 2015-258122, NE), (CONACyT, Ciencia de Frontera 2019-7357, RG) and CONACyT scholarship 853509 (AP). The work was also supported by SEP-CINVESTAV FIDSC2018/143 to RC.

ACKNOWLEDGMENTS

We thank Leyberth Fernández-Herrera for technical assistance for the extraction of brevetoxins. Special thanks to Andrew Turner (Centre for Environment Fisheries and Aquaculture Science; CEFAS, United Kingdom) by PbTxs composition.

SUPPLEMENTARY MATERIAL

The Supplementary Material for this article can be found online at: https://www.frontiersin.org/articles/10.3389/fimmu.2021.634497/full#supplementary-material

REFERENCES

1. FAO. *The State of World Fisheries and Aquaculture 2020*. Rome: Sustainability in action (2020). p. 206. doi: 10.4060/ca9229en
2. Helm MM. *Cultured Aquatic Species Information Programme. Crassostrea gigas (Thunberg, 1793)*. Rome: FAO, Fisheries and Aquaculture Department (2015). Available online at: http://www.fao.org/fishery/culturedspecies/Crassostrea_gigas/en (accessed March 20, 2020).
3. Barbosa Solomieu V, Renault T, Travers M. Mass mortality in bivalves and the intricate case of the Pacific oyster, *Crassostrea gigas*. *J Invertebr Pathol.* (2015) 131:2–10. doi: 10.1016/j.jip.2015.07.011
4. Zannella C, Mosca F, Mariani F, Franci G, Folliero V, Galdiero M, et al. Microbial diseases of bivalve mollusks: infections, immunology and antimicrobial defense. *Mar Drugs.* (2017) 15:182. doi: 10.3390/md15060182
5. Lassudriea M, Hégaret H, Wikfors GH, Mirella da Silva P. Effects of marine harmful algal blooms on bivalve cellular immunity and infectious diseases: a review. *Dev Comp Immunol.* (2020) 108:103660. doi: 10.1016/j.dci.2020.103660
6. Bacheré E, Gueguen Y, Gonzalez M, de Lorgeril J, Garnier J, Romestand B. Insights into the anti-microbial defense of marine invertebrates: the penaeid shrimps and the oyster *Crassostrea gigas*. *Immunol Rev.* (2004) 198:149–68. doi: 10.1111/j.0105-2896.2004.00115.x
7. Guo X, He Y, Zhang L, Lelong C, Jouaux A. Immune and stress responses in oysters with insights on adaptation. *Fish Shellfish Immunol.* (2015) 46:107–19. doi: 10.1016/j.fsi.2015.05.018
8. Guo X, Ford SE. Infectious diseases of marine molluscs and host responses as revealed by genomic tools. *Philos Trans R Soc Lond B Biol Sci.* (2016) 371:20150206. doi: 10.1098/rstb.2015.0206
9. Canesi L, Gallo G, Gavioli M, Pruzzo C. Bacteria–hemocyte interactions and phagocytosis in marine bivalves. *Microsc Res Tech.* (2002) 57:469–76. doi: 10.1002/jemt.10100
10. Cheng TC. Bivalves. In: Ratcliffe NA, Rowley AF, editors. *Invertebrate Blood Cells*. Vol. I. London: Academic Press (1981). p. 231–300.
11. Auffret M. Bivalve hemocyte morphology. In: Fisher WS, editor. *Disease Processes in Marine Bivalve Molluscs*. Vol. 18. Bethesda, MD: American Fisheries Society (1988). p. 169–77.
12. Hine PM. The inter-relationships of bivalve haemocytes. *Fish Shellfish Immunol.* (1999) 9:367–85. doi: 10.1006/fsim.1998.0205
13. Auffret M. Bivalves as models for marine immunotoxicology. In: Tryphonas H, Fournier M, Blakley BR, Smits JEG, Brousseau P, editors. *Investigative Immunotoxicology*. Chapter 3. Boca Raton, FL: CRC Press (2005). p. 29–48.
14. Song L, Wang L, Qiu L, Zhang H. Bivalve immunity. In: Soderhall K, editor. *Invertebrate Immunity*. Vol. 708. New York, NY: Springer (2010). p. 44–65.
15. Fisher WS. Structure and function of oyster hemocytes. In: Brehelin M, editor. *Immunity in Invertebrates*. Berlin: Springer (1986). p. 25–35.
16. Canesi L, Ciacci C, Betti M, Scarpato A, Citterio B, Pruzzo C, et al. Effects of PCB congeners on the immune function of *Mytilus* hemocytes: alterations of tyrosine kinase-mediated cell signalling. *Aquat Toxicol.* (2003) 63:293–306. doi: 10.1016/S0166-445X(02)00186-8
17. Canesi L, Ciacci C, Lorusso LC, Betti M, Guarnieri T, Tavolari S, et al. Immunomodulation by 17b-Estradiol in bivalve hemocytes. *Am J Physiol Regul Integr Comp Physiol.* (2006) 291:R664–73. doi: 10.1152/ajpregu.00139.2006
18. Tang D, Kang R, Berghe TV, Vandenabeele P, Kroemer G. The molecular machinery of regulated cell death. *Cell Res.* (2019) 29:347–64. doi: 10.1038/s41422-019-0164-5
19. Tsuchiya K. Inflammasome-associated cell death: pyroptosis, apoptosis, and physiological implications. *Microbiol Immunol.* (2020) 64:252–69. doi: 10.1111/1348-0421.12771
20. Raff M. Cell suicide for beginners. *Nature.* (1998) 396:119–22. doi: 10.1038/24055
21. Fink SL, Cookson BT. Apoptosis, pyroptosis, and necrosis: mechanistic description of dead and dying eukaryotic cells. *Infect Immun.* (2005) 73:1907–16. doi: 10.1128/IAI.73.4.1907-1916.2005
22. Elmore S. Apoptosis: a review of programmed cell death. *Toxicol Pathol.* (2007) 35:495–516. doi: 10.1080/01926230701320337
23. Fuchs Y, Steller H. Programmed cell death in animal development and disease. *Cell.* (2011) 147:742–58. doi: 10.1016/j.cell.2011.10.033
24. Jorgensen I, Rayamajhi M, Miao EA. Programmed cell death as a defence against infection. *Nat Rev Immunol.* (2017) 17:151–64. doi: 10.1038/nri.2016.147
25. Sunila I, LaBanca J. Apoptosis in the pathogenesis of infectious diseases of the eastern oyster *Crassostrea virginica*. *Dis Aquat Org.* (2003) 56:63–170. doi: 10.3354/dao056163
26. Sokolova IM, Evans S, Hughes FM. Cadmium-induced apoptosis in oyster hemocytes involves disturbance of cellular energy balance but no mitochondrial permeability transition. *J Exp Biol.* (2004) 207:3369–80. doi: 10.1242/jeb.01152

27. Terahara K, Takahashi KG. Mechanisms and immunological roles of apoptosis in molluscs. *Curr Pharm Des*. (2008) 14:131–7. doi: 10.2174/138161208783378725
28. Sokolova IM. Apoptosis in molluscan immune defense. *Invertebr Surviv J*. (2009) 6:49–58.
29. Kiss T. Apoptosis and its functional significance in molluscs. *Apoptosis*. (2010) 15:313–21. doi: 10.1007/s10495-009-0446-3
30. Zhang L, Li L, Zhang G. Gene discovery, comparative analysis and expression profile reveal the complexity of the *Crassostrea gigas* apoptosis system. *Dev Compar Immunol*. (2011) 35:603–10. doi: 10.1016/j.dci.2011.01.005
31. Romero A, Novoa B, Figueras A. The complexity of apoptotic cell death in mollusks: an update. *Fish Shellfish Immunol*. (2015) 46:79–87. doi: 10.1016/j.fsi.2015.03.038
32. Creagh EM, Conroy H, Martin SJ. Caspase-activation pathways in apoptosis and immunity. *Immunol Rev*. (2003) 193:10–21. doi: 10.1034/j.1600-065X.2003.00048.x
33. Siegel RM. Caspases at the crossroads of immune-cell life and death. *Nat Rev Immunol*. (2006) 6:308–17. doi: 10.1038/nri1809
34. Cookson BT, Brennan MA. Pro-inflammatory programmed cell death. *Trends Microbiol*. (2001) 9:113–4. doi: 10.1016/S0966-842X(00)01936-3
35. Bergsbaken T, Fink SL, Cookson BT. Pyroptosis: host cell death and inflammation. *Nat Rev Microbiol*. (2009) 7:99–109. doi: 10.1038/nrmicro2070
36. Miao EA, Rajan JV, Aderem A. Caspase-1-induced pyroptotic cell death. *Immunol Rev*. (2011) 243:206–14. doi: 10.1111/j.1600-065X.2011.01044.x
37. Qu T, Huang B, Zhang L, Li L, Xu F, Huang W, et al. Identification and functional characterization of two executioner caspases in *Crassostrea gigas*. *PLoS ONE*. (2014) 9:e89040. doi: 10.1371/journal.pone.0089040
38. Jorgensen I, Miao EA. Pyroptotic cell death defends against intracellular pathogens. *Immunological Rev*. (2015) 265:130–42. doi: 10.1111/imr.12287
39. Kerr J, Wyllie A, Currie A. Apoptosis: a basic biological phenomenon with wide ranging implications in tissue kinetics. *Br J Cancer*. (1972) 26:239–57. doi: 10.1038/bjc.1972.33
40. Wyllie AH, Kerr JFR, Currie AR. Cell death: the significance of apoptosis. *Int Rev Cytol*. (1980) 68:251–306. doi: 10.1016/S0074-7696(08)62312-8
41. Wyllie AH, Morris RG, Smith AL, Dunlop D. Chromatin cleavage in apoptosis: association with condensed chromatin morphology and dependence on macromolecular synthesis. *J Pathol*. (1984) 142:67–77. doi: 10.1002/path.1711420112
42. Fink SL, Cookson BT. Caspase-1-dependent pore formation during pyroptosis leads to osmotic lysis of infected host macrophages. *Cell Microbiol*. (2006) 8:1812–25. doi: 10.1111/j.1462-5822.2006.00751.x
43. Wang Q, Imamura R, Motani K, Kushiyama H, Nagata S, Suda T. Pyroptotic cells externalize eat-me and release find-me signals and are efficiently engulfed by macrophages. *Int Immunol*. (2013) 25:363–72. doi: 10.1093/intimm/dxs161
44. Ryter SW, Choi AMK. Cell death and repair in lung disease. In: McManus LM, Mitchell RN, editors. *Pathobiology of Human Disease*. Amsterdam: Academic Press (2014). p. 2558–74. doi: 10.1016/b978-0-12-386456-7.05302-8
45. Vasconcelos NM, Van Opdenbosch N, Van Gorp H, Parthoens E, Lamkanfi M. Single-cell analysis of pyroptosis dynamics reveals conserved GSDMD-mediated subcellular events that precede plasma membrane rupture. *Cell Death Differ*. (2018) 26:146–61. doi: 10.1038/s41418-018-0106-7
46. da Silva PM, Hégaret H, Lambert C, Wikfors GH, Le Goic N, Shumway SE, et al. Immunological responses of the Manila clam (*Ruditapes philippinarum*) with varying parasite (*Perkinsus olseni*) burden, during a long-term exposure to the harmful alga, *Karenia selliformis*, and possible interactions. *Toxicon*. (2008) 51:563–73. doi: 10.1016/j.toxicon.2007.11.006
47. Galimany E, Sunila I, Hégaret H, Ramón M, Wikfors GH. Pathology and immune response of the blue mussel (*Mytilus edulis* L.) after an exposure to the harmful dinoflagellate *Prorocentrum minimum*. *Harmful Algae*. (2008) 7:630–8. doi: 10.1016/j.hal.2008.01.001
48. Galimany E, Sunila I, Hégaret H, Ramón M, Wikfors GH. Experimental exposure of the blue mussel (*Mytilus edulis* L.) to the toxic dinoflagellate *Alexandrium fundyense*: histopathology, immune responses, and recovery. *Harmful Algae*. (2008) 7:702–11. doi: 10.1016/j.hal.2008.02.006
49. Hégaret H, Smolowitz RM, Sunila I, Shumway SE, Alix J, Dixon M, et al. Combined effects of a parasite, QPX, and the harmful-alga, *Prorocentrum minimum* on northern quahogs, *Mercenaria mercenaria*. *Mar Environ Res*. (2010) 69:337–44. doi: 10.1016/j.marenvres.2009.12.008
50. Mello DF, Proença LAO, Barracco MA. Comparative study of various immune parameters in three bivalve species during a natural bloom of *Dinophysis acuminata* in Santa Catarina Island, Brazil. *Toxins*. (2010) 2:1166–78. doi: 10.3390/toxins2051166
51. Romero A, Estévez-Calvar N, Dios S, Figueras A, Novoa B. New insights into the apoptotic process in mollusks: characterization of caspase genes in *Mytilus galloprovincialis*. *PLoS ONE*. (2011) 6:e17003. doi: 10.1371/journal.pone.0017003
52. Mello DF, de Oliveira ES, Vieira RC, Simoes E, Trevisan R, Dafre AL, et al. Cellular and transcriptional responses of *Crassostrea gigas* hemocytes exposed *in vitro* to brevetoxin (PbTx-2). *Mar Drugs*. (2012) 10:583–97. doi: 10.3390/md10030583
53. Moreira R, Balseiro P, Planas JV, Fuste B, Beltran S, Novoa B, et al. Transcriptomics of *in vitro* immune-stimulated hemocytes from the manila clam *Ruditapes philippinarum* using high-throughput sequencing. *PLoS ONE*. (2012) 7:e35009. doi: 10.1371/journal.pone.0035009
54. Prado-Alvarez M, Romero A, Balseiro P, Dios S, Novoa B, Figueras A. Morphological characterization and functional immune response of the carpet shell clam (*Ruditapes decussatus*) haemocytes after bacterial stimulation. *Fish Shellfish Immun*. (2012) 32:69–78. doi: 10.1016/j.fsi.2011.10.019
55. Medhioub W, Ramondenc S, Vanhove A, Vergnes A, Masseret E, Savar V, et al. Exposure to the neurotoxic dinoflagellate, *Alexandrium catenella,* induces apoptosis of the hemocytes of the oyster, *Crassostrea gigas*. *Mar Drugs*. (2013) 11:4799–814. doi: 10.3390/md11124799
56. Prado-Alvarez M, Flórez-Barrós F, Méndez J, Fernandez-Tajes J. Effect of okadaic acid on carpet shell clam (*Ruditapes decussatus*) haemocytes by *in vitro* exposure and harmful algal bloom simulation assays. *Cell Biol Toxicol*. (2013) 29:189–97. doi: 10.1007/s10565-013-9246-1
57. Tanguy M, McKenna P, Gauthier-Clerc S, Pellerin J, Danger JM, Siah A. Sequence analysis of a normalized cDNA library of *Mytilus edulis* hemocytes exposed to *Vibrio splendidus* LGP32 strain. *Results Immunol*. (2013) 3:40–50. doi: 10.1016/j.rinim.2013.04.001
58. Estrada N, Ascencio F, Shoshani L, Contreras RG. Apoptosis of hemocytes from lions-paw scallop *Nodipecten subnodosus* induced with paralyzing shellfish poison from *Gymnodinium catenatum*. *Immunobiology*. (2014) 219:964–74. doi: 10.1016/j.imbio.2014.07.006
59. Simoes E, Vieira RC, Schramm MA, Mello DF, De Almeida Pontinha V, da Silva PM, et al. Impact of harmful algal blooms (*Dinophysis acuminata*) on the immune system of oysters and mussels from Santa Catarina, Brazil. *J Mar Biol Assoc UK*. (2014) 95:773–81. doi: 10.1017/S0025315414001702
60. Prego-Faraldo MV, Valdiglesias V, Laffon B, Eirín-López JM, Méndez J. *In vitro* analysis of early genotoxic and cytotoxic effects of okadaic acid in different cell types of the mussel *Mytilus galloprovincialis*. *J Toxicol Environ Health Part A*. (2015) 78:814–24. doi: 10.1080/15287394.2015.1051173
61. Abi-Khalil C, Finkelstein DS, Conejero G, Du Bois J, Destoumieux-Garzon D, Rolland JL. The paralytic shellfish toxin, saxitoxin, enters the cytoplasm and induces apoptosis of oyster immune cells through a caspase-dependent pathway. *Aquat Toxicol*. (2017) 190:133–41. doi: 10.1016/j.aquatox.2017.07.001
62. Rey-Campos M, Moreira R, Gerdol M, Pallavicini A, Novoa B, Figueras A. Immune tolerance in *Mytilus galloprovincialis* hemocytes after repeated contact with *Vibrio splendidus*. *Front Immunol*. (2019) 10:1894. doi: 10.3389/fimmu.2019.01894
63. Hummert C, Ritscher M, Reinhardt K, Luckas B. Analysis of the characteristic PSP profiles of *Pyrodinium bahamense* and several strains of *Alexandrium* by HPLC based on ion-pair separation, post-column oxidation, and fluorescence detection. *Chromatographia*. (1997) 45:312–6. doi: 10.1007/BF02505576
64. Yu, RC, Hummert C, Luckas B, Qian PY, Zhou MJ. A modified HPLC method for analysis of PSP toxins in algae and shellfish from China. *Chromatographia*. (1998) 48:671–6. doi: 10.1007/BF02467597
65. AOAC International. AOAC Official Method 959.08, Paralytic shellfish poison: biological method. In: Horwitz W, editor. *Official Methods of*

Analysis of AOAC International, 17th ed. Gaithersburg, MD: AOAC International. (2000). p. 59–61.
66. Heredia-Tapia A, Arredondo-Vega BO, Nuñez-Vázquez EJ, Yasumoto T, Yasuda M, Ochoa JL. Isolation of *Prorocentrum lima* (Syn. *Exuviaella lima*) and diarrhetic shellfish poisoning (DSP) risk assessment in the Gulf of California, Mexico. *Toxicon.* (2002) 40:1121–7. doi: 10.1016/S0041-0101(02)00111-3
67. Guillard RRL, Ryther JH. Studies of marine planktonic diatoms. I. *Cyclotella nana* Hustedt and *Detonula confervacea* Cleve. *Can J Microbiol.* (1962) 8:229–39. doi: 10.1139/m62-029
68. Guillard RRL. Culture of phytoplankton for feeding marine invertebrates. In: Smith WL, Chanley MH, editors. *Culture of Marine Invertebrate Animals*. New York, NY: Plenum Press (1975). p. 26–60.
69. Quilliam MA, Hardstaff WR, Ishida N, McLachlan JL, Reeves AR, Ross NW, et al. Production of diarrhetic shellfish poisoning (DSP) toxins by *Prorocentrum lima* in culture and development of analytical methods. In: Yasumoto T, Oshima Y, Fukuyo Y, editors. *Harmful and Toxic Algal Blooms*. Paris: IOC-UNESCO (1996). p. 289–92.
70. Lewis RJ. Detection of ciguatoxins and related benthic dinoflagellate toxins: *in vivo* and *in vitro* methods. In: Hallegraeff GM, Anderson DM, Cembella AD, editors. *IOC Manual on Harmful Marine Microalgae: Manual and Guides.* Paris: UNESCO (1995). p. 135–61.
71. Le Du, J, Tovar-Ramírez D, Núnez-Vázquez EJ. Embryotoxic effects of dissolved okadaic acid on the development of Longfin yellowtail *Seriola rivoliana*. *Aquat Toxicol.* (2017) 190:210–6. doi: 10.1016/j.aquatox.2017.07.012
72. Blackburn SI, Hallegraef GM, Bolch CJS. Vegetative reproduction and sexual life cycle of the toxic dinoflagellate *Gymnodinium catenatum* from Tasmania. *Australia J Phycol.* (1989) 25:577–90. doi: 10.1111/j.1529-8817.1989.tb00264.x
73. McNabb PS, Selwood AI, van Ginkel R, Boundy M, Holland PT. Determination of brevetoxins in shellfish by LC/MS/MS: single-laboratory validation. *J AOAC Int.* (2012) 95:1097–105. doi: 10.5740/jaoacint.11-272
74. APHA. *Subcommittee on Laboratory Methods for the Examination of Shellfish. Method for the Bioassay of Gymnodinium breve toxin(s) in Shellfish. Recommended Procedures for the Examination of Sea Water and Shellfish*. 4th ed. Washington, DC: American Public Health Association (1970). p. 61–8.
75. Sambrook J, Fritsch EF. Maniatis T. *Molecular Cloning: A Laboratory Manual*. 2nd ed. Vol. 1, 2 and 3. New York, NY: Cold Spring Harbor Laboratory Press (1989). p. 1669.
76. Riss TL, Moravec RA. Use of multiple assay endpoints to investigate the effects of incubation time, dose of toxin, and plating density in cell-based cytotoxicity assays. *Assay Drug Dev Technol.* (2004) 2:51–62. doi: 10.1089/154065804322966315
77. Fairbairn, DW, O'Neill KL. The neutral comet assay is sufficient to identify an apoptotic window by visual inspection. *Apoptosis*. (1996) 1:91–4. doi: 10.1007/BF00142083
78. Pfaffl MW. Relative expression software tool (REST(C)) for group-wise comparison and statistical analysis of relative expression results in real-time PCR. *Nucleic Acids Res.* (2002) 30:36. doi: 10.1093/nar/30.9.e36
79. Feig C, Peter ME. How apoptosis got the immune system in shape. *Eur J Immunol.* (2007) 37(S1):S61–70. doi: 10.1002/eji.200737462
80. Hildeman D, Jorgensen T, Kappler J, Marrack P. Apoptosis and the homeostatic control of immune responses. *Curr Opin Immunol.* (2007) 19:516–21. doi: 10.1016/j.coi.2007.05.005
81. Birge RB, Ucker DS. Innate apoptotic immunity: the calming touch of death. *Cell Death Differ.* (2008) 15:1096–102. doi: 10.1038/cdd.2008.58
82. Estrada N, Rodríguez-Jaramillo C, Contreras G, Ascencio F. Effects of induced paralysis on hemocytes and tissues of the giant lions-paw scallop by paralyzing shellfish poison. *Mar Biol.* (2010) 157:1401–15. doi: 10.1007/s00227-010-1418-4
83. Manfrin C, De Moro G, Torboli V, Venier P, Pallavicini S, Gerdol M. Physiological and molecular responses of bivalves to toxic dinoflagellates. *Invertebr Surviv J.* (2012) 9:184–99.
84. Mello DF, da Silva PM, Barracco MA, Soudant P, Hegaret H. Effects of the dinoflagellate *Alexandrium minutum* and its toxin (saxitoxin) on the functional activity and gene expression of *Crassostrea gigas* hemocytes. *Harmful Algae.* (2013) 26:45–51. doi: 10.1016/j.hal.2013.03.003
85. Prado-Alvarez M, Flórez-Barrós F, Sexto-Iglesias A, Méndez J, Fernandez-Tajes J. Effects of okadaic acid on haemocytes from *Mytilus galloprovincialis*: a comparison between field and laboratory studies. *Mar Environ Res.* (2012) 81:90–3. doi: 10.1016/j.marenvres.2012.08.011
86. Astuya A, Carrera C, Ulloa V, Aballay A, Núñez-Acuña G, Hégaret H, et al. Saxitoxin modulates immunological parameters and gene transcription in *Mytilus chilensis* hemocytes. *Int J Mol Sci.* (2015) 16:15235–50. doi: 10.3390/ijms160715235
87. Detree C, Núñez-Acuña G, Roberts S, Gallardo-Escárate C. Uncovering the complex transcriptome response of *Mytilus chilensis* against saxitoxin: implications of harmful algal blooms on mussel populations. *PLoS ONE.* (2016) 11:e0165231. doi: 10.1371/journal.pone.0165231
88. Goedken M, Morsey B, Sunila I, Dungan C, De Guise S. The effects of temperature and salinity on apoptosis of *Crassostrea virginica* hemocytes and *Perkinsus marinus*. *J Shellfish Res.* (2005) 24:177–83. doi: 10.2983/0730-8000(2005)24[177:TEOTAS]2.0.CO;2
89. Goedken M, Morsey B, Sunila I, De Guise S. Immunomodulation of *Crassostrea gigas* and *Crassostrea virginica* cellular defense mechanisms by *Perkinsus marinus*. *J Shellfish Res.* (2005) 24:487–96. doi: 10.2983/0730-8000(2005)24[487:IOCGAC]2.0.CO;2
90. Cherkasov AS, Grewal S, Sokolova IM. Combined effects of temperature and cadmium exposure on haemocyte apoptosis and cadmium accumulation in the eastern oyster *Crassostrea virginica* (Gmelin). *J Therm Biol.* (2007) 32:162–70. doi: 10.1016/j.jtherbio.2007.01.005
91. Hsiang YH, Lihou MG, Liu LF. Arrest of replication forks by drug-stabilized topoisomerase I-DNA cleavable complexes as a mechanism of cell killing by camptothecin. *Cancer Res.* (1989) 49:5077–82.
92. Kabir J, Lobo M, Zachary I. Staurosporine induces endothelial cell apoptosis via focal adhesion kinase dephosphorylation and focal adhesion disassembly independent of focal adhesion kinase proteolysis. *Biochem J.* (2002) 367:145–55. doi: 10.1042/bj20020665
93. Morris EJ. Induction of neuronal apoptosis by camptothecin, an inhibitor of DNA topoisomerase-I: evidence for cell cycle-independent toxicity. *J Cell Biol.* (1996) 134:757–70. doi: 10.1083/jcb.134.3.757
94. Traganos F, Seiter K, Feldman E, Halicka HD, Darzynkiewicz Z. Induction of apoptosis by camptothecin and topotecan. *Ann NY Acad Sci.* (1996) 803:101–10. doi: 10.1111/j.1749-6632.1996.tb26380.x
95. Belmokhtar CA, Hillion J, Ségal-Bendirdjian E. Staurosporine induces apoptosis through both caspase-dependent and caspase-independent mechanisms. *Oncogene.* (2001) 20:3354–62. doi: 10.1038/sj.onc.1204436
96. Stepczynska A, Lauber K, Engels IH, Janssen O, Kabelitz D, Wesselborg S, et al. Staurosporine and conventional anticancer drugs induce overlapping, yet distinct pathways of apoptosis and caspase activation. *Oncogene.* (2001) 20:1193–202. doi: 10.1038/sj.onc.1204221
97. Fadok VA, Bratton DL, Frasch SC, Warner ML, Henson PM. The role of phosphatidylserine in recognition of apoptotic cells by phagocytes. *Cell Death Differ.* (1998) 5:551–62. doi: 10.1038/sj.cdd.4400404
98. Lee SH, Meng XW, Flatten KS, Loegering DA, Kaufmann SH. Phosphatidylserine exposure during apoptosis reflects bidirectional trafficking between plasma membrane and cytoplasm. *Cell Death Differ.* (2012) 20:64–76. doi: 10.1038/cdd.2012.93
99. Mariño G, Kroemer G. Mechanisms of apoptotic phosphatidylserine exposure. *Cell Res.* (2013) 23:1247–8. doi: 10.1038/cr.2013.115
100. Li Z, Venegas V, Nagaoka Y, Morino E, Raghavan P, Audhya A, et al. Necrotic cells actively attract phagocytes through the collaborative action of two distinct PS-exposure mechanisms. *PLoS Genet.* (2015) 11:e1005285. doi: 10.1371/journal.pgen.1005285
101. Gong YN, Guy C, Olauson H, Becker JU, Yang M, Fitzgerald P, et al. ESCRT-III acts downstream of MLKL to regulate necroptotic cell death and its consequences. *Cell.* (2017) 169:286–300.e216. doi: 10.1016/j.cell.2017.03.020
102. Hengartner MO. The biochemistry of apoptosis. *Nature.* (2000) 407:770–6. doi: 10.1038/35037710
103. Li C, Qu T, Huang B, Ji P, Huang W, Que H, et al. Cloning and characterization of a novel caspase-8-like gene in *Crassostrea gigas*. *Fish Shellfish Immun.* (2015) 46:486–92. doi: 10.1016/j.fsi.2015.06.035
104. Xu J, Jiang S, Li Y, Li M, Cheng Q, Zhao D, et al. Caspase-3 serves as an intracellular immune receptor specific for lipopolysaccharide

in oyster *Crassostrea gigas*. *Dev Comp Immunol*. (2016) 61:1–12. doi: 10.1016/j.dci.2016.03.015
105. Vogel C, Marcotte EM. Insights into the regulation of protein abundance from proteomic and transcriptomic analyses. *Nat Rev Genet*. (2014) 13:227–32. doi: 10.1038/nrg3185
106. Fantuzzi G, Dinarello CA. Interleukin-18 and interleukin-1β: two cytokine substrates for ICE (caspase-1). *J Clin Immunol*. (1999) 19:1–11.
107. Frantz S. Targeted deletion of caspase-1 reduces early mortality and left ventricular dilatation following myocardial infarction. *J Mol Cell Cardiol*. (2003) 35:685–94. doi: 10.1016/S0022-2828(03)00113-5
108. Miao EA, Leaf IA, Treuting PM, Mao DP, Dors M, Sarkar A, et al. Caspase-1-induced pyroptosis is an innate immune effector mechanism against intracellular bacteria. *Nat Immunol*. (2010) 11:1136–42. doi: 10.1038/ni.1960
109. Yina S, Zhongjie C, Chenghua L, Weiwei Z, Xuelin Z, Ming G. A novel caspase-1 mediates inflammatory responses and pyroptosis in sea cucumber *Apostichopus japonicus*. *Aquaculture*. (2019) 513:734399. doi: 10.1016/j.aquaculture.2019.734399
110. Yang G, Wang J, Luo T, Zhang X. White spot syndrome virus infection activates Caspase 1-mediated cell death in crustacean. *Virology*. (2019) 528:37–47. doi: 10.1016/j.virol.2018.12.004
111. Lu G, Yu Z, Lu M, Liu D, Wang F, Wu Y, et al. The self-activation and LPS binding activity of executioner caspase-1 in oyster *Crassostrea gigas*. *Dev Compar Immunol*. (2017) 77:330–9. doi: 10.1016/j.dci.2017.09.002
112. Narahashi T. Mechanism of tetrodotoxin and saxitoxin action. In: Tiu AT, editor. *Handbook of Natural Toxins. Marine Toxins and Venoms*. Vol. 3. New York, NY: Marcel Dekker Inc. (1988). p. 185–210.
113. Bricelj VM, Shumway SE. Paralytic shellfish toxins in bivalve molluscs: occurrence, transfer kinetics, and biotransformation. *Rev Fish Sci*. (1998) 6:315–83. doi: 10.1080/10641269891314294
114. FAO. Food and Agriculture Organization of the United Nations. *Marine Biotoxins. 2. Paralytic Shellfish Poisoning (PSP)*. Roma: FAO (2004). p. 281.
115. Band-Schmidt CJ, Durán-Riveroll LM, Bustillos-Guzmán JJ, Leyva-Valencia I, López-Cortés DJ, Núñez-Vázquez EJ, et al. Paralytic toxin producing dinoflagellates in latin america: ecology and physiology. *Front Mar Sci*. (2019) 6:42. doi: 10.3389/fmars.2019.00042
116. Shin HH, Li Z, Réveillon D, Rovillon GA, Mertens KN, Hess P, et al. Centrodinium punctatum (Dinophyceae) produces significant levels of saxitoxin and related analogs. *Harmful Algae*. (2020) 100:101923. doi: 10.1016/j.hal.2020.101923
117. Wiese M, D'Agostino PM, Mihali TK, Moffitt MC, Neilan BA. Neurotoxic alkaloids: saxitoxin and its analogs. *Mar Drugs*. (2010) 8:2185–211. doi: 10.3390/md8072185
118. Xiang Z, Qu F, Qi L, Zhang Y, Tong Y, Yu Z. Cloning, characterization and expression analysis of a caspase-8 like gene from the Hong Kong oyster, *Crassostrea hongkongensis*. *Fish Shellfish Immun*. (2013) 35:1797–803. doi: 10.1016/j.fsi.2013.08.026
119. Baden DG, Adams DJ. Brevetoxins: chemistry, mechanism of action, and method of detection. In: Botana LM, editor. *Seafood and Freshwater Toxins: Pharmacology, Physiology and Detection*. New York, NY: Marcel Dekker Incorp. (1983). p. 505–32.
120. Wang DZ. Neurotoxins from marine dinoflagellates: a brief review. *Mar Drugs*. (2008) 6:349–71. doi: 10.3390/md6020349
121. Sayer A, Hu Q, Bourdelais AJ, Baden DG, Gibson JE. The effect of brevenal on brevetoxin-induced DNA damage in human lymphocytes. *Arch Toxicol*. (2005) 79:683–8. doi: 10.1007/s00204-005-0676-2
122. Haystead TAJ, Sim ATR, Carling D, Honnor RC, Tsukitani Y, Cohen P, et al. Effects of the tumour promoter okadaic acid on intracellular protein phosphorylation and metabolism. *Nature*. (1989) 337:78–81. doi: 10.1038/337078a0
123. Van Apeldoorn ME. *Diarrheic Shellfish Poisoning*: A Review. RIVM/CSR Report 05722A00. Netherlands. (1998). p. 47.
124. Fujiki H, Suganuma M. Tumor promotion by inhibitors of protein Z phosphatases 1 and 2A: the okadaic acid class of compounds. *Adv Cancer Res*. (1993) 61:143–94. doi: 10.1016/S0065-230X(08)60958-6
125. Van Egmond HP, Aune T, Lassus P, Speijers G, Waldock M. Paralytic and diarrheic shellfish poisons: occurrence in Europe, toxicity, analysis and regulation. *J Nat Toxins*. (1993) 2:41–83.
126. Nuydens R, De Jong M, Van Den Kieboom G, Heers C, Dispersyn G, Cornelissen F, et al. Okadaic acid-induced apoptosis in neuronal cells: evidence for an abortive mitotic attempt. *J Neurochem*. (2002) 70:1124–33. doi: 10.1046/j.1471-4159.1998.70031124.x
127. Lerga A, Richard C, Delgado MD, Cañelles M, Frade P, Cuadrado MA, et al. Apoptosis and mitotic arrest are two independent effects of the protein phosphatases inhibitor okadaic acid in K562 leukemia cells. *Biochem Bioph Res Co*. (1999) 260:256–64. doi: 10.1006/bbrc.1999.0852
128. Traoré A, Baudrimont I, Ambaliou S, Dano SD, Creppy EE. DNA breaks and cell cycle arrest induced by okadaic acid in Caco-2 cells, a human colonic epithelial cell line. *Arch Toxicol*. (2001) 75:110–7. doi: 10.1007/s002040000188
129. Rami BG, Chin LS, Lazio BE, Singh SK. Okadaic-acid-induced apoptosis in malignant glioma cells. *Neurosurg Focus*. (2003) 14:e4. doi: 10.3171/foc.2003.14.2.5
130. Cabado AGM, Leira F, Vieytes MR, Vieites JM, Botana LM. Cytoskeletal disruption is the key factor that triggers apoptosis in okadaic acid-treated neuroblastoma cells. *Arch Toxicol*. (2004) 78:74–85. doi: 10.1007/s00204-003-0505-4
131. Parameswaran N, Spielman WS, Brooks DP, Nambi P. Okadaic acid stimulates caspase-like activities and induces apoptosis of cultured rat mesangial cells. *Mol Cell Biochem*. (2004) 260:7–11. doi: 10.1023/B:MCBI.0000026041.41078.32
132. Pérez-Gómez A. The marine toxin dinophysistoxin-2 induces differential apoptotic death of rat cerebellar neurons and astrocytes. *Tox Sci*. (2004) 80:74–82. doi: 10.1093/toxsci/kfh139
133. Lago J, Santaclara F, Vieites JM, Cabado AG. Collapse of mitochondrial membrane potential and caspases activation are early events in okadaic acid-treated Caco-2 cells. *Toxicon*. (2005) 46:579–86. doi: 10.1016/j.toxicon.2005.07.007
134. Jayaraj R, Gupta N, Rao PV. Multiple signal transduction pathways in okadaic acid induced apoptosis in HeLa cells. *Toxicology*. (2009) 256:118–27. doi: 10.1016/j.tox.2008.11.013
135. Chen L. Okadaic acid induces apoptosis through the PKR, NF-κB and caspase pathway in human osteoblastic osteosarcoma MG63 cells. *Toxicol Vitro*. (2011) 25:1796–802. doi: 10.1016/j.tiv.2011.09.014
136. Ferron PJ, Hogeveen K, Fessard V, Hégarat L. Comparative analysis of the cytotoxic effects of okadaic acid-group toxins on human intestinal cell lines. *Mar Drugs*. (2014) 12:4616–34. doi: 10.3390/md12084616
137. Romero-Geraldo R, García-Lagunas N, Hernández-Saavedra NY. Effects of *in vitro* exposure to diarrheic toxin producer *Prorocentrum lima* on gene expressions related to cell cycle regulation and immune response in *Crassostrea gigas*. *PLoS ONE*. (2014) 9:e97181. doi: 10.1371/journal.pone.0097181
138. Svensson S, Särngren A, Förlin L. Mussel blood cells, resistant to the cytotoxic effects of okadaic acid, do not express cell membrane p-glycoprotein activity (multixenobiotic resistance). *Aquat Toxicol*. (2003) 65:27–37. doi: 10.1016/S0166-445X(03)00097-3
139. Lamkanfi M, Kanneganti TD, Van Damme P, Vanden Berghe T, Vanoverberghe I, Vandekerckhove J, et al. Targeted peptide centric proteomics reveals caspase-7 as a substrate of the caspase-1 inflammasomes. *Mol Cell Proteomics*. (2008) 7:2350–63. doi: 10.1074/mcp.M800132-MCP200
140. Feldmeyer L, Keller M, Niklaus G, Hohl D, Werner S, Beer HD. The inflammasome mediates UVB-induced activation and secretion of interleukin-1beta by keratinocytes. *Curr Biol*. (2007) 17:1140–5. doi: 10.1016/j.cub.2007.05.074
141. Rossini GP, Sgarbi N, Malaguti C. The toxic responses induced by okadaic acid involve processing of multiple caspase isoforms. *Toxicon*. (2001) 39:763–70. doi: 10.1016/S0041-0101(00)00202-6
142. Gomez-Leon J, Villamil L, Lemos ML, Novoa B, Figueras A. Isolation of *Vibrio alginolyticus* and *Vibrio splendidus* from aquacultured carpet shell clam (*Ruditapes decussatus*) larvae associated with mass mortalities. *Appl Environ Microbiol*. (2005) 71:98–104. doi: 10.1128/AEM.71.1.98-104.2005
143. Travers MA, Boettcher Miller K, Roque A, Friedman CS. Bacterial diseases in marine bivalves. *J Invert Pathol*. (2015) 131:11–31. doi: 10.1016/j.jip.2015.07.010

144. Dubert J, Barja JL, Romalde JL. New insights into pathogenic vibrios affecting bivalves in hatcheries: present and future prospects. *Front Microbiol.* (2017) 8:762. doi: 10.3389/fmicb.2017.00762
145. Ina-Salwany MY, Al-Saari N, Mohamad A, Fathin-Amirah M, Mohd A, Amal MNA, et al. Vibriosis in fish: a review on disease development and prevention. *J Aquat Anim Health*. (2019) 31:3–22. doi: 10.1002/aah.10045
146. Muñoz CA, Amador A, Rodríguez-Jaramillo C, Ochoa N, Hernández J, Ascencio F, et al. *Biochemistry, Pathogenicity and Genome of Vibrio and Other Pathogenic Halophilic Bacteria Associated With Marine Aquaculture in Mexico*. Latin American & Caribbean Aquaculture, Mazatlan (2017).
147. Palacios A. *Expresión de caspasas por efecto de toxinas marinas en hemocitos del ostión del Pacífico, Crassostrea gigas (Thunberg, 1793)* (dissertation/thesis). La Paz, Mexico (2017). p. 80.
148. Lucero A. *Genómica comparativa de bacterias patógenas halófilas aisladas de granjas acuícolas de Baja California Sur* (dissertation/master's thesis). Centro de Investigaciones Biológicas del Noroeste, La Paz, Mexico (2020). p. 144.
149. Huang WB, Ren HL, Gopalakrishnan S, Xu DD, Qiao K, Wang KJ. First molecular cloning of a molluscan caspase from variously colored abalone (*Haliotis diversicolor*) and gene expression analysis with bacterial challenge. *Fish Shellfish Immun*. (2010) 28:587–95. doi: 10.1016/j.fsi.2009.12.016
150. Lee Y, De Zoysa M, Whang I, Lee S, Kim Y, Oh C, et al. Molluscan death effector domain (DED)-containing caspase-8 gene from disk abalone (*Haliotis discus discus*): molecular characterization and expression analysis. *Fish Shellfish Immun.* (2011) 30:480–7. doi: 10.1016/j.fsi.2010.11.014
151. Chávez-Mardones J, Gallardo-Escárate C. Immune response of apoptosis-related cysteine peptidases from the red abalone *Haliotis rufescens* (HrCas8 and HrCas3): molecular characterization and transcription expression. *Fish Shellfish Immun*. (2014) 39:90–8. doi: 10.1016/j.fsi.2014.04.027
152. Scaffidi P, Misteli T, Bianchi ME. Release of chromatin protein HMGB1 by necrotic cells triggers inflammation. *Nature.* (2002) 418:191–5. doi: 10.1038/nature00858
153. Shi Y, Evans JE, Rock KL. Molecular identification of a danger signal that alerts the immune system to dying cells. *Nature.* (2003) 425:516–21. doi: 10.1038/nature01991
154. Los FCO, Randis TM, Aroian RV, Ratner AJ. Role of pore-forming toxins in bacterial infectious diseases. *Microbiol Mol Biol R.* (2013) 77:173–207. doi: 10.1128/MMBR.00052-12
155. Cohen H, Baram N, Edry-Botzer L, Munitz A, Salomon D, Gerlic M. Vibrio pore-forming leukocidin activates pyroptotic cell death via the NLRP3 inflammasome. *Emerg Microbes Infect*. (2020) 9:278–90. doi: 10.1080/22221751.2020.1720526
156. Bossaller L, Chiang PI, Schmidt-Lauber C, Ganesan S, Kaiser WJ, Rathinam VA, et al. Cutting edge: FAS (CD95) mediates noncanonical IL-1beta and IL-18 maturation via caspase-8 in an RIP3-independent manner. *J Immunol.* (2012) 189:5508–12. doi: 10.4049/jimmunol.1202121
157. Gurung P, Malireddi RK, Anand PK, Demon D, Vande Walle L, Liu Z, et al. Toll or interleukin-1 receptor (TIR) domain-containing adaptor inducing interferon-b (TRIF)-mediated caspase-11 protease production integrates Toll-like receptor 4 (TLR4) protein- and Nlrp3 inflammasome-mediated host defense against enteropathogens. *J Biol Chem.* (2012) 287:34474–83. doi: 10.1074/jbc.M112.401406
158. Antonopoulos C, El Sanadi C, Kaiser WJ, Mocarski ES, Dubyak GR. Proapoptotic chemotherapeutic drugs induce noncanonical processing and release of IL-1beta via caspase-8 in dendritic cells. *J Immunol.* (2013) 191:4789–803. doi: 10.4049/jimmunol.1300645
159. Man SM, Tourlomousis P, Hopkins L, Monie TP, Fitzgerald KA, Bryant CE. Salmonella infection induces recruitment of caspase-8 to the inflammasome to modulate IL-1b production. *J Immunol.* (2013) 191:5239–46. doi: 10.4049/jimmunol.1301581
160. Gurung P, Anand PK, Malireddi RK, Vande Walle L, Van Opdenbosch N, Dillon CP, et al. FADD and caspase-8 mediate priming and activation of the canonical and noncanonical Nlrp3 inflammasomes. *J Immunol.* (2014) 192:1835–46. doi: 10.4049/jimmunol.1302839
161. Philip NH, Dillon CP, Snyder AG, Fitzgerald P, Wynosky-Dolfi MA, Zwack EE, et al. Caspase-8 mediates caspase-1 processing and innate immune defense in response to bacterial blockade of NF- B and MAPK signaling. *PNAS.* (2014) 111:7385–90. doi: 10.1073/pnas.1403252111
162. Shenderov K, Riteau N, Yip R, Mayer-Barber KD, Oland S, Hieny S, et al. Cutting edge: endoplasmic reticulum stress licenses macrophages to produce mature IL-1beta in response to TLR4 stimulation through a caspase-8- and TRIF-dependent pathway. *J Immunol.* (2014) 192:2029–33. doi: 10.4049/jimmunol.1302549
163. Gurung P, Kanneganti TD. Novel roles for caspase-8 in IL-1β and inflammasome regulation. *Am J Pathol.* (2015) 185:17–25. doi: 10.1016/j.ajpath.2014.08.025
164. Gurcel L, Abrami L, Girardin S, Tschopp J, van der Goot FG. Caspase-1 activation of lipid metabolic pathways in response to bacterial pore-forming toxins promotes cell survival. *Cell.* (2006) 126:1135–45. doi: 10.1016/j.cell.2006.07.033

Conflict of Interest: The authors declare that the research was conducted in the absence of any commercial or financial relationships that could be construed as a potential conflict of interest.

frontiers in Immunology

ORIGINAL RESEARCH
published: 09 April 2021
doi: 10.3389/fimmu.2021.661823

A New C-Type Lectin Homolog SpCTL6 Exerting Immunoprotective Effect and Regulatory Role in Mud Crab *Scylla paramamosain*

Wanlei Qiu[1], *Fangyi Chen*[1,2,3*], *Roushi Chen*[1], *Shuang Li*[1], *Xuewu Zhu*[1], *Ming Xiong*[1,2,3] *and Ke-Jian Wang*[1,2,3]

[1] State Key Laboratory of Marine Environmental Science, College of Ocean & Earth Sciences, Xiamen University, Xiamen, China, [2] State-Province Joint Engineering Laboratory of Marine Bioproducts and Technology, College of Ocean & Earth Sciences, Xiamen University, Xiamen, China, [3] Fujian Innovation Research Institute for Marine Biological Antimicrobial Peptide Industrial Technology, College of Ocean & Earth Sciences, Xiamen University, Xiamen, China

OPEN ACCESS

Edited by:
Chaozheng Li,
Sun Yat-Sen University, China

Reviewed by:
WeiWei Li,
East China Normal University, China
Jing Xing,
Ocean University of China, China

***Correspondence:**
Fangyi Chen
chenfangyi@xmu.edu.cn

Specialty section:
This article was submitted to Comparative Immunology, a section of the journal Frontiers in Immunology

Received: *31 January 2021*
Accepted: *16 March 2021*
Published: *09 April 2021*

Citation:
Qiu W, Chen F, Chen R, Li S, Zhu X, Xiong M and Wang K-J (2021) A New C-Type Lectin Homolog SpCTL6 Exerting Immunoprotective Effect and Regulatory Role in Mud Crab Scylla paramamosain. Front. Immunol. 12:661823. doi: 10.3389/fimmu.2021.661823

C-type lectin (CTL), a well-known immune-related molecule, has received more and more attention due to its diverse functions, especially its important role in development and host defense of vertebrate and invertebrate. Since the research on crab CTLs is still lack, we screened a new CTL homolog, named SpCTL6 from mud crab *Scylla paramamosain*. The full-length cDNA sequence of SpCTL6 was 738 bp with a 486 bp of ORF, and the deduced amino acids were 161 aa. SpCTL6 was predicted to have a 17 aa signal peptide and its mature peptide was 144 aa (MW 16.7 kDa) with pI value of 5.22. It had typical CTL structural characteristics, such as a single C-type lectin-like domain, 4 conserved cysteines, similar tertiary structure to that of vertebrate CTLs and a mutated Ca^{2+} binding motif Gln-Pro-Thr (QPT), clustering into the same branch as the crustacean CTLs. SpCTL6 was highly expressed in the entire zoeal larval stages and widely distributed in adult crab tissues with the highest transcription level in testis. During the molting process of juvenile crabs, the expression level of SpCTL6 was remarkably increased after molting. SpCTL6 could be significantly upregulated in two larval stages (Z1 and megalopa) and adult crab testis under immune challenges. Recombinant SpCTL6 (rSpCTL6) was successfully obtained from eukaryotic expression system. rSpCTL6 exhibited binding activity with PAMPs (LPS, lipoteichoic acid, peptidoglycan, and glucan) and had a broad spectrum bacterial agglutination activity in a Ca^{2+}-dependent manner. In addition, rSpCTL6 could enhance the encapsulation activity of hemocytes and has no cytotoxic effect on hemocytes. Although rSpCTL6 had no bactericidal activity on *Vibrio alginolyticus*, rSpCTL6 treatment could significantly reduce the bacterial endotoxin level *in vitro* and greatly improved the survival of *S. paramamosain* under *V. alginolyticus* infection *in vivo*. The immunoprotective effect of rSpCTL6 might be due to the regulatory role of rSpCTL6 in immune-related genes and immunological parameters. Our study

provides new information for understanding the immune defense of mud crabs and would facilitate the development of effective strategies for mud crab aquaculture disease control.

Keywords: C-type lectin, SpCTL6, development, immunoprotective effect, regulatory role

INTRODUCTION

Mud crabs, *Scylla paramamosain*, due to their deliciousness, rich nutrition and high commodity value, have become an important global economic fishery species, which are mainly distributed in the Western Indo-Pacific (1). The capture fishery of mud crabs has been unable to meet the market demand, and the mud crab aquaculture industry has emerged and developed rapidly (2, 3). In 2018, the aquaculture production of mud crabs in China (157,712 tons) far exceeded that of the captured ones (79,444 tons), making it the most productive crab among marine aquaculture crabs in China (4). Although the total production of mud crabs has increased significantly in recent years, the artificial breeding technology of mud crab seedlings is still one of the main scientific and technological problems that have not been solved yet. High mortality occurs frequently during the developmental stage, especially the metamorphosis stage of the larvae [the survival rate was only about 10% from hatching to first-stage crabs (5)], the molting stage of juvenile crabs, and the reproductive molting process, which is closely related to the vulnerability of *S. paramamosain* to pathogens in these processes (6–8). In the past few decades, the research on mud crab immune system has made considerable progress, and many efforts have been made to encourage the development of mud crab aquaculture, such as the use of probiotics, immune-stimulants, and natural products, as reviewed in-depth previously (6). However, these strategies are limited, and we are still far away from understanding the molecular mechanisms of mud crab immunity.

C-type lectin (CTL), a well-known immune-related molecule, has received more and more attention due to its diverse functions, especially its important role in development and host defense of vertebrate and invertebrate (9, 10). Having at least one CTL-like domain (CTLD) is an indispensable feature of the CTLs superfamily (11). Most reported CTLs showed Ca^{2+}-dependent carbohydrate binding activity and were considered as pattern recognition receptors (PRRs), with a few exceptions (9). Since the first CTL was discovered in bovine in 1906, more than a thousand CTL members have been identified in Metazoa, with dozens or even hundreds of CTL homologous genes in their genomes (10, 12). In vertebrate, these highly diverse CTLs have been demonstrated to play an important role in the regulation of innate and adaptive immunity, through non-self-recognizing or mediating intercellular communication and interaction, and could act as effector molecules exhibiting directly antibacterial activity (9, 13, 14). And CTLs with single CTLD in invertebrate are also well-studied, with insects and crustaceans as representatives (10). Similarly, the immune function of CTLs in invertebrates is evolutionarily conserved. They participate in both cellular and humoral immunity of invertebrates, such as promoting hemocyte phagocytosis, mediating hemocyte encapsulation, nodule formation, activating the phenol oxidase (PO) system and ultimately leading to melanization, direct bactericidal activity, regulating immune signal transduction pathways and the expression of immune effectors etc., as summarized in detail previously (10, 15, 16).

Currently, several crustacean genomes have been sequenced and assembled, such as the Pacific white shrimp *Litopenaeus vannamei* (17), the marbled crayfish *Procambarus virginalis* (18), the Chinese mitten crab *Eriocheir sinensis* (19), and the swimming crab *Portunus trituberculatus* (20), which would greatly facilitate the research on crustacean CTLs. So far, more than 90 crustacean CTLs have been reported. Among them, significant progress has been made in the study of shrimp CTLs, whose immune-related functions, molecular mechanisms involved in host-virus (WSSV) interactions, and the expression regulatory mechanism have been thoroughly discussed, providing a valuable reference for the research on other crustacean CTLs (15, 16). In crabs, numerous studies in CTLs have also been conducted, such as the *E. sinensis* CTLs (21–26), and the *P. trituberculatus* CTLs (27–30).

For the mud crab *S. paramamosain*, a total of six CTLs (SpCTLs) have been reported, including SpLec1 and SpLec2 (31), Sp-lectin3 and Sp-lectin4 (32), SpCTL-B (33), SpCTL5 (34). Analysis of SpCTLs coding sequences showed that they all contained only one CTLD, and four of them had signal peptides (SpLec1, SpLec2, Sp-lectin3 and Sp-lectin4), which is common in most crustacean CTLs. Conserved carbohydrate recognition motifs have also been found in SpCTLs, such as QPD (Gln-Pro-Asp) in Sp-lectin4 (32), EPD (Glu-Pro-Asp) in SpCTL-B (33). All SpCTLs were predominantly distributed in the hepatopancreas of adult mud crabs, which is an important immune organ. Among them, SpLec1 and SpLec2, Splectin3 and Sp-lectin4 were also distributed in the embryo and larval stage of crabs, indicating that they might play an important role in the development of crabs. Immune stimulations [such as *Vibrio parahaemolyticus*, *Vibrio alginolyticus*, LPS, Poly (I:C)] could significantly induce the expression of SpCTLs. Recombinant SpCTL protein expression was only performed in SpCTL-B (rSpCTL-B) and SpCTL5 (rSpCTL5) using prokaryotic expression system. *In vitro* functional studies showed that both rSpCTL-B and rSp-CTL5 showed bacterial agglutination activity in a Ca^{2+}-dependent manner, while only rSpCTL-B exhibited potent antibacterial activity. When the expression of SpCTL-B was inhibited by RNAi, the bacterial load in hemocytes increased significantly, and several immune-related genes [including SpSTAT and five antimicrobial peptides (AMPs)] were down-regulated, indicating its role in the immune response and regulation (33). Although some progress has been made in *S. paramamosain* CTLs, the functions and molecular mechanisms

of SpCTLs are still largely unknown. Therefore, more SpCTLs are expected to be screened and more in-depth studies are needed.

In this study, a new CTL homolog, named SpCTL6 was identified from mud crab *S. paramamosain*. The full-length cDNA sequence was obtained. The expression profiles of SpCTL6 gene was analyzed by absolute quantitative PCR (qPCR) and relative qPCR. The recombinant protein (rSpCTL6) was expressed in *Pichia pastoris* eukaryotic expression system and purified by affinity chromatography. The binding, hemagglutination, agglutination, and encapsulation activity analysis of rSpCTL6 were performed *in vitro*. In addition, the cytotoxicity and the endotoxin level of *V. alginolyticus* after rSpCTL6 treatment were determined. The immunoprotective effect and the regulatory role of rSpCTL6 in *S. paramamosain* challenged with *V. alginolyticus* were evaluated through analyzing the survival rate of crabs, the bacterial clearance ability in gills and hepatopancreas, the expression of immune-related genes and the enzymatic activity of immunological parameters including phenol oxidase (PO), lysozyme (LZM), peroxidase (POD), superoxide dismutase (SOD), alkaline phosphatase (AKP), and acid phosphatase (ACP). This study aims to enrich the knowledge of crab CTLs through in-depth study of its function, immune protective effect and related mechanism, providing important information for understanding the immune defense of mud crabs and facilitating the development of effective strategies for mud crab aquaculture disease control.

MATERIALS AND METHODS

Animals, Sample Collection and Immune Challenge

Adult male and female mud crabs (*S. paramamosain*) weighing about 300 ± 30 g were purchased from a crab farm in Zhangzhou City, Fujian Province, China. The hemocytes were prepared as previously described (35). Multiple tissues of crabs (n=5) were sampled (including gills, hepatopancreas, midgut, eyestalks, subcuticular epidermis, heart, muscle, stomach, thoracic ganglion, female crab gonadal tissues (ovaries, spermatheca, and reproductive duct) and male crab gonadal tissues (testis, anterior vas deferens, seminal vesicle, posterior vas deferens, ejaculation ducts, posterior ejaculation ducts) and ready for total RNA extraction. The various stages of crab development, including embryonic stages (Em1-Em5), zoeal larval stages (Z1-Z5), megalopa stage, three juvenile stages (JU1, JU2, and JU3), the molting process of juvenile crabs including premolt and postmolt samples (JU1 developed to JU2, JU2 developed to JU3) (n=5) were collected from a crab breeding farm in Beihai City, Guangxi Province, China. The different larval stages have their unique features, which can be easily identified as described in detail previously (36, 37).

Two larval stages (Z1 larvae and megalopa) were selected for immune challenge experiments. Thousands of Z1 larvae or megalopa were randomly divided into 6 petri dishes (1.5 L), and 700 mL of sterilized sea water was added. The experiment included three different groups: the control group (sea water), the bacterial infection group (5×10^6 colony-forming units (CFU)/mL *V. alginolyticus*), and the LPS stimulation group [200 ng/mL LPS (Sigma, USA)]. The larvae were sampled at 3 h, 6 h, 9 h, 12 h, and 24 h after challenge. Five biological parallel samples (n=5) were set up at each time point (each parallel sample contained dozens of larvae). They were immediately put into liquid nitrogen and then stored at -80°C for later use.

The purchased adult male crabs (300 ± 30 g) were acclimated at 23 ± 2 °C for several days before the challenge experiment. Ninety crabs were randomly divided into three groups (30 crabs for each group), including the control group, the *V. alginolyticus* infection group (3×10^6 CFU/crab), and the LPS stimulation group (0.5 mg/kg·crab). For the control group, 100 μL of crab saline (4.96 mM NaCl, 9.52 mM KCl, 0.8 mM $MgSO_4$, 16.2 mM $CaCl_2$, 0.84 mM $MgCl_2$, 5.95 mM $NaHCO_3$, 20 mM HEPES, pH 7.4) was injected. Testis (n=5) were sampled in each group at 3, 6, 12, 24, 48 and 72 h post-injection (hpi) and then stored in -80 °C for later use.

Total RNA of the collected samples were extracted using Trizol reagent (Thermo Fisher Scientific, USA) according to the manufacturer's instructions. RNA quality was evaluated by NanoDrop 2000 spectrophotometer (Thermo Fisher Scientific, USA), and PrimeScript™ RT reagent kit with gDNA eraser (TaKaRa, Japan) was used for cDNA synthesis.

Cloning of the Full-Length cDNA Sequence of SpCTL6

The cDNA of adult male crab testis was synthesized as described above. The 5′ and 3′ RACE cDNA were prepared using SMARTer® RACE 5′/3′ Kit (Clontech, USA). The coding sequence (CDS) of SpCTL6 was obtained from the transcriptome database established by our laboratory. A pair of primers (SpCTL6-CDS-F and SpCTL6-CDS-R, as shown in **Table 1**) were designed to amplify SpCTL6 CDS and testis cDNA was used as a template. The PCR was carried out as follows: 95°C, 5 min; 30 cycles of 95°C, 30 s, 62°C, 30 s, 72°C 1 min; 72°C for 5 minute. And primers (SpCTL6-5-R1, SpCTL6-5-R2, SpCTL6-3-F1, SpCTL6-3-F2, as shown in **Table 1**) were synthesized to amplify the 5′ and 3′ cDNA ends of SpCTL6 using nested PCR and touchdown PCR. The first round of PCR used pairs of primers (SpCTL6-5-R1/Long primer for 5′ RACE PCR, SpCTL6-3-F1/Long primer for 3′ RACE PCR) and the second round of PCR used SpCTL6-5-R2/Short primer for 5′ RACE PCR, SpCTL6-3-F2/Short primer for 3′ RACE PCR, respectively. The Long primer and Short primer were provided by SMARTer® RACE 5′/3′ Kit. The touch down PCR procedure was performed as followed: 95°C, 5 min; 30 cycles of 95°C, 30 s, 68°C -0.5/cycle, 30 s, 72°C, 2 min; 72°C, 10 min; 16°C 5 min. The PCR products were then purified and sequenced by Sangon Biotech (Shanghai) Co., Ltd.

Bioinformatics and Phylogenetic Analysis of SpCTL6

The homology of the SpCTL6 gene sequence with other sequences was analyzed by the basic local alignment search

TABLE 1 | Sequences of primers used in this study.

Primer name	Primer sequences (5′-3′)
SpCTL6-CDS-F	ATGCTGCGCGTGTACTGCCTCCTCC
SpCTL6-CDS-R	TCAGAAGGCGTGGACCTCGTTCTGA
SpCTL6-5-R1	AGCCACGTGGTTGTAATCGAA
SpCTL6-5-R2	AAGCACATGTAGTTGAGCACG
SpCTL6-3-F1	TTGACGACCGTGCCCTTAG
SpCTL6-3-F2	GCCCTTAGCCCCAACTCTATT
Long primer	CTAATACGACTCACTATAGGGCAAGCA GTGGTATCAACGCAGAGT
Short primer	CTAATACGACTCACTATAGGGC
SpCTL6-qPCR-F	ACGACGCCTCCTGGTTTTGG
SpCTL6-qPCR-R	GGCGTGGACCTCGTTCTGAC
SpSOD-F	GGGGATGGGAAACAACTCTGGAT
SpSOD-R	GGTGCCTTGGTTAAATACACGGTGC
SpALF6-F	TCAAGGGAGACGTGTGGTGC
SpALF6-R	TGGCGAAGTCTGCGATAGCC
SpCrustin3-F	ACCTGCCTGGCCATTACGTG
SpCrustin3-R	CCCACCACAGGGAGTGTTGC
GADPH-qPCR-F	CTCCACTGGTGCCGCTAAGGCTGTA
GADPH-qPCR-R	CAAGTCAGGTCAACCACGGACACAT
rSpCTL6-*EcoR*I-F	CGGAATTCGCGTGCCCTGCCCCCTTTGT
rSpCTL6-*Not*I-R	ATAAGAATGCGGCCGCTCA**GTGGTGGTG GTGGTGGTG**GAAGGCGTGGACCTCGTTC

tool (BLAST) of NCBI (http://www.ncbi.nlm.nih.gov/blast). The signal peptide and conserved domain of SpCTL6 were predicted by SignalP 4.1 Server (http://www.cbs.dtu.dk/services/SignalP/) and SMART database (http://smart.embl-heidelberg.de/), respectively. Expasy (http://web.expasy.org/protparam) was used to calculate the theoretical molecular weight (MW) and isoelectric point (pI) of SpCTL6. The secondary and tertiary structures of SpCTL6 were predicted by UCL (http://bioinf.cs.ucl.ac.uk/psipred/) and SWISS-MODEL (https://swissmodel.expasy.org/), respectively. Multiple sequence alignment between SpCTL6 and other CTLs was performed using Clustal X 2.1 software. The phylogenetic tree was constructed using the neighbor joining method of MEGA 6.0, and the reliability was evaluated by 1000 bootstraps.

Quantitative Real-Time PCR Analysis of the Expression Profiles of SpCTL6

The expression profiles of SpCTL6 gene in various adult crab tissues and different developmental stages were determined by absolute quantitative real-time PCR (qPCR) and the expression changes of SpCTL6 during the molting stages of juvenile crabs and the response patterns of SpCTL6 gene to LPS and *V. alginolyticus* challenge were analyzed by relative qPCR. GAPDH gene of *S. paramamosain* (GenBank accession number: JX268543.1) was employed as the internal reference gene in relative qPCR assay. Gene-specific primers (SpCTL6-qPCR-F/SpCTL6-qPCR-R, GADPH-qPCR-F/GADPH-qPCR-R, listed in **Table 1**) were designed. The SpCTL6 CDS plasmid was used to generate its standard curve. qPCR was performed on Qtower 2.2 (Analytik Jena, Germany) as followed: 50 °C for 2 min, 95 °C for 10 min, 40 cycles of 95 °C for 15 s, 60 °C for 1 min. The absolute copy numbers of SpCTL6 gene were calculated according to the linear regression of the standard curve. The data for relative qPCR was analyzed using the algorithm of the $2^{-\Delta\Delta Ct}$ method (38).

Expression and Purification of Recombinant SpCTL6 (rSpCTL6) in *Pichia Pastoris* Eukaryotic Expression System

The mature peptide sequence of SpCTL6 was constructed into the pPIC9K vector using primers rSpCTL6-*EcoR*I-F/rSpCTL6-*Not*I-R (as shown in **Table 1**). The recombinant plasmid was linearized by restriction enzyme *Sac* I, and then transformed into competent *P. pastoris* cells by electroporation. A positive clone was picked and cultured to logarithmic growth phase at 28 °C in YPD medium (2% tryptone, 1% yeast extract, 2% D-glucose). Then the medium was replaced with BMGY medium (10 g yeast extract, 20 g tryptone were dissolved in 700mL water, autoclaved for 20 min, cooled to room temperature, and the following mixture were added: 100 mL 1 M potassium phosphate buffer (pH 6.0), 100 mL 10 YNB, 100 mL10% glycerine, 2 mL 500×biotin) until it cultured to logarithmic then *P. pastoris* cells were induced by 0.5% methanol in BMMY (dissolve 10 g yeast extract, 20 g tryptone in 700 mL water, autoclaviate for 20 min, cool to room temperature, add the following mixture: 100 mL 1 M potassium phosphate buffer (pH 6.0), 100 mL 10 YNB, 100 mL10% methanol, 2 mL 500×biotin). After 24 hours of induction, the supernatant was collected and dialyzed against buffer (50 mM phosphate buffer, 50 mM NaCl, pH 9.0). The target protein was purified by ÄKTA Pure system (GE Healthcare Life Sciences, USA) using a HisTrap™ FF Crude column (GE Healthcare Life Sciences, USA). The purity of rSpCTL6 was analyzed by SDS-PAGE, and the sequence was confirmed by the Mass Spectrometry Center of the School of Life Sciences, Xiamen University. The protein concentration was determined by Bradford assay kit (Beyotime Institute of Biotechnology, China). All recombinant protein rSpCTL6 were stored at -80°C for later use.

Hemagglutination, Bacterial Agglutination, Binding, and Encapsulation Assay

Hemagglutination Assay

The blood of mouse was collected in a centrifuge tube containing sodium citrate. After washing 3 times with TBS buffer, the blood was re-suspended in TBS buffer at a concentration of 2% (v/v), and then transferred to a 96-well type V hemagglutination plate. Four groups were set up (rSpCTL6 with or without 10 mM $CaCl_2$ groups, TBS with 10 mM $CaCl_2$ group, and BSA with10 mM $CaCl_2$ group). rSpCTL6 was added at a series of dilution concentrations (from 0.75 μg/mL to 100 μg/mL). An equal volume of BSA (100 μg/mL) and TBS with 10 mM $CaCl_2$ were added as control groups. Hemagglutination was observed after incubation at 4°C for 1 h. Each group had three biological parallels. The independent experiment was repeated at least three times.

Bacterial Agglutination Assay

Gram-positive bacteria (*Staphylococcus aureus*), and Gram-negative bacteria (*Pseudomonas aeruginosa*, *Pseudomonas fluorescens*, *Aeromonas hydrophila*, *Vibrio harveyi*, *Vibrio fluvialis*, *V. parahaemolyticus*, and *V. alginolyticus*) were selected to investigate the agglutination activity of rSpCTL6. All the bacteria were cultured to the logarithmic growth phase,

washed 3 times with TBS, and re-suspended in 0.1 M $NaHCO_3$ (pH 9.0). They were then incubated with a final concentration of 0.1 mg/mL FITC (Sigma, USA) for 30 min at room temperature, and washed 3 times with TBS to remove unlabeled FITC. The concentration of the bacteria was adjusted to 10^8 CFU/mL. Four groups were set up (rSpCTL6 with or without 10 mM $CaCl_2$ groups, TBS with 10 mM $CaCl_2$ group, and BSA with10 mM $CaCl_2$ group). The FITC-labeled bacteria were incubated with 10 μL of rSpCTL6 (40 μg/mL) at room temperature in the dark for 1 h. An equal volume of BSA (40 μg/mL) and TBS with 10 mM $CaCl_2$ were added as control groups. The agglutination results were observed with an inverted fluorescence microscope (Zeiss, Germany). Each group had three biological parallels. The independent experiment was repeated at least three times.

Binding Assay

A modified enzyme-linked immune sorbent assay (ELISA) was carried out as previously described (39). Briefly, LPS, peptidoglycan (PGN), lipoteichoic acid (LTA) and glucan (GLU) were diluted with an ELISA coating solution to a working concentration of 20 μg/mL, and then added to a 96-well ELISA plate. The plate was coated overnight at 4°C, blocked with 5% skim milk at 37°C for 2 h, and then added with a series dilution of rSpCTL6 (0~100 μg/mL) at 37°C for 2 h. There were 3 parallels for each concentration of protein. Mouse anti-His antibody (1:5000, prepared in 1% skim milk) was added and incubated at 37 °C for 2 h followed by incubation with goat anti-mouse HRP antibody (1:5000). TMB solution was added and incubated at 37 °C for 10-30 min. The reaction was stopped with 2 M H_2SO_4. The absorbance at 450 nm was measured using a microplate reader (TECAN GENios, GMI, USA). Each group had three biological parallels. The independent experiment was repeated at least three times.

Encapsulation Assay

In order to evaluate the encapsulation activity of rSpCTL6, the Ni-NTA agarose beads [Senhui Microsphere Technology (Suzhou) Co., Ltd, China] was used. Four groups were also set up (rSpCTL6 with or without 10 mM $CaCl_2$ groups, TBS with 10 mM $CaCl_2$ group, and BSA with10 mM $CaCl_2$ group). The beads were first equilibrated in TBS, then incubated with different amounts of rSpCTL6 (25 μg-200 μg) at 4 °C overnight, and washed with TBS 3 times. A 24-well culture plate was pre-coated with 1% agarose. The hemocytes were isolated from *S. paramamosain* as previously described (35), and added to the plate for at least 10 min to allow them settle down. The beads containing proteins were then added and incubated at 26 °C. Encapsulation was detected after 6 and 24 h under a light microscope (LEICA DMi1, Germany). Each group had three biological parallels. The independent experiment was repeated at least three times.

V. Alginolyticus Endotoxin Assay

The endotoxin level of *V. alginolyticus* was detected by the Toxin Sensor™ Chromogenic LAL Endotoxin Assay Kit (GenScript, USA) following the manufacturer's instructions. *V. alginolyticus* was collected when reaching to the logarithmic growth phase and adjusted to a concentration of 10^7 CFU/mL. They were then incubated with different concentration of rSpCTL6 (10.5, 21, 42, 84 μM) at room temperature for 1 h and analyzed by a spectrophotometer at an absorbance of 545 nm (Agilent Technologies. Malaysia). Each concentration of rSpCTL6 treatment had three biological parallels. The independent experiment was repeated at least three times.

Cytotoxicity Assay

The hemocytes of adult crabs were primarily cultured as previously described (40, 41). About 1×10^5 cells/well were inoculated on a 96-well cell culture plate at 26 °C and cultured overnight. Different concentration of rSpCTL6 (3 μM, 6 μM, 12 μM, 24 μM, 48 μM) were added. After 24 h of incubation, the CellTiter 96® AQueous Kit (Promega) was used to evaluate the viability of hemocytes. Each concentration of rSpCTL6 treatment had three biological parallels. The independent experiment was repeated at least three times.

Effect of rSpCTL6 on Mud Crab *S. Paramamosain* Infected by *V. Alginolyticus*

Mortality Test

To investigate whether rSpCTL6 has an immunoprotective effect on *S. paramamosain*, a bacterial challenge experiments was performed in male mud crabs (100 ± 10 g). *V. alginolyticus* (2×10^7 CFU $crab^{-1}$) were first injected into the base of the right fourth leg of the crabs (n=105). After bacterial injection, 105 crabs were randomly divided into three groups (n=35) (control group, 10 μg $crab^{-1}$ rSpCTL6 treatment group and 20 μg $crab^{-1}$ rSpCTL6 treatment group). Two hours later, rSpCTL6 (10 μg $crab^{-1}$ or 20 μg $crab^{-1}$) was injected, and an equal volume of the crab saline was injected as the control group. Survival crabs were recorded at different time point (3 h, 6 h, 9 h, 24 h, 36 h, 48 h, 60 h, 72 h, 96 h, 120 h), and a mortality curve was drawn by GraphPad Prism 8.3.0 version. The independent experiment was repeated twice.

Bacterial Load Assay

The bacterial load in two crab tissues (gills and hepatopancreas) of different groups (control group and 20 μg $crab^{-1}$ rSpCTL6 treatment group) was determined at selected time points after treatment (3 h, 6 h, and 24 h). Briefly, gills and hepatopancreas (n=3) were sampled from experimental crabs (treated with crab saline or 20 μg $crab^{-1}$ rSpCTL6 after 2 h of bacterial injection), and approximately 100 mg of each tissue was homogenized in 1 mL of PBS solution, then diluted to an appropriate concentration, and spread on an agar plate [containing 2216E cultured medium (Qingdao Hope Bio Tech., China)], and cultured at 28 °C overnight. The bacterial CFU of all plates were counted and recorded. Each sample had three biological parallels and three different dilutions.

Enzymatic Activity Assay

The gills and hepatopancreas were sampled (n=3) and homogenized as described above and various enzymatic activity assays were performed according to the manufacturer's instructions of the corresponding protease detection kits

[including PO, lysozyme (LZM), peroxidase (POD), superoxide dismutase (SOD), alkaline phosphatase (AKP), acid phosphatase (ACP) assays (Nanjing Jiancheng, China)].

Immune-Related Genes Expression Analysis

Several immune-related genes were selected to study their expression pattern after treatment (including signaling pathway genes (*Sp*Toll2, Relish, *Sp*Dorsal, STAT), AMPs [*Sp*Crustin3, *Sp*Crustin5, *Sp*ALF2, *Sp*ALF6), cytokine gene (LITAF), antioxidant gene (*Sp*SOD)]. The specific primers and genbank accession numbers for these genes were summarized in **Tables 1** and **S1**. Relative qPCR was performed as described above.

Statistical Analysis

GraphPad Prism 8.0 Software was applied for analyzing relative qPCR assay and enzymatic activity assay using multiple t test - one per row. The mortality curve was drawn by GraphPad Prism 8.0 Software and analyzed using the Kaplan-Meier Log rank test. Difference was considered as significant at $p < 0.05$. All data were displayed as mean ± standard deviation (SD).

RESULTS

Sequence and Structure Analysis of SpCTL6

The full-length cDNA sequence of SpCTL6 was 738 bp with a 486 bp of ORF, and the deduced amino acids was 161 aa (**Figure 1A**). SpCTL6 was predicted to have a 17 aa signal peptide and its mature peptide was 144 aa (MW 16.7 kDa) with pI value of 5.22, which contained a conserved CTLD (**Figures 1A, B**). Its tertiary structures were predicted, which has a double-loop structure, 2 α-helices and 5 β-sheets (**Figure 1C**). The phylogenetic analysis showed that SpCTL6 was clustered into the same branch as the crustacean CTLs (**Figure 1D**). Multiple sequences alignment analysis showed that it has 4 conserved cysteines and a Gln-Pro-Thr (QPT) motif (**Figure 1E**).

The Expression Profiles of SpCTL6

Based on qPCR analysis, SpCTL6 mRNA was at a relatively low level in the embryonic stage (Em1-Em4) of *S. paramamosain*. Its copy numbers gradually increased from the Em5 stage, reached the highest levels in the Z1 stage (about 1×10^6 copies/μL), maintained a high level (over 0.7×10^6 copies/μL) throughout the zoea larval stage, and then gradually reduced from the megalopa stage to juvenile crabs (**Figure 2A**). During the molting process of juvenile crabs, the expression of SpCTL6 was significantly upregulated after molting (JU1 developed to JU2, and JU2 developed to JU3) (**Figure 2B**). As reported, high mortality occurs frequently during the developmental stages, especially the metamorphosis stage of the larvae (5). Among them, Z1 is the larvae that has just hatched from embryo, and megalopa is the last larval stage undergoing metamorphosis from zoeal stage, which are two important metamorphosis stages. Therefore, we chose these two stages as representatives to investigate the immune response of SpCTL6 in the larval stages. After LPS stimulation, in the Z1 stage of *S. paramamosain*, SpCTL6 was significantly down-regulated at 3 h and up-regulated at 24 h, while the expression of SpCTL6 did not show any change under the challenge of *V. alginolyticus* (**Figures 2C, E**). In the megalopa stage, the transcription level of SpCTL6 mRNA was remarkably increased at 12 h after LPS or bacterial challenge (**Figures 2D, F**).

The absolute qPCR results also showed that SpCTL6 was widely distributed in various tissues of male and female adult crabs, with the highest expression level in the testis of male adult crabs (**Figures 3A, B**). When adult male crabs were injected with LPS or *V. alginolyticus*, the expression of SpCTL6 was significantly down-regulated at 3 h and up-regulated at 72 h after LPS stimulation, and up-regulated at 3 h after bacterial challenge (**Figures 3C, D**).

Recombinant SpCTL6 (rSpCTL6) Obtained From *P. pastoris* Eukaryotic Expression System

We successfully obtained recombinant SpCTL6 (rSpCTL6) from the *P. pastoris* eukaryotic expression system. SDS-PAGE analysis showed that a specific positive band appeared at a position slightly larger than the 15 kDa marker, corresponding to the predicted mature peptide size (16.7 kDa), and the purity of rSpCTL6 was high as shown in **Figure 4A**. In addition, the results from the mass spectrometry also confirmed that the purified protein was the target protein rSpCTL6 (**Figure S1**).

rSpCTL6 Showed Hemagglutination, Bacterial Agglutination, Binding, and Encapsulation Activity *In Vitro*

For the type V hemagglutination plate used in hemagglutination assay, if the erythrocytes are observed to settle at the bottom of the plate, it indicates that the reaction is negative, that is, the erythrocytes have not agglutinated. The results showed that in the presence of 10 mM Ca^{2+}, rSpCTL6 at a low concentration of 12.5 μg/mL could cause significant agglutination of mouse erythrocytes, not to mention higher concentrations (25, 50, and 100 μg/mL) (**Figure 4B**). In the 0 mM Ca^{2+} group and the control group, obvious sedimentation of erythrocytes was observed (**Figure 4B**). Therefore, the hemagglutination activity of rSpCTL6 was Ca^{2+} dependent. Similarly, rSpCTL6 could agglutinate all the selected bacteria (including several Vibrio species commonly found in aquaculture) in a Ca^{2+}-dependent manner (**Figure 4D**). While the control groups (TBS and BSA) and rSpCTL6 without $CaCl_2$ group could not induce agglutination of tested bacteria.

As shown in **Figure 4C**, rSpCTL6 had binding affinity to several tested microbial surface molecules (LPS, LTA, PGN, and GLU). The calculated apparent dissociation constants (Kd) were 1.876 μM for LTA, 2.160 μM for LPS, 2.804 μM for PGN, 2.957 μM for GLU, respectively, which indicated that rSpCTL6 had the highest binding affinity for LTA.

rSpCTL6 pre-coated with Ni-NTA agarose beads was used to perform the encapsulation assay *in vitro*. The results showed that

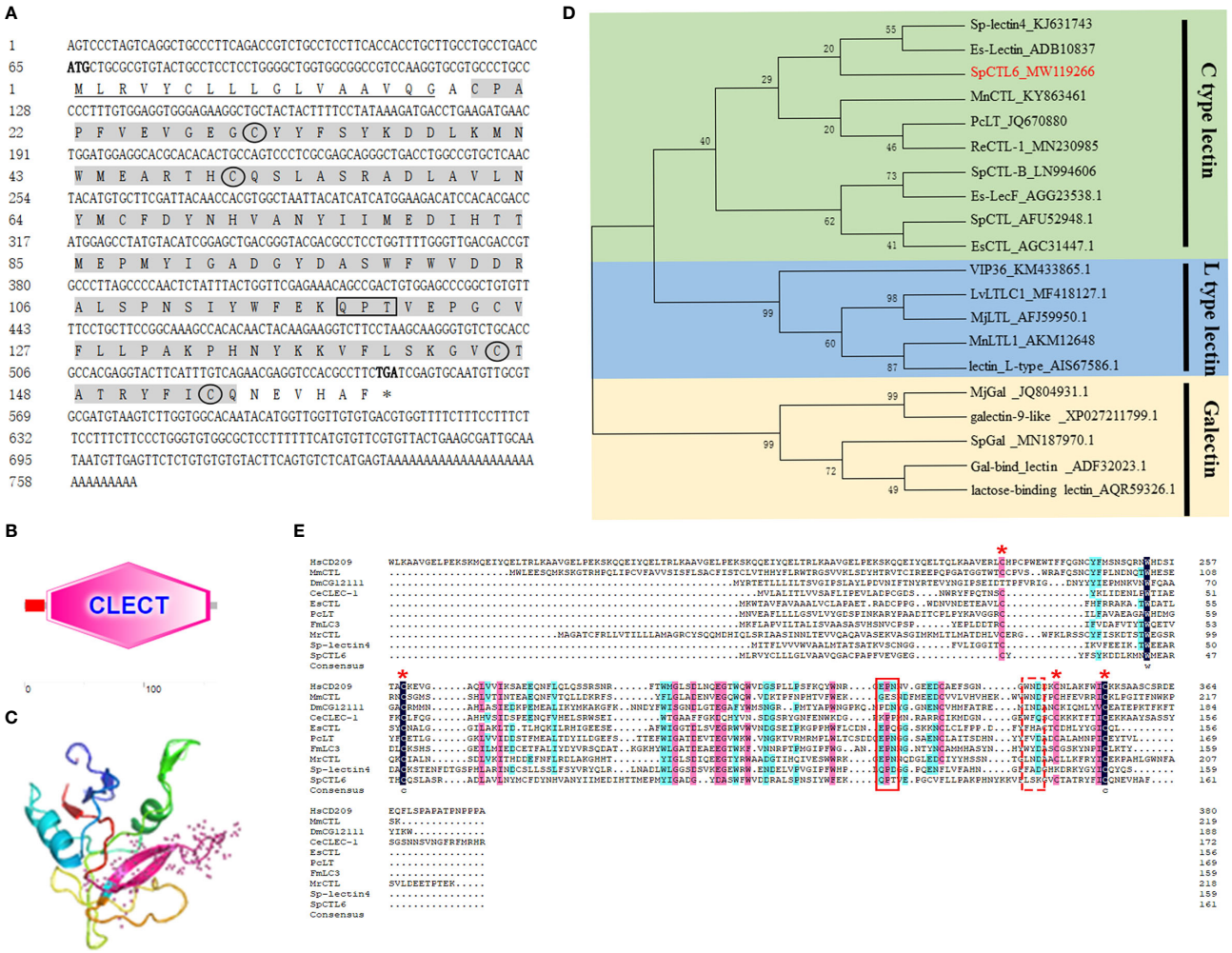

FIGURE 1 | Bioinformatics and phylogenetic analysis of SpCTL6. **(A)** The nucleotide sequence and deduced amino sequence of SpCTL6 from *Scylla paramamosain*. Start codon (ATG) and stop codon(TGA) are marked in bold. The signal peptide is underlined and the CTLD is shade with gray. Four conserved residues are circled and the carbohydrate binding motif (QPT) is boxed. **(B)** Schematic representation of the structural domain of SpCTL6 protein predicted by SMART. **(C)** A predicted three-dimensional model of SpCTL6 by SWISS-MODEL program. **(D)** Phylogenetic tree analysis of SpCTL6. A neighbor-joining phylogenetic tree of lectins was constructed using MEGA ver.6.0 software with 1000 bootstrap replications. SpCTL6 was shown in red. **(E)** Multiple sequence alignment of CTLs from various species. Amino acids residues that are completely conserved are shaded in dark blue, and similar amino acids are shaded in red or light blue. Four conserved cysteine residues involved in the formation of the disulfide bridges are marked with red asterisks, the carbohydrate binding motif (QPT) is boxed with solid line and the WND motif is boxed with dot line. The information of the sequences are listed as follows: HsCD209 (*Homo sapiens*, AAI10616), MmCTL (*Mus musculus* AAD05125), DmCG12111 (*Drosophila melanogaster*, AAF46391), CeCLEC-2 (*C. elegans*, CCD61973), EsCTL (*E. sinensis*, JX841199), PcLT (*Procambarus clarkia*, JQ670880), FmLC3 (*Fenneropenaeus merguiensis*, JF430082), MrCTL (*Macrobrachium rosenbergii*, KX495215), Sp-lectin4 (*S. paramamosain*, KJ631743), SpCTL6 (*S. paramamosain*, MW119266).

there was no obvious hemocytes encapsulating around the beads in the control groups and the encapsulation ratio was very low (TBS and BSA, with or without Ca^{2+} group) (**Figures 5A, B**). While in 200 μg rSpCTL6 treatment group, after 6 h of incubation, dozens of hemocytes were recruited around the beads, the color of the beads became light dark, and the encapsulation ratio was about 7% (**Figures 5A, B**). Especially, in the presence of 10 mM Ca^{2+}, 200 μg rSpCTL6 treatment for 6 h resulted in an encapsulation ratio of about 98% and the beads color became black dark (**Figures 5A, B**). The encapsulation ratio of 24 h rSpCTL6 treatment without or with Ca^{2+} reached about 40% and 99.6%, respectively (**Figures 5A, B**). And the encapsulation activity of rSpCTL6 exhibited in a dose-dependent manner (**Figure S2**).

rSpCTL6 Had No Cytotoxicity on Hemocytes of *S. Paramamosain* and Could Reduce the *V. Alginolyticus* Endotoxin Level *In Vitro*

The cytotoxicity of rSpCTL6 on hemocytes of *S. paramamosain* was evaluated. The results showed that different concentrations

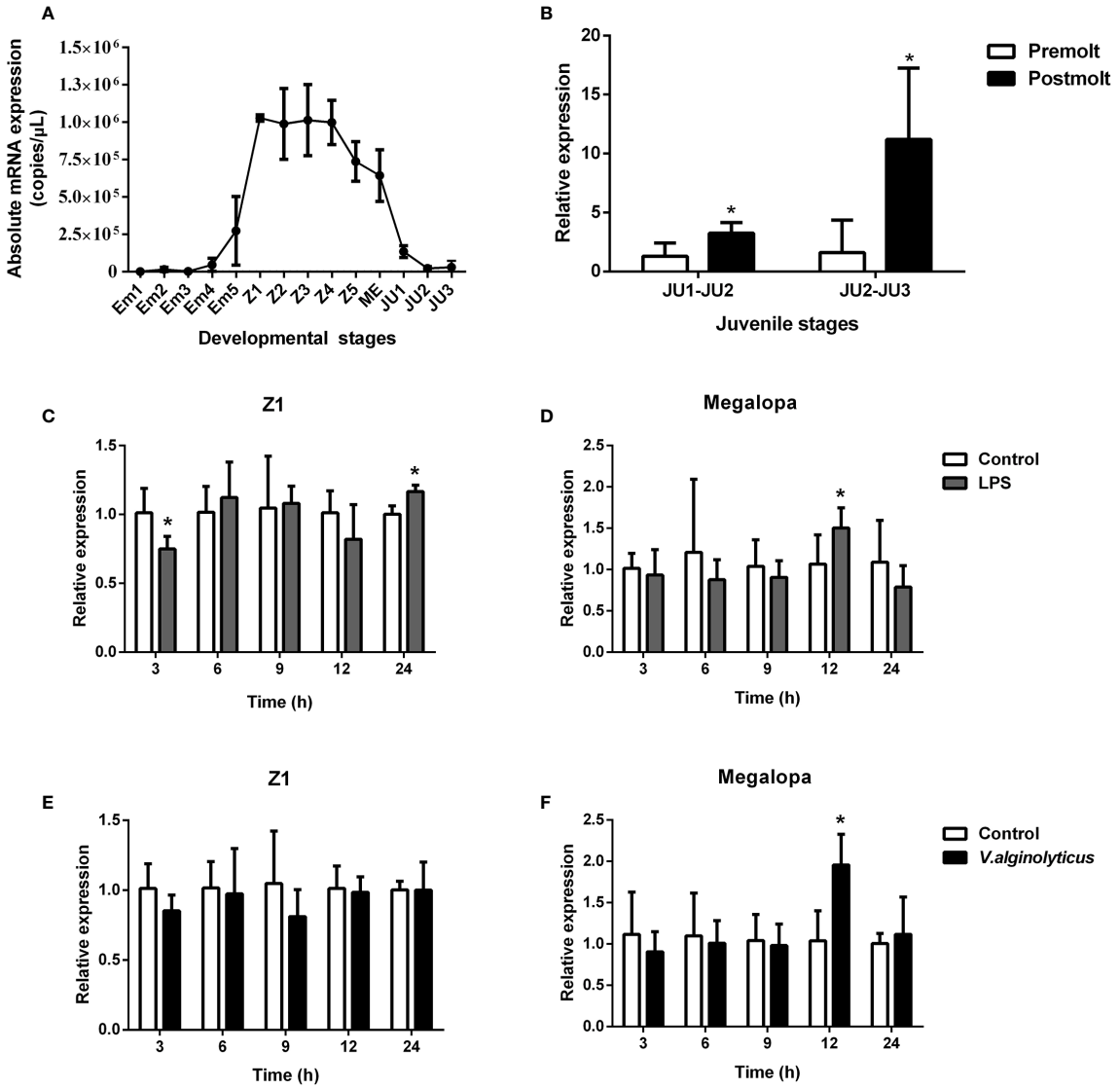

FIGURE 2 | Expression profiles of SpCTL6 gene in the developmental stages of *S. paramamosain*. **(A)** The expression of SpCTL6 in the different developmental stages of *S. paramamosain* was determined by absolute qPCR (n=5). Em1-Em5: embryonic stage 1-5; Z1-Z5: zoeal larval stage 1-5; ME: megalopa; JU: juvenile crab. **(B)** The expression of SpCTL6 in molting process of juvenile crabs was analyzed by relative qPCR (n=5); The expression pattern of SpCTL6 in Z1 (n=5) and megalopa (n=5) after LPS **(C, D)** and *V. alginolyticus* **(E, F)** challenges was analyzed by relative qPCR. Significant difference was indicated by asterisks as $^*p < 0.05$.

of rSpCTL6 (from 1.5 μM to 48 μM) had no cytotoxic effect on the primarily cultured crab hemocytes (**Figure 6A**), which would provide evidence for the safety use of this protein in subsequent *in vivo* study.

In addition, it was found that low concentration rSpCTL6 treatment (10.5 μM) could significantly reduce the endotoxin level of *V. alginolyticus*, which also showed a dose-dependent manner, that is, higher protein treatment concentration, lower bacterial endotoxin level (**Figure 6B**). And under the treatment of 84 μM rSpCTL6, the endotoxin level was reduced by about 70% (**Figure 6B**).

The Immunoprotective Effect of rSpCTL6 on Mud Crab *S. Paramamosain* Challenged with *V. Alginolyticus*

In order to investigate the immunoprotective effect of rSpCTL6 and its regulatory role on the immune system of mud crab *S. paramamosain* under bacterial infection, a series of assays were conducted, including mortality test, bacterial load assay, enzymatic activity assay, and immune-related genes expression analysis.

The schematic diagram of the bacterial challenge and treatment process was shown in **Figure 6C**. The mud crab mortality curve was drawn (**Figure 6C**). The results showed

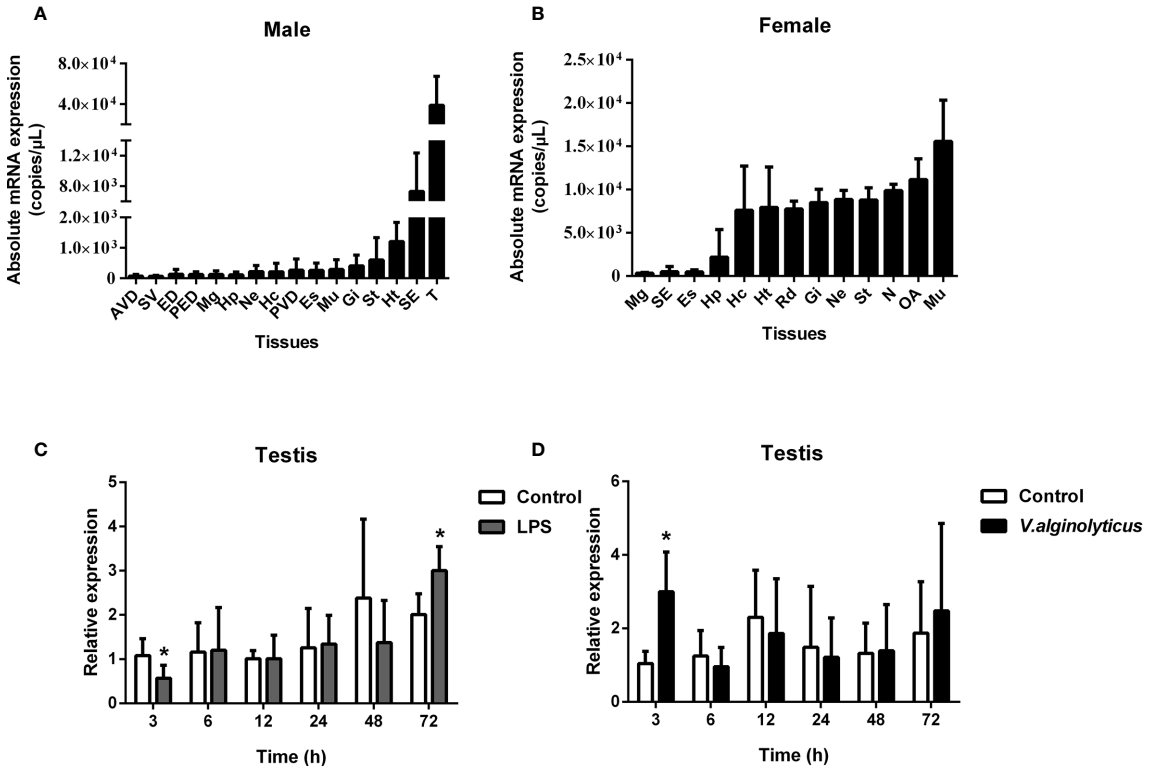

FIGURE 3 | Expression profiles of SpCTL6 gene in *S. paramamosain* adult. Tissue distribution of SpCTL6 in male **(A)** and female **(B)** crabs (n=5). The expression pattern of SpCTL6 in male testis after LPS **(C)** and *V. alginolyticus* **(D)** challenges (n=5). Significant difference was indicated by asterisks as $*p < 0.05$. AVD, anterior vas deferens; SV, seminal vesicle; ED, ejaculatory duct; PED, posterior ejaculatory duct; Mg, midgut; Hp, hepatopancreas; Ne, thoracic ganglion; Hc, hemocytes; PVD, posterior vas deferens; Es, eye stalk; Mu, muscle; Gi, gills; St, stomach; Ht, heart; SE, subcuticular; T, testis; RD, reproductive duct; N: spermathecae; OA, ovaries.

that in the crab saline group, the survival rate dropped sharply in the early stage, and reached about 54% survival rate after 24 h of treatment. While for the rSpCTL6 treatment groups (10 μg crab^{-1} or 20 μg crab^{-1}), the survival rate at 24 h was 80% and 85.7%, respectively (P<0.0001) (**Figure 6C**). 120 h after treatment, the survival rate of the crab saline group was only 11%, while 42.8% for the 10 μg rSpCTL6 crab^{-1} treatment group and 62.9% for the 20 μg rSpCTL6 crab^{-1} treatment group (P<0.0001) (**Figure 6C**). These results indicated that rSpCTL6 treatment could significantly increase the survival of mud crab *S. paramamosain* infected with *V. alginolyticus*.

The bacterial loads in gills and hepatopancreas of *S. paramamosain* after bacterial infection and different treatments were determined. As shown in **Figure 6D**, rSpCTL6 treatment at different time points (3 h, 6 h, and 24 h) could significantly reduce the bacterial number in gills and hepatopancreas of crabs. For example, 3 h after treatment, the bacterial counts in gills and hepatopancreas of the control group were around 1.19×10^4 CFU and 1.58×10^4 CFU, while the corresponding bacterial counts in rSpCTL6 treatment group decreased to 1.32×10^3 CFU, 1.53×10^3 CFU, respectively. With the treatment time increased (from 3 h to 24 h), the amount of bacteria gradually decreased, no matter in the control group or the treatment group (**Figure 6D**).

The Regulatory Role of rSpCTL6 on Mud Crab *S. Paramamosain* Infected by *V. Alginolyticus*

In order to further investigate the molecular mechanism of the immunoprotective effect of rSpCTL6, we analyzed the activity of several immunological parameters and the expression of genes involved in mud crab immunity. The results showed that the activity of two antioxidant enzymes SOD and POD was significantly upregulated at 3 h and 24 h after rSpCTL6 treatment, respectively (**Figure 7A**). For ACP and AKP, their response time was also different, whose activity was remarkably increased at 6 h and 24 h after rSpCTL6 treatment, respectively (**Figure 7A**). In addition, both LZM and PO activity were found to have significant enhancement at two time points (3 h and 24 h after rSpCTL6 treatment) (**Figure 7A**).

We randomly chose several typical immune-related genes to analyze their gene expression modulations in hemocytes and hepatopancreas of *S. paramamosain* after rSpCTL6 treatment. The results showed that among them, three genes (including *Sp*SOD, *Sp*Crustin3 and *Sp*ALF6) were significantly upregulated in both hemocytes and hepatopancreas at 3 h after rSpCTL6 treatment, with *Sp*Crustin3 upregulated at 24 h in hepatopancreas (**Figure 7B**). While the expression of other

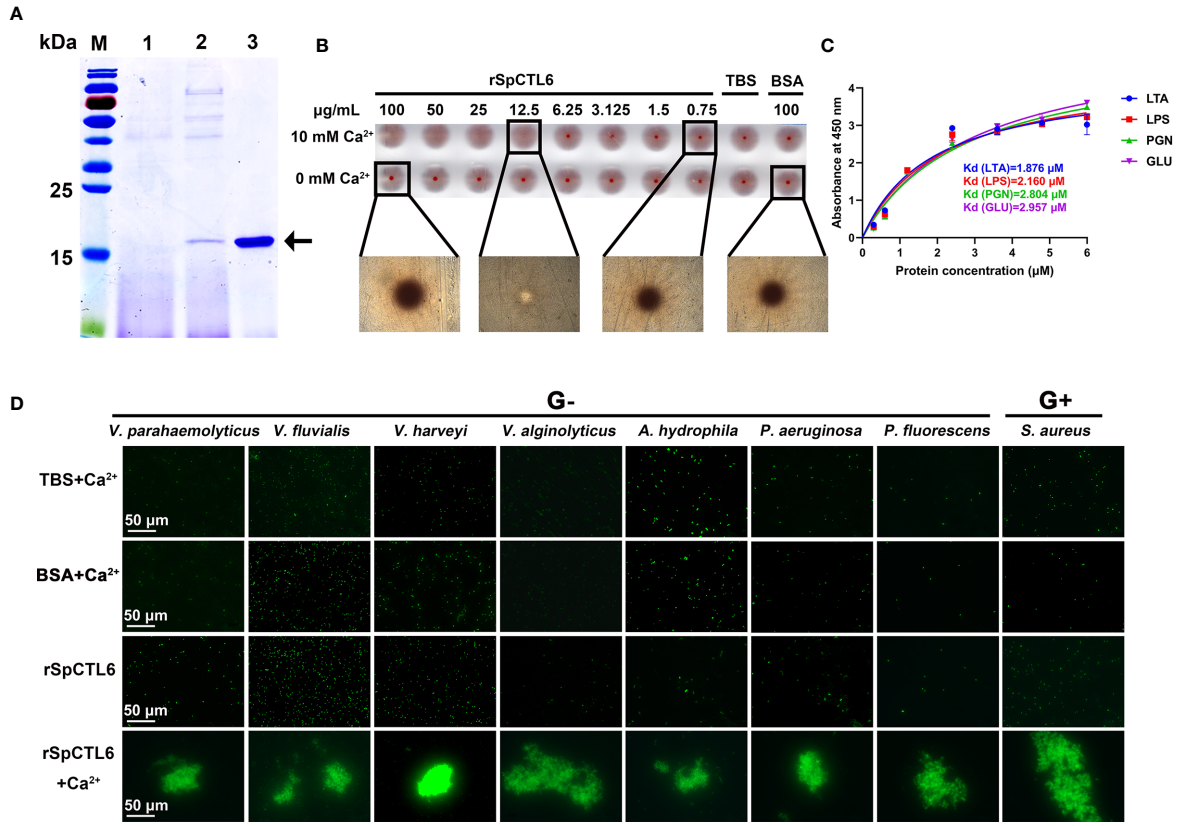

FIGURE 4 | Analysis of hemagglutination, agglutination and binding activity of rSpCTL6. **(A)** Expression and purification of recombinant SpCTL6. Lane M: protein molecular standard; lane 1: negative control for rSpCTL6 without methanol induction; lane 2: expression of rSpCTL6 after methanol induction; lane 3: purified rSpCTL6. **(B)** Agglutination activity of rSpCTL6 on mouse erythrocytes. **(C)** Binding activity of rSpCTL6 to PAMPs (LTA for lipoteichoic acid, LPS for lipopolysaccharide, PGN for peptidoglycan, GLU for glucan). **(D)** Bacterial agglutinating activity of rSpCTL6 on FITC-labeled Gram-negative bacteria (G^-) *V. parahaemolyticus*, *V. fluvialis*, *V. harveyi*, *V. alginolyticus*, *A hydrophila*, *P. aeruginosa*, *P. fluorescens*, and Gram-positive bacteria (G^+) *S. aureus*. The concentration of $CaCl_2$ was 10 mM. TBS and BSA were used as control groups.

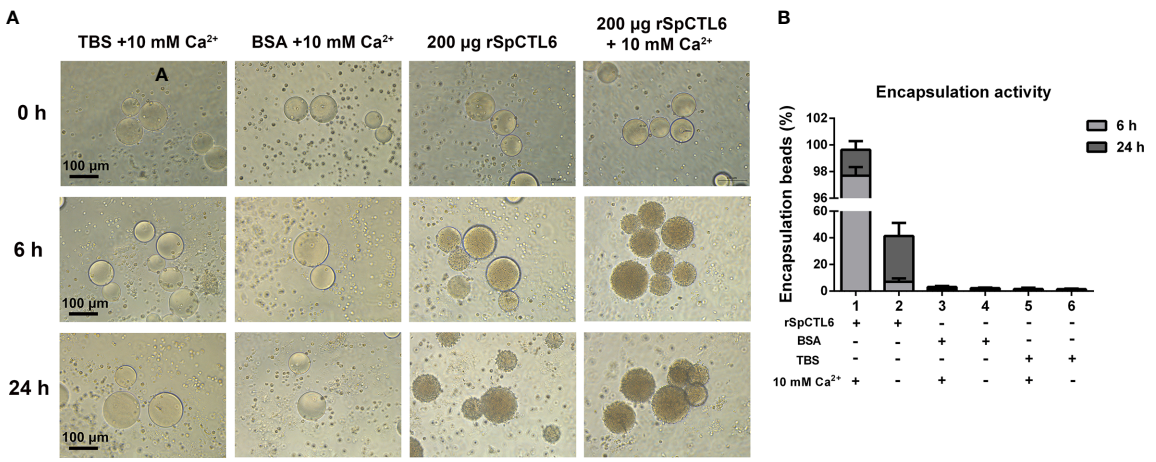

FIGURE 5 | Analysis of encapsulation activity of rSpCTL6. The agrose beads pre-coated with rSpCTL6 were observed for encapsulation by crab hemocytes at 0, 6 and 24 h post-incubation **(A)**. The beads coated with TBS and BSA were used as control groups. **(B)** The percentage of beads encapsulated by hemocytes after 6 h and 24 h of incubation.

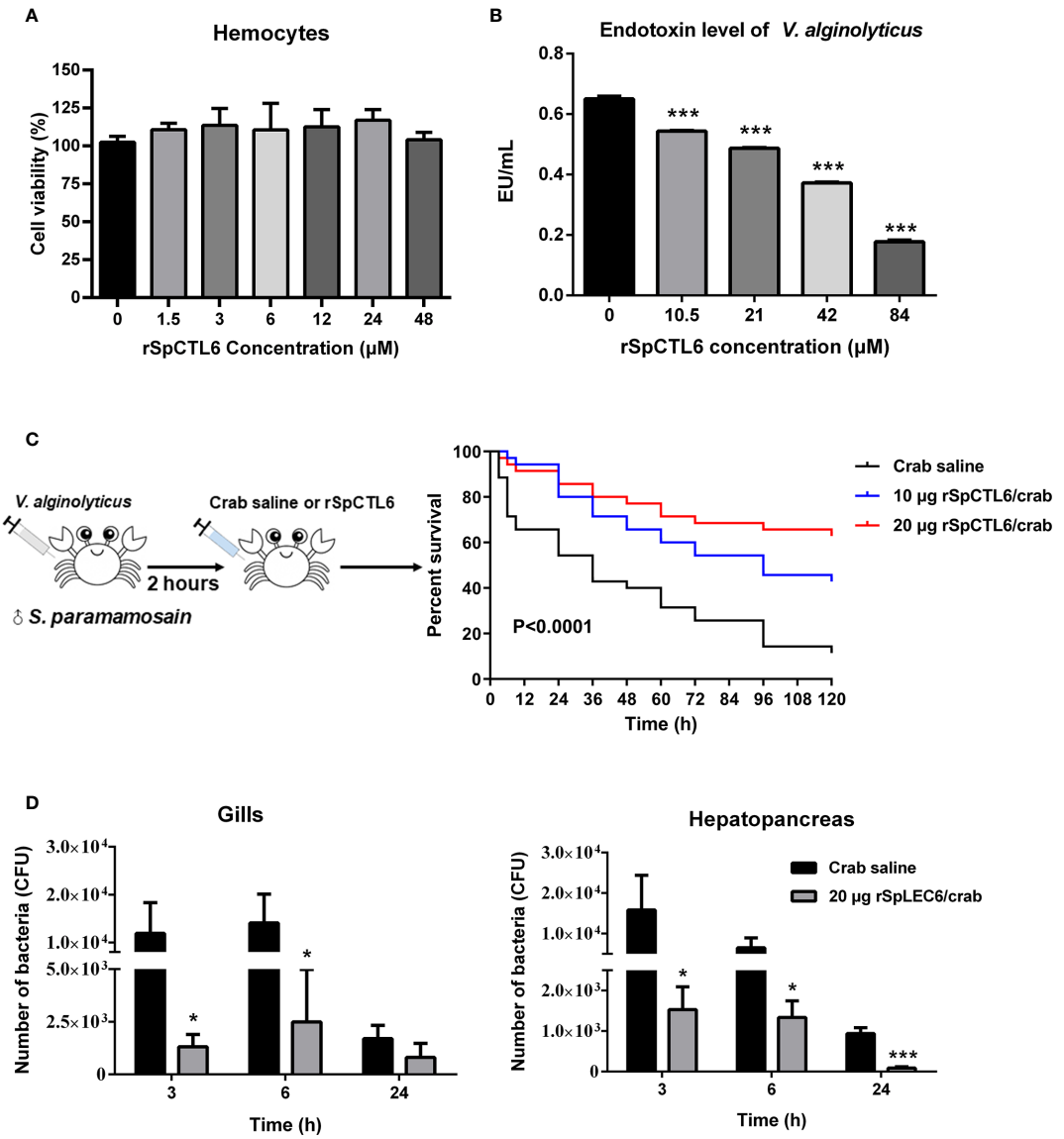

FIGURE 6 | Evaluation of cytotoxicity and endotoxin level of *V. alginolyticus* after rSpCTL6 treatment *in vitro* and the immunoprotective effect of rSpCTL6 in *S. paramamosain*. Cytotoxic effect of rSpCTL6 on crab hemocytes **(A)** and endotoxin level of *V. alginolyticus* after rSpCTL6 treatment *in vitro* **(B)**. The survival curve of mud crabs after rSpCTL6 treatment **(C)**. Male crabs were challenged with *V. alginolyticus*, and SpCTL6 was injected (10 μg crab^{-1} or 20 μg crab^{-1}) at 2 h post bacterial challenge (n=35). Bacterial clearance of *V. alginolyticus* in the gills and hepatopancreas **(D)**. The bacterial burden in the gills and hepatopancreas were determined at 3, 6 and 24 hpi. * represented $p < 0.05$ and *** represented $p < 0.001$.

selected genes showed no changes, except for *Sp*ALF2 down-regulated at 24 h in hemocytes (**Figure S3**).

DISCUSSION

Although the genome of *S. paramamosain* is not available, cDNA library construction and transcriptome analysis has become a powerful tool to identify functional genes (35, 42–44). Since the research on SpCTLs is still lack, we screened a new CTL homolog, named SpCTL6 from the embryonic and larval developmental transcriptome database established in our laboratory. It was found that the transcription level of this newly selected CTL gene was relatively high in the entire Zoeal larval stages, and gradually decreased when it developed into megalopa stage and juvenile crabs, which attracted our attention to investigate its function. Subsequent verification by qPCR also confirmed the reliability of the transcriptome data, indicating that SpCTL6 might play important roles in the development of zoeal larval stages. We then cloned the full-length cDNA of SpCTL6 and determined its expression profiles. In addition, we obtained the recombinant protein (rSpCTL6) from eukaryotic

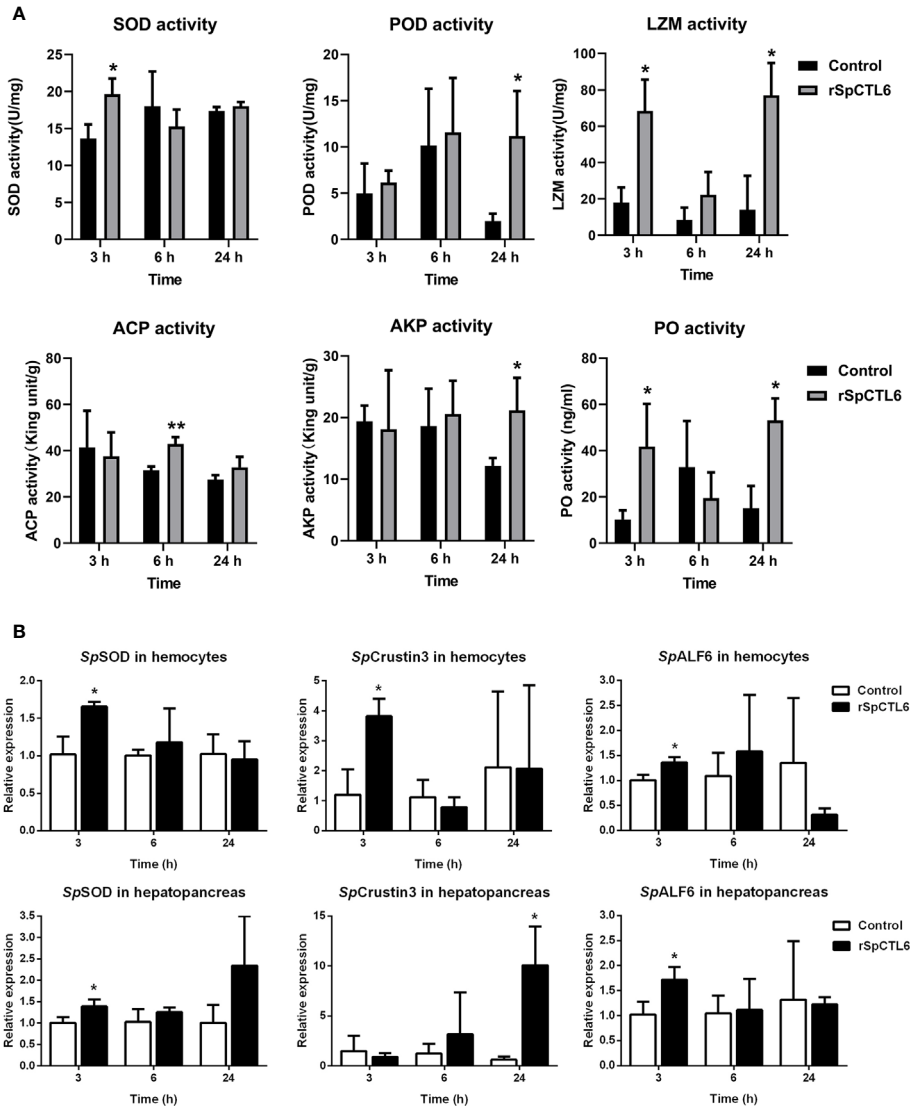

FIGURE 7 | The regulatory role of rSpCTL6 in *S. paramamosain*. Enzymatic activity analysis (SOD, POD, LZM, ACP, AKP, and PO) in hepatopancreas after rSpCTL6 treatment of *S. paramamosain* challenged with *V. alginolyticus* (n=3) **(A)**. The immune-related gene (*Sp*SOD, *Sp*Crustin3 and *Sp*ALF6) expression in hemocytes and hepatopancreas were examined (n=3) **(B)**. Significant difference between rSpCTL6 treatment group and the crab saline injection group was indicated by asterisks as $^*p < 0.05$.

expression system and the immune-related function of rSpCTL6 *in vitro* and *in vivo* were elucidated.

Most reported crustacean CTLs have signal peptides, as well as SpCTL6 in this study, indicating that they might belong to secreted expression proteins and act as PRRs, opsonins or effectors to help eliminate invading pathogens (10). In vertebrates, CTL has 4 highly conserved cysteines (Cys), which form disulfide bridges to stabilize its double-loop tertiary structure with 2 α-helices and 5 β-sheets (11). Besides, there are 4 Ca^{2+}-binding sites and site 2 has been confirmed to participate in carbohydrate binding through two typical motifs [EPN (Glu-Pro-Asn) or QPD (Gln-Pro-Asp), and WND (Trp-Asn- Asp)] (11). However, since there is no report on crystal structure analysis of crustacean CTLs, we could only obtain information from their structural prediction and sequence alignment with other CTLs. It is found that crustacean CTLs are diverse, in which those conserved motifs in vertebrate are usually mutated, such as EPK (Glu-Pro-Lys), EPS (Glu-Pro-Ser), EPQ (Glu -Pro-Gln), QPG (Gln-Pro-Gly), QPS (Gln-Pro-Ser), QPN (Gln-Pro-Asn), QPT (Gln-Pro-Thr), as summarized in detail in shrimp CTLs (15). Among SpCTLs, only Sp-lectin4 has a typical QPD motif (32), while SpCTL-B contains EPD (Glu-Pro-Asp) motif (33), which is not found in SpLec1, SpLec2, Sp-lectin3 and SpCTL5 (31, 32, 34). For SpCTL6 in the study, although its amino acid identity is relatively low compared with other crustacean CTLs, it had typical CTL structural

characteristics, such as a single CTLD, 4 conserved Cys, similar tertiary structure to that of vertebrate CTLs and the mutated Ca^{2+} binding motif (QPT), clustering into the same branch as the crustacean CTLs, which provided evidence that SpCTL6 is a novel CTL homolog.

In recent years, a large number of studies have focused on the immune function of CTLs, but the role of CTLs in development cannot be ignored. At present, relevant researches have been carried out on insects. It was reported that a CTL HaCTL3 from the cotton bollworm *Helicoverpa armigera* played an important role in larval growth and development through modulating ecdysone and juvenile hormone signaling (45). Knock-down the expression of Tcctl5 led to developmental defects of *Tribolium castaneum*, such as reduced survival rate in early adults, and loss of locomotor activity in adults (46). The schlaff (slf) gene coding a putative C-type lectin was necessary for the adhesion between the horizontal cuticle layers of Drosophila (47). So far, research on the function of crustacean CTLs in the development are few and not in-depth. In *S. paramamosain*, it was found that SpLec1 and SpLec2 had certain expression in the zoeal stages of *S. paramamosain*, while Sp-lectin3 and Sp-lectin4 were widely distributed in embryos, larvae and crablet stages (31, 32). *V. parahaemolyticus* challenge could up-regulated the expression of SpLec1 and SpLec2 in megalopa stage of *S. paramamosain*, indicating their role in development and immune response (31). In the study, we systematically analyzed the expression of SpCTL6 in the entire embryonic (Em1-5) and larval stages (Z1-Z5, megalopa) and three stages of juvenile crabs (JU1-3). The absolute copy number of SpCTL6 during zoeal stages reached $0.7\sim1\times10^6$ copies/μL. Such a high transcription level indicated that SpCTL6 might be involved in the modulation of zoeal stage development. However, whether the development-related signaling pathways (such as ecdysone and juvenile hormone signaling) could also be modulated by SpCTL6 similar to HaCTL3 requires further investigation. The upregulated expression pattern of SpCTL6 in Z1 and megalopa stages under immune challenges further demonstrated that SpCTL6 might exert dual roles (developmental modulation and immune response) in the early development of *S. paramamosain*. In addition, during the molting process of juvenile crabs, the expression SpCTL6 was significantly upregulated after molting (JU1 developed to JU2, and JU2 developed to JU3). Since crabs are vulnerable to infection by foreign microorganisms during molting, they might adopt certain strategies, such as increasing the expression of immune factors (including SpCTL6) to resist pathogens. Though the underlying molecular mechanism is still unclear, the results obtained in this study provide new insights into the role of crustacean CTLs in development.

The currently reported crustacean CTLs are widely distributed in various tissues, most of which are predominantly expressed in the hepatopancreas, and some CTLs mainly distributed in hemocytes and gills, or other tissues (heart, gills, intestine, stomach, brain) (15, 21, 30, 33, 34). However, there are few reports on the specific high expression of CTLs in the gonads of crustaceans. Interestingly, SpCTL6 was highly expressed in the testis of adult male crabs (its absolute copy number was the highest compared with other male tissues and all female tissues), which is quite different from reported crustacean CTLs. In other aquatic invertebrates, it was found that two CTLs, AjCTL-1 from sea cucumber *Apostichopus japonicus* and AiCTL-9 from scallop *Argopecten irradians* also had the highest expression level in gonad (48, 49). Wang et al. performed a genome-wide survey on the lectin domain containing proteins (LDCPs) of oyster *Crassostrea gigas* and found that C-type lectin domain containing proteins (CTLPs) were the most abundant proteins (50). Among them, 40 CTLPs were highly expressed in male gonad, indicating their important role in the reproductive immunity (50). Similar screening methods can also be used in the discovery of crustacean CTLs, which would help us further understand the function of this superfamily. Due to the lack of model animals, it is relatively difficult to investigate the molecular mechanism of functional genes in aquatic invertebrates. In the model organism *Caenorhabditis elegans*, a CTLP IRG-7 was demonstrated to regulate the immune response of reproductive systems of *C. elegans* to defense against pathogens (51). In *S. paramomosain*, several male-specific immune effectors antimicrobial peptides (AMPs) have been identified in our previous studies, including scygonadin (52–54), SCY2 (55), and scyreprocin (39). All of them have been revealed to participate in the reproductive immunity of mud crabs. In the present study, SpCTL6 was found to be significantly regulated in the testis under LPS or *V. alginolyticus* challenge, indicating that it participated in the immune response of *S. paramamosain*. Therefore, we speculated that the high expression of SpCTL6 in male gonad might also be involved in mud crab reproductive immunity, which will be further studied in the future.

Most functional studies of crustacean CTLs have been conducted through obtaining the recombinant proteins and analyzing the *in vitro* activity (including antimicrobial, binding, agglutination, and encapsulation activities etc.) (10, 15). Prokaryotic expression system is widely used in the recombinant expression of crustacean CTL proteins, and the vectors included pET-32a, pET-21a, and pGEX-4T-1 etc. (33, 34, 56). As we all know, the yeast eukaryotic expression system is also a commonly used protein expression system, which can undergo mRNA splicing and post-translational modifications for eukaryotic organisms, thereby would better mimic the existing form of the protein *in vivo* (57). In particular, the correct spatial structure and modification are very important for protein function. In this study, we obtained high-purity recombinant SpCTL6 (rSpCTL6) from *P. pastoris* eukaryotic expression system, and confirmed it using mass spectrometry, which provides a critical guarantee for our further functional study.

As PRRs, crustacean CTLs exhibited strong binding activity with pathogen associated molecular patterns (PAMPs, such as LPS, LTA, PGN and GLU) and bacteria, some of which had direct bactericidal activity. In swimming crab *P. trituberculatus* and Chinese mitten crab *E. sinensis*, several CTLs showed both binding activity with PAMPs and bacteria, such as PtCLec1, PtCTL-2, PtCTL-3, EsCTL1, EsCTL2, and EsCTLDcp (22, 23,

27, 30). SpCTL-B in *S. paramamosain* could bind to a variety of bacteria, including Gram-positive bacteria *S. aureus* and *Streptococcus hemolyticus*, Gram-negative bacteria *E. coli*, *V. parahaemolyticus*, *V. alginolyticus*, *A. hydrophila* and fungi *Saccharomyces cerevisiae* (33). Several crab CTLs showed potent antibacterial activity, such as SpCTL-B (33), PtCLec1 (30), rEsLecH (21), EsLecA and EsLecG (25). For rSpCTL6, it had binding activity with 4 PAMPs 9LPS, LTA, PGN, and GLU) with moderate binding affinity ["moderate" was defined as Kd value of 100 nM to 10 μM) (58)]. However, rSpCTL6 could not bind to bacteria and had no obvious antimicrobial activity (data not shown), indicating that it might exert immune functions through other molecular mechanisms.

Agglutination activity is also the hallmark biological function of CTLs. By recognizing molecules on the surface of bacteria, CTLs can directly immobilize pathogens and agglutinate them, so that pathogens will not spread in the body. A large number of studies have shown that most CTLs rely on calcium ions to exert or enhance their agglutination activity (10). Crab CTLs exhibited a broad spectrum of bacterial agglutination activity in Ca^{2+}-dependent manner, especially on several typical aquaculture pathogens, such as *V. alginolyticus*, *V. parahaemolyticus*, *V. vulnificus*, and *A. hydrophila* (22, 23, 27, 30, 33). Among them, EsLecA, EsLecG and EsLecD agglutinated *E. coli* and *P. pastoris* without relying on calcium ions, and the addition of Ca^{2+} could significantly enhance their agglutinating activity (25, 59). In addition, PtCLec1, PtCTL4 and PtCTL1 had hemagglutination activity on rabbit erythrocytes in the presence of Ca^{2+} (28–30). Similar broad spectrum bacterial agglutination activity was also found in rSpCTL6, which could agglutinate 5 common pathogens in aquaculture (*A. hydrophila*, *V. harveyi*, *V. fluvialis*, *V. parahaemolyticus*, and *V. alginolyticus*), and rSpCTL6 had hemagglutination activity on mouse erythrocytes in a Ca^{2+}-dependent manner.

When some large pathogens such as parasites invade the crustacean, the host hemocytes will wrap around them, forming a multiple cell layers, so that those pathogens cannot move freely in the host, and then they will be killed by melanin or endotoxin released by hemocytes (60). Therefore, hemocyte encapsulation ability play an important role in cellular immunity of invertebrates (61). Studies have found that crustacean CTLs can enhance the ability of hemocytes to encapsulate large pathogens and then followed by melanization (15). Agarose beads are usually used as invading objects to evaluate the effect of CTLs on the encapsulation activity of hemocytes. When the agarose beads were incubated with PtCTL-2 and PtCTL-3 from *P. trituberculatus* separately, and then the hemocytes were added, the hemocytes encapsulated 57% and 45% of agarose beads respectively, while the control group had no obvious coating effect (27). In *E. sinensis*, EsLecA, EsLecG, EsLecD and EsLecF could also activate the encapsulation activity of hemocytes on agarose beads (25, 59, 62). The results showed that after 24 h of incubation, almost 100% of EsLecD-coated agarose beads were encapsulated by hemocytes, which might be due to the high binding affinity of EsLecD to hemocyte surface molecules (59). Similarly, in our study, rSpCTL6 significantly enhanced the hemocyte encapsulation on agarose beads and might cause hemocyte melanization to help eliminate invading pathogens, indicating its important role in cellular immunity of *S. paramamosain*.

Research on the function of recombinant CTLs *in vitro* is far from enough, and elucidating the immune protective and regulatory effects of CTL proteins *in vivo* will provide important evidences for further understanding their immune functions. Most of the reported crustacean CTLs conducted the *in vivo* bacterial clearance assay to evaluate the *in vivo* effects of recombinant CTLs. They first pre-incubated the bacteria and recombinant CTL protein for a period of time, and then co-injected them into animals, and finally counted the numbers of living bacteria in the hemolymph. The results showed that this treatment could remarkably accelerate the bacteria clearance, such as rPtCLec1 (30), EsCTL1 and EsCTL2 (22), EsCTLDcp (23) in crab, PcLec3 (63), PcLec4 (64), MnCTL (56), MrCTL (65), LvCTL3 (66), FmLC4 (67), and FcLec4 (68) in crayfish, prawn and shrimp. Whether CTLs can significantly improve the survival rate of animals under pathogenic infection is an important evidence to clarify their immune protective effects. PcLec4 overexpression *in vivo* exhibited obviously higher survival rate (50% at the ninth day) than that of the control groups (10% at the ninth day) (64). Pre-incubated rPcLT and WSSV could effectively protect crayfish *Procambarus clarkii* from WSSV infection, with a much higher survival rate (around 75%) than that of the control groups (3-5%) (69). Injection of WSSV or *V. alginolyticus* together with rLvCTL3 could significantly reduce the mortality of *L. vannamei* infected by WSSV and *V. alginolyticus* (66). In our study, the treatment method was different from those reports mentioned above. We first infected the crabs with *V. alginolyticus* and 2 hours later, injected rSpCTL6 or crab saline into the crabs. We would like to know the *in vivo* protective effect of rSpCTL6 under pathogenic infection. The results showed that rSpCTL6 treatment could also enhance the bacterial clearance in gills and hepatopancreas. In addition, rSpCTL6 treatment could greatly improve the survival of infected crabs [increased by about 50% (62.9% in rSpCTL6 treatment group, 11% in the control group in 120h)], which would provide a valuable information for the disease control in mud crab aquaculture.

At present, the regulatory role of crustacean CTLs in the immune system has been extensively studied mainly through the use of RNA interference (RNAi), which is a powerful tool for revealing the molecular mechanism of functional genes (15). In crabs, such as in *E. sinensis*, RNAi of EsLecH could down-regulate the expression of several AMPs (including Es-DWD1, EsALF, and EsALF-2) and phosphorylation of JNK (21). When the mRNA level of JNK was inhibited, the addition of rEsLecH could not cause changes in AMP expression, indicating that EsLecH required JNK signaling to perform its regulation function (21). Knock down of PtCLec1 from *P. trituberculatus* could regulate the expression of genes involved in phagocytosis, proPO system, complement system, Toll and IMD pathways, and AMPs, indicating its key regulatory role in the innate immunity of *P. trituberculatus* (30). In rPcLT treatment shrimp, PO and SOD activity increased significantly at different time points (69). In *S. paramamosain*,

several AMPs (SpHistin, SpALF4, SpALF5 and SpALF6), spSTAT and hemocyte phagocytosis were all regulated by SpCTL-B (also evaluated through RNAi), suggesting that SpCTL-B played important roles both in the humoral and cellular immunity of mud crabs (33). In order to understand the underlying molecular mechanism of the immunoprotective effect of SpCTL6, we further analyzed the expression of immune-related genes and several immunological parameters after rSpCTL6 treatment. We found that the expression of two AMP genes SpCrustin3 and SpALF6, an antioxidant gene SOD, and all the tested parameters (including SOD, POD, LZM, ACP, AKP, and PO activity) had been upregulated, indicating the regulatory role of rSpALF6 in the innate immunity of *S. paramamosain*. However, the underlying regulatory mechanism of CTLs is complicated and we are still far from understanding it. As shown in a previous study, it was found that the silencing of LvLdlrCTL (a CTL containing a low-density lipoprotein receptor (LDLR) class A domain) from *L. vannamei* down-regulated the expression of 3 AMPs (crustin, ALF3, and PEN3), but 2 other AMPs (PEN2 and PEN4) were upregulated (70). Similarly, in our study, 2 AMPs (*Sp*Crustin3 and *Sp*ALF6) were upregulated at 3 h in the hemocytes, while another AMP *Sp*ALF2 was down-regulated at 24 h in the hemocytes after rSpCTL6 treatment. In the early stage (3 h and 6 h after rSpCTL6 treatment), the bacterial load in crabs was still high (**Figure 6D**), which might require increased enzyme activity and expression of AMPs to resist bacteria. Our results corresponded to this hypothesis, for example, the activities of a variety of immunological parameters in the hepatopancreas (including SOD, LZM, ACP and PO) and several immune-related genes in hemocytes (including *Sp*SOD, *Sp*Crustin3, *Sp*ALF6) were upregulated at 3 h or 6 h after rSpCTL6 treatment, suggesting that rSpCTL6 might activate the innate immune system of *S. paramamosain*, thereby quickly eliminating the invading bacteria. And at the 24 h time point, the number of bacteria decreased to a low level, we speculated that crabs need to adopted anti-inflammatory strategies to help the body recover. Therefore, the downregulation of *Sp*ALF2 might be due to the need for anti-inflammatory response and the maintenance of homeostasis, which requires further in-depth investigation.

In summary, this study characterized a new CTL homolog SpCTL6 from mud crab *S. paramamosain*. SpCTL6 was highly expressed in the entire zoeal larval stages and widely distributed in adult crab tissues with the highest transcription level in testis. It could be significantly upregulated in two larval stages (Z1 and megalopa stages) and adult crab testis under immune challenges. During the molting process of juvenile crabs, the expression level of SpCTL6 was remarkably increased after molting. Recombinant SpCTL6 was successfully obtained from eukaryotic expression system. rSpCTL6 exhibited binding activity with PAMPs and had a broad spectrum of bacterial agglutination activity in a Ca^{2+}-dependent manner. rSpCTL6 could enhance the encapsulation activity of hemocytes and it had no cytotoxic effect on hemocytes. Furthermore, rSpCTL6 treatment could significantly reduce the endotoxin level of *V. alginolyticus in vitro* and greatly improved the survival of *S. paramamosain* under bacterial infection. The immunoprotective effect of rSpCTL6 might be due to the regulatory role of rSpALF6 in the immune-related genes and immunological parameters. Our study provides important information for understanding the immune defense of mud crabs and would facilitate the development of effective strategies for mud crab aquaculture disease control.

DATA AVAILABILITY STATEMENT

The original contributions presented in the study are included in the article/**Supplementary Material**. Further inquiries can be directed to the corresponding author.

ETHICS STATEMENT

The animal study was reviewed and approved by the Laboratory Animal Management and Ethics Committee of Xiamen University.

AUTHOR CONTRIBUTIONS

WQ: Data curation, formal analysis, investigation, and methodology. RC, SL, XZ, and MX: Investigation and methodology. FC: Conceptualization, funding acquisition, project administration, supervision; writing–original draft, and writing–review and editing. KW: Funding acquisition, project administration, and writing–review and editing. All authors contributed to the article and approved the submitted version.

FUNDING

This study was supported by grants (grant # U1805233/ # 41806162) from the National Natural Science Foundation of China (NSFC), the Fundamental Research Funds from Central Universities (grant # 20720190109), the Fujian Marine Economic Development 395 Subsidy Fund Project (Grant # FJHJF-L-2019-1) from the Fujian Ocean and Fisheries Department and a grant (# 3502Z20203012) from the Xiamen Science and Technology Planning Project.

ACKNOWLEDGMENTS

We thank laboratory engineers Hui Peng and Zhiyong Lin for providing technical assistance. We thank Yaying Wu, Zheni Xu and C.C. Xie for mass spectrometry experiments and data analysis.

SUPPLEMENTARY MATERIAL

The Supplementary Material for this article can be found online at: https://www.frontiersin.org/articles/10.3389/fimmu.2021.661823/full#supplementary-material

REFERENCES

1. Mirera OD. Trends in exploitation, development and management of artisanal mud crab (*Scylla serrata*-Forsskål-1775) fishery and small-scale culture in Kenya: An overview. *Ocean Coast Manage* (2011) 54:844–55. doi: 10.1016/j.ocecoaman.2011.08.001
2. Azra MN, Ikhwanuddin M. A review of maturation diets for mud crab genus *Scylla* broodstock: Present research, problems and future perspective. *Saudi J Biol Sci* (2016) 23:257–67. doi: 10.1016/j.sjbs.2015.03.011
3. Hungria DB, Tavares CPD, Pereira LA, da Silva UDT, Ostrensky A. Global status of production and commercialization of soft-shell crabs. *Aquacult Int* (2017) 25:2213–26. doi: 10.1007/s10499-017-0183-5
4. Ministry of Agriculture and Rural Affairs of the People's Republic of China, Fisheries Administration; National Fisheries Technology Promotion Station, China; Chinese Fisheries Society. *China Fishery Statistical Yearbook 2019*. China Agriculture Press (2019). pp. 1–152.
5. Hamasaki K, Obata Y, Dan S, Kitada S. A review of seed production and stock enhancement for commercially important portunid crabs in Japan. *Aquacult Int* (2011) 19:217–35. doi: 10.1007/s10499-010-9387-7
6. Chen F, Wang K. Characterization of the innate immunity in the mud crab *Scylla paramamosain*. *Fish Shellfish Immunol* (2019) 93:436–48. doi: 10.1016/j.fsi.2019.07.076
7. Quinitio ET, de la Cruz JJ, Eguia MRR, Parado-Estepa FD, Pates G, Lavilla-Pitogo CR. Domestication of the mud crab *Scylla serrata*. *Aquacult Int* (2011) 19:237–50. doi: 10.1007/s10499-010-9381-0
8. Ye HH, Tao Y, Wang GZ, Lin QW, Chen XL, Li SJ. Experimental nursery culture of the mud crab *Scylla paramamosain* (Estampador) in China. *Aquacult Int* (2011) 19:313–21. doi: 10.1007/s10499-010-9399-3
9. Robinson MJ, Sancho D, Slack EC, LeibundGut-Landmann S, Reis e Sousa C. Myeloid C-type lectins in innate immunity. *Nat Immunol* (2006) 7:1258–65. doi: 10.1038/ni1417
10. Pees B, Yang WT, Zarate-Potes A, Schulenburg H, Dierking K. High innate immune specificity through diversified C-type lectin-like domain proteins in invertebrates. *J Innate Immun* (2016) 8:129–42. doi: 10.1159/000441475
11. Zelensky AN, Gready JE. The C-type lectin-like domain superfamily. *FEBS J* (2005) 272:6179–217. doi: 10.1111/j.1742-4658.2005.05031.x
12. Kilpatrick DC, 187-97. Animal lectins: a historical introduction and overview. *Biochim Biophys Acta* (2002) 1572:187–97. doi: 10.1016/S0304-4165(02)00308-2
13. van Gisbergen KP, Ludwig IS, Geijtenbeek TB, van Kooyk Y. Interactions of DC-SIGN with Mac-1 and CEACAM1 regulate contact between dendritic cells and neutrophils. *FEBS Lett* (2005) 579:6159–68. doi: 10.1016/j.febslet.2005.09.089
14. Vaishnava S, Yamamoto M, Severson KM, Ruhn KA, Yu X, Koren O, et al. The antibacterial lectin RegIIIgamma promotes the spatial segregation of microbiota and host in the intestine. *Science* (2011) 334:255–8. doi: 10.1126/science.1209791
15. Wang XW, Wang JX. Diversity and multiple functions of lectins in shrimp immunity. *Dev Comp Immunol* (2013) 39:27–38. doi: 10.1016/j.dci.2012.04.009
16. Wang XW, Vasta GR, Wang JX. The functional relevance of shrimp C-type lectins in host-pathogen interactions. *Dev Comp Immunol* (2020) 109:103708. doi: 10.1016/j.dci.2020.103708
17. Zhang XJ, Yuan JB, Sun YM, Li SH, Gao Y, Yu Y, et al. Penaeid shrimp genome provides insights into benthic adaptation and frequent molting. *Nat Commun* (2019) 10:356. doi: 10.1038/s41467-018-08197-4
18. Gutekunst J, Andriantsoa R, Falckenhayn C, Hanna K, Stein W, Rasamy J, et al. Clonal genome evolution and rapid invasive spread of the marbled crayfish. *Nat Ecol Evol* (2018) 2:567–73. doi: 10.1038/s41559-018-0467-9
19. Song L, Bian C, Luo Y, Wang L, You X, Li J, et al. Draft genome of the Chinese mitten crab, *Eriocheir sinensis*. *Gigascience* (2016) 5:5. doi: 10.1186/s13742-016-0112-y
20. Tang B, Zhang D, Li H, Jiang S, Zhang H, Xuan F, et al. Chromosome-level genome assembly reveals the unique genome evolution of the swimming crab (*Portunus trituberculatus*). *Gigascience* (2020) 9:1–10. doi: 10.1093/gigascience/giz161
21. Zhu YT, Zhang X, Wang SC, Li WW, Wang Q. Antimicrobial functions of EsLecH, a C-type lectin, via JNK pathway in the Chinese mitten crab, *Eriocheir sinensis*. *Dev Comp Immunol* (2016) 61:225–35. doi: 10.1016/j.dci.2016.04.007
22. Huang Y, Huang X, Wang Z, Tan JM, Hui KM, Wang W, et al. Function of two novel single-CRD containing C-type lectins in innate immunity from *Eriocheir sinensis*. *Fish Shellfish Immunol* (2014) 37:313–21. doi: 10.1016/j.fsi.2014.02.001
23. Huang Y, An L, Hui KM, Ren Q, Wang W. An LDLa domain-containing C-type lectin is involved in the innate immunity of *Eriocheir sinensis*. *Dev Comp Immunol* (2014) 42:333–44. doi: 10.1016/j.dci.2013.10.004
24. Wang L, Wang L, Zhang D, Li F, Wang M, Huang M, et al. A novel C-type lectin from crab *Eriocheir sinensis* functions as pattern recognition receptor enhancing cellular encapsulation. *Fish Shellfish Immunol* (2013) 34:832–42. doi: 10.1016/j.fsi.2012.12.010
25. Jin XK, Li S, Guo XN, Cheng L, Wu MH, Tan SJ, et al. Two antibacterial C-type lectins from crustacean, *Eriocheir sinensis*, stimulated cellular encapsulation *in vitro*. *Dev Comp Immunol* (2013) 41:544–52. doi: 10.1016/j.dci.2013.07.016
26. Guo HZ, Zou PF, Fu JP, Guo Z, Zhu BK, Nie P, et al. Characterization of two C-type lectin-like domain (CTLD)-containing proteins from the cDNA library of Chinese mitten crab *Eriocheir sinensis*. *Fish Shellfish Immunol* (2011) 30:515–24. doi: 10.1016/j.fsi.2010.11.027
27. Huang M, Mu C, Wu Y, Ye F, Wang D, Sun C, et al. The functional characterization and comparison of two single CRD containing C-type lectins with novel and typical key motifs from *Portunus trituberculatus*. *Fish Shellfish Immunol* (2017) 70:398–407. doi: 10.1016/j.fsi.2017.09.029
28. Lu J, Yu Z, Mu C, Li R, Song W, Wang C. Characterization and functional analysis of a novel C-type lectin from the swimming crab *Portunus trituberculatus*. *Fish Shellfish Immunol* (2017) 64:185–92. doi: 10.1016/j.fsi.2017.03.013
29. Zhang X, Lu J, Mu C, Li R, Song W, Ye Y, et al. Molecular cloning of a C-type lectin from *Portunus trituberculatus*, which might be involved in the innate immune response. *Fish Shellfish Immunol* (2018) 76:216–23. doi: 10.1016/j.fsi.2018.01.051
30. Su Y, Liu Y, Gao F, Cui Z. A novel C-type lectin with a YPD motif from *Portunus trituberculatus* (PtCLec1) mediating pathogen recognition and opsonization. *Dev Comp Immunol* (2020) 106:103609. doi: 10.1016/j.dci.2020.103609
31. Jiang K, Zhang D, Zhang F, Sun M, Qi L, Zhang S, et al. Isolation of the C-type lectin like-domain cDNAs from the mud crab *Scylla paramamosain* Estampador, 1949, and its expression profiles in various Tissues, during larval development, and under Vibrio challenge. *Crustaceana* (2012) 85:817–34. doi: 10.1163/156854012X650269
32. Duan LP, Huang B, Zhou LH, Liang Y, Nie P, Huang WS. Molecular cloning, characterization and expression of two novel lectins in mud crab, *Scylla paramamosain*. *Acta Hydrobiol Sin* (2015) 39:321–30. doi: 10.7541/2015.43
33. Wei X, Wang L, Sun W, Zhang M, Ma H, Zhang Y, et al. (SpCTL-B) regulates the expression of antimicrobial peptides and promotes phagocytosis in mud crab *Scylla paramamosain*. *Dev Comp Immunol* (2018) 84:213–29. doi: 10.1016/j.dci.2018.02.016
34. Zhang W, Zhang Z, Mu C, Li R, Ye Y, Zhang H, et al. Molecular cloning, characterization, and expression of a C-type lectin from *Scylla paramamosain*, which might be involved in the innate immune response. *Fish Shellfish Immunol* (2019) 93:251–7. doi: 10.1016/j.fsi.2019.07.035
35. Chen FY, Liu HP, Bo J, Ren HL, Wang KJ. Identification of genes differentially expressed in hemocytes of *Scylla paramamosain* in response to lipopolysaccharide. *Fish Shellfish Immunol* (2010) 28:167–77. doi: 10.1016/j.fsi.2009.10.017
36. Zeng C, Li S, Zeng H. Studies on the morphology of the larvae of *Scylla serrata* (Forskal). *J Zhanjiang Ocean Univ* (2001) 2:1–6.
37. Huang S, Li W. Study on the larval development of *Scylla serrata* (Forskal). *J Fisheries China* (1965) 4:24–30.
38. Livak KJ, Schmittgen TD. Analysis of relative gene expression data using real-time quantitative PCR and the 2^{-DDCT} Method. *Methods* (2001) 25:402. doi: 10.1006/meth.2001.1262
39. Yang Y, Chen F, Chen HY, Peng H, Hao H, Wang KJ. A novel antimicrobial peptide scyreprocin from mud crab *Scylla paramamosain* showing potent antifungal and anti-biofilm activity. *Front Microbiol* (2020) 11:1589. doi: 10.3389/fmicb.2020.01589
40. Deepika A, Makesh M, Rajendran KV. Development of primary cell cultures from mud crab, *Scylla serrata*, and their potential as an in vitro model for the

replication of white spot syndrome virus. *In Vitro Cell Dev Biol: Anim* (2014) 50:406–16. doi: 10.1007/s11626-013-9718-x
41. Qiao K, Zhang YQ, Wang SP, Zhe AN, Hao H, Chen FY, et al. The optimization of primary hemocyte culture of *Scylla paramamosain*. *China Anim Husbandry Vet Med* (2014) 41:145–9.
42. Cheng CH, Ma HL, Deng YQ, Feng J, Jie YK, Guo ZX. Effects of *Vibrio parahaemolyticus* infection on physiological response, histopathology and transcriptome changes in the mud crab (*Scylla paramamosain*). *Fish Shellfish Immunol* (2020) 106:197–204. doi: 10.1016/j.fsi.2020.07.061
43. Liu S, Chen G, Xu H, Zou W, Yan W, Wang Q, et al. Transcriptome analysis of mud crab (*Scylla paramamosain*) gills in response to Mud crab reovirus (MCRV). *Fish Shellfish Immunol* (2017) 60:545–53. doi: 10.1016/j.fsi.2016.07.033
44. Xie C, Chen Y, Sun W, Ding J, Zhou L, Wang S, et al. Transcriptome and expression profiling analysis of the hemocytes reveals a large number of immune-related genes in mud crab *Scylla paramamosain* during *Vibrio parahaemolyticus* infection. *PloS One* (2014) 9:e114500. doi: 10.1371/journal.pone.0114500
45. Wang W, Wang G, Zhuo X, Liu Y, Tang L, Liu X, et al. C-type lectin-mediated microbial homeostasis is critical for *Helicoverpa armigera* larval growth and development. *PloS Pathog* (2020) 16:e1008901. doi: 10.1371/journal.ppat.1008901
46. Li J, Bi J, Zhang P, Wang Z, Zhong Y, Xu S, et al. Functions of a C-type lectin with a single carbohydrate-recognition domain in the innate immunity and movement of the red flour beetle, *Tribolium castaneum*. *Insect Mol Biol* (2021) 30:90–101. doi: 10.1111/imb.12680
47. Zuber R, Shaik KS, Meyer F, Ho HN, Speidel A, Gehring N, et al. The putative C-type lectin Schlaff ensures epidermal barrier compactness in *Drosophila*. *Sci Rep* (2019) 9:5374. doi: 10.1038/s41598-019-41734-9
48. Wei X, Liu X, Yang J, Wang S, Sun G, Yang J. Critical roles of sea cucumber C-type lectin in non-self recognition and bacterial clearance. *Fish Shellfish Immunol* (2015) 45:791–9. doi: 10.1016/j.fsi.2015.05.037
49. Wang L, Wang L, Yang J, Zhang H, Huang M, Kong P, et al. A multi-CRD C-type lectin with broad recognition spectrum and cellular adhesion from *Argopecten irradians*. *Dev Comp Immunol* (2012) 36:591–601. doi: 10.1016/j.dci.2011.10.002
50. Wang W, Gong C, Han Z, Lv X, Liu S, Wang L, et al. The lectin domain containing proteins with mucosal immunity and digestive functions in oyster *Crassostrea gigas*. *Fish Shellfish Immunol* (2019) 89:237–47. doi: 10.1016/j.fsi.2019.03.067
51. Yunger E, Safra M, Levi-Ferber M, Haviv-Chesner A, Henis-Korenblit S. Innate immunity mediated longevity and longevity induced by germ cell removal converge on the C-type lectin domain protein IRG-7. *PloS Genet* (2017) 13:e1006577. doi: 10.1371/journal.pgen.1006577
52. Wang KJ, Huang WS, Yang M, Chen HY, Bo J, Li SJ, et al. A male-specific expression gene, encodes a novel anionic antimicrobial peptide, scygonadin, in *Scylla serrata*. *Mol Immunol* (2007) 44:1961–8. doi: 10.1016/j.molimm.2006.09.036
53. Wang KJ, Huang WS, Yang M, Cai JJ. Scygonadin, a novel male-specific anionic antibacterial protein from *Scylla serrata* (forskål, 1775). *FASEB J* (2006) 20:A974–4. doi: 10.1096/fasebj.20.5.A974-a
54. Huang WS, Wang KJ, Yang M, Cai JJ, Li SJ, Wang GZ. Purification and part characterization of a novel antibacterial protein Scygonadin, isolated from the seminal plasma of mud crab, *Scylla serrata* (forskål, 1775). *J Exp Mar Biol Ecol* (2006) 339:37–42. doi: 10.1016/j.jembe.2006.06.029
55. Qiao K, Xu WF, Chen HY, Peng H, Zhang YQ, Huang WS, et al. A new antimicrobial peptide SCY2 identified in *Scylla Paramamosain* exerting a potential role of reproductive immunity. *Fish Shellfish Immunol* (2016) 51:251–62. doi: 10.1016/j.fsi.2016.02.022
56. Huang X, Li T, Jin M, Yin S, Wang W, Ren Q. Identification of a *Macrobrachium nipponense* C-type lectin with a close evolutionary relationship to vertebrate lectins. *Mol Immunol* (2017) 87:141–51. doi: 10.1016/j.molimm.2017.04.009
57. Thakur R, Shankar J. Strategies for gene expression in prokaryotic and eukaryotic system. In: VC Kalia, AK Saini, editors. *Metabolic Engineering for Bioactive Compounds: Strategies and Processes*. Singapore: Springer Singapore (2017). p. 223–47.
58. Watson JD, Baker TA, Bell SP, Gann A, Levine M, Losick R. *Molecular Biology of the Gene 5th ed.* Benjamin Cummings: Cold Spring Harbor Laboratory Press (1976).
59. Guo XN, Jin XK, Li S, Yu AQ, Wu MH, Tan SJ, et al. A novel C-type lectin from *Eriocheir sinensis* functions as a pattern recognition receptor with antibacterial activity. *Fish Shellfish Immunol* (2013) 35:1554–65. doi: 10.1016/j.fsi.2013.08.021
60. Cerenius L, Soderhall K. The prophenoloxidase-activating system in invertebrates. *Immunol Rev* (2004) 198:116–26. doi: 10.1111/j.0105-2896.2004.00116.x
61. Nappi A, Poirie M, Carton Y. The role of melanization and cytotoxic by-products in the cellular immune responses of *Drosophila* against parasitic wasps. *Adv Parasitol* (2009) 70:99–121. doi: 10.1016/S0065-308X(09)70004-1
62. Jin XK, Guo XN, Li S, Wu MH, Zhu YT, Yu AQ, et al. Association of a hepatopancreas-specific C-type lectin with the antibacterial response of *Eriocheir sinensis*. *PloS One* (2013) 8:e76132. doi: 10.1371/journal.pone.0076132
63. Zhang XW, Wang Y, Wang XW, Wang L, Mu Y, Wang JX. A C-type lectin with an immunoglobulin-like domain promotes phagocytosis of hemocytes in crayfish *Procambarus clarkii*. *Sci Rep* (2016) 6:29924. doi: 10.1038/srep29924
64. Zhang XW, Liu YY, Mu Y, Ren Q, Zhao XF, Wang JX. Overexpression of a C-type lectin enhances bacterial resistance in red swamp crayfish *Procambarus clarkii*. *Fish Shellfish Immunol* (2013) 34:1112–8. doi: 10.1016/j.fsi.2013.01.020
65. Huang X, Feng JL, Jin M, Ren Q, Wang W. C-type lectin (MrCTL) from the giant freshwater prawn *Macrobrachium rosenbergii* participates in innate immunity. *Fish Shellfish Immunol* (2016) 58:136–44. doi: 10.1016/j.fsi.2016.08.006
66. Li M, Li C, Ma C, Li H, Zuo H, Weng S, et al. Identification of a C-type lectin with antiviral and antibacterial activity from pacific white shrimp *Litopenaeus vannamei*. *Dev Comp Immunol* (2014) 46:231–40. doi: 10.1016/j.dci.2014.04.014
67. Utarabhand P, Thepnarong S, Runsaeng P. Lipopolysaccharide-specific binding C-type lectin with one CRD domain from *Fenneropenaeus merguiensis* (FmLC4) functions as a pattern recognition receptor in shrimp innate immunity. *Fish Shellfish Immunol* (2017) 69:236–46. doi: 10.1016/j.fsi.2017.08.028
68. Wang XW, Zhao XF, Wang JX. C-type lectin binds to beta-integrin to promote hemocytic phagocytosis in an invertebrate. *J Biol Chem* (2014) 289:2405–14. doi: 10.1074/jbc.M113.528885
69. Chen DD, Meng XL, Xu JP, Yu JY, Meng MX, Wang J. PcLT, a novel C-type lectin from *Procambarus clarkii*, is involved in the innate defense against *Vibrio alginolyticus* and WSSV. *Dev Comp Immunol* (2013) 39:255–64. doi: 10.1016/j.dci.2012.10.003
70. Liang Z, Yang L, Zheng J, Zuo H, Weng S, He J, et al. A low-density lipoprotein receptor (LDLR) class A domain-containing C-type lectin from *Litopenaeus vannamei* plays opposite roles in antibacterial and antiviral responses. *Dev Comp Immunol* (2019) 92:29–34. doi: 10.1016/j.dci.2018.11.002

Conflict of Interest: The authors declare that the research was conducted in the absence of any commercial or financial relationships that could be construed as a potential conflict of interest.

frontiers in Immunology

REVIEW
published: 13 May 2021
doi: 10.3389/fimmu.2021.667787

A Comprehensive Review on Crustaceans' Immune System With a Focus on Freshwater Crayfish in Relation to Crayfish Plague Disease

Younes Bouallegui *

LR01ES14 Laboratory of Environmental Biomonitoring, Faculty of Sciences of Bizerte, University of Carthage, Bizerte, Tunisia

Freshwater crayfish immunity has received great attention due to the need for urgent conservation. This concern has increased the understanding of the cellular and humoral defense systems, although the regulatory mechanisms involved in these processes need updating. There are, however, aspects of the immune response that require clarification and integration. The particular issues addressed in this review include an overall description of the oomycete *Aphanomyces astaci*, the causative agent of the pandemic plague disease, which affects freshwater crayfish, and an overview of crustaceans' immunity with a focus on freshwater crayfish. It includes a classification system of hemocyte sub-types, the molecular factors involved in hematopoiesis and the differential role of the hemocyte subpopulations in cell-mediated responses, including hemocyte infiltration, inflammation, encapsulation and the link with the extracellular trap cell death pathway (ETosis). In addition, other topics discussed include the identity and functions of hyaline cells, the generation of neoplasia, and the emerging topic of the role of sessile hemocytes in peripheral immunity. Finally, attention is paid to the molecular execution of the immune response, from recognition by the pattern recognition receptors (PRRs), the role of the signaling network in propagating and maintaining the immune signals, to the effector elements such as the putative function of the Down syndrome adhesion molecules (Dscam) in innate immune memory.

Keywords: hemocytes, hyaline cells, hematopoiesis, etosis, *Aphanomyces astaci*

OPEN ACCESS

Edited by:
Luciane M. Perazzolo, Federal University of Santa Catarina, Brazil

Reviewed by:
Jing Xing, Ocean University of China, China
WeiWei Li, East China Normal University, China

***Correspondence:**
Younes Bouallegui
bouallegui_younes@outlook.com

Specialty section:
This article was submitted to Comparative Immunology, a section of the journal Frontiers in Immunology

Received: *14 February 2021*
Accepted: *27 April 2021*
Published: *13 May 2021*

Citation:
Bouallegui Y (2021) A Comprehensive Review on Crustaceans' Immune System With a Focus on Freshwater Crayfish in Relation to Crayfish Plague Disease. Front. Immunol. 12:667787. doi: 10.3389/fimmu.2021.667787

INTRODUCTION

The large decline in the number of the European indigenous freshwater crayfish caused by repetitive outbreaks has brought such organisms close to extinction (e.g., *Astacus astacus*) (1–3). Scientists have raised their concerns about the natural stock of endangered crayfish species, boosting investigations to uncover the causes for conservation purposes. The crayfish plague disease, reported as the main threat to this species is linked to the accidental or commercial relocation of invasive species like the North American species (e.g., *Pacifastacus leniusculus* and *Procambarus clarkii), a* vector of the oomycete *Aphanomyces astaci*, the causative agent of the disease (4–6). The disease's most characteristic symptoms are common spots of melanin in the cuticle of infected or

dead individuals. Extensive studies have demonstrated that such melanin spots (i.e., melanization) are the result of the immune response aiming to enclose the pathogen in melanin sheaths to prevent it from invading and grow into the hemocoel (7–11). *A. astaci* is capable of infecting indigenous and invasive crayfish species equally, however, the latter are less vulnerable (*P. leniusculus, C. quadricarinatus, and Procambarus clarkii*) (1, 8, 12). However, vulnerable indigenous European species like *A. astacus*, mostly showed very few or almost no formation of melanized spots, while the development of hyphae was recorded. The differential immune response between indigenous and invasive species is among the main clues that need to be studied and has driven investigations related to crayfish immunity (4, 13, 14). In this context, the activation of the prophenoloxidase (ProPO) system, the process responsible for melanin formation, has been extensively studied (15–21). Interestingly, previous studies have demonstrated that encapsulation is a mandatory process that triggers the activation of the ProPO system (22–24). However, functional mechanisms linking cooperative actions of the humoral- and cell-mediated responses of the innate immunity, need to be considered further (18, 25). In doing so, the relationships between melanization, pathogen encapsulation, and immune cell production (i.e., hematopoiesis) need to be elucidated and integrated to the reported decrease in the number of circulating hemocytes (i.e., total hemocyte count [THC]), during infection (14–17, 26–31). In this context, the immune modulation of freshwater crayfish against *A. astaci* is still hampered by a smaller integration of the components of functional defenses (17, 32). In this review we tried to compile different components of the crayfish immune response, related strategies, and debated topics in one paper, aiming to make a comprehensive and integrated synopsis of the crayfish immune system available that might advance the understanding of this topic.

APHANOMYCES ASTACI: CAUSATIVE AGENT OF THE CRAYFISH PLAGUE DISEASE

The pathogen *Aphanomyces astaci* (Shikora, 1906) is a pathogenic oomycete native to North America and only colonizes aquatic decapods. It is listed among the world's 100 worst invasive alien species (3, 33). The oomycetes, the so-called water molds, belong to the genus *Aphanomyces* and are members of the *Ooomycotina*, *Eumycota* family, which are not true fungi but more closely related to brown algae and diatoms (8, 33). *A. astaci* is a non-septate, branching fungus belonging to the *Saprolegniaceae* family, with 7-10 micron thick hyphae and biflagellate zoospores assuring their asexual reproduction. The life cycle comprises a relatively short-lived swimming zoospore stage that ends with encasement (12). Encysted spores drop or retract their flagella to be able to encase into the cell wall covered by sticky substances assuring their adherence to the host. Shortly after, a period of hyphal growth within the host starts and the emerging hyphae penetrate the host's cuticle (8, 12). So far, 5 strains of *A. astaci* have been identified and characterized to belong to 5 different genotypes thanks to random amplified polymorphic DNA (RAPD) (2, 34, 35). Such genotypes are referred to as groups 1, 2, 3, and 4, or as the *Astacus* strain, the *Pacifastacus* strain I, the *Pacifastacus* strain II, and the *Procambarus* strain, which can be abbreviated to As, PsI, PsII, Pc, and Or, respectively. The As-strain is referred to as *Astacus*, and is the first genus from which this strain was identified since the original host has not yet been identified or found. The original host of PsI and PsII is the crayfish species *Pacifastacus leniusculus* (Dana, 1852), the original hosts of the Pc and Or genotypes are *Procambarus clarkii* (Girard, 1852), and *Orconectes limosus* (Rafinesque, 1817), respectively (2, 10, 34, 36, 37). The As-genotype was thought to be responsible for the first outbreaks in Europe following its transmission in the 19th century. In contrast to North American crayfish species, which maintain a relatively stable interaction with *A. astaci*, Asian, Australian, and European crayfish species are highly susceptible to the pathogen. However, recent reports have recorded differential virulence of different *A. astaci* strains to different European species (36, 37). Laboratory experiments demonstrated that PsI was found to be the most virulent causing all the noble crayfish *Astacus astacus* to die within few days, while the As strain was found to be the less virulent in general (36). Overall, a devastating impact on European-native crayfish species has been recorded, which drastically declined their natural stock and so far has led to numerous species being listed at "risk of extinction" (34). Many studies have attributed this drastic effect to the inability of such species to respond efficiently to prevent the spread of *A. astaci*. Thus, the oomycete is capable of killing almost 100% of the individuals within an infected population in a few days (8, 10, 12). Infected individuals of vulnerable species are incapable of preventing hyphae growth in their hemocoel, in contrast to resistant species, which have been reported to extensively respond by triggering their immune system after interaction with the oomycete cell wall (1,3-β-glucan). This stimulates the activation of the prophenoloxidase system producing cytotoxic compounds and melanin to ensure the encapsulation of the pathogen in the cuticle and prevent it from completely colonizing the hemocoel (8, 34). There is no efficient treatment for the disease, nor has there been a successful strategy recorded to help mitigate the pathogen's effects. However, a deep understanding of defense mechanisms, which has greatly increased nowadays, is still the most promising way to design an accurate strategy to overcome this threatening situation.

EPIDEMIOLOGY AND PREVALENCE OF THE PATHOGEN *APHANOMYCES ASTACI*

Aphanomyces astaci outside of North America is considered as an alien species. The first evidence for its introduction into Europe marked by the first mass mortality among European native crayfishes occurred in 1859 in the Po River basin in northern Italy, which has deeply threatened populations of the Italian white-clawed crayfish *Austropotamobius pallipes* (38).

These followed later by several outbreaks in the Plateau des Langres at the Franco-German frontier area, in 1874 (38). The following decades, witnessed steady spreads of the pathogen to other European countries following main two directions, down the Danube river into the Balkans ending in the Black Sea, and across North Germany into Russia. From there, the distribution occurred toward the south again to the Black Sea, and onto north-west to Finland and, in 1907, to Sweden. And since, that time it has spread across most of Europe. However, in 1960s, the first pandemics were reported in Spain, and two decades later the disease spread far to the British Isles, Turkey, Greece and Norway (39). Currently, the distribution of *A. astaci*, is confirmed to be present in other continents rather than native, and classic localities across Europe, like South America, Japan (40). Introductions of invasive crayfish species in many sites around the world for aquaculture purposes have been usually found to be coupled by A. astaci. However, no further data has been recorded about the distribution of A. astaci in Africa, Central America, South America, and other parts of east and south Asia (40). Australia and New Zealand have not experienced any outbreaks of crayfish plague to date and are currently considered plague free area (40). The actual distribution of A. astaci is therefore likely to be far broader than the distribution table would suggest.

Very recently, the occurrence of chronic infections in native European crayfish populations were documented, however such phenomenon still newly reported, and underlying mechanisms and factors remain scarce and need to be investigated further (1, 11, 37). Recent assessments on the potential of freshwater crabs, and shrimp (11, 37, 41) to be as alternative hosts have been conducted to rule out non-lethal effects in the absence of any mass mortality. The following is an integrated illustration of the recent findings on the crayfish immune system.

GENERAL DESCRIPTION OF CRAYFISH IMMUNITY

Like all invertebrates, crustaceans, including crayfish, only rely on innate immunity, which constitutes humoral- and cellular-mediated responses (**Figure 1**) (17, 18, 29, 30, 42). Lack of acquired (specific) immune response in crayfish is due to the lack of myeloid lineage cells being able to produce immunoglobulins (specific antibodies) against specific pathogens in the event of

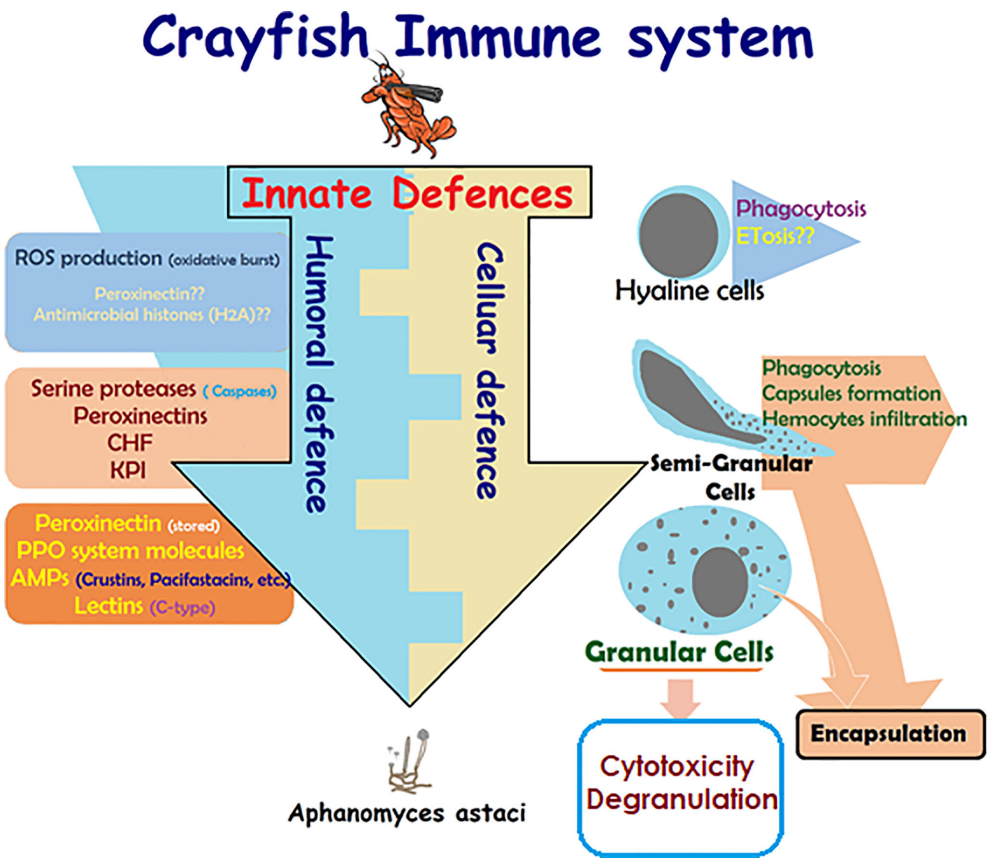

FIGURE 1 | Schematic presentation of crayfish immune response. Presentation of the main constituents of crayfish immune response alongside the cooperative action of the cellular-mediated and humoral-mediated responses and their corresponding factors (4, 5, 14, 17, 18, 26, 28–30, 42–54).

repetitive infections (lack of memory). This lack of acquired immune response was found to be balanced by the enrichment of different cell-mediated strategies and several multi-type humoral factors, both constituting the innate defenses of the crayfish immunity (**Figure 1**) [e.g., multiple pathogen recognition receptors (PRRs)] (28, 42). These defenses are activated in a cooperative way in order to initiate effective defensive actions and can be classified according to two main responses: a humoral-mediated response involving humoral factors produced and released by the immune cells (antimicrobial peptides, hydrolytic enzymes, and molecules of the ProPO system, etc.), and a cell-mediated response that requires a direct action of the cell itself, such as phagocytosis, initiating the cell death pathway mechanisms (e.g., cytotoxicity, encapsulation) (**Figure 1**).

Cell-Mediated Immune Response

Cell-mediated responses require the direct action of the cell itself to neutralize alien invaders through mechanisms like phagocytosis, cell death pathways (e.g., apoptosis and autophagy), and inflammatory response (e.g., nodule formation and encapsulation). These strategies share a common prerequisite, which is hemocyte infiltration (hemocytosis), or the excessive migration of hemocytes from circulation to the infection site.

Changes in hemocytes' shape and/or features, in addition to surveying the total hemocyte number (THC), and differential hemocyte count (DHC), as well as the assessment of defensive activities like phagocytosis, cell viability, cytotoxicity, and different physiological changes, have been considered useful assays to investigate the crayfish immune response modulation (4, 26, 43–45). Hemocytosis requires extensive recruitment and infiltration of hemocytes into tissues where infections/stress have been detected (25, 30, 32, 55, 56). Hemocyte infiltration may result in structural modifications of the histology of target tissue near the infection-surrounding microenvironment (56–66). Inflammatory response and histopathological assessments linked to hemocyte infiltration have been integrated into a single quantitative index using multiple histopathological traits for a more sensitive discrimination of the health status of assessed organisms like bivalves and fish aiming to develop an accurate system for assessing the health status of farmed animals (67–70). However, very few studies have been conducted on crayfish histopathology. Interestingly, studies using hemocyte parameters as a tool for assessing the modulation of the immune response in crustacean (mainly THC and DHC describing the fall in the number of circulating hemocytes due to their recruitment to infected tissues, to block pathogens from disseminating the hemocel), could be inter-correlated with quantitative histopathological assessments for more accurate hemocyte parameter data and integrative conclusions (4, 14, 15, 18, 24, 26).

It is worth noting that the activation of melanin production by the ProPO system in crustacean defenses might be disrupted due to a lack of the appropriate number of hemocytes needed to fulfill such a role. This finding has been highlighted in *Astacus astacus* infected with *Aphanomyces astaci*, and has been linked to the lack of melanization in infected tissues that present hyphae development, which is not the case in invasive species like *Pacifastacus leniusculus* (species showing resistance to *A. astaci*) (4, 5, 46). In this context, it would be interesting to illustrate the characteristics of hemocytes (and their different sub-populations), the key element of the crayfish immune response, which will be detailed in the following sections.

CLASSIFICATION OF HEMOCYTE SUB-POPULATIONS

Morphological Characterization/ Classification

Hemocytes, the key element of the crayfish immunity, participate in almost every defensive activity through direct action (e.g., phagocytosis, capsule formation), in addition to their production of most humoral factors (17). Hemocytes have been described and characterized since the early 1880s by Carus as reported in (47). Hemocyte sub-populations were classified in general following morphological characterization according to the size of the cell, and the structural complexity of their cytoplasm (i.e., nucleus/cytoplasm ratio and the presence/absence of granules) (15, 24, 26, 71). Such characterization was mostly consolidated by a functional/cytochemical classification of each sub-population (i.e., dependent on the main defensive action and/or enzymatic activity through their enclosed granules, like peroxidase) (72–74). Last but not least, despite the significant progress recorded in these studies, the final number of crayfish hemocyte subpopulations has not yet been firmly determined. However, the oldest and most accepted clustering system presents three hemocyte sub-types: hyaline cells (HC) also called hyalinocytes, semi granular cells or hemocytes (SGC), and granular cells or hemocytes (GC), also called granulocytes (26, 48, 49). The general characteristics are summarized in **Table 1** below. Hyaline cells (HC) are described as the smallest cell type,

TABLE 1 | Summary of the three hemocyte sub-populations' characteristics.

Hemocyte sub-populations	Size (mean Ø)	Characteristics (structural complexity of cytoplasm)
Hyaline cells (HC)	10 µm	• Oval-shaped cells • High nucleus-to-cytoplasm ratio • Euchromatic centered nucleus • Very few granules
Semi-granular cells (SGC)	15 µm	• Low nucleus-to-cytoplasm ratio • Elongated cells • Large central nucleus • Well-developed organelles (rough endoplasmic reticulum) • Numerous granules
Granular cells (GC)	21 µm	• Very low nucleus-to-cytoplasm ratio • Spindle-shaped cells • Enclosed nucleus; finely dispersed nucleoplasm • Large, well developed, structureless lemon-like granules

while SGC typically feature an elongated shape. On the other hand, GC is described as the largest cell-type (43–46, 50, 51).

Functional Characterization

Functional activities of each hemocyte sub-type still are still the cause of some controversy (5, 14). This classification started to be elucidated by the early 1980s, however, separation techniques developed by Smith and Söderhäll at that time (1983) greatly advanced the detailed description of said functional activities (26). In this context, hyaline cells were described as phagocytic cells, semi granular cells were the main type ensuring encapsulation, and granular cells were mainly specialized in storing/releasing active molecules such as prophenoloxidase (pro-PO) system molecules within/from their well-developed granules (14, 15, 18, 24, 26, 27). However, all the sub-types mentioned were reported to be involved in the immune response with differential efficiencies toward mechanistic processes (18, 43, 45, 52–54). For example, for the most studied crayfish species (e.g., *Astacus astacus, Pacifastacus leniusculus*, *Cherax quadricarinatus*, and *Procambarus clarkii*), semi granular cells are described as the most important family in immune reactivity, involving capsule formation, encapsulation and assuring moderate phagocytic activity in addition to melanization through activation of ProPO cascading reactions (4, 14, 43, 45). ProPO activation is the main role of granular cells that do not present any phagocytic activity. The phagocytic function has been mainly allocated to hyaline cells (**Figure 1**). Unfortunately, many investigations (*in vitro* and *in vivo*) reported controversial data about the functional activity of hyaline cells (43, 45) and this is due to their very small presence in circulation. The scarce presence/putative function of hyaline cells and their importance has been exacerbated by the lineage paradigm of different types of immune cells, which consists of immune cell proliferation exclusively occurs in the hematopoietic tissue, therefore only very well differentiated and mature cells are released into circulation. Mature semi-granular as well as granular cells cannot be fully activated until released into circulation (47, 53, 75). Unfortunately, HC are cells with the characteristics of immature undifferentiated cells (presenting proliferative phenotype, expressing PCNA; commonly called pro-hemocytes). HC, have been described to be released under certain circumstances, mainly after an immune challenge (46, 47) and so they have drawn attention to the existence and functions of such cell types (detailed in the following sections).

Molecular Markers of Different Hemocyte Sub-populations

Further, many transcriptomic and proteomic studies have helped classify hemocyte cell-types, following specific molecular markers expressed by each type, and have improved their functional characterization (5, 46, 76). The PIRunt transcription factor has been reported as not being expressed in less mature cells, whereas it is marked simultaneously with the ProPO in the SGC and CG. More extension of ProPO to GC has been demonstrated. Furthermore, immunohistochemical studies reported the presence of superoxide dismutase (SOD) in SGC and GC, however, mRNA expression studies demonstrated that GC produces SOD (as monomers), which attaches to the outside of SGC (dimeric). More specifically, a Kazal-type proteinase inhibitor (KPI) and crustacean hematopoietic factor (CHF) were reported as being exclusively expressed by SGC (more details can be found in 5, 73, 62, 76). Very recent studies have shown that hemocytes of the freshwater crayfish *P. leniusculus* express two types of transglutaminases, commonly named Pl_TGase1 and Pl_TGase2, and have evidenced that such TGs are specific to different hemocyte sub-populations (77). Pl_TGase1 was only expressed in SGC, but not expressed by all SGCs, and Pl_TGase2 was only expressed in GC, and again not expressed by all GCs (77).

It's worth to note that benefit from advanced single-cell RNA-sequencing (scRNAseq) technologies, in recent years, provide substantial improvement in reporting the hemocyte sub-type of the fly Drosophila, which has been largely renewed from only three sub-types: plasmatocytes, crystal cells, and lamellocytes to generating a comprehensive gene expression profiles for the drosophila circulating' hemocytes. In fact, Fu et al. have identified two new hemocytes' sub-types in Drosophila: thanacytes and primocytes with differential sets of genes (78). However, thanacytes expresses genes involved in distinct responses to different types of bacteria, while primocytes expresses cell fate, and signaling genes, potentially involved in keeping stem cells in the circulating blood. In addition to four other novel plasmatocytes subtypes (Ppnþ, CAH7þ, Lspþ and reservoir plasmatocytes), each with unique molecular markers and distinct predicted functions (78). Further study conducted by Tattikota et al., aimed to use scRNAseq in mapping hemocytes across different inflammatory conditions in larvae. Subsequently, different genes expression-based states of plasmocytes have been resolved (79). In addition, a rare subsets of crystal cells expressing the fibroblast growth factor (FGF) ligand branchless, and lamellocytes expressing receptor breathless, have been reported. FGF components are required for mediating effective immune responses against parasitoid wasp eggs. As perspective, scRNAseq analysis consists a very urgent needed analysis that should be performed to decipher the gene expression profiles for a systems-level understanding of the diversity of crayfish hemocytes, and their functions.

Production of Hemocyte Sub-populations: The Hematopoiesis

Hematopoietic processes are among the most studied and have been really well described in studies related to crayfish immunity, aiming to decipher mechanisms underlying insufficient immune response against diseases like the plague disease (75, 80–82). Overall, investigations conducted by Söderhälls (Kenneth and Irene) and coworkers, resulted in an almost complete overview of molecular mechanisms that generate different hemocyte sub-families (47, 53, 82). In brief, the hematopoietic tissue in *P. leniusculus* contains four to five cell lineages arranged in lobules surrounded by connective tissue localized starting around the brain and following the ophthalmic artery to the posterior HPT, and ending by covering the dorsal part of the stomach (**Figure 2**)

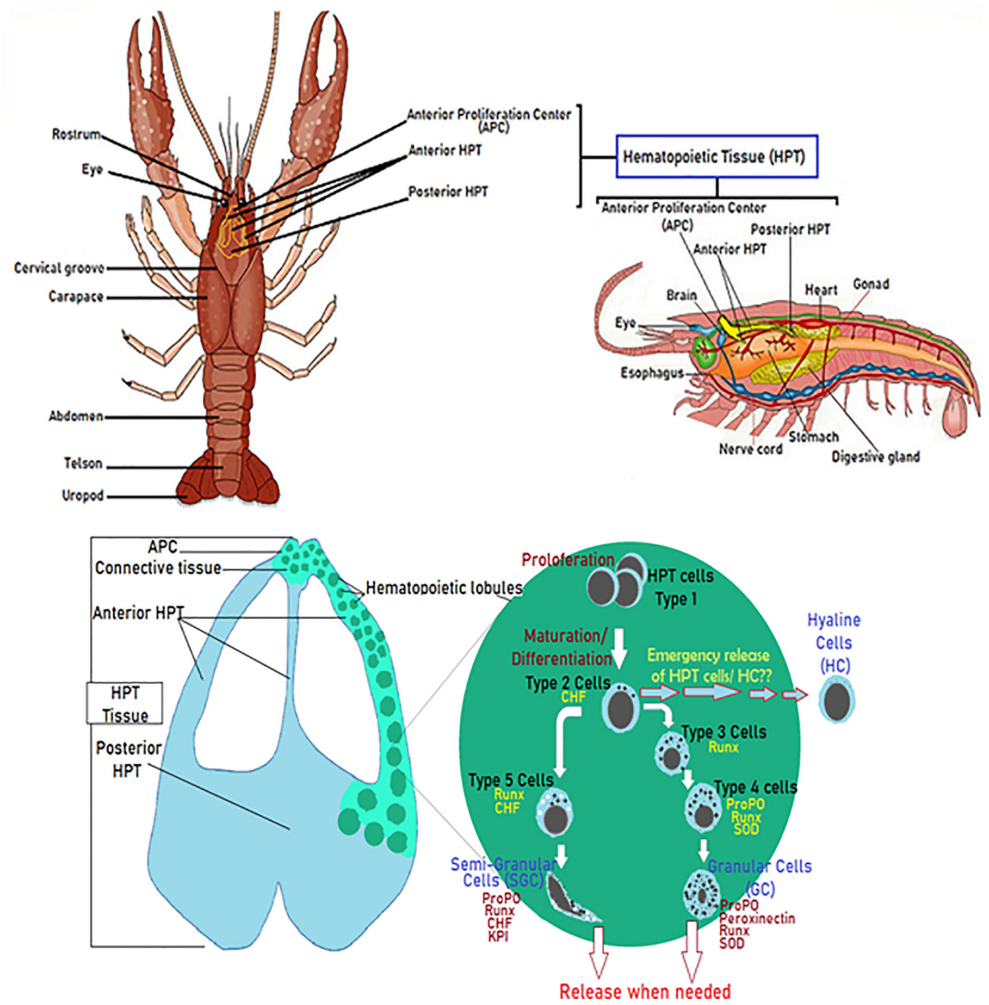

FIGURE 2 | Diagram of the hematopoietic tissue (HPT) illustrating the hematopoiesis' mechanistic steps. Schematic localization and presentation of the different parts of the HPT and the hematopoietic lobules illustrating the different phases of hemocyte production and how different cell types (Type I-V) acquire their specific molecular markers (47, 53, 75, 80–84).

(47, 53). HPT cells are clustered into lobules of 10 cell clusters for each lobule (47, 75, 80, 83, 84). Cell morphology within such lobules is similar to different areas of the posterior HPT, with low mitotic activity in the center tissue that surrounds the ophthalmic artery. In contrast, high mitotic activity has been detected along the edges of HPT and the anterior proliferation center (APC), (**Figure 2**) (47, 75, 83). HPT cells clustered into as type I to type V cells, with type I have the characteristics of undifferentiated cells without or with few granules (high mitotic figures and expression of PCNA), located in the apical part of the lobule where proliferation (extensive division) of precursor/stem cell occurs. Tending towards the center of the lobule, cells being more determined, and differentiated. Type II-IV cells are distally arranged starting with the type II cells, all presenting granules. Type III and IV found between lobules separated from each other, do not show divisive activities and ready to be easily freed as mature hemocytes into circulation (47, 82). Type V showed granules morphologically distinct from other types (**Figure 2**) (47, 75, 80, 82, 83).

The hematopoiesis involves several key molecular factors like Astakines (1 and 2), cytokine-like proteins that contain a prokineticin domain (PK), and playing the role of the growth factor hormone to stimulate the production and release of new hemocytes into circulation. Astakines acts through the reduction of the activity of transglutaminase (TGs) (**Figure 3**) (75, 83–89). TGs are Ca2+-dependent cross-linking enzymes with substrate is the type IV collagen, involved in coagulation and controlling hematopoiesis and extracellular matrix organization in crayfish (84, 88, 91, 92). TGs aims to inhibit stem cell differentiation and migration, which is closely dependent to ROS signaling (**Figure 3**). Astakine 1 was shown to stimulate differentiation along with SGC, through inducing the crustacean hematopoietic factor (CHF) to inhibits stem cell apoptosis and stimulates their differentiation and migration (75). Although, Astakine 2 most

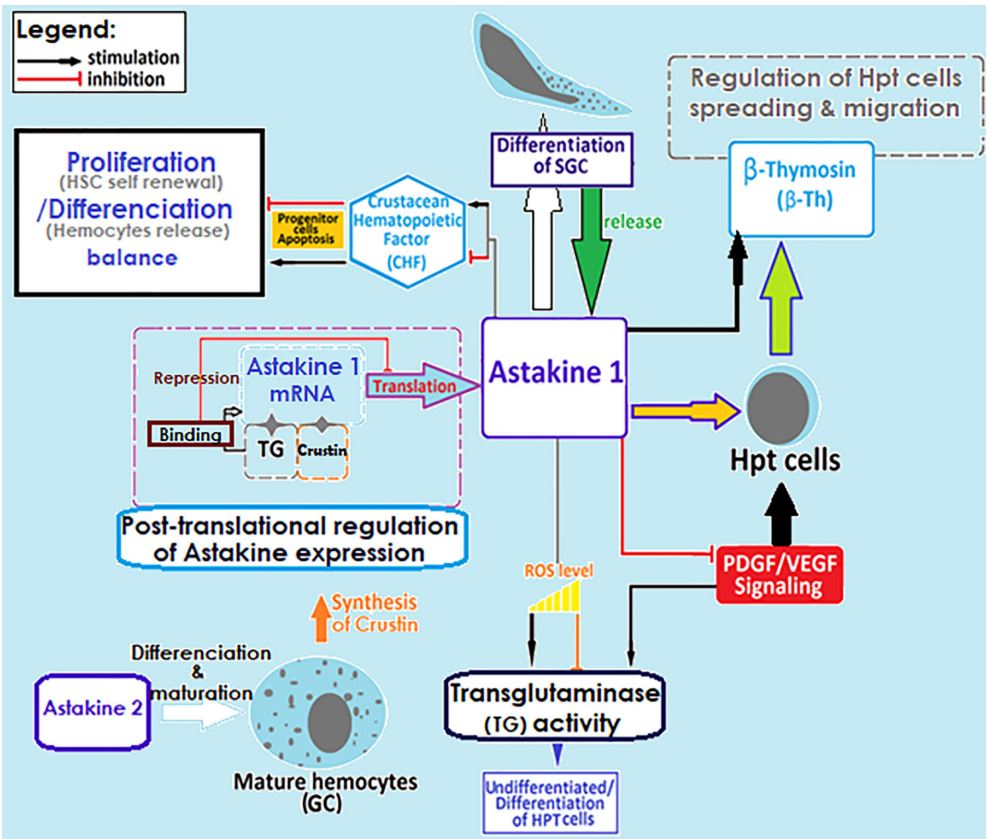

FIGURE 3 | Regulation of crayfish hematopoietic mechanisms. Molecular factors involved in the regulation of hemocyte production. SGC, semi granular cells; GC, granular cells; TG, transglutaminase; ROS, reactive oxygen species; HPT cell, hematopoietic cells; HSC, hematopoietic stem cells (29, 45, 47, 75, 83–97).

probably plays a role in the differentiation of GC (47, 75, 89). Astakine expression and release were reported to be induced by a bacterial infection (LPS), fungal challenge, and tissue injury (84, 86, 87, 91). Moreover, crayfish' hemocytes reported as to be precursor for new neuron formation, and renewal of the nervous system in adult crayfish (93–95). Also, β-thymosin proteins are known for their actin-binding activity, and have been reported to interfere with Astakine in inducing hemocytes production and migration from the HPT (**Figure 3**) (96). In this same context, it is important to highlight the role of transglutaminase and crustin, a cysteine-rich anti-microbial peptide, as RNA binding proteins with a down-regulation role in post-transcriptional regulations for Astakine 1 expression (47, 97) (**Figure 3**).

INTEGRATION OF THE CRAYFISH' IMMUNE COMPONENTS INTO FUNCTIONAL MECHANISMS

Role of Hemocyte Sub-populations in Mounting an Encapsulation

A large parasite that cannot be phagocytosed nor engulfed by hemocytes triggers the recruitment of new hemocytes into the infection site to isolate the invader by what is known as encapsulation. Such a process is usually accompanied by the activation of the ProPO system and the formation of a melanin sheath around the pathogen, which should be digested by quinones resulting from PO cascading reactions. These aim to neutralize the pathogen and prevent it from disseminating the hemocel (16, 21, 26, 98). Overall, inflammation consists of several successive steps starting with the recognition step of pathogens and/or sensing tissue damages (16, 17, 28, 30), followed by the recruitment of immune cells to the infected/damaged site, where additional effector molecules, such as clotting proteins (e.g., peroxinectins and transglutaminase), would be generated and released by these cells to consolidate pathogen isolation (i.e., capsule formation) (4, 14, 26, 84, 85, 88, 92, 99, 100) (**Figure 3**). These activities may also initiate further recruitment of neo-formed hemocytes through the secretion of cytokine-like proteins (Astakine 1 and 2), which stimulate stem cell proliferation and new hemocyte maturation (83, 85). However, Persson et al. (14) demonstrated in an *in vitro* assessment that capsule formation is mainly assured by semi-granular cells that are recruited and flattened to form aggregates around different spherules. Such capsules later develop into densely packed layers, which is not the case with granular cells forming less stable structures (4). In that same report, hyaline

cells are described as the type that never participates in any aggregate formation (4). Other studies have reported that the hemocyte type involved in encapsulation depends on insect order (101). Dubovskiy et al. (101) stated that granular cells are the first to come in contact with and aggregate around the invader, therefore releasing clotting proteins to facilitate the termination of the process (101). In the same context, Jiravanichpaisal et al. (18) found that granular and semi-granular cells in crayfish are cooperatively involved in encapsulation, whereas no functional involvement has been allocated to hyaline cells (**Figure 1**) (18, 30, 32, 102).

Prospective Role of the Extracellular Trap Cell Death Pathway (ETosis) in Encapsulation

Recent reports have highlighted the potential participation of HC in initiating encapsulation (32, 103). This finding has been demonstrated through the involvement of HC in implementing the extracellular trap cell death pathway (ETosis) in the crab *Carcinus maenas* (104, 105). In this context, it's worth highlighting that ETosis is a phenomenon which was first described in mammals and which can be triggered by inflammatory cells like neutrophils and other mammalian innate immune cells (105, 106). Such a phenomenon entails an extracellular expulsion of chromatin out of the nucleus intending to entrap and kill foreign invaders like bacteria, fungi, viruses, and parasites. ETosis requires the involvement and production of reactive oxygen species (ROS) through the NADPH oxidase enzyme complex and myeloperoxidase (32, 105). The inflammatory condition is described to favor the initiation of the process by de-condensing the nucleus within the cell and then expelling the cloud-like mesh of chromatin into the extracellular environment in a controlled manner (104, 105). Such material was found to be accompanied by antimicrobial agents (as antimicrobial peptides from granules and histones with antimicrobial functions as well) (107). ETosis has been recently found in some arthropods, bivalves, and cnidarians (103–105, 107). ETosis in the crab has been proved to be caused by the prohemocytes (homolog of HC in crayfish) (32, 103). Interestingly, SGC also seems to have the ability to release chromatin (103). Most importantly, ETosis greatly facilitates the encapsulation process through the entrapment of pathogens by expelled chromatin, and aids in assembling the flattened layers of hemocytes to form a sort of sheath around the foreign entity using the externalized chromatin as a scaffold during the early stage of encapsulation (32, 104, 105). Peroxinectins and histones (mainly H2A) were also found to be greatly involved in the early stages of encapsulation (103, 105, 107). The ETosis pathway needs to be investigated in crayfish to be confirmed as a potential immune strategy that could be assured or at least require to be initiated through the involvement of HC.

Sessile Hemocytes—Potential Role in the Immune Response

In contrast to circulating hemocytes in invertebrates, which are referred to as free wandering cells in the hemolymph, sessile hemocytes, also known as fixed phagocytes, are hemocytes that can migrate, infiltrate and inhabit different tissues and organs, due to the open circulatory system of invertebrates (30, 45, 101, 108, 109). Therefore, sessile hemocytes can inhabit in, and sometimes even be fixed to, different tissues (e.g., as in the central channel of the gills, arterioles, and hepatopancreas) (18, 110). Recently, the involvement of such cells in determining a proper immune response has been extensively studied, raising a putative role in immune defenses (108, 109). Amongst others, sessile hemocytes have been described to be involved in phagocytic activities aiming to clear foreign materials and substances from the hemocoel, and to accumulate debris within their giant vacuoles in some organs like the gills, and from the epithelium of the hepatopancreas (18, 30, 45, 110). More interestingly, a potential role of replenishment for circulating hemocytes, following immune challenge, has been suggested as a putative strategy *via* a third route rather than hematopoiesis (30, 45). Otherwise, still to be confirmed as a role of sessile hemocytes is that of signal delivery following pathogen recognition (through PRRs). This assumption has been corroborated by the fact that fixed hemocytes have resulted from the circulating hemocytes' ability to migrate, attach and penetrate the basement membrane by extravasations into infection sites, even before the pathogen enters, as reviewed in Butt et al. (102). Recent studies have aimed at investigating the immune functions of sessile hemocytes from three different organs of Kuruma shrimp and have demonstrated the fact that such hemocytes differentially expressed immune-related genes compared to circulating hemocytes (108, 109). From the above, it's highly important to note the ability of "peripheral" hemocytes of the eastern oyster *Crassostrea virginica* (described as pallial hemocytes; compared to those designated as sessile hemocytes in crustaceans) to ensure exchanges with circulatory hemocytes (111, 112). Such exchanges have been described as bi-directional transepithelial migrations, which proved to regulate the pathogenesis of its obligate parasite *Perkinsus marinus* (111, 112). Interestingly, it has been demonstrated that such peripheral hemocytes share common general characteristics with circulating ones but also display some differences in their cell surface phenotypes (112–114). Overall, reporting the characteristics and role of sessile hemocytes in crayfish defense strategies would help in improving the understanding of the crayfish immune response.

HYALINE CELLS AND NEOPLASIA-INTERFERENCE WITH THE IMMUNE RESPONSE

Since the development of the hemocyte' classification system into sub-populations in crayfish, there has been much debate about the function of hyaline cells (HC), in spite of their very little shown phagocytic activity (5, 26, 43, 45, 46, 53, 82). Recent studies have suggested that HC are in fact free wandering prohemocytes that might be released into circulation only under certain circumstances. This hypothesis has led to much

debate about HC's identity, which is described as having hematopoietic cells' characteristics' (undifferentiated, expressing PCNA) (43, 45, 47, 76). This, in the light of the paradigm that clustering cell proliferation (excessive divisions), as can be exclusively occurs in the hematopoietic tissue, have strongly increased controversy over the identity of HC (32, 46, 52, 53, 85, 103), could be explained by the possible triggering of a neoplastic disease (e.g., lymphoma-like disease or hemic neoplasia) (32, 43, 45). However, chronic inflammatory conditions like excessive release of Astakine1 (role of growth factor hormone), besides the recorded involvement of PDGV-factor within signaling processes, which may stimulate an angiogenesis profile, favoring appearance of neoplastic features (83, 115). It is worth noting that cells with peculiar shapes that mark the initiation of neoplasia and occurrence in crustaceans, have been already reported, which might be assumed as a potential process explaining the hemocytes' loss of immune capacity despite the recovery recorded in terms of number (i.e., increased THC after infections/challenges within different scenarios) (116).

Unfortunately, neoplasia in crayfish, and in crustaceans in general, hasn't been studied much. The scarcity of information on tumors in crustaceans has been attributed to the lack of accurate descriptions by experienced crustacean pathologists, and to the absence in most reported cases of histopathological examinations (116–119). Neoplastic features mostly exhibit nodules containing numerous anaplastic and hypertrophied/giant cells, with either one large nucleus or several small nuclei. At the tissue level, possible tissue lesions presenting structural disorganization and high amounts of undifferentiated pleomorphic cells with hypertrophied nuclei and prominent nucleoli, in addition to bizarre multipolar mitotic figures have been reported (116–119). Despite the few documented case studies reporting crustacean neoplasia, a lack of accurate assessments has also been attributed to researchers' backgrounds, having only previously reported some cases of neoplasia in assessments that were primarily concerned with other topics.

In this same context, it's worth noting that studying the immune capacity of hemocytes should be considered while checking their expression of p53/63 and heat shock proteins (HSPs), such as HSP70 and HSP90, as biomarkers of neoplastic transformations.

MOLECULAR COMPONENTS OF CRAYFISH IMMUNITY

Pattern Recognition Receptors (PRRs)

So far it has been demonstrated that the activation of an effective, immune response requires the cooperative processing of molecular components in three mechanistic levels, which are the initiation process, response propagation through signal networking, and finally, the stimulation of effector molecules to neutralize pathogens (**Figure 4**).

However, the initiation step constitutes an accurate recognition of the pathogens or their associated cell walls (PAMPs like LPS and β-glucans) by the receptors of cells/epithelium on the external surfaces, enriched with components of innate immunity (PRRs). Many PRRs have been identified so far in freshwater crayfish such as toll-like receptors, β-glucan binding proteins (LGBP), lectins, integrins, and Down syndrome cell adhesion molecules (Dscams). Fortunately, the TLRs are one of the well-conserved families of PRRs that perform a recognition role of diverse classes of pathogens including fungi, bacteria, and viruses. Several Toll receptors and related proteins have been identified in different freshwater crayfish, for example, Toll receptor 3 from *A. astacus* (120), PcToll1, 2, 3, 4, 5, and 6 from *Procambarus clarkii* (121–127). Crayfish PRRs represent lectins as an important class of molecules with a role of non-self-recognition, however, lectins are proteins that bind to sugar using a characteristics carbohydrate recognition domain (CRD). In fact, among the 13 animal classes of lectins identified (according to their structural characteristics), crayfish lectins were reported to belong to at least three structural groups. Pc-Lec2 & 3 from *P. clarkii* as C-type lectins (126, 128), PcL-lectin

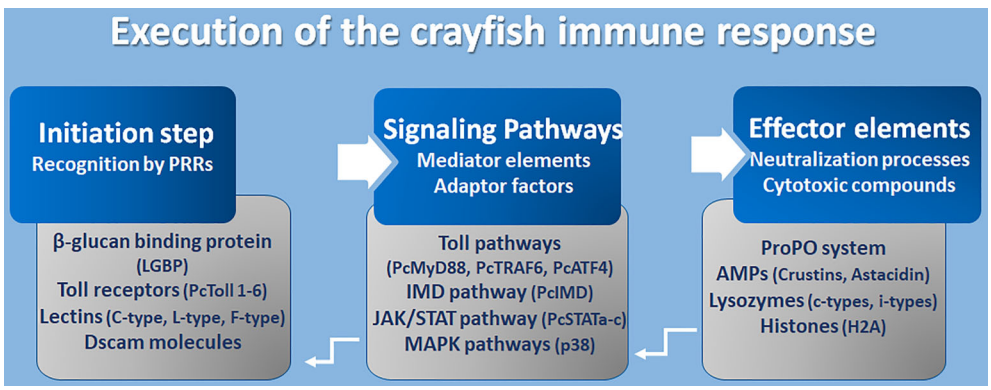

FIGURE 4 | Execution of crayfish immune response. Coordination of the immune response at molecular level (8, 16, 17, 97, 106, 120–141).

from *P. clarkii* as L-type lectins (129), and PlFLP1 & 2 from *Pacifastacus leniusculus* as Ficolin-like lectins (130). Because of their role in activating the ProPO system, LGBP are the most studied type of PRRs and have been identified to belong to the typical β-1,3-glucanase related protein (BGRP) family that participates in the recognition of a wide range of pathogens, including bacteria and fungi like the *A. astaci*, the causative agent of the plague disease in crayfish [further details are found in (126)]. Additionally, the Down syndrome cell adhesion molecules (Dscam), the largest Ig superfamily (IgSF) members, have been identified in arthropods including crustaceans (131). It's interesting to highlight that Dscam can produce thousands of isoforms (142). Dscam, presents membrane-bound and soluble forms (mDscam and sDscam), which are distinguished only by the presence/absence of transmembrane and cytoplasmic tail regions. Studies in the Chinese mitten crab *Eriocheir sinensis*, demonstrated that alternative splicing of Dscam can generate pathogen-specific isoforms with diverse epitopes in response to immune challenge, that potentially be able to recognize a broad spectrum of ligands. In fact, Li et al. (142) demonstrated that the mRNA and protein expressions of EsDscam were significantly upregulated after bacterial challenge, leading to produce isoforms found to bind specifically with the original bacteria to facilitate efficient clearance *via* phagocytosis by hemocytes. Li et al. (143) have elucidated that pathogen-induced particular soluble Dscam isoforms specifically binding with the original bacteria *via* epitope II, and then interact with membrane-bound Dscam that share the same extracellular regions *via* epitope I to promote phagocytosis. The cascading signal transduction mechanisms that activate post-Dscam binding pathogens remain not fully characterized. Dscams have been recorded in freshwater crayfish such as *Cherax quadricarinatus* and *P. leniusculus*, and have been proposed as key candidates for a somatically diversified receptor system speculated to be a hypervariable pattern-recognition receptor in crayfish immunity, playing the role of the cell surface receptor that triggers phagocytosis and opsonins due to the detection of soluble Dscam isoforms in crustacean hemolymphs (131, 132). Such findings have highlighted the putative involvement of Dscams as immunological effectors that promote immune memory through their ability to produce variable Ig domain combinations to promote the specificity of recognition and binding to a variety of pathogens through such splicing capacity (126, 144).

Mediators and Signaling Adaptors

A successful recognition step conducted by PRR members activates several downstream reactions aiming to propagate the immune response signals. Such networking is assured through a multitude of intermediate factors and mediator molecules of the Toll pathway, immune deficiency (IMD) pathway, Janus kinase-signal transducer activator of transcription (JAK/STAT) pathways, Mitogen-activated protein kinases (MAPKs) pathways, and the cytokines-like network. Many transcripts that have been assigned to the Toll pathways have been recorded for *A. astacus* (120). Up to now, many Toll intermediate homologs and signaling pathway components, such as those of the TLR4 signaling pathway (the cytosolic adaptor PcMyD88, tumor necrosis factor 6 (PcTRAF6), and PcATF4) have been identified in the red swamp crayfish *P. clarkii* (124, 133). However, some other key components which are necessary in TLR4 signaling, such as IRAK4, IRAK1, TRAF6, TAK1, and IRB, or their corresponding counterparts, remain unidentified in crustaceans (126). Besides, some other intermediate molecules belonging to other signaling pathways like the IMD pathway, the JAK/STAT and MAPK pathways, have been described in studies elucidating immunity against Gram-negative bacteria and triggering defenses through peptidoglycan (PG) receptors, and in response to white spot syndrome virus (WSSV) in *P. clarkii* (117, 126). The WSSV challenge modulates the PcIMD expression. The IMD pathway, which has a conserved function for regulating antimicrobial peptides' (AMP) expression in crayfish against Gram-negative bacteria, has also been reported to be involved in regulating the expression of crustins and lysozyme genes against WSSV (133). In addition, three different cDNA isoforms designated as PcSTATa, PcSTATb, and PcSTATc, belonging to the JAK/STAT signaling pathway, have proved to play a crucial role against WSSV in the red swamp crayfish *Procambarus clarkii* by modulating the expression levels of anti-lipopolysaccharide factors (PcALF1, PcALF2, PcALF3, PcALF4, PcALF5, and PcALF6) and crustin (PcCrus1, PcCrus2, PcCrus3, and PcCrus4) (134). Furthermore, the involvement of p38-MAPKinase, belonging to the serine/threonine protein kinases (MAPKs) (e.g., ERKs, JNKs, and p38s), in triggering the immune response in *P. clarkii* as results of exposure to cadmium has been demonstrated. As such, MAPKs could be irritated by various extracellular stimulations (e.g., inflammatory cytokines, pathogen infections, and environmental stress) (135).

The Effector Elements of Immunity

Immune components leading to the implementation of functional defenses against pathogens, like the ProPO system, and their related activation molecules such as serine proteases and proteases inhibitors, together with their intermediate regulators, have been thoroughly investigated (8, 24, 136). The ProPO system activates the copper-containing enzyme phenoloxidase (PO) to oxidize phenols into quinones, which in turn are catalyzed into melanin. This process was found to be involved in wound healing and encapsulation as part of antifungal defenses [further details can be found in (8, 21, 27)].

AMPs are widely distributed small cationic polypeptides that exert an anti-pathogenic effect on a broad spectrum of pathogens. Crustacean AMPs can generally be classified into four groups according to their amino acid compositions and structural properties (106, 127) (1): single-domain amphipathic linear α-helical structure AMPs, including astacidins which are proline-rich peptides like astacidin 2 from *P. leniusculus* (137), and Pc-astacidin from *P. clarkii* (127) (2); single-domain peptides enriched with cysteine residues that are able to form at least one disulfide bridge between the B-sheets (3); AMPs with multi-domain linear α-helical peptides enriched with certain amino acids, generally proline and/or glycine residues, including crustins, characterized by their acidic protein (WAP) domain at

C-terminus, such as Pl-crustin 1 & 2 in *P. leniusculus*, and Pc-crustin 4 in *P. clarkii* (138, 139), and procambarins, the glycine-rich peptide described in *P. clarkia* (140); and (4) unconventional AMPs including proteins/protein-fragments with antimicrobial functions like H2A histones and anti-lipopolysaccharide factors (ALFs) (reviewed in 121, 126). Lastly, at least two types of invertebrate (i-types) lysozymes, Pclysi 1 and 2, have been identified in *P. clarkii* (141). However, all lysozyme types described in crustaceans are of the chicken type (C-type) (126). Lysozymes are important factors with antimicrobial functions defined by their muramidase activity, hydrolyzing β-1,4-glycosidic linkage between N-acetylmuramic acid and N-acetylglucosamine, thus causing the lysis of peptidoglycan bacterial walls.

FORWARD-LOOKING SUMMARY OF DEVELOPMENTS IN THE FIELD

This review presents an extensive and up-to-date knowledge of crayfish immunity molecular components aiming to advance our understanding the defense mechanisms to evoke the old dilemma of plague disease, to enhance the resistance of endangered native European crayfishes. Unfortunately, early preventive strategies, like boosting crayfish immune responses, have not been fairly explored. Assessments of crayfish's immune responses should be considered in light of the recent updates on signaling pathways and processes that were found to be involved in different anti-pathogenic defenses. It is also interesting to highlight what is described as host-pathogen interactions as an underlying factor influencing the adjustment of an effective immune response. However, a recent study conducted by Zheng et al. (145) demonstrated the involvement of the Toll pathways in the early detection of fungal infection, even before the pathogen penetrates the host cuticle. The *Locusta migratoria manilensis* can activate the Toll signaling pathway by upregulating the Spaetzle and Cactus members of the upstream PRRs of the Toll pathway following a challenge by β-1, 3-glucan (laminarin) from the cell wall of the fungus *Metarhizium acridum* when applied onto the host cuticle, even before fungal penetration (145). Such findings pave the way for further investigations taking into account the already described different signaling pathways in crayfish to increase our understanding of host-pathogen interactions in resolving the dilemma of crayfish plague disease. Yet, this aim could be more widen with integrative assessments taking into account the integration of the immune components into functional mechanisms. In doing so, understanding the importance of cellular versus humoral defenses in crayfish immune response is timely needed. This implies that greater emphasis needs to be placed on understanding the molecular mechanisms underlying cellular involvement in innate immune defenses of susceptible crayfish species. Such, may constitute a basis for wider assessments to overcome current limitations in forming immune priming strategies against *A. astaci* and to enhance conservation efforts of the endangered species. In this context, prospective acquirement of a specific immune response, named immunological memory of innate immunity, has been evidenced in many invertebrates, including crustaceans. However, deciphering the mechanisms of such memory is yet to be fully investigated. The main proposed underpinning molecular mechanistic is epigenetic re-programming or modification on gene expression due to different factors other than DNA mutations, which also remain elusive. To this end, an overreaching goal aiming to survey the modifications in the molecular mechanisms underlying the immunity of European freshwater crayfish, by exploring a potential transgenerational transfer of resistance traits against *A. astaci*, may consolidate breeding programs and crayfish production in captivity, thus enhancing European crayfish conservation.

AUTHOR CONTRIBUTIONS

The author confirms being the sole contributor of this work and has approved it for publication.

ACKNOWLEDGMENTS

The author would like to thank Prof. Irene Söderhäll (Invertebrate infection biology Lab, Department of Organismal Biology, Uppsala University, Sweden) for her time and consideration to review this manuscript and for her valuable recommendations and assistance during the editing of this paper. The author also thanks Mrs. Nayua Abdelkefi Zorrilla for the proofreading and editing the English language of the manuscript.

REFERENCES

1. Jussila J, Makkonen J, Vainikka A, Kortet R, Kokko H. Latent Crayfish Plague (Aphanomyces astaci) Infection in a Robust Wild Noble Cray Fish (Astacus astacus) Population. *Aquaculture* (2011) 321(1–2):17–20. doi: 10.1016/j.aquaculture.2011.08.026
2. Makkonen J, Jussila J, Kokko H. The Diversity of the Pathogenic Oomycete (Aphanomyces astaci) Chitinase Genes Within the Genotypes Indicate Adaptation to its Hosts. *Fungal Genet Biol* (2012) 49(8):635–42. doi: 10.1016/j.fgb.2012.05.014
3. Makkonen J, Kokko H, Vainikka A, Kortet R, Jussila J. Dose-Dependent Mortality of the Noble Crayfish (Astacus astacus) to Different Strains of the Crayfish Plague (Aphanomyces astaci). *J Invertebrate Pathol* (2014) 115:86–91. doi: 10.1016/j.jip.2013.10.009
4. Persson M, Cerenius L, Söderhäll K. The Influence of Haemocyte Number on the Resistance of the Freshwater Crayfish, Pacifastacus leniusculus dana, to the Parasitic Fungus Aphanomyces astaci. *J Fish Dis* (1987) 10(6):471–7. doi: 10.1111/j.1365-2761.1987.tb01098.x
5. Cerenius L, Bangyeekhun E, Keyser P, Söderhäll I, Söderhäll K. Host Prophenoloxidase Expression in Freshwater Crayfish is Linked to Increased Resistance to the Crayfish Plague Fungus, Aphanomyces astaci. *Cell Microbiol* (2003) 5:353–7. doi: 10.1046/j.1462-5822.2003.00282.x
6. Edgerton BF, Henttonen P, Jussila J, Mannonen A, Paasonen P, Taugbol T, et al. Understanding the Causes of Disease in European

Freshwater Crayfish. *Conserv Biol* (2004) 18:1466–74. doi: 10.1111/j.1523-1739.2004.00436.x
7. Nyhlèn L, Unestam T. Wound Reactions and Aphanomyces Crayfish Cuticle Astaci Growth in. *J Invertebrate Pathol* (1980) 197:187–97. doi: 10.1016/0022-2011(80)90023-3
8. Cerenius L, Andersson MG, Söderhäll K. *Aphanomyces astaci and Crustaceans Oomycete Genetics and Genomics: Diversity, Interactions, and Research Tools*. K Lamour, S Kamoun, editors. United States: John Wiley & Sons, Inc (2008) p. 425–33. doi: 10.1002/9780470475898.ch21
9. Longshaw M. Diseases of Crayfish: A Review. *J Invertebrate Pathol* (2011) 106(1):54–70. doi: 10.1016/j.jip.2010.09.013
10. Gruber C, Kortet R, Vainikka A, Hyvärinen P, Rantala MJ, Pikkarainen A, et al. Variation in Resistance to the Invasive Crayfish Plague and Immune Defence in the Native Noble Crayfish. *Annales Zoologici Fennici* (2014) 51 (4):371–89. doi: 10.5735/086.051.0403
11. Svoboda J, Mrugała A, Kozubíková-Balcarová A, Petrusek A. Hosts and Transmission of the Crayfish Plague Pathogen Aphanomyces astaci: A Review. *J Fish Dis* (2017) 40(1):127–40. doi: 10.1111/jfd.12472
12. Oidtmann B, Heitz1 E, Rogers D, Hoffmann RW. Transmission of Crayfish Plague. *Dis Aquat Organisms* (2002) 52(2):159–67. doi: 10.3354/dao052159
13. Smith VJ, Ratcliffe NA. Host Defence Reactions of the Shore Crab, Carcinus maenas (L.), *In Vitro*. *J Marine Biol Assoc United Kingdom* (1978) 58(2):367–79. doi: 10.1017/S0025315400028046
14. Persson M, Vey A, Söderhäll K. Encapsulation of Foreign Particles In Vitro by Separated Blood Cells From Crayfish, Astacus Leptodactylus. *Cell Tissue Res* (1987) 247(2):409–15. doi: 10.1007/BF00218322
15. Johansson MW, Söderhäll K. Cellular Immunity in Crustaceans and the proPO System. *Parasitol Today* (1989) 5(6):171–6. doi: 10.1016/0169-4758(89)90139-7
16. Cerenius L, Söderhäll K. The Prophenoloxidase-Activating System in Invertebrates. *Immunol Rev* (2004) 198:116–26. doi: 10.1111/j.0105-2896.2004.00116.x
17. Cerenius L, Söderhäll K. Crayfish Immunity – Recent Findings. *Dev Comp Immunol* (2018) 80:94–8. doi: 10.1016/j.dci.2017.05.010
18. Jiravanichpaisal P, Lee BL, Söderhäll K. Cell-Mediated Immunity in Arthropods: Hematopoiesis, Coagulation, Melanization and Opsonization. *Immunobiology* (2006) 211(4):213–36. doi: 10.1016/j.imbio.2005.10.015
19. Kan H, Kim CH, Kwon HM, Park JW, Roh KB, Lee H, et al. Molecular Control of Phenoloxidase-Induced Melanin Synthesis in an Insect. *J Biol Chem* (2008) 283(37):25316–23. doi: 10.1074/jbc.M804364200
20. Roh KB, Kim C-H, Lee H, Kwon H-M, Park J-W, Ryu J-H, et al. Proteolytic Cascade for the Activation of the Insect Toll Pathway Induced by the Fungal Cell Wall Component. *J Biol Chem* (2009) 284(29):19474–81. doi: 10.1074/jbc.m109.007419
21. Cerenius L, Kawabata S-i, Lee BL, Nonaka M, Söderhäll K. Proteolytic Cascades and Their Involvement in Invertebrate Immunity. *Trends Biochem Sci* (2010) 35(10):575–83. doi: 10.1016/j.tibs.2010.04.006
22. Söderhäll K, Wingren A, Johansson MW, Bertheussen K. The Cytotoxic Reaction of Hemocytes From the Freshwater Crayfish, Astacus astacus. *Cell Immunol* (1985) 94(2):326–32. doi: 10.1016/0008-8749(85)90256-4
23. Söderhäll K, Smith VJ, Johansson MW. Exocytosis and Uptake of Bacteria by Isolated Haemocyte Populations of Two Crustaceans: Evidence for Cellular Co-Operation in the Defence Reactions of Arthropods. *Cell Tissue Res* (1986) 245(1):43–9. doi: 10.1007/BF00218085
24. Kobayashi M, Johansson MW, Söderhäll K. The 76 Kd Cell-Adhesion Factor From Crayfish Haemocytes Promotes Encapsulation *In Vitro*. *Cell Tissue Res* (1990) 260(1):13–8. doi: 10.1007/BF00297485
25. Jiravanichpaisal P, Söderhäll K, Söderhäll I. Inflammation in Arthropods. *Curr Pharm Design* (2011) 16(38):4166–74. doi: 10.2174/138161210794519165
26. Smith VJ, Söderhäll K. Induction of Degranulation and Lysis of Haemocytes in the Freshwater Crayfish, Astacus astacus by Components of the Prophenoloxidase Activating System *In Vitro*. *Cell Tissue Res* (1983) 233 (2):295–303. doi: 10.1007/BF00238297
27. Cerenius L, Lee BL, Söderhäll K. The proPO-system: Pros and Cons for its Role in Invertebrate Immunity. *Trends Immunol* (2008) 26(6):263–71. doi: 10.1016/j.it.2008.02.009
28. Cerenius L, Söderhäll K. Arthropoda: Pattern Recognition Proteins in Crustacean Immunity. In: EL Cooper, editor. *Advances in Comparative Immunology*. Cham: Springer (2018). p. 213–24. doi: 10.1007/978-3-319-76768-0
29. Lin X, Kim YA, Lee BL, Söderhäll K, Söderhäll I. Identification and Properties of a Receptor for the Invertebrate Cytokine Astakine, Involved in Hematopoiesis. *Exp Cell Res* (2009) 315(7):1171–80. doi: 10.1016/j.yexcr.2009.01.001
30. Rowley AF. *The Immune System of Crustaceans, Encyclopedia of Immunobiology*. Amsterdam, Netherlands: Elsevier (2016). doi: 10.1016/B978-0-12-374279-7.12005-3
31. Liu H, Söderhäll K, Jiravanichpaisal P. Antiviral Immunity in Crustaceans. *Fish Shellfish Immunol* (2009) 27(2):79–88. doi: 10.1016/j.fsi.2009.02.009
32. Smith VJ. *Immunology of Invertebrates: Cellular. Els*. Chichester, UK: John Wiley & Sons, Ltd (2016) p. 1–13. doi: 10.1002/9780470015902.a0002344.pub3
33. Jussila J, Vainikka A, Kortet R, Kokko H. Crayfish Plague Dilemma: How to be a Courteous Killer? *Boreal Environ Res* (2014) 19(3):235–44.
34. Martín-Torrijos L, Campos Llach M, Pou-Rovira Q, Diéguez-Uribeondo J. Resistance to the Crayfish Plague, Aphanomyces astaci (Oomycota) in the Endangered Freshwater Crayfish Species, Austropotamobius Pallipes. *PloS One* (2017) 12(7):1–13. doi: 10.1371/journal.pone.0181226
35. Panteleit J, Keller NS, Diéguez-Uribeondo J, Makkonen J, Martín-Torrijos L, Patrulea V, et al. Hidden Sites in the Distribution of the Crayfish Plague Pathogen Aphanomyces astaci in Eastern Europe: Relicts of Genetic Groups From Older Outbreaks? *J Invertebrate Pathol* (2018) 157:117–24. doi: 10.1016/j.jip.2018.05.006
36. Becking T, Mrugała A, Delaunay C, Svoboda J, Raimond M, Viljamaa-Dirks S, et al. Effect of Experimental Exposure to Differently Virulent Aphanomyces astaci Strains on the Immune Response of the Noble Crayfish Astacus astacus. *J Invertebrate Pathol* (2015) 132:115–24. doi: 10.1016/j.jip.2015.08.007
37. Svoboda J, Mrugała A, Kozubíková-Balcarová E, Kouba A, Diéguez-Uribeondoc J, Petrusek A, et al. Resistance to the Crayfish Plague Pathogen, Aphanomyces astaci, in Two Freshwater Shrimps. *J Invertebrate Pathol* (2014) 121:97–104. doi: 10.1016/j.jip.2014.07.004
38. Filipova L, Petrusek A, Matasova K, Delaunay C, Grandjean F. Prevalence of the Crayfish Plague Pathogen Aphanomyces astaci in Populations of the Signal Crayfish Pacifastacus leniusculus in France: Evaluating the Threat to Native Crayfish. *PloS One* (2013) 8:e70157. doi: 10.1371/journal.pone.0070157
39. Alderman DJ. Geographical Spread of Bacterial and Fungal Diseases of Crustaceans. *Rev Scientifique Et Technique l'Office Int Des Epizooties* (1996) 15:603–32. doi: 10.20506/rst.15.2.943
40. Martín-Torrijos L, Kawai T, Makkonen J, Jussila J, Kokko H, Diéguez-Uribeondo J. Crayfish Plague in Japan: A Real Threat to the Endemic Cambaroides Japonicus. *PloS One* (2018) 13(4):e0195353. doi: 10.1371/journal.pone.0195353
41. Schrimpf A, Schmidt T, Schulz R. Invasive Chinese Mitten Crab (Eriocheir Sinensis) Transmits Crayfish Plague Pathogen (Aphanomyces astaci). *Aquat Invasions* (2014) 9:203–9. doi: 10.3391/ai.2014.9.2.09
42. Ratcliffe NA, Rowley AF, Fitzgerald SW, Rhodes CP. Invertebrate Immunity: Basic Concepts and Recent Advances. *Int Rev Cytology* (1985) 97(C):183–350. doi: 10.1016/S0074-7696(08)62351-7
43. Giulianini PG, Bierti M, Lorenzon S, Battistella S, Ferrero EA. Ultrastructural and Functional Characterization of Circulating Hemocytes From the Freshwater Crayfish Astacus Leptodactylus: Cell Types and Their Role After *In Vivo* Artificial non-Self-Challenge. *Micron* (2007) 38(1):49–57. doi: 10.1016/j.micron.2006.03.019
44. Giglio A, Manfrin C, Zanetti M, Aquiloni L, Simeon E, Bravin MK, et al. Effects of X-ray Irradiation on Haemocytes of Procambarus clarkii (Arthropoda: Decapoda) Males. *Eur Zoological J* (2018) 85(1):26–35. doi: 10.1080/24750263.2017.1423119
45. Li F, Chang X, Xua L, Yang F. Different Roles of Crayfish Hemocytes in the Uptake of Foreign Particles. *Fish Shellfish Immunol* (2018) 77:112–9. doi: 10.1016/j.fsi.2018.03.029
46. Wu C, Söderhäll I, Kim YA, Liu H, Söderhäll K. Hemocyte-Lineage Marker Proteins in a Crustacean, the Freshwater Crayfish, Pacifastacus leniusculus. *Proteomics* (2008) 8(20):4226–35. doi: 10.1002/pmic.200800177

47. Söderhäll I. Crustacean Hematopoiesis. *Dev Comp Immunol* (2016) 58:129–41. doi: 10.1016/j.dci.2015.12.009
48. Mix MC, Sparks AK. Hemocyte Classification and Differential Counts in the Dungeness Crab, Cancer Magister. *J Invertebrate Pathol* (1980) 35(2):134–43. doi: 10.1016/0022-2011(80)90176-7
49. Söderhäll K, Smith VJ. Separation of the Haemocyte Populations of *Carcinus maenas* and Other Marine Decapods, and Prophenoloxidase Distribution. *Dev Comp Immunol* (1983) 7:229–39. doi: 10.1016/0145-305x(83)90004-6
50. Ding Z, Du J, Ou J, Li W, Wu T, Xiu Y, et al. Classification of Circulating Hemocytes From the Red Swamp Crayfish Procambarus clarkii and Their Susceptibility to the Novel Pathogen Spiroplasma Eriocheiris *In Vitro*. *Aquaculture* (2012) 356–357:371–80. doi: 10.1016/j.aquaculture.2012.04.042
51. Lv S, Xu J, Zhao J, Yin N, Lu B, Li S, et al. Classification and Phagocytosis of Circulating Haemocytes in Chinese Mitten Crab (Eriocheir Sinensis) and the Effect of Extrinsic Stimulation on Circulating Haemocytes *In Vivo*. *Fish Shellfish Immunol* (2014) 9(2):415–22. doi: 10.1016/j.fsi.2014.05.036
52. Hammond JA, Smith VJ. Lipopolysaccharide Induces DNA-synthesis in a Sub-Population of Hemocytes From the Swimming Crab, Liocarcinus Depurator. *Dev Comp Immunol* (2002) 26(3):227–36. doi: 10.1016/s0145-305x(01)00069-6
53. Söderhäll I, Bangyeekhun E, Mayo S, Söderhäll K. Hemocyte Production and Maturation in an Invertebrate Animal; Proliferation and Gene Expression in Hematopoietic Stem Cells of Pacifastacus leniusculus. *Dev Comp Immunol* (2003) 27(8):661–72. doi: 10.1016/S0145-305X(03)00039-9
54. Cerenius L, Kawabata Sc, Soöerhäll K. Biological and Immunological Aspects of Innate Defence Mechanisms Activated by (1,3)β-Glucans and Related Polysaccharides in Invertebrates. In: *Chemistry, Biochemistry, and Biology of 1-3 Beta Glucans and Related Polysaccharides*. Cambridge, Massachusetts, United States: Elsevier Inc. Academic press (2009). p. 563–77. doi: 10.1016/B978-0-12-373971-1.00017-0
55. Smith VJ, Ratcliffe NA. Pathological Changes in the Nephrocytes of the Shore Crab, Carcinus maenas, Following Injection of Bacteria. *J Invertebrate Pathol* (1981) 38(1):113–21. doi: 10.1016/0022-2011(81)90041-0
56. Powell A, Rowley AF. Tissue Changes in the Shore Crab Carcinus maenas as a Result of Infection by the Parasitic Barnacle Sacculina Carcini. *Dis Aquat Organisms* (2008) 80(1):75–9. doi: 10.3354/dao01930
57. Edgerton BF, Owens L. Histopathological Surveys of the Redclaw Freshwater Crayfish, Cherax quadricarinatus, in Australia. *Aquaculture* (1999) 180(1–2):23–40. doi: 10.1016/S0044-8486(99)00195-7
58. Stentiford GD, Feist SW. A Histopathological Survey of Shore Crab (Carcinus maenas) and Brown Shrimp (Crangon Crangon) From Six Estuaries in the United Kingdom. *J Invertebrate Pathol* (2005) 88(2):136–46. doi: 10.1016/j.jip.2005.01.006
59. Sharshar KM. Histopathological and Pcr Diagnostc Techniques for Detection of White Spot Syndrome Virus in Different Tissues of Procambarus clarkii -. *Egyptian J Exp Biol (Zoology)* (2008) 4(0):307–16.
60. Jiravanichpaisal P, Roos S, Edsman L, Liu L, Söderhäll K. A Highly Virulent Pathogen, Aeromonas Hydrophila, From the Freshwater Crayfish Pacifastacus leniusculus. *J Invertebrate Pathol* (2009) 101(1):56–66. doi: 10.1016/j.jip.2009.02.002
61. Wei K, Yang J. Oxidative Damage of Hepatopancreas Induced by Pollutiondepresses Humoral Immunity Response in the Freshwater Crayfish Procambarus clarkii. *Fish Shellfish Immunol* (2015) 43(2):510–9. doi: 10.1016/j.fsi.2015.01.013
62. Wei KQ, Yang JX. Histological Alterations and Immune Response in the Crayfish Procambarus clarkii Given rVP28-incorporated Diets. *Fish Shellfish Immunol* (2011) 31(6):1122–8. doi: 10.1016/j.fsi.2011.10.002
63. Ding Z, Yao W, Du J, Ren Q, Li W, Wu T, et al. Histopathological Characterization and *in Situ* Hybridization of a Novel Spiroplasma Pathogen in the Freshwater Crayfish Procambarus clarkii. *Aquaculture* (2013) 380–383:106–13. doi: 10.1016/j.aquaculture.2012.12.007
64. Wren M, Gagnon ZE. A Histopathological Study of Hudson River Crayfish, Orconectes virilis, Exposed to Platinum Group Metals. *J Environ Sci Health - Part A Toxic/Hazardous Substances Environ Eng* (2014) 49(2):135–45. doi: 10.1080/10934529.2013.838836
65. Samnejhad A, Afsharnasab M, Kakoolaki S, Sepahdari A. Effect of Aeromonas Hydrophila Infection With High and Normal Water Temperature on Total Hemocyte Count, Total Plasma Protein and Histopathological Differences in Freshwater Crayfish Astacus Leptodactylus. *Survey Fisheries Sci* (2016) 2(2):45–65. doi: 10.18331/sfs2016.2.2.4
66. Silva MAS, Almeida Neto ME, Ramiro BO, Santos ITF, Guerra RR. Histomorphologic Characterization of the Hepatopancreas of Freshwater Prawn Macrobrachium rosenbergii (De Man, 1879). *Arquivo Brasileiro Medicina Veterinaria e Zootecnia* (2018) 70(5):1539–46. doi: 10.1590/1678-4162-10497
67. Bernet D, Schmidt H, Meier W, Burkhardt-Holm P, Wahli T. Histopathology in Fish: Proposal for a Protocol to Assess Aquatic Pollution. *J Fish Dis* (1999) 22(1):25–34. doi: 10.1046/j.1365-2761.1999.00134.x
68. Costa PM, Diniz MS, Caeiro S, Lobo J, Martins M, Ferreira AM, et al. Histological Biomarkers in Liver and Gills of Juvenile Solea Senegalensis Exposed to Contaminated Estuarine Sediments: A Weighted Indices Approach. *Aquat Toxicol* (2009) 92(3):202–12. doi: 10.1016/j.aquatox.2008.12.009
69. Bouallegui Y, Ben-Younes R, Bellamine H, Oueslati R. Histopathology and Analyses of Inflammation Intensity in the Gills of Mussels Exposed to Silver Nanoparticles: Role of Nanoparticle Size, Exposure Time, and Uptake Pathways. *Toxicol Mech Methods* (2017) 27(8):582–91. doi: 10.1080/15376516.2017.1337258
70. Bouallegui Y, Ben-Younes R, Bellamine H, Oueslati R. Histopathological Indices and Inflammatory Response in the Digestive Gland of the Mussel Mytilus Galloprovincialis as Biomarker of Immunotoxicity to Silver Nanoparticles. *Biomarkers* (2018) 23(3):277–87. doi: 10.1080/1354750X.2017.1409803
71. Stara A, Kouba A, Velisek J. Biochemical and Histological Effects of Sub-Chronic Exposure to Atrazine in Crayfish Cherax Destructor. *Chemico Biological Interact* (2018) 291(June):95–102. doi: 10.1016/j.cbi.2018.06.012
72. Lanz H, Tsutsumi V, Aréchiga H. Morphological and Biochemical Characterization of Procambarus clarki Blood Cells. *Dev Comp Immunol* (1993) 17:389–97. doi: 10.1016/0145-305X(93)90030-T
73. Matozzo V, Marin MG. The Role of Haemocytes From the Crab Carcinus Aestuarii (Crustacea, Decapoda) in Immune Responses: A First Survey. *Fish Shellfish Immunol* (2010) 28(4):534–41. doi: 10.1016/j.fsi.2009.12.003
74. Matozzo V, Mrin MG. First Cytochemical Study of Haemocytes From the Crab Carcinus a Estuarii (Crustacea, Decapoda). *Eur J Histochem* (2010) 54 (1):44–9. doi: 10.4081/ejh.2010.e9
75. Lin X, Söderhäll I. Crustacean Hematopoiesis and the Astakine Cytokines. *Blood* (2011) 117(24):6417–24. doi: 10.1182/blood-2010-11-320614
76. Söderhäll I, Junkunlo K. A Comparative Global Proteomic Analysis of the Hematopoietic Lineages in the Crustacean Pacifastacus leniusculus. *Dev Comp Immunol* (2019) 92:170–8. doi: 10.1016/j.dci.2018.11.016
77. Junkunlo K, Söderhäll K, Söderhäll I. Transglutaminase 1 and 2 are Localized in Different Blood Cells in the Freshwater Crayfish Pacifastacus leniusculus. *Fish Shellfish Immunol* (2020) 104:83–91. doi: 10.1016/j.fsi.2020.05.062
78. Fu Y, Huang X, Zhang P, Van de Leemput J, Han Z. Single-Cell RNA Sequencing Identifies Novel Cell Types in Drosophila Blood. *J Genet Genomics* (2020) 47:175–86. doi: 10.1016/j.jgg.2020.02.004
79. Tattikota SG, Cho B, Liu Y, Hu Y, Barrera V, Steinbaugh MJ, et al. A Single-Cell Survey of Drosophila Blood. *eLife* (2020) 9:e54818. doi: 10.7554/eLife.54818
80. van de Braak CB, Botterblom MH, Liu W, Taverne N, van der Knaap WP, Rombout JH. The Role of the Haematopoietic Tissue in Haemocyte Production and Maturation in the Black Tiger Shrimp (Penaeus monodon). *Fish Shellfish Immunol* (2002) 12(3):253–72. doi: 10.1006/fsim.2001.0369
81. Lin X, Soderhall K, Soderhall I. Invertebrate Hematopoiesis: An Astakine-Dependent Novel Hematopoietic Factor. *J Immunol* (2011) 186(4):2073–9. doi: 10.4049/jimmunol.1001229
82. Johansson MW, Keyser P, Sritunyalucksana K, Söderhäll K. Crustacean Haemocytes and Haematopoiesis. *Aquaculture* (2000) 191(1–3):45–52. doi: 10.1016/S0044-8486(00)00418-X
83. Lin X, Novotny M, Söderhäll K, Söderhäll I. Ancient Cytokines, the Role of Astakines as Hematopoietic Growth Factors. *J Biol Chem* (2010) 285 (37):28577–86. doi: 10.1074/jbc.M110.138560

84. Junkunlo K, Söderhäll K, Söderhäll I. Clotting Protein – An Extracellular Matrix (ECM) Protein Involved in Crustacean Hematopoiesis. *Dev Comp Immunol* (2018) 78:132–40. doi: 10.1016/j.dci.2017.09.017
85. Söderhäll I, Kim Y-A, Jiravanichpaisal P, Lee S-Y, Söderhäll K. An Ancient Role for a Prokineticin Domain in Invertebrate Hematopoiesis. *J Immunol* (2005) 174(10):6153–60. doi: 10.4049/jimmunol.174.10.6153
86. Lin X, Söderhäll K, Söderhäll I. Transglutaminase Activity in the Hematopoietic Tissue of a Crustacean, Pacifastacus leniusculus, Importance in Hemocyte Homeostasis. *BMC Immunol* (2008) 9:1–11. doi: 10.1186/1471-2172-9-58
87. Junkunlo K, Söderhäll K, Söderhäll I, Noonin C. Reactive Oxygen Species Affect Transglutaminase Activity and Regulate Hematopoiesis in a Crustacean. *J Biol Chem* (2016) 291(34):17593–601. doi: 10.1074/jbc.M116.741348
88. Sirikharin R, Junkunlo K, Söderhäll K, Söderhäll I. Role of Astakine1 in Regulating Transglutaminase Activity. *Dev Comp Immunol* (2017) 76:77–82. doi: 10.1016/j.dci.2017.05.015
89. Ericsson L, Irene S. Astakines in Arthropods E Phylogeny and Gene Structure. *Dev Comp Immunol* (2018) 81:141–51. doi: 10.1016/j.dci.2017.11.005
90. Junkunlo K, Söderhäll K, Söderhäll I. Transglutaminase Inhibition Stimulates Hematopoiesis and Reduces Aggressive Behavior of Crayfish, Pacifastacus leniusculus. *J Biol Chem* (2019) 294(2):708–15. doi: 10.1074/jbc.RA118.005489
91. Chen M-Y, Hu K-Y, Huang C-C, Song Y-L. More Than One Type of Transglutaminase in Invertebrates? A Second Type of Transglutaminase is Involved in Shrimp Coagulation. *Dev Comp Immunol* (2005) 29:1003–16. doi: 10.1016/j.dci.2005.03.012
92. Cerenius L, Söderhäll K. Coagulation in Invertebrates. *J Innate Immun* (2011) 3:3–8. doi: 10.1159/000322066
93. Beltz BS, Zhang Y, Benton JL, Sandeman DC. Adult Neurogenesis in the Decapod Crustacean Brain: A Hematopoietic Connection? *Eur J Neurosci* (2011) 34:870–83. doi: 10.1111/j.1460-9568.2011.07802.x
94. Benton JL, Kery R, Li J, Noonin C, Söderhäll I, Beltz BS. Cells From the Immune System Generate Adult-Born Neurons in Crayfish. *Dev Cell* (2014) 30(3):322–33. doi: 10.1016/j.devcel.2014.06.016
95. Noonin C. Involvement of Serotonin in Crayfish Hematopoiesis. *Dev Comp Immunol* (2018) 86:189–95. doi: 10.1016/j.dci.2018.05.006
96. Saelee N, Noonin C, Nupan B, Junkunlo K, Phongdara A, Lin X, et al. B -Thymosins and Hemocyte Homeostasis in a Crustacean. *PloS One* (2013) 8 (4):e60974. doi: 10.1371/journal.pone.0060974
97. Chang YT, Lin CY, Tsai CY, Siva VS, Chu CY, Tsai HJ, et al. The New Face of the Old Molecules: Crustin Pm4 and Transglutaminase Type I Serving as RNPs Down-Regulate Astakine-Mediated Hematopoiesis. *PLoS ONE* (2013) 8(8):e72793. doi: 10.1371/journal.pone.0072793
98. Liu H, Jiravanichpaisal P, Cerenius L, Lee BL, Söderhäll I, Söderhäll K. Phenoloxidase is an Important Component of the Defense Against Aeromonas Hydrophila Infection in a Crustacean, Pacifastacus leniusculus. *J Biol Chem* (2007) 282(46):33593–8. doi: 10.1074/jbc.M706113200
99. Hall M, Wang R, van Antwerpen R, Sottrup-Jensen L, Söderhäll K. The Crayfish Plasma Clotting Protein: A Vitellogenin-Related Protein Responsible for Clot Formation in Crustacean Blood. *Proc Natl Acad Sci USA* (1999) 96(5):1965–70. doi: 10.1073/pnas.96.5.1965
100. Ang RW, Iang ZL, All MH. A Transglutaminase Involved in the Coagulation System of the Freshwater Crayfish, Pacifastacus leniusculus. Tissue Localisation and cDNA Cloning. *Fish Shellfish Immunol* (2001) 11(7):623–37. doi: 10.1006/fsim.2001.0341
101. Dubovskiy IM, Kryukova NA, Glupov VV, Ratcliffe NA. 'Encapsulation and Nodulation in Insects. *Invertebrates Survival J* (2016) 13:229–46. doi: 10.25431/1824-307X/isj.v13i1.229-246
102. Butt TM, Coates CJ, Dubovskiy IM, Ratcliffe NA. Entomopathogenic Fungi: New Insights Into Host-Pathogen Interactions. *Adv Genet* (2016) 94:307–64. doi: 10.1016/bs.adgen.2016.01.006
103. Robb CT, Dyrynda EA, Gray RD, Rossi AG, Smith VJ. Invertebrate Extracellular Phagocyte Traps Show That Chromatin is an Ancient Defence Weapon. *Nat Commun* (2014) 5:1–11. doi: 10.1038/ncomms5627
104. Brinkmann V, Reichard U, Goosmann C, Fauler B, Uhlemann Y, Weiss DS, et al. Neutrophil Extracellular Traps Kill Bacteria. *Science* (2004) 303 (5663):1532–5. doi: 10.1126/science.1092385
105. Brinkmann V, Zychlinsky A. Neutrophil Extracellular Traps: Is Immunity the Second Function of Chromatin? *J Cell Biol* (2012) 198(5):773–83. doi: 10.1083/jcb.201203170
106. Rosa RD, Barracco MA. Antimicrobial Peptides in Crustaceans. *Invertebrate Survival J* (2010) 7(2):262–84.
107. Poirier AC, Schmitt P, Rosa RD, Vanhove AS, Kieffer-Jaquinod S, Rubio TP, et al. Antimicrobial Histones and DNA Traps in Invertebrate: Evidences in Crassostrea gigas. *J Biol Chem* (2014) 289(36):24821–31. doi: 10.1074/jbc.M114.576546
108. Koiwai K, Kondo H, Hirono I. The Immune Functions of Sessile Hemocytes in Three Organs of Kuruma Shrimp Marsupenaeus Japonicus Differ From Those of Circulating Hemocytes. *Fish Shellfish Immunol* (2018) 78:109–13. doi: 10.1016/j.fsi.2018.04.036
109. Koiwai K, Kondo H, Hirono I. Isolation and Molecular Characterization of Hemocyte Sub – Populations in Kuruma Shrimp Marsupenaeus japonicus. *Fisheries Sci* (2019) 85:521–32. doi: 10.1007/s12562-019-01311-5
110. Cerenius L, Soderhall K. Crustacean Immune Responses and Their Implications for Disease Control, Infectious Disease. In: B Austin, editor. *Aquaculture: Prevention and Control*. Cambridge, UK: Sawston, Woodhead Publishing Series in Food Science, Technology and Nutrition (2012). doi: 10.1016/B978-0-85709-016-4.50002-7
111. Lau YT, Gambino L, Santos B, Pales Espinosa E, Allam B. Regulation of Oyster (Crassostrea virginica) Hemocyte Motility by the Intracellular Parasite Perkinsus marinus: A Possible Mechanism for Host Infection. *Fish Shellfish Immunol* (2018) 78:18–25. doi: 10.1016/j.fsi.2018.04.019
112. Lau YT, Gambino L, Santos B, Pales Espinosa E, Allam B. Transepithelial Migration of Mucosal Hemocytes in Crassostrea virginica and Potential Role in Perkinsus Marinus Pathogenesis. *J Invertebrate Pathol* (2018) 153:122–9. doi: 10.1016/j.jip.2018.03.004
113. Pales Espinosa E, Corre E, Allam B. Pallial Mucus of the Oyster Crassostrea virginica Regulates the Expression of Putative Virulence Genes of its Pathogen Perkinsus Marinus. *Int J Parasitol* (2014) 44(5):305–17. doi: 10.1016/j.ijpara.2014.01.006
114. Pales Espinosa E, Koller A, Allam B. Proteomic Characterization of Mucosal Secretions in the Eastern Oyster, Crassostrea virginica. *J Proteomics* (2016) 132:63–76. doi: 10.1016/j.jprot.2015.11.018
115. Junkunlo K, Söderhäll K, Noonin C, Söderhäll I. PDGF/VEGF-Related Receptor Affects Transglutaminase Activity to Control Cell Migration During Crustacean Hematopoiesis. *Stem Cells Dev* (2017) 26(20):1449–59. doi: 10.1089/scd.2017.0086
116. Vogt G. How to Minimize Formation and Growth of Tumours: Potential Benefits of Decapod Crustaceans for Cancer Research. *Int J Cancer* (2008) 123(12):2727–34. doi: 10.1002/ijc.23947
117. Lightner DV, Brock JA. A Lymphoma-Like Neoplasm Arising From Hematopoietic Tissue in the White Shrimp, Penaeus Vannamei Boone (Crustacea: Decapoda). *J Invertebrate Pathol* (1987) 49(2):188–93. doi: 10.1016/0022-2011(87)90159-5
118. Sparks AK, Morado JF. A Putative Carcinoma-Like Neoplasm in the Hindgut of a Red King Carb, Paralithodes camtschatica. *J Invertebrate Pathol* (1987) 50(1):45–52. doi: 10.1016/0022-2011(87)90144-3
119. Victor B. Histopathological Progression of Hemic Neoplasms in the Tropical Crab Paratelphusa hydrodromous (Herbst) Treated With Sublethal Cadmium Chloride. *Arch Environ Contamination Toxicol* (1993) 25(1):48–54. doi: 10.1007/BF00230710
120. Theissinger K, Falckenhayn C, Blande D, Toljamo A, Gutekunst J, Makkonen J, et al. De Novo Assembly and Annotation of the Freshwater Crayfish Astacus astacus Transcriptome. *Marine Genomics* (2016) 28:7–10. doi: 10.1016/j.margen.2016.02.006
121. Wang Z, Chen YH, Dai YJ, Tan JM, Huang Y, Lan JF, et al. A Novel Vertebrates Toll-like Receptor Counterpart Regulating the Anti-Microbial Peptides Expression in the Freshwater Crayfish, Procambarus clarkii. *Fish Shellfish Immunol* (2015) 43(1):219–29. doi: 10.1016/j.fsi.2014.12.038
122. Lan JF, Zhao LJ, Wei S, Wang Y, Lin L, Li XC. PcToll2 Positively Regulates the Expression of Antimicrobial Peptides by Promoting PcATF4 Translocation Into the Nucleus. *Fish Shellfish Immunol* (2016) 58:59–66. doi: 10.1016/j.fsi.2016.09.007
123. Huang Y, Li T, Jin M, Yin S, Hui KM, Ren Q. Newly Identified PcToll4 Regulates Antimicrobial Peptide Expression in Intestine of Red Swamp

Crayfish Procambarus clarkii. *Gene* (2017) 610:140–7. doi: 10.1016/j.gene.2017.02.018
124. Huang Y, Chen Y, Hui K, Ren Q. Cloning and Characterization of Two Toll Receptors (PcToll5 and PcToll6) in Response to White Spot Syndrome Virus in the Red Swamp Crayfish Procambarus clarkii. *Front Physiol* (2018) 9:936. doi: 10.3389/fphys.2018.00936
125. Habib YJ, Zhang Z. The Involvement of Crustaceans Toll-Like Receptors in Pathogen Recognition. *Fish Shellfish Immunol* (2020) 102:169–76. doi: 10.1016/j.fsi.2020.04.035
126. Huang Y, Ren Q. Research Progress in Innate Immunity of Freshwater Crustaceans. *Dev Comp Immunol* (2020) 104:103569. doi: 10.1016/j.dci.2019.103569
127. Rončević T, Čikeš-Čulić V, Maravić A, Capanni F, Gerdol M, Pacor S, et al. Identification and Functional Characterization of the Astacidin Family of Proline-Rich Host Defence Peptides (PcAst) From the Red Swamp Crayfish (Procambarus clarkii, Girard 1852). *Dev Comp Immunol* (2020) 105:103574. doi: 10.1016/j.dci.2019.103574
128. Wang XW, Zhang HW, Li X, Zhao XF, Wang JX. Characterization of a C-type Lectin (PcLec2) as an Upstream Detector in the Prophenoloxidase Activating System of Red Swamp Crayfish. *Fish Shellfish Immunol* (2011) 55:241–7. doi: 10.1016/j.fsi.2010.10.012
129. Dai Y, Wang Y, Zhao L, Qin Z, Yuan J, Qin Q, et al. A Novel L-type Lectin was Required for the Multiplication of WSSV in Red Swamp Crayfish (Procambarus clakii). *Fish Shellfish Immunol* (2016) 55:48–55. doi: 10.1016/j.fsi.2016.05.020
130. Wu C, Söderhäll K, Söderhäll I. Two Novel Ficolin-Like Proteins Act as Pattern Recognition Receptors for Invading Pathogens in the Freshwater Crayfish Pacifastacus leniusculus. *Proteomics* (2011) 11(11):2249–64. doi: 10.1002/pmic.201000728
131. Ng TH, Kurtz J. Dscam in Immunity: A Question of Diversity in Insects and Crustaceans. *Dev Comp Immunol* (2020) 105:103539. doi: 10.1016/j.dci.2019.103539
132. Armitage SAO, Peuß R, Kurtz J. Dscam and Pancrustacean Immune Memory - a Review of the Evidence. *Dev Comp Immunol* (2015) 48 (2):315–23. doi: 10.1016/j.dci.2014.03.004
133. Lan JF, Zhou J, Zhang XW, Wang ZH, Zhao XF, Ren Q, et al. Characterization of an Immune Deficiency Homolog (IMD) in Shrimp (Fenneropenaeus Chinensis) and Crayfish (Procambarus clarkii). *Dev Comp Immunol* (2013) 41(4):608–17. doi: 10.1016/j.dci.2013.07.004
134. Huang Y, Ren Q. Molecular Cloning and Functional Analysis of Three STAT Isoforms in Red Swamp Crayfish Procambarus clarkii. *Dev Comp Immunol* (2020) 108:103670. doi: 10.1016/j.dci.2020.103670
135. Shen H, Hu Y, Ma Y, Zhou X, Xu Z, Shui Y, et al. In-Depth Transcriptome Analysis of the Red Swamp Crayfish Procambarus clarkii. *PloS One* (2014) 9 (10):e110548. doi: 10.1371/journal.pone.0110548
136. Wu C, Charoensapsri W, Nakamura S, Tassanakajon A, Söderhäll I, Söderhäll K. An MBL-like Protein may Interfere With the Activation of the proPO-system, an Important Innate Immune Reaction in Invertebrates. *Immunobiology* (2013) 218(2):159–68. doi: 10.1016/j.imbio.2012.02.011
137. Jiravanichpaisal P, Lee SY, Kim YA, Andrén T, Söderhäll I. Antibacterial Peptides in Hemocytes and Hematopoietic Tissue From Freshwater Crayfish Pacifastacus leniusculus: Characterization and Expression Pattern. *Dev Comp Immunol* (2007) 31(5):441–55. doi: 10.1016/j.dci.2006.08.002
138. Donpudsa S, Rimphanitchayakit V, Tassanakajon A, Söderhäll I, Söderhäll K. Characterization of Two Crustin Antimicrobial Peptides From the Freshwater Crayfish Pacifastacus leniusculus. *J Invertebrate Pathol* (2010) 104(3):234–8. doi: 10.1016/j.jip.2010.04.001
139. Du ZQ, Li B, Shen XL, Wang K, Du J, Yu XD, et al. A New Antimicrobial Peptide Isoform, Pc-crustin 4 Involved in Antibacterial Innate Immune Response in Fresh Water Crayfish, Procambarus clarkii. *Fish Shellfish Immunol* (2019) 94:861–70. doi: 10.1016/j.fsi.2019.10.003
140. Zeng Y. Procambarin: A Glycine-Rich Peptide Found in the Haemocytes of Red Swamp Crayfish Procambarus clarkii and its Response to White Spot Syndrome Virus Challenge. *Fish Shellfish Immunol* (2013) 35(2):407–12. doi: 10.1016/j.fsi.2013.04.048
141. Zhang HW, Sun C, Sun SS, Zhao XF, Wang JX. Functional Analysis of Two Invertebrate-Type Lysozymes From Red Swamp Crayfish, Procambarus clarkii. *Fish Shellfish Immunol* (2010) 29(6):1066–72. doi: 10.1016/j.fsi.2010.08.023
142. Li X-J, Yang L, Li D, Zhu Y-T, Wang Q, Li W-W. Pathogen Specific Binding Soluble Down Syndrome Cell Adhesion Molecule (Dscam) Regulates Phagocytosis Via Membrane Bound Dscam in Crab. *Front Immunol* (2018) 9:801. doi: 10.3389/fimmu.2018.00801
143. Li D, Wan Z, Li X, Duan M, Yang L, Ruan Z, et al. Alternatively Spliced Down Syndrome Cell Adhesion Molecule (Dscam) Controls Innate Immunity in Crab. *J Biol Chem* (2019) 294:16440–50. doi: 10.1074/jbc.RA119.010247
144. Chang YH, Kumar R, Ng TH, Wang HC. What Vaccination Studies Tell Us About Immunological Memory Within the Innate Immune System of Cultured Shrimp and Crayfish. *Dev Comp Immunol* (2018) 80:53–66. doi: 10.1016/j.dci.2017.03.003
145. Zheng X, Li S, Si Y, Hu J, Xia Y. Locust can Detect β-1, 3-Glucan of the Fungal Pathogen Before Penetration and Defend Infection *via* the Toll Signaling Pathway. *Dev Comp Immunol* (2020) 106:103636. doi: 10.1016/j.dci.2020.103636

Conflict of Interest: The author declares that the research was conducted in the absence of any commercial or financial relationships that could be construed as a potential conflict of interest.

frontiers in Immunology

BRIEF RESEARCH REPORT
published: 13 May 2021
doi: 10.3389/fimmu.2021.634152

Differentially Expressed Genes in Hepatopancreas of Acute Hepatopancreatic Necrosis Disease Tolerant and Susceptible Shrimp (*Penaeus vannamei*)

*Hung N Mai, Luis Fernando Aranguren Caro, Roberto Cruz-Flores, Brenda Noble White and Arun K. Dhar**

Aquaculture Pathology Laboratory, School of Animal & Comparative Biomedical Sciences, The University of Arizona, Tucson, AZ, United States

OPEN ACCESS

Edited by:
Kunlaya Somboonwiwat, Chulalongkorn University, Thailand

Reviewed by:
Ikuo Hirono, Tokyo University of Marine Science and Technology, Japan
Yeong Yik Sung, University of Malaysia Terengganu, Malaysia
Parin Chaivisuthangkura, Srinakharinwirot University, Thailand

***Correspondence:**
Arun K. Dhar
adhar@email.arizona.edu

Specialty section:
This article was submitted to Comparative Immunology, a section of the journal Frontiers in Immunology

Received: *27 November 2020*
Accepted: *15 April 2021*
Published: *13 May 2021*

Citation:
Mai HN, Caro LFA, Cruz-Flores R, White BN and Dhar AK (2021) Differentially Expressed Genes in Hepatopancreas of Acute Hepatopancreatic Necrosis Disease Tolerant and Susceptible Shrimp (Penaeus vannamei). Front. Immunol. 12:634152. doi: 10.3389/fimmu.2021.634152

Acute hepatopancreatic necrosis disease (AHPND) is a lethal disease in marine shrimp that has caused large-scale mortalities in shrimp aquaculture in Asia and the Americas. The etiologic agent is a pathogenic *Vibrio* sp. carrying binary toxin genes, *pir*A and *pir*B in plasmid DNA. Developing AHPND tolerant shrimp lines is one of the prophylactic approaches to combat this disease. A selected genetic line of *Penaeus vannamei* was found to be tolerant to AHPND during screening for disease resistance. The mRNA expression of twelve immune and metabolic genes known to be involved in bacterial pathogenesis were measured by quantitative RT-PCR in two populations of shrimp, namely P1 that showed susceptibility to AHPND, and P2 that showed tolerance to AHPND. Among these genes, the mRNA expression of chymotrypsin A (ChyA) and serine protease (SP), genes that are involved in metabolism, and crustin-P (CRSTP) and prophenol oxidase activation system 2 (PPAE2), genes involved in bacterial pathogenesis in shrimp, showed differential expression between the two populations. The differential expression of these genes shed light on the mechanism of tolerance against AHPND and these genes can potentially serve as candidate markers for tolerance/susceptibility to AHPND in *P. vannamei*. This is the first report of a comparison of the mRNA expression profiles of AHPND tolerant and susceptible lines of *P. vannamei*.

Keywords: AHPND, *Penaeus vannamei*, AHPND tolerant P vannamei, shrimp immunity, immune genes

INTRODUCTION

Acute hepatopancreatic necrosis disease (AHPND) is a lethal disease of marine shrimp that emerged in China in 2009. Since then it was reported in other countries including Vietnam, Thailand, Mexico, Philippines, Bangladesh, US and South-Korea (1–7). The etiologic agent was initially identified as *Vibrio parahaemolyticus* carrying plasmid-borne binary toxin genes, *pir*A and *pir*B (8, 9). Subsequently other species of *Vibrio* including *V. harveyi* and *V. owensii* have been reported to cause AHPND (10, 11). The clinical signs of AHPND include atrophy and pale

discoloration of hepatopancreas, soft shell, gut with discontinuous or no content, and often 100% of mortality occurs in shrimp farms experiencing AHPND outbreaks (12–14). Histopathology of the hepatopancreas tissue from AHPND affected shrimp reveals three different stages of disease development, namely initial, acute/terminal and chronic phases. In the initial phase, elongation of epithelial cells in hepatopancreas is common, whereas during the acute/terminal phase necrosis of tubular epithelial cells and inflammatory responses are observed (13). The chronic phase of AHPND is characterized by the epithelial necrosis and bacterial inflammation in the tubules which is similar to septic hepatopancreatic necrosis (SHPN) (15).

It has widely been accepted that shrimp protect themselves from microbial pathogens by innate immunity that encompass humoral and cellular responses. Recently, it has been reported that the $PirA^{VP}$- and $PirB^{VP}$ binary toxin encoded by *V. parahaemolyticus* can be neutralized by either hemocyanin or anti-lipopolysaccharide factor (16). In addition, the interaction between immune and metabolism appears to play a role in AHPND response in hepatopancrease in shrimp (17, 18). Until now, due to the lack of AHPND- tolerant lines of shrimp, no effort could be made to examine the gene expression profiles of AHPND- susceptible and tolerant lines of shrimp.

Recently, a line of *P. vannamei* shrimp has been identified that displays tolerance to AHPND (15). In this study, we initially compared the mRNA expression of twelve metabolic/immune related genes between AHPND-tolerant and-susceptible lines of *P. vannamei* by reverse transcriptase quantitative PCR (RT-qPCR). These genes are known to be involved in bacterial pathogenesis (19–24). The expression of seven genes that showed statistically significant differences between the tolerant and susceptible lines were validated. The results showed that there is a significant difference in the expression of these genes between AHPND-tolerant and-susceptible lines of *P. vannamei*. The potential implications of differential expression of these genes are discussed in the context of immunity and pathogenesis.

MATERIALS AND METHODS

Bioassay 1- Assessing AHPND Tolerance in *P. vannamei*

Vibrio parahemolyticus (Strain 13-028A/3) (Vp_{AHPND}) was used for the experimental challenges following a previously published protocol (15). Three *P. vannamei* family lines were obtained from a commercial supplier as a part of an on-going family line screening for AHPND-tolerance. Each line was stocked separately into a total of nine 1000 L tanks in triplicate. From each of these three lines, we screened 56, 57 and 78 organisms from lines one, two and three respectively. A Specific Pathogen Free (SPF) *P. vannamei* (N=60, average weight 3 g) (AHPND susceptible line, population P1, were obtained from a commercial supplier in the USA and stocked into two 90L tanks and used as positive controls for AHPND challenge. A third tank containing SPF shrimps of the same genetic line (N=64) was used as negative control. An immersion challenge was performed using an inoculum load of 10^6 cfu/ml (15). The experiment was terminated at 7 days post-inoculation. The mortality in each tank was recorded daily, and a subset of moribund and surviving animals was examined by routine H&E histology.

Histopathology

Moribund *P. vannamei* were fixed in Davidson's alcohol-formalin-acetic acid (AFA) fixative. The samples were processed, embedded in paraffin, sectioned (4 μm thick) and analyzed in accordance with standard methods (25).

Bioassay 2- Initial Gene Expression Analyses

To evaluate gene expression in the AHPND-tolerant and-susceptible lines, a second challenge was conducted. A total of 46 animals were utilized from P1 (n= 42, average weight 5g) with 21 animals challenged with VP_{AHPND}, 21 animals utilized as negative controls and 4 animals sampled for gene expression analysis prior to challenge. The tolerant line was named population P2 (n=20, average weight 9g), with 9 animals challenged with VP_{AHPND}, 9 unchallenged as negative controls and 2 animals sampled for gene expression analysis prior to challenge. All shrimp from each family were tagged in the 4th abdominal segment with uniquely colored elastomer tags to allow visual identification. Both families were then held in a single 1000L tank and challenged by immersion, as described above. The negative controls were held in a single 1000L tank but were not challenged.

Twenty-four hours after challenge, animals were collected for gene expression analysis. Limited numbers (N=4) of the susceptible P1 line were available for sampling due to the typically high mortality rates observed in AHPND challenges in the first 24 hours. Two shrimp were collected from the tolerant population P2 at 24 hours post-infection to leave enough animals in the tank for a survival comparison at termination. In order to keep the sample numbers equal, a pool of 10 challenged animals from P2 group in the initial family line challenge were pooled as 2 samples for a total of 4 samples.

Measuring the Expression Levels of Candidate Immune and Metabolic Genes in AHPND Challenged *P. vannamei*

Four shrimp samples per population were collected from each treatment for RNA extraction using RNAzol following the manufacturer's protocol (MRC, Ohio, USA). The RNA was treated with DNase 1 (Invitrogen, USA). One μg of DNase treated RNA was used for cDNA synthesis using Superscript IV and following the manufacturer's recommendation (Invitrogen, USA). After that, cDNA was subjected to gene expression analysis.

The mRNA expression of β-glucan binding protein (BGBP) (AY249858.1), Crustin-P (CRSTP) (AY488497), C-type lectin 1-like (CTL1-like) (DQ858900.1), Extracellular Copper/Zinc Superoxide dismutase (EC-SOD) (HM371157), Kazal protease inhibitor (KPI) (AY544986), lipopolysaccharide and β-1,3-glucan-

binding protein (LGBP) (EU102286.1), Penaidin 2 (PEN2) (Y14925), Prophenol oxidase activation system 2 (PPAE2) (AWF98992.1), Serpin8 (SEP8) (KU853046.1), serine protease (SP) (AY368151), Chymotrypsin A (ChyA) (Y10664), Chymotrypsin B (ChyB) (Y10665) and two toxin genes of *V. parahaemolyticus* (i.e. *pir*A and *pir*B toxin genes, KM067908) were measured by quantitative PCR (StepOnePlus Real-time PCR system, Applied biosystems, USA) using PowerUPTM SYBR Green Master Mix (Applied Biosystem, USA). The reaction mixture contained 10 µl of PowerUP™ SYBR Green Master Mix, 0.8 µl (0.4 µM) of each primer, 2.0 µl of cDNA and 6.4 µl of sterile water in a reaction volume of 20 µl. The thermal profile for the reaction was 2 minutes at 50°C, 2 minutes at 95°C followed by 40 cycles of 3 seconds at 95°C and 30 seconds at 60°C. The primer sequence for each gene is given in **Supplementary Table S1**. In addition, literature search of the responses to pathogens of studied genes was provided in **Supplementary Table S4**. Each sample was run in duplicate and the mean Ct value was used for gene expression analysis. Expression levels of each gene in various populations are shown relative to the expression in corresponding control treatments according to the formula of Livak and Schmittgen (26). For evaluating the gene expression between challenged animals coming from P1 and P2 population, the expression levels of each gene were shown relative to the expression in the P1 negative control. The expression value was converted to Log based 2 prior to statistical analysis. The genes showing statistical difference in expression level in Bioassay 2 were validated in Bioassay 3.

Bioassay 3- Gene Expression Validation

Two hundred shrimp (average wt. 2 g) with the same genetic characteristics of the AHPND tolerant shrimp line (P2) from Bioassay 2 were stocked in two 1000 L-tanks (100 shrimp/tank) in which one tank was challenged with VP_{AHPND}. The remaining tank was used as negative control. Forty SPF shrimp (AHPND susceptible shrimp) (average wt. ~1.5 g) (P1) were stocked in two 90L-tanks (20 shrimp/tank), one tank was challenged with VP_{AHPND}. The remaining tank was used as negative control. The AHPND challenge protocol was the same as described previously. After 24 hours, nine shrimp from each tank were collected for gene expression analyses.

Statistical Analysis

The statistical significances in the difference in Log based 2 value of gene expression between control and challenged animals in each population and between challenged animals in P1 and P2 populations was determined by using Student's t-test with $P<0.05$, SPSS v.16 software. The mortality data was analyzed using Kaplan-Meier method, SPSS v.16 software.

RESULTS

Bioassay 1- Assessing AHPND Tolerance in *P. vannamei*

In experimental AHPND challenge, the survival rate in the AHPND-tolerant P2 population was over five times higher compared to the AHPND-susceptible P1 population (72% *vs.* 12.5%). Meanwhile, the survival rate in negative control was 95.45% (**Supplementary Figure S1**). The histopathology of the P1 and P2 populations are presented in **Figure 1**. The Davidson-fixed shrimp from the healthy, negative controls from P1 and P2 displayed normal structure of tubules and epithelial cells in the hepatopancreas including high levels of lipid droplets (R-cells), secretory vacuoles (B-cells) and absence of AHPND (**Figures 1A, B**). In contrast, shrimp from the P1 population challenged with Vp_{AHPND} displayed lesions typical of AHPND in the acute phase, including a multifocal necrosis and massive sloughing of HP tubule epithelial cells in the hepatopancreas. At this stage, bacterial colonization was not observed (**Figure 1C**). Shrimp from the P2 population displayed the typical VP_{AHPND} chronic phase characterized by SHPN-like lesions (**Figure 1D**).

Bioassay 2- Initial Gene Expression Analyses, Measuring the mRNA Expression of Immune and Metabolic Genes in *P. vannamei*

Interestingly, there was no significant difference in the expression levels of *pir*A/*pir*B genes between P1 and P2 population ($P>0.05$) (**Figure 2**).

The mRNA expression of a set of immune and metabolic genes (i.e. SEP8, BGBP, CRSTP, CTL1-like, KPI, LGBP, EC-SOD, PEN2, PPAE2, SP, ChyA and ChyB) were measured by RT-qPCR in control animals and challenged animals in each population. We also compared the levels of gene expression in AHPND susceptible P1 and AHPND tolerant P2 populations.

The *V. parahaemolyticus* infection led to the significant upregulation of expression of LGBP, PPAE2, and ChyA transcripts in the P1 population ($P<0.05$) whereas SP mRNA showed significant down regulated expression ($P<0.05$). The mRNA levels of BGBP, CRSTP, CTL1-like, KPI, PEN2, EC-SOD, SEP8 and ChyB in the challenged and un-challenged groups did not show significant differences ($P>0.05$) (**Figure 3A**).

In the P2 population, *V. parahaemolyticus* infection led to the significant downregulated expression of LGBP mRNA ($P<0.05$). The expression of BGBP, SEP8, CTL1-like, CRSTP, KPI, EC-SOD, PPAE2, PEN2, SP, ChyA and ChyB showed no significant difference between challenged and un-challenged groups ($P>0.05$) (**Figure 3B**).

When the mRNA expression levels were compared between AHPND challenged animals from the P1 and P2 populations, there were significant differences in the expression profiles of some genes. For example, while the susceptible P1 population showed significantly higher levels of expression of ChyA, CRSTP, CTL1-like, LGBP and PPAE2 ($P<0.05$) (**Figure 3C**), the AHPND-tolerant population P2 showed higher expression of SP and ChyB compared to the susceptible P1 population ($P<0.05$) (**Figure 3C**) (**Supplementary Table S2**).

Bioassay 3- Gene Expression Validation

The genes showing significant differences in expression levels between susceptible and tolerant shrimp were selected for

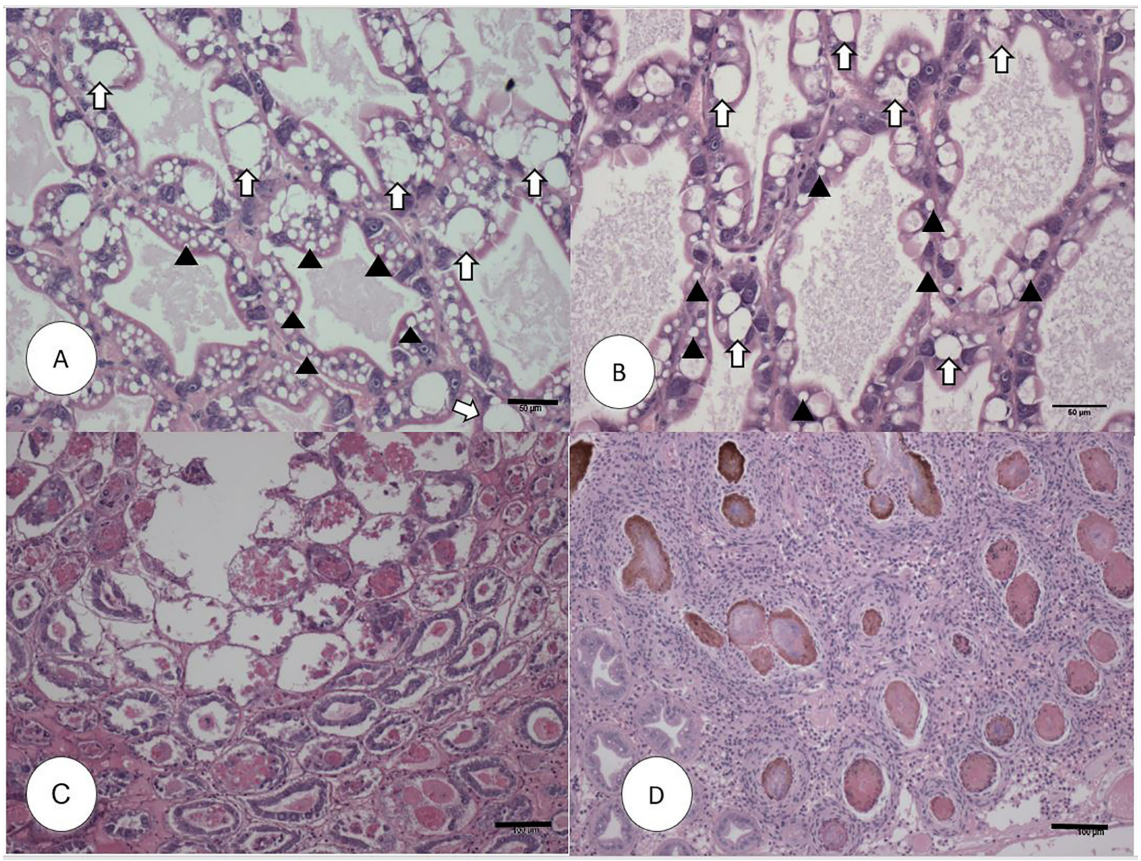

FIGURE 1 | H&E (Mayer–Bennet hematoxylin and eosin-phloxine) histology of *Penaeus vannamei* from Bioassay 1. *Penaeus vannamei* from negative control tank from the P1 **(A)** and P2 populations **(B)** showing intact tubules and epithelial R-cells (arrowhead) and B-cells (white arrow). Acute phase infection of AHPND in shrimp from P1 population **(C)** showing a severe sloughing of epithelial tubule cells into the lumen. Terminal phase of AHPND infection in shrimp from P2 population **(D)** showing a severe intertubular hemocytic infiltration surrounding the affected melanized tubules. Scale bars for **(A**, **B)** = 50 μm; **(C**, **D)** = 100 μm.

validations in Bioassay 3. In the P1 population, the expression of CTL1-like, CRSTP, SP and ChyB were significantly down regulated (P<0.05) meanwhile PPAE2 and ChyA expression levels were significantly up regulated (P<0.05) (**Figure 4A**). LGBP expression level was not significant during the experiment (P>0.05) (**Figure 4A**).

In P2 population, PPAE2, ChyA and LGBP expression levels were significantly up regulated (P<0.05). In contrast, the expression levels of CRSTP and SP were down regulated (P<0.05) (**Figure 4B**). CTL1-like and ChyB expression were not significantly different during the experiment (P>0.05) (**Figure 4B**).

By comparison, P1 and P2 challenged animals showed the same expression pattern in both Bioassay 2 and Bioassay 3. The expression levels of CRSTP, PPAE2 and ChyA were significantly higher in P1 population (P<0.05). LGBP expression level was higher in P1 population but not significantly different (P>0.05). Meanwhile, SP had a significant higher expression level in P2 population than P1 population (P<0.05) (**Figure 4C**). ChyB expression level was higher in P2 population than P1 population even though there was no significant difference observed during the experiment (P>0.05) (**Figure 4C**) (**Supplementary Table S3**).

DISCUSSION

Bacterial pathogenesis in crustaceans is well studied and genes involved in humoral and cellular immunity are known. We decided to take advantage of this background knowledge by measuring the expression of genes that are well known to be involved in defense and metabolic responses during bacterial infections in shrimp. Coincidentally, we had access to AHPND-tolerant lines of *P. vannamei* and considering the lethal nature of AHPND-causing *V. parahaemolyticus* we explored if genes known to be involved in other bacterial pathogenesis in shrimp are also involved in AHPND pathogenesis. To our knowledge, a recently published paper is the first report of the development of AHPND resistant/tolerant lines of *P. vannamei*, Aranguren Caro et al. (15), and as of today, there is no report of looking into the gene expression profiles of AHPND-tolerant *vs*. susceptible lines.

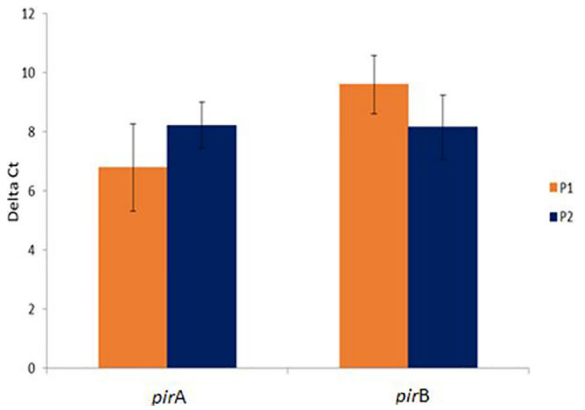

FIGURE 2 | Comparative *pir*A- and *pir*B- toxin genes expression in challenged animals from Bioassay 2 in the P1 and P2 populations. The levels of mRNA expression is expressed as a normalized mean Ct value. The data is presented as ΔMean Ct ± SD. Statistical significance between P1 and P2 populations for each of the candidate gene was determined using Student's t-test.

It is now widely accepted that the etiology of AHPND is the insecticidal binary toxin-like genes carried by plasmid DNA in *Vibrio* spp (11, 12, 27). An AHPND resistant/tolerant shrimp line would be ideal in controlling the disease in shrimp aquaculture. Tinwongger and colleagues (16) showed that shrimp exposed to formalin killed cells (FKC) of AHPND causing *V. parahaemolyticus* can survive upon AHPND challenge, and anti-lipopolysaccharide factor AV-R isoform (LvALF AV-R) showed significantly higher expression in the hepatopancreas from the survivor. Interestingly, only four out of two hundred shrimp (2%) survived after feeding with FKC diet, and only three shrimp from the survivor group were used for gene expression analysis. Despite examining a limited number of animals, the authors were successful in identifying genes that could be potentially involved in AHPND pathogenesis. In this study, three bioassays were performed. Bioassay 1 was performed to identify an AHPND tolerant line, P2, using mortality and histopathology as end point data of the bioassay. The P2 population suffered 28% mortality compared to the susceptible line P1 that experienced 87.5% mortality. The bioassay was repeated using the same AHPND-susceptible (P1) and tolerant line (P2) (i.e. Bioassay 2) to examine the mRNA expression of twelve candidate immune and metabolic genes. When the expression of these genes were compared before and after challenge within a population, P1 and P2, a number of genes showed differential expression. However, when the expression profiles were compared between P1 and P2 populations after AHPND-challenge, seven candidate genes showed differential expression. These genes are likely involved in AHPND pathogenesis. In order to further validate the expression of these seven genes, a third bioassay was conducted (i.e. Bioassay 3) and samples were collected for the gene expression validation. The data shed light on the molecular basis of AHPND pathogenesis and enabled to identify potential markers for AHPND tolerance/susceptibility, as discussed below.

Bioassay 1

The mortality data in the Bioassay 1 showed that the survival rate of the P2 population was over five times higher than P1 population indicating that P2 population is indeed an AHPND tolerant line. The mortality data was consistent with the histopathology findings that cellular damage in the hepatopancreas was far greater in animals from the P1 compared to the P2 population. For example, sloughing of the epithelial cells in the hepatopancreatic tubules followed by massive infiltration of bacterial cells that are considered pathognomonic for AHPND was clearly evident by H&E histology in animals from P1 population (**Figure 1**), whereas in the P2 population, the lesions present in the hepatopancreas resembled more of a chronic infection as seen during SHPN. The differences in mortality and histopathology data led to examining the expression profiles of twelve metabolic and immune-related genes in these two populations. Interestingly, some genes in the tolerant shrimp such as CRST-P, SP, ChyB and LGBP showed the discrepancies in the trend of expression between Bioassay 2 and Bioassay 3. However, only LGBP expression significantly down-regulated in tolerant shrimp from Bioassay 2 meanwhile LGBP expression in tolerant shrimp from Bioassay 3 showed significantly up-regulated. The reasons for discrepancies could be different animals reacting differently to the same pathogen although they are similar genetic line. That would be the reason we had to do validation test with larger number animals.

Gene Expression in *P. vannamei* From Bioassay 2 *vs*. Bioassay 3

The expression of twelve candidate genes known to be involved in other bacterial diseases were examined to determine if similar genes are involved in AHPND pathogenesis. It was interesting to note that there was no significant difference in the expression levels of *pir*A or *pir*B toxin genes between the P1 and P2 populations suggesting that the animals from the two populations were exposed to equivalent levels of toxin. Thus, the difference in tolerance was most likely due to the difference in immune response between the two populations.

It is known that shrimp, like other invertebrates, elicit cellular and humoral immune responses when exposed to microbes or non-self-protein containing pathogen associated molecular patterns (PAMP) (28, 29). PAMP is easily recognized by pattern recognition proteins including BGBP, LGBP and CTL (19, 30–33). Several studies indicate that the expression of BGBP, LGBP and CTL are up-regulated in shrimp challenged with pathogens such as bacteria, viruses and fungi (34–37).

In Bioassay 2, when the mRNA expressions of BGBP, LGBP and CTL1-like genes were compared between AHPND-susceptible P1 and AHPND-tolerant P2 populations, LGBP and CTL1-like genes were found to be upregulated in P1 compared to P2 population. However, there was no difference in BGBP expression between the two populations (**Figure 3**). Interestingly, in Bioassay 3, although LGBP expression was higher in P1 than P2 populations as in Bioassay 2 samples, the difference in expression was not statistically significant

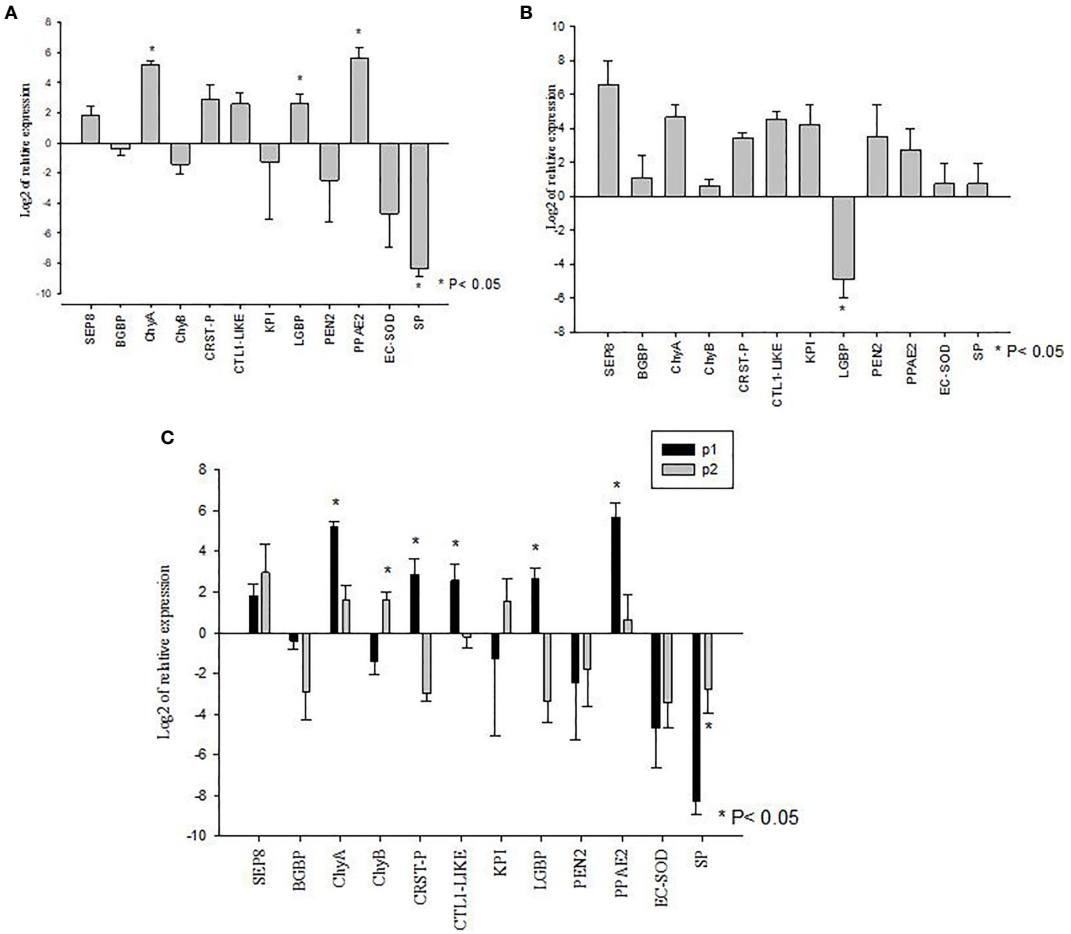

FIGURE 3 | Gene expression profiles of metabolic and immune genes in shrimp *Penaeus vannamei* from Bioassay 2. **(A)** The mRNA expression profile in AHPND susceptible (P1) population following experimental challenge. **(B)** The mRNA expression profile in AHPND tolerant (P2) population following experimental challenge. Expression levels of each gene are shown relative to the expression in correspond control treatment **(C)** Comparison of gene expression profile from AHPND susceptible (P1) vs. AHPND resistant/tolerant (P2) population. Expression levels of each gene are shown relative to the expression in P1 negative control treatment. The data is presented as log2 of relative expression ± SD. Statistical significance between control and challenged animals for each of the candidate gene was determined using Student's t-test. *P<0.05. BGBP, β-glucan binding protein; CRST P, Crustin P; CTL, C-type lectin 1-like; ECSOD, Extracellular Copper/Zinc Superoxide dismutase; KPI, Kazal protease inhibitor; LGBP, Lipopolysaccharide and β-1,3-glucan-binding protein; PEN2, Penaidin 2; PPAE2, Prophenol oxidase activation system 2; SEP, Serpin8; SP, Serine protease; ChyA, Chymotrypsin A; ChyB, Chymotrypsin B.

(p=0.365). In contrary, CTL1-like gene did not show any differential expression between the two populations (**Figure 4**), as observed in samples derived from Bioassay 2 (**Figure 3**). These discrepancies highlight two important facts: (i) it is critical to validate gene expression data with biological samples derived from independent bioassays, and (ii) it is important to validate initial findings with larger sample sets, as in Bioassay 3 compared to Bioassay 2. These gives further credence to the mRNA expression findings reported in this study.

In shrimp, upon microbial infection pattern recognition protein(s) circulating in the hemolymph triggers immune response by activating proPO cascade and releasing antimicrobial peptides such as PEN and CRSTP to eliminate the invading pathogen(s) (20). Although PEN and CRSTP were shown to have antimicrobial activities against *Vibrio* spp. and Gram positive bacteria in penaeid shrimp (21, 23, 38), neither of these genes were significantly upregulated in the challenged animals in Bioassay 2. In shrimp, PEN2 is mostly detected in hemocytes and to a lesser level in hepatopancreas. Since we examined the gene expression in hepatopancreas tissue, it is possible that for this reason PEN2 was not found to be differentially expressed. Interestingly, CRSTP which is also predominantly expressed in hemocytes and less in hepato pancreas showed significantly higher expression in AHPND susceptible P1 compared to AHPND tolerant P2 populations in both Bioassays 2 and 3. It remains to be determined if higher CRSTP expression in the susceptible population is due to increased bacterial cell deaths and consequently the release of $PirAB^{VP}$ toxin in the infected animals.

The proPO activation is an important event in crustacean immunity to eliminate pathogens from the circulatory system (39, 40). The final event in the proPO activation process is the

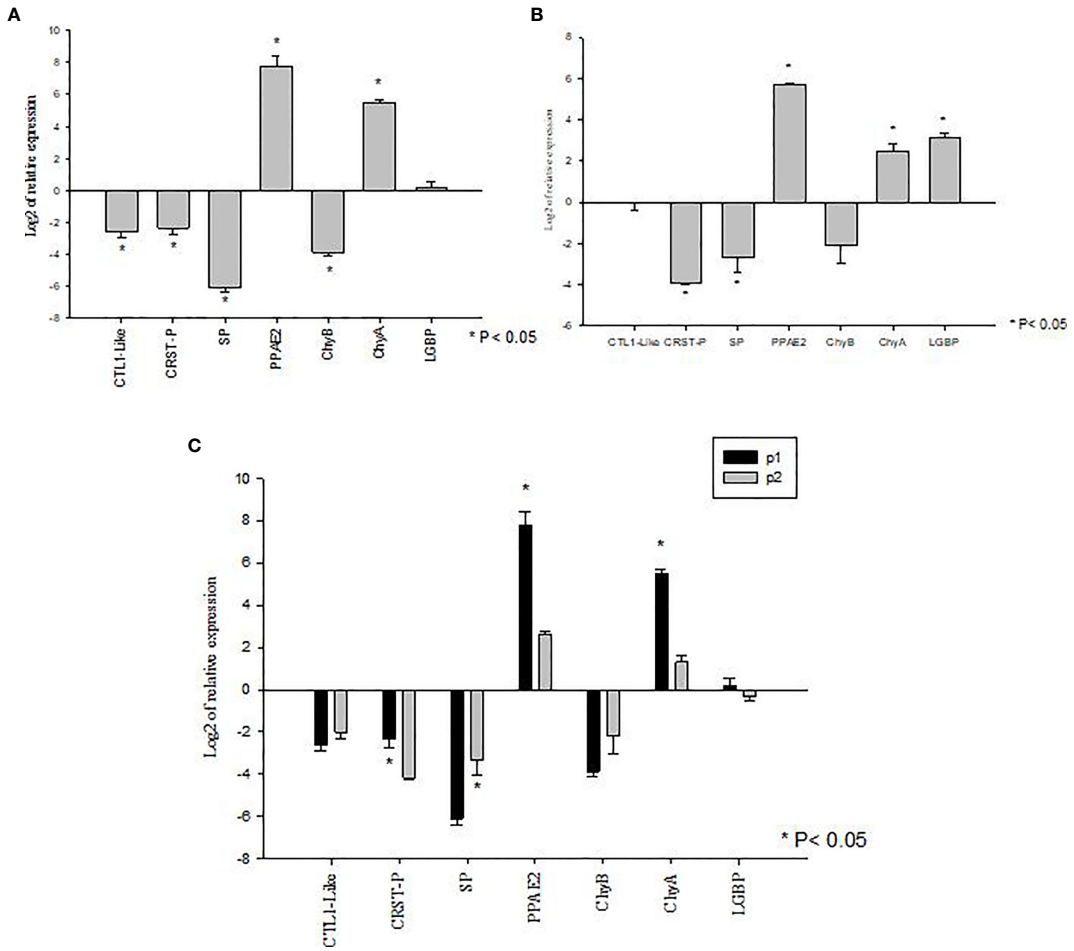

FIGURE 4 | Validation of gene expression profiles of metabolic and immune genes in *Penaeus vannamei* from Bioassay 3 **(A)** The mRNA expression profile in *P. vannamei* AHPND susceptible (P1) population (Panel **A**) and AHPND resistant/tolerant (P2) population (Panel **B**) following experimental challenge. Expression level of each gene is shown relative to the expression in correspond control treatment **(C)** Comparison of gene expression profile from AHPND susceptible (P1) vs AHPND resistant/tolerant (P2) population. Expression levels of each gene are shown relative to the expression in P1 negative control treatment. The data are presented as $\log_2$ of relative expression ± SD. Statistical significance between control and challenged animals for each of the candidate gene was determined using Student's t-test. *P<0.05. CRST P, Crustin P; CTL, C-type lectin 1-like; LGBP, Lipopolysaccharide and β-1,3-glucan-binding protein; PPAE2, Prophenol oxidase activation system 2; SP, Serine protease; CHYA, Chymotrypsin A; CHYB, Chymotrypsin B.

conversion of proPO to phenoloxidase (PO) by the PPAE (26, 41, 42). In both Bioassays 2 and 3, PPAE2 showed significantly higher expression after AHPND challenge in P1 compared to P2 populations. The finding is consistent with a previously published report in *P. monodon* where PPAE2 expression in the stomach showed significant upregulation at 24 hour post-challenge with AHPND causing *V. parahaemolyticus* (43). In a separate study, Apitanyasai et al. (44) suggested an overreaction of the proPO cascade causes damage to host cells during AHPND infection and leads to higher mortality. The higher expression of PPAE2 in AHPND susceptible P1 population supports this observation. Taken together, this evidence suggests that upon infection with Vp_{AHPND}, not only the expression of antimicrobial peptide like CRSTP but also the genes involved in the proPO pathway are elevated in AHPND susceptible compared to tolerant animals.

It is known that the activation of proPO leads to production of quinones and other intermediate reactions which polymerizes quinones to melanin resulting in pathogen capsulation (45). Quinone, however, also causes cell death by inducing reactive oxygen species (ROS) production (46–48). In crustacean, ROS can be scavenged by an anti-oxidant system involving enzymes of the SOD family (49–51). The EC-SOD expression in the animals studied was not significantly modulated upon AHPND challenge. The proPO cascade is also modulated by a series of protease inhibitors such as KPI and SEP8 to prevent the over activation (52, 53). Again, both KPI and SEP8 mRNA levels in animals from the P1 and P2 populations were not significantly different. It is tempting to speculate that for the lack of modulation of efforts in EC-SOD, proPO cascade activation led to cell toxicity more in P1 compared to P2 population. It is also possible that killing of Vp_{AHPND} cells leads to further release of

PirAB toxin from the inactivated bacterial cells exerting lethal effects in genetically susceptible animals.

The involvement of PO activity in the susceptibility of invertebrates due to bacterial toxins has been well documented in many insect species. For example, cabbage loopers (*Trichoplusia ni*) is inherently susceptible to the Cry toxin secreted from *Bacillus thuringiensis*. However, the Cry toxin resistance is negatively correlated with the PO activity in *B. thuringiensis* challenged *T.ni* (54). In addition, the effectiveness of biological insecticide is also higher in lepidopteran species that show high PO activity (55). Recently, it has been reported that during VP_{AHPND} infection resulting in AHPND, reduction in activation of the proPO system by a serine protease inhibitor, *Lv*Serpin7, results in reduction of the toxic effects compared to an unregulated activation of the PO cascade (44).

Apart from the difference in immune gene expression, the expression of metabolic genes also showed differences between healthy and AHPND-challenged animals in each population and between challenged animals in populations P1 *vs* P2. The expression of ChyB and SP were down regulated whereas ChyA expression was up regulated in AHPND challenged shrimp in both P1 and P2 populations and in both Bioassays 2 and 3. These results are consistent with the findings from a recent study in which SP was shown to be upregulated in AHPND tolerant *P. monodon* (18). In addition, Chymotrypsin is upregulated in AHPND susceptible *P. vannamei* after 24 hour of infection (17) which is also in agreement with our findings.

Recently, the crystal structure of $PirAB^{VP}$ toxin shows homology to the structure of the Cry toxin released by *B. thuringiensis* (56), and it is known that the Cry protein is activated by protease enzymes (56–58). The tertiary structure of $PirAB^{VP}$ involves a heterotetrameric interaction between two $PirA^{VP}$ and two $PirB^{VP}$. It has been hypothesized that $PirA^{VP}$ plays a role in receptor binding while $PirB^{VP}$ is involved in pore formation in the cell membrane (59). *In silico* analysis (https://web.expasy.org/peptide_cutter/) showed that the $PirA^{VP}$ toxin contains twelve and nine putative sites that are likely to be cleaved by chymotrypsin and trypsin, respectively (**Supplementary Figure S2**). Meanwhile, $PirB^{VP}$ toxin contains 53 and 36 sites cleaved by chymotrypsin and trypsin, respectively. Multiple alignments between Cry toxin and $PirA^{VP}$ showed that 3 out of 12 and 3 out of 9 cleaved sites for chymotrypsin and trypsin were conserved. Meanwhile, the multiple alignment between Cry toxin and $PirB^{VP}$ showed that 9 out of 53 and 1 out of 36 cleaved sites for chymotrypsin and trypsin were conserved (**Supplementary Figure S2**). It is interesting to note that SP expression showed higher levels in the AHPND tolerant than AHPND susceptible *P. vannamei* in this study and this enzyme belongs to trypsin family (60). It remains to be determined if SP is involved in cleaving $PirAB^{VP}$ toxins to de-activate the toxin. If so, a higher expression of this enzyme in AHPND tolerant population (P2) may prevent the activation of toxin from exerting a lethal effect.

To summarize, we compared the gene expression profiles of two populations of *P. vannamei* that differ in susceptibility to AHPND. The two populations showed a major difference in survival upon experimental challenge. The difference in susceptibility was further evidenced by the differences observed by histopathology. In order to understand the molecular mechanisms governing tolerance and susceptibility, a set of candidate genes that are known to be involved in bacterial pathogenesis and in metabolism in crustaceans were evaluated. Seven genes that showed differential expression in Bioassay 2 were further evaluated in a follow-up challenge, Bioassay 3. The pattern of differential expression between the susceptible (P1) and tolerant (P2) population in Bioassays 2 and 3 were in agreement. Despite the fact that the mRNA expression of only handful genes were measured and a limited number of animals were screened, the information, *albeit* limited, provides valuable insight in *V. parahaemolyticus* pathogenesis and sheds light on how susceptible and tolerant populations of *P. vannamei* respond differently to Vp_{AHPND}. To our knowledge, this is the first report looking into the differences in gene expression profiles between AHPND tolerant and susceptible lines in *P. vannamei*.

DATA AVAILABILITY STATEMENT

The original contributions presented in the study are included in the article/**Supplementary Material**, further inquiries can be directed to the corresponding author.

AUTHOR CONTRIBUTIONS

AD conceived the idea. HM and AD designed the study. HM and RC-F performed gene expression analyses. HM wrote the manuscript. LA performed histopathological examine. BN carried out experimental challenge experiment. HM, RC-F, LA, and AD reviewed the manuscript. All authors contributed to the article and approved the submitted version.

FUNDING

Funding for this research was provided by Aquaculture Pathology Laboratory Diagnostic Fund. Part of this work is also supported by the USDA National Institute of Food and Agriculture, Hatch/Multistate project 1018120.

ACKNOWLEDGMENTS

The authors would like to thank Mr. Paul Schofield and Mr. Tanner Padilla for their support in conducting the AHPND experimental challenges and Ms. Jasmine Millabas for preparing the histological slides.

SUPPLEMENTARY MATERIAL

The Supplementary Material for this article can be found online at: https://www.frontiersin.org/articles/10.3389/fimmu.2021.634152/full#supplementary-material

REFERENCES

1. De La Peña LLD, Cabillon NARN, Catedral DDD, Amar EEC, Usero RRC, Monotilla WWD, et al. Acute Hepatopancreatic Necrosis Disease (AHPND) Outbreaks in Penaeus Vannamei and P. Monodon Cultured in the Philippines. *Dis Aquat Organ* (2015) 116:251–4. doi: 10.3354/dao02919
2. Dhar AK, Piamsomboon P, Aranguren Caro LFL, Kanrar S, Adami R, Juan Y-SY. First Report of Acute Hepatopancreatic Necrosis Disease (AHPND) Occurring in the USA. *Dis Aquat Organ* (2019) 132:241–7. doi: 10.3354/dao03330
3. Han J, Choi S, Han S, Chan S, Jin H, Lee C, et al. Genomic and Histopathological Characteristics of Vibrio Parahaemolyticus Isolated From an Acute Hepatopancreatic Necrosis Disease Outbreak in Paci Fi C White Shrimp (Penaeus Vannamei) Cultured in Korea. *Aquaculture* (2020) 524:735284. doi: 10.1016/j.aquaculture.2020.735284
4. Joshi J, Srisala J, Truong VH, Chen IT, Nuangsaeng B, Suthienkul O, et al. Variation in Vibrio parahaemolyticus Isolates From a Single Thai Shrimp Farm Experiencing an Outbreak of Acute Hepatopancreatic Necrosis Disease (AHPND). *Aquaculture* (2014) 428–429:297–302. doi: 10.1016/j.aquaculture.2014.03.030
5. Nunan L, Lightner D, Pantoja C, Gomez-jimenez S. Detection of Acute Hepatopancreatic Necrosis Disease (AHPND) in Mexico. *Dis Aquat Organ* (2014) 111:81–6. doi: 10.3354/dao02776
6. Thitamadee S, Prachumwat A, Srisala J, Jaroenlak P, Salachan PV, Sritunyalucksana K, et al. Review of Current Disease Threats for Cultivated Penaeid Shrimp in Asia. *Aquaculture* (2016) 452:69–87. doi: 10.1016/j.aquaculture.2015.10.028
7. MME E, MM A, NJ P, MK B, Rahman M. Molecular Identification of AHPND Positive Vibrio Parahaemolyticus Causing an Outbreak in South-West Shrimp Farming Regions of Bangladesh. *J Bangladesh Acad Sci* (2017) 41:127–35. doi: 10.3329/jbas.v41i2.35492
8. Han JE, Tang KFJ, Aranguren LF, Piamsomboon P. Characterization and Pathogenicity of Acute Hepatopancreatic Necrosis Disease Natural Mutants, Pirabvp(-) V. Parahaemolyticus, and Pirabvp(+) V. Campbellii Strains. *Aquaculture* (2017) 470:84–90. doi: 10.1016/j.aquaculture.2016.12.022
9. Tran L, Nunan L, Redman RRMR, Mohney LLL, Pantoja CCR, Fitzsimmons K, et al. Determination of the Infectious Nature of the Agent of Acute Hepatopancreatic Necrosis Syndrome Affecting Penaeid Shrimp. *Dis Aquat Organ* (2013) 105:45–55. doi: 10.3354/dao02621
10. Liu L, Ge M, Zheng X, Tao Z, Zhou S, Wang G. Investigation of Vibrio Alginolyticus, V. Harveyi, and V. Parahaemolyticus in Large Yellow Croaker, Pseudosciaena Crocea (Richardson) Reared in Xiangshan Bay, China. *Aquac Rep* (2016) 3:220–4. doi: 10.1016/j.aqrep.2016.04.004
11. Jesús M, Ana DAV, Francisco J, Fabiola ZM, Manuel J, Norberto AJG. Pir A - and Pirb - Like Gene Identification in Micrococcus Luteus Strains in Mexico. *J Fish Dis* (2018) 11:1667–73. doi: 10.1111/jfd.12874
12. Han JE, Tang KFJ, Tran LH, Lightner DV. Photorhabdus Insect-Related (Pir) Toxin-Like Genes in a Plasmid of Vibrio Parahaemolyticus, the Causative Agent of Acute Hepatopancreatic Necrosis Disease (AHPND) of Shrimp. *Dis Asian Aquac* (2015) 113:33–40. doi: 10.3354/dao02830
13. Soto-Rodriguez SA, Gomez-Gil B, Lozano-Olvera R, Betancourt-Lozano M, Morales-Covarrubias MS. Field and Experimental Evidence of Vibrio Parahaemolyticus as the Causative Agent of Acute Hepatopancreatic Necrosis Disease of Cultured Shrimp (Litopenaeus Vannamei) in Northwestern Mexico. *Appl Environ Microbiol* (2015) 81:1689–99. doi: 10.1128/AEM.03610-14
14. Lai H, Hann T, Ando M, Lee C, Chen I, Chiang Y, et al. Fish & Shell Fi Sh Immunology Pathogenesis of Acute Hepatopancreatic Necrosis Disease (AHPND) in Shrimp. *Fish Shellfish Immunol* (2015) 47:1006–14. doi: 10.1016/j.fsi.2015.11.008
15. Fernando L, Caro A, Mai HN, Noble B, Dhar AK. Acute Hepatopancreatic Necrosis Disease (VP AHPND), a Chronic Disease in Shrimp Penaeus Vannamei Population Raised in Latin America. *J Invertebr Pathol* (2020) 174:107424. doi: 10.1016/j.jip.2020.107424
16. Tinwongger S, Thawonsuwan J, Kondo H, Hirono I. Fish and Shell Fi Sh Immunology Identi Fi Cation of an Anti-Lipopolysaccharide Factor AV-R Isoform (Lv Alf Av- R) Related to Vp _ PirAB-like Toxin Resistance in Litopenaeus Vannamei. *Fish Shellfish Immunol* (2019) 84:178–88. doi: 10.1016/j.fsi.2018.10.005
17. Vela E, Jua L, Id ISR, Id HV, Valdes-lopez O, Luna-gonza A. Transcriptomic Analysis of Pacific White Shrimp (Litopenaeus Vannamei, Boone 1931) in Response to Acute Hepatopancreatic Necrosis Disease Caused by Vibrio Parahaemolyticus. *PloS One* (2019) 14:1–28, e0220993. doi: 10.1371/journal.pone.0220993
18. Soo C, Chiew T, Devadas S, Shariff M, Din M, Bhassu S. Differential Transcriptome Analysis of the Disease Tolerant Madagascar – Malaysia Crossbred Black Tiger Shrimp, Penaeus Monodon Hepatopancreas in Response to Acute Hepatopancreatic Necrosis Disease (AHPND) Infection : Inference on Immune Gene Response. *Gut Pathog* (2019) 11:1–13. doi: 10.1186/s13099-019-0319-4
19. Lee SY, Wang R, So K. A Lipopolysaccharide- and -1, 3-Glucan-Binding Protein From Hemocytes of the Freshwater Crayfish Pacifastacus Leniusculus. *J Biol Chem* (2000) 275:1337–43. doi: 10.1074/jbc.275.2.1337
20. Bernard D, Söderhäll K. β-1, 3-Glucan-Binding Proteins From Plasma of the Fresh-Water Crayfishes Astacus Astacus and Procambarus Clarkii Author (s): Bernard Duvic and Kenneth Söderhäll Published by: Oxford University Press on Behalf of The Crustacean Society Stable URL: Htt. *J Crustac Biol* (1993) 13:403–8. doi: 10.2307/1548783
21. Shockey JE, O'Leary NA, de la Vega E, Browdy CL, Baatz JE, Gross PS. The Role of Crustins in Litopenaeus Vannamei in Response to Infection With Shrimp Pathogens: An In Vivo Approach. *Dev Comp Immunol* (2009) 33:668–73. doi: 10.1016/j.dci.2008.11.010
22. Amparyup P, Charoensapsri W, Tassanakajon A. Fish & Shell Fi Sh Immunology Prophenoloxidase System and its Role in Shrimp Immune Responses Against Major Pathogens. *Fish Shellfish Immunol* (2013) 34:990–1001. doi: 10.1016/j.fsi.2012.08.019
23. Vandenbulcke F, Saulnier D, Bache E, Mun M. Expression and Distribution of Penaeidin Antimicrobial Peptides are Regulated by Haemocyte Reactions in Microbial Challenged Shrimp. *Eur J Biochem* (2002) 2689:2678–89. doi: 10.1046/j.1432-1033.2002.02934.x
24. Charoensapsri W, Amparyup P, Hirono I, Aoki T, Tassanakajon A. Pm PPAE2, a New Class of Crustacean Prophenoloxidase (proPO) -Activating Enzyme and its Role in PO Activation. *Dev Comp Immunol* (2011) 35:115–24. doi: 10.1016/j.dci.2010.09.002
25. Aranguren LF, Mai HN, Noble B, Dhar AK. Acute Hepatopancreatic Necrosis Disease (VPAHPND), a Chronic Disease in Shrimp (Penaeus Vannamei) Population Raised in Latin America. *J Invertebr Pathol* (2020) 174:107424. doi: 10.1016/j.jip.2020.107424
26. Livak KJ, Schmittgen TD. Analysis of Relative Gene Expression Data Using Real- Time Quantitative PCR and the 2(-Delta Delta C(T)) Method. *Methods* (2001) 408:402–8. doi: 10.1006/meth.2001.1262
27. Kondo H, Van PT, Dang LT. Draft Genome Sequence of Non- Vibrio Parahaemolyticus Acute Diseased Shrimp in Vietnam. *Genome Announc* (2015) 3:2014–5. doi: 10.1128/genomeA.00978-15
28. Hauton C. The Scope of the Crustacean Immune System for Disease Control. *J Invertebrate Pathol* (2012) 110:251–60. doi: 10.1016/j.jip.2012.03.005
29. Jiravanichpaisal P, Lee BL, Söderhäll K. Cell-Mediated Immunity in Arthropods: Hematopoiesis, Coagulation, Melanization and Opsonization. *Immunobiology* (2006) 211:213–36. doi: 10.1016/j.imbio.2005.10.015
30. Wang X, Wang J. Fish & Shell Fi Sh Immunology Pattern Recognition Receptors Acting in Innate Immune System of Shrimp Against Pathogen Infections. *Fish Shellfish Immunol* (2013) 34:981–9. doi: 10.1016/j.fsi.2012.08.008
31. Yu X, Kanost MR. Immulectin-2, a Pattern Recognition Receptor That Stimulates Hemocyte Encapsulation and Melanization in the Tobacco Hornworm, Manduca Sexta. *Dev Comp Immunol* (2004) 28:891–900. doi: 10.1016/j.dci.2004.02.005
32. Beschin A, Bilej M, Hanssens F, Raymakers J, Van Dyck E, Revets H, et al. Identification and Cloning of a Glucan- and Lipopolysaccharide-Binding Protein From Eisenia Foetida Earthworm Involved in the Activation of Prophenoloxidase Cascade. *J Biol Chem* (1998) 273:24948–54. doi: 10.1074/jbc.273.38.24948
33. Kim Y, Ryu J-H, Han S-J, Choi K-H, Nam K-B, Jang I-H, et al. Gram-Negative Bacteria-binding Protein, a Pattern Recognition Receptor for Lipopolysaccharide and B -1, 3-Glucan That Mediates the Signaling for the Induction of Innate Immune Genes in Drosophila Melanogaster Cells. *J Biol Chem* (2000) 275:32721–7. doi: 10.1074/jbc.M003934200
34. Roux MM, Pain A, Klimpel KR, Dhar AK. The Lipopolysaccharide and B-1, 3-Glucan Binding Protein Gene is Upregulated in White Spot Virus-Infected Shrimp (Penaeus Stylirostris). *J Virol* (2002) 76:7140–9. doi: 10.1128/JVI.76.14.7140-7149.2002

35. Zhao Z-Y, Yin Z-X, Xu X-P, Weng S-P, Rao X-Y, Dai Z-X, et al. A Novel C-Type Lectin From the Shrimp Litopenaeus Vannamei Possesses Anti-White Spot Syndrome Virus Activity. *J Virol* (2009) 83:347–56. doi: 10.1128/JVI.00707-08
36. Cheng W, Liu C, Tsai C, Chen J. Molecular Cloning and Characterisation of a Pattern Recognition Molecule, Lipopolysaccharide- and B -1, 3-Glucan Binding Protein (LGBP) From the White Shrimp Litopenaeus Vannamei. *Fish Shellfish Immunol* (2005) 18:297–310. doi: 10.1016/j.fsi.2004.08.002
37. Amparyup P, Sutthangkul J, Charoensapsri W, Tassanakajon A. Pattern Recognition Protein Binds to Lipopolysaccharide and β-1,3-glucan and Activates Shrimp Prophenoloxidase System. *J Biol Chem* (2012) 287:10060–9. doi: 10.1074/jbc.M111.294744
38. Destoumieux D, Bulet P, Strub J, Van Dorsselaer A, Bache E. Recombinant Expression and Range of Activity of Penaeidins, Antimicrobial Peptides From Penaeid Shrimp. *Enviromental Microbiol* (1999) 346:335–46. doi: 10.1046/j.1432-1327.1999.00855.x
39. Sritunyalucksana K, Söderhäll K. The proPO and Clotting System in Crustaceans. *Aquaculture* (2000) 191:53–69. doi: 10.1016/S0044-8486(00)00411-7
40. Cerenius L, Kawabata S, Lee BL, Nonaka M. Proteolytic Cascades and Their Involvement in Invertebrate Immunity. *Trends Biochem Sci* (2010) 35:575–83. doi: 10.1016/j.tibs.2010.04.006
41. Wang R, Lee SY, Cerenius L, So K. Properties of the Prophenoloxidase Activating Enzyme of the Freshwater Crayfish, Pacifastacus Leniusculus. *Eur J Biochem* (2001) 902:895–902. doi: 10.1046/j.1432-1327.2001.01945.x
42. Charoensapsri W, Amparyup P, Hirono I, Aoki T, Tassanakajon A. Gene Silencing of a Prophenoloxidase Activating Enzyme in the Shrimp, Penaeus Monodon, Increases Susceptibility to Vibrio Harveyi Infection. *Dev Comp Immunol* (2009) 33:811–20. doi: 10.1016/j.dci.2009.01.006
43. Soonthornchai W, Chaiyapechara S, Klinbunga S. Differentially Expressed Transcripts in Stomach of Penaeus Monodon in Response to AHPND Infection. *Dev Comp Immunol* (2016) 65:53–63. doi: 10.1016/j.dci.2016.06.013
44. Apitanyasai K, Chang C, Hann T, Siong Y, Liou J. Penaeus Vannamei Serine Proteinase Inhibitor 7 (Lv Serpin7) Acts as an Immune Brake by Regulating the proPO System in AHPND-a Ff Ected Shrimp. *Dev Comp Immunol* (2020) 106:103600. doi: 10.1016/j.dci.2019.103600
45. Cerenius L, Lee BL, So K. The proPO-system: Pros and Cons for its Role in Invertebrate Immunity. *Trends Immunol* (2008) 29:263–71. doi: 10.1016/j.it.2008.02.009
46. Hergenhahn H, Aspant A, Soderhalltt K. Purification and Characterization of a high-MA Proteinase Inhibitor of Pro-Phenol Oxidase Activation From Crayfish Plasma. *Biochem J* (1987) 248:223–8. doi: 10.1042/bj2480223
47. Kan H, Kim C-H, Kwon H-M, Park J-W, Roh K-B, Lee H, et al. Molecular Control of Phenoloxidase-induced Melanin Synthesis in an Insect. *J Biol Chem* (2008) 283:25316–23. doi: 10.1074/jbc.M804364200
48. Saibu M, Sagar S, Green I, Ameer F, Meyer M. Evaluating the Cytotoxic Effects of Novel Quinone Compounds. *Anticancer Res* (2014) 34:4077–86.
49. Fridovich I. Superoxide Radical and Superoxide Dismutases. *Annu Rev Biochem* (1995) 64:97–112. doi: 10.1146/annurev.bi.64.070195.000525
50. Hart PJ, Balbirnie MM, Ogihara NL, Nersissian AM, Weiss MS, Valentine JS, et al. A Structure-Based Mechanism for Copper - Zinc Superoxide Dismutase †,‡. *Biochemistry* (1999) 38:2167–78. doi: 10.1021/bi982284u
51. Chakravarthy N, Aravindan K, Kalaimani N. Intracellular Copper Zinc Superoxide Dismutase (icCuZnSOD) From Asian Seabass (Lates Calcarifer): Molecular Cloning, Characterization and Gene Expression With Reference to Vibrio Anguillarum Infection. *Dev Comp Immunol* (2012) 36:751–5. doi: 10.1016/j.dci.2011.11.002
52. Wedde M, Weise C, Kopacek P, Franke P, Vilcinskas A. Purification and Characterization of an Inducible Metalloprotease Inhibitor From the Hemolymph of Greater Wax Moth Larvae, Galleria Mellonella. *Eur J Biochem* (1998) 225:535–43. doi: 10.1046/j.1432-1327.1998.2550535.x
53. Kanost MR. Serine Proteinase Inhibitors in Arthropod Immunity. *Dev Comp Immunol* (1999) 23:291–301. doi: 10.1016/S0145-305X(99)00012-9
54. Ericsson JD, Janmaat AF, Lowenberger C, Myers JH. Is Decreased Generalized Immunity a Cost of Bt Resistance in Cabbage Loopers Trichoplusia N? *J Invertebr Pathol* (2009) 100:61–7. doi: 10.1016/j.jip.2008.10.007
55. Damas G, Oppert B. Comparative Evaluation of Phenoloxidase Activity in Different Larval Stages of Four Lepidopteran Pests After Exposure to Bacillus Thuringiensis. *J Insect Sci* (2012) 12:1–11. doi: 10.1673/031.012.8001
56. Lin S, Hsu K, Wang H. Structural Insights Into the Cytotoxic Mechanism of Vibrio Parahaemolyticus PirA Vp and PirB Vp Toxins. *Mar Drugs* (2017) 15:9–12. doi: 10.3390/md15120373
57. Loseva O, Ibrahim M, Candas M, Koller CN, Bauer LS, Bulla LA Jr. Changes in Protease Activity and Cry3Aa Toxin Binding in the Colorado Potato Beetle: Implications for Insect Resistance to Bacillus Thuringiensis Toxins. *Insect Biochem Mol Biol* (2002) 32:567–77. doi: 10.1016/S0965-1748(01)00137-0
58. Sa J, Real MD, Bravo A. Role of Toxin Activation on Binding and Pore Formation Activity of the Bacillus Thuringiensis Cry3 Toxins in Membranes of Leptinotarsa Decemlineata (Say). *Biochim Biophys Acta* (2004) 1660:99–105. doi: 10.1016/j.bbamem.2003.11.004
59. Lin SJ, Chen Y-F, Hsu K-C, Chen Y-L, Ko T-P, Lo C-F, et al. Structural Insights to the Heterotetrameric Interaction Between the Vibrio Parahaemolyticus PirA Vp and PirB Vp Toxins and Activation of the Cry-Like Pore-Forming Domain. *Toxins (Basel)* (2019) 11. doi: 10.3390/toxins11040233
60. Vargas-albores F, So K, Jime F. Characterisation of a Serine Proteinase From Penaeus Vannamei Haemocytes. *Fish Shellfish Immunol* (2005) 18:101–8. doi: 10.1016/j.fsi.2004.02.001

Conflict of Interest: The authors declare that the research was conducted in the absence of any commercial or financial relationships that could be construed as a potential conflict of interest.

frontiers in Immunology

MINI REVIEW
published: 11 June 2021
doi: 10.3389/fimmu.2021.674216

Mini Review: Virus Interference: History, Types and Occurrence in Crustaceans

César Marcial Escobedo-Bonilla *

Laboratory of Pathology and Molecular Diagnostics, Aquaculture Department, Instituto Politécnico Nacional - CIIDIR Unidad Sinaloa, Guasave, Mexico

Virus interference is a phenomenon in which two viruses interact within a host, affecting the outcome of infection of at least one of such viruses. The effect of this event was first observed in the XVIII century and it was first recorded even before virology was recognized as a distinct science from microbiology. Studies on virus interference were mostly done in the decades between 1930 and 1960 in viruses infecting bacteria and different vertebrates. The systems included *in vivo* experiments and later, more refined assays were done using tissue and cell cultures. Many viruses involved in interference are pathogenic to humans or to economically important animals. Thus the phenomenon may be relevant to medicine and to animal production due to the possibility to use it as alternative to chemical therapies against virus infections to reduce the severity of disease/mortality caused by a superinfecting virus. Virus interference is defined as the host resistance to a superinfection caused by a pathogenic virus causing obvious signs of disease and/or mortality due to the action of an interfering virus abrogating the replication of the former virus. Different degrees of inhibition of the superinfecting virus can occur. Due to the emergence of novel pathogenic viruses in recent years, virus interference has recently been revisited using different pathogens and hosts, including commercially important farmed aquatic species. Here, some highly pathogenic viruses affecting farmed crustaceans can be affected by interference with other viruses. This review presents data on the history of virus interference in hosts including bacteria and animals, with emphasis on the known cases of virus interference in crustacean hosts.

Life Science Identifiers (LSIDs)
Escherichia coli [(Migula 1895) Castellani & Chalmers 1919]
Aedes albopictus (Skuse 1894)
Liocarcinus depurator (Linnaeus 1758): urn:lsid:marinespecies.org:taxname:107387
Penaeus duorarum (Burkenroad 1939): urn:lsid:marinespecies.org:taxname:158334
Carcinus maenas (Linnaeus 1758): urn:lsid:marinespecies.org:taxname:107381
Macrobrachium rosenbergii (De Man 1879): urn:lsid:marinespecies.org:taxname:220137
Penaeus vannamei (Boone 1931): urn:lsid:zoobank.org:pub:C30A0A50-E309-4E24-851D-01CF94D97F23
Penaeus monodon (Fabricius 1798): urn:lsid:zoobank.org:act:3DD50D8B-01C2-48A7-B80D-9D9DD2E6F7AD
Penaeus stylirostris (Stimpson 1874): urn:lsid:marinespecies.org:taxname:584982

Keywords: virus interference, tissue cultures, cell cultures, bacteria hosts, vertebrate hosts, crustacean hosts

OPEN ACCESS

Edited by:
Luciane M. Perazzolo, Federal University of Santa Catarina, Brazil

Reviewed by:
Xiaobo Zhang, Zhejiang University, China
Didier Bouchon, University of Poitiers, France

***Correspondence:**
César Marcial Escobedo-Bonilla
cesar_escobedomx@yahoo.com

Specialty section:
This article was submitted to Comparative Immunology, a section of the journal Frontiers in Immunology

Received: *28 February 2021*
Accepted: *31 May 2021*
Published: *11 June 2021*

Citation:
Escobedo-Bonilla CM (2021) Mini Review: Virus Interference: History, Types and Occurrence in Crustaceans. Front. Immunol. 12:674216. doi: 10.3389/fimmu.2021.674216

INTRODUCTION

Virus interference is a phenomenon observed before the dawn of virology itself and even before proper experimental methods were available in the decade of 1950 (1, 2). The earliest records indicating the presence of interference between two pathogens go back to the XVI century when Montaigne observed that one disease could be cured by another. In the XVIII century it was reported that the severity of smallpox infection in children was reduced when they had secondary yaws. In the XIX century, cowpox vaccination prevented the full manifestation of smallpox infection. Also, vaccination reduced symptoms of whooping cough in children (3).

Virus interference was first described in plants in 1929 by McKinney where the yellow-mosaic tobacco virus did not replicate in plants already infected with the common mosaic virus (4). In animals, the first observations of virus interference were done in 1935 by Magrassi studying two strains of herpesvirus in rabbit with different tissue tropism. Rabbits infected with non-encephalitogenic strains of herpesvirus were resistant to infection by an encephalitogenic strain inoculated in the brain. The same year, a study done by Hoskins with strains of yellow fever virus with different tropism showed that monkeys infected with a neurotropic strain were protected against a lethal infection with a pantropic strain (4, 5). Another study done in 1937 by Findlay and MacCallum with the Rift Valley fever virus in rhesus monkeys, protected them from an infection with the unrelated yellow fever virus (5–7). In viruses infecting bacteria (bacteriophages), the first virus interference reports were done in 1942 (8, 9). Here, a strain of *Escherichia coli* [(Migula 1895) Castellani & Chalmers 1919], was used as host upon which two distinct bacteriophage strains (by replication speed and size of inhibition halo produced), were able to replicate. The interference experiments showed that using equal amounts of these two viruses (α and γ), virus γ inhibited replication of virus α by 67%. Also, the interference did not occur by differences in virus adsorption by the cells, and the time at which virus γ was inoculated after virus α influenced the interference, with longer times (4 - 6 min) showing less interference (8). Since these earliest works, subsequent records of virus interference have been documented between homologous and heterologous viruses in human cells as well as in animal hosts.

Different *in vitro* and *in vivo* systems have been used to study virus-virus interactions resulting in interference. These have included avian chorio-allantoic membranes (1, 10), prokaryotic (8, 9) and eukaryotic cell cultures (4, 11), and animal hosts such as mosquitoes (1), insect larvae (12), mice, rats, hamsters, rabbits, horses, primates, including man (1, 4, 7), ferrets (13), and more recently, fish (14) and crustaceans (15). Fish and shellfish are appreciated food commodities with significant commercial value and are produced in aquaculture facilities throughout the world (16). These studies show that under natural conditions, virus coinfections often occur within a single host (17–22) and virus replication of the coinfecting viruses can occur within the same or different cellular compartments (1, 3, 17).

Virus interference is a virus-virus interaction in which the infection and/or replication of one virus is altered by the presence of another virus within the same host (4, 5, 7, 8, 19). Such interaction can occur *in vivo* or *in vitro*. This type of virus interactions may affect the pathogenesis of at least one of the viruses (18, 19). Most of the knowledge on quantitative interference derives from work on myxoviruses in chick embryos or on tissue cultures. Moreover, interference reported in embryonated eggs or in tissue cultures does not involve antibody production, therefore ensuring that the virus interference is independent of immune responses (1).

Interference Experiments *In Vivo*

The *in vivo* interference experiments in monkeys were first done in 1935 and 1937 (4–7). The *in vivo* interference assays in vertebrates may be covert by the presence of immune defense responses and the production of molecules that may be confused with virus interference. Such molecules include antibodies, production of innate immune responses, interferons (IFNs) and other cytokines, cellular immune responses or immunostimulation (1, 5, 10, 19, 23). Also, some interference experiments may have induced the genetic recombination of less virulent virus strains, producing a mock interference result (1, 19).

Despite these drawbacks, the virus interference phenomenon has been reported *in vivo* using various vertebrate hosts such as mice, guinea pigs, hamsters, rabbits, foxes, hedgehogs, ferrets, goats, calves, chick embryos, chickens and non-human primates (1, 3, 6, 13, 24–26) (**Table 1**). In all these cases, the interference was due to virus components and not to any innate or specific host immune response (1, 13). Examples of this are described in Types of Virus Interference. A study showed that production of virus-specific IFN-γ was not the cause of the observed interference in heterotypic viruses. Lymph nodes of ferrets infected with influenza B virus showed IFN-γ responses to this virus but not to Influenza A (H3N2) virus and vice versa; ferrets infected with Influenza A (H3N2) virus had IFN-γ responses specific to this virus but not to Influenza B virus (26). The *in vivo* experiments found that one particle of interfering virus was enough to cause interference of the superinfective virus in different homologous and heterologous systems (1, 3, 23, 27).

Interference Experiments *In Vitro*

Virus interference was first studied in 1939 using animal cell and tissue cultures with different viruses (4, 7). Cell and tissue cultures represent a more standardized and easier way to determine virus interference than *in vivo* experiments with animals (4). These systems were used to test the interference of various pairs of homologous (same species or immunologically related) or heterologous (different species or immunologically distinct) virus interactions resulting in interference (1, 3, 4, 17, 24). The first tissue cultures were comprised by the chick chorio-allantoic membrane (8), minced mouse embryos or chick embryos without nervous tissues (3, 4, 7). Hence, cultures were not composed by a homogeneous cell type. Nonetheless, in these types of culture systems, the interference was evaluated through the replication inhibition of the superinfecting virus by the interfering virus. Interference of the cultured viruses was additionally evaluated by the corresponding virus titers *in vivo* using susceptible hosts (3, 4, 7). Later, using modern continuous cell cultures (e.g. continuous mouse L cell cultures; rabbit kidney cell line RK13, Vero-Green monkey

TABLE 1 | Virus interference in different animal hosts using different experimental systems.

Experimental system	Host	Interfering virus	Superinfective virus	Reference
Cell culture	*Escherichia coli*	Bacteriophage T2 "γ"	Bacteriophage T1 "α"	(8)
Cell culture	*Escherichia coli*	Bacteriophage "T2 "γ"	Bacteriophage T1 "α"	(9)
Cell culture	*Escherichia coli*	Bacteriophage T7 "δ"	Bacteriophage T1 "α"	(18)
Tissue culture	chick embryo tissues	Influenza A strain W.S.	Influenza A neurotropic variant "neuroflu"	(7)
Tissue culture	Chick embryo	Yellow fever virus strain 17DD	Yellow fever virus strain Asibi	(4)
Tissue culture	Chick embryo	Yellow fever virus strain 17DD	West Nile virus	(4)
Tissue culture	Chick embryo	Yellow fever virus strain 17DD	Venezuelan equine encephalomyelitis virus	(4)
Tissue culture	Chick embryo	West-Nile virus	Venezuelan equine encephalomyelitis virus	(4)
Tissue culture	Chick embryo	Yellow fever virus strain 17DD	Influenza A virus strain PR8	(4)
Tissue culture	Chick chorio-allantoic membrane	Influenza A virus	Heterologous Influenza	(1)
Tissue culture	Mouse lung	Influenza A virus	Heterologous Influenza	(1)
Tissue culture	Chick chorio-allantoic membrane	Influenza A virus	Newcastle disease virus	(1)
Tissue culture	Chick chorio-allantoic membrane	Influenza A virus	Mumps	(1)
Tissue culture	Chick chorio-allantoic membrane	Influenza A virus	Venezuelan equine encephalomyelitis virus	(1)
Tissue culture	Chick chorio-allantoic membrane	Newcastle disease virus	Influenza A virus	(1)
Cell culture	Chick embryo cells	Vesicular stomatitis virus New Jersey strain	Vesicular stomatitis virus Indiana strain	(27)
Tissue culture	Primary rabbit kidney cells	Rubella virus	Vaccinia virus	(11)
Tissue culture	Primary rabbit kidney cells	Rubella virus	Vesicular stomatitis virus	(11)
Cell culture	Rabbit kidney cell line PK13	Rubella virus	Vaccinia virus	(11)
Cell culture	Rabbit kidney cell line PK13	Rubella virus	Vesicular stomatitis virus	(11)
Cell culture	Vero-Green Monkey kidney cells	Vesicular stomatitis virus	Vesicular stomatitis virus	(26)
Cell culture	293T human cells	Human parainfluenza 3 virus	Homologous virus	(28)
Tissue culture	Chick embryo	Avian influenza virus	Newcastle disease virus	(29)
Cell culture	C6/36 *Aedes albopictus* cells	Sindbis virus	Dengue virus	(30)
Cell culture	BHK-21 cells	Pest des petits ruminants virus	Foot and mouth disease virus	(24)
Cell culture	Vero cells	Foot and mouth disease virus	Pest des petits ruminants virus	(24)
In vivo	Rhesus monkey	Yellow fever virus, neurotropic strain	Yellow fever virus, viscerotropic strain	Hoskins 1935 (4)
In vivo	Rabbit	Non-encephalitogenic Herpes simplex virus	Encephalitogenic herpes simplex virus	Magrassi 1935 (4)
In vivo	Rhesus monkey	Rift Valley fever virus	Yellow fever virus	(6)
In vivo	Mouse	Rift Valley fever virus	Yellow fever virus	(6)
In vivo	Mouse	Coxsackie	Poliomyelitis virus	(1)
In vivo	Rat	Saint Louis encephalitis	Eastern equine encephalomyelitis virus	(1)
In vivo	Rat	Japanese B encephalitis	Eastern equine encephalomyelitis virus	(1)
In vivo	Rabbit	Western equine encephalomyelitis virus	Eastern equine encephalomyelitis virus	(1)
In vivo	Guinea pigs	Western equine encephalomyelitis virus	Eastern equine encephalomyelitis virus	(1)
In vivo	Man	Dengue virus	Yellow fever virus	(1)
In vivo	Mosquito	Dengue virus	Yellow fever virus	(1)
In vivo	Chick embryo	Influenza A virus	Western equine encephalomyelitis virus	(25)
In vivo	Ferret	Influenza A virus (H_1N_1)	Influenza B virus	(31)
In vivo	Ferret	Influenza A virus (H_1N_1)	Influenza A virus (H_3N_2)	(31)
In vivo	Ferret	Influenza A virus (H_3N_2)	Influenza A virus (H_1N_1)	(31)
In vivo	Ferret	Influenza B/Malaysia (B/Vic) virus	Influenza B/Florida (B/Yam) virus	(13)
In vivo	Ferret	Influenza B/Florida (B/Yam) virus	Influenza B/Malaysia (B/Vic) virus	(13)
In vivo	Ferret	Influenza B/Brisbane (B/Vic) virus	Influenza B/Massachusetts (B/Yam) virus 3	(13)
In vivo	Ferret	Influenza B/Massachusetts (B/Yam) virus	Influenza B/Brisbane (B/Vic) virus	(13)

(Continued)

TABLE 1 | Continued

Experimental system	Host	Interfering virus	Superinfective virus	Reference
In vivo	Ferret	Influenza B/Brisbane (B/Vic) virus	Influenza B/Phuket (B/Yam) virus	(13)
In vivo	Ferret	Influenza B/Phuket (B/Yam) virus	Influenza B/Brisbane (B/Vic) virus	(13)
In vivo	Shrimp	Taura syndrome virus	Yellow head virus	(32)
In vivo	Shrimp	Infectious hypodermal and haematopoietic necrosis virus	White spot syndrome virus	(15, 33–35)
In vitro	Shrimp	Infectious hypodermal and haematopoietic necrosis virus	White spot syndrome virus	(36)
In vivo	Crab	Unknown virus	Unknown virus	(37)

kidney cells), experiments were carried out to determine the interference using different animal viruses (11), showing that interference actually occurs between various types of viruses and that such an interference was not caused in tissue or cell cultures by immunologic factors such as neutralizing antibodies, humoral immunity (3, 4) or the presence of soluble antiviral molecules such as IFNs (5, 7, 10, 11, 28, 29).

In such culture systems, cells pre-infected with an interfering sublethal virus (28) or a defective interfering virus (29) become resistant to infection by a cell-destructing virus (28, 29). Moreover, experiments done in chick embryo cell cultures using vesicular stomatitis virus (VSV), showed that only one interfering virus particle is needed to block infection of a superinfecting virus. Also, similar to what was previously reported for bacteriophages (8), an all or nothing effect was observed in these experiments (27, 29). The virus interference between rubella virus and vaccinia or VSV was not caused by the presence of IFN in primary rabbit kidney cell cultures or when using an excessive amount of IFN in the continuous rabbit kidney cell line PK13 (11). In these culture systems, interference was found between homologous and heterologous viruses (**Table 1**). Examples of such studies include tests between strains of avian influenza A virus with strains of Newcastle disease virus in chicken embryos (25), and the interference of Sindbis virus inoculated 1 h before challenge with dengue virus using *Aedes albopictus* (Skuse 1894) C6/36 cell cultures (30).

TYPES OF VIRUS INTERFERENCE

Different studies were done to determine virus interference in various hosts. These include bacterial cells, animal cell and tissue cultures and *in vivo* experiments (**Table 1**). Since the earliest studies on virus - virus interference, it was suggested that the interference mechanism may not be one but many (1, 3, 18, 23). Recently, different situations of virus - virus interactions were analyzed and three main categories of virus-virus interactions were proposed: (a) direct interactions of viral genes or gene products, (b) alterations in the host environment leading to indirect virus interactions, and (c) immunological interactions occurring only in animals with adaptive immune systems (19). This classification of virus-virus interactions do not deal with virus interference but rather the possible outcomes of such interactions. Nonetheless, the first category includes the main type of the virus interference phenomenon reported in bacterial and animal hosts.

Direct Interactions of Viral Genes or Gene Products

This category consist of the physical interaction of nucleic acids or proteins of one virus with genes or gene products of another infecting virus. This category includes the superinfection exclusion event, which is the main example of virus interference.

Superinfection Exclusion

This type of virus interaction occurs when a primary viral infection induces resistance to subsequent infections by similar viruses (19). This interaction results in the most commonly reported virus interference event and it has been described among various virus types including bacteriophages, flaviviruses, orthomyxoviruses, paramyxoviruses, retroviruses, hepadnaviruses, arboviruses, and plant viruses (1, 3, 4, 18, 19). Not all the different exclusion mechanisms have been unraveled, but those known depend on direct interaction of products of the primary infection with the secondary infecting virus.

Examples of this type of virus interference include viruses infecting bacterial cells (bacteriophages). Bacteria (*E. coli*) simultaneously infected with two different types of T bacteriophages showed interference, as one single interfering virus particle was able to inhibit replication of a super-infective virus in any bacterial cell (8, 9, 18).

These experiments revealed various features on the mechanism of virus interference in bacterial cells: (i) the interference was not due to differences in virus adsorption to cells, penetration into the host cell or competition for a key enzyme (8, 18, 23); (ii) the virus interference did not induce cross-immunity (8); (iii) one cell never released both virus types. Only one type of virus was produced from any one infected cell. This was called the mutual exclusion effect (1, 18, 23); (iv) the mutual exclusion effect is an "all or none" event (8); (v) The depressor effect (1, 18, 23) results in reduced yield of both viruses produced in an infected cell, compared to their normal replication yield. Later it was proposed that both the mutual exclusion and depressor effect occurs as result of the superinfecting virus not getting access to the cell division machinery, instead of the hypothesis of the key-enzyme proposed by Delbrück and Luria (3, 18, 23). The mutual exclusion effect described in bacterial cells, may be analogous to the interference reported in some animal viruses (8, 18) given that the two viruses replicate in the same cellular compartment.

Examples of superinfection exclusion in animal hosts include various homologous interfering viruses such as influenza virus (1, 23), viscerotropic and neurotropic yellow fever virus and Theiler virus (1). Interference in homologous viruses is connected to virulence changes between two variants of the same virus. This can be evaluated by the protection of the host against the virulent variant or by determining the presence of viral progeny of the virulent strain. Here, the interfering agent always is an active virus.

The interference of homologous viruses is far more difficult to distinguish from the immunological effects and genetic interactions than for heterologous interference, since both the interfering and superinfecting viruses are antigenically equivalent (1). Nonetheless, the homologous interference can be recognized from immune responses. Studies done on homologous interference between neurotropic and viscerotropic yellow fever virus showed that the cross-protection was achieved in similar ways between the yellow fever and Rift Valley fever viruses, thus separating this effect from immune responses (1, 4, 6). In contrast, a study done by Magrassi in 1935 (4) using nonencephalitogenic and encephalitogenic herpesvirus strains, displayed the same phenomenon in neuronal pathways, but this experiment called for the possible role of antibody immunity. The difference between the yellow fever and the herpesvirus systems lie in the time interval from inoculation of the interfering and the superinfecting viruses, which was long enough to allow the stimulation of antibody-producing cells by the primary inoculum (1). Other studies showed that the dose of the superinfecting virus may have further stimulated a secondary antibody response. A study where animals were inoculated with Western Equine Encephalitis (WEE) virus after intracerebral challenge with active WEE virus, showed that the challenge virus may have become an antigen booster dose which offered protection (1).

On the other hand, most of the works done on virus interference have been done in heterologous virus systems in different hosts (1, 4, 11). This type of interference has also been reported in aquatic organisms such as crustaceans (15, 31, 38). In these studies, important information about timing and dosing of interfering and superinfective viruses was obtained, despite the fact that the interference event not always was quantified or clearly observed as inhibition of replication. Instead, interference was shown as protection against disease and/or mortality caused by the superinfecting virus (1). The degree of protection is dependent on the host-virus system and the severity of the disease leading to pathological manifestations of death, both *in vivo* or *in vitro*. Another criterion for heterologous virus interference is the lack of immunogenicity against the virus pairs by the host, or the independence of interference to any relationship to antigenic reactions and antibody production. This type of interference has been reported among viruses that are antigenically and taxonomically distinct (1).

Some experiments in animals have raised the doubt of whether viruses sharing some antigenic properties may induce reciprocal resistance. For example, the previous exposure to one type of poliovirus in monkeys or human may sensitize them in such way that vaccination with a different type activates neutralizing antibodies against all three poliovirus types. The consecutive infection with different arthropod-borne viruses which share complement-fixing (CF) and hemagglutinating (HA) antigens produces broadly cross-reacting neutralizing antibodies (1). Nonetheless, a clear distinction between specific immunity and interference as the basis for host resistance was shown by studies on Eastern Equine Encephalomyelitis (EEE) and WEE viruses (1). Mice, guinea pigs or rabbits inoculated with formalin-killed WEE virus induced long-lasting protection against intracerebral challenge of the homologous, but not the heterologous virus. The homologous challenge produced a transient infection which end was associated with a type-specific antibody response (1). After this abortive infection, the animals resisted an intracerebral superinfection with massive doses of the heterologous virus. This resistance was potent for some short time periods and was not associated with anamnestic antibody response. Hence this resistance was due to virus interference (1). Influenza virus gives another example of heterologous virus interference on "minor" cross-reacting antigens and antibodies that do not offer protection against different strains, or even a single serotype. Here, the presence of protective antibodies boost rather than inhibit lingering infection. Hence this result showed that interference was the mechanism of cross protection (1).

Helper-Dependent Virus

This interaction is another example of the category of direct interactions of viral genes or gene products. This occurs in any virus that may lack replication ability at some degree and hence requires the gene products of another virus to produce infection. This interaction does not produce virus interference, but it allows a defective virus to successfully replicate and exit the cell. An example of this interaction occurs in the bacteriophage P4, which is able to replicate its own genome in the presence of a coinfecting phage (P2), thus providing capsid components and cell lysis (19).

In vertebrates, an adeno-associated virus (AAV) is a replication-defective parvovirus that usually requires a host cell that is coinfected with an adenovirus or herpesvirus in order to produce virions to be released from the host cell. Later, it was discovered that AAV is not completely replication defective, since genotoxic stress and other factors may also make a host cell permissive for AAV progeny production (19).

In invertebrates, this type of virus-virus interaction was reported between two RNA viruses in the freshwater prawn *Macrobrachium rosenbergii* (De Man 1879) causing muscle whitening in the abdomen and sometimes cephalothorax, resulting in massive mortalities to postlarvae (20). Animals with the white tail disease had the two viruses replicating in cytoplasm of connective tissues and muscle cells. The *Macrobrachium rosenbergii* Nodavirus (MrNV) is icosaedrical with 27 nm diameter and its genome composed by two equimolar linear single-stranded (ss) RNA molecules of ≈ 3200 and 1250 nucleotides, respectively (20). The extra-small virus (XSV) also found in diseased animals has icosahedral shape, size of 15 nm and a genomic single linear ss RNA with size ≈ 900 bases (20). *In vitro* assays in fish cell line SSN-1 showed that MrNV alone infected cells and produced cytopathic effects. Infection resulted in synthesis of capsid proteins but no genome replication was observed and virions were empty despite that virus RNA was detected by RT-PCR. Supernatant of infected

cells did not cause infection nor cytopathic effect in cell cultures, suggesting a role of XSV to complete MrNV viral replication. Further assays showed that higher amounts of MrNV resulted in higher yields of both MrNV and XSV, and signs of disease only appeared at high MrNV replication rates. These data indicate the essential role of MrNV in the disease and suggest a cooperative interaction of XSV with MrNV to complete its replication (20).

Cell Receptor Blockade

Another possible mechanism of virus interference is the cell receptor blockade (3). This mechanism postulates the adsorption of virus to cellular receptors as the first step of infection, with the subsequent destruction of the receptor by a viral enzyme. This creates a breach in the cellular defense which allows the entry of the virus into the cell (1, 3). A recent study done *in vitro* described the interference mechanism of human parainfluenza type 3. Here, the neuraminidase activity was needed to establish homologous interference in 293T cells (39).

Autointerference

This event causes protection or reduced virus replication in hosts inoculated with large virus doses, which in smaller quantities induce disease and high replication rates. This phenomenon was described first by Pasteur on the rabies virus in rabbits, but has also been reported for other virus-host systems such as Influenza B in chick embryos, and yellow fever, dengue and Rift Valley fever in mice (1). In tissue and cell cultures, autointerference has been observed in egg-adapted influenza strains on chick embryo lung monolayers, VSV in chick embryo monolayers, WEE in mice L cells. In most virus systems, autointerference is the result of virus infection that are not completely adapted to the experimental hosts, or which have mixtures of particles with different properties (e.g. different tissue tropism, varying particle virulence or completeness). These differences may result in inhibition of replication of the virulent component and hence, host protection from infection. In influenza viruses, experimental support exists of intrinsic viral heterogeneity, and these variations are the cause of the production of incomplete virions, which induce the autointerference (1).

VIRUS INTERFERENCE IN CRUSTACEANS

The culture of aquatic organisms such as fish, crustaceans and mollusks has been done in countries such as China, Egypt or Italy for thousands of years (40–42), but as a science and as commercial industry, aquaculture of marine and brackishwater species is probably the most recent animal production activity (43, 44). The first viral pathogens described in wild crustaceans date back to 1966 in the crab *Liocarcinus depurator* (Linnaeus 1758) (45). Later, other viruses were found in this species, and in the marine shrimp *Penaeus duorarum* (Burkenroad 1939), the virus *Baculovirus penaei* (46) was first described (46, 47). Since its beginnings, aquaculture has been affected by several viruses which have caused important damages to the industry (48). At present, the main cultured crustaceans are marine shrimp, freshwater prawns and crabs (16). Crustaceans do not have an adaptive immune system but only an efficient innate defense system to recognize and eliminate foreign materials, including microorganisms (49). Several reports exist on the coinfection of two viruses in wild or farmed crustaceans (20–22, 37, 50) which suggests the high probability of virus-virus interactions in these hosts. In fact, a few events of virus interference have been reported in crustaceans and are presented below.

Virus Interference in Crabs

One unidentified pathogenic virus infecting hemocytes in the crab *Carcinus maenas* (Linnaeus 1758) was first mentioned in 1971 and later found to display autointeference in the same host (51, 52). The virus caused impaired hemolymph clotting and death of infected animals. Nonetheless, a majority of animals showing disease recovered and regained clotting function, about half of them at 4 - 6 d post infection (dpi). Despite recovery, crabs still had virus in hemolymph as late as 40 dpi. Low virus dilutions did not cause signs of infection but higher dilutions (10^{-2} and 10^{-3}) did. This effect is similar to the phenomenon of autointerference observed in vertebrates. Autointerference was tested with undiluted and diluted hemolymph samples and it was observed when the more diluted samples caused disease faster than the undiluted ones. All six samples of whole hemolymph taken late in the course of disease did not show the normal dilution effect or even showed a reversal. Further, none of the fresh sera samples taken showed the expected normal dilution effect, and five out of six (83%) showed autointerference. This phenomenon could not be determined to be caused by the virus, from an associated virus or by the innate defense system (52).

Virus Interference in Marine Shrimp

Marine shrimp is an important commodity and is produced in aquaculture facilities in many countries worldwide. The main farmed species are the Pacific white shrimp *Penaeus vannamei* (Boone 1931) and the black tiger shrimp *Penaeus monodon* (Fabricius 1798) among others (53). Many virus diseases have been reported in these species and several of them have caused important epizootics with large economic losses (48). Due to the importance of these hosts, virus interference acquire relevance since it may help to reduce or impair the impact of highly pathogenic viruses. Hence, better documented cases of virus interference exist in these species.

Interference Between Taura Syndrome Virus and Yellow-Head Virus

Taura syndrome virus (TSV) has a single stranded, positive-sense linear RNA genome and replicates in cytoplasm (54). It infects epithelia and connective tissues of integument, gills, foregut and hindgut of shrimp (55) and caused massive mortalities in wild and farmed Pacific white shrimp in Latin American and Asian countries (44). *Yellow-head virus* (YHV) has a single-stranded positive sense RNA genome and also replicates in cytoplasm (56). It causes systemic infection in gills, lymphoid organ, head soft tissues, eyestalk, nerve tissues, heart, midgut, hepatopancreas, connective tissues and muscle of shrimp (32, 57). This virus still causes mortality to infected shrimp.

These viruses have similar cell tropism indicating that they may compete upon coinfection. An experimental challenge was done with specific pathogen-free shrimp inoculated first with TSV-infected tissues *per os* to produce chronically-infected shrimp. Then, after 27, 37 or 47 dpi shrimp were challenged intramuscularly with a lethal dose (10^4 genome copies) of YHV. Results showed that virus interference occurred between TSV and YHV and survival of shrimp treated with TSV was significantly higher than YHV positive controls at the different times evaluated. The highest survival occurred when YHV was inoculated at 27 d after TSV inoculation (31). *In situ* hybridization assays showed that shrimp were infected with the two viruses but their tissue distribution was different. Presence of TSV was restricted to lymphoid organ due to its chronic stage, whereas YHV was found in cuticular epithelium, connective tissues and lymphoid organ. In this organ, TSV was mostly present in tubules while YHV was distributed in adjacent areas of the tubules, and severe necrosis by YHV was not seen in the interference shrimp (31).

Interference Between IHHNV and WSSV

Probably the most studied virus interference event in shrimp is between *infectious hypodermal and haematopoietic necrosis virus* (IHHNV) (38), also known as *Penstylhamaparvovirus* 1 (58), and *white spot syndrome virus* 1 (WSSV) (59). The IHHNV has a linear single-stranded DNA genome of 4.1 kilobases (60). This virus replicates in nuclei of infected cells in organs of ectodermal and mesodermal origin (61). It caused massive mortalities to farmed Pacific blue shrimp *Penaeus stylirostris* (Stimpson 1874) and disease to *P. vannamei* and *P. monodon* (61). The WSSV genome is circular, double-stranded DNA of size between 293 - 307 kilobase pairs. Its large virion (210 - 380 nm length x 70 - 167 nm width) is enveloped, non-occluded, bacilliform with a tail-like appendage at one end (62). WSSV is a systemic pathogen replicating in organs of ectodermal and mesodermal origin. This virus still is a major threat to shrimp aquaculture worldwide.

The first evidence of interference was found in experiments done in juvenile Pacific blue shrimp *P. stylirostris* (15). Shrimp were pre infected with IHHNV by *per os* route and between 27 - 49 d later, they were challenged *per os* with WSSV infected tissues. Shrimp pre-infected with IHHNV showed survival between 25 and 44% compared to 0% in controls inoculated only with WSSV. Survival differences were due to the line of shrimp used, which were crosses of IHHNV susceptible and IHHNV resistant lines, and an IHHNV susceptible line, being this the one with lowest survival. In surviving shrimp, IHHNV viral load was much higher than that of WSSV (10^9 vs 10^2 copies), whereas moribund and dead shrimp had higher WSSV load than IHHNV (10^7 vs 10^4), respectively. The protective effect of IHHNV infection lasted at least 6 weeks.

Another study evaluated the interference of IHHNV or inactivated WSSV against WSSV in *P. vannamei* postlarvae. Shrimp treated with IHHNV at nauplius V or zoea I stages or treated with formalin-inactivated WSSV showed a delay in shrimp mortality from day 4 until the end of the experiment, indicating an interfering effect of such treatments. Nonetheless, shrimp treated with IHHNV or inactivated WSSV had 4 and 4.7% survival at 10 d post WSSV challenge, respectively. Surviving shrimp had similar virus loads between IHHNV and WSSV (9.0×10^1 - 1.2×10^2 vs 4.4×10^2 - 6.0×10^2, respectively), whereas moribund shrimp had higher WSSV load (1.5×10^4 - 2.3×10^4 vs 2.2×10^9 - 9.0×10^8, respectively) (33).

The interference between IHHNV and WSSV inoculated *per os* in juvenile *P. vannamei* was evaluated at different times after IHHNV inoculation (0 to 50 d). Shrimp challenged only with WSSV died at 3 dpi, whereas shrimp treated with IHHNV between 30 and 50 d before WSSV challenge died at 5 dpi. The virus load in shrimp treated with IHHNV showed an increase during the 50 d peaking at 40 d with an average IHHNV virus load of 2.6×10^9 copies μg^{-1} DNA. Shrimp challenged with WSSV showed a reduction in IHHNV load (2.7×10^7 and 9.7×10^7 copies μg^{-1} DNA) compared to shrimp inoculated only with IHHNV (2.5×10^8 - 2.6×10^9 copies μg^{-1} DNA) at 30 and 40 d, respectively. A delay in mortality due to WSSV infection was a function of IHHNV virus load and duration of infection. A significant delay in mortality occurred when IHHNV load was higher than 10^8 copies μg^{-1} DNA at the time of WSSV challenge (34).

Another work was done in batches of *P. monodon* juveniles pre-infected with IHHNV and another batch of IHHNV-negative shrimp. Both groups were challenged with WSSV by cohabitation with WSSV-infected shrimp. Results showed significant differences in time of mortality between the two groups: 10.3 ± 2.7 d in the IHHNV-negative group and 14.7 ± 4.9 d in the IHHNV-infected group. Significant differences in WSSV load were found in the two groups: $1.74 \times 10^7 \pm 1.78 \times 10^7$ copies in the IHHNV-negative group and $2.74 \times 10^6 \pm 2.41 \times 10^6$ copies in the IHHNV-infected group (35).

An *in vitro* assay was done to determine the interference mechanism of IHHNV and WSSV using a competitive ELISA assay with *P. vannamei* gill cells cultures. Digoxigenin-labeled WSSV and unlabeled IHHNV were used. Gill cell membranes added with unlabeled IHHNV interfered with digoxigenin-labeled WSSV, indicating an interfering effect of IHHNV with WSSV by competition for binding to the cellular membrane. An inverse assay using labeled IHHNV and unlabeled WSSV on gill cell membranes also showed that unlabeled WSSV interfered attachment of labeled IHHNV to cell membranes even in a higher degree. This suggests that WSSV also competes with IHHNV for binding to the cellular membrane (36).

DISCUSSION

Virus interference is an old and interesting research subject, of which mechanisms in many pairs of viruses are still to be uncovered. The use of modern cell cultures and the development of novel *in vitro* systems to study virus-virus interference may help to unravel such mechanisms. Virus interference might have different mechanisms, of which virus exclusion - either mutual or affecting one of the viruses – may be the most common. This type of interference has been recorded in homologous and heterologous viruses in different vertebrate hosts.

In crustaceans, virus interference is rather a novel phenomenon which so far has been limited by the lack of continuous cell cultures to study virus-host and virus-virus interactions. Efforts to understand the mechanism of interference between pathogenic viruses with less pathogenic ones have been done both *in vivo* (32–35) and *in vitro* (36). Nonetheless, the *in vivo* study of virus interference in these hosts has gained renewed interest as it may provide a new means to control lethal viral pathogens in the absence of an adaptive immune system and lack of effective antiviral treatments. Due to the heavy impact of WSSV outbreaks in farmed shrimp worldwide since the dawn of the XXI century, different methods aimed to curb the disease have been explored. The fact that shrimp previously infected with IHHNV may induce a reduction in severity of WSSV disease and/or mortality, makes this interference a possible natural control method against WSSV. Hence, the phenomenon gained a renewed interest and was investigated between 2003 and 2016, which has been the most recent research trend on the subject. Moreover, WSSV continues to be a major threat to shrimp aquaculture, whereas the Pacific white shrimp appears to have reduced its susceptibility to IHHNV disease (63, 64). Two recent studies showed that these viruses compete by mutual exclusion for cellular receptors (35, 36). Both IHHNV and WSSV produce systemic infections in shrimp, but some differences between the infection and replication steps may influence the outcome of the interaction. WSSV replicates fast, inducing disease and mortality within 3-5 dpi (62). In contrast, IHHNV has a slower replication, which varies from 7-15 dpi and it seldom induces mortality (64). Further, WSSV may use additional cell receptors to enter cells, as it has a broad crustacean host range, in contrast to IHHNV which may enter cells with one of the four polypeptides present on its virion (60). *In vivo* experiments to evaluate interference between these viruses would have to be done at different stages of IHHNV replication and then challenge with WSSV, or inoculating viruses with different doses and/or inoculation routes to determine the best conditions to induce virus interference and higher shrimp survival.

It is possible that the exclusion interference also occurs in the virus pairs reported for crustaceans such as TSV and YHV. These RNA viruses have similar tissue tropism and replicate in the same cell location. A reduced YHV replication and damage was observed in target organs such as lymphoid organ, gill epithelium and foregut of shrimp preinfected with TSV. Although in chronic TSV infection, the virus is not found in many epithelial tissues, still it was able to hinder YHV replication in other target tissues (31).

Research in invertebrate viruses is important because they are often dangerous agents able to cause disease and massive mortalities to many species of economic interest. Nonetheless, they also have potential to be used as control agents of pests and invasive species (65). Further, recent advances in high throughput sequencing has allowed a sharp progress in sequence capacity resulting in increased number of species with complete genome sequences, including viruses. RNA-seq has proved very useful identifying novel viruses in complex or unusual samples. Two main sequence strategies are used for identifying new viral sequences: (i) short read sequencing (i.e. Illumina) which has high throughput and sequencing depth, allowing the identification of a wide range of novel virus sequences or variants of known viruses affecting invertebrates, especially those of economic importance in animal production, affecting species of ecological importance, and/or disease agents in humans (65). This strategy makes it possible to analyze a great number of samples in an economic fashion. (ii) Long reads sequencing is used to decipher incomplete genome assemblies from highly complex samples containing mixed host and pathogen DNA. With these strategies it has been possible to determine whole-genome sequencing of numerous organisms including several previously unknown viruses (65).

The diversity of viral communities can be determined using environmental DNA (eDNA). This method requires the analysis of DNA/RNA obtained from the environment or organisms, including soil, water, host tissues, feces and other samples. Two common eDNA methods are amplicon-based (metabarcoding) or whole shotgun metagenomics/metatranscriptomics. The former amplifies and sequences variable regions of conserved genes (i.e. mitochondrial cytochrome oxidase I and 16S, 18S and 28S ribosomal RNA) or mitochondrial intergenic regions that are shared across a group or sub-groups of a selected organism. The diversity of the resulting sequences are used to assign operational taxonomic units (OTUs). In the case of viruses which lack these conserved regions, the latter method is used to study viral communities in environmental samples (65).

In conclusion, virus interference is an old phenomenon that implies the interaction of two viruses within a host cell, resulting in the inhibition of replication of at least one of the viruses. This phenomenon may have various mechanisms, of which three have been reported. The exclusion interference may be common in viruses infecting animals. Heterologous virus interference between a low and a highly pathogenic viruses has been reported in farmed shrimp and it could be used as a natural control strategy against highly pathogenic viruses. As sequencing technology advances, better knowledge on environmental and crustacean virus diversity will be gained, and also in virus genome organization and gene interactions between host - pathogen and virus - virus interactions, may help elucidate the mechanisms that drive this phenomenon.

AUTHOR CONTRIBUTIONS

The author confirms being the sole contributor of this work and has approved it for publication.

FUNDING

The present work was supported by Instituto Politecnico Nacional projects SIP20200533 and SIP20210092. COFAA-IPN provided financial support to publish this article.

REFERENCES

1. Schlesinger RW. Interference Between Animal Viruses. In: FM Burnet, WM Stanley, editors. *The Viruses: Biochemical, Biological and Biophysical Properties*, vol. 3. New York: Academic Press (1959). p. 157–94.
2. van Helvort T. When did Virology Start? *Am Soc Microbiol News* (1996) 62:142–5.
3. Lennette EH. Interference Between Animal Viruses. *Annu Rev Microbiol* (1951) 5(1):277–94. doi: 10.1146/annurev.mi.05.100151.001425
4. Lennette EH, Koprowski H. Interference Between Viruses in Tissue Culture. *J Exp Med* (1946) 83(3):195–219. doi: 10.1084/jem.83.3.195
5. Isaacs A, Burke DC. Viral Interference and Interferon. *Br Med Bull* (1959) 15 (3):185–8. doi: 10.1093/oxfordjournals.bmb.a069760
6. Findlay GM, MacCallum FO. An Interference Phenomenon in Relation to Yellow Fever and Other Viruses. *J Pathol Bacteriol* (1937) 44(2):405–24. doi: 10.1002/path.1700440216
7. Andrewes CH. Interference by One Virus With the Growth of Another in Tissue-Culture. *Br J Exp Pathol* (1942) 23(4):214–20.
8. Delbrück M, Luria SE. Interference Between Bacterial Viruses IInterference Between Two Bacterial Viruses Acting Upon the Same Host, and the Mechanism of Virus Growth. *Arch Biochem* (1942) 1(1):111–42.
9. Luria SE, Delbrück M. Interference Between Bacterial Viruses II. Interference Between Inactivated Bacterial Virus and Active Virus From the Same Strain and of a Different Strain. *Arch Biochem* (1942) 1(2):207–18.
10. Isaacs A, Lindenmann J, Andrewes CH. Virus InterferenceI. The Interferon. *Proc R Soc London Ser B - Biol Sci* (1957) 147(927):258–67. doi: 10.1098/rspb.1957.0048
11. De Somer P, Billiau A, DeClerck E, Schonne E. Rubella Virus Interference and Interferon Production. *Antonie van Leeuwenhoek* (1967) 33:237–45. doi: 10.1007/BF02045569
12. Hackett KJ, Boore A, Deming C, Buckley E, Camp M, Shapiro M. *Helicoverpa Armigera* Granulovirus Interference With Progression of H. Zea Nucleopolyhedrovirus Disease in *H. Zea* Larvae. *J Invertebr Pathol* (2000) 75:99–106. doi: 10.1006/jipa.1999.4914
13. Laurie KL, Horman W, Carolan LA, Chan KF, Layton D, Bean A, et al. Evidence for Viral Interference and Cross-Reactive Protective Immunity Between Influenza B Virus Lineages. *J Infect Dis* (2018) 217:548–59. doi: 10.1093/infdis/jix509
14. Chinchar VG, Logue O, Antao A, Chinchar GD. Channel Catfish Reovirus (CRV) Inhibits Replication of Channel Catfish Herpesvirus (CCV) by Two Distinct Mechanisms: Viral Interference and Induction of an Anti-Viral Factor. *Dis Aquat Org* (1998) 33:77–85. doi: 10.3354/dao033077
15. Tang KFJ, Durand SV, White BL, Redman RM, Mohney LL, Lightner DV. Induced Resistance to White Spot Syndrome Virus Infection in Penaeus Stylirostris Through Pre-Infection With Infectious Hypodermal and Hematopoietic Necrosis Virus–a Preliminary Study. *Aquaculture* (2003) 216 (1-4):19–29. doi: 10.1016/S0044-8486(02)00498-2
16. Stentiford GD. Diseases of Commercially Exploited Crustaceans: Cross-Cutting Issues for Global Fisheries and Aquaculture. *J Invertebr Pathol* (2011) 106:3–5. doi: 10.1016/j.jip.2010.10.001
17. Anderson K. Dual Virus Infection of Single Cells. *Am J Pathol* (1942) 18 (4):577–83.
18. Delbrück M. Interference Between Bacterial Viruses. III. The Mutual Exclusion Effect and the Depressor Effect. *J Bacteriol* (1945) 50(2):151–70. doi: 10.1128/jb.50.2.151-170.1945
19. DaPalma T, Doonan BP, Trager NM, Kasman LM. A Systematic Approach to Virus-Virus Interactions. *Virus Res* (2010) 149:1–9. doi: 10.1016/j.virusres.2010.01.002
20. Bonami JR, Sri Widada J. Viral Diseases of the Giant Fresh Water Prawn *Macrobrachium Rosenbergii*: A Review. *J Invertebr Pathol* (2011) 106:131–42. doi: 10.1016/j.jip.2010.09.007
21. Texeira-Lopes MA, Nogueira Vieira-Girão PR, Da Cruz Freire JE, Castelo Branco IR, Farias Costa FH, Rádis-Baptista G. Natural Co-Infection With Infectious Hypodermal and Hematopoietic Necrosis Virus (IHHNV) and Infectious Myonecrosis Virus (IMNV) in *Litopenaeus Vannamei* in Brazil. *Aquaculture* (2011) 312:212–6. doi: 10.1016/j.aquaculture.2011.01.005
22. Senapin S, Phiwsaiya K, Gangnonngiw W, Briggs M, Sithigorngul P, Flegel TW. Dual Infections of IMNV and MrNV in Cultivated Penaeus Vannamei From Indonesia. *Aquaculture* (2013) 372-375:70–3. doi: 10.1016/j.aquaculture.2012.10.027
23. Wagner RR. Viral Interference. Some Considerations of Basic Mechanisms and Their Potential Relationship to Host Resistance. *Bacteriol Rev* (1960) 24 (1):151–6. doi: 10.1128/br.24.1.151-166.1960
24. Kumar N, Barua S, Riyesh T, Chaubey KK, Rawat KD, Khandelwal N, et al. Complexities in Isolation and Purification of Multiple Viruses From Mixed Viral Infections: Viral Interference, Persistence and Exclusion. *PloS One* (2016) 11(5):e0156110–e0156110. doi: 10.1371/journal.pone.0156110
25. Ge S, Zheng D, Zhao Y, Liu H, Liu W, Sun Q, et al. Evaluating Viral Interference Between Influenza Virus and Newcastle Disease Virus Using Real-Time Reverse Transcription–Polymerase Chain Reaction in Chicken Eggs. *Virol J* (2012) 9(1):128. doi: 10.1186/1743-422X-9-128
26. Laurie KL, Guarnaccia TA, Carolan LA, Yan AWC, Aban M, Petrie S, et al. Interval Between Infections and Viral Hierarchy are Determinants of Viral Interference Following Influenza Virus Infection in a Ferret Model. *J Infect Dis* (2015) 212:1701–10. doi: 10.1093/infdis/jiv260
27. Bellett AJD, Cooper PD. Some Properties of the Transmissible Interfering Component of Vesicular Stomatitis Virus Preparations. *J Gen Microbiol* (1959) 21(3):498–509. doi: 10.1099/00221287-21-3-498
28. Ho M. Role of Infection in Viral Interference. *Arch Internal Med* (1962) 110 (5):159–65. doi: 10.1001/archinte.1962.03620230099014
29. Sekellick MJ, Marcus PI. Viral Interference by Defective Particles of Vesicular Stomatitis Virus Measured in Individual Cells. *Virology* (1980) 104(1):247–52. doi: 10.1016/0042-6822(80)90385-2
30. Salas-Benito JS, De Nova-Ocampo M. Review Article: Viral Interference and Persistence in Mosquito-Borne Flaviviruses. *J Immunol Res* (2015) 2015 (873404):14. doi: 10.1155/2015/873404
31. Aranguren LF, Tang KL, Lightner DV. Protection From Yellow Head Virus (YHV) Infection in *Penaeus Vannamei* Pre-Infected With Taura Syndrome Virus (TSV). *Dis Aquat Org* (2012) 98(3):185–92. doi: 10.3354/dao02448
32. Munro J, Owens L. Yellow Head-Like Viruses Affecting the Penaeid Aquaculture Industry: A Review. *Aquac Res* (2007) 38(9):893–908. doi: 10.1111/j.1365-2109.2007.01735.x
33. Melena J, Bayot B, Betancourt I, Amano Y, Panchana F, Alday-Sanz V, et al. Pre-Exposure to Infectious Hypodermal and Haematopoietic Necrosis Virus or to Inactivated White Spot Syndrome Virus (WSSV) Confers Protection Against WSSV in *Penaeus Vannamei* (Boone) Post-Larvae. *J Fish Dis* (2006) 29:589–600. doi: 10.1111/j.1365-2761.2006.00739.x
34. Bonnichon V, Lightner DV, Bonami JR. Viral Interference Between Infectious Hypodermal and Hematopoietic Necrosis Virus and White Spot Syndrome Virus in Litopenaeus Vannamei. *Dis Aquat Org* (2006) 72:179–84. doi: 10.3354/dao072179
35. Molthathong S, Jitrakorn S, Joyinda Y, Boonchird C, Withchayachamnarnkul B, Pongtippatee P, et al. Persistence of *Penaeus Stylirostris* Densovirus Delays Mortality Caused by White Spot Syndrome Virus Infection in Black Tiger Shrimp (*Penaeus Monodon*). *BMC Vet Res* (2013) 9:33. doi: 10.1186/1746-6148-9-33
36. Yan DC, Huang J, Yang B, Sun HS, Wang YY, Liu X. Competition of Infectious Hypodermal and Haematopoietic Necrosis Virus (IHHNV) With White Spot Syndrome Virus (WSSV) for Binding to Shrimp Cellular Membrane. *J Fish Dis* (2016) 39(10):1225–9. doi: 10.1111/jfd.12489
37. Feijó RG, Kamimura MT, Oliveira-Nieto JM, Vila-Nova CMVM, Gomes ACS, Coelho M, et al. Infectious Myonecrosis Virus and White Spot Syndrome Virus Co-Infection in Pacific White Shrimp (*Litopenaeus Vannamei*) Farmed in Brazil. *Aquaculture* (2013) 380-383:1–5. doi: 10.1016/j.aquaculture.2012.11.026
38. Cotmore SF, Agbandje-McKenna M, Canuti M, Chiorini JA, Eis-Hubinger A-M, Hughes J, et al. Ictv Virus Taxonomy Profile: Parvoviridae. *J Gen Virol* (2019) 100(3):367–8. doi: 10.1099/jgv.0.001212
39. Horga MA, Gusella GL, Greengard O, Poltoratskaia N, Porotto M, Moscona A. Mechanism of Interference Mediated by Human Parainfluenza Virus Type 3 Infection. *J Virol* (2000) 74(24):11792–9. doi: 10.1128/JVI.74.24.11792-11799.2000
40. Pillay TVR, Kutty MN. Aquaculture. In: *Principles and Practices*, *2nd*. Oxford, U.K: Blackwell Publishing Co. (2005). p. 7–13.
41. Stickney RR, Treece GD. History of Aquaculture. In: JH Tidwell, editor. *Aquaculture Production Systems*. Ames, Iowa: Wiley-Blackwell (2012). p. 15–50.
42. Lucas JS. Introduction. In: JS Lucas, PC Southgate, CS Tucker, editors. *Aquaculture: Farming Aquatic Animals and Plants*, *3rd ed*. West Sussex: John Wiley & Sons Ltd. (2019). p. 1–19.

43. Argue BJ, Arce SM, Lotz JM, Moss SM. Selective Breeding of Pacific White Shrimp (*Litopenaeus Vannamei*) for Growth and Resistance to Taura Syndrome Virus. *Aquaculture* (2002) 204:447–60. doi: 10.1016/S0044-8486(01)00830-4
44. Escobedo-Bonilla CM. Emerging Infectious Diseases Affecting Farmed Shrimp in Mexico. *Austin J Biotechnol Bioeng* (2016) 3(2):1062–4.
45. Johnson PT. A Viral Disease of the Blue Crab, *Callinectes Sapidus*: Histopathology and Differential Diagnosis. *J Invertebr Pathol* (1977) 29:201–9. doi: 10.1016/0022-2011(77)90194-X
46. Couch JA. An Enzootic Nuclear Polyhedrosis Virus of Pink Shrimp: Ultrastructure, Prevalence, and Enhancement. *J Invertebr Pathol* (1974) 24 (3):311–31. doi: 10.1016/0022-2011(74)90139-6
47. Harrison RL, Herniou EA, Jehle JA, Theilmann DA, Burand JP, Becnel JJ, et al. Ictv Virus Taxonomy Profile: Baculoviridae. *J Gen Virol* (2018) 99(9):1185–6. doi: 10.1099/jgv.0.001107
48. Lightner DV. Virus Diseases of Farmed Shrimp in the Western Hemisphere (the Americas): A Review. *J Invertebr Pathol* (2011) 106:110–30. doi: 10.1016/j.jip.2010.09.012
49. Lee SY, Söderhäll K. Early Events in Crustacean Innate Immunity. *Fish Shellfish Immunol* (2002) 12:421–37. doi: 10.1006/fsim.2002.0420
50. Owens L, Liessmann L, La Fauce K, Nyguyen T, Zeng C. Intranuclear Bacilliform Virus and Hepatopancreatic Parvovirus (PmergDNV) in the Mud Crab *Scylla Serrata* (Forskal) of Australia. *Aquaculture* (2010) 310:47–51. doi: 10.1016/j.aquaculture.2010.10.028
51. Bang FB. Transmissible Disease, Probably Viral in Origin, Affecting the Amebocytes of the European Shore Crab, Carcinus Maenas. *Infect Immun* (1971) 3(4):617–23. doi: 10.1128/iai.3.4.617-623.1971
52. Bang FB. Pathogenesis and Autointerference in a Virus Disease of Crabs. *Infect Immun* (1974) 9(6):1057–61. doi: 10.1128/iai.9.6.1057-1061.1974
53. FAO. The State of World Fisheries and Aquaculture 2018. In: *Meeting the Sustainable Development Goals*. Rome: FAO (2018). p. 1–210 +XVII.
54. Valles SM, Chen Y, Firth AE, Guérin DMA, Hashimoto Y, Herrero S, et al. Ictv Virus Taxonomy Profile: Dicistroviridae. *J Gen Virol* (2017) 98(3):355–6. doi: 10.1099/jgv.0.000756
55. Hasson KW, Lightner DV, Mohney LL, Redman RM, Poulos BT, White BM. Taura Syndrome Virus (TSV) Lesion Development and the Disease Cycle in the Pacific White Shrimp Penaeus Vannamei. *Dis Aquat Org* (1999) 36:81–93. doi: 10.3354/dao036081
56. Walker PJ, Cowley JA, Dong X, Huang J, Moody N, Ziebuhr J, et al. Ictv Virus Taxonomy Profile: Roniviridae. *J Gen Virol* (2021) 102(1):1–2. doi: 10.1099/jgv.0.001514
57. Duangsuwan P, Tinikul Y, Chotwiwatthanakun C, Vanichviriyakit R, Sobhon P. Changes in the Histological Organization and Spheroid Formation in Lymphoid Organ of *Penaeus Monodon* Infected With Yellow Head Virus. *Fish Shellfish Immunol* (2008) 25:560–9. doi: 10.1016/j.fsi.2008.08.008
58. Pénzes JJ, Söderlund-Venermo M, Canuti M, Eis-Hübinger AM, Hughes J, Cotmore SF, et al. Reorganizing the Family Parvoviridae: A Revised Taxonomy Independent of the Canonical Approach Based on Host Association. *Arch Virol* (2020) 165(9):2133–46. doi: 10.1007/s00705-020-04632-4
59. Wang H-C, Hirono I, Maningas MBB, Somboonwiwat K, Stentiford G, Consortium IR. Ictv Virus Taxonomy Profile: Nimaviridae. *J Gen Virol* (2019) 100(7):1053–4. doi: 10.1099/jgv.0.001248
60. Bonami JR, Trumper B, Mari J, Brehelin M, Lightner DV. Purification and Characterization of the Infectious Hypodermal and Haematopoietic Necrosis Virus of Penaeid Shrimps. *J Gen Virol* (1990) 71:2657–64. doi: 10.1099/0022-1317-71-11-2657
61. Lightner DV, Redman RM, Bell TA. Infectious Hypodermal and Hematopoietic Necrosis, a Newly Recognized Virus Disease of Penaeid Shrimp. *J Invertebr Pathol* (1983) 42:62–70. doi: 10.1016/0022-2011(83)90202-1
62. Escobedo-Bonilla CM, Alday-Sanz V, Wille M, Sorgeloos P, Pensaert MB, Nauwynck HJ. A Review on the Morphology, Molecular Characterization, Morphogenesis and Pathogenesis of White Spot Syndrome Virus. *J Fish Dis* (2008) 31(1):1–18. doi: 10.1111/j.1365-2761.2007.00877.x
63. Flegel TW. Update on Viral Accommodation, a Model for Host-Viral Interaction in Shrimp and Other Arthropods. *Dev Comp Immunol* (2007) 31:217–31. doi: 10.1016/j.dci.2006.06.009
64. Escobedo-Bonilla CM, Rangel-Ibarra JL. Susceptibility to an Inoculum of Infectious Hypodermal and Haematopoietic Necrosis Virus (IHHNV) in Three Batches of Whiteleg Shrimp *Litopenaeus Vannamei* (Boone, 1931). *Zookeys* (2014) 457:355–65. doi: 10.3897/zookeys.457.6715
65. van Aerle R, Santos EM. Advances in the Application of High-Throughput Sequencing in Invertebrate Virology. *J Invertebr Pathol* (2017) 147:145–56. doi: 10.1016/j.jip.2017.02.006

Conflict of Interest: The author declares that the research was conducted in the absence of any commercial or financial relationships that could be construed as a potential conflict of interest.

frontiers in Immunology

ORIGINAL RESEARCH
published: 11 June 2021
doi: 10.3389/fimmu.2021.679767

Hepatopancreas-Specific Lectin Participates in the Antibacterial Immune Response by Regulating the Expression of Antibacterial Proteins

Xiao-Tong Cao[1†], *Xiao-Yi Pan*[2†], *Meng Sun*[3], *Yan Liu*[3] *and Jiang-Feng Lan*[1*]

[1] Shandong Provincial Key Laboratory of Animal Biotechnology and Disease Control and Prevention, College of Animal Science and Veterinary Medicine, Shandong Agricultural University, Taian, China, [2] Key Laboratory of Healthy Freshwater Aquaculture, Ministry of Agriculture and Rural Affairs; Key Laboratory of Fish Health and Nutrition of Zhejiang Province; Zhejiang Institute of Freshwater Fisheries, Huzhou, China, [3] College of Fisheries, Huazhong Agricultural University, Wuhan, China

The hepatopancreas is an important digestive and immune organ in crustacean. There were low but stable numbers of microbes living in the hemolymph of crustacean, whereas the organs (including hepatopancreas) of crustacean were immersed in the hemolymph. It is very important to study the immune mechanism of the hepatopancreas against bacteria. In this study, a novel CTL (HepCL) with two CRDs, which was mainly expressed in the hepatopancreas, was identified in red swamp crayfish (*Procambarus clarkii*). HepCL binds to bacteria *in vitro* and could enhance bacterial clearance *in vivo*. Compared with the C-terminal CRD of HepCL (HepCL-C), the N-terminal CRD (HepCL-N) showed weaker bacterial binding ability *in vitro* and stronger bacterial clearance activity *in vivo*. The expression of some antimicrobial proteins, such as FLP, ALF1 and ALF5, was downregulated under knockdown of HepCL or blocked with Anti-HepCL after challenge with *Vibrio* in crayfish. These results demonstrated that HepCL might be involved in the antibacterial immune response by regulating the expression of antimicrobial proteins.

Keywords: C-type lectin, *Procambarus clarkii*, antimicrobial peptides, *Vibrio parahaemolyticus*, hepatopancreas

OPEN ACCESS

Edited by:
Luciane M. Perazzolo, Federal University of Santa Catarina, Brazil

Reviewed by:
Li Lin, Zhongkai University of Agriculture and Engineering, China
Jin-Xing Wang, Shandong University, China

***Correspondence:**
Jiang-Feng Lan
jflan@sdau.edu.cn

[†]*These authors have contributed equally to this work*

Specialty section:
This article was submitted to Comparative Immunology, a section of the journal Frontiers in Immunology

Received: *12 March 2021*
Accepted: *31 May 2021*
Published: *11 June 2021*

Citation:
Cao X-T, Pan X-Y, Sun M, Liu Y and Lan J-F (2021) Hepatopancreas-Specific Lectin Participates in the Antibacterial Immune Response by Regulating the Expression of Antibacterial Proteins. Front. Immunol. 12:679767. doi: 10.3389/fimmu.2021.679767

INTRODUCTION

In the natural environment, vertebrates and invertebrates are exposed to various bacterial communities all the time, and their autoimmune systems play a key role in defending against pathogen infection (1–3). In vertebrates, innate immunity and adaptive immunity resist pathogen infection together. Invertebrates lack the typical antibody and T/B cell-based immune recognition system. The innate immune system of invertebrates plays an important role in defending against infectious agents (4–7). Pattern recognition receptors (PRRs) can trigger the innate immune response, such as Toll-like receptors and lectins (8–10). Among these PRRs, C-type lectins (CTLs) play an important role in the recognition of microbe-associated molecular patterns (MAMPs). In vertebrates, mannose-binding lectin (MBL), possesses a collagenous domain that can bind to the MBL-associated serine protease (MASP) to activate the complement system (11, 12).

CTLs have been characterized in many organisms, including vertebrates and invertebrates, and they primarily exert their function through the carbohydrate recognition domain (CRD) (13). Most

CTLs contain a single CRD, and several of the CTLs have more CRDs. CTLs from invertebrates effectively participate not only in the recognition of pathogenic microbial glycans but also in antimicrobial functions, such as bacterial clearance, phagocytosis, cell adhesion, and prophenoloxidase activation (14–19). Fc-hsL with one CRD, a hepatopancreas-specific lectin, acts as a pattern recognition receptor in antibacterial defense (20). *Hc*Lec4 with four CRDs participate in antibacterial immune responses by regulating antimicrobial peptides (AMPs) expression in *Hyriopsis cumingii* (21). In *Anopheles gambiae*, two CTLs, CTL4 and CTLMA2 cooperate to exert anti-Gram-negative bacteria function (22). FcLec4 cooperates with β-integrin to promote hemocytic phagocytosis in *Fenneropenaeus chinensis* (19). It has been reported that CTLs could be involved in antifungal responses (23). Some CTLs have been reported to be directly or indirectly involved in the activation of the immune signaling pathways (24, 25). LvCTL1 possesses anti-white spot syndrome virus activity by binding to virus proteins in *Litopenaeus vannamei* (26). In contrast, some transmembrance C-type lectins promote *Mycobacterium tuberculosis* (27) and certain virus entry into host cells (28–31). CD45 phosphatase homolog recruits mosGCTL-1 to promote West Nile virus (WNV) infection in mosquitoes (32).

In crustaceans, especially shrimp, bacteria exist not only in the digestive tract but also in the hemolymph (33, 34). These bacteria possess a potential risk to shrimp farming. The hepatopancreas plays a key role in digestive and immune processes in shrimp. However, how shrimp restrain the proliferation of microbiota in the hepatopancreas needs to be further revealed. It has reported that CTL33 regulates intestinal homeostasis by mediating biofilm formation in *Marsupenaeus japonicas* (35). mosGCTLs binds gut microbiome and offset AMP activity to maintain gut microbiota homeostasis in *Aedes aegypti* (36). In this study, HepCL (GenBank No. MW727280), a novel CTL with two CRDs, mainly expressed in the hepatopancreas, was identified from red swamp crayfish (*Procambarus clarkii*). Bacterial clearance assays, bacterial binding assays and pathological sections were performed to analyze the role of HepCL in the antibacterial immune response in hepatopancreas. This study provides a new perspective for crustacean hepatopancreas resistance to bacterial infection.

MATERIALS AND METHODS

Vibrio Challenge and Tissue Collection

Healthy red swamp crayfish (10-15 g) were obtained from a fish farm in Weishan, Shandong Province, China. These crayfish were acclimated in laboratory aquarium tanks with aerated freshwater at 22°C for one week before being involved in this study. Organs (hemocytes, hepatopancreas, gills, stomach and intestine) were collected from at least three crayfish for further analyses, and total RNA was extracted with RNAiso Plus (Takara, China). For hemocyte collection, hemolymph was extracted with a syringe containing 1 ml cold anticoagulant buffer [0.14 M NaCl, 0.1 M glucose, 30 mM trisodium citrate, 26 mM citric acid, and 10 mM ethylene diamine tetra acetic acid (EDTA), pH 4.6] at 4°C (37) and immediately centrifuged at 800 g for 5 min (4°C). For bacterial challenge assays, each crayfish was injected in the abdomen with 25 μl of *Vibrio parahaemolyticus* (1×10^7 CFU in PBS). The total RNA and protein of the hepatopancreas were separately extracted from 10 healthy crayfish and collected at 12 h post injection (hpi). cDNA was synthesized by using the PrimeScript RT-PCR Kit (Vazyme, China) for quantitative real-time PCR (qRT-PCR) analysis. The assay was performed in triplicate.

Expression and Purification of Recombinant HepCL

In the experiment on prokaryotic recombinant expression, primers (HepCL-EX-F/R, HepCL-N-EX-F/R, HepCL-C-EX-F/R, **Table 1**) were used to amplify fragments of HepCL (957 bp), HepCL-N (345 bp), and HepCL-C (519 bp). PCR was programmed at 95°C for 5 min, 35 cycles at 95°C for 30 s, 58°C for 30 s, 72°C for 50 s, and one cycle at 72°C for 10 min. The DNA fragments were linked to the vector pGEX-4T-1. Recombinant HepCL, HepCL-N, and HepCL-C were expressed in *Escherichia coli* (*E. coli*) BL21 cells (TransGen, China). The recombinant proteins were purified by affinity chromatography using GST resin (Sangon, China) following the method described in previous papers (38). HepCL polyclonal antibodies were prepared by the company using recombinant proteins (Frdbio, China).

Tissue Distribution and Expression Profiles

The tissue distribution of HepCL in normal crayfish was analyzed by qRT-PCR and western blot. For qRT-PCR, a pair of primers (HepCL-RT-F/R, **Table 1**) was used to detect the

TABLE 1 | Primers used in this study.

Primers	Sequences (5'-3')
HepCL-EX-F	TACTCAGGATCCATGGACTGTCCCTAC
HepCL-EX-R	TACTCACTCGAGCTA GGT AGC CATGCA
HepCL-N-EX-F	TACTCAGGATCCATGGACTGTCCCTAC
HepCL-N-EX-R	TACTCACTCGAGTTA AAATTCGCATAA
HepCL-C-EX-F	TACTCAGGATCCATGGCGTGTGAGGCA
HepCL-C-EX-R	TACTCACTCGAGCTAGGTAGCCATGCA
HepCL-RT-F	GGTTTAGTGCTGGACGGAGTT
HepCL-RT-R	CTGGGCGACATCATAGGTG
Lys-i1-RT-F	GTCAACCCACCCTCAATAAC
Lys-i1-RT-R	CTTGTGAATCAGGGCGTA
ALF1-RT-F	GAAGCGATGACGAGGAGCAAT
ALF1-RT-R	GACGGGTTGGCACAAGAGC
ALF2-RT-F	CAAACTGGGCGGGTTATGG
ALF2-RT-R	TGACGAAGTCCCTGGTGGC
ALF5-RT-F	GGGGAGGTGAGGCTACT
ALF5-RT-R	TTCCTGCTCGGTGATG
FLP-RT-F	CGACAAGACCGTCAAGGC
FLP-RT-R	ATCTGTGTTCGTTTTTTATTTT
18S-RT-F	TCTTCTTAGAGGGATTAGCGG
18S-RT-R	AAGGGGATTGAACGGGTTA
HepCL-RNAi-F	GCGTAATACGACTCACTATAGG ACGACCAAGCAATAGAAA
HepCL-RNAi-R	GCGTAATACGACTCACTATAGG CACAGGGAATTAAATCAAAC
GFP-RNAi-F	GCGTAATACGACTCACTATAGGTGGTCCCAATTCTCGTGGAAC
GFP-RNAi-R	GCGTAATACGACTCACTATAGGCTTGAAGTTGACTTGATGCC

transcriptional levels of HepCL with 18S rRNA (with primers 18S-RT-F/R, **Table 1**) as an internal control. The qRT-PCR procedure was as follows: 94°C for 2 min, 40 cycles at 94°C for 15 s and 60°C for 30 s. The results were analyzed by using the $2^{-\Delta\Delta Ct}$ method (39). Sodium dodecyl sulfate polyacrylamide gel electrophoresis (SDS-PAGE) was used to analyze protein samples, and then the proteins were transferred onto nitrocellulose (NC) membranes followed by blocking in nonfat milk (4% in TBS: 150 mM NaCl, 10 mM Tris-HCl, pH 7.4) for 2 h. The NC membranes were incubated overnight with primary antibody (rabbit anti-HepCL or β-actin antiserum), washed three times with TBST (0.02% Tween 20 in TBS) and then with TBS. The specific polyclonal antiserum of HepCL and β-actin were prepared in our lab by immunizing rabbit with the purified GST-HepCL and His-actin. The NC membrane was incubated with HRP goat anti-rabbit IgG (1/10,000 diluted in TBS) (Proteintech, China) for 1 h. After washing with TBST and TBS as above, the protein bands were detected using ChemiLuminescence (CWbio, China). qRT-PCR and western blot were also used to detect HepCL expression patterns after *Vibrio* infection following the methods described above.

RNA Interference Assay

The specific primers HepCL-RNAi-F/R and GFP-RNAi-F/R (**Table 1**) were used in this assay. A commercial transcription T7 kit (Thermo, USA) was used to synthesize dsRNA following a previously reported method (40). Crayfish were divided into three groups (3 crayfish/group) and injected with dsHepCL (20 μg) or dsGFP. The normal group was the group of unchallenged crayfish. Total RNA from the hepatopancreas was extracted to evaluate the RNAi efficacy at 48 h after the injection of dsRNA.

Bacterial Clearance Assay

Crayfish were divided into two groups (3 crayfish/group) and injected with 50 μg of (1 μg/μl) HepCL. GST-Tag was used as a control. One hour after injection, the crayfish were challenged with 25 μl *Vibrio* (1×10^9 CFU/ml). Thirty minutes after bacterial injection, the hemolymph of each crayfish was collected, and 50 μl of the hemolymph was cultured on solid Luria-Bertani (LB) plates at 37°C overnight. The numbers of bacteria on each plate were counted. HepCL was knockeddown *in vivo*, and then the bacterial clearance assay was performed as above. The experiment was repeated three times.

To study the role of the different domains of HepCL in antibacterial immune responses, crayfish were divided into four groups (3 crayfish/group) and injected with 50 μg of (1 μg/μl) HepCL, HepCL-N, or HepCL-C protein. GST-Tag was used as control. The experiment was carried out as above.

Survival Rate Assay

To analyze the function of HepCL, crayfish (60 crayfish per group, 10-15 g) were divided into two groups to evaluate the crayfish survival rate. The experimental group was injected with recombinant HepCL (50 μl, 1 μg/μl) and then challenged with *Vibrio* (25 μl 1×10^7 CFU/ml in PBS) within 1 h after the first injection. GST-Tag was used as a control. The number of dead crayfish was monitored every day, and the cumulative survival rates of the two groups of crayfish were calculated.

Pathological Analysis of the Hepatopancreas After Challenge with *Vibrio*

Crayfish were divided into six groups (6 crayfish per group), one group was not treated as control, and 50 μg of HepCL, HepCL-N, HepCL-C or GST-Tag protein were injected into other five group crayfish. Overnight-cultured *Vibrio* or heat-inactivated *Vibrio* were washed three times with PBS and diluted to 10^7 CFU/ml, and then, 50 μl *Vibrio* or heat-inactivated *Vibrio* was injected into each crayfish 1 h after protein injection. Hepatopancreases were collected after 24 hpi and fixed with 4% paraformaldehyde solution. Then, all samples were sent to the company (Google, China) for pathological sections, then pathological sections of hepatopancreas were observed and analyzed under microscope in our lab.

Bacterial Binding Assay

Six kinds of bacteria were involved in the bacterial binding assay (gram-positive bacteria: Staphylococcus aureus, Bacillus subtilis and Streptococcus agalactiae; and gram-negative bacteria: Edwardsiella piscicida, V. parahaemolyticus and Aeromonas hydrophila). All bacteria were cultivated overnight, harvested at 3000 rpm for 10 min by centrifugation, and then washed three times with PBS. The HepCL, HepCL-N, HepCL-C or GST-Tag proteins were mixed and incubated with different bacteria (10^7 CFU/ml) respectively at 37°C for 30 min at a final concentration of 50 μg/ml. The samples were centrifuged at 3000 rpm for 10 min and washed three times with PBS. Finally, bacterial pellets in each tube were resuspended in 20 μl of PBS and boiled with 2 × loading buffer for 5 min. Western blot was used to determine the binding activity of HepCL, HepCL-N, and HepCL-C to the bacteria with anti-GST-Tag (Cwbio, China).

Expression Analysis of Antibacterial Proteins After Blocked HepCL or HepCL Was Knockeddown

The expression levels of antibacterial proteins were detected at 6 h after *Vibrio* or *S. aureus* infection in the hepatopancreas of crayfish. The expression levels of FLP, ALF1, ALF2, ALF5 and Lys-i1 were detected by qRT-PCR with specific primers (**Table 1**). After blocked HepCL with Anti-HepCL, the expression levels of antibacterial proteins were detected at 6 h after challenge with *Vibrio* in the hepatopancreas of crayfish. Anti-actin was used as control. The assay was repeated three times.

To further verify the role of HepCL in regulation the expression of AMPs, it was knockeddown. And then the expression levels of antibacterial proteins were detected in hepatopancreas of HepCL-knockdown crayfish at 6 h post *Vibrio* challenge. dsGFP was used as control. The assay was repeated three times.

RESULTS

Tissue Distribution and Expression Profiles of HepCL

The tissue distribution of HepCL was analyzed in hemocytes, hepatopancreas, gills, stomach and intestine by qRT-PCR and western blot. HepCL was observed mainly in the hepatopancreas at the mRNA level (**Figure 1A**). HepCL was mainly expressed in the hepatopancreas at the protein level, and it was also detected in the stomach and intestine (**Figure 1B**).

Expression patterns of HepCL after challenge with *Vibrio* were analyzed with qRT-PCR and western blot. The results showed that the expression level of HepCL was upregulated at 12 h after *Vibrio* challenge in the hepatopancreas (**Figures 1C, D**).

HepCL Influence Survival Rate and Bacterial Clearance

To further study the role of HepCL in the anti*Vibrio* immune response *in vivo*, survival assay and bacterial clearance assay were performed. The results showed that after knockdown of HepCL (**Figure 2A**), the number of bacteria in dsHepCL injection crayfish increased significantly compared with that in the control crayfish (**Figure 2B**). As shown in **Figure 2C**, the number of bacteria in HepCL injection crayfish decreased significantly compared with that in the control crayfish. The survival assay showed that the crayfish began to die on the first day after injection. All of the crayfish in the GST-Tag injection group died within six days, whereas half of the crayfish survived in the HepCL injection group at six day after injection (**Figure 2D**). These results suggest that HepCL improved the survival rate of crayfish and enhanced bacterial clearance in crayfish.

Histological Section Analysis

To further analyze the role of HepCL in the hepatopancreas, GST-Tag+ *Vibrio*, HepCL+*Vibrio*, HepCL-N+*Vibrio*, HepCL-C+ *Vibrio* and HepCL+Dead *Vibrio* were injected into crayfish. The hepatopancreas tissue of each crayfish was fixed for histological sectioning at 24 hpi. As shown in **Figure 3B**, vacuolization in the hepatopancreas was found, and the connection between the lobules of the hepatopancreas was broken after *Vibrio* infection. The pathological tissue morphology of each crayfish injected with HepCL+*Vibrio* (**Figure 3C**), HepCL-N+*Vibrio* (**Figure 3D**) or HepCL+Dead *Vibrio* (**Figure 3F**), revealed shrinkage and a cell infiltration inflammatory response in the hepatopancreas compared with that of control and injected HepCL-C+ *Vibrio* (**Figure 3E**) crayfish. Obvious tissue damage was present in the hepatopancreas of *Vibrio*-infected crayfish. The hepatopancreas of crayfish injected with HepCL showed a stronger inflammatory response than those injected with other proteins.

Influence of the Different Domains of HepCL on Bacterial Clearance

To identify the role of the two domains of HepCL in the antibacterial immune response. Bacterial clearance was observed in the hemolymph and hepatopancreas after HepCL, HepCL-N or HepCL-C protein injection. Crayfish were injected

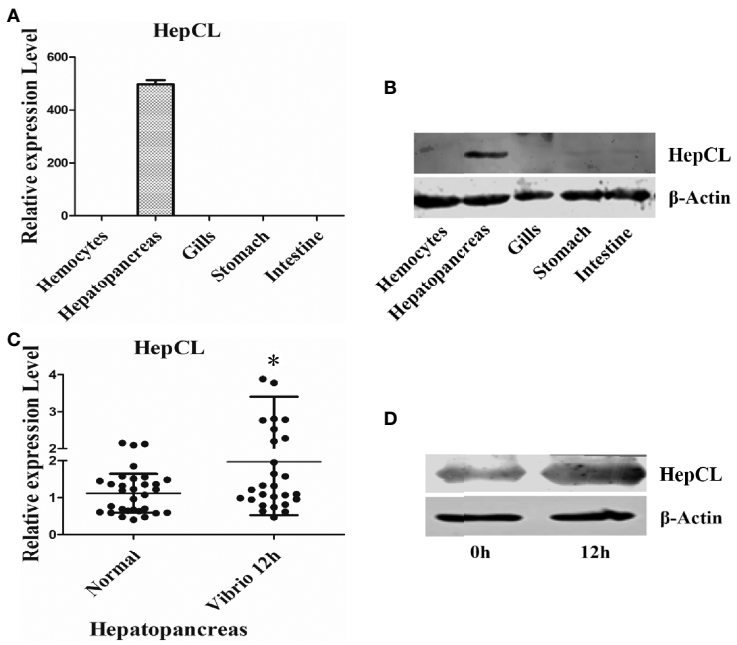

FIGURE 1 | Tissue distribution and expression profile of HepCL. **(A, B)** The tissues distribution of HepCL was detected by qRT-PCR and western blot. **(C, D)** Expression profile of HepCL were analyzed after challenged with *Vibrio* at 12 h also detected by qRT-PCR and western blot in hepatopancreas. 18S rRNA (mRNA level) and β-Actin (protein level) were used as the control. The asterisk represented the significant difference, $p < 0.05$.

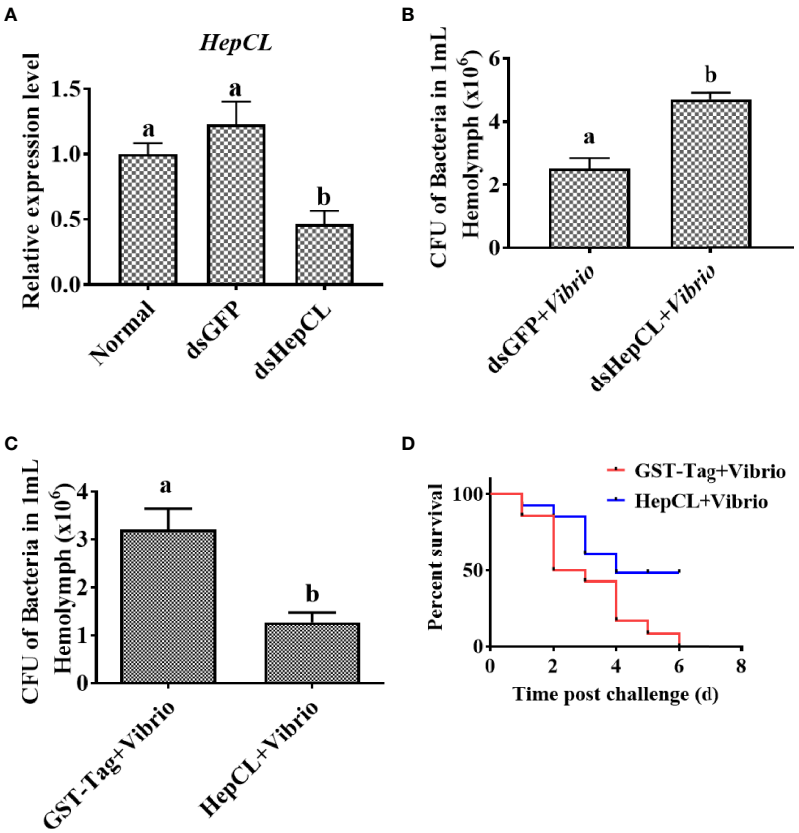

FIGURE 2 | HepCL influence survival rate and bacterial clearance capacity of crayfish. **(A)** After HepCL was knocked down, bacterial clearance experiments were performed. qPCR was used to analyze the interference effect of HepCL. **(B)** After hep was knocked down, the residual bacteria in crayfish were counted, dsGFP was used as control. **(C)** The bacterial clearance capacity of the crayfish was analyzed after HepCL was injected into Crayfish, GST- Tag protein was used as control. **(D)** The survival rate was counted after HepCL and *Vibrio* injected, GST-Tag was used as the control. Differences among the groups were analyzed using a t-test, different letters indicate significant differences $p < 0.05$.

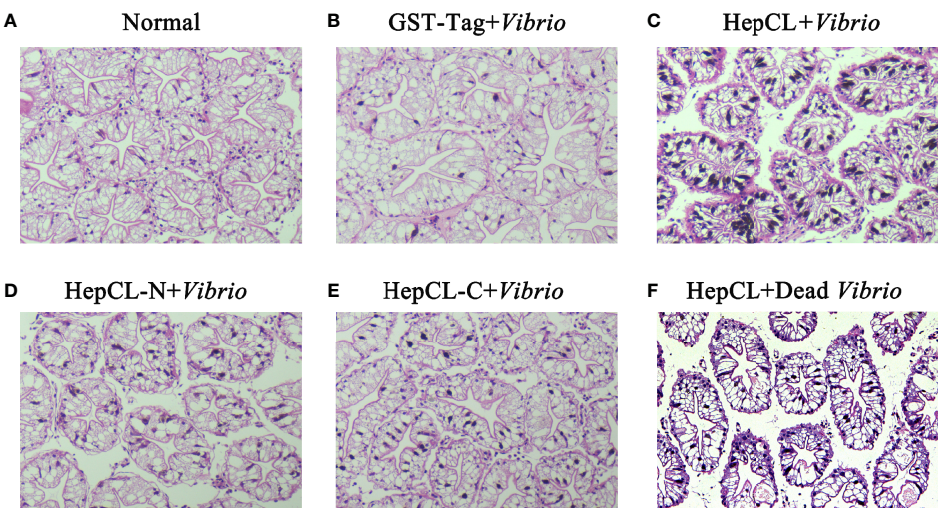

FIGURE 3 | Histological section analysis of hepatopancreas. H&E stain was used in this assay. Proteins (GST-Tag **(B)**, HepCL **(C)**, HepCL-N **(D)**, HepCL-C **(E)** were injected into crayfish, then crayfish was challenged with 10^6 *Vibrio*. **(F)** After protein HepCL injection, the crayfish was injected with heat-inactivated *Vibrio* (Dead *Vibrio*). Normal crayfish was used as control **(A)**.

with the corresponding proteins and then infected with *Vibrio* 1 h after the first injection. Thirty minutes after infection, hemolymph and hepatopancreas homogenates were collected. The bacterial clearance activity of crayfish injected with HepCL or HepCL-N was more effective than those crayfish injected with HepCL-C in both the hemolymph (**Figure 4A**) and hepatopancreas (**Figure 4B**). These results suggest that N-terminal CRD (HepCL-N) plays a key role in maintaining bacterial homeostasis.

Bacterial Binding Analysis

It has reported that CTLs could bind the bacteria, then promote phagocytosis or inhibit bacteria proliferation. To gain further insight into the role of HepCL in antibacterial immunity, the bacterial binding activities of HepCL, HepCL-N and HepCL-C were analyzed by western blot using the six kinds of bacteria. As shown in **Figure 5**, HepCL, HepCL-N and HepCL-C could bind to all the tested bacteria, while the binding activity of HepCL-N was weaker than that of HepCL and HepCL-C. These results suggest that HepCL-C contributed more bacterial binding activity.

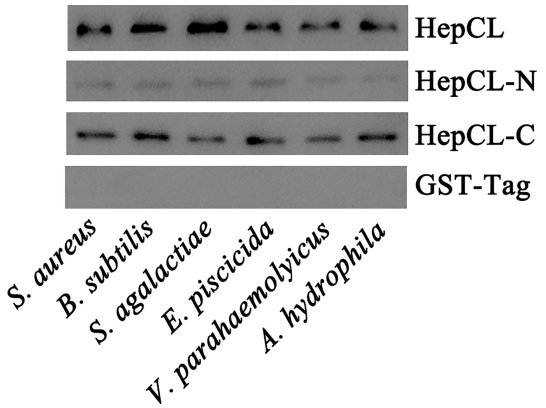

FIGURE 5 | Bacterial binding assay. Six kinds of bacteria *S. aureus, B subtilis and S. agalactiae, E piscicida, V. parahaemolyticus and A hydrophila*, were used to analyze the binding activity of recombinant HepCL, HepCL-N, HepCL-C by western blot, and detected with anti-GST-Tag antibody. GST-Tag was involved as control.

HepCL Regulates the Expression of Antimicrobial Proteins

HepCL did not show any activity in inhibiting bacterial proliferation (data not shown). We wanted to know whether HepCL is involved in anti-bacterial immunity as a regulatory factor. We analyzed whether HepCL regulates the expression of antimicrobial proteins. The antimicrobial proteins expression levels were detected after *Vibrio* and *S. aureus* infection. The result showed that the expression levels of all antimicrobial proteins which were tested, were significantly upregulated (**Figure 6A**). To analyze the possible mechanism of HepCL in antibacterial immunity, the expression levels of antimicrobial proteins were analyzed, in Anti-HepCL injection- or HepCL knockeddown-crayfish at 6 h after *Vibrio* challenge (**Figure 7A**). The expression levels of five antimicrobial proteins were evaluated, including four antimicrobial peptides (ALF1, ALF2, ALF5 and Lys-i1) and a ficolin-like protein (FLP), after *Vibrio* challenge in crayfish. The results showed that in Anti-HepCL injection crayfish the expression levels of FLP, ALF1, ALF5 and Lys-i1 were downregulated (**Figures 6B, C, E, F**), while the expression levels of ALF2 was not (**Figure 6D**) compared with those in the Anti-actin injection crayfish. In dsHepCL injection crayfish, the expression levels of FLP, ALF1 and ALF5 were downregulated (**Figures 7B, C, E**), while the expression levels of ALF2 and Lys-i1 were not (**Figures 7D, F**) compared with those

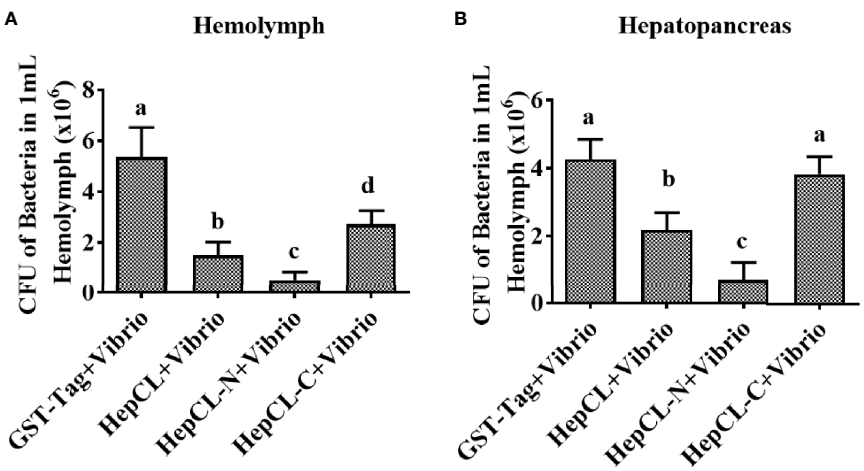

FIGURE 4 | Bacterial clearance assay. Bacterial clearance assay was involved to study the function of different domain of HepCL in antibacterial immunity. Crayfish were injected with HepCL, HepCL-N, HepCL-C 1 h later challenged with *Vibrio*, after 30 mpi, hemocytes **(A)** and hepatopancreas **(B)** were collected and the number of bacteria was counted. The group of GST-tag was used as control. Differences between groups were analyzed using one-way analysis of variance (ANOVA). Different letters indicate significant differences ($p < 0.05$).

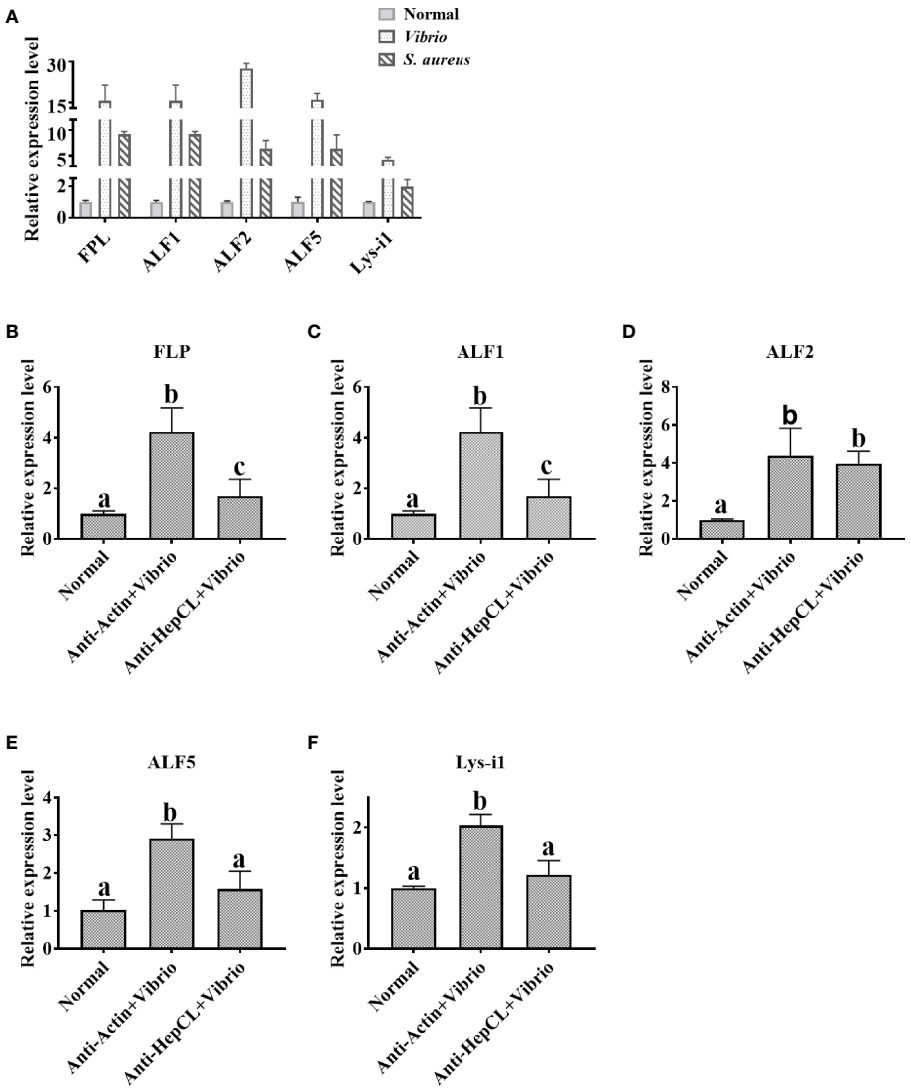

FIGURE 6 | The expression levels of antimicrobial proteins after Anti-HepCL-*Vibrio* injection. **(A)** The expression levels of FLP, ALF1, ALF2, ALF5 and Lys-i1 were analyzed by qRT-PCR after *Vibrio* and *S. aureus* infection. **(B–F)** The expression levels of FLP, ALF1, ALF2, ALF5 and Lys-i1 was analyzed when blocked HepCL with Anti-HepCL after *Vibrio* infection, Anti-actin was used as control. Differences between groups were analyzed using one-way analysis of variance (ANOVA). Different letters indicate significant differences $p < 0.05$.

in the dsGFP injection group. All the above results indicated that block and knockdown of HepCL specifically downregulated the expression of some antimicrobial proteins.

DISCUSSION

Invertebrates possess an innate immune system, lack acquired immune system that is dependent on immunoglobulin (41). Pathogen-associated molecular patterns (PAMPs) are detected by host pattern recognition receptors (PRRs) in innate immunity. C-type lectins are important pattern recognition receptors in the innate immune system of invertebrates. Lectins are generally expressed in lymphocytes and act as immunoglobulins (42, 43). Some insect lectins can bind to bacterial lipopolysaccharides by O-specific chains (44). A hepatopancreas specific C-type lectin (*Pm*LT) binds to bacteria and activates the innate immunity of *Penaeus monodon* (45). CTL33, mainly in stomach and intestine, mediated biofilm formation by intestinal bacteria was reported, providing a new view into the homeostasis of intestinal regulation in invertebrates (35). MjHeCL inhibits the proliferation of the hemolymph microbiota in maintaining a healthy status (18). The hepatopancreas is one of the major digestive and immune tissues of shrimp. In this study, we identified a C-type lectin from crayfish, HepCL, with two different CRDs that was primarily expressed in the hepatopancreas and plays a very important role in the crayfish antibacterial immune response.

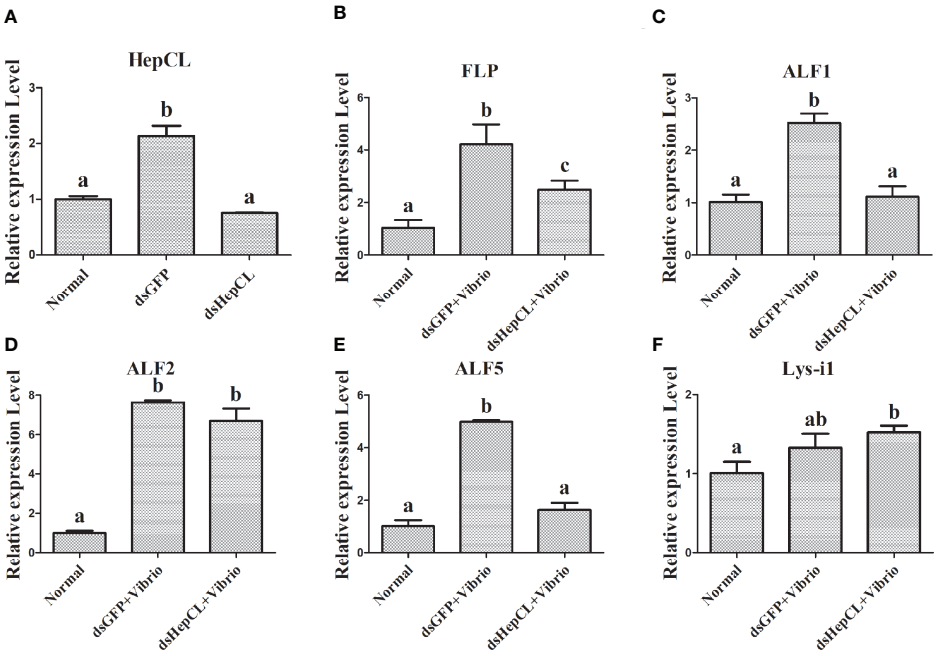

FIGURE 7 | The expression levels of antimicrobial proteins after knockdown of HepCL. **(A)** qPCR was used to analyzes the effect of HepCL was knockeddown. **(B–F)** The expression levels of FLP, ALF1, ALF2, ALF5 and Lys-i1 was analyzed under knockdown of HepCL after *Vibrio* infection by qPCR, dsGFP was used as control. Differences between groups were analyzed using one-way analysis of variance (ANOVA). Different letters indicate significant differences $p < 0.05$.

HepCL was primarily expressed in the hepatopancreas at mRNA and protein level, and it was detected low expression at protein level in stomach and intestine (**Figures 1A, B**). There is a signal peptide at the N-terminus of HepCL. These results suggest that HepCL may be a secretory protein that is synthesized from the hepatopancreas and secreted into circulatory hemolymph.

Previous studies have shown that most CTLs play a key role in immune responses, and their expression levels can be upregulated after challenge by pathogenic microorganisms. *Vibrio* infection could cause pathological changes in the hepatopancreas of shrimp. Ficolin-like protein (FLP1), a type of lectin, could protect the connection between the lobule from *Vibrio* infection in crayfish (46). As shown in **Figure 3B**, *Vibrio* infection induced an obvious inflammatory response in the hepatopancreas. There were obvious hepatopancreatic tube shrinkage and cell infiltration when injected with HepCL and HepCL-N, compared with that which injected with GST or HepCL-C (**Figure 3**). STAT3 signaling hyperactivation occurs in most human cancers and is connected with a poor prognosis (47). These results suggest that HepCL may be closely related to the activation of inflammatory response.

The histopathological analysis prompted us to consider the possibility that HepCL may be connected with other immune responses. CRDs usually contain key motifs, such as EPN (Glu-Pro-Asn), EPS (Glu-Pro-Ser), LND (Leu-Asn-Asp), and QAP (Glu-Ala-Pro), which bind to polysaccharides (9, 48). HepCL contains two dissimilar CRDs. HepCL and the C-terminal CRD (HepCL-C) showed strong binding activity, but the N-terminal CRD (HepCL-N) with "EPS and LND" motifs was weak (**Figure 5**). The bacterial clearance efficiency of the HepCL-N injection crayfish was higher than that of the HepCL-C injection crayfish (**Figure 4**). CfLec-3 from scallop with three CRDs that occurred obvious different functions, as CRD1 showed strong binding activity, while CRD2/3 showed more function in facilitating hemocyte mediated opsonisation (49). Our results suggest that other molecules which may be regulated by HepCL, rather than CRDs itself, play a direct antimicrobial role. Thus, we speculate that the N-terminal CRD (HepCL-N) may trigger the innate immune response, while the C-terminal CRD (HepCL-C) plays a role in the recognition of MAMPs.

Previous studies showed that Ab and MBL are classical opsonins in mammals, and in invertebrates, some CTLs were also reported as opsonins, pattern recognition or effector molecules to exert immune functions (50–52). In the current study, we found that HepCL could bind to bacteria and enhance bacterial clearance activity in crayfish, but it did not inhibit bacterial proliferation *in vitro* (data not shown). Further study showed that HepCL could regulate the expression of antimicrobial proteins (**Figures 6**, **7**). Invertebrates lack an acquired immune system, and effector molecules such as antimicrobial peptides (AMPs) play important roles in innate immunity (53). The rapid synthesis and release of active AMPs is a significant strategy in invertebrate host defenses. In *M. japonicas*, *Mj*CC-CL upregulates the expression of AMPs *via* the JAK/STAT signaling pathway in the antibacterial response (24). HcLec4 is involved in the regulation of AMP expression (21). MjHeCL binds to hemocytes to modulate the expression of AMPs (18). A new AMP inhibits *A. hydrophila* infection in crayfish, and new insights

into the maturation of AMPs were revealed (54). We speculated that HepCL may modulate the expression of antimicrobial proteins to exert an antibacterial immune response.

Previous studies showed that Fibrinogen-related proteins are mainly function as PRRs in invertebrates and vertebrates (55, 56). Two ficolin-like proteins function as pattern recognition receptors in the innate immunity of crayfish (57). A Fibrinogen-related protein (FREP) in *M. japonicus* was reported that plays an important role in the antibacterial immunity by binding bacteria and enhancing bacterial clearance (58). Our previous results showed that ficolin (FLP) could bind to bacteria and inhibit the replication of bacteria in *P. clarkii* (46). Some shrimp ALFs, which is a type of AMPs, have important motifs interact with LPS in antibacterial immunity (mainly Gram-negative bacteria) (59). ALF5 inhibits proliferation of microbiota by binding to RPS4 and MscL of *E. coli* in Crayfish (60). In this project, the expression levels of two AMPs (ALF1 and ALF5) and FLP were upregulated in *Vibrio* and *S. aureus* infection crayfish (**Figure 6A**), while the expression levels of them were downregulated after challenge with *Vibrio* in Anti-HepCL injection crayfish (**Figure 6**) and HepCL knockeddown crayfish (**Figure 7**). When the crayfish was injected with HepCL protein, the number of bacteria in the crayfish decreased than those in control crayfish (**Figure 2C**), while in the crayfish of HepCL was knockeddown, the number of bacteria in the crayfish increased than those in control crayfish (**Figure 2B**). The present study revealed that HepCL might be involved in the antibacterial immune response by regulating the expression of antimicrobial proteins rather than by the classical inhibition of bacterial replication and decreasing pathological changes. Hyperactivation of the immune system (overly strong or long-lasting activation) can subsequently lead to organ dysfunction and increased susceptibility to secondary infections (61). An inflammatory storm caused by the high expression of antimicrobial molecules in a short period of time leads to cell infiltration. The underlying mechanism by which HepCL regulates the expression of antibacterial proteins needs further study.

DATA AVAILABILITY STATEMENT

The datasets presented in this study can be found in online repositories. The names of the repository/repositories and accession number(s) can be found below: https://www.ncbi.nlm.nih.gov/genbank/, 2437240.

AUTHOR CONTRIBUTIONS

All authors listed have made a substantial, direct, and intellectual contribution to the work, and approved it for publication.

FUNDING

This work was supported by grants from the open project of Agriculture Ministry Key Laboratory of Healthy Freshwater Aquaculture (No. ZJK201804), the National Key Research and Development Program of China (No. 2020YFD0900303), Technical Innovation Project of Hubei province (No. 2018ABA103), Research on Public Welfare Technology Application Projects of Zhejiang Province (No. 2017C32012).

REFERENCES

1. Maynard CL, Elson CO, Hatton RD, Weaver CT. Reciprocal Interactions of the Intestinal Microbiota and Immune System. *Nature* (2012) 489:231–41. doi: 10.1038/nature11551
2. Duron O, Hurst GD. Arthropods and Inherited Bacteria: From Counting the Symbionts to Understanding How Symbionts Count. *BMC Biol* (2013) 11:45. doi: 10.1186/1741-7007-11-45
3. Kamada N, Seo SU, Chen GY, Núñez G. Role of the Gut Microbiota in Immunity and Inflammatory Disease. *Nat Rev Immunol* (2013) 13:321–35. doi: 10.1038/nri3430
4. Loker ES, Adema CM, Zhang SM, Kepler TB. Invertebrate Immune Systems–Not Homogeneous, Not Simple, Not Well Understood. *Immunol Rev* (2004) 198:10–24. doi: 10.1111/j.0105-2896.2004.0117.x
5. Vasta GR, Ahmed H, Odom EW. Structural and Functional Diversity of Lectin Repertoires in Invertebrates, Protochordates and Ectothermic Vertebrates. *Curr Opin Struct Biol* (2004) 14:617–30. doi: 10.1016/j.sbi.2004.09.008
6. Hanington PC, Forys MA, Dragoo JW, Zhang SM, Adema CM, Loker ES. Role for a Somatically Diversified Lectin in Resistance of an Invertebrate to Parasite Infection. *Proc Natl Acad Sci U S A* (2010) 107:21087–92. doi: 10.1073/pnas.1011242107
7. Amparyup P, Sutthangkul J, Charoensapsri W, Tassanakajon A. Pattern Recognition Protein Binds to Lipopolysaccharide and β-1,3-glucan and Activates Shrimp Prophenoloxidase System. *J Biol Chem* (2016) 291:10949. doi: 10.1074/jbc.A111.294744
8. Christophides GK, Vlachou D, Kafatos FC. Comparative and Functional Genomics of the Innate Immune System in the Malaria Vector*Anopheles Gambiae*. *Immunol Rev* (2004) 198:127–48. doi: 10.1111/j.0105-2896.2004.0127.x
9. Zelensky AN, Gready JE. The C-type Lectin-Like Domain Superfamily. *FEBS J* (2005) 272:6179–217. doi: 10.1111/j.1742-4658.2005.05031.x
10. Wang Z, Chen YH, Dai YJ, Tan JM, Huang Y, Lan JF, et al. A Novel Vertebrates Toll-like Receptor Counterpart Regulating the Anti-Microbial Peptides Expression in the Freshwater Crayfish, *Procambarus Clarkii*. *Fish Shellfish Immunol* (2015) 43:219–29. doi: 10.1016/j.fsi.2014.12.038
11. Ali YM, Lynch NJ, Haleem KS, Fujita T, Endo Y, Hansen S, et al. The Lectin Pathway of Complement Activation is a Critical Component of the Innate Immune Response to Pneumococcal Infection. *PloS Pathog* (2012) 8: e1002793. doi: 10.1371/journal.ppat.1002793
12. Cedzynski M, Swierzko AS, Kilpatrick DC. Factors of the Lectin Pathway of Complement Activation and Their Clinical Associations in Neonates. *J BioMed Biotechnol* (2012) 2012:363246. doi: 10.1155/2012/363246
13. Robinson MJ, Sancho D, Slack EC, LeibundGut-Landmann S, Reis e Sousa C. Myeloid C-type Lectins in Innate Immunity. *Nat Immunol* (2006) 7:1258–65. doi: 10.1038/ni1417
14. Shagin DA, Barsova EV, Bogdanova E, Britanova OV, Gurskaya N, Lukyanov KA, et al. Identification and Characterization of a New Family of C-type Lectin-Like Genes From Planaria *Girardia tigrina*. *Glycobiology* (2002) 12:463–72. doi: 10.1093/glycob/cwf056
15. Yu XQ, Kanost MR. Immulectin-2, a Lipopolysaccharide-Specific Lectin From an Insect, *Manduca Sexta*, is Induced in Response to Gram-Negative Bacteria. *J Biol Chem* (2000) 275:37373–81. doi: 10.1074/jbc.M003021200
16. Watanabe A, Miyazawa S, Kitami M, Tabunoki H, Ueda K, Sato R. Characterization of a Novel C-Type Lectin*Bombyx Mori* Multibinding Protein, From the B. Mori Hemolymph: Mechanism of Wide-Range Microorganism Recognition and Role in Immunity. *J Immunol* (2006) 177:4594–604. doi: 10.4049/jimmunol.177.7.4594

17. Ao J, Ling E, Yu XQ. *Drosophila* C-type Lectins Enhance Cellular Encapsulation. *Mol Immunol* (2007) 44:2541–48. doi: 10.1016/j.molimm.2006.12.024
18. Wang XW, Xu JD, Zhao XF, Vasta GR, Wang JX. A Shrimp C-Type Lectin Inhibits Proliferation of the Hemolymph Microbiota by Maintaining the Expression of Antimicrobial Peptides. *J Biol Chem* (2014) 289:11779–90. doi: 10.1074/jbc.M114.552307
19. Wang XW, Zhao XF, Wang JX. C-Type Lectin Binds to β-Integrin to Promote Hemocytic Phagocytosis in an Invertebrate. *J Biol Chem* (2014) 289:2405–14. doi: 10.1074/jbc.M113.528885
20. Sun YD, Fu LD, Jia YP, Du XJ, Wang Q, Wang YH, et al. A Hepatopancreas-Specific C-Type Lectin From the Chinese Shrimp*Fenneropenaeus Chinensis* Exhibits Antimicrobial Activity. *Mol Immunol* (2008) 45:348–61. doi: 10.1016/j.molimm.2007.06.355
21. Zhao LL, Wang YQ, Dai YJ, Zhao LJ, Qin QW, Lin L, et al. A Novel C-Type Lectin With Four Crds is Involved in the Regulation of Antimicrobial Peptide Gene Expression in*Hyriopsis Cumingii*. *Fish Shellfish Immunol* (2016) 55:339–47. doi: 10.1016/j.fsi.2016.06.007
22. Schnitger AK, Yassine H, Kafatos FC, Osta MA. Two C-type Lectins Cooperate to Defend*Anopheles Gambiae* Against Gram-negative Bacteria. *J Biol Chem* (2009) 284:17616–24. doi: 10.1074/jbc.M808298200
23. Höft MA, Hoving JC, Brown GD. Signaling C-Type Lectin Receptors in Antifungal Immunity. *Curr Top Microbiol Immunol* (2020) 429:63–101. doi: 10.1007/82_2020_224
24. Sun JJ, Lan JF, Zhao XF, Vasta GR, Wang JX. Binding of a C-type Lectin's Coiled-Coil Domain to the Domeless Receptor Directly Activates the JAK/STAT Pathway in the Shrimp Immune Response to Bacterial Infection. *PloS Pathog* (2017) 13:e1006626. doi: 10.1371/journal.ppat.1006626
25. Geng T, Lu F, Wu H, Wang Y, Lou D, Tu N, et al. C-Type Lectin 5, a Novel Pattern Recognition Receptor for the JAK/STAT Signaling Pathway in *Bombyx Mori*. *J Invertebr Pathol* (2021) 179:107473. doi: 10.1016/j.jip.2020.107473
26. Zhao ZY, Yin ZX, Xu XP, Weng SP, Rao XY, Dai ZX, et al. A Novel C-Type Lectin From the Shrimp*Litopenaeus Vannamei* Possesses Anti-White Spot Syndrome Virus Activity. *J Virol* (2009) 83:347–56. doi: 10.1128/JVI.00707-08
27. Tailleux L, Schwartz O, Herrmann JL, Pivert E, Jackson M, Amara A, et al. Dc-SIGN is the Major Mycobacterium Tuberculosis Receptor on Human Dendritic Cells. *J Exp Med* (2003) 197:121–27. doi: 10.1084/jem.20021468
28. Halary F, Amara A, Lortat-Jacob H, Messerle M, Delaunay T, Houlès C, et al. Human Cytomegalovirus Binding to DC-SIGN is Required for Dendritic Cell Infection and Target Cell Trans-Infection. *Immunity* (2002) 17:653–64. doi: 10.1016/s1074-7613(02)00447-8
29. Klimstra WB, Nangle EM, Smith MS, Yurochko AD, Ryman KD. Dc-SIGN and L-SIGN can Act as Attachment Receptors for Alphaviruses and Distinguish Between Mosquito Cell- and Mammalian Cell-Derived Viruses. *J Virol* (2003) 77:12022–32. doi: 10.1128/jvi.77.22.12022-12032.2003
30. Tassaneetrithep B, Burgess TH, Granelli-Piperno A, Trumpfheller C, Finke J, Sun W, et al. Dc-SIGN (Cd209) Mediates Dengue Virus Infection of Human Dendritic Cells. *J Exp Med* (2003) 197:823–29. doi: 10.1084/jem.20021840
31. Miller JL, de Wet BJ, Martinez-Pomares L, Radcliffe CM, Dwek RA, Rudd PM, et al. The Mannose Receptor Mediates Dengue Virus Infection of Macrophages. *PloS Pathog* (2008) 4:e17. doi: 10.1371/journal.ppat.0040017
32. Cheng G, Cox J, Wang P, Krishnan MN, Dai J, Qian F, et al. A C-type Lectin Collaborates With a CD45 Phosphatase Homolog to Facilitate West Nile Virus Infection of Mosquitoes. *Cell* (2010) 142:714–25. doi: 10.1016/j.cell.2010.07.038
33. Gomez-Gil B, Tron-Mayén L, Roque A, Turnbull JF, Inglis V, Guerra-Flores AL. Species of *Vibrio* Isolated From Hepatopancreas, Haemolymph and Digestive Tract of a Population of Healthy Juvenile *Penaeus Vannamei*. *Aquaculture* (1998) 163:0–9. doi: 10.1016/s0044-8486(98)00162-8
34. Fagutao FF, Koyama T, Kaizu A, Saito-Taki T, Kondo H, Aoki T, et al. Increased Bacterial Load in Shrimp Hemolymph in the Absence of Prophenoloxidase. *FEBS J* (2009) 276:5298–306. doi: 10.1111/j.1742-4658.2009.07225.x
35. Zhang YX, Zhang ML, Wang XW. C-Type Lectin Maintains the Homeostasis of Intestinal Microbiota and Mediates Biofilm Formation by Intestinal Bacteria in Shrimp. *J Immunol* (2021) 206:1140–50. doi: 10.4049/jimmunol.2000116
36. Pang X, Xiao X, Liu Y, Zhang R, Liu J, Liu Q, et al. Mosquito C-type Lectins Maintain Gut Microbiome Homeostasis. *Nat Microbiol* (2016) 1:16023. doi: 10.1038/nmicrobiol.2016.23
37. Söderhäll K, Smith VJ. Separation of the Haemocyte Populations of Carcinus Maenas and Other Marine Decapods, and Prophenoloxidase Distribution. *Dev Comp Immunol* (1983) 7:229–39. doi: 10.1016/0145-305x(83)90004-6
38. Dai YJ, Wang YQ, Zhao LL, Qin ZD, Yuan JF, Qin QW, et al. A Novel L-Type Lectin was Required for the Multiplication of WSSV in Red Swamp Crayfish (*Procambarus Clakii*). *Fish Shellfish Immunol* (2016) 55:48–55. doi: 10.1016/j.fsi.2016.05.020
39. Livak KJ, Schmittgen TD. Analysis of Relative Gene Expression Data Using Real-Time Quantitative PCR and the 2(-Delta Delta C(T)) Method. *Methods* (2001) 25:402–8. doi: 10.1006/meth.2001.1262
40. Lan JF, Li XC, Sun JJ, Gong J, Wang XW, Shi XZ, et al. Prohibitin Interacts With Envelope Proteins of White Spot Syndrome Virus and Prevents Infection in the Red Swamp Crayfish*Procambarus Clarkii*. *J Virol* (2013) 87:12756–65. doi: 10.1128/JVI.02198-13
41. Hoffmann JA. The Immune Response of *Drosophila*. *Nature* (2003) 426:33–8. doi: 10.1038/nature02021
42. Wang XW, Wang JX. Crustacean Hemolymph Microbiota: Endemic, Tightly Controlled, and Utilization Expectable. *Mol Immunol* (2015) 68:404–11. doi: 10.1016/j.molimm.2015.06.018
43. Huang Y, Ren Q. Research Progress in Innate Immunity of Freshwater Crustaceans. *Dev Comp Immunol* (2020) 104:103569. doi: 10.1016/j.dci.2019.103569
44. Shin SW, Park DS, Kim SC, Park HY. Two Carbohydrate Recognition Domains of*Hyphantria Cunea* Lectin Bind to Bacterial Lipopolysaccharides Through O-Specific Chain. *FEBS Lett* (2000) 467:70–4. doi: 10.1016/s0014-5793(00)01127-3
45. Ma TH, Benzie JA, He JG, Chan SM. *Pm*LT, a C-type Lectin Specific to Hepatopancreas is Involved in the Innate Defense of the Shrimp*Penaeus Monodon*. *J Invertebr Pathol* (2008) 99:332–41. doi: 10.1016/j.jip.2008.08.003
46. Dai YJ, Wang YQ, Zhang YH, Liu Y, Li JQ, Wei S, et al. The Role of Ficolin-Like Protein (*Pc*FLP1) in the Antibacterial Immunity of Red Swamp Crayfish (*Procambarus Clarkii*). *Mol Immunol* (2017) 81:26–34. doi: 10.1016/j.molimm.2016.11.017
47. Johnson DE, O'Keefe RA, Grandis JR. Targeting the IL-6/JAK/STAT3 Signalling Axis in Cancer. *Nat Rev Clin Oncol* (2018) 15:234–48. doi: 10.1038/nrclinonc.2018.8
48. Cambi A, Koopman M, Figdor CG. How C-type Lectins Detect Pathogens. *Cell Microbiol* (2005) 7:481–8. doi: 10.1111/j.1462-5822.2005.00506.x
49. Yang J, Huang M, Zhang H, Wang L, Wang H, Wang L, et al. Cflec-3 From *Scallop*: An Entrance to non-Self Recognition Mechanism of Invertebrate C-Type Lectin. *Sci Rep* (2015) 5:10068. doi: 10.1038/srep10068
50. Thiel S, Gadjeva M. Humoral Pattern Recognition Molecules: Mannan-Binding Lectin and Ficolins. *Adv Exp Med Biol* (2009) 653:58–73. doi: 10.1007/978-1-4419-0901-5_5
51. Tian YY, Liu Y, Zhao XF, Wang JX. Characterization of a C-type Lectin From the Cotton Bollworm*Helicoverpa Armigera*. *Dev Comp Immunol* (2009) 33:772–9. doi: 10.1016/j.dci.2009.01.002
52. Goh YS, Grant AJ, Restif O, McKinley TJ, Armour KL, Clark MR, et al. Human IgG Isotypes and Activating Fcγ Receptors in the Interaction of Salmonella Enterica Serovar Typhimurium With Phagocytic Cells. *Immunology* (2011) 133:74–83. doi: 10.1111/j.1365-2567.2011.03411.x
53. Zhou J, Fang NN, Zheng Y, Liu KY, Mao B, Kong LN, et al. Identification and Characterization of Two Novel C-type Lectins From the Larvae of Housefly, *Musca Domestica* L. *Arch Insect Biochem Physiol* (2018) 98:e21467. doi: 10.1002/arch.21467
54. Zhao BR, Zheng Y, Gao J, Wang XW. Maturation of an Antimicrobial Peptide Inhibits *Aeromonas Hydrophila* Infection in Crayfish. *J Immunol* (2020) 204:487–97. doi: 10.4049/jimmunol.1900688
55. Adema CM, Hertel LA, Miller RD, Loker ES. A Family of Fibrinogen-Related Proteins That Precipitates Parasite-Derived Molecules is Produced by an Invertebrate After Infection. *Proc Natl Acad Sci U S A* (1997) 94:8691–6. doi: 10.1073/pnas.94.16.8691
56. Runza VL, Schwaeble W, Männel DN. Ficolins: Novel Pattern Recognition Molecules of the Innate Immune Response. *Immunobiology* (2008) 213:297–306. doi: 10.1016/j.imbio.2007.10.009
57. Wu C, Söderhäll K, Söderhäll I. Two Novel Ficolin-Like Proteins Act as Pattern Recognition Receptors for Invading Pathogens in the Freshwater

Crayfish*Pacifastacus Leniusculus*. *Proteomics* (2011) 11:2249–64. doi: 10.1002/pmic.201000728
58. Sun JJ, Lan JF, Shi XZ, Yang MC, Yang HT, Zhao XF, et al. A Fibrinogen-Related Protein (FREP) is Involved in the Antibacterial Immunity of*Marsupenaeus Japonicus*. *Fish Shellfish Immunol* (2014) 39:296–304. doi: 10.1016/j.fsi.2014.05.005
59. Rosa RD, Vergnes A, de Lorgeril J, Goncalves P, Perazzolo LM, Sauné L, et al. Functional Divergence in Shrimp Anti-Lipopolysaccharide Factors (Alfs): From Recognition of Cell Wall Components to Antimicrobial Activity. *PloS One* (2013) 8:e67937. doi: 10.1371/journal.pone.0067937
60. Yin CM, Pan XY, Cao XT, Li T, Zhang YH, Lan JF. A Crayfish Alf Inhibits the Proliferation of Microbiota by Binding to RPS4 and MscL of *E. Coli*. *Dev Comp Immunol* (2021) 121:104106. doi: 10.1016/j.dci.2021.104106
61. Medzhitov R, Schneider DS, Soares MP. Disease Tolerance as a Defense Strategy. *Science* (2012) 335:936–41. doi: 10.1126/science.1214935

Conflict of Interest: The authors declare that the research was conducted in the absence of any commercial or financial relationships that could be construed as a potential conflict of interest.

Advantages of publishing in Frontiers

OPEN ACCESS
Articles are free to read for greatest visibility and readership

FAST PUBLICATION
Around 90 days from submission to decision

HIGH QUALITY PEER-REVIEW
Rigorous, collaborative, and constructive peer-review

TRANSPARENT PEER-REVIEW
Editors and reviewers acknowledged by name on published articles

Frontiers
Avenue du Tribunal-Fédéral 34
1005 Lausanne | Switzerland

Visit us: www.frontiersin.org
Contact us: frontiersin.org/about/contact

REPRODUCIBILITY OF RESEARCH
Support open data and methods to enhance research reproducibility

DIGITAL PUBLISHING
Articles designed for optimal readership across devices

FOLLOW US
@frontiersin

IMPACT METRICS
Advanced article metrics track visibility across digital media

EXTENSIVE PROMOTION
Marketing and promotion of impactful research

LOOP RESEARCH NETWORK
Our network increases your article's readership